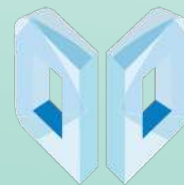


BMC Oral Health Digital Dentistry

Collection of Scientific Papers - Year 2019

Official Journal of the
International Digital Dentistry Society

Digital Dentistry Section Editor:
Francesco Mangano



Digital
Dentistry
Society

BMC Oral Health



SUMMARY

- 7** Anne Menard
Editorial
- 9** Francesco Mangano
Editorial
- 11** Ju-Won Kim, Jong-Cheol Kim, Chun-Gi Jeong, Kyeong-Jun Cheon, Seoung-Won Cho, In-Young Park and Byoung-Eun Yang
The accuracy and stability of the maxillary position after orthognathic surgery using a novel computer-aided surgical simulation system (19:18)
- 24** Francesca Gazzani, Chiara Pavoni, Paola Cozza and Roberta Lione
Stress on facial skin of class III subjects during maxillary protraction: a finite element analysis (19:31)
- 30** Alexey Unkovskiy, Eugen Wahl, Anne Teresa Zander, Fabian Huettig and Sebastian Spintzyk
Intraoral scanning to fabricate complete dentures with functional borders: a proof-of-concept case report (19:46)
- 37** Thomas Spielau, Uli Hauschild and Joannis Katsoulis
Computer-assisted, template-guided immediate implant placement and loading in the mandible: a case report (19:55)
- 46** Zhongpeng Yang, Tianmin Xu and Ruoping Jiang
Deviations in palatal region between indirect and direct digital models: an in vivo study (19:66)
- 58** Agostino Guida , Mariagrazia Maglione, Anna Crispo, Francesco Perri, Salvatore Villano, Ettore Pavone, Corrado Aversa, Francesco Longo, Florinda Feroce, Gerardo Botti and Franco Ionna
Oral lichen planus and other confounding factors in NBI during routine inspection of oral cavity for early detection of oral squamous cell carcinoma: a retrospective pilot study (19:70)
- 67** Francesco Guido Mangano , Uli Hauschild, Giovanni Veronesi, Mario Imburgia, Carlo Mangano and Oleg Admakin
Trueness and precision of 5 intraoral scanners in the impressions of single and multiple implants: a comparative in vitro study (19:101)
- 81** Avi Meirowitz, Yoli Bitterman, Sharon Levy, Eitan Mijiritsky and Eran Dolev
An in vitro evaluation of marginal fit of zirconia crowns fabricated by a CAD-CAM dental laboratory and a milling center (19:103)
- 87** Peter Gehrke , Konstantin Bleuel, Carsten Fischer and Robert Sader
Influence of margin location and luting material on the amount

SUMMARY

of undetected cement excess on CAD/CAM implant abutments and cement-retained zirconia crowns: an in-vitro study (19:111)

99

Fernando Zarone , Maria Irene Di Mauro, Pietro Ausiello, Gennaro Ruggiero and Roberto Sorrentino

Current status on lithium disilicate and zirconia: a narrative review (19:134)

113

Marco Farronato, Cinzia Maspero, Valentina Lanteri, Andrea Fama, Francesco Ferrati, Alessandro Pettenuzzo and Davide Farronato

Current state of the art in the use of augmented reality in dentistry: a systematic review of the literature (19:135)

128

Hytham N. Fageeh , Abdullah A. Meshni, Hassan A. Jamal, Reghunathan S. Preethanath and Esam Halboub

The accuracy and reliability of digital measurements of gingival recession versus conventional methods (19:154)

136

Gerardo Pellegrino, Carlo Mangano, Roberto Mangano, Agnese Ferri, Valerio Taraschi and Claudio Marchetti

Augmented reality for dental implantology: a pilot clinical report of two cases (19:158)

144

Silvia Caruso, Alessandro Nota, Shideh Ehsani,

Elena Maddalone, Kenji Ojima and Simona Tecco

Impact of molar teeth distalization with clear aligners on occlusal vertical dimension: a retrospective study (19:182)

149

M. L. Menéndez López-Mateos, J. Carreño-Carreño, J. C. Palma, J. A. Alarcón, C. Menéndez López-Mateos and M. Menéndez-Núñez

3D photographic analysis of the face in European adults from southern Spain with normal occlusion: reference anthropometric measurements (19:196)

157

Ting Dong, Lunguo Xia, Chenglin Cai, Lingjun Yuan, Niansong Ye and Bing Fang

Accuracy of in vitro mandibular volumetric measurements from CBCT of different voxel sizes with different segmentation threshold settings (19:206)

164

Francesca Cattoni, Giulia Teté, Alessandro Mauro Calloni, Fabio Manazza, Giorgio Gastaldi and Paolo Cappare

Milled versus moulded mock-ups based on the superimposition of 3D meshes from digital oral impressions: a comparative in vitro study in the aesthetic area (19:230)

172

Ashraf Ayoub and Yeshwanth Pulijala

The application of virtual reality and augmented reality in Oral & Maxillofacial Surgery (19:238)

- 180** Francesca Gazzani , Roberta Lione, Chiara Pavoni, Gianluca Mampieri and Paola Cozza

Comparison of the abrasive properties of two different systems for interproximal enamel reduction: oscillating versus manual strips (19:247)

- 187** Vladimir Yu. Reshetnyak, Olga V. Nesterova, Oleg I. Admakin, Denis A. Dobrokhoto, Irina N. Avertseva, Samira A. Dostdar and Dinara F. Khakimova

Evaluation of free and total fluoride concentration in mouthwashes via measurement with ion-selective electrode (19:251)

- 195** Jaafar Mouhyi, Maurice Albert Salama, Francesco Guido Mangano, Carlo Mangano, Bidzina Margiani and Oleg Admakin

A novel guided surgery system with a sleeveless open frame structure: a retrospective clinical study on 38 partially edentulous patients with 1 year of follow- up (19:253)

- 212** Yiran Jiang and Gui Chen

Reliability and validity of miniscrews as references in cone-beam computed tomography and intraoral scanner digital models: study on goat heads (19:259)

- 219** Akinori Tasaka, Yuuki Uekubo, Tomoharu Mitsui, Takao Kasahara, Takuya Takanashi, Shinya Homma, Satoru Matsunaga, Shinichi Abe, Masao Yoshinari, Yasutomo Yajima, Kaoru

Sakurai and Shuichiro Yamashita

Applying intraoral scanner to residual ridge in edentulous regions: in vitro evaluation of inter-operator validity to confirm trueness (19:264)

- 229** Edoardo Ferrari Cagidiaco, Simone Grandini, Cecilia Goracci and Tim Joda

A pilot trial on lithium disilicate partial crowns using a novel prosthodontic functional index for teeth (FIT) (19:276)

- 237** G. Joós-Kovács , B. Vecsei, Sz. Körmendi, V. A. Gyarmathy, J. Borbély and P. Hermann

Trueness of CAD/CAM digitization with a desktop scanner – an in vitro study (19:280)

- 251** Antonio Scarano , Marco Stoppaccioni and Tommaso Casolino

Zirconia crowns cemented on titanium bars using CAD/CAM: a five-year follow-up prospective clinical study of 9 patients (19:286)

- 261** Proceeding of the International Digital Dentistry Society Word Congress, Baden Baden 2019

EDITORIAL

BMC, BMC Series and BMC Oral Health

Dr. Anne Menard, BMC Oral Health General Editor

What is BMC?

BMC, which was previously known as BioMed Central, is a pioneer publisher in terms of open access. BMC is now part of Springer Nature, an academic publishing group which was created in 2015 through the merger of Springer Science plus Business Media and Holtzbrinck Publishing Group's Nature Publishing Group, Palgrave Macmillan, and Macmillan Education.

In 1999, BMC committed to making high quality research open to everyone who needed access to, thereby establishing open access research.

BMC has a portfolio of approximately 300 peer-reviewed journals, in the fields of science, technology, engineering and medicine. The BMC Series is part of BMC.

What is the BMC Series?

The BMC Series is a collection of high-quality, peer-reviewed journals covering all scientific and clinical disciplines, focusing on the needs of the research communities which they serve.

The BMC Series:

- Offers an efficient and fair peer review service
- Provides a home for all publishable research within the series
- Innovates in approaches to peer review and publication
- Promotes transparency and open research
- Partners with our authors, editors and reviewers to make scientific knowledge widely available

The ethos of the BMC Series is different to many other publishers, as we do not judge papers based on their scientific originality or interest, however, the authors must be aiming to answer a valid scientific question.

The BMC Series includes 65 subject journals, including BMC Oral Health.

BMC Oral Health is an open access, peer-reviewed journal that considers articles on all aspects of the prevention, diagnosis and management of disorders of the mouth, teeth and gums, as well as related molecular genetics, pathophysiology, and epidemiology.

Our sections include:

- Clinical oral healthcare research
- Delivery, management and promotion of oral health and dental care
- Dental techniques; tools, materials and surgical research
- Epidemiology of oral health
- Oral microbiology
- Digital Dentistry

The benefits of publishing with BMC Oral Health lie within the ethos of the BMC Series: we provide a home for research which perhaps does not meet the novelty limit of some other publishers; we are open access, which makes published research widely available, globally, in turn, leading to the research being more citable; we provide waivers to authors who are from lower- or middle- income countries, allowing them to publish their valuable research, we also provide waivers to members of our affiliated society, the Digital Dentistry Society, who are producing ground-breaking research in the relatively modern field of digital dentistry.

EDITORIAL

BMC Oral Health: Digital Dentistry

Prof. Francesco Mangano, Section Editor, Digital Dentistry, BMC Oral Health

Dear Friends and Colleagues,

I hope you are well.

In 2017, I have proposed to the General Editor of BMC Oral Health to open a Section inside the Journal, entirely dedicated to Digital Dentistry. At that time, I was already an Associate Editor of the Journal, but I felt the need to introduce a new and fascinating topic like Digital Dentistry in the BMC world, and I believed that opening a Section dedicated to it was timely and necessary. As a Dentist, the Digital Revolution has radically transformed my professional life and I really believed it was necessary – and still it is – to gather scientific evidence on new devices, software, materials and protocols introduced with the advent of digital technologies. The Digital Dentistry Section published the first article in June 2017 and it was immediately a huge success, with 30.000 downloads and several citations in a very short timeframe.

Now, after three years of hard work and dedication, together with the BMC Editorial Office, the Associated Editors and the Reviewers, the Digital Dentistry Section is extremely successful, as it attracts several high quality submissions from researchers and clinicians from all over the world. The papers published in the Digital Dentistry section are very interesting for the readers, as evidenced by the large number of downloads; in addition, they are frequently cited by other researchers, and this has contributed to double the Journal's impact factor from 1.0 to 2.0.

In 2018, BMC Oral Health has become the flagship Journal of the Digital Dentistry Society (DDS). The Digital Dentistry Society (DDS) is the most important international scientific society for Digital Dentistry, with around 400 Active Members in 45 different countries, and the active involvement of some of the most prestigious dental Universities and Research Institutes worldwide.

In a moment of deep transformation, with dentistry becoming digital, the role of the Digital Dentistry Society (DDS) is key. In fact, the Digital Dentistry Society (DDS) aims to scientifically validate the new digital protocols and workflows, to educate and support dentists all over

the world. At the same time, the Digital Dentistry Society (DDS) is a reference point for the leading manufacturers and companies of the dental world, since it provides a network of researchers and clinicians that is able to support them.

The relationship between the Digital Dentistry Society (DDS) and BMC Oral Health could not be more productive and successful, as demonstrated by the large number of scientific papers published over these years. As Editor of the Digital Dentistry Section of BMC Oral Health, I am very happy to share with you this collection of scientific articles, published during 2019. I hope you will find it interesting and it will stimulate your passion for digital technologies even more.

The Third Digital Dentistry Society Consensus Conference



Digital
Dentistry
Society

October 2nd-3rd 2020

Serralunga D'Alba (IT)

The aim of DDS Consensus Conference is to define the **“State of the Art of Digital Technologies in Daily Dental Practice”**.

Program

THURSDAY 1 OCTOBER 2020

Reception of the participants at Hotel Boscareto, Serralunga d'Alba.

FRIDAY 2 OCTOBER 2020

8:45-9:00 **Introduction to the Consensus Conference**
Carlo Mangano, President of the Digital Dentistry Society

9:00-10:00 **Accuracy of cone beam computed tomographies (CBCT)**
Reinhilde Jacobs (University of Leuven, Belgium)
Discussion Panel: Scott Ganz (USA), Thomas Fortin (France), Fabrizia Luongo (Italy)

10:00-11:00 **Accuracy of intraoral scanners (IOS)**
Janos Vag (Semmelweis University, Hungary)
Discussion Panel: Vyandas Rutkunas (Lithuania), Mario Imburgia (Italy), Mahmoud Ezzat (Egypt), Walter Renne (USA)

11:00-12:00 **Accuracy of milling units and 3D printers**
Francesco Mangano (Sechenov First State Medical University of Moscow, Russia)
Discussion Panel: Piotr Nagadowsky (Poland), Carlo Mangano (Italy), Jaafar Mouhyi (Morocco)

12:00-14:00 **Lunch break**

14:00-15:00 **Marginal fit of CAD/CAM restorations: single crowns, partial prostheses, full arches**
Marco Ferrari (University of Siena, Italy)
Discussion Panel: Fernando Zarone (Italy), Julian Caplan (UK), Uli Hauschild (Germany), Eitan Mijiritsky (Israel)

15:00-16:00 **Digital occlusion**
Robert Kerstein (New York, USA)
Discussion Panel: Henriette Lerner (Germany), Miguel Stanley (Portugal), Jameel Gardee (UK), Maxim Jaisson (France)

16:00-17:00 **Dynamic navigation in implant dentistry**
Luigi Stefanelli (University La Sapienza, Rome, Italy)
Discussion Panel: Gerardo Pellegrino (Italy), Jerome Lipowicz (France), Giuseppe Luongo (Italy)

17:00-18:00 **Digital technologies in maxillofacial surgery**
Devorah Schwartz-Arad (Tel Aviv, Israel)
Discussion Panel: Ashraf Ayoub (Scotland), Claudio Marchetti (Italy), Pasquale Piombino (Italy), Katalyn Nagy (Hungary)

20:00 **Gala Dinner**

SATURDAY 3 OCTOBER 2020

9:00-10:00 **Digital technologies in Orthodontics**
Giampietro Farronato (University of Milan, Italy)
Discussion Panel: Matteo Beretta (Italy), Isabelle Savoye (Belgium), Flavia Preda (Belgium), Pablo Ramirez (Spain), Jose Navarro (Spain)

10:00-13:00 **Innovation from the partners**
Partners speech

Location



Serralunga d'Alba is famous for Barolo and Barbaresco wine, cheese, and truffles — particularly the white truffle of Alba. Because of its cultural landscapes, part of the Langhe belongs now to the UNESCO's World Heritage: an outstanding living testimony to winegrowing and winemaking traditions that stem from a long history.

RESEARCH ARTICLE

Open Access



The accuracy and stability of the maxillary position after orthognathic surgery using a novel computer-aided surgical simulation system

Ju-Won Kim^{1,4,5†}, Jong-Cheol Kim^{1,2†}, Chun-Gi Jeong², Kyeong-Jun Cheon^{1,4}, Seoung-Won Cho^{1,4}, In-Young Park^{3,4,5} and Byoung-Eun Yang^{1,4,5*}

Abstract

Background: Many reports have been published on orthognathic surgery (OGS) using computer-aided surgical simulation (CASS). The purpose of this study was to evaluate the accuracy of the maxillary repositioning and the stability of the maxilla in patients who underwent OGS using a newly developed CASS program, a customized osteotomy guide, and a customized miniplate.

Methods: Thirteen patients who underwent OGS from 2015 to 2017 were included. All patients underwent a bimaxillary operation. First, a skull-dentition hybrid 3D image was rendered by merging the cone beam computed tomography (CBCT) images with the dentition scan file. After virtual surgery (VS) using the FaceGuide® program, patient-customized osteotomy guides and miniplates were then fabricated and used in the actual operation. To compare the VS with the actual surgery and postoperative skeletal changes, each reference point marked on the image was compared before the operation (T0) and three days (T1), four months (T2), and a year (T3) after the operation, and with the VS (Tv). The differences between ΔTv (Tv-T0) and $\Delta T1$ (T1-T0) were statistically compared using tooth-based reference points. The superimposed images of Tv and T1 were also investigated at eight bone-based reference points. The differences between the reference points of the bone surface were examined to evaluate the stability of the miniplate on the maxilla over time.

Results: None of the patients experienced complications. There were no significant differences between the reference points based on the cusp tip between ΔTv and $\Delta T1$ ($p > 0.01$). Additionally, there were no significant differences between the Tv and T1 values of the bone surface ($p > 0.01$). The mean difference in the bone surface between Tv and T1 was 1.01 ± 0.3 mm. Regarding the stability of the miniplate, there were no significant differences between the groups. The difference in the bone surface between T1 and T3 was -0.37 ± 0.29 mm.

(Continued on next page)

* Correspondence: omsyang@gmail.com; face@hallym.or.kr

[†]Ju-Won Kim and Jong-Cheol Kim contributed equally to this work.

¹Division of Oral and Maxillofacial Surgery, Hallym University Sacred Heart Hospital, 11, Gwanpyeong-ro 170beon-gil, Dongan-gu, Anyang-si, Gyeonggi-do, 14066 Anyang, Republic of Korea

⁴Graduate School of Clinical Dentistry, Hallym University, Chuncheon, Republic of Korea

Full list of author information is available at the end of the article



© The Author(s). 2019 **Open Access** This article is distributed under the terms of the Creative Commons Attribution 4.0 International License (<http://creativecommons.org/licenses/by/4.0/>), which permits unrestricted use, distribution, and reproduction in any medium, provided you give appropriate credit to the original author(s) and the source, provide a link to the Creative Commons license, and indicate if changes were made. The Creative Commons Public Domain Dedication waiver (<http://creativecommons.org/publicdomain/zero/1.0/>) applies to the data made available in this article, unless otherwise stated.

(Continued from previous page)

Conclusions: VS was performed using the FaceGide® program, and customized materials produced based on the VS were applied in actual OGS. The maxilla was repositioned in almost the same manner as in the VSP plan, and the maxillary position remained stable for a year.

Keywords: Orthognathic surgery, Virtual surgery, Computer-aided surgical simulation, Patient-customized osteotomy guide (PCG), Patient-customized Miniplate (PCM)

Background

Skeletal malocclusion affects oral health and is highly associated with dental trauma and masticatory difficulties as secondary effects of parafunction and teeth crowding [1]. Orthognathic surgery (OGS) is used to resolve imbalances involved in the craniofacial structure and skeletal malocclusion, thereby improving the oral and facial function and aesthetics of the patient. The efforts of both orthodontists and surgeons can dramatically improve the quality of life of patients experiencing functional and aesthetic discomfort. However, jaw misplacement by a surgeon during OGS is difficult for an orthodontist to revise after the operation. During traditional bimaxillary OGS, the maxilla is first moved, and the mandible is relocated relative to the maxilla. Therefore, it is most important to move the maxilla to a planned position during OGS. Efforts to achieve such outcomes include freehand relocation [2] and the use of an internal reference point, which are currently applied by several surgeons. However, external reference points are the most accurate method to use during LeFort I osteotomy [3]. In recent years, the progress in OGS has mainly resulted from the use of a virtual surgery plan (VSP) to accurately reposition the bone segments [4]. There are problems associated with conventional OGS and several reasons why VSPs are favored. An analysis of dentofacial deformity is based on the information obtained through several preoperative examinations. Once the analysis is completed, subsequent surgical planning is initiated using a visual treatment objective (VTO), which determines where each component should be positioned in relation to the fixed reference structure (skull base) and another. When the VTO involves the movement of only a single jaw, either the maxilla or mandible, a simple hinge articulator is sufficient for mock surgery. However, when the VTO involves the movement of both jaws, a semi-adjustable articulator is used as these articulators can better reproduce the centric relation (CR) and centric occlusion within an acceptable anatomical average. The most difficult aspect in performing model surgery is in the repositioning of the maxillary cast during bimaxillary surgery [5]. After the mock surgery is performed according to the surgical plan, two surgical occlusal splints (an intermediate splint (IMS) and a final splint) are made for bimaxillary surgery. Occlusal splints

(or wafers) locate the dental arches in any preplanned relationships and eliminate unreliable intraoperative guesswork [6]. As the first step in simulating a bimaxillary surgery, a face-bow transfer procedure is required to transfer the maxilla to a semi-adjustable articulator. However, it is impossible to transfer the patient's maxillary dentition to the articulator and accurately reproduce the patient's anatomy [7–10]. In addition, it is difficult to achieve complete three-dimensional (3D) movement in a model surgery in cases of patients with severe facial anomalies, even though the face-bow is used to correctly reproduce the patient's actual maxillary position in the articulator. During the model surgery, the upper arm of the semi-adjustable articulator is used as a reference for moving the maxillary cast. However, the most common technique for repositioning the maxilla in the operating room is the use of an external reference point with the help of the IMS. Therefore, the substantive reference for repositioning the maxilla is the mandible. In most cases, OGS requiring maxillary movement is performed under general anesthesia. Some researchers have reported that the position of the mandible deviates from its normal position under general anesthesia [11, 12]. Even if a face-bow transfer is performed well enough to accurately reflect the anatomy of the patient, the model surgery is performed well, and the IMS is made perfectly, errors may occur when the surgeon uses the mandible as a reference and repositions the maxilla using only the IMS. Therefore, considerable time is required to determine the desired position of the maxilla when conventional bimaxillary surgery is planned. Recently, computer-aided surgical simulation (CASS) and device manufacturing using computer-aided design (CAD) and computer-aided manufacturing (CAM) technologies have attracted attention for precise OGS [13, 14]. Herein, we performed a VS using FaceGide® (MegaGen Co., Daegu, Korea), a CASS program, instead of a model surgery and face-bow transfer in preparation for OGS. In addition, patient-customized miniplates (PCMs) were used instead of the IMS. The purpose of this study was to evaluate the surgical accuracy and long-term stability of maxillary repositioning using the FaceGide® system by comparing cone beam computed tomography (CBCT) images over time.

Methods

Subjects

Thirteen patients were selected from a list of medical records. The sample consisted of seven females and six males with a mean age of 22.9 ± 3.3 years (range, 18–29). The patients were selected according to the following inclusion criteria: (1) patients who underwent surgery between February 2015 and August 2017; (2) those who completed presurgical orthodontic treatment; and (3) patients who underwent bimaxillary surgery to treat skeletal malocclusion. The exclusion criteria were as follows: (1) patients with cleft palate or craniofacial anomalies; (2) patients who had not undergone surgery with FaceGide®; and (3) patients who were unwilling to participate in this study. All medical practices conformed to the Declaration of Helsinki as a medical protocol. The study protocol was approved by the hospital's Institutional Review Board (IRB No. 2018–06-016). All patient data were anonymized and de-identified prior to the analysis. Detailed patient characteristics are presented in Table 1.

Preoperative procedures and virtual OGS

Our protocol for OGS with the FaceGide® system was as follows (Fig. 1). Clinical photographs of the patient were taken after a clinical examination. CBCT (Alphard 3030, Asahi, Inc., Kyoto, Japan) was performed two weeks before the surgery to obtain a 3D image of the patient. All images were obtained with the Frankfort plane parallel to the horizontal plane, a field of view of 200×200 mm, a voxel size of 0.39 mm and exposure conditions of 80 kVp, 5 mA, and 17 s. The patients were scanned wearing a CR wax bite to ensure that their condyles were scanned in the CR position, that is, with the condyle resting in the glenoid fossa. With CBCT, a

patient's dental structure cannot be obtained accurately due to bracketing, blurring, and enlargement of the image. Almost all orthodontic patients wear fixed metal orthodontic appliances or have metallic brackets, which produce striped artifacts that distort the view of the dentition and occlusions during scanning. Therefore, a conventional impression was taken, and a pair of stone casts was fabricated for each patient. The surface image of the casts was then digitized into surface tessellation language (STL) format using a desktop model scanner (Freedom HD; Dof, Inc., Seoul, Korea). The CBCT images were transformed into DICOM format, and three-dimensionally reconstructed. Then, the CBCT reconstruction and the dental cast scan files were sent to the digital center. Subsequently, the DICOM and STL files were imported into a planning software program. The patient's CBCT scan and the scanned image of the patient's dental cast were registered. Semiautomatic merging started with registration of the image of the teeth obtained from the dental cast to the CBCT image of the teeth, which is relatively accurate. The images were merged process via manual registration by selecting three anatomical landmarks from the dentition. The contour of the dental cast image placed on the CBCT image was examined, and fine adjustments were made if necessary. The next step was reorientation of the skull image to reconcile the views of the surgeon, the orthodontist, and the digital technician. In this way, the final virtual hybrid skull-dentition 3D image (virtual face) was obtained. The reorientation image was sent to the surgeon, and telecommunication with the digital technician took place via the computer screen. The position of the osteotomy, the movement of the bone segment, the position of the customized plate, and the

Table 1 Patient characteristics and surgery descriptions

Patient No.	Age	Sex	Characteristics	Surgery
Pt 01	28	F	FA (Lt side ^a), Angle III	Lefort I, BSSO, Genio
Pt 02	24	F	FA (Rt side ^a), Angle I	Lefort I, BSSO
Pt 03	24	M	Angle III	Lefort I, BSSO, Genio
Pt 04	29	M	FA (Lt side ^a), Angle III	Lefort I, BSSO
Pt 05	24	F	FA (Rt side ^a), Angle I	Lefort I, SSO(Rt), HRO(Lt), Genio
Pt 06	20	M	FA (Lt side ^a), Angle III	Lefort I, HRO(Rt), SSO(Lt), Genio
Pt 07	20	M	FA (Lt side ^a), Angle III	Lefort I, BVSSO
Pt 08	26	F	Angle III	Lefort I, BSSO
Pt 09	22	F	FA (Rt side ^a), Angle III	Lefort I, BSSO
Pt 10	18	F	FA (Lt side ^a), Angle III	Lefort I, BSSO
Pt 11	21	M	FA (Rt side ^a), Angle III	Lefort I, BSSO
Pt 12	21	M	FA (Rt side ^a), Angle III	Lefort I, BSSO
Pt 13	21	F	FA (Rt side ^a), Angle I	Lefort I, BSSO

FA Facial asymmetry, Angle Angle malocclusion classification, Lefort I, Lefort I osteotomy, BSSO Bilateral sagittal split ramus osteotomy, HRO Horizontal ramus osteotomy, Genio Genioplasty, BVSSO Bilateral vertical sagittal ramus osteotomy. ^aThe direction indicated in parentheses following FA is the deviation direction

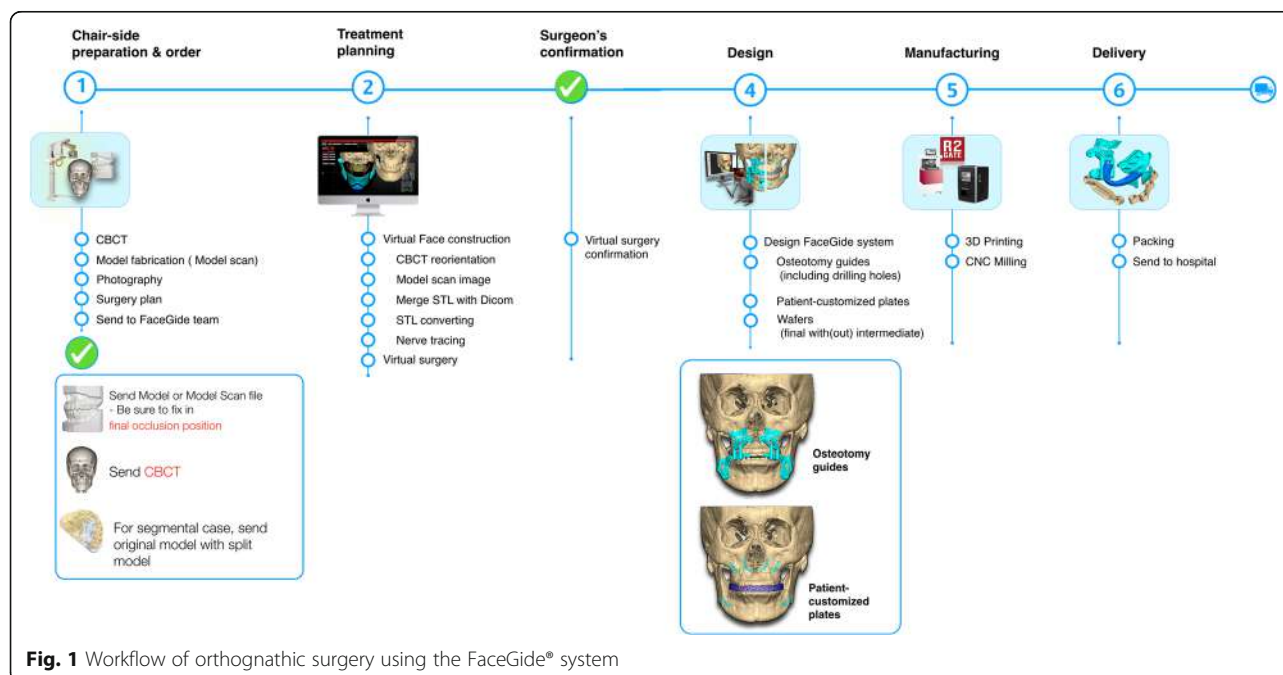


Fig. 1 Workflow of orthognathic surgery using the FaceGide® system

final occlusion were determined. After the final confirmations were made, virtual materials (such as the patient-customized osteotomy guides (PCGs), PCMs, and splints) were designed (Fig. 2). After the surgeon checked them, their images were exported as STL files.

Then, the actual materials were produced by a rapid prototyping machine (S30 3D printer, Rapid Shape GmbH, Heimsheim, Germany) and a computer numerical control (CNC) machine (ARDEN, TPS Korea Ltd., Gwangju, Republic of Korea).

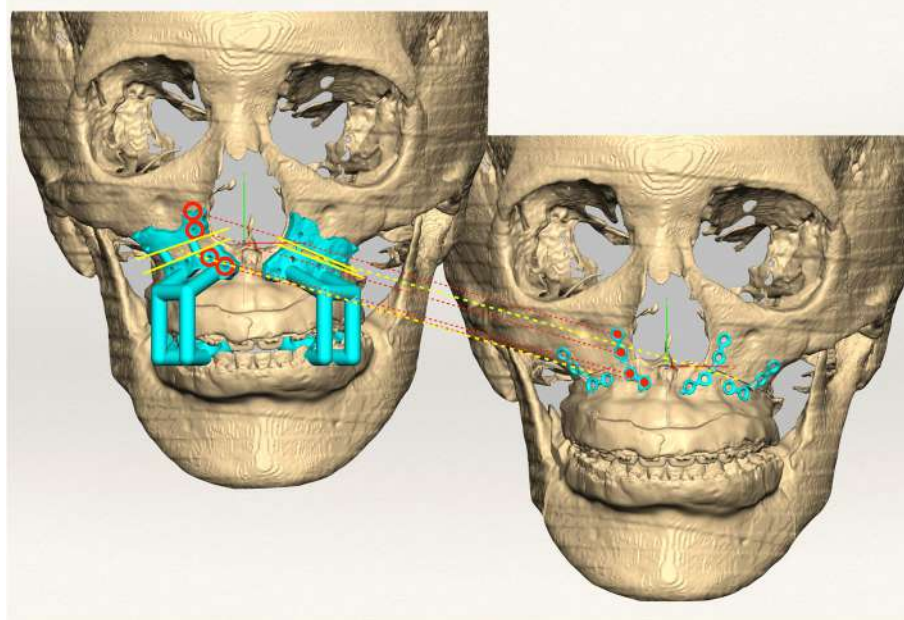


Fig. 2 Patient-customized osteotomy guides (PCGs) and patient-customized miniplates (PCMs) designed for surgery (Pt 12 of Table 1). The patient had a longer maxilla on the right side; therefore, the amount of bone removed after the osteotomy was greater on the right side. The yellow lines indicate the osteotomy line. There were 16 holes in the PCGs for the insertion of the bone screws. The empty red circle is the location of the screw holes in the PCGs, and the red circle on the right is the site of screw insertion. In the virtual face on the right side (where the maxillary bone is moved), the screws are marked, and the PCGs were designed after the image was constructed based on the virtual face on the left side (without moving the maxilla)

Actual OGS

All physical components and reports regarding the VS showing the PCGs (including drilling holes) and PCMs were sent to the surgeon before the OGS. These materials were then delivered to the operating room for sterilization (Fig. 3a, b). The maxilla was repositioned and fixed with four L-shaped PCMs and monocortical self-drilling screws. The customized maxillary miniplates have holes corresponding to the drilling holes in the PCGs. As a result, bone holes are precisely formed using PCGs, and prefabricated miniplates are fitted to these holes (Fig. 3c, d). The PCM was positioned by merely inserting a self-drilling screw into the predrilled hole to ensure that there was no stress on the miniplate when the other screws were inserted. Mandibular surgery was performed in the same manner used for the maxilla, and customized mandibular miniplates corresponding to the osteotomy guides were used. After the ramus osteotomy, the distal segments of the mandible were repositioned using the final splint. Proximal segment positioning devices were used for proximal segment repositioning [15]. After maxillomandibular fixation (MMF) with rubber bands, the mandible was stabilized with customized miniplates. MMF was maintained for three days. Operations were performed by a single surgeon (BE.Y).

Outcome evaluation

3D CBCT images were obtained before the surgery (T0) and three days (T1), four months (T2) and one year (T3) after the surgery. The 3D image of the virtual OGS is

denoted as Tv (T virtual). The predicted results and achieved outcomes were evaluated by comparing the eight landmarks (the center point between the cusp tips of the upper central incisors, the cusp tips of the upper canines, the mesiobuccal cusp tips of the upper first molars, the anterior nasal spine (ANS), the posterior nasal spine (PNS) and the A point) specified on the four sets of CBCT images. Each coordinate value was marked according to the trigonal system (x, y, z) and recorded in the program (Geomagic Freeform Plus, 3D Systems, North Carolina, USA) (Fig. 4). The X-axis represents the left and right directions, the Y-axis represents the up and down directions, and the Z-axis represents the front and back relationships. An individual t-test was performed for statistical comparisons between ΔTv (Tv-T0) and $\Delta T1$ (T1-T0). The STL files from each period were evaluated using PolyWorks Inspector™ (InnovMetric Software, Inc., Quebec, Canada) to measure differences in the bone surface. Because superimposition must be performed based on a nonsurgically exposed region, such as the cranium, we used the virtually planned final position of the maxilla and the postoperative position of the maxilla for surface registration. Eight reference points were examined to compare the maxillary changes at T1, Tv, T2, and T3. T2 and T3 were times when orthodontic treatment had already begun. Therefore, measurements were based on the bone reference points rather than the tooth positions because the tooth positions changed at all time points. Measurements were made on the maxillary bone surface in front of the tooth

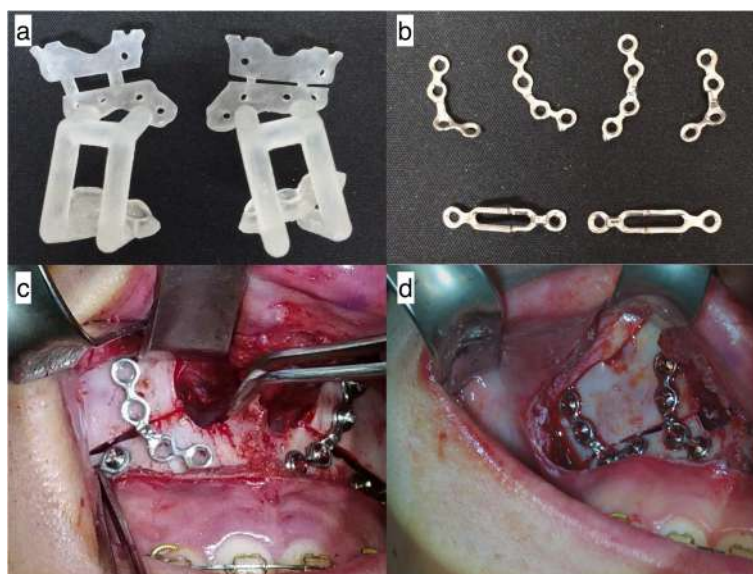
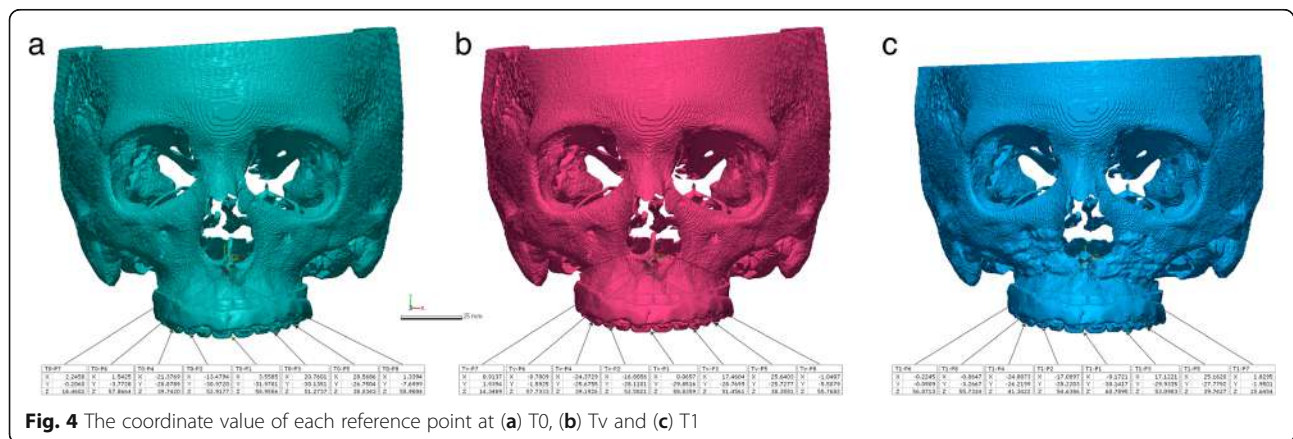
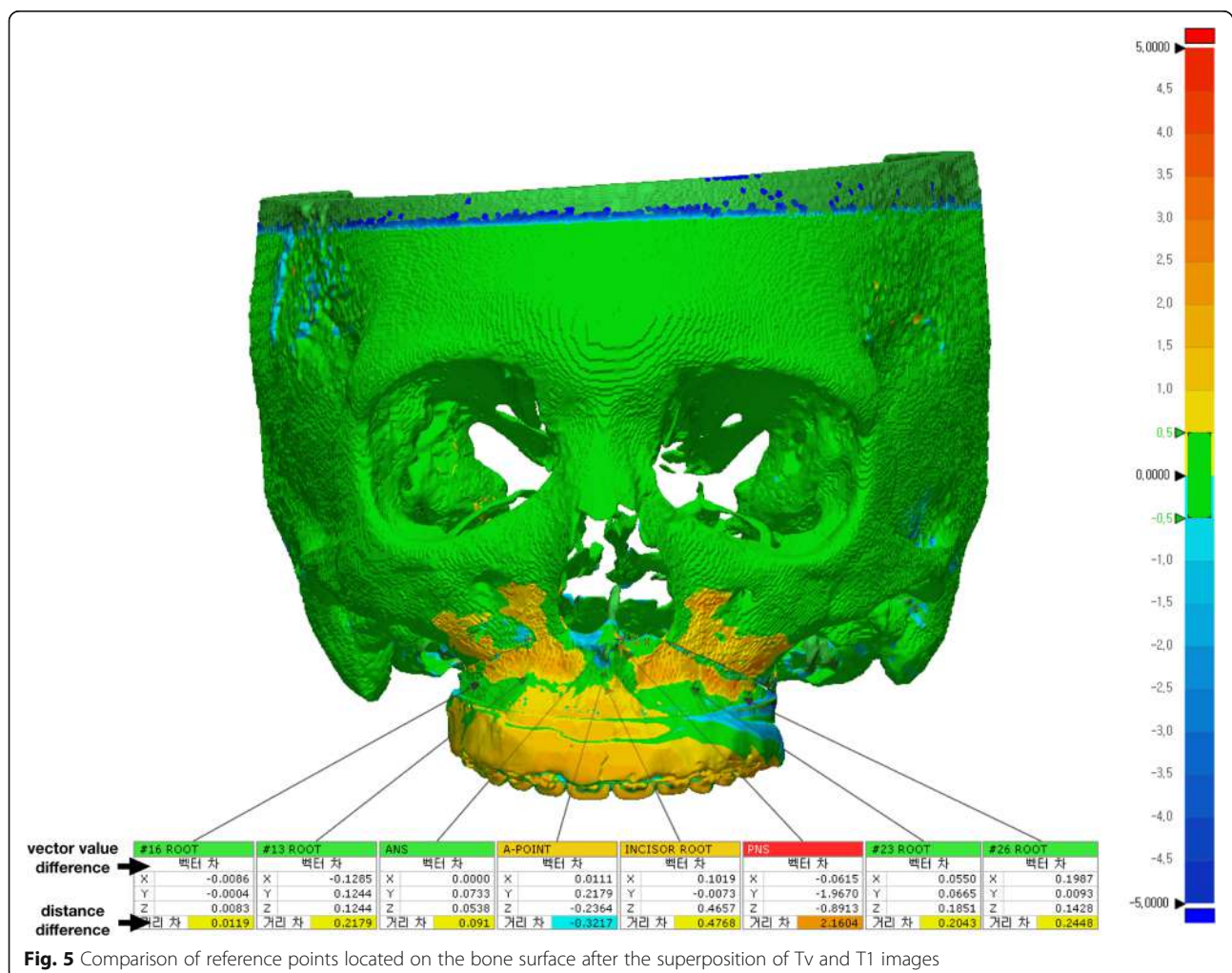


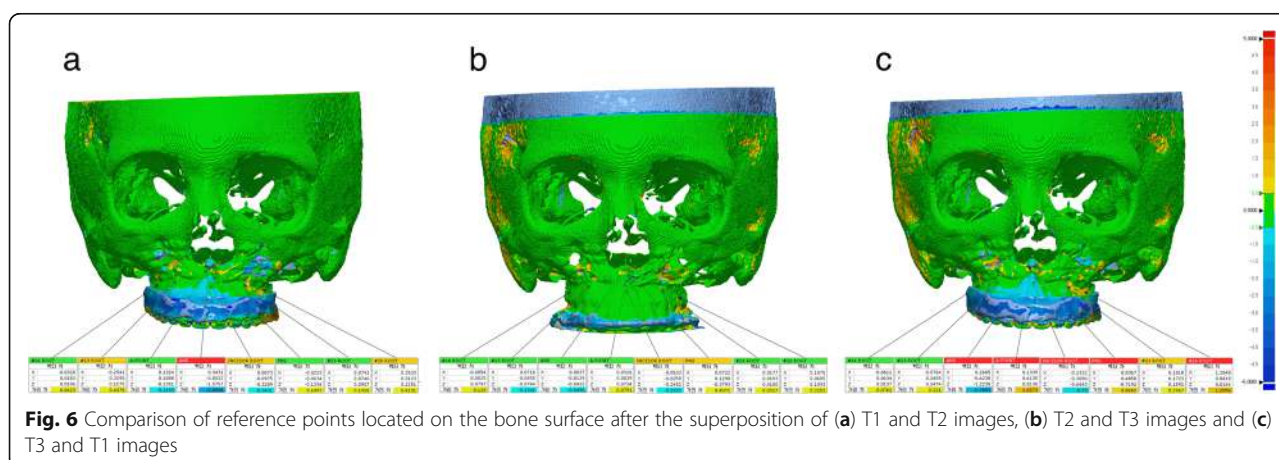
Fig. 3 The actual maxillary osteotomy guides and patient-customized miniplates (PCMs) on the patient (Pt 12). **(a)** Osteotomy guides fabricated using a 3D printer. **(b)** PCMs. The PCMs below were used for the mandibular surgery. **(c)** The PCM was applied to the right maxilla. The holes in the PCMs were aligned with preformed holes on the bone surface. **(d)** PCMs in place



root (the midpoint of the upper central incisors and canines and the mesiobuccal root of the first molars) instead of the cusp tip (5 sites) of the teeth among the eight reference points used in Geomagic Freeform Plus. The direct bone distance between the actual operation (T1) and VS (Tv) was measured (Fig. 5), and statistical

comparisons between the coordinate values of the reference points were also investigated. Independent t-tests were used to compare values. Images were obtained at three time points (T1, T2, and T3) and then superimposed (Fig. 6). The three groups (T1 and T2, T2 and T3, T1 and T3) were compared to assess the postoperative





stability of the maxilla. One-way ANOVA with Tukey's multiple comparison tests was used for comparisons among the three groups. Data were analyzed using the Statistical Package for Social Sciences (SPSS, version 23.0, IBM Co., Armonk, NY, USA). *P*-values less than 0.01 were considered significant.

Results

Satisfactory clinical outcomes were achieved in all patients, and VS was successfully reproduced in the actual surgery for all patients. All 13 patients were also satisfied by the postoperative results, including the occlusion and facial profile. No complications, such as malocclusion, tooth loss, sensory disturbance of the infraorbital nerve or infection, occurred during the follow-up period. The differences between ΔT_v (Tv-T0) and ΔT_1 (T1-T0) are shown in Table 2. There were no significant differences between the time points (Fig. 7). The Tv and T1 coordinate values for the bone reference points and the direct distances are shown in Table 3. There were no significant differences among the coordinate values. The mean distance difference at all reference points between Tv and T1 was 1.01 ± 0.3 mm (Fig. 8). The greatest

difference was at the PNS, although the difference was not significant. There were no significant differences among the three groups (T1 and T2, T2 and T3, T1 and T3) regarding the stability of the maxilla. The mean difference between T1 and T3 was -0.37 ± 0.29 mm (Table 4) (Fig. 9).

Discussion

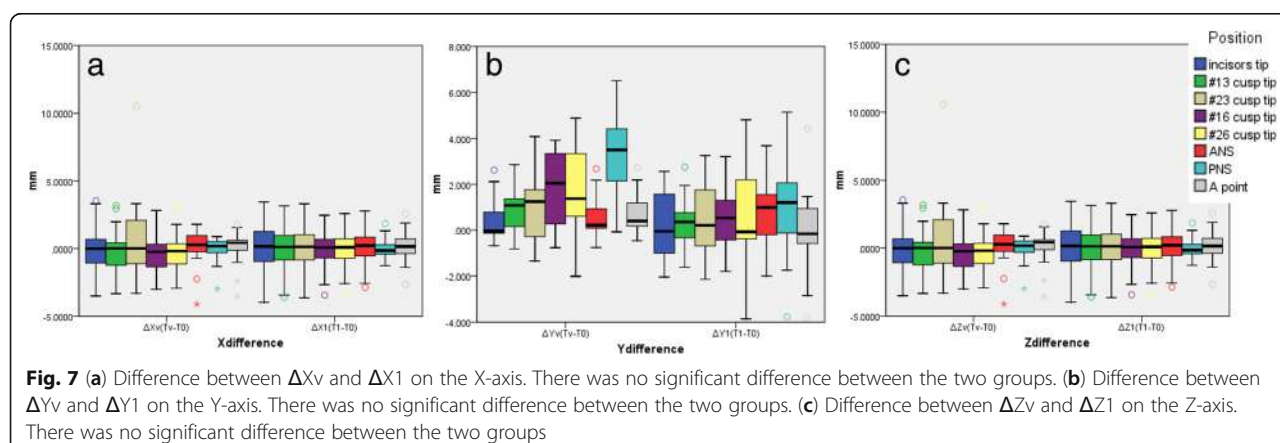
In this study, we report virtual surgical simulation with FaceGide® incorporating PCGs (including drilling holes for screws), PCMs and a customized final splint. In our series, the surgical transfer of the VSP by FaceGide® showed good accuracy, and the final position of the maxilla measured at the points associated with the root of the tooth (bone surface) was 0.94 ± 0.17 mm from the mean value. The ANS, PNS, and A point may show large differences between Tv and T1 because they are the sites of bone removal during the actual operation. However, the error was still approximately 1.01 ± 0.3 mm, even when these points were included.

With the introduction of CBCT, which reduces the hardware costs and radiation doses, 3D imaging can be used as a standard tool for diagnosis and treatment

Table 2 Distance difference between ΔT_v (Tv-T0) and ΔT_1 (T1-T0)

	n	ΔX_v (Tv-T0)		ΔX_1 (T1-T0)		<i>p</i>	ΔY_v (Tv-T0)		ΔY_1 (T1-T0)		<i>p</i>	ΔZ_v (Tv-T0)		ΔZ_1 (T1-T0)		<i>p</i>
		Average	SD	Average	SD		Average	SD	Average	SD		Average	SD	Average	SD	
Incisor tip	13	-0.004	2.097	0.003	2.293	0.994	0.468	1.075	0.216	1.426	0.616	0.034	0.370	1.166	1.649	0.024
#13 cusp tip	13	-0.059	1.909	-0.071	2.075	0.988	0.910	1.042	0.271	1.226	0.165	0.148	0.522	1.334	1.515	0.014
#23 cusp tip	13	0.790	3.522	-0.026	2.126	0.482	0.996	1.636	0.491	1.770	0.458	0.019	0.664	1.044	1.921	0.082
#16 cusp tip	13	-0.161	1.603	-0.257	1.731	0.885	1.843	1.759	0.509	1.482	0.047	0.397	0.702	1.494	1.385	0.018
#26 cusp tip	13	-0.083	1.571	-0.190	1.716	0.87	1.940	2.018	0.756	2.386	0.185	0.224	0.867	1.051	2.002	0.185
ANS	13	-0.042	1.598	-0.045	1.576	0.997	0.661	0.988	0.730	1.470	0.89	1.655	1.442	1.177	1.805	0.462
PNS	13	-0.178	1.080	0.092	0.882	0.492	3.263	1.736	1.100	2.428	0.015	1.723	1.487	1.618	1.508	0.859
A point	13	-0.027	1.518	-0.016	1.539	0.99	0.767	0.950	-0.107	2.054	0.18	1.409	1.250	1.447	1.093	0.94

ANS anterior nasal spine, PNS posterior nasal spine, SD standard deviation



planning [16]. Although it is possible to obtain much information from this 3D diagnostic method, the IMS is generally used in conventional bimaxillary OGS. Increased use of the IMS can cause postoperative problems because the inherent thickness of the splint may result in a degree of autorotation after the splint's removal [17]. Additionally, Perez et al. reported that the temporomandibular joint (TMJ) is not a discrete ball-and-socket joint. The mandibular condyle rotates and translates within the TMJ [18]. Therefore, repositioning the maxilla in relation to the position of the mandible may have several limitations. The mandible and maxilla can be fixed together with an IMS during OGS, but a certain amount of space can develop as a result of the mobility of the mandibular condyle. Therefore, the maxilla cannot be precisely positioned relative to the base of the skull using only an IMS, and the surgeon must take time to adjust it manually. In addition, inaccuracy of the IMS can arise from the model surgery stage. Model surgery depends on the accurate recording of the occlusion in the retruded position and the face-bow transfer to the articulator. These recordings both have inherent inaccuracy. Bailly et al. measured the angulation of the occlusal plane to the Frankfort plane on a Hanau articulator and compared this with lateral cephalograms; they found a mean difference of 5 degrees, which corresponded to 70% of the error during the face-bow transfer [19]. Ellis et al. reported that the average case had an inaccuracy of almost 7 degrees in the angulation of the occlusal plane [20]. The accuracy of the 3D position of the upper first molar was highly variable using four different Hanau face-bows [21]. When using a conventional articulator for OGS, it is essential that the angle between the occlusal plane and the Frankfort horizontal plane for the patient is the same as the angle between the occlusal plane and the upper member of the articulator on the maxillary model. OGS using the FaceGide® system can reduce errors related to

mock surgery because it does not use such an articulator during preoperative preparation.

The surgical method presented in this study using the FaceGide® system is not necessary for all patients with craniofacial deformity. Rustemeyer et al. reported that a 2D cephalometric analysis and a 3D mock operation are sufficient for accurate planning and will ensure good results for experienced surgeons [22]. We agree with this opinion, and if the patient has no facial asymmetry or requires only single-jaw surgery, conventional OGS can produce good results. However, if major 3D movements are indicated, including changes to the transverse occlusal plane or major rotation of the jaws, a navigation system should be chosen for complex 3D planning and controlling the position of the maxilla during surgery [23]. Most of the patients in this study had facial asymmetry. Therefore, the use of the FaceGide® system was recommended for surgery, and complex 3D movement of the jaws was performed. Our method of OGS using the FaceGide® system is very original, albeit not new. The principle of the FaceGide® system that we present is based on the combination of previously mentioned processes and is associated with predrilling determined by a reverse approach [24]. In a study by Xia et al., the final state was made into a medical replica after the VS, and the ready-made plates were bent according to the outline of this replica. During the actual operation, drilling for screw insertion was performed using the navigation system [24]. Use of the FaceGide® system is the same as the reverse approach of that reported by Xia et al., but customized miniplates and corresponding osteotomy guides (including drilling guides) are used. Similar processes involving predrilling and positioning osteotomy guides or prebent plates in OGS have been reported [25–28].

Ellis reported that the average accuracy of maxillary positioning in the horizontal plane deviated 2 mm from what was planned when external references were used,

Table 3 Differences in coordinate value and distance between Tv and T1 with PolyWorks Inspector™

n	Coordinate value difference										Distance difference							
	Xv		X1		Yv		Y1		Zv		Z1		Tv and T1					
	Average	SD	Average	SD	Average	SD	Average	SD	Average	SD	Average	SD	Average	SD				
Incisor root	13	-0.657	0.884	-0.551	0.915	0.765	-9.498	5.583	-9.597	5.651	0.964	58.596	8.086	58.848	7.659	0.936	0.820	0.694
#13 root	13	-17.639	1.749	-17.733	1.460	0.883	-7.312	6.825	-7.604	6.622	0.913	51.769	8.050	51.777	7.815	0.998	0.819	0.904
#23 root	13	16.208	1.621	16.401	1.454	0.752	-7.477	5.886	-7.805	5.734	0.887	51.706	8.526	51.660	8.078	0.989	0.817	1.196
#16 root	13	-29.700	2.270	-29.747	2.389	0.959	-9.119	7.143	-9.787	6.847	0.810	37.436	10.435	37.069	10.678	0.930	1.196	1.303
#26 root	13	28.993	2.451	28.921	2.730	0.944	-8.716	6.300	-9.482	6.117	0.756	35.991	9.303	36.135	9.043	0.968	1.022	1.661
ANS	13	-0.602	1.157	-0.440	0.989	0.705	0.091	6.152	-0.209	6.423	0.904	59.772	8.377	58.865	8.015	0.78	0.883	1.793
PNS	13	-1.104	2.046	-0.969	1.893	0.863	1.708	6.314	0.552	5.860	0.633	18.227	9.234	17.670	8.905	0.877	1.661	1.489
A point	13	-0.863	0.944	-0.804	0.828	0.866	-4.078	6.194	-4.453	6.243	0.879	57.691	8.034	57.723	7.693	0.992	0.860	1.071
ANS anterior nasal spine, PNS posterior nasal spine, SD standard deviation																		

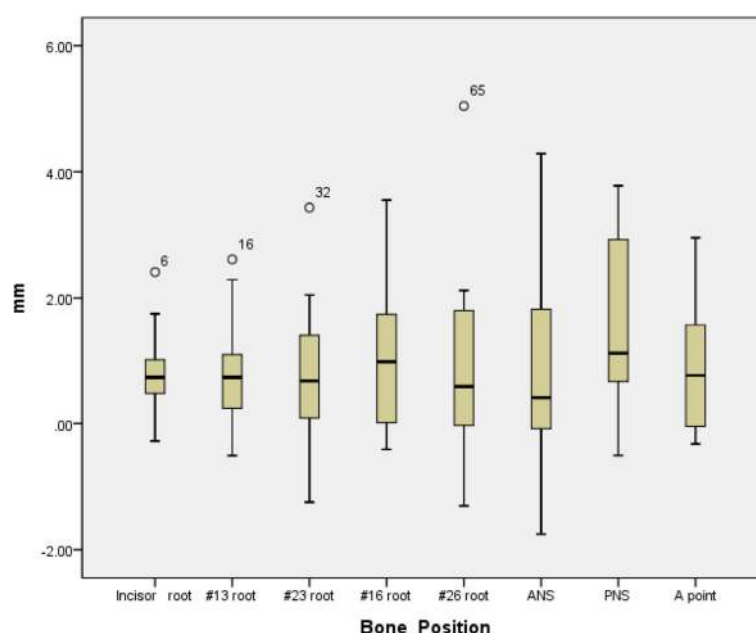


Fig. 8 Differences between T1 and T2 at each bone reference point

whereas the vertical accuracy ranged from 0.5 to 1 mm [29]. Jacobson et al. reported that a 2-mm or greater discrepancy was noted for 20 to 30% of 46 patients who underwent LeFort I osteotomy [30]. With the development of CAD and CAM, VSPs and 3D-printed navigation templates have been proposed as alternatives to conventional model surgery [31]. Sun et al. performed a clinical study using an orthognathic surgical template made from a 3D printer and VSP and reported that the mean vertical, lateral, and anteroposterior errors in the anterior maxillary region were 0.57 mm, 0.35 mm, and 0.5 mm, respectively [32]. Although our study shows a higher error than that of Sun et al.'s study, the difference may have been due to the use of different measurement methods, and our error was smaller than that reported in previous studies [29, 30] that used conventional methods. During the entire process, errors in surface

rendering, data integration (merging dentition and CBCT data), and setting 3D coordinates in the virtual space or during guide, surgical splint and miniplate fabrication (3D printing or milling process) are related to accuracy. Accuracy can be improved with the use of a systemic process during surgical planning and preparation. Zinser et al. reported that the mean vertical, lateral, and anteroposterior errors compared with the anterior maxillary region were 0.23 mm, 0.04 mm, and 0.09 mm, respectively, and that the vertical, lateral, and anteroposterior errors compared with the posterior maxillary region were 0.15 mm, 0.04 mm, and 0.1 mm, respectively [33]. Our results are not comparable because we did not use the same measurement approach that was used by Zinser et al. However, in our study, the differences between the VS and the actual surgery were 0.26 mm, 0.47 mm, and 1.11 mm in the anterior

Table 4 Distance difference between T1 and T2, T2 and T3, and T1 and T3

	N	T1 and T2		T2 and T3		T1 and T3		p
		Average	SD	Average	SD	Average	SD	
Incisor root	13	-0.109	1.037	-0.117	0.237	-0.529	0.982	0.352
# 13 root	13	0.393	0.930	-0.044	0.236	-0.165	0.617	0.089
#23 root	13	0.271	0.556	-0.057	0.197	-0.145	0.680	0.113
#16 root	13	-0.053	0.591	-0.016	0.183	-0.138	0.896	0.880
#26 root	13	0.354	1.066	0.010	0.322	-0.446	1.389	0.153
ANS	13	-0.823	1.811	-0.105	0.496	-0.821	1.449	0.316
PNS	13	0.083	0.770	-0.179	0.623	-0.043	0.845	0.741
A point	13	0.030	0.910	-0.005	0.164	-0.665	0.808	0.028

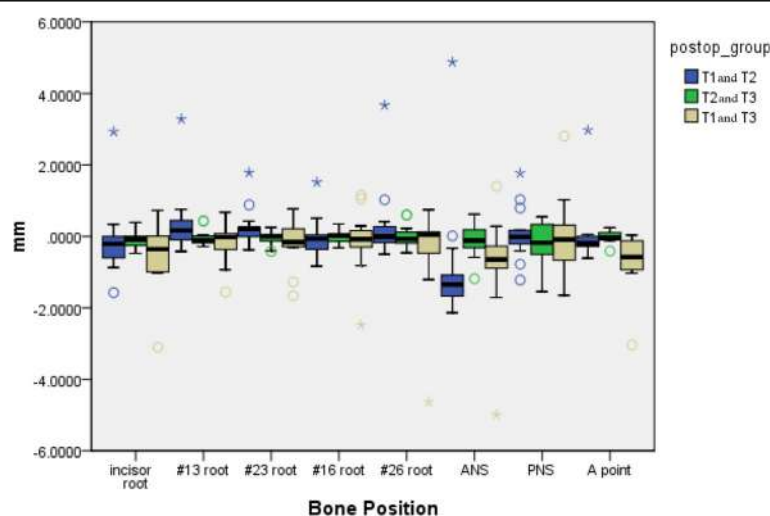


Fig. 9 Comparison of the three groups after the superposition of T1, T2, and T3 images. There were no significant differences among the three groups

maxillary region (incisor tip, #13 cusp tip and #23 cusp tip) and 0.02 mm, 1.6 mm, and 0.6 mm in the posterior maxillary region (#16 cusp tip, #26 cusp tip and PNS).

We are aware that this study may have limitations. The small number of patients in this retrospective study limits the ability to draw definite conclusions. One reason for the small sample size was the utilization of strict inclusion and exclusion criteria, which resulted in the exclusion of the majority of patients who underwent OGS in the department during the study period. However, image analysis using 3D comparison programs is highly reproducible and can yield significant results even with a small number of cases. There were some trial and error in the operation using the FaceGide® system. There were no significant differences between ΔT_v and ΔT_0 , but in some cases, the Y coordinate value of the PNS was somewhat different from that of the other sites. Therefore, even when the operation is performed using this system, more attention should be paid when the posterior part of the maxilla is moved. In three patients, the maxilla was unstable after fixation, so the ready-made miniplates were added for reinforcement. In some cases in which the surgeon was unfamiliar with the newly developed system, wide-diameter screws were used because of a widening of the holes after drilling. However, this problem could be solved by drilling with a small-diameter round burr and self-drilling screws. PCGs with an arm that originates from the cusp of the teeth can also confirm the accuracy of the bone contact (Fig. 2). Minor mispositioning of the PCGs is impossible to detect by the naked eye and can result in erroneous cuts. Therefore, this type of PCG is believed to be more accurate than a bone-only supported guide because it is supported by both the bone surface and the cusp of the

teeth, but further research regarding its accuracy is needed. The accuracy of OGS using CASS is influenced by reproduction of the VS in the actual surgery. Individual errors can originate from internal sources, including the CBCT image quality, file conversion process, computer design software, and interactions between mechanical components, and external sources, such as the adaption of the osteotomy guide, customized plate, and splints and the surgeon's experience. The accumulation of such errors produces the total deviation between the planned and postoperative outcomes. However, this study demonstrates the suitable accuracy and stability of OGS using the FaceGide® system.

The facial surgery protocol using FaceGide® has advantages similar to those of other CASS systems. Digital diagnosis and VS data files can be transmitted to the surgeon and orthodontists for final adjustments [33]. Such exchanges have the advantage of allowing the creation of an interdisciplinary platform that centralizes the technical and surgical domains of expertise and produces financial and operative efficiency, all within a digital environment [31]. Because the site of the bone screw insertion is designed to avoid the root of the tooth, it is unlikely that root damage will occur when conventional methods are used. Some clinicians may claim that using CASS can expose the patient to increased radiation [34]. However, it can eliminate the need for additional radiographic examinations, which is indicated when there are doubts about the final surgical position. It is well known that the radiation dose of most CBCT systems used to acquire DICOM data is considered minimal [35]. There have been reports of the use of one piece of customized plate in the maxilla that have claimed accuracy [36–38]. However, the

amount of titanium used in one-piece plates is greater than the amount of titanium used in conventional maxillary fixation methods. Hosoki et al. reported that the detailed mechanism of action of allergy and hypersensitivity to metallic materials is not known but is related to the total exposure to specific metallic ions [39]. In this study, four customized L-shaped miniplates were used, and they remained stable for more than one year without any bone changes. An excessive amount of titanium can cause a foreign body reaction. The volume of titanium used in our study is equal to or less than the volume of titanium used in the conventional fixation method of LeFort I osteotomy. Although not reported in this study, the PCMs were removed in three patients one year after surgery and did not cause clinical problems. Future studies involving PCM removal will be conducted. Unlike conventional surgery, the use of PCGs in our study allowed us to remove the necessary amount of bone, thereby increasing contact between bone segments. Our method was less invasive than conventional methods, and the patients recovered rapidly and were able to return quickly to normal life.

Conclusions

The maxillary bone should be positioned according to a planned position during OGS to achieve a successful operation. We performed OGS using the FaceGide® system, which is a newly developed CASS system. The repositioning of the maxilla was clinically accurate, and stable results were maintained one year after the operation. Currently, the quality of the surgical result still depends on the skill of the individual surgeon in carrying out the surgical plan. However, surgeons with average experience will be able to achieve acceptable treatment results using the FaceGide® system (via a VSP and manufacturing of the related materials). In other words, 3D evaluation, virtual simulation, and CAD-CAM technology can benefit both doctors and patients. The development of digital technologies will continue to support the adoption of computer-assisted techniques in medicine and dentistry.

Abbreviations

3D: Three-dimensional; CAD: Computer-aided design; CAM: Computer-aided manufacturing; CASS: Computer-aided surgical simulation; CBCT: Cone beam computed tomography; CNC: Computer numerical control; CR: Centric relation; IMS: Intermediate splint; OGS: Orthognathic surgery; PCG: Patient-customized osteotomy guide; PCM: Patient-customized miniplate; SD: Standard deviation; STL: Surface tessellation language; VSP: Virtual surgical plan; VTO: Visual treatment objective

Acknowledgments

We would like to thank Dr. Jun-Young You, Ph.D., (Director of "Gnatho Oral and Maxillofacial Surgery Clinic," Seoul, Republic of Korea) for advice on the reorientation method based on CBCT and OGS.

Funding

This study was supported by the Hallym University Research Fund (HURF-2017-42) in relation to English proofreading.

Availability of data and materials

The dataset used and/or analyzed during the present study available from the corresponding author on reasonable request.

Authors' contributions

All the authors made substantial contributions to the present study. JWK, JCK, and BEY contributed to the conception and design of the study and acquisition, analysis, and interpretation of the data; they were also involved in writing and editing the manuscript. KJC and SWC acquired all the CBCT data, and KJC, SWC, and IYP analyzed and interpreted all the data; together, they were the major contributors to preparing and writing the manuscript. CGJ acquired data with the FaceGide® program and the PolyWorks Inspector™ program. BEY performed the statistical evaluation and revised the manuscript before submission. All the authors have read and approved the final manuscript.

Ethics approval and consent to participate

This study protocol was approved by the Hallym University Sacred Heart Hospital Institutional Review Board (IRB No. 2018-06-016). IRB approved this retrospective study, and informed consent was waived by the study subjects because all the patient data were anonymized and de-identified before the analysis.

Consent for publication

Not applicable.

Competing interests

The authors declare that they have no competing interests in relation to the present work.

Publisher's Note

Springer Nature remains neutral with regard to jurisdictional claims in published maps and institutional affiliations.

Author details

¹Division of Oral and Maxillofacial Surgery, Hallym University Sacred Heart Hospital, 11, Gwanpyeong-ro 170beon-gil, Dongan-gu, Anyang-si, Gyeonggi-do, 14066 Anyang, Republic of Korea. ²Mir Dental Hospital, 12 Gongpyoungro Jung-gu Daegu, 41940 Daegu, Republic of Korea. ³Division of Orthodontics, Hallym University Sacred Heart Hospital, Anyang, Republic of Korea. ⁴Graduate School of Clinical Dentistry, Hallym University, Chuncheon, Republic of Korea. ⁵Institute of Clinical Dentistry, Hallym University, Chuncheon, Republic of Korea.

Received: 1 October 2018 Accepted: 4 January 2019

Published online: 15 January 2019

References

- Joshi N, Hamdan AM, Fakhouri WD. Skeletal malocclusion: a developmental disorder with a life-long morbidity. *J Clin Med Res*. 2014;6:399.
- Luhr H, Kubein-Meesenburg D. Rigid skeletal fixation in maxillary osteotomies. Intraoperative control of condylar position *Clin Plast Surg*. 1989;16:157–63.
- Polido WD, Ellis E, Sinn DP. An assessment of the predictability of maxillary repositioning. *Int J Oral Maxillofac Surg*. 1991;20:349–52.
- Stokbro K, Aagaard E, Torkov P, Bell R, Thygesen T. Virtual planning in orthognathic surgery. *Int J Oral Maxillofac Surg*. 2014;43:957–65.
- Ellis E. Accuracy of model surgery: evaluation of an old technique and introduction of a new one. *J Oral Maxillofac Surg*. 1990;48:1161–7.
- Harris M, Hunt N. Fundamentals of orthognathic surgery and non surgical facial aesthetics. 3rd ed: World Scientific; 2018.
- Yohn K. The face bow is irrelevant for making prostheses and planning orthognathic surgery. *J Am Dent Assoc*. 2016;147:421–6.
- Bowley JF, Michaels GC, Lai TW, Lin PP. Reliability of a facebow transfer procedure. *J Prosthet Dent*. 1992;67:491–8.
- Gold B, Setchell D. An investigation of the reproducibility of face-bow transfers. *J Oral Rehabil*. 1983;10:495–503.

10. Zizelmann C, Hammer B, Gellrich N-C, Schweska-Polly R, Rana M, Bucher P. An evaluation of face-bow transfer for the planning of orthognathic surgery. *J Oral Maxillofac Surg*. 2012;70:1944–50.
11. Boucher L, Jacoby J. Posterior border movements of the human mandible. *J Prosthet Dent*. 1961;11:836–41.
12. McMillen LB. Border movements of the human mandible. *J Prosthet Dent*. 1972;27:524–32.
13. Gelesko S, Markiewicz MR, Weimer K, Bell RB. Computer-aided orthognathic surgery. *Atlas Oral Maxillofac Surg Clin North Am*. 2012;20:107–18.
14. Zhang W, Li B, Gui H, Zhang L, Wang X, Shen G. Reconstruction of complex mandibular defect with computer-aided navigation and orthognathic surgery. *J Craniofac Surg*. 2013;24:e229–e33.
15. Kim JW, Kim JC, Cheon KJ, Cho SW, Kim YH, Yang BE. Computer-aided surgical simulation for yaw control of the mandibular condyle and its actual application to orthognathic surgery: a one-year follow-up study. *Int J Environ Res Public Health*. 2018;15.
16. Mah J: The genesis and development of CBCT for dentistry. In.; 2014. <https://www.semanticscholar.org/paper/The-Genesis-and-Development-of-CBCT-for-Dentistry/11fda347e7b4348865ef5535e1506c6491b9022>.
17. Bryan DC, Hunt NP. Surgical accuracy in orthognathic surgery. *Br J Oral Maxillofac Surg*. 1993;31:343–9 discussion 9–50.
18. Perez D, Ellis E. Sequencing bimaxillary surgery: mandible first. *J Oral Maxillofac Surg*. 2011;69:2217–24.
19. Bailey J, Nowlin T. Accuracy of the Frankfort plane transfer to the Hanau articulator. *J Dent Res*. 1981;531.
20. Ellis E, Tharanon W, Gambrell K. Accuracy of face-bow transfer: effect on surgical prediction and postsurgical result. *J Oral Maxillofac Surg*. 1992;50:562–7.
21. O'malley A, Milosevic A. Comparison of three facebow/semi-adjustable articulator systems for planning orthognathic surgery. *Br J Oral Maxillofac Surg*. 2000;38:185–90.
22. Rustemeyer J, Groddeck A, Zwerger S, Bremerich A. The accuracy of two-dimensional planning for routine orthognathic surgery. *Br J Oral Maxillofac Surg*. 2010;48:271–5.
23. Santler G. 3-D COSMOS: a new 3-D model based computerised operation simulation and navigation system. *J Craniomaxillofac Surg*. 2000;28:287–93.
24. Xia JJ, Gateno J, Teichgraeber JF. A new paradigm for complex midface reconstruction: a reversed approach. *J Oral Maxillofac Surg*. 2009;67:693–703.
25. Olszewski R, Tranduy K, Reyckler H. Innovative procedure for computer-assisted genioplasty: three-dimensional cephalometry, rapid-prototyping model and surgical splint. *Int J Oral Maxillofac Surg*. 2010;39:721–4.
26. Polley JW, Figueroa AA. Orthognathic positioning system: intraoperative system to transfer virtual surgical plan to operating field during orthognathic surgery. *J Oral Maxillofac Surg*. 2013;71:911–20.
27. Dérand P, Rännar L-E, Hirsch J-M. Imaging, virtual planning, design, and production of patient-specific implants and clinical validation in craniomaxillofacial surgery. *Craniomaxillofac Trauma Reconstr*. 2012;5:137.
28. Zhou LB, Shang HT, He LS, Bo B, Liu GC, Liu YP, et al. Accurate reconstruction of discontinuous mandible using a reverse engineering/ computer-aided design/rapid prototyping technique: a preliminary clinical study. *J Oral Maxillofac Surg*. 2010;68:2115–21.
29. Ellis E. Bimaxillary surgery using an intermediate splint to position the maxilla. *J Oral Maxillofac Surg*. 1999;57:53–6.
30. Jacobson R, Sarver DM. The predictability of maxillary repositioning in LeFort I orthognathic surgery. *Am J Orthod Dentofac Orthop*. 2002;122:142–54.
31. Xia JJ, Phillips CV, Gateno J, Teichgraeber JF, Christensen AM, Gliddon MJ, et al. Cost-effectiveness analysis for computer-aided surgical simulation in complex cranio-maxillofacial surgery. *J Oral Maxillofac Surg*. 2006;64:1780–4.
32. Sun Y, Luebbbers H-T, Agbaje JO, Schepers S, Vrielinck L, Lambrechts I, et al. Accuracy of upper jaw positioning with intermediate splint fabrication after virtual planning in bimaxillary orthognathic surgery. *J Craniofac Surg*. 2013; 24:1871–6.
33. Zinser MJ, Mischkowski RA, Sailer HF, Zöller JE. Computer-assisted orthognathic surgery: feasibility study using multiple CAD/CAM surgical splints. *Oral Surg Oral Med Oral Pathol Oral Radiol*. 2012;113:673–87.
34. Yeh J-K, Chen C-H. Estimated radiation risk of cancer from dental cone-beam computed tomography imaging in orthodontics patients. *BMC oral health*. 2018;18:131.
35. Bagheri SC, Jo C. Clinical review of Oral and maxillofacial surgery-E-book. Elsevier Health Sciences. 2013.
36. Mazzoni S, Bianchi A, Schiariti G, Badiali G, Marchetti C. Computer-aided design and computer-aided manufacturing cutting guides and customized titanium plates are useful in upper maxilla waferless repositioning. *J Oral Maxillofac Surg*. 2015;73:701–7.
37. Suojanen J, Leikola J, Stoor P. The use of patient-specific implants in orthognathic surgery: a series of 32 maxillary osteotomy patients. *J Craniomaxillofac Surg*. 2016;44:1913–6.
38. Heufelder M, Wilde F, Pietzka S, Mascha F, Winter K, Schramm A, et al. Clinical accuracy of waferless maxillary positioning using customized surgical guides and patient specific osteosynthesis in bimaxillary orthognathic surgery. *J Craniomaxillofac Surg*. 2017;45:1578–85.
39. Hosoki M, Nishigawa K, Miyamoto Y, Ohe G, Matsuka Y. Allergic contact dermatitis caused by titanium screws and dental implants. *J Prosthodont Res*. 2016;60:213–9.

Ready to submit your research? Choose BMC and benefit from:

- fast, convenient online submission
- thorough peer review by experienced researchers in your field
- rapid publication on acceptance
- support for research data, including large and complex data types
- gold Open Access which fosters wider collaboration and increased citations
- maximum visibility for your research: over 100M website views per year

At BMC, research is always in progress.

Learn more biomedcentral.com/submissions




RESEARCH ARTICLE

Open Access



Stress on facial skin of class III subjects during maxillary protraction: a finite element analysis

Francesca Gazzani^{1*} , Chiara Pavoni^{1,2}, Paola Cozza^{1,2} and Roberta Lione^{1,2}

Abstract

Background: Maxillary protraction with facemask (FM) is an orthopedic approach for treatment of Class III growing patients. Aim of the present investigation was to analyze tension loads produced by two different facial mask (FM) designs on facial skin of subject with skeletal Class III.

Methods: A three-dimensional (3D) geometry of Delaire and Petit FM models were reconstructed from the original Computer Aided Design (CAD) 3D prototype using software package (ANSYS 5.7). A traction load of 9.8 N inclined of 30° to the occlusal plane was applied combining analytical FM models with a 3D facial model. Resulting stresses and deformations on the skin layer were tested through the von Mises yield criterion.

Results: Overall tensions were mostly developed on the chin area, while lower stresses were observed on forehead area for both FM designs. When Delaire FM model was tested, maximum stresses were observed on the upper border of the chin cup corresponding to the inferior lip and to marginal gingiva of lower incisors. After Petit FM application, maximum stresses were more extensively localized at the level of both upper border and central area of the chin. Stresses measured on the chin area were significantly higher with Petit FM when compared with Delaire FM (44 KPa versus 29 KPa, respectively).

Conclusions: Delaire FM determined lower stresses and tensile tensions than Petit FM model. Highest tensions were observed at the level of chin cup area for both Delaire and Petit FM. Stresses following Delaire FM application were mostly observed on the upper border of the chin cup, while Petit FM determined stresses more extensively distributed to the central area of the chin.

Keywords: FEM analysis, Face mask, Maxillary protraction, Facial skin stresses

Background

Introduction

Face-mask (FM) therapy is the most recommended orthopedic approach for early treatment of skeletal Class III malocclusion [1–5]. Many articles [1–5] described favorable and stable outcomes on dento-skeletal structures and on soft tissue profile of maxillary protraction protocol. During orthopedic treatment, tensile forces are applied on maxillary sutures allowing a forward displacement of the maxilla and an improvement of the sagittal dento-skeletal relationship [6, 7]. Orthopedic therapy requires the

application of heavy forces ranging from 7.8 N to 9.8 N (800–1000 g, respectively) that often cause skin irritation and even mild swelling [7, 8]. Original FM model was firstly described by Jean Delaire [9, 10] and it consists of two extra-oral plastic supports connected to a metallic framework composed by two lateral vertical bars and one cross bar. Some years later, Petit [11] introduced a modified model of Delaire FM with a single rod running in the mid-line between the chin and forehead plastic cups. Recently, three-dimensional (3D) Finite Element Analysis (FEA) [6, 7, 12] has been used in order to evaluate the displacement and stress distribution of orthopedic forces applied on maxillofacial structures. Gautam et al. [6] highlighted that the highest loads produced by FM therapy were mostly localized along naso-maxillary, frontonasal and, fronto-maxillary

* Correspondence: francescagazzani@hotmail.it

¹Department of Clinical Sciences and Translational Medicine, University of Rome 'Tor Vergata', Via Collazia 29, 00183 Rome, Italy

Full list of author information is available at the end of the article



© The Author(s). 2019 **Open Access** This article is distributed under the terms of the Creative Commons Attribution 4.0 International License (<http://creativecommons.org/licenses/by/4.0/>), which permits unrestricted use, distribution, and reproduction in any medium, provided you give appropriate credit to the original author(s) and the source, provide a link to the Creative Commons license, and indicate if changes were made. The Creative Commons Public Domain Dedication waiver (<http://creativecommons.org/publicdomain/zero/1.0/>) applies to the data made available in this article, unless otherwise stated.

sutures. Gazzani et al. [13] evaluated mechanical properties of Delaire FM and the stresses generated on device components during orthopedic treatment, by means of FEA. Some of the major complications related to maxillary protraction treatment are due to poor adaptation and low fit of FM on the face and to skin irritation determined by the extra-oral cups. The discomfort in wearing the FM device affects patients' compliance with negative consequences on treatment effectiveness.

Purpose of the study

Hence, the aim of the present FEA study was to analyze tension loads produced by two FM designs and their effects on the chin and forehead skin area during orthopedic maxillary protraction.

Methods

Finite element analysis (FEA)

The FEA was performed defining the following parameters:

- geometrical features of both Delaire and Petit FMs;
- geometrical feature of 3D facial model prototype;
- material properties for each element of the FMs;
- support bone properties;
- mesh (number, shape and size of the elements used to discretize the FMs);
- constraints and loads applied on the system.

The ANSYS 5.7 software (Ansys Inc., Canonsburg, PA, USA) was used for the FEA. The software solved the steady state condition of a rigid body in the space

considering the input data. In particular, the system of algebraic equations was solved iteratively until the convergence of the solution was reached. Regarding the output data, stress and strain state induced by FM rigid bodies on the facial prototype were evaluated. Two analytical models were developed by considering Delaire-FM (M0774–01 Leone S.p.A., Florence, Italy) and Petit-FM (M0772–1 Leone S.p.A., Florence, Italy) (Fig. 1). Each component of the two models was constructed and assembled using Rhinoceros 4.0 CAD software (Robert McNeel & Associates, Seattle, WA, USA) and then exported to ANSYS 14.0 (Ansys Inc., Canonsburg, PA, USA) for the FEA (Fig. 2). For the 3D facial model, a human head prototype was chosen from Rhinoceros software and then modified considering a support bone with Young's Modulus of 18,000 MPa and a 3 mm skin layer with Young's Modulus of 0.64 MPa [14]. However, only forehead and chin areas of the model were considered and imported in ANSYS in order to simplify the FEA. In the 3D facial model an ideal occlusal plane was simulated for force application. The occlusal plane was orientated respect the ala-tragus line considering the facial model positioned in natural head position (NHP). For both Delaire and Petit FM, a 9.8 N (4.9 N for each side) loading force was applied with a 30° downward inclination respect to the occlusal plane to replicate the clinical application of the FM [3–5, 13, 15]. The FEA static simulation was conducted applying both FM types on 3D facial model. Thus, stress and load distribution on the skin areas were evaluated by using a static load. The mesh phase and the loads were developed by means of the interactive interface of the software.

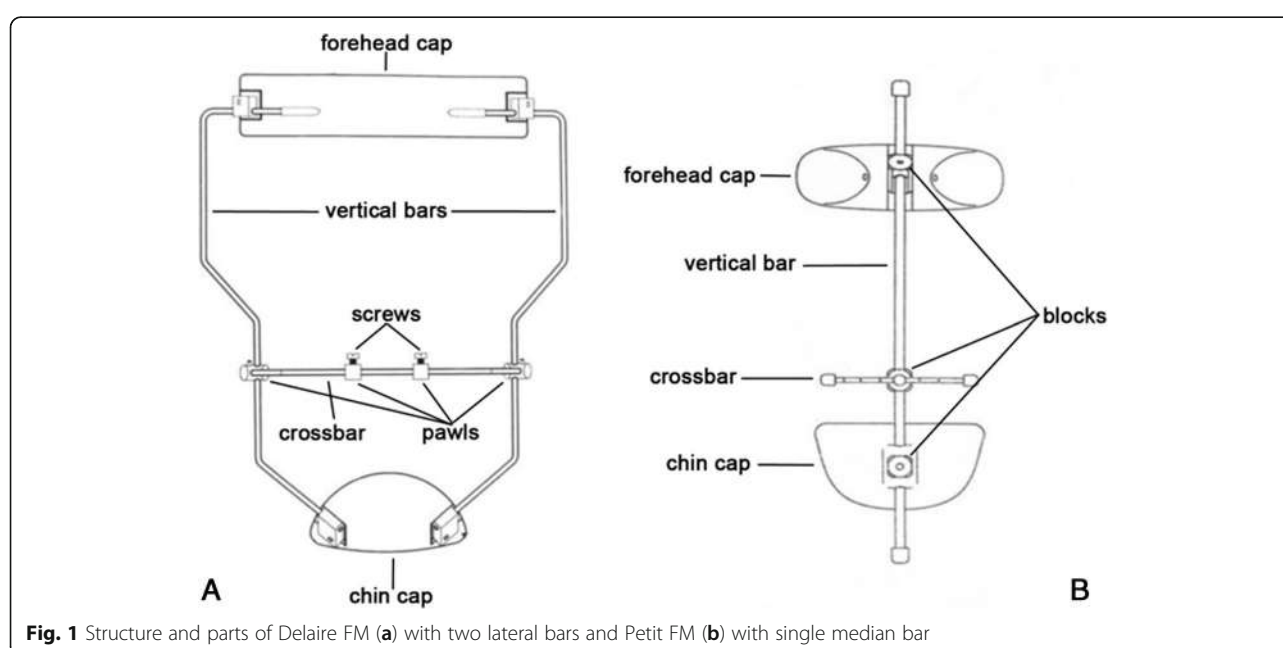


Fig. 1 Structure and parts of Delaire FM (a) with two lateral bars and Petit FM (b) with single median bar

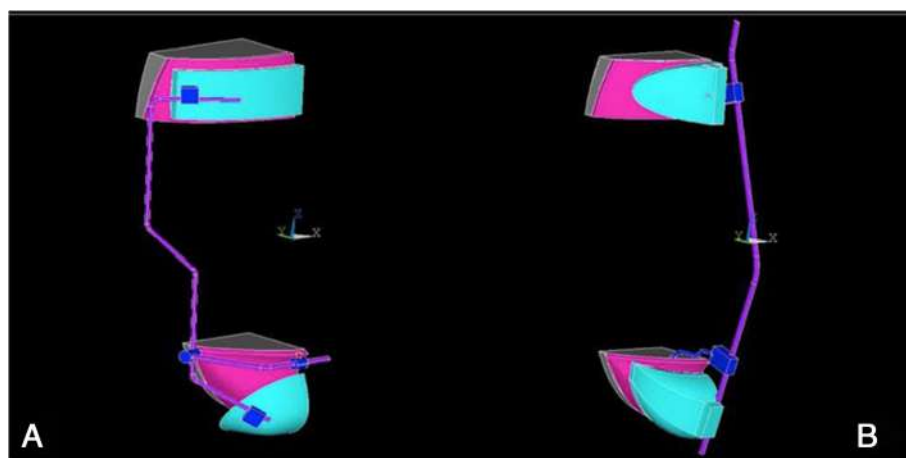


Fig. 2 3D models of Delaire FM (a) and Petit FM (b) designed by using ANSYS 5.7

Evaluation of load and stress distribution

In order to underline the load and stress distribution on the forehead and chin areas, von Mises yield criterion was evaluated on the skin layer delimited externally by the FMs cups and internally by the bone structure. The amount of elastic energy absorption was calculated for 9.8 N inclined of 30° to the occlusal plane to quantify the deformation state induced on the skin areas involved by the two FM models.

Results

The results of the von Mises yield criterion are shown in Figs. 3 and 4 and Table 1. For both FM models, greater tensions were recorded at the level of the chin cup with higher stresses and deformations observed for the Petit FM (29 KPa and 44 KPa, for Delaire and Petit FM, respectively) (Table 1). When Delaire FM was tested, maximum stresses were observed on the upper border of the chin cup corresponding to the inferior lip and to marginal gingiva of lower incisors (Fig. 3A). Moreover, maximum stresses tended to decrease constantly as moving away from this area. Similarly, tensile strength distribution analysis showed maximum stresses in correspondence of chin cup area after Petit FM application (Fig. 4A). In particular, tensile tensions were more extensively distributed and localized in correspondence of both upper border and central area of the chin. Within all tests performed, lower stresses were observed in the forehead area respect to the chin area (Figs. 3B, 4B). Heavier tensions developed on the forehead were at least three times lower than the maximum stresses affecting the chin (7 KPa and 3 KPa, induced by Delaire and Petit FM, respectively).

Discussion

FM therapy represents the gold standard for correcting skeletal Class III malocclusion in growing subjects [1–5, 16–19]. Several factors play a substantial role in terms of efficacy and effectiveness of orthopedic Class III treatment, including individual skeletal pattern, protraction device adaptation, patients' compliance, and device wear-time [20–24]. Stocker et al. [23] and Ozkalayci and Cicek [24] analyzed wearing time and patient compliance with FM reporting a significantly lower wearing time than the prescribed instructions. The not customized design of both FM models can cause poor device adaptation to the patient's face. The less adhesion of the device could determine skin irritations and mild swelling, with negative effects on patient compliance [1–5]. Stresses and load distribution developed on skeletal structures during orthopedic protraction treatment were widely analyzed [6, 7, 25]. More recently, in a previous investigation stresses developed during maxillary protraction and their effects on FM structure were evaluated by means of FEM analysis [13]. The absence of permanent plastic deformations and efficacy persistence of FM components highlighted the importance of a careful management of the device during treatment in order to grant its best performance. Although adverse effects on facial skin are known and very frequent in daily practice, however no data are available in literature regarding distributions and effects of tensile forces on facial skin. To our knowledge, both Petit and Delaire FM can lead to skin irritations caused by the plastic forehead and chin pads. Plastic supports of FM should be adjusted to fit patient's face maximizing the contact surface with the skin for a homogeneous distribution of the loads applied and avoiding skin wounds. Overall results of the present study highlighted higher tensile tensions at the level of the chin cup after the application of

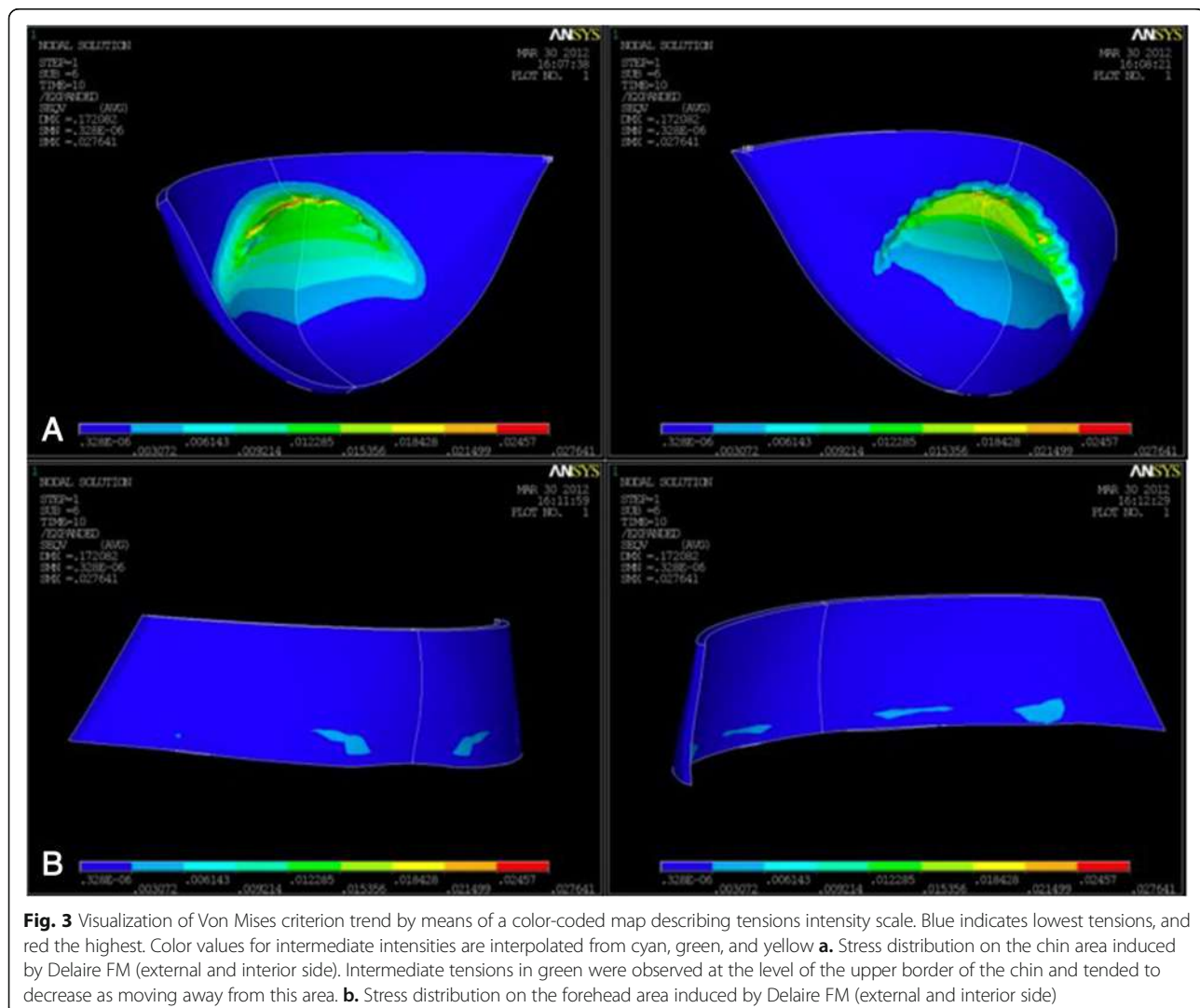
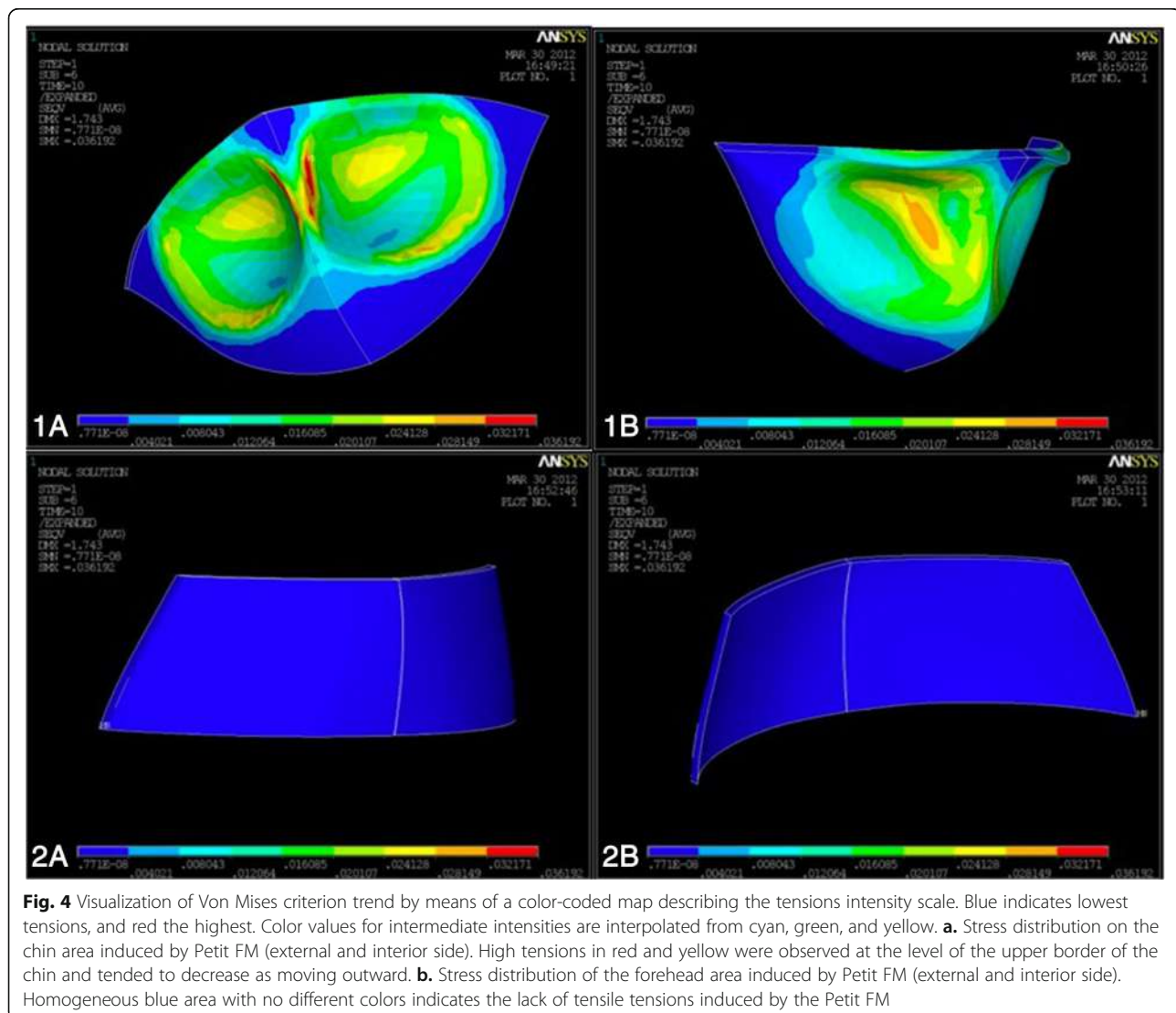


Fig. 3 Visualization of Von Mises criterion trend by means of a color-coded map describing tensions intensity scale. Blue indicates lowest tensions, and red the highest. Color values for intermediate intensities are interpolated from cyan, green, and yellow **a.** Stress distribution on the chin area induced by Delaire FM (external and interior side). Intermediate tensions in green were observed at the level of the upper border of the chin and tended to decrease as moving away from this area. **b.** Stress distribution on the forehead area induced by Delaire FM (external and interior side)

the Petit FM when compared with the Delaire FM (44 kPa and 29 kPa, respectively) (Table 1). More extended chin support of Delaire design reduced the intensity of the residual tensions and stresses developed on the patient skin face, while smaller chin support of Petit FM tended to increase the tensile tensions on the face exposing the patient to more skin irritation. Lower tensile tensions decrease the risk of skin irritations, but also maximize orthopedic forces transmission to the bone structure [2]. Moreover, tensile tensions were localized on the whole chin cup area with Petit FM, while more extended chin cup pads of Delaire FM determined maximum stresses in correspondence of its upper border. In both FM models' analysis, tensions registered on forehead region resulted particularly low and thus, clinically irrelevant, especially when Petit FM was tested. Maximum stresses ranged from 3 kPa (Petit FM) to 7 kPa (Delaire FM) and were mostly localized on the lower area, near to the eyebrows (Table 1).

Color uniformity observed on the forehead support indicates the absence of significant stresses induced by applying Petit FM (Fig. 4B). Forehead caps can be considered negligible in terms of discomfort and fit if compared with the chin supports. Tensile strength analysis confirmed good adaptation for both FM designs. It can be supposed that all tensions and stresses developed during orthopedic protraction are maximized and focused on the chin area near the center of load application, especially in the Petit structure. The results of the present FEA investigation suggested that Petit FM appears clinically less comfortable than the Delaire model with a higher risk of skin irritation and mild swelling on the chin. On the other hand, a prolonged stress applied by the border of the chin cap could interfere with the periodontal health of the lower incisors [26]. An external compression on the labial mental groove exerted by the chin pad could transmit a compression on the lower incisors' marginal gingiva with



resulting processes of gingival retraction. According to the findings of the present study, FM designs with more extended chin supports should be preferred to achieve wearing comfort. As previously suggested [8] a clinician-made customization of the chin cup using a poly-vinyl siloxane could be used to uniform the contact surfaces of the orthopedic device structure improving its performance and control of the load distribution.

Limitations of the current study were due to the 3D facial model used to perform FEM analysis of forces induced by different FM models. Standardization of 3D

Table 1 Maximum tensions on the skin areas

Mask type	Max. tension on chin skin surface	Max. tension on forehead skin surface
Delaire	29 kPa	6 kPa
Petit	44 kPa	3 kPa

kPa, kilopascal. 1 kPa correspond to 1000 Pa

model did not provide data about how forces distribution could change on different facial biotype. Further clinical studies will be necessary to analyzed stresses and loads distribution of orthopedic forces induced by maxillary protraction considering different facial patterns and biotypes in order to grant optimum management and customized fit of the device.

Conclusion

Highest tensions were observed at the level of chin cup area than at the level of forehead cups for both Delaire and Petit FM. Stresses following Delaire FM application were mostly observed on the upper border of the chin cup at the level of the inferior lip and lower incisor marginal gingiva. Petit FM produced higher tensile tensions than the Delaire design on the chin cup with stresses more extensively distributed to the central area of the chin.

Abbreviations

3D: Three Dimensional; CAD: Computer Aided Design; FEA: Finite Element Analysis; FM: Face Mask; KPa: KiloPascal; N: Newton

Acknowledgements

The authors wish to thank to Dr. Gabriele Scommegna for his advices in performing the experimental analysis and, Engineers Marouue J. and Gervasi G.L. for their competence and scientific support.

Funding

Not applicable.

Availability of data and materials

The datasets used and/or analyzed during the current study are available from the corresponding author on reasonable request.

Authors' contributions

FG analyzed and interpreted the data obtained, and was a major contributor in writing the manuscript. CP, RL, PC interpreted the data obtained and were a supervisor in writing the paper. All authors read and approved the final manuscript.

Ethics approval and consent to participate

Not applicable.

Consent for publication

Not applicable.

Competing interests

The authors declare that they have no competing interests.

Publisher's Note

Springer Nature remains neutral with regard to jurisdictional claims in published maps and institutional affiliations.

Author details

¹Department of Clinical Sciences and Translational Medicine, University of Rome 'Tor Vergata', Via Collazia 29, 00183 Rome, Italy. ²Department of Dentistry UNSBC, Tirana, Albania.

Received: 9 January 2019 Accepted: 4 February 2019

Published online: 13 February 2019

References

- De Toffol L, Pavoni C, Baccetti T, Franchi L, Cozza P. Orthopedic treatment outcomes in class III malocclusion. A systematic review. *Angle Orthod*. 2008; 78(3):561–73.
- Pavoni C, Masucci C, Cerroni S, Franchi L, Cozza P. Short-term effects produced by rapid maxillary expansion and facemask therapy in class III patients with different vertical skeletal relationships. *Angle Orthod*. 2015; 85(6):927–33.
- Pavoni C, Mucedero M, Baccetti T, Franchi L, Polimeni A, Cozza P. The effects of facial mask/bite block therapy with or without rapid palatal expansion. *Prog Orthod*. 2009;10:20–8.
- Franchi L, Pavoni C, Cerroni S, Cozza P. Thin-plate spline analysis of mandibular morphological changes induced by early class III treatment: a long-term evaluation. *Eur J Orthod*. 2014;36(4):425–30.
- Masucci C, Franchi L, Defraia E, Mucedero M, Cozza P, Baccetti T. Stability of rapid maxillary expansion and facemask therapy: a long-term controlled study. *AJODO*. 2011;140:493–500.
- Gautam P, Valiathan A, Adhikari R. Maxillary protraction with and without maxillary expansion: a finite element analysis of sutural stresses. *AJODO*. 2009;136(3):361–6.
- Kim KY, Bayome M, Park JH, Kim KB, Mo S-S, Kook Y-A. Displacement and stress distribution of the maxillofacial complex during maxillary protraction with buccal versus palatal plates: finite element analysis. *Eur J Orthod*. 2015; 37(3):275–83.
- Cacciatore G, Poletti L, Ghislanzoni LH. A chairside customized chin cup. *J Clin Orthod*. 2013;47(6):352.
- Delaire J. Manufacture of the "orthopedic mask". *Rev Stomatol Chir Maxillofac*. 1971;72(5):579–82.
- Delaire J. Treatment of class III with dentofacial orthopedic mask. *Acta Odontol Venez*. 1979;17(2–3):168–200.
- Petit HP. Adaptation following accelerated facial mask therapy. In: McNamara JA Jr, Ribbens KA, Howe RP, eds. *Clinical Alteration of the Growing Face*. 1983. Monograph 14, craniofacial growth series. Ann Arbor, Mich: Center for Human Growth and Development, University of Michigan;
- Staderini E, Patini R, De Luca M, Gallenzi P. Three-dimensional stereophotogrammetric analysis of nasolabial soft tissue effects of rapid maxillary expansion: a systematic review of clinical trials. *Acta Otorhinolaryngol Ital*. 2018;38(5):399–408.
- Gazzani F, Pavoni C, Giancotti A, Cozza P, Lione R. Facemask performance during maxillary protraction: a finite element analysis (FEA) evaluation of load and stress distribution on Delaire facemask. *Progr in Orthod*. 2018; 9: 19(1):21;
- Agache PG, Monneur C, Leveque JL, De Rigal J. Mechanical properties and Young's modulus of human skin in vivo. *Arch Dermatol Res*. 1980;269(3): 221–32.
- Yepes E, Quintero P, Rueda ZV, Pedroza A. Optimal force for maxillary protraction facemask therapy in the early treatment of class III malocclusion. *Eur J Orthod*. 2014;36(5):586–94M.
- Alcan T, Keles A, Erverdi N. The effects of a modified protraction headgear on maxilla. *AJODO*. 2000;117(1):27–38.
- Lione R, Buongiorno M, Laganà G, Cozza P, Franchi L. Early treatment of class III malocclusion with RME and facial mask: evaluation of dentoalveolar effects on digital dental casts. *Eur J Paediatr Dent*. 2015;16(3):210–20.
- Ngan P. Early timely treatment of class III malocclusion. *Semin Orthod*. 2005; 11:140–5.
- Cozza P, Baccetti T, Mucedero M, Pavoni C, Franchi L. Treatment and posttreatment effects of a facial mask combined with a bite- block appliance in class III malocclusion. *Am J Orthod Dentofac Orthop*. 2010;138:300–10.
- Franchi L, Baccetti T, Tollaro I. Predictive variables for the outcome of early functional treatment of class III malocclusion. *AJODO*. 1997;112(1):80–6.
- Nanda R, Kierl M. Prediction of cooperation in orthodontic treatment. *AJODO*. 1992;102(1):15–21.
- Campbell P. The dilemma of class III treatment: early or late? *Angle Orthod*. 1983;53(3):175–19.
- Stocker B, Willmann JH, Wilmes B, Vasudavan S, Drescher D. Wear-time recording during early class III facemask treatment using TheraMon chip technology. *AJODO*. 2016;150(3):533–40.
- Ozkalayci N, Cicek O. When Do Skeletal Class III Patients Wear Their Reverse Pull Headgears? *Biomed Res. Int*. 2017. <https://doi.org/10.1155/2017/3546262>;
- Park JH, Bayome M, Zahrowski JJ, Kook Y-A. Displacement and stress distribution by different bone-borne palatal expanders with facemask: a 3-dimensional finite analysis. *Am J Orthod Dentofac Orthop*. 2017;151(1):105–17.
- Parenti S, Checchi V, Molinari C, Bonetti GA. Periodontal side effect during orthopedic face mask therapy. *Inter J Orthod*. 2015;26(4).

Ready to submit your research? Choose BMC and benefit from:

- fast, convenient online submission
- thorough peer review by experienced researchers in your field
- rapid publication on acceptance
- support for research data, including large and complex data types
- gold Open Access which fosters wider collaboration and increased citations
- maximum visibility for your research: over 100M website views per year

At BMC, research is always in progress.

Learn more biomedcentral.com/submissions



CASE REPORT

Open Access



Intraoral scanning to fabricate complete dentures with functional borders: a proof-of-concept case report

Alexey Unkovskiy^{1,2*} , Eugen Wahl¹, Anne Teresa Zander¹, Fabian Huettig¹ and Sebastian Spintzyk³

Abstract

Background: The utilization of intraoral scanning for manufacturing of complete dentures (CD) has been reported recently. However, functional border molding still cannot be supported digitally. A proof-of-concept trial shows two possible pathways to overcome this limitation by integrating a relining procedure into the digital workflow for CD manufacturing.

Case presentation: Intraoral scans and additional facial scans were performed with two various scanning systems for the rehabilitation of an edentulous male patient. The obtained raw data was aligned and used for the computer aided design (CAD) of the CD. The virtually constructed dentures were materialized in two various ways, considering rapid manufacturing and digital relining approaches in order to apply functionally molded borders.

Conclusion: The use of intraoral edentulous jaws scans in combination with the digital relining procedure may allow for fabrication of CD with functional borders within a fully digital workflow.

Keywords: Case report, Complete denture; intraoral scanning, Additive manufacturing, 3D printing, Computer aided design

Background

During the past decade, prosthetic dentistry was seriously impacted by computer driven technologies, which has also touched upon the rehabilitation of edentulous patients [1]. Fabrication of complete dentures (CD) by means of computer aided design (CAD) and manufacturing (CAM) has been proven to be feasible [2, 3]. A better fit to the underlying tissues [4] and a reduced number of appointments till a final denture delivery [5, 6] were reported to be the main advantages towards the conventional production chain. However, the long-term clinical performance of digitally produced CD was not evaluated until now, and the existing software solutions still require further improvements [7].

Within numerous digital protocols, recently introduced for CD fabrication, CAD/CAM substitutes many of the steps of a conventional production chain [8]. For instance, occlusal rims (OR) and functional impressions (with border moldings) can be digitalized with the use of laboratory scanners for the data input [7, 9]. Then, a denture is constructed virtually in specific CAD software [10, 11]. The facial scans can be obtained for the virtual esthetic evaluation and digital try-in session [9, 12]. A denture prototype can be fabricated by means of additive manufacturing (AM) for the chairside try-in session [8, 13]. A final denture assembly is manufactured using subtractive or additive manufacturing methods [14, 15]. These approaches, however, should be perhaps regarded as “partially digital”, as they consider no intraoral scanning of maxilla and mandible alveolar parts and necessitate analog elements, such as impressions, within the workflow.

In the last years, the intraoral scanning has been widely applied in prosthetic dentistry as an alternative to the conventional impression taking [16–18]. Very recently, a few techniques for the direct capturing of edentulous jaws

* Correspondence: dr.unkovskiy@gmail.com

¹Department of Prosthodontics at the Centre of Dentistry, Oral Medicine, and Maxillofacial Surgery with Dental School, Tuebingen University Hospital, Osianderstr. 2-8, 72076 Tuebingen, Germany

²Department of Dental Surgery, Sechenov First Moscow State Medical University, Bolshaya Pirogovskaya Street, 19c1, 119146 Moscow, Russia

Full list of author information is available at the end of the article



© The Author(s). 2019 **Open Access** This article is distributed under the terms of the Creative Commons Attribution 4.0 International License (<http://creativecommons.org/licenses/by/4.0/>), which permits unrestricted use, distribution, and reproduction in any medium, provided you give appropriate credit to the original author(s) and the source, provide a link to the Creative Commons license, and indicate if changes were made. The Creative Commons Public Domain Dedication waiver (<http://creativecommons.org/publicdomain/zero/1.0/>) applies to the data made available in this article, unless otherwise stated.

have been introduced, but do not cover the functional mucosa reflections [19–21]. Furthermore, the reliability and reproducibility of some of these techniques are questionable [22]. The unfeasibility of digital functional impression taking and modest precision are considered herein as main limitations [8, 23]. Some clinical cases have shown the pathway till delivery of the definitive CD: Utilizing intraoral scans in a fully digital workflow either considering no functional borders molding [15], or a using finger to stretch the mucosa and capture its reflections [24]. Such technique was reported to provide a denture with sufficient retention, however, major concern here may be the overextension of the plica intermedia and neglecting of the functional movements.

The present clinical case describes two technical proof-of-concept approaches for fabrication of CDs with functional borders in a fully digital workflow utilizing intraoral scanning.

Case presentation

A fully edentulous male patient received conventional CDs and gave his informed written consent to participate in this feasibility trial. The edentulous upper and lower jaws were scanned with the TRIOS3 intraoral scanner (3Shape, Copenhagen, Denmark) (Software version 1.4.7.5) (Fig. 1). The lips were retracted with a Brånemark cheekholder and saliva was constantly removed with an aspirator during intraoral scanning [25]. The “zig-zag” scanning technique was used in this clinical case [24, 26]. The occlusal vertical dimension (OVD) was oriented on the physiological rest position and an occlusion rim (OR) was made with Silaplast putty silicone material (Detax, Ettlingen, Germany). The central, canine, and smile lines were marked with cuts in the

silicone on the facial surface of the OR. This OR was digitized extraorally with the same scanner (TRIOS3). In order to capture the facial anatomy, three scans with the OR being placed in the mouth were performed with neutral face, smiling face, and with cheekholders using the priti®mirror scanner (priti®denta, Leinfelden-Echterdingen, Germany). The pathway for raw data matching and virtual denture design using both available dental CAD solutions: DentalCAD software (Version 2.2 Valetta, Exocad, Darmstadt, Germany) and 3Shape Dental System (3shape, Copenhagen, Denmark) is described in Fig. 2. The obtained virtual denture design was used to produce two final denture sets utilizing the following technical approaches.

“The rapid manufacturing (RM-) approach”

The virtual models of denture bases without tooth anatomy were milled from Organic PMMA Eco Pink discs (Organical CAD CAM, Berlin, Germany) with Organic Desktop 8 milling unit (Organical CAD CAM, Berlin, Germany). To ensure the proper positioning of the standard artificial teeth (Bonartic NFC+, Candulor, Glattpark, Switzerland) in the denture basis, a transfer key was designed in the Zbrush software (Pixologic, Los Angeles, CA, USA). Figure 3a based on the 3D datasets of the artificial teeth set.

In addition, undercuts on the prostheses’ models were blocked out with a virtual clay tool. An U-shaped bulk was superimposed onto the denture virtual model, so that it covered the artificial teeth, and both retromolar and palatal surfaces. The denture model was cut out from the bulk with the Boolean function constituting the transfer key. This dataset was printed with a direct light processing (DLP) Solflex 170 3D printer (W2P Engineering,

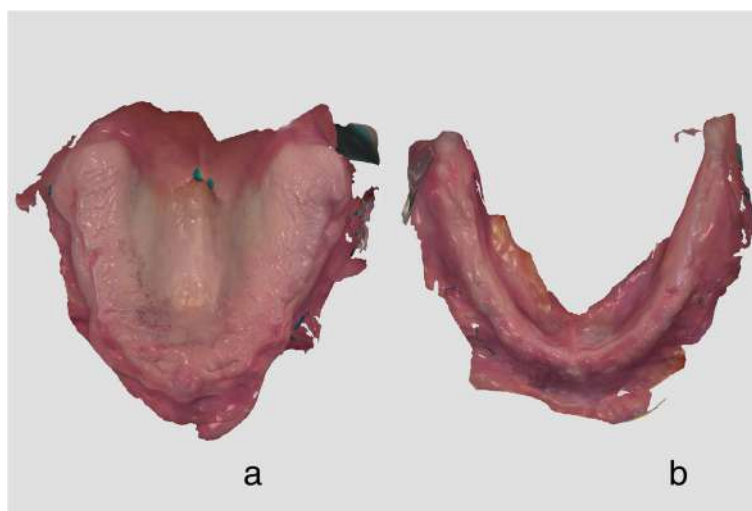


Fig. 1 Intraoral scans of edentulous upper (a) and lower (b) jaws in native format in 3Shape scanning software obtained using the “zig-zag” technique

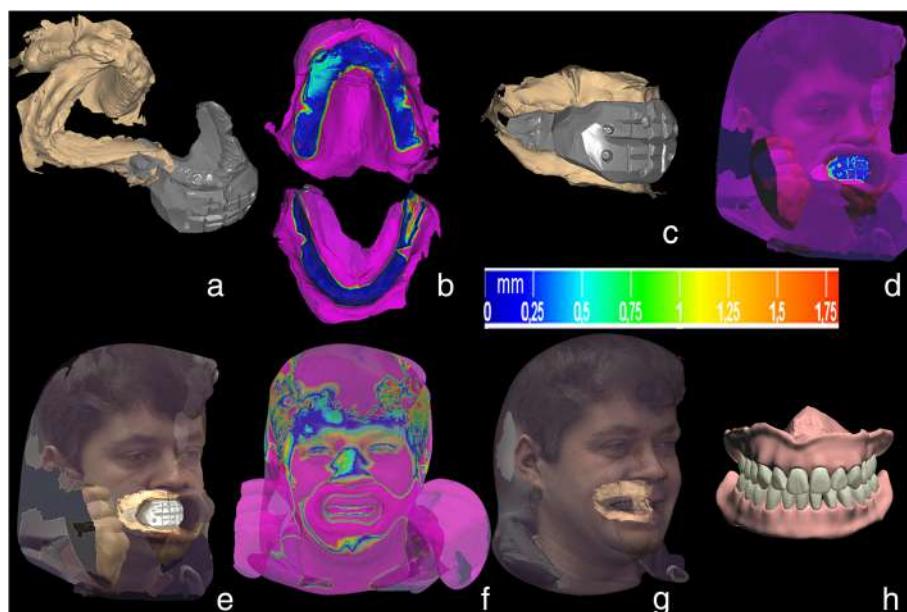


Fig. 2 CAD pathway in DentalCAD software (Exocad). **a**: unmatched upper and lower jaws scans and scan of OR; **b**: initial alignment of the both jaw scans with OR using “three points alignment” protocol and the final alignment with “best-fit protocol”. The deviation of the reference areas ranged between 0 and 0.25 mm, as indicated in the scale; **c**: aligned scans of upper and lower jaws with OR; **d**: alignment of OR with the “cheek retractor facial scan” using reference lines on the OR; **e**: aligned OR with the “cheek retractor facial scan” **f**: alignment of the “cheek retractor facial scan” with “smile facial scan” using common reference points (chin, eyes, dorsum nasi); **g**: aligned upper and lower jaw scans embedded into the “smile facial scan” as a result of “d” and “f”; **h**: the whole dataset was transferred into the Dental System software (3Shape, Copenhagen, Denmark) for the digital design of two dentures

Vienna, Austria) using V-Print model material (Voco, Cuxhaven, Germany). Afterwards, the chosen artificial teeth were fixed into the corresponding sockets with the cold curing Aesthetic Blue PMMA (Candulor, Glattpark, Switzerland). The printed transfer key was placed upon the teeth and was pressed onto the denture bases (Fig. 3b). After the PMMA excesses were removed the, dentures were put under pressure (2.5 Bar, 40 °C, 20 min). The dentures were then polished (Fig. 3c).

“The digital relining (DR) approach”

This approach encompasses a chairside try-in session. For this purpose, the denture prototype with tooth anatomy was printed with the DLP Solflex 170 3D printer (W2P Engineering, Vienna, Austria) using Solflex prov A2 material (W2P Engineering, Vienna, Austria) (50 µm layer thickness, printing time 5 h). Pink wax (Modelierwachs, Omnident, Rodgau Nieder-Roden, Germany) was applied to imitate the gingiva for a more realistic perception (Fig. 4).



Fig. 3 “The rapid manufacturing (RM) approach” (exemplarily upper denture). **a**: the virtual design of a transfer key in Zbrush software (Pixologic, Los Angeles, CA, USA) to ensure the proper teeth positioning; **b**: transfer key put on the denture base and being supported upon the tuber and palatal surfaces; artificial teeth are put into corresponding sockets; **c**: polished denture with artificial teeth in situ being fixed with cold curing PMMA



Fig. 4 Printed denture prototype with tooth anatomy for the DR approach

During the try-in session, the general esthetics and function were checked, including the OVD, occlusion, and the bases extension. Due to suboptimal retention of the prototypes' bases, they were relined with a Silasoft N silicone material (Detax, Ettlingen, Germany) (Fig. 5a). The silicone excesses that spread over the flanges onto the prototype basis were cut out with a scalpel. The relined prototypes were scanned extraorally with the TRIOS3 scanner (3Shape, Copenhagen, Denmark) (Fig. 5b). The obtained datasets were aligned with the existing 3D denture constructions through the matching surfaces, e.g. teeth and basis in the DentalCAD

software (Exocad, Darmstadt, Germany) (Fig. 5c). The matched surfaces were merged together and further adjusted in the Zbrush software (Pixologic, Los Angeles, CA, USA). The relined and adjusted virtual denture models were printed with a Solflex 170 DLP printer (W2P Engineering, Vienna, Austria) with pink resin (Base pink, NextDent, Soesterberg, Netherlands) (50 μ m layer thickness, 7 h 50 min printing time for both dentures) (Fig. 5d). The artificial teeth were then fixed into the bases the same way it was done in "RM-approach" described above (Fig. 5e).

Discussion and conclusions

The digitalization of the CD manufacturing began with the advent of specific CAD software, which allowed for CAM of denture bases and artificial teeth in either a subtractive or additive way [8]. The implementation of the facial scanning into the workflow allowed for the virtual try-in session and contributed to the predictability of the final outcome [11, 12]. The primary data acquisition step, however, remained rather analog and implied conventional impression taking, which was afterwards scanned extraorally [9]. In 2013, the feasibility of a direct digital impression of edentulous jaws was shown extraorally [23], however differences up to 591.8 μ m to the original model were revealed from this work. With the advent of more sophisticated intraoral scanning devices, the precision of direct digital data acquisition has increased, and minor deviations up to 125 μ m were reported

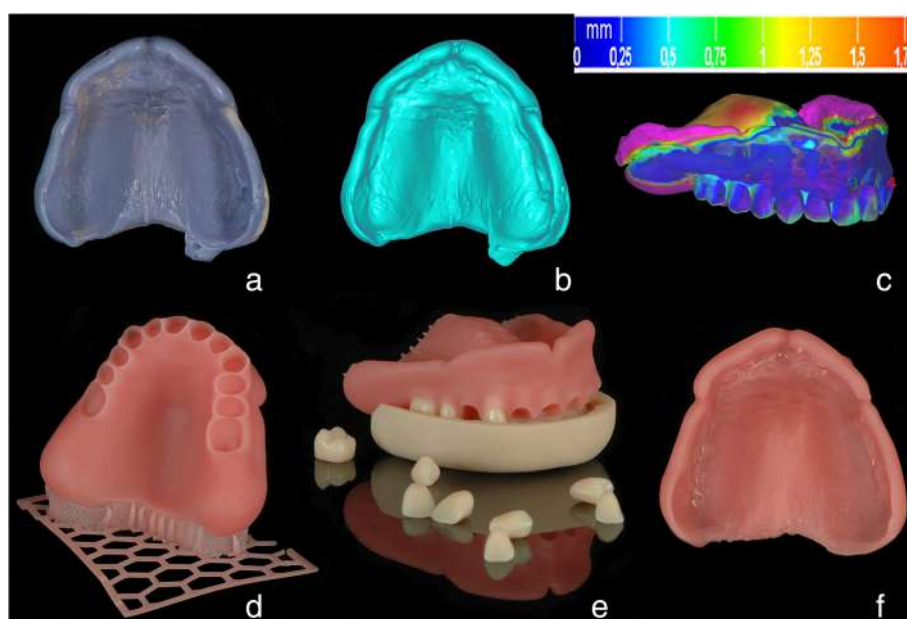


Fig. 5 "The digital relining (DR-) approach". **a**: relined denture prototype; **b**: virtual model of the relined surface obtained with a Trios scanner; **c**: alignment of the relined surface with the existing denture design through the reference teeth and basis surfaces using the best-fit protocol (DentalCAD, Exocad, Darmstadt, Germany); **d**: "digitally relined" denture basis fabricated with Solflex 170 3D printer 'as is' (W2P Engineering, Vienna, Austria); **e**: fitting the artificial teeth into the corresponding sockets using a transfer key; **f**: 3D printed final denture surface with functional borders

[27]. In the last few years, the buccal-occlusal-palatal (BOP) [26] and “zig-zag” [20] techniques have been mainly used for the intraoral scanning of edentulous jaws. Thereby, the BOP has shown greater trueness but lower precision [28]. A specific pathway was described for an intraoral scanning of a maxillary edentulous jaw considering special markers on the palatal surface to avoid “overlapping effects” [21]. In the present clinical case the intraoral digital impressions of edentulous maxilla were performed with “zig-zag” technique. No visual overlapping effect was detected in the data sets. The scanning process of the edentulous mandible took more time, as it is devoid of anatomical landmarks. Care was taken to retract the cheeks and tongue, to remove the saliva from the mouth floor and keep the palatal surface dry.

Even if the direct scan of the jaws still supports no functional impression, a CD manufactured in such a digital workflow was reported to have a good retention [15]. Thereby, the surface tension between the denture basis and underlying tissue may play a bigger role, than the sealing effect by means of custom formed denture borders [17]. Goodacre et al. have reported that the stretching of the mucosa with the finger, while performing the intraoral scan, may be useful to capture sufficient amount of mucosa reflections and achieve a good peripheral seal. Here, two aspects may be of major concern. First, care must be taken not to overextend the plica intermedia, while manipulating it freely in order to avoid the excessive displacement of the tissue of the vestibule [29]. Second, a traditional functional impression encompasses not only the manual manipulation of the mucosa by the operator, but also the border molding movements performed by the patient himself [30].

Aside from retention, valid orientation of the obtained jaw scans prerequisites a successful, reproducible digital workflow for CD manufacturing. This order implies a transfer of the jaw relation, which is challengeable to perform intraorally. As demonstrated by Kanazawa et al., the reduction of OR dimensions can simplify the scanning process at least for the manufacturing of custom impression trays [31]. However, such an approach hinders the transfer of esthetical lines as well as the alignment and connection of facial and jaw scans. Therefore in the present feasibility study, the OR with the marked esthetical lines was digitalized extraorally and acted as an index object for orientation and CAD alignments. The extraoral scanning process with the intraoral scanner surprisingly was not associated with any difficulties. The OR could be captured with one scanning sequence. For the alignment of OR with the “cheekholder facial scan”, the three-point protocol was used for the initial alignment, followed by the best-fit protocol for the definitive one. The deviation range of the reference areas was between 0 and 0.25 mm, which was considered

to be accurate enough to start the CAD stage. During the try-in stage, no deviations in either the occlusion between the prototypes or the orientation of the occlusal plane were revealed. If there should be any inaccuracies in the virtual alignment of the whole dataset, they could be fixed on the try-in stage utilizing the DR approach. However, the RM approach would be more susceptible to any kind of inaccuracies in the data alignment. Minor corrections in terms of OVD and occlusion scheme may be applied chairside. In case of greater deviations, the production process should be started from the very beginning.

The present clinical case shows two pathways to fabricate CD with functional borders in a digital workflow, using intraoral scanning for initial data acquisition and facial scans for the aesthetical adjustment. These techniques result in comparable dentures and require one intraoral scanner, three CAD solutions, and a DLP 3D printer (Fig. 6). Unfortunately, no universal software solution for CAD of CD is available today. Whereas the 3Shape software includes the data library with prefabricated teeth in 3D format, it supports no raw data alignment and integration of the facial 3D scans for the fully 3D smile design. Thus, in order to design a CD with prefabricated teeth (i.e. Candulor), utilizing at the same time the facial 3D scans for the aesthetical adjustment, one is obliged to use a combination of 3Shape and Exocad software solutions.

The RM approach showed the shortest pathway from data acquisition to the final denture delivery within a fully digital workflow in only two appointments. However, as this approach implies no try-in session, the final esthetical outcome is hardly predictable and relies only upon the consistency of the digital try-in session in the CAD software. In the present case, the upper denture fabricated within the RM approach with no border molding showed a poor retention. Thus, a relining procedure with all functional probes can be performed in analog workflow either directly or indirectly [32].

The DR approach considered the virtual relining procedure as an inherent step. This step does not require any additional appointment as it can be performed during the try-in session. The virtual image of the relined surface can be obtained chairside in the same appointment with the intraoral scanner and requires no further hardware investments, i.e. a labor-scanner. A faithful alignment of the scanned relined surface and the existing denture design is of major concern and depend heavily of the square of the matching surface. For this reason, all the silicone excesses that spread over the prototype flanges were cut out with the scalpel in order to increase the matching surface.

The other setback of this approach is the fact that no CAD software today supports the merging procedure of



Fig. 6 Two upper jaw dentures with custom borders made in a digital workflow utilizing the intraoral jaw scans. **a**: digitally relined and printed (DR approach); **b**: milled and relined in the analog way (RM approach)

the relined surface with the initial denture design and allows for designing of a transfer index. For this reason, additional software must be used, i.e. the Zbrush, which is capable of aligning and merging of two virtual meshes. Thus, the certain CAD skills and expertise is required. This fact can be considered as the limitation of the described technique and calls for the CAD software enhancement.

The upper denture fabricated within the DR approach demonstrated – as expected – clinically sufficient retention, as the peripheral sealing effect was achieved due to denture flanges customized extension. A perfect retention of the lower denture is commonly hard to achieve [33]. A lingual occlusal scheme without the canine guidance was considered in this case, alternatively to the bilateral balanced occlusion [34, 35].

Within the current technique, the acquired digital set up must be arranged in the CAD software, prior to the prostheses designing process. The setup includes OR, upper and lower jaw scans, a “cheekholder facial scan”, and a “smile scan”. Meaning, the four subsequent alignment procedures may constitute a potential error source. In the present clinical case, the deviation between the matching areas ranged between 0 and 0.25 mm. A systematic study with a greater sample size must address the reliability of this technique.

This clinical trial reveals the current state of technology in a digital workflow of CD fabrication and highlights the possibilities and limitations of the intraoral scans utilization. The RM approach allowed for a quicker workflow within two appointments, but it is questionable as a definitive treatment option due to shortcomings in retention and poor predictability of the esthetic outcome. Thus, the integration of a relining procedure with functional impression – as shown in DR approach – may enhance the denture retention made in

a digital workflow, starting with the intraoral scanning. The digital underlining technique shown still implies the conventional functional probes, restricting the unambiguously fully digital workflow.

The two introduced technical approaches revealed that there is still no optimal CAD solution, which would cover such aspects of CD design, as integration of facial scans, fabrication of transfer index, merging of the separate meshes and integration of prefabricated tooth libraries. Furthermore, these approaches require a certain financial investments in both hard- (one intraoral scanner, one facial scanner, one 3D printer) and software (three commercial CAD solutions).

Abbreviations

CAD: Computer aided design; CAM: Computer aided manufacturing; CD: Complete denture; DR: Digital relining; OR: Occlusal rim; OVD: Occlusal vertical dimension; PMMA: Poly-methylmethacrylate; RM: Rapid manufacturing

Acknowledgements

The authors thank the Way2Production Company (W2P), especially Dr. S. Gruber and S. Schueller for their technical support. We also thank MDT Mr. E. Kroewerath from University Hospital Tuebingen for his useful technical advice.

Funding

This trial received no funding.

Availability of data and materials

The datasets used and/or analyzed during the current study are available from the corresponding author on reasonable request.

Authors' contributions

All authors contributed not only to the manuscript preparation and finalization, but also conducting the case, data acquisition and evaluation as follows: AU designed and performed the clinical case, including 3D data acquisition and CAD design as well as try-in; drafted the manuscript. FH supervised the regulatory affairs and design to conduct the case, revised the manuscript. EW performed the postprocessing of the prostheses and gave technical input to the manuscript. AZ screened and informed patients for participation, performed the conventional part of the treatment, try-in stages and the aftercare, and contributed with critical revisions to the manuscript. SS supervised the 3D hardware, handled the 3D data to coordinate the production process with the manufacturer, and critically

revised the manuscript. All authors of this paper have read and approved the final version submitted.

Ethics approval and consent to participate

Not applicable.

Consent for publication

The patient gave his written informed consent for participation in this study and publication of the gathered data.

Competing interests

The authors declare that they have no competing interests.

Publisher's Note

Springer Nature remains neutral with regard to jurisdictional claims in published maps and institutional affiliations.

Author details

¹Department of Prosthodontics at the Centre of Dentistry, Oral Medicine, and Maxillofacial Surgery with Dental School, Tuebingen University Hospital, Osianderstr. 2-8, 72076 Tuebingen, Germany. ²Department of Dental Surgery, Sechenov First Moscow State Medical University, Bolshaya Pirogovskaya Street, 19c1, 119146 Moscow, Russia. ³Section Medical Materials Science and Technology, Tuebingen University Hospital, Osianderstr. 2-8, 72076 Tuebingen, Germany.

Received: 9 November 2018 Accepted: 25 February 2019

Published online: 13 March 2019

References

- Bidra AS, Taylor TD, Agar JR. Computer-aided technology for fabricating complete dentures: systematic review of historical background, current status, and future perspectives. *J Prosthet Dent*. 2013;109:361–6.
- Maeda Y, Minoura M, Tsutsumi S, Okada M, Nokubi T. A CAD/CAM system for removable denture. Part I: fabrication of complete dentures. *Int J Prosthodont*. 1994;7:17–21.
- Busch M, Kordass B. Concept and development of a computerized positioning of prosthetic teeth for complete dentures. *Int J Comput Dent*. 2006;9:113–20.
- Steinmassl O, Dumfahrt H, Grunert I, Steinmassl PA. CAD/CAM produces dentures with improved fit. *Clin Oral Investig*. 2018;22:2829–35.
- Kattadiyil MT, Jekki R, Goodacre CJ, Baba NZ. Comparison of treatment outcomes in digital and conventional complete removable dental prosthesis fabrications in a predoctoral setting. *J Prosthet Dent*. 2015;114:818–25.
- Infante L, Yilmaz B, McGlumphy E, Finger I. Fabricating complete dentures with CAD/CAM technology. *J Prosthet Dent*. 2014;111:351–5.
- Bonnet G, Batisse C, Bessadet M, Nicolas E, Veyrune JL. A new digital denture procedure: a first practitioners appraisal. *BMC Oral Health*. 2017;17:155.
- Schweiger J, Stumbaum J, Edelhoff D, Guth JF. Systematics and concepts for the digital production of complete dentures: risks and opportunities. *Int J Comput Dent*. 2018;21:41–56.
- Schweiger J, Guth JF, Edelhoff D, Stumbaum J. Virtual evaluation for CAD-CAM-fabricated complete dentures. *J Prosthet Dent*. 2017;117:28–33.
- Contrepois M, Sireix C, Soenen A, Pia JP, Lasserre JF. Complete denture fabrication with CAD/CAM technology: a case report. *Int J Esthet Dent*. 2018;13:66–85.
- Joda T, Muller P, Zimmerling F, Schimmel M. Die CAD/CAM-gefertigte Totalprothese mit dem «digital denture professional system». *Swiss Dent J*. 2016;126:899–919.
- Hassan B, Greven M, Wismeijer D. Integrating 3D facial scanning in a digital workflow to CAD/CAM design and fabricate complete dentures for immediate total mouth rehabilitation. *J Adv Prosthodont*. 2017;9:381–6.
- Han W, Li Y, Zhang Y, Lv Y, Zhang Y, Hu P, et al. Design and fabrication of complete dentures using CAD/CAM technology. *Medicine (Baltimore)*. 2017;96:e5435.
- Lin WS, Harris BT, Pellerito J, Morton D. Fabrication of an interim complete removable dental prosthesis with an in-office digital light processing three-dimensional printer: a proof-of-concept technique. *J Prosthet Dent*. 2018;120:331–4.
- Lo Russo L, Salami A. Single-arch digital removable complete denture: a workflow that starts from the intraoral scan. *J Prosthet Dent*. 2017;120:20–4.
- Virard F, Venet L, Richert R, Pfeffer D, Viguie G, Bienfait A, et al. Manufacturing of an immediate removable partial denture with an intraoral scanner and CAD-CAM technology: a case report. *BMC Oral Health*. 2018;18:120.
- Bosniac P, Rehmann P, Wostmann B. Comparison of an indirect impression scanning system and two direct intraoral scanning systems in vivo. *Clin Oral Investig*. 2018. <https://doi.org/10.1007/s00784-018-2679-4>.
- Park GH, Son K, Lee KB. Feasibility of using an intraoral scanner for a complete-arch digital scan. *J Prosthet Dent*. 2018. <https://doi.org/10.1016/j.prosdent.2018.07.014>.
- Hayama H, Fueki K, Wadachi J, Wakabayashi N. Trueness and precision of digital impressions obtained using an intraoral scanner with different head size in the partially edentulous mandible. *J Prosthodont Res*. 2018;62:347–52.
- Fang Y, Fang JH, Jeong SM, Choi BH. A technique for digital impression and bite registration for a single edentulous arch. *J Prosthodont*. 2018. <https://doi.org/10.1111/jopr.12786>.
- Fang JH, An X, Jeong SM, Choi BH. Digital intraoral impression technique for edentulous jaws. *J Prosthet Dent*. 2017. <https://doi.org/10.1016/j.prosdent.2017.05.008>.
- Lee JH. Comments regarding: Fang JH, An X, Jeong SM, Choi BH. Digital intraoral impression technique for edentulous jaws. *J Prosthet Dent* 2017; doi: <https://doi.org/10.1016/j.prosdent.2017.05.008>. [Epub ahead of print]. *J Prosthet Dent* 2018;119:499–500.
- Patzelt SB, Vonau S, Stampf S, Att W. Assessing the feasibility and accuracy of digitizing edentulous jaws. *J Am Dent Assoc*. 2013;144:914–20.
- Goodacre BJ, Goodacre CJ, Baba NZ. Using intraoral scanning to capture complete denture impressions, tooth positions, and centric relation records. *Int J Prosthodont*. 2018;31:377–81.
- Goodacre BJ, Goodacre CJ. Using intraoral scanning to fabricate complete dentures: first experiences. *Int J Prosthodont*. 2018;31:166–70.
- Mutwalli H, Braian M, Mahmood D, Larsson C. Trueness and precision of three-dimensional digitizing intraoral devices. *Int J Dent*. 2018;2018:5189761.
- Iturrate M, Eguiraun H, Etxaniz O, Solaberrieta E. Accuracy analysis of complete-arch digital scans in edentulous arches when using an auxiliary geometric device. *J Prosthet Dent*. 2018. <https://doi.org/10.1016/j.prosdent.2018.09.017>.
- Muller P, Ender A, Joda T, Katsoulis J. Impact of digital intraoral scan strategies on the impression accuracy using the TRIOS pod scanner. *Quintessence Int*. 2016;47:343–9.
- Ma L. Border molding-teach me what I am blind to (Moffatt). *Adv Dent & Oral Health*. 2017;6:555697.
- Rao S, Chowdhary R, Mahoorkar S. A systematic review of impression technique for conventional complete denture. *J Indian Prosthodont Soc*. 2010;10:105–11.
- Kanazawa M, Iwaki M, Arakida T, Minakuchi S. Digital impression and jaw relation record for the fabrication of CAD/CAM custom tray. *J Prosthodont Res*. 2018;62:509–13.
- Rathi A, Banerjee R, Radke U, Lahoti S, Sahni S. Knowledge and attitude about relining of complete dentures in clinical practice: a cross-sectional study. *J Indian Prosthodont Soc*. 2018;18:174–80.
- van der Bilt A, Burgers M, van Kampen FM, Cune MS. Mandibular implant-supported overdentures and oral function. *Clin Oral Implants Res*. 2010;21:1209–13.
- Loh PJ, Levey C. Occlusal schemes for complete dentures. *Evid Based Dent*. 2018;19:116–7.
- Lemos CAA, Verri FR, Gomes JML, Santiago Junior JF, Moraes SLD, Pellizzer EP. Bilateral balanced occlusion compared to other occlusal schemes in complete dentures: a systematic review. *J Oral Rehabil*. 2018;45:344–54.

CASE REPORT

Open Access



Computer-assisted, template-guided immediate implant placement and loading in the mandible: a case report

Thomas Spielau^{1*}, Uli Hauschild² and Joannis Katsoulis³

Abstract

Background: Computer-assisted implant planning has become an important diagnostic and therapeutic tool in modern dentistry. This case report emphasizes the possibilities in modern implantology combining virtual implant planning, guided surgery with tooth and implant supported templates, immediate implant placement and loading.

Case presentation: A straight forward approach was followed for the mandible presenting with hopeless lower incisors. Diagnosis, decision making and treatment approach were based on clinical findings and detailed virtual three-dimensional implant planning. Extractions of the hopeless mandibular incisors, immediate and guided implant placement of six standard implants, and immediate loading with a provisional fixed dental prosthesis (FDP) were performed fulfilling patient's functional and esthetic demands. The final computer assisted design / computer assisted manufacturing (CAD/CAM) FDP with a titanium framework and composite veneering was delivered after 6 months. At the 1-year recall the FDP was free of technical complications. Stable bony conditions and a healthy peri-implant mucosa could be observed.

Conclusions: Computer assisted implantology including three-dimensional virtual implant planning, guided surgery, and CAD/CAM fabrication of provisional and final reconstructions allowed for a concise treatment workflow with predictable esthetic and functional outcomes in this mandibular full-arch case. The combination of immediate implant placement and immediate loading was considerably more complex and required a high level of organization between implantologist, technician and patient. After the usage of a first tooth-supported surgical template with subsequent extraction of the supporting teeth, a second surgical template stabilized on the previously inserted implants helped to transfer the planned implant position in the extraction sites with a guided approach.

Keywords: Virtual implant planning, Guided surgery, Immediate placement, Immediate loading, CAD/CAM

Background

Computer assisted implantology (CAI) was introduced more than 25 years ago and aimed to facilitate implant planning and to avoid intraoperative complications such as mandibular nerve damage, sinus perforations, fenestrations, or dehiscence [1–4]. Based on a computerized tomography (CT) scan and a digitized tooth setup, the prosthetically ideal implant positions can be planned virtually with the help of a guided surgery software allowing for three dimensional visualization prior to implant surgery [2, 5, 6].

Furthermore, the possibility to transfer the virtually planned implant position to the real clinical situation is provided by a stereolithographically fabricated surgical template [3, 7]. While only few guided implant placement systems were available at the time, today, multiple CAI software are available on the market. Several in-vitro, cadaver and clinical studies have reported on the accuracy of guided implant placement [8–10]. Although the current state of software and hardware technology has improved, inaccuracies in implant placement may occur and depend on different factors such as the template support (bone, mucosa, teeth, implants), intrinsic factors of the surgical guide (tolerance in diameter between the drill and the guide sleeve, fabrication

* Correspondence: info@ergozahn.de

¹Implantology, Oral Surgery; Private dental office, Johannesstrasse 7-9, 474623 Kevelaer, Germany

Full list of author information is available at the end of the article



© The Author(s). 2019 **Open Access** This article is distributed under the terms of the Creative Commons Attribution 4.0 International License (<http://creativecommons.org/licenses/by/4.0/>), which permits unrestricted use, distribution, and reproduction in any medium, provided you give appropriate credit to the original author(s) and the source, provide a link to the Creative Commons license, and indicate if changes were made. The Creative Commons Public Domain Dedication waiver (<http://creativecommons.org/publicdomain/zero/1.0/>) applies to the data made available in this article, unless otherwise stated.



Fig. 1 Panoramic radiograph of the initial dental status

accuracy of the guide) [11, 12] and human related factors during the workflow of virtual planning and guided surgery [7, 13]. The guided surgery approach is still controversially discussed [14–16] even though the procedure may be performed in a safe and predictable way [17, 18]. However, a systematic and concise approach performing the single steps in the treatment sequence may allow for more accurate implant positioning as type of guide and fixation have an important influence [19, 20]. Additionally, the use of multiple templates with different supports, i.e. teeth and implant support combined in a sequenced order is believed to improve accuracy compared to a mucosa supported approach alone [21].

While some patients wish to be informed in detail about the specific treatment steps, most of them want to know whether they would have to leave the dental office without teeth at some point of the treatment. In this context, immediate implant placement after tooth extraction and immediate implant loading with a fixed provisional reconstruction may help the patient as time after extractions and osseointegration is consolidated. In guided surgery protocols, minimally invasive placement and immediate loading has been a possible treatment step from the beginning [3, 4]. Postoperative morbidity after flapless surgery is significantly reduced compared to

the traditional open approach, especially in edentulous patients [17, 22, 23]. Later during the treatment, reconstructions fabricated with the help of computer assisted design / computer assisted manufacturing (CAD/CAM) provide high quality and aesthetic materials. Although CAI and CAD/CAM procedures have facilitated towards a straight forward workflow in the rehabilitation of edentulous patients, immediate implant placement and immediate loading protocols combined are complex and required a high level of organization between the implantologist, the technician and the patient.

The aim of the present case report was to illustrate the feasibility of combined immediate implant placement and loading approach using CAI in the rehabilitation of a patient with a partially dentate mandible asking for a comprehensive treatment and, specifically, not accepting being edentulous all the while.

Case report

Initial status und treatment concept

The partially dentate 74-year old patient presented with masticatory problems due a removable partial denture (RPD) with insufficient stability in combination with chronic pain condition in the lower front teeth area. She asked for a comprehensive treatment and did not accept to be edentulous at any stage of the treatment. The patient was a non-smoker and -with the help of antihypertensive (Candecor comp. 32 mg/12,5 mg,) and anticoagulant medication (quick 30; Marcourmar)- in good general health.

The dental status showed an acceptable oral hygiene, some teeth with increased mobility grade III (41/31/32 and 18, 28) and local periodontal problems including horizontal bone loss (42/41/31/32/33, 18/17, 27/28). The teeth 42 and 33 were healthy and not mobile. The alveolar crest in the lateral



Fig. 2 Initial dental status; **a** right side; **b** left side

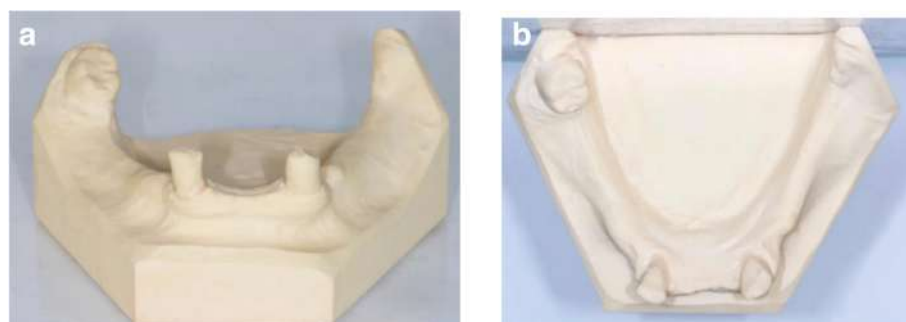


Fig. 3 Occlusal and frontal view of the study models after extraction of the 3 incisors 41,31 and 32; **a** front view, **b** occlusal view

mandible area showed clinically a wide shape with thick keratinized mucosa. The initial panoramic radiograph revealed stable crestal bone in the lateral mandible area (Figs. 1, 2 and 3). Thus, focusing on the lower jaw, the single tooth prognosis was fair for the teeth 47, 42 and 33 and hopeless for the teeth 41/31/32 [24].

During decision making for the final treatment plan different options were discussed with the patient. Various treatment options including a removable dental prosthesis were discussed with the patient. To keep the patient's wish for a fixed reconstruction and to never become edentulous in any treatment phase and considering the prognosis of the remaining mandibular teeth, the decision was made to prepare a provisional fixed prosthesis with an immediate loading approach extracting the teeth 42 and 33 for prosthodontic reasons but maintaining tooth 47.

Digital implant planning (Table 1)

After extraction of the painful and extremely mobile lower front teeth 41/31/32 and adaptation of the existing RPD, a cone beam computed tomography (CBCT) (Pax-Uni 3D, Orangedental GmbH & Co. KG, Biberach, Germany) with a 5 × 8 cm field of view

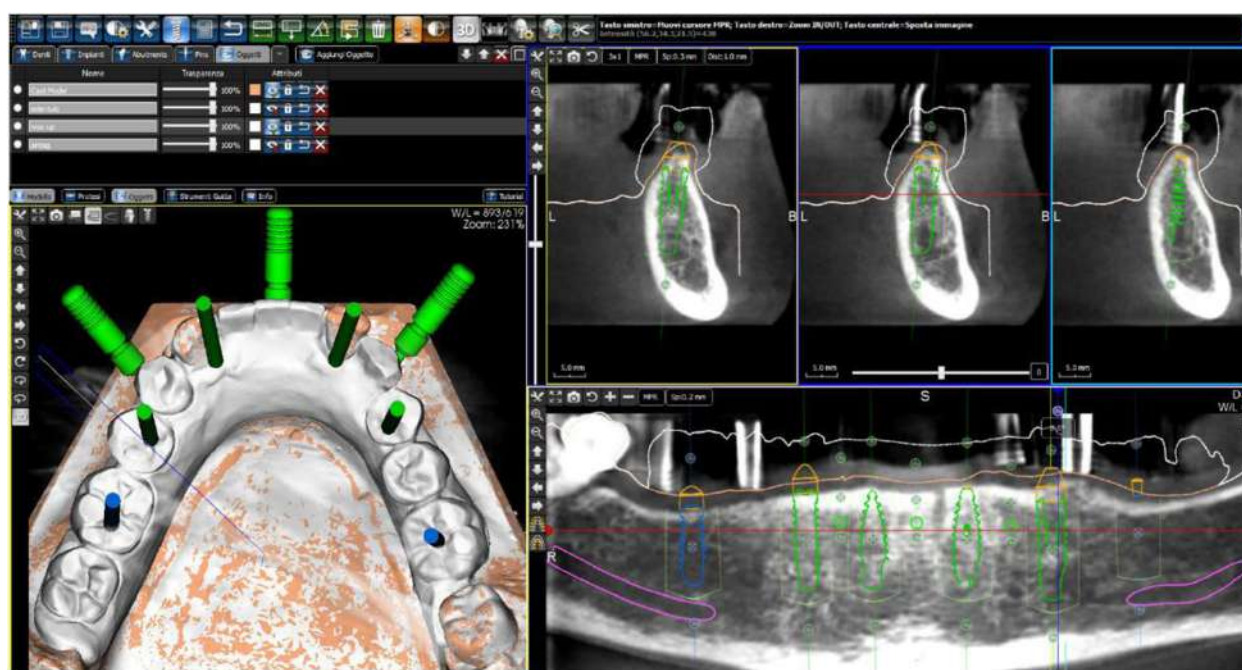
and 85KV/5.5 mA/0.2 mm Voxel was performed to proceed with the detailed implant planning (Fig. 4). Based on the anatomical conditions and prosthetic planning (i.e. tooth setup for the provisional RPD), six implants were virtually planned (3Diagnosys, 3DIEMME, Cantu, Italy) in the FDI (Fédération Dentaire Internationale) positions 46, 44, 42, 33, 35, and 36. As the implant positions 42 and 33 interfered with the teeth 43 and 33, a two-step procedure with two surgical templates was planned for the guided implant placement (Fig. 5a, b). The templates were fabricated stereolithographically (DS3000, XFAB, DWS srl, Thiene, Italy) according to the virtual implant planning. Based on the same digital file (Fig. 6a, b) a provisional fixed dental prosthesis (FDP) was prepared preoperatively allowing for an intraoral adaptation between the abutments and the framework to achieve a passive fit (Fig. 7a-d).

Immediate implant placement

During the day of surgery, a single dose of antibiotic (2 g of amoxicillin and clavulanic acid) was administered prophylactically 1 h prior to surgery. This treatment continued for five days (1 g amoxicillin and clavulanic acid twice a day). Prior to the start of

Table 1 Material and software used for the planning and realization of the treatment

CBCT	Pax-Uni 3D	Orangedental GmbH & Co. KG, Biberach a. d. Riß, Germany
Virtual implant planning	3Diagnosys®	3DIEMME, Cantu, Italy
Implants	Thommen ELEMENT RC 4.5 × 9.5 mm	Thommen Medical AG, Grenchen, Switzerland
CAD	Exocad	Exocad GmbH, Darmstadt, Deutschland
CAM	M1 Wet	Zirkonzahn, Gais, Italy
Provisional FDP	Prefabricated titanium abutments CAD/CAM CoCr framework Composite veneering & teeth	Thommen Medical AG, Grenchen, Switzerland Sintermetall, Zirkonzahn Srl, Gais, Italy SR Nexco Paste, Ivoclar Vivadent AG, Schaan, Liechtenstein
Final FDP	CAD/CAM CoCr framework Composite veneering & teeth	Sintermetall, Zirkonzahn Srl, Gais, Italy SR Nexco Paste, Ivoclar Vivadent AG, Schaan, Liechtenstein



Planning

Fig. 4 Screen shot of the virtual implant planning (FDA) positions 36,35,33,42,and,46 occlusal, sectional and panoramic views

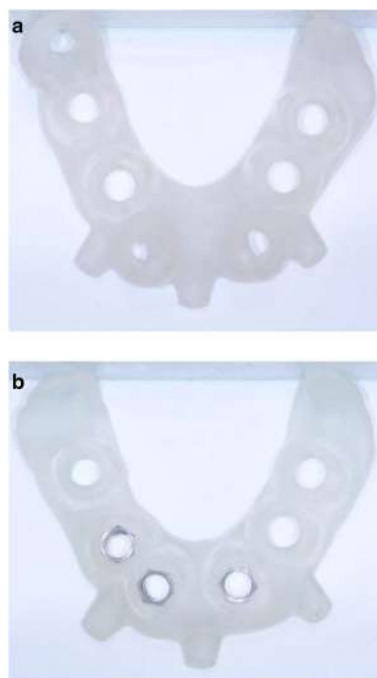


Fig. 5 CAD/CAM fabricated surgical guides no. 1 (a, tooth and mucosa supported) and no. 2 (b, implant and mucosa supported)

surgery, the patient rinsed with 0.2% chlorhexidine for 1 min. Local anesthesia was induced by using a 4% articaine solution with epinephrine 1:100.000.

The two-step approach comprised the flapless guided insertion of the four posterior implants (Thommen Element RC 4.5 × 9.5 mm, Thommen Medical AG, Grenchen, Switzerland), with the first surgical template that was tooth supported (Fig. 8a). The template was then removed and the teeth 42 and 33 previously supporting the guide were extracted. Thereafter, the second surgical template was positioned and stabilized on the four posterior implants with the help of specific abutments and the same anchor pins (Fig. 8b), thus allowing to place the anterior implant 42 and 33 (Thommen Element RC 4.5 × 9.5 mm) guided and immediately after extractions. All the implants were inserted with a torque of 35Ncm and proved good primary stability.

Immediate loading

After removal of the second surgical template, the standard titanium abutments were mounted on the implants with a torque of 15Ncm (Fig. 9a). The gaps between the abutments and the FDP were filled with Dual-Composite material and the screw retained immediate provisional FDP delivered. The occlusion

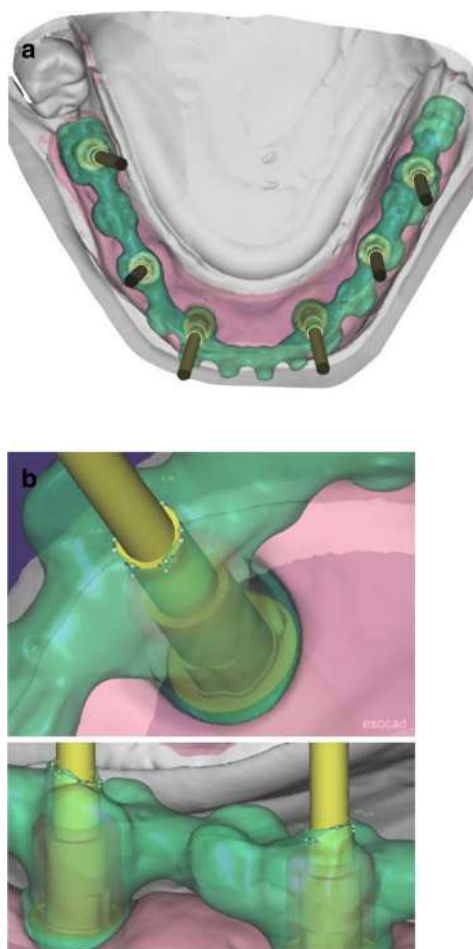


Fig. 6 Occlusal view showing CAD of the provisional FDP framework (a) and close-up view from the interface between the CAD framework and the prefabricated titanium abutments (b)

required only minor adaptations due to the accurate digital preoperative planning (Fig. 9b). The postoperative panoramic radiograph (OPT) showed the parallel axes of the six implants (Fig. 10).

Final fixed prosthesis

All the six implants osseointegrated successfully without complications. After 6 months with the provisional FDP a conventional impression was taken (screw retained impression copings, open tray technique, polyether material) to fabricate the final FDP on a new precise cast (Fig. 11), which was then digitized with a laboratory scanner (Deluxe Scanner, Open Technologies, Rezzato, Italy). The final framework was designed with straight connection to the implant platforms and with a cut-back allowing for the veneering material (Fig. 12a, b). While the cobalt-chromium framework was fabricated using

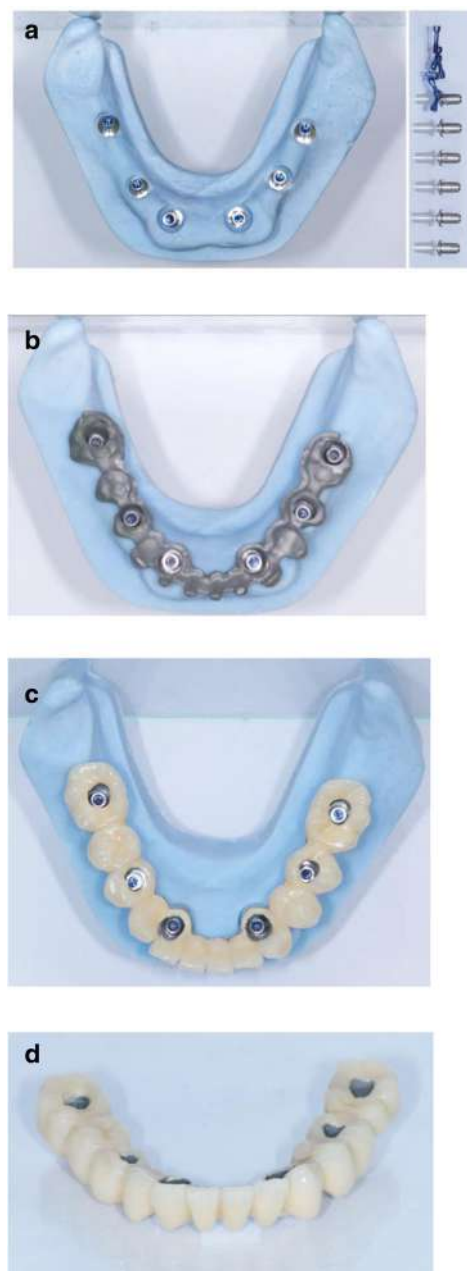


Fig. 7 CAD/CAM model with the prefabricated titanium abutments (a), the CAD/CAM cobalt-chromium framework (b), and the composite veneered provisional FDP (c, d) before bonding to the abutments

CAD/CAM technology (Exocad, Exocad gmbH, Deutschland / M1 Wet, Zirkonzahn, Italy) the veneering was performed manually allowing for an individual characterization of the teeth (Fig. 13a-d). The models were fabricated with a laser stereolithography printer (XFAB, DWS srl, Thiene, Italy) using an ABS-like polymer (RD096B, DWS srl, Thiene,

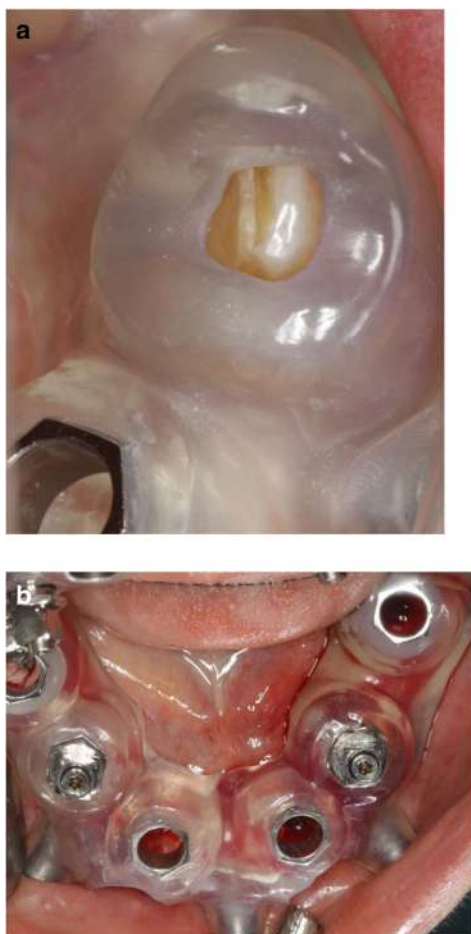


Fig. 8 Close-up view of the CAD/CAM guide no. 1 in-situ (tooth and mucosa supported) showing the perfect fit on tooth 33 (a), and occlusal view (b) of the CAD/CAM guide no. 2 (implant and mucosa supported) after extraction of the teeth 42/33 and placement of the implants 44/35

Italy). Healthy mucosal conditions were present at the delivery of the final CAD/CAM reconstruction made from cobalt-chromium and composite veneering material (Fig. 14a-f). The accurately fitting FDP was screw retained with 25Ncm and the screw access area covered with composite material. The OPT at the day of delivery showed optimal prosthetic and osseous conditions (Fig. 15). The patient followed a regular maintenance program at the dental hygienist twice a year.

At the one year follow-up appointment, healthy mucosal and stable crestal peri-implant conditions could be observed (Fig. 16). The patient was very pleased with the esthetic and functional outcome. Thus, the performed treatment was successful and showed stable results without complications or need for maintenance service after the first year.

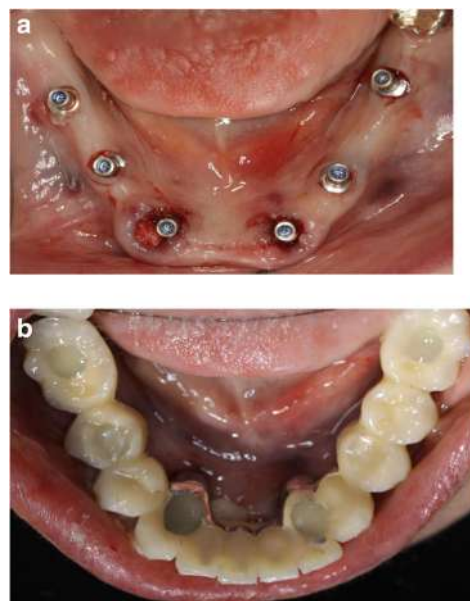


Fig. 9 a; Occlusal views of the abutments and b; the immediate provisional reconstruction that were passively bond in-situ

Discussion

The use of CAI software in the preoperative virtual three-dimensional implant planning allowed for guided and immediate implant placement, and proved to be especially beneficial in the presented mandibular full-arch case. While there are some studies that investigated outcomes of immediately loaded implants placed in edentulous patients using computer-assisted template-guided surgery to support a FDP [25], only few case reports are available in literature describing the entire workflow, the patients state in detail, and the usage of guided surgery templates with subsequent immediate loading [3, 4]. The considerably more complex combination of immediate implant placement and immediate loading required a high level of organization between implantologist and technician, minimizing patient's compliance. Pozzi et al. reported excellent results with CAD/CAM cross-arch Zirconia bridges on

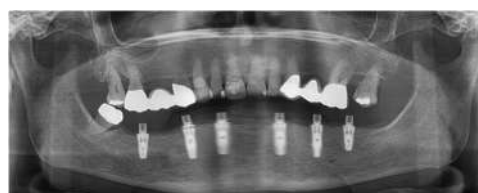


Fig. 10 Postoperative panoramic radiograph



Fig. 11 Frontal view showing the screw retained post at impression taking 24 weeks after implant placement

immediately loaded implants placed with computer-assisted/template-guided surgery [26]. Several investigators presented analyses of recent studies in this context elaborating the factors that influence mainly the accurate implant placement but also the comparable outcome of the reconstructions after guided implant placement [15, 20, 21, 27–31]. In the present case report, two CAD/CAM surgical templates were combined in this partially dentate patient with extraction of the teeth 42/33 and immediate implants performed in a sequenced order. The first scanner-based template was teeth and mucosa supported enabling a higher template stability and, thus,

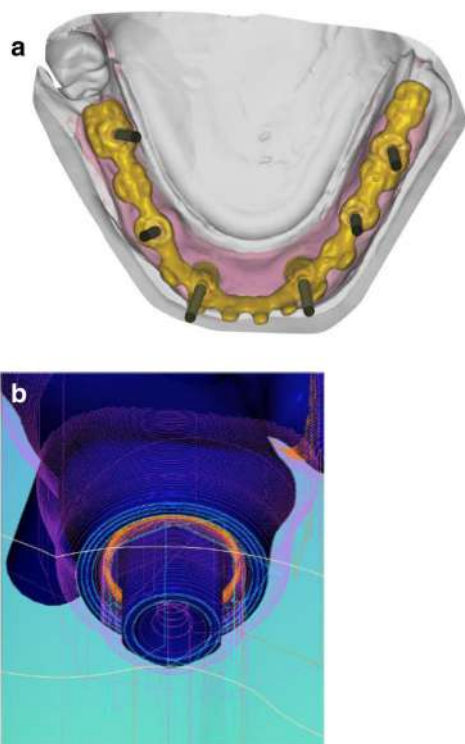


Fig. 12 Occlusal view showing CAD of the final FDP (a) and detailed screen-shot of the interface geometry (b)

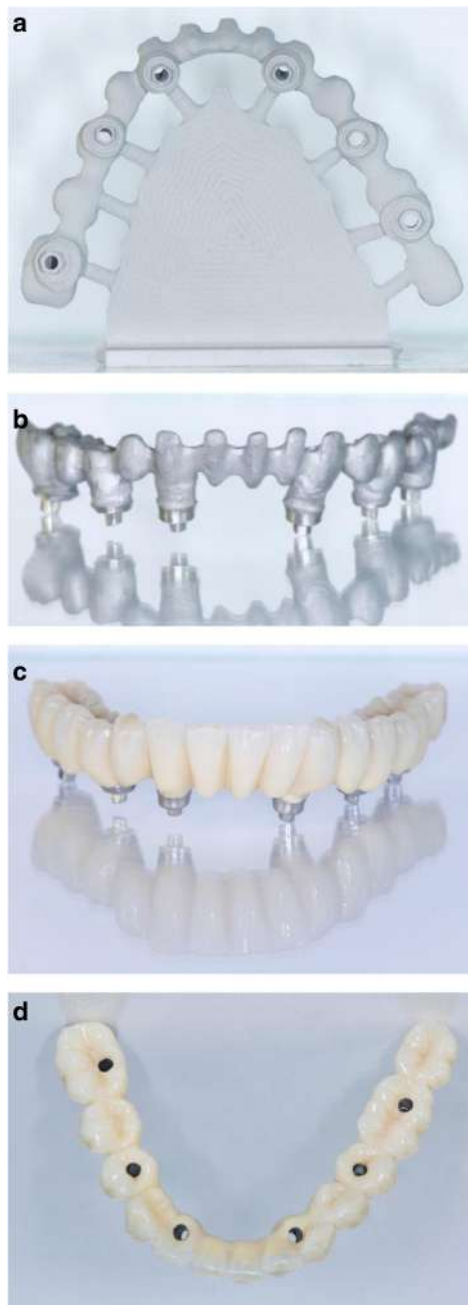


Fig. 13 CAD/CAM fabricated one-piece cobalt-chromium framework before (a, b) and after veneering with composite (Nexco Ivoclar) i.e. final FDP (c, d)

more accurate guided osteotomies and implant placement. Four posterior implants were placed with this approach allowing to support the second surgical template after extraction of the anterior teeth 42/33. The stability on these four points was high as the implants 42/33 showed a torque value of 35 to 40 Ncm each. The subsequent two anterior immediate implants were thus placed perfectly guided.



Fig. 14 Occlusal, frontal and lateral views at the day of delivery showing healthy peri-implant mucosal conditions (a) and the final CAD/CAM reconstruction in situ (b-e)

Different factors contributed to this insertion torque such as the depth of the planned implant position in a more apical area than the extraction site, the minimally invasive tooth extraction, the macroscopic implant geometry and the osteotomy protocol with a smaller drilling diameter compared to the implant diameter (as proposed by the company), the accurate performance of the single steps in the pre- and intraoperative phases, and the bone density in the anterior mandibular area. The prefabricated provisional FDP was prepared to connect the abutments to the FDP intraorally, which was easily to be performed given the accurate result of the implant positions. With this approach the passive fit of the FDP was maximized, the clinical chairside efforts (in terms of abutment connection and occlusal adaptations) were minimal and the predictability was very high compared to different limitations and problems reported in a recent review [32].

The preoperative communication between the dentist and the technician during the decision making and planning phase were essential for the concise timing in the clinic, ensuring highest surgical and prosthodontic



Fig. 15 Panoramic radiograph at delivery of the final CAD/CAM FDP



Fig. 16 Panoramic radiograph at the 12-months recall appointment

performance accuracy in this particular case. Therefore, up-to-date software and hardware with the knowledge to apply information to the specific products was required. This case report supports the need for minimally traumatic or flapless surgery, optimal implant positioning and immediate loading, as summarized in a recent review on randomized controlled trials [33].

Conclusions

The present case report emphasized the efficient workflow and the predictable outcome using computer assisted implantology. The fabrication of an immediate provisional FDP and, subsequently, the final CAD/CAM reconstruction was facilitated by CAI fulfilling patient's wish of being continuously restored during the complete treatment.

Abbreviations

CAD/CAM: Computer assisted design / computer assisted manufacturing; CAI: Computer assisted implantology; CBCT: Cone beam computed tomography; CT: Computerized tomography; FDI: Fédération Dentaire Internationale; FDP: Fixed dental prosthesis; RPD: Removable partial denture

Acknowledgements

The authors declare no conflict of interest related to this case report. Thommen Medical AG is acknowledged for its logistical and administrative help during the treatment.

Funding

No funding body was involved in the design of the study and collection, analysis, and interpretation of data and in writing the manuscript.

Availability of data and materials

Not applicable

Authors' contributions

TS has made substantial contributions to conception, acquisition of data, and interpretation of data. He has been involved in drafting the manuscript. He has given final approval of the version to be published and agreed to be accountable for all aspects of the work in ensuring that questions related to the accuracy or integrity of any part of the work are appropriately investigated and resolved. UH has made substantial contributions to conception, acquisition of data, and interpretation of data. He has been involved in revising the manuscript critically for important intellectual content. He has given final approval of the version to be published and agreed to be accountable for all aspects of the work in ensuring that questions related to the accuracy or integrity of any part of the work are appropriately investigated and resolved. JK has made substantial contributions to analysis and interpretation of data. He has been involved in drafting the manuscript or revising it critically for important intellectual content. He has been involved in revising the manuscript critically for important intellectual content. He has given final approval of the version to be published and agreed to be accountable for all aspects of the work in ensuring that questions related to the accuracy or integrity of any part of the work are appropriately investigated and resolved.

Ethics approval and consent to participate

Not applicable

Consent for publication

The patient in this case report has given written informed consent for publication.

Competing interests

The authors declare that they have no competing interests.

Publisher's Note

Springer Nature remains neutral with regard to jurisdictional claims in published maps and institutional affiliations.

Author details

¹Implantology, Oral Surgery; Private dental office, Johannesstrasse 7-9, 474623 Kevelaer, Germany. ²Department of Postgraduate Education, Faculty of Oral and Dental Medicine at J.W. Goethe-University Frankfurt am Main, Frankfurt am Main, Germany. ³Department of Reconstructive Dentistry and Gerodontology, School of Dental Medicine, University of Bern, Bern, Switzerland.

Received: 7 January 2019 Accepted: 26 March 2019

Published online: 11 April 2019

References

1. Verstreken K, Van Cleynenbreugel J, Martens K, Marchal G, van Steenberghe D, Suetens P. An image-guided planning system for endosseous oral implants. *IEEE Trans Med Imaging*. 1998;17(5):842–52.
2. Verstreken K, Van Cleynenbreugel J, Marchal G, Naert I, Suetens P, van Steenberghe D. Computer-assisted planning of oral implant surgery: a three-dimensional approach. *Int J Oral Maxillofac Implants*. 1996;11(6): 806–10.
3. van Steenberghe D, Naert I, Andersson M, Brajnovic I, Van Cleynenbreugel J, Suetens P. A custom template and definitive prosthesis allowing immediate implant loading in the maxilla: a clinical report. *Int J Oral Maxillofac Implants*. 2002;17(5):663–70.
4. Tardieu PB, Vrielinck L, Escolano E. Computer-assisted implant placement. A case report: treatment of the mandible. *Int J Oral Maxillofac Implants*. 2003; 18(4):599–604.
5. Avrampou M, Mericske-Stern R, Blatz MB, Katsoulis J. Virtual implant planning in the edentulous maxilla: criteria for decision making of prosthesis design. *Clin Oral Implants Res*. 2012;24(Suppl A100):152–9. <https://doi.org/10.1111/j.1600-0501.2011.02407.x>. Epub 2012 Feb 13.
6. Katsoulis J, Pazera P, Mericske-Stern R. Prosthetically driven, computer-guided implant planning for the edentulous maxilla: a model study. *Clin Implant Dent Relat Res*. 2009;11(3):238–45.
7. Vercruyssen M, Fortin T, Widmann G, Jacobs R, Quirynen M. Different techniques of static/dynamic guided implant surgery: modalities and indications. *Periodontology*. 2000. 2014;66(1):214–27.
8. Vasak C, Watzak G, Gahleitner A, Strbac G, Schemper M, Zechner W. Computed tomography-based evaluation of template (NobelGuide)-guided implant positions: a prospective radiological study. *Clin Oral Implants Res*. 2011;22(10):1157–63.
9. Van Assche N, van Steenberghe D, Guerrero ME, Hirsch E, Schutyser F, Quirynen M, et al. Accuracy of implant placement based on pre-surgical planning of three-dimensional cone-beam images: a pilot study. *J Clin Periodontol*. 2007;34(9):816–21.
10. Cassetta M, Stefanelli LV, Giansanti M, Calasso S. Accuracy of implant placement with a stereolithographic surgical template. *Int J Oral Maxillofac Implants*. 2012;27(3):655–63.
11. Van Assche N, Quirynen M. Tolerance within a surgical guide. *Clin Oral Implants Res*. 2010;21(4):455–8.
12. Cassetta M, Di Mambro A, Giansanti M, Stefanelli LV, Cavallini C. The intrinsic error of a stereolithographic surgical template in implant guided surgery. *Int J Oral Maxillofac Surg*. 2013;42(2):264–75.
13. Cassetta M, Di Mambro A, Giansanti M, Stefanelli LV, Barbato E. How does an error in positioning the template affect the accuracy of implants inserted using a single fixed mucosa-supported stereolithographic surgical guide? *Int J Oral Maxillofac Surg*. 2014;43(1):85–92.
14. Schneider D, Marquardt P, Zwahlen M, Jung RE. A systematic review on the accuracy and the clinical outcome of computer-guided template-based implant dentistry. *Clin Oral Implants Res*. 2009;20(Suppl 4):73–86.
15. D'Haese J, Ackhurst J, Wismeijer D, De Bruyn H, Tahmaseb A. Current state of the art of computer-guided implant surgery. *Periodontology*. 2000. 2017; 73(1):121–33.
16. Di Giacomo GA, da Silva JV, da Silva AM, Paschoal GH, Cury PR, Szarf G. Accuracy and complications of computer-designed selective laser sintering surgical guides for flapless dental implant placement and immediate definitive prosthesis installation. *J Periodontol*. 2012;83(4):410–9.
17. Tallarico M, Esposito M, Khanari E, Caneva M, Meloni SM. Computer-guided vs freehand placement of immediately loaded dental implants: 5-year postloading results of a randomised controlled trial. *Eur J Oral Implantol*. 2018;11(2):203–13.
18. Tallarico M, Meloni SM. Retrospective analysis on survival rate, template-related complications, and prevalence of Peri-implantitis of 694 anodized implants placed using computer-guided surgery: results between 1 and 10 years of follow-up. *Int J Oral Maxillofac Implants*. 2017;32(5):1162–71.
19. Tallarico M, Kim YJ, Cocchi F, Martinolli M, Meloni SM. Accuracy of newly developed sleeve-designed templates for insertion of dental implants: a prospective multicenters clinical trial. *Clin Implant Dent Relat Res*. 2019; 21(1):108–13.
20. Zhou W, Liu Z, Song L, Kuo CL, Shafer DM. Clinical factors affecting the accuracy of guided implant surgery—a systematic review and meta-analysis. *J Evid Based Dent Pract*. 2018;18(1):28–40.
21. Seo C, Juodzbalys G. Accuracy of guided surgery via stereolithographic mucosa-supported surgical guide in implant surgery for edentulous patient: a systematic review. *J Oral Maxillofac Res*. 2018;9(1):e1.
22. Nkenke E, Eitner S, Radespiel-Troger M, Vairaktaris E, Neukam FW, Fenner M. Patient-centred outcomes comparing transmucosal implant placement with an open approach in the maxilla: a prospective, non-randomized pilot study. *Clin Oral Implants Res*. 2007;18(2):197–203.
23. Fortin T, Bosson JL, Isidori M, Blanchet E. Effect of flapless surgery on pain experienced in implant placement using an image-guided system. *Int J Oral Maxillofac Implants*. 2006;21(2):298–304.
24. Samet N, Jotkowitz A. Classification and prognosis evaluation of individual teeth—a comprehensive approach. *Quintessence Int*. 2009;40(5):377–87.
25. Meloni SM, Tallarico M, Pisano M, Khanari E, Canullo L. Immediate loading of fixed complete denture prosthesis supported by 4-8 implants placed using guided surgery: a 5-year prospective study on 66 patients with 356 implants. *Clin Implant Dent Relat Res*. 2017;19(1):195–206.
26. Pozzi A, Holst S, Fabbri G, Tallarico M. Clinical reliability of CAD/CAM cross-arch zirconia bridges on immediately loaded implants placed with computer-assisted/template-guided surgery: a retrospective study with a follow-up between 3 and 5 years. *Clin Implant Dent Relat Res*. 2015; 17(Suppl 1):e86–96.
27. Sigcho Lopez DA, Garcia I, Da Silva SG, Cruz LD. Potential deviation factors affecting stereolithographic surgical guides: a systematic review. *Implant Dent*. 2019;28(1):68–73.
28. Bover-Ramos F, Vina-Almunia J, Cervera-Ballester J, Penarrocha-Diago M, Garcia-Mira B. Accuracy of implant placement with computer-guided surgery: a systematic review and meta-analysis comparing cadaver, clinical, and in vitro studies. *Int J Oral Maxillofac Implants*. 2018;33(1):101–15.
29. Marliere DAA, Demetrio MS, Picinini LS, De Oliveira RG, Chaves Netto HDM. Accuracy of computer-guided surgery for dental implant placement in fully edentulous patients: a systematic review. *Eur J Dent*. 2018;12(1):153–60.
30. Pozzi A, Polizzi G, Moy PK. Guided surgery with tooth-supported templates for single missing teeth: a critical review. *Eur J Oral Implantol*. 2016;9(Suppl 1):S135–53.
31. Raico Gallardo YN, da Silva-Olivio IRT, Mukai E, Morimoto S, Sesma N, Cordaro L. Accuracy comparison of guided surgery for dental implants according to the tissue of support: a systematic review and meta-analysis. *Clin Oral Implants Res*. 2017;28(5):602–12.
32. Tahmaseb A, Wismeijer D, Coucke W, Derksen W. Computer technology applications in surgical implant dentistry: a systematic review. *Int J Oral Maxillofac Implants*. 2014;29(Suppl):25–42.
33. Colombo M, Mangano C, Mijiritsky E, Krebs M, Hauschild U, Fortin T. Clinical applications and effectiveness of guided implant surgery: a critical review based on randomized controlled trials. *BMC Oral Health*. 2017;17(1):150.

RESEARCH ARTICLE

Open Access



Deviations in palatal region between indirect and direct digital models: an in vivo study

Zhongpeng Yang^{1,2}, Tianmin Xu^{1,2} and Ruoping Jiang^{1,2*} 

Abstract

Background: Studies focusing on accuracy of intraoral digital models in the palatal region are scarce. The present study aimed to investigate the influence of different scanning sequences on palatal trueness and to assess deviation and distribution character of trueness in palate.

Methods: Overall, 35 participants accepted three types of procedures to acquire upper digital models. Indirect models digitalised from plaster models were considered as the reference. Two direct digital models were acquired using TRIOS 3 POD intraoral scanners, namely Groups Tr1 and Tr2, wherein intraoral scanning differed in terms of palatal scanning sequences. Based on a modified dental-level superimposition method, 3D measurements of trueness in palate and palatal vault region (PVR) for palatal stable regional superimposition in Groups Tr1 and Tr2, respectively, were performed. Absolute deviations were measured for trueness, while signed deviations were analysed for shape distortion. Colour-coded maps were used for quantitative analysis of deviation distribution pattern. Paired t test was used to analyse differences in palatal trueness between different scanning sequences. One-way repeated-measures analysis of variance and Bonferroni test were used to compare trueness measurements among different superimposition methods. Intraclass correlation coefficient (ICC) was used to verify reproducibility of the proposed method.

Results: Palatal trueness in Group Tr1 ($118.59 \pm 37.67 \mu\text{m}$) was slightly less accurate than that ($108.25 \pm 33.83 \mu\text{m}$) in Group Tr2 ($p = 0.012 < 0.05$). Trueness of PVR in Groups Tr1 ($127.35 \pm 54.11 \mu\text{m}$) and Tr2 ($118.17 \pm 49.52 \mu\text{m}$) did not differ significantly ($p = 0.149$). Moreover, no significant difference was noted in distortion of the palatal region and PVR in Groups Tr1 and Tr2 ($p = 0.582$ and 0.615 , respectively). A similar pattern of palatal trueness was noted in a majority of participants (22/35). For 3D palatal trueness measurement, there were different applications for different superimposition methods. ICC for the proposed method was > 0.90 .

Conclusions: Scanning sequences can affect palatal trueness. Palatal scanning should be initiated at the palatal side of the posterior teeth where the initial scan begins. For 3D PVR superimposition, distal boundary of the selected region should be adjusted mesially whilst referring to intraoral digital models.

Trial registration: The trial has been registered (registration No: [R000039467](https://www.clinicaltrials.gov/ct2/show/study?term=R000039467), Trial ID: UMIN000034617, date of registration: 2018/10/24'retrospectively registered').

Keywords: Intraoral scan, Digital model, Palatal soft tissue, Model superimposition, Trueness

* Correspondence: jiangruoping@126.com

¹National Engineering Laboratory for Digital and Material Technology of Stomatology, Peking University School and Hospital of Stomatology, No.22 Zhongguancun South Avenue, Haidian District, Beijing 100081, China

²Department of Orthodontics, Peking University School and Hospital of Stomatology, No.22 Zhongguancun South Avenue, Haidian District, Beijing 100081, China



© The Author(s). 2019 **Open Access** This article is distributed under the terms of the Creative Commons Attribution 4.0 International License (<http://creativecommons.org/licenses/by/4.0/>), which permits unrestricted use, distribution, and reproduction in any medium, provided you give appropriate credit to the original author(s) and the source, provide a link to the Creative Commons license, and indicate if changes were made. The Creative Commons Public Domain Dedication waiver (<http://creativecommons.org/publicdomain/zero/1.0/>) applies to the data made available in this article, unless otherwise stated.

Background

Dental treatment of any type usually necessitates evaluation of the intraoral situation. With introduction of intraoral scanners in dentistry, direct acquisition of digital impressions is gaining popularity [1] as it provides advantages of reducing the number of procedures required as well as storage space. Several studies have investigated the accuracy of intraoral scans, which encompasses two parameters, namely ‘trueness’ and ‘precision’ [2–5]. Numerous factors can affect accuracy of intraoral scans; typically, these can be categorised into three types—scanning principles [6], scanning environment [7, 8] and process of data synthesis [6, 7, 9–14]. When performing a direct scan of the oral environment, trueness can be $> 200\ \mu\text{m}$ [7], while precision can be $> 1000\ \mu\text{m}$ [8]. Moreover, attention must be paid to scanning strategies used since these strategies have a marked influence on accuracy and distribution of deviations in full-arch intraoral scans [11–13]. Larger deviations are observed in regions wherein continuous full-arch scanning is terminated [12]. Since it is not possible to change scanning principles or avoid oral environment factors, application of an appropriate scanning strategy may help improve the accuracy of intraoral scanning.

Most studies on accuracy have focused on dental hard tissues, ranging from single tooth crown to full arches [2–12, 15]. Irrespective of statistical differences between intraoral digital and conventional impressions, direct digital dental model is clinically acceptable [1–4]. However, much less attention is paid to soft tissue accuracy of intraoral digital models. Numerous appliances used in prosthodontics and orthodontics need to cover certain parts of the palatal region, such as removable partial dentures, obturators, retainers and Hyrax appliances [16–19]. In addition, characteristics of the palatal region can be utilised to study human identification, articulo-metry and the impact of oral habits [20–22]. Furthermore, because of multiple features of palatal rugae and the sufficient area of the entire palatal region, dental changes of orthodontic treatment are usually evaluated using 3D superimposition in a specific palatal region [23–25]. By using stationary mini-screws as a reference, Chen et al. (2011) [25] found a reliable palatal region with $500\text{-}\mu\text{m}$ deviations for assessing dental changes in adults. This method is called ‘3D palatal vault regional (PVR) superimposition,’ which is now widely used in clinical practice. Therefore, owing to non-substitutability of the palatal region in various clinical fields, it is essential to identify deviation and its distribution of accuracy in intraoral palatal scanning.

Nevertheless, the soft tissue accuracy of intraoral scanning has not been validated yet owing to scarcity of relevant studies. According to an *in vivo* study by Gan et al. (2016) [10], trueness of digital impression acquired by

TRIOS POD scanners in the palatal region ($130.54 \pm 33.95\ \mu\text{m}$) was less accurate than that in the dentition ($80.01 \pm 17.78\ \mu\text{m}$). A similar trueness of intraoral palatal scans was identified by Deferm et al. (2018) [26]. Moreover, to our knowledge, there is no research focusing on the stable palatal region for superimposition of intraoral scanning.

To our knowledge, to date, none of studies on scanning strategies have focused on palatal soft tissues. Even the User Guide (3 Shape, Denmark) does not provide any specific description of palatal scanning strategy. Therefore, the effect of scanning sequences on the palatal region should be clarified so that it would be clear to estimate the region displaying a higher deviation in terms of scanning sequences.

To date, the two most relevant studies on 3D measurement of accuracy of intraoral scanning in the palatal region have used surface-based registration between intraoral digital models and digitalised plaster models by using a best-fit algorithm [10, 26]. Deferm et al. (2018) [26] measured palatal accuracy by using model superimposition at a full-arch level. While the global superimposition method was used in the other study [10], the details about the selected area for superimposition were unclear. Since the accuracy of intraoral digital impression on dentition has been verified as substantially high [1–4], dentition can be used for surface-based registration to measure accuracy in the palatal region. However, intraoral scans appear to have greater divergences in certain specific dental regions, particularly in the distal end of the arch, the anterior region and interproximal surfaces [2–4, 8, 12, 14]. Moreover, gypsum casts from polyvinyl siloxane (PVS) impressions showed increasing deviations of both trueness and precision at the distal end of the arch [3]. Therefore, in order to avoid relatively less accurate dental regions and to involve more surface characters, a modified dental-level superimposition method was proposed in this study.

Aims of this *in vivo* study were (i) to compare accuracy of 3D measurement of intraoral palatal scans among different superimposition methods; (ii) to investigate the influence on trueness of intraoral palatal scans by using different scanning sequences; and (iii) to assess deviation and its distribution character of trueness in the palatal and PVR region.

Methods

Participants

Thirty-seven students from the School of Stomatology were recruited in this study. Eventually, 35 volunteers successfully finished entire data acquisition. Informed consent was obtained from all participants.

Inclusion criteria were as follows:

1. Age between 18 and 30 years;
2. Permanent dentition, including premolars symmetrically extracted for past orthodontic treatment with retention stage ended;
3. Good oral hygiene; and
4. Good cooperation to finish all data acquisition.

Exclusion criteria were as follows:

1. Undergoing orthodontic treatment or finished orthodontic treatment for no more than 2 years;
2. With more than one-third of tooth defect on a single tooth;
3. With large amounts of metal restorations;
4. With severe crowding or obvious spaces;
5. With palatal defect or lesion;
6. With an abnormally large arch width between bilateral upper first molars; and
7. Moderate to severe periodontitis or obvious gingivitis.

Digital model acquisition

To acquire digital models of the upper jaws, each participant underwent three different processes as follows. Figure 1 presents a flow diagram of the same.

1. Group S: Indirect digital models were utilised as reference. Impressions were recorded using PVS material (DMG Silagum, Germany) by experienced operators in a one-step process, and cast models were fabricated using type IV gypsum (Heraeus, Germany). These plaster models were digitalised using a model scanner (3 Shape R700, Denmark), the accuracy of which is 20 µm [27].
2. Group Tr1: Direct intraoral scans of the upper jaws were performed using an intraoral scanner (3 Shape TRIOS 3 POD, Denmark). The upper dentition was scanned according to the recommended protocol [13], following the sequence of ¹occlusal–²palatal–³buccal surfaces in a slow zigzag manner. The upper left second molar was set as the starting point for the initial scan. Whilst scanning palatal soft tissues, scanning was initiated from the palatal side of upper central incisors in a zigzag manner, in accordance with guidelines from a previous study [10].
3. Group Tr2: Direct intraoral scans of upper jaws were performed using the same intraoral scanner. The upper dentition was scanned using the same method as in Group Tr1. Palatal scanning was performed from palatal side of the upper second molar to palatal side of the opposite arch, finishing

the entire palatal scanning at the distal end of the second molars by continuously narrowing down the scope in an inverted U manner. The palatal scanning sequence was similar to that described by Pavoni C et al. [28].

All intraoral scans were performed by one trained researcher. Re-scans were performed if any defects were identified with image stitching.

3D superimposition measurement

The models were imported in STL format into a 3D scan data metrology and modelling software (Rapid-Form 2006, INUS Technology, Inc., Korea) and were split into three parts for following measurements (Fig. 1).

- (1) Upper dentition (D): The upper dentition was selected by removing soft tissue along the gingival margin, except for existing third molars.
- (2) Palatal region (P): For selection of the palatal region, in view of characters of hard palatal anatomy, the distal boundary was set at the level of the mid-gingival margin of second molars. Models were trimmed by the orthogonal plane with horizontal and mid-sagittal planes at the distal boundary. The horizontal plane was created by the midpoints of gingival-margin of bilateral second molars and the point of gingival papilla of upper incisors. While, the mid-sagittal plane was perpendicular to the horizontal plane through the midline of palate. Subsequently, the palatal segment was selected along the gingival margin.
- (3) Palatal vault region (PVR): The palatal vault region was selected in accordance with borders suggested by Chen G et al. (2011) [25].

Subsequently, trueness of D, P, and PVR was separately measured. According to definition, trueness of intraoral scanning was determined by means of divergence between indirect and direct digital models in this study. Thus, trueness in the palatal region (P) in Group Tr1 was termed 'Tr1-S (P)', and so were the rest of the descriptions.

Various features of 3D measurement by different superimposition methods need to be discussed further.

3D measurement by superimposition methods on different levels

Because scanning sequence in Group Tr1 was consistent with that reported in a previous study [10], trueness in Group Tr1 was analysed. Four types of registration levels were considered.

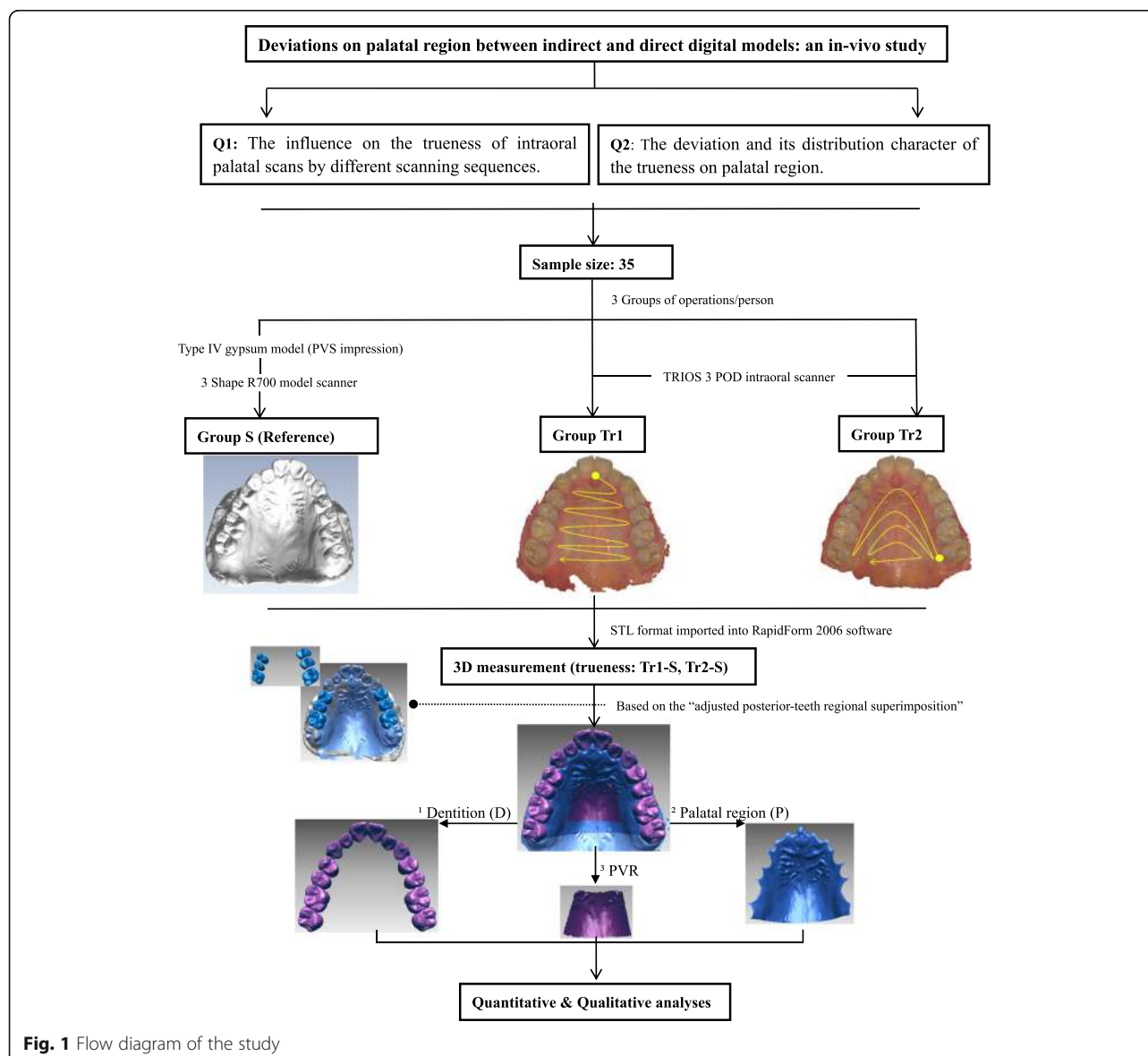


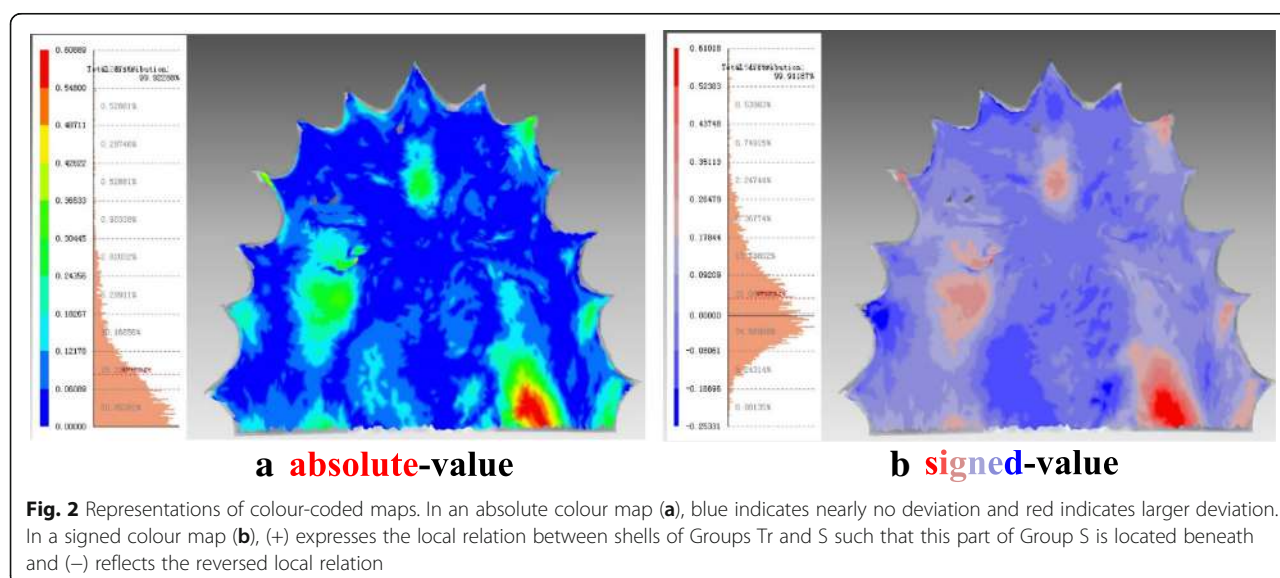
Fig. 1 Flow diagram of the study

- (1) Adjusted dental-level: For 3D measurement of accuracy of intraoral digital impression in the palatal region, certain surfaces of non-free-end posterior teeth were selected for regional superimposition. This method was termed as 'upper posterior-teeth regional superimposition (UPRS)' (Fig. 1). Relatively accurate regions of dentition were selected for regional superimposition, namely buccal, occlusal and palatal surfaces of upper posterior teeth except the distal free-end teeth. Second molars were permitted if premolars were missing.

Reproducibility of this method was analysed by repeatedly selecting surfaces for secondary 3D measurement of trueness in the palatal region.

- (2) Dental-level: The entire upper dentition was considered as a relatively accurate region for model superimposition.
- (3) Palatal-level: Irrespective of the entire upper jaw, palatal regions were selected from the two models and directly superimposed.
- (4) Upper jaw-level: Irrespective of differences in features, the entire upper jaws were globally superimposed.

All 3D measurements were displayed in absolute-value and signed-value colour-coded maps (Fig. 2). Data from a calibrated scale was used for quantitative analyses, wherein mean absolute deviations were measured for trueness and mean signed deviations were analysed for distortion in shape.



Quantitative and qualitative analyses of trueness in the palatal region

Based on UPRS, trueness of intraoral digital models in the palatal region in Groups Tr1 and Tr2 was measured and statistically compared. In addition, trueness in PVR was measured and analysed independently. Moreover, colour maps were used for qualitative analyses, in an attempt to derive conclusions on deviation distribution/patterns of trueness of intraoral palatal scans.

Statistical analysis

For quantitative analyses, data were statistically analysed using IBM SPSS Statistics (version 19, IBM Corp., USA). According to the formula (Fig. 3) [29], the sample size met the demand of paired t-test under the circumstances of $\alpha = 0.05$ and power = 0.80, which required at least 32 participants. It was also sufficient for one-way analysis of variance (ANOVA), wherein the sample size per group was 14 subjects, as estimated using a statistical analysis software (PASS 11, NCSS, U.S.).

One-way repeated-measures ANOVA and Bonferroni post hoc test were used to analyse differences among the four superimposition methods in terms of trueness measurement for the palatal region. On the other hand, paired t test was used to analyse the influence of

scanning sequences on palatal trueness and compare the trueness between palatal and dental regions. p values < 0.05 were considered statistically significant. Moreover, the intraclass correlation coefficient (ICC) was calculated to verify reproducibility of the superimposition in each region. The reproducibility of 3D measurements in absolute and signed-colour maps was represented by that of Palatal-level superimposition method.

Results

Participant characteristics

The study population included 9 men and 26 women, with an age range of 24–27 years. Seventeen participants had undergone orthodontic treatment, of whom, 7 had their premolars extracted. The mean arch width between bilateral upper first molars was 36.68 mm.

Comparison of 3D measurement among different superimposition methods

3D measurements had satisfied reproducibility. ICCs for absolute-deviation and signed-deviation measurements were separately 1.000 (95% confidence interval [CI] 0.999, 1.000) and 0.901 (95% CI 0.805, 0.950).

Measured using four methods, trueness of intraoral digital models in Group Tr1 is summarised in Table 1. Based on ICCs, the reproducibility could be ordered as following: Palatal-level (1.000, 95% CI 0.999, 1.000) > Dental level (0.998, 95% CI 0.995, 0.999) > Upper Jaw-level (0.982, 95% CI 0.965, 0.991) > Adjusted-dental level (0.938, 95% CI 0.876, 0.969).

By using one-way repeated-measures ANOVA, differences in trueness measurement for the palatal region

$$N = \left[\frac{(t_{\alpha/2} + t_{\beta})S}{\delta} \right]^2$$

Fig. 3 Formula of two-tailed paired t-test sample size

Table 1 Trueness of intraoral digital impression in Group Tr1 measured using different superimposition methods

Methods	Absolute-value (μm)			Signed-value (μm)		
	Palatal region	Dentition	<i>p</i> value	Palatal region	Dentition	<i>p</i> value
Adjusted-dental level	118.59 \pm 37.67	69.22 \pm 21.62	.000*	14.56 \pm 93.32	35.26 \pm 18.27	0.209
Dental-level	115.27 \pm 36.03	64.92 \pm 19.50	.000*	1.40 \pm 90.38	24.09 \pm 14.61	0.164
Palatal-level	80.48 \pm 26.23	–	–	12.11 \pm 25.40	–	–
Upper Jaw-level	94.89 \pm 28.18	70.53 \pm 22.33	.000*	7.55 \pm 55.24	24.13 \pm 26.26	0.210

**p* values < 0.05 indicate statistical significance

measured using the aforementioned methods were analysed as follows:

- (1) For absolute deviations (Fig. 4-a), significant differences were identified among the four methods. By Bonferroni test, significant difference was noted among all methods ($p < 0.0005$), except for comparisons between adjusted dental-level and dental-level methods.
- (2) For signed deviations (Fig. 4-b), no significant difference was found among the four methods. Moreover, by Bonferroni test, no significant difference was noted among the methods, except for comparisons between adjusted dental-level and dental-level methods ($p = 0.004 < 0.05$).

Furthermore, for 3D measurement of trueness in dentition, all methods except the palatal-level method were analysed using ANOVA:

- (1) For absolute deviations (Fig. 5-a), significant differences were noted among all three methods. In addition, by Bonferroni test, significant differences were noted among each method ($p < 0.0005$), except for comparison between adjusted dental-level and upper jaw-level methods.
- (2) For signed deviations (Fig. 5-b), significant differences were observed among all three methods. In addition, by Bonferroni test, significant differences were noted between each method, except for comparisons between dental-level and upper jaw-level methods.

For comparison of trueness between palatal region and dentition (Table 1), significant differences were noted in measurements of absolute deviations, while no significant difference was noted in measurements of signed deviations.

Influence of different intraoral scanning sequences on palatal trueness

The influence of different scanning sequences on palatal trueness was investigated based on the UPRS method. Measurements of palatal trueness in Groups Tr1 and Tr2 are enlisted in Table 2.

Comparison of palatal trueness between different scanning sequences

On comparing absolute deviations, deviations in Group Tr1 were larger than those in Group Tr2. The difference in mean values was 10.34 μm (95% CI 2.44, 18.25 μm) and was statistically significant ($p = 0.012 < 0.05$).

On comparing signed deviations, no significant difference was noted between the two groups ($p = 0.582$).

Comparison of PVR trueness between different scanning sequences

On comparing absolute deviations, no significant difference was noted between the two groups ($p = 0.149$). Moreover, compared with palatal trueness, the mean absolute deviation of trueness of PVR was larger without statistical significance. In Group Tr2, the difference in mean values between PVR and palatal trueness was 9.93 μm (95% CI - 1.72, 21.57 μm).

On comparing signed deviations, no significant difference was found between the two groups ($p = 0.615$). Moreover, compared with palatal trueness, the mean signed deviation of PVR trueness was smaller without statistical significance. In Group Tr2, the difference in mean values between PVR and palatal trueness was 10.32 μm (95% CI - 33.56, 12.92 μm).

Patterns of deviation distribution of palatal trueness

Characteristics of deviation distribution on the palate

On observing colour-maps, a majority (22/35) of participants from both groups presented a similar pattern of palatal trueness (Fig. 6-a,b). Three local regions were more likely to present larger deviations, ordered by frequency and deviations as follows.

- (i) Middle one-third of the palatal region at the level of second premolars and the distal part on unilateral or bilateral sides (Fig. 6-a①): the largest deviation usually appeared at the distal level of the mid-gingival margin of first molars (Fig. 6-a②). Largest deviations were typically $\geq 500 \mu\text{m}$,

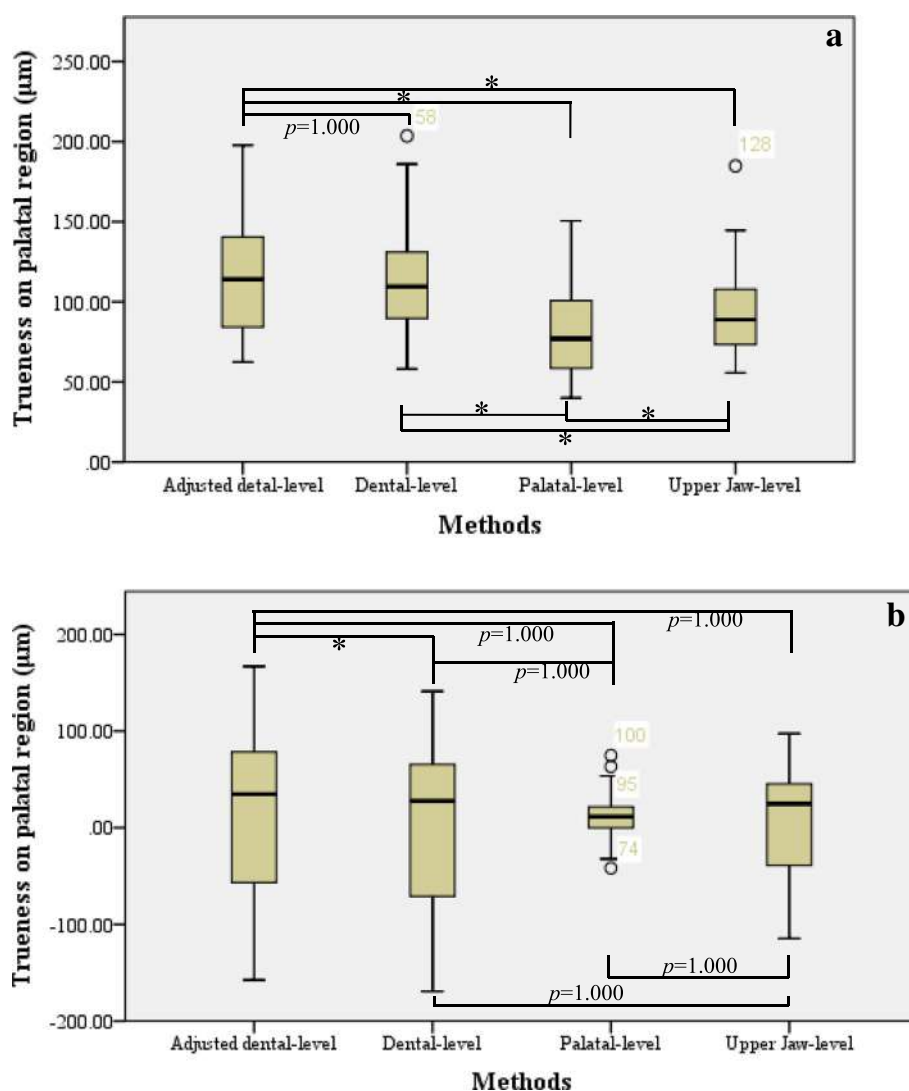


Fig. 4 Comparison of trueness in palatal region in Group Tr1 between different superimposition methods. **a.** Absolute deviations of trueness in palatal region: in tests of within-subject effects, $F(1.383, 47.009) = 41.986$, $p < 0.0005$, $\eta^2 = 0.553$. **b.** Signed deviations of trueness in palatal region: in tests of within-subject effects, $F(1.162, 39.506) = 0.730$, $p = 0.418$, $\eta^2 = 0.021$. Note: Information shown in the boxplot are median, quartiles, minimum and maximum; the circle represents the outlier; asterisk (*) indicates statistical significance ($p < 0.05$)

whereas certain deviations were even close to 1000 μm .

- (ii) Incisive papilla and the following part at the level between canines and first premolars (Fig. 6-a③): here, the deviations were seldom $> 500 \mu\text{m}$.
- (iii) Gingival margin: deviations were irregularly distributed.

In addition, directions of larger deviations were almost positive. However, only a few cases (8/22) met all characteristics of the pattern.

Moreover, deviation distribution in the rest of the cases (13/35) was irregular and was noted at the level of first and second molars if there were obvious deviations.

The deviations were typically $\leq 500 \mu\text{m}$, except for one case in Group Tr1 with negative deviations ranging 485.91–813.95 μm over the left middle one-third of the palatal region at the level of first and second molars.

Characteristics of deviation distribution on PVR

On lateral sides of PVR, it revolves part of middle one-third of the palatal region (Fig. 6-a,c). Therefore, larger deviations appeared at the sides of PVR, particularly those at the distal level of the mid-gingival margin of first molars, which could be $> 500 \mu\text{m}$ and were usually positive. However, the same direction was not found for relatively small deviations.

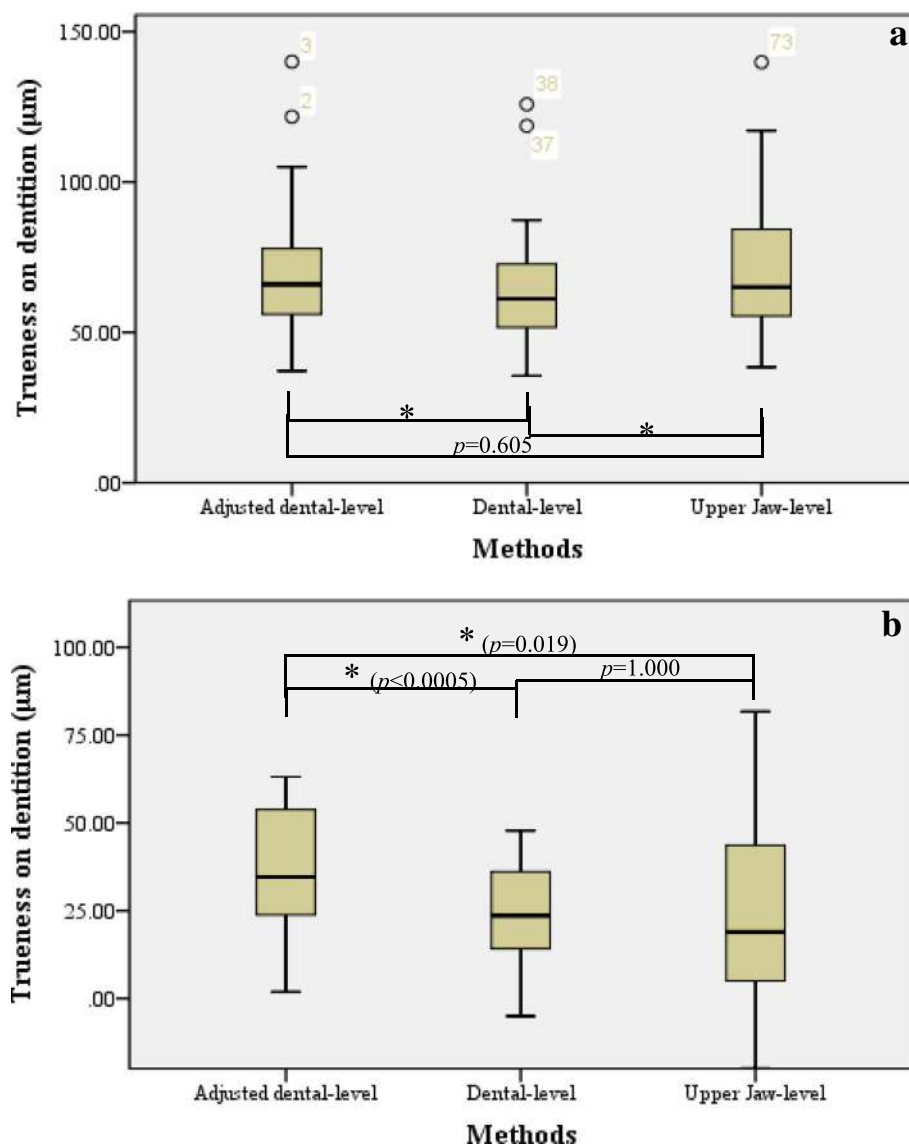
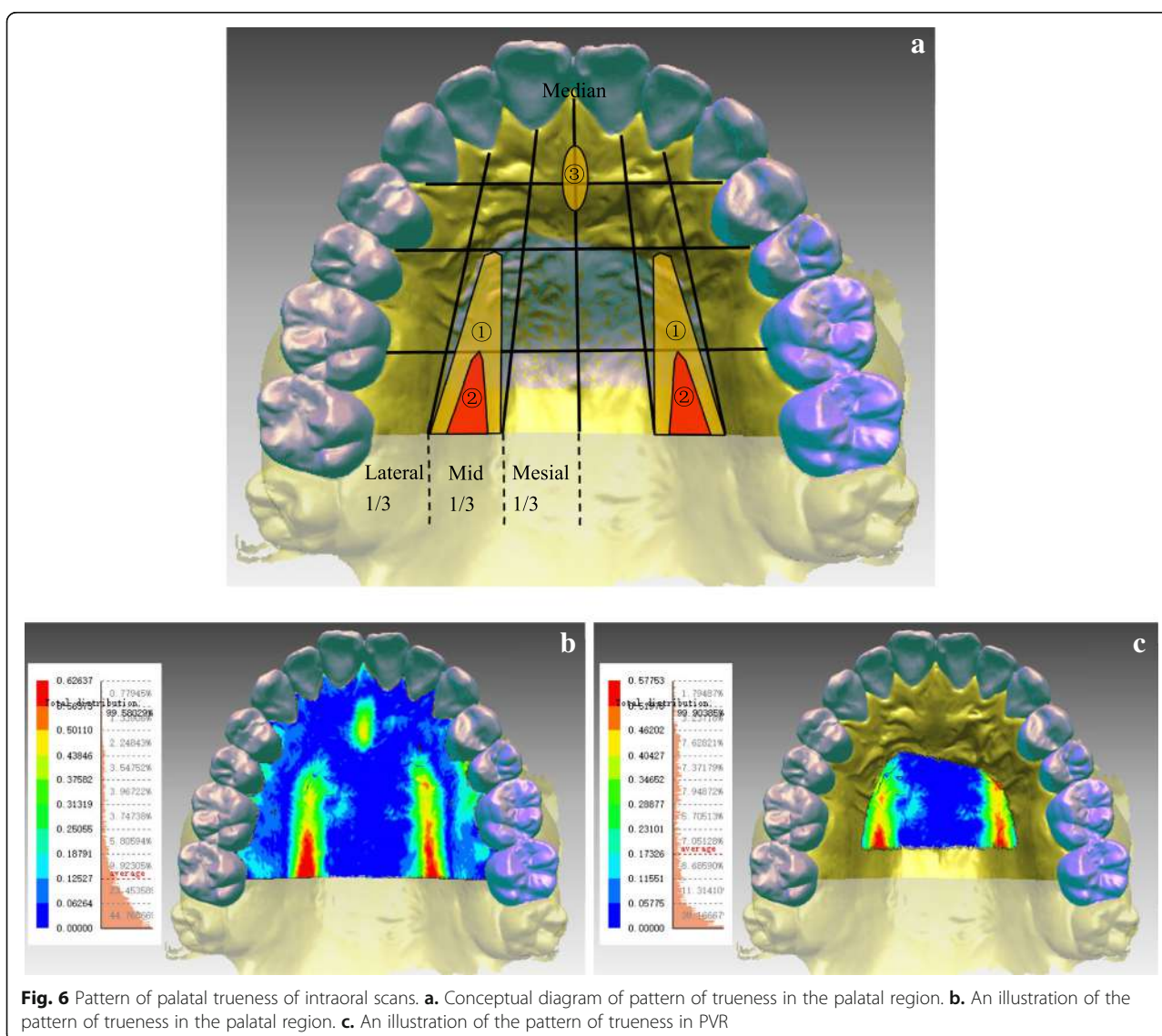


Fig. 5 Comparison of trueness in dentition in Group Tr1 between different superimposition methods. **a.** Absolute deviations of trueness in dentition: in tests of within-subject effects, $F(2, 68) = 20.439$, $p < 0.0005$, $\eta^2 = 0.375$. **b.** Signed deviations of trueness in dentition: in tests of within-subject effects, $F(1.270, 43.167) = 8.971$, $p = 0.002$, $\eta^2 = 0.209$. Note: Information shown in the boxplot are median, quartiles, minimum and maximum; the circle represents the outlier; asterisk (*) indicates statistical significance ($p < 0.05$)

Table 2 Comparison of palatal trueness between different intraoral scanning sequences measured using the UPRS method

N = 35	Absolute-value (μm)			Signed-value (μm)		
	Palatal region (P)	PVR	p value	Palatal region (P)	PVR	p value
Tr1-S (P)	118.59 ± 37.67	127.35 ± 54.11	0.129	14.56 ± 93.32	13.13 ± 126.00	0.898
Tr2-S (P)	108.25 ± 33.83	118.17 ± 49.52	0.092	18.01 ± 80.69	7.70 ± 112.76	0.373
p value	0.012*	0.149		0.582	0.615	

*p values < 0.05 indicate statistical significance



Discussion

Methodology

Digital models can be acquired using three methods [29]: directly by intraoral scanning; impressions or plaster models digitalised using laboratory scanners; and digital models extracted directly from cone-beam computed tomography (CBCT) data or acquired using CBCT scans as well as laboratory scanners. Owing to radiation exposure and less accurate dental measurements [30, 31], the CBCT approach was not used in this study.

For 3D measurement of accuracy, the best method is model superimposition [4] with common use of a best-fit algorithm [15] as we did. Based on the normals technique [32, 33], 3D measurement was performed using the 'shell-shell deviation' function with high reproducibility.

A modified dental-level regional superimposition was proposed in this study. For participants who had undergone orthodontic treatment with premolar extraction, second molars were included in order to increase feature points for regional superimposition because the longer arch length, the larger the deviation of accuracy of dentition [7, 9]. Although the reproducibility was lower than that of the other three methods, according to the ICC value and its 95% confidence interval, the level of reliability of this method could be concluded as 'good' to 'excellent' [34].

Applications can be analysed using characters of superimposition and the measurements. (1) Both adjusted dental-level and dental-level methods are based on the prerequisite that the morphology of dentition in the intraoral digital impression is accurate [1–4]. When evaluating palatal trueness measured using

these two methods, trueness in dentition should also be taken into consideration. Compared with the dental-level method, the adjusted dental-level method was more likely to represent distinct deviations and deformation on dentition (both with statistical significance). This maybe because there were more dental local deviations observed in intraoral digital impressions than in conventional impressions [2, 3]. Thus, it would highlight local deviations when relatively accurate regions were chosen for superimposition. (2) For the palatal-level method, the measurement of palatal trueness was the smallest. However, the outcome of this method cannot be extended to application in the entire upper jaw because of tendency of the best-fit algorithm to find a position with the least difference between two shells as well as less anatomical features on the palate compared with the dentition. (3) For the upper jaw-level method, it did not distinguish differences of surface characters and area between the palatal region and the dentition. Therefore, the most notable result of this method was that absolute deviations of trueness in the palatal region were statistically larger than those in the dentition. It was further verified that differences existed between trueness in the palatal region and the dentition, which was consistent with results reported by Gan N et al. [10].

Of note, when assessing palatal deformation (signed deviations) of intraoral digital impression, standard deviations (SDs) were distinctly higher than means, indicating that local deformation between the palatal region of intraoral digital models and plaster models was relatively unstable and irregular.

Influence of different intraoral scanning sequences on palatal trueness

Because of more characters on posterior teeth and for image stitching based on additional feature points, in Group Tr2, palatal scanning was initiated on the palatal side of posterior teeth. Patterns of deviation distribution in both groups were similar in a majority of participants (22/35). The statistical difference in palatal trueness between Group Tr1 and Group Tr2 was primarily in values of larger deviations. Indeed, the process of image stitching is essential. The impact of scanning sequences on accuracy of dentition can be seen at regions with larger deviations; this results because of error accumulation during the process of image stitching [12, 13]. Palatal scanning in both groups was terminated at the molar level. Thus, the stitching error was converged at the distal end of the palate. Although there is no correlation between palatal trueness and arch width, deviations of palatal precision will increase with increasing arch width [10]. In Group Tr1, the entire palatal scan was finished by repeatedly scanning across the palate with increasing

arch width. On the other hand, in Group Tr2, palatal scanning was finished by repeatedly scanning along the arch with decreasing scanning scope. Of note, the process of image stitching in Group Tr2 had three advantages: (i) there were more feature points at the beginning of palatal scanning; (ii) the possibility of deformation at palatal margins decreased by merging with the initial arch scan at the beginning of the palatal scan; and (iii) the scanning scope was decreasing in the process. It reduced the instability and error accumulation of scanning across the palate.

Regarding PVR, the region considered stable for model superimposition in orthodontics, there was no notable impact of different scanning sequences (Table 2). This indicates that it is reliable to use this region for superimposition of intraoral digital models regardless of which scanning sequences were performed. Above all, although the average difference of palatal trueness between the two scanning sequences was merely 10.34 μm , which is insufficient for it to be clinically significant. From the view of operation convenience and local deviations, we recommend the palatal scanning sequence in Group Tr2.

Palatal trueness and its pattern of deviation distribution

Compared with findings from recent studies [10, 26], the measurement of palatal trueness in this study was smaller. This might be because selection of the studied palatal region was different from the aforementioned studies. In this study, the distal end was set at the level of the mid-gingival margin of second molars, with a mesial movement of half a tooth. The limitation of a plaster model was taken into consideration. (i) An *in vitro* study showed that there was slight deformation (50 μm) at the distal end of the arch (second molars) in plaster models [4], implying that some deformation of the palate might have occurred at the same level. (ii) Anatomically, there are more glands in the submucosa of the posterior region than that of the anterior region of the hard palate. In addition, greater palatine foramina are always located on the palatal side of third molars [35], where neurovascular bundles go through and then migrate mesially under the palatine mucoperiosteum. Therefore, the palatal shape at the level of second molars in conventional impression might be greatly affected by flexibility.

Regarding characteristics of deviation distribution of palatal trueness, findings were similar to that reported by Gan et al. [10], wherein positive deviations were noted at the palatal rugae and the two sides of the palatal vault. These regions and the direction of deviations implied that the uneven flexibility of palatal soft tissues during the impression procedure might lead to larger deviations. Moreover, whether the patterns were similar

or not, regions with the largest deviations were consistent, namely the distal level of the mid-gingival margin of first molars, which was always the termination level of palatal scanning along with accumulation of scanning errors. However, nowadays, conventional impressions are still used as the reference, and hence, the pattern is interfered by the limitation of impact of flexibility.

PVR trueness and its clinical significance

Compared with palatal trueness, the mean absolute deviation of PVR trueness was slightly higher, and the mean signed deviation of PVR trueness was closer to 0 μm with a larger discrete degree. This indicated that the area proportion of more obvious deformation in PVR was slightly higher than that in the entire palate. Regardless of scanning sequences, PVR trueness of $122.76 \pm 48.51 \mu\text{m}$ was noted (95% CI 106.10, 139.42 μm). Although a deviation of $> 500 \mu\text{m}$ is considered clinically significant [14], when assessing treatment changes by 3D PVR superimposition between plaster model and intraoral digital model, an error of 123 μm would make a difference with the development of Precision Medicine, such as a digital plan for teeth movement.

For 3D PVR superimposition [25], anterior and posterior boundaries of the selected region are the third palatal rugae and the distal end of first molars, respectively; lateral boundaries begin at the lateral one-third of the third palatal rugae and are parallel to the occlusal line of posterior teeth. By observation, larger deviations appeared at the lateral sides of PVR, particularly those at the distal level of the mid-gingival margin of first molars (Fig. 6-a,c). Therefore, although it would be reliable to use this region for superimposition of intraoral digital models, adjustments should be made when applying 3D PVR superimposition for plaster and intraoral digital models. In order to avoid the region of larger deformation and to maintain more distinctive structures, the distal boundary of the selected region for superimposition should be set at the level of the mid-gingival margin of first molars.

Limitations

A major limitation of this study was the influence of flexibility of palatal mucosa on the reference model. To overcome this, selection of the palatal region was accordingly adjusted. However, from the viewpoint of characteristics of deviation distribution, the influence of flexibility during the impression procedure was still unavoidable. Another limitation was sex-imbalance in samples (9 males: 26 females). The area of the palate might be slightly larger in males. To counteract the possible effect of sex-imbalance on transversal and antero-posterior dimensions of palate, it is better to balance sex distribution in samples. However, the statistical

methods applied in this study were about self-control, less impacted by sex distribution. Furthermore, only one type of intraoral scanner was investigated in this study. In future, comparison among different intraoral scanners should be made to explore the divergency in reproducing palatal morphology.

Conclusions

When evaluating accuracy of intraoral scanning in the palatal region, the superimposition method should be appropriately adjusted. Palatal trueness is affected by scanning sequences. We recommended that palatal scanning should be initiated at the palatal side of the posterior teeth where the initial scan begins, and the entire palatal scan should be finished along with the arch. Furthermore, when assessing treatment changes by using model superimposition of plaster and intraoral digital models, the average systematic 3D error was 123 μm . For 3D PVR superimposition, we recommend to adjust the distal boundary of the selected region mesially, at the level of the mid-gingival margin of first molars, whilst referring to intraoral digital models.

Abbreviations

CBCT: Cone-beam computed tomography; ICC: Intraclass correlation coefficient; PVR: Palatal vault region; PVS: Polyvinyl-siloxane; STL: Standard tessellation language; UPRS: Upper posterior-teeth regional superimposition; VSE: Vinyl siloxanether

Acknowledgements

This paper was proofread by a native English professional with science background at Elixigen Corporation.

Funding

This study was supported by Z181100001718112 project by Beijing Municipal Science & Technology Commission with design and data collection.

Availability of data and materials

Datasets used and/or analysed during the present study are available from the corresponding author on reasonable request. All data generated or analysed during this study are included in this published article.

Authors' contributions

ZPY was a major contributor in conducting research and writing the manuscript. ZPY recruited volunteers, collected data and analysed and interpreted the data. TMX and RPJ supervised the research and revised important parts of the manuscript. All authors read and approved the final manuscript.

Ethics approval and consent to participate

The study protocol was approved by the Ethics Committee of Peking University Biomedical Sciences (PKUSSIRB-201733018). The informed consent obtained from all participants was written.

Consent for publication

Not applicable

Competing interests

The authors declare that they have no competing interests.

Publisher's Note

Springer Nature remains neutral with regard to jurisdictional claims in published maps and institutional affiliations.

Received: 7 November 2018 Accepted: 31 March 2019

Published online: 27 April 2019

References

- Fan Z, Suh KJ, Lee KM. Validity of intraoral scans compared with plaster models: an in-vivo comparison of dental measurements and 3D surface analysis. *PLoS One*. 2016. <https://doi.org/10.1371/journal.pone.0157713>.
- Ender A, Mehl A. Full arch scans: conventional versus digital impressions—an in-vitro study. *Int J Comput Dent*. 2011;14(1):11–21.
- Ender A, Mehl A. Accuracy of complete-arch dental impressions: a new method of measuring trueness and precision. *J Prosthet Dent*. 2013;109(2):121–8.
- Ender A, Attin T, Mehl A. In vivo precision of conventional and digital methods of obtaining complete-arch dental impressions. *J Prosthet Dent*. 2016;115(3):313–20.
- Treesh JC, Liacouras PC, Taft RM, et al. Complete-arch accuracy of intraoral scanners. *J Prosthet Dent*. 2018;120(3):382–8.
- Park JM. Comparative analysis on reproducibility among 5 intraoral scanners: sectional analysis according to restoration type and preparation outline form. *J Adv Prosthodont*. 2016;8(5):354–62.
- Solaberrieta E, Garmendia A, Brizuela A, et al. Intraoral digital impressions for virtual occlusal records: section quantity and dimensions. *Biomed Res Int*. 2016; <https://doi.org/10.1155/2016/7173824>.
- Flügge TV, Schlager S, Nelson K, et al. Precision of intraoral digital dental impressions with iTero and extraoral digitization with the iTero and a model scanner. *Am J Orthod Dentofac Orthop*. 2013;144(3):471–8.
- Su TS, Sun J. Comparison of repeatability between intraoral digital scanner and extraoral digital scanner: an in-vitro study. *J Prosthodont Res*. 2015; 59(4):236–42.
- Gan N, Xiong Y, Jiao T. Accuracy of intraoral digital impressions for whole upper jaws, including full dentitions and palatal soft tissues. *PLoS One*. 2016; 11(7) <https://doi.org/10.1371/journal.pone.0158800>.
- Ender A, Mehl A. Influence of scanning strategies on the accuracy of digital intraoral scanning systems. *Int J Comput Dent*. 2013;16(1):11–21.
- Anh JW, Park JM, Chun YS, et al. A comparison of the precision of three-dimensional images acquired by 2 digital intraoral scanners: effects of tooth irregularity and scanning direction. *Korean J Orthod*. 2016;46(1) <https://doi.org/10.4041/kjod.2016.46.1.3>.
- Müller P, Ender A, Joda T, et al. Impact of digital intraoral scan strategies on the impression accuracy using the TRIOS pod scanner. *Quintessence Int*. 2016. <https://doi.org/10.3290/j.qia.35524>.
- Park JM, Choi SA, Myung JY, et al. Impact of orthodontic brackets on the intraoral scan data accuracy. *Biomed Res Int*. 2016;2016(1):1–6 <https://doi.org/10.1155/2016/5075182>.
- Güth JF, Keul C, Stimmelmayer M, et al. Accuracy of digital models obtained by direct and indirect data capturing. *Clin Oral Investig*. 2013;17(4):1201–8.
- Kattadiyil MT, Mursic Z, Alrumaih H, et al. Intraoral scanning of hard and soft tissues for partial removable dental prosthesis fabrication. *J Prosthet Dent*. 2014;112(3):444–8.
- Londono J, Abreu A, Baker PS, et al. Fabrication of a definitive obturator from a 3D cast with achairside digital scanner for a patient with severe gag reflex: a clinical report. *J Prosthet Dent*. 2015;114(5):735–8.
- Al MN, Jones Q, Eggbeer D, et al. Fabrication of a resin appliance with alloy components using digital technology without an analog impression. *Am J Orthod Dentofacial Orthop*. 2015;148(5):862–7.
- Graf S, Cornelis MA, Hauber GG, et al. Computer-aided design and manufacture of hyrax devices: can we really go digital? *Am J Orthod Dentofacial Orthop*. 2017;152(6):870–4.
- Taneva ED, Johnson A, Viana G, et al. 3D evaluation of palatal rugae for human identification using digital study models. *J Forensic Dent Sci*. 2015; 7(3):244–52.
- Chen WR, Chang YC, Best CT, et al. Super-imposing maxillary and palatal locations for electroarticulometry: a SIMPLE method. *J Acoust Soc Am*. 2015; 138(2):161–6.
- Lione R, Franchi L, Huanca Ghislanzoni LT, et al. Palatal surface and volume in mouth-breathing subjects evaluated with three-dimensional analysis of digital dental casts—a controlled study. *Eur J Orthod*. 2015;37(1):101–4.
- Choi DS, Jeong YM, Jang I, et al. Accuracy and reliability of palatal superimposition of three-dimensional digital models. *Angle Orthod*. 2010; 80(4):497–503.
- Choi JJ, Cha BK, Jostbrinkmann PG, et al. Validity of palatal superimposition of 3-dimensional digital models in cases treated with rapid maxillary expansion and maxillary protraction headgear. *Korean J Orthod*. 2012;42(5): 235–41.
- Chen G, Chen S, Zhang XY, et al. Stable region for maxillary dental cast superimposition in adults, studied with the aid of stable miniscrews. *Orthod Craniofac Res*. 2011;14(2):70–9.
- Deferm JT, Schreurs R, Baan F, et al. Validation of 3D documentation of palatal soft tissue shape, color, and irregularity with intraoral scanning. *Clin Oral Investig*. 2018;22(3):1303–9.
- Martin CB, Chalmers EV, McIntyre GT, et al. Orthodontic scanners: what's available? *Br J Orthod*. 2015;42(2):136–43.
- Pavoni C, Paoloni V, Ghislanzoni LTH, et al. Geometric morphometric analysis of the palatal morphology in children with impacted incisors: a three-dimensional evaluation. *Angle Orthod*. 2017;87(3):404–8.
- Yan-Yan Ni, Zhang JX. How to determine permissible error δ value properly when computing sample sizes in hypothesis tests. *J Evid Based Med*. 2011; 11(6):370–4.
- Wesemann C, Muallah J, Mah J, et al. Accuracy and efficiency of full-arch digitalization and 3D printing: a comparison between desktop model scanners, an intraoral scanner, a CBCT model scan, and stereolithographic 3D printing. *Quintessence Int*. 2017;48(1):41–50.
- De WO, Rangel FA, Fudalej PS, et al. Reproducibility and accuracy of linear measurements on dental models derived from cone-beam computed tomography compared with digital dental casts. *Am J Orthod Dentofac Orthop*. 2014;146(3):328–36.
- Majid Z, Chong AK, Setan H. Important considerations for craniofacial mapping using laser scanners. *Photogramm Rec*. 2007;22(120):1–19.
- Miller L, Morris DO, Berry E. Visualizing three-dimensional facial soft tissue changes following orthognathic surgery. *Eur J Orthod*. 2007;29(1):14–20.
- Koo TK, Li MY. A guideline of selecting and reporting Intraclass correlation coefficients for reliability research. *J Chiropr Med*. 2016;15(2):155–63.
- Ikuta S, Renata C, Rubira-Bullen F, et al. Position of the greater palatine foramen: an anatomical study through cone beam computed tomography images. *Surg Radiol Anat*. 2013;35(9):837–42.

Ready to submit your research? Choose BMC and benefit from:

- fast, convenient online submission
- thorough peer review by experienced researchers in your field
- rapid publication on acceptance
- support for research data, including large and complex data types
- gold Open Access which fosters wider collaboration and increased citations
- maximum visibility for your research: over 100M website views per year

At BMC, research is always in progress.

Learn more biomedcentral.com/submissions




RESEARCH ARTICLE

Open Access



Oral lichen planus and other confounding factors in narrow band imaging (NBI) during routine inspection of oral cavity for early detection of oral squamous cell carcinoma: a retrospective pilot study

Agostino Guida^{1*} , Mariagrazia Maglione¹, Anna Crispo², Francesco Perri³, Salvatore Villano¹, Ettore Pavone¹, Corrado Aversa¹, Francesco Longo¹, Florinda Feroce⁴, Gerardo Botti⁴ and Franco Ionna¹

Abstract

Background: Narrow Band Imaging is a noninvasive optical diagnostic tool. It allows the visualization of sub-mucosal vasculature; four patterns of shapes of submucosal capillaries can be recognized, increasingly associated with neoplastic transformation. With such characteristics, it has showed high effectiveness for detection of Oral Squamous Cell Carcinoma. Still, scientific literature highlights several bias/confounding factors, such as Oral Lichen Planus. We performed a retrospective observational study on patients routinely examined with Narrow Band Imaging, investigating for bias, confounding factors and conditions that may limit its applicability.

Methods: Age, sex, smoking, use of dentures, history of head & neck radiotherapy, history of Oral Squamous Cell Carcinoma, site of the lesion and thickness of the epithelium of origin were statistically evaluated as possible bias/confounding factors. Pearson's Chi-squared test, multivariate logistic regression, Positive Predictive Value, Negative Predictive Value, Sensitivity, Specificity, Positive Likelihood Ratio, Negative Likelihood Ratio and accuracy were calculated, normalizing the cohort with/without patients affected by Oral Lichen Planus, to acknowledge its role as bias/confounding factor.

Results: Five hundred fifty-six inspections were performed on 106 oral cavity lesions from 98 patients. Age, sex, smoking, use of dentures and anamnesis of Oral Squamous Cell Carcinoma were not found to influence Narrow Band Imaging. History of head & neck radiotherapy was not assessed due to insufficient sample. Epithelium thickness does not seem to interfere with feasibility. Presence of Oral Lichen Planus patients in the cohort led to false positives but not to false negatives. Among capillary patterns, number IV was the most significantly associated to Oral Squamous Cell Carcinoma ($p < 0.001$), not impaired by the presence of Oral Lichen Planus patients in the cohort (accuracy: 94.3, 95% confidence interval: 88.1–97.9%; odds ratio: 261.7, 95% confidence interval: 37.7–1815.5).

Conclusion: Narrow Band Imaging showed high reliability in detection of Oral Squamous Cell Carcinoma in a cohort of patients with oral cavity lesions not normalized for bias/confounding factors. Still, Oral Lichen Planus may lead to false positives. Narrow Band Imaging could help in the follow-up of patients with multiple lesions through detection of capillary pattern IV, which seems to be the most significantly associated to neoplastic epithelium.

Keywords: Narrow band imaging, Oral squamous cell carcinoma, Oral potentially malignant disease, Early diagnosis, Follow-up, Oral lichen planus

* Correspondence: a.guida@istitutotumori.na.it

¹Maxillofacial and ENT Surgery Department, Istituto Nazionale Tumori – IRCCS “Fondazione G. Pascale”, via M. Semmola, Naples, Italy

Full list of author information is available at the end of the article



© The Author(s). 2019 **Open Access** This article is distributed under the terms of the Creative Commons Attribution 4.0 International License (<http://creativecommons.org/licenses/by/4.0/>), which permits unrestricted use, distribution, and reproduction in any medium, provided you give appropriate credit to the original author(s) and the source, provide a link to the Creative Commons license, and indicate if changes were made. The Creative Commons Public Domain Dedication waiver (<http://creativecommons.org/publicdomain/zero/1.0/>) applies to the data made available in this article, unless otherwise stated.

Background

Narrow Band Imaging (NBI), a recently introduced non-invasive optical diagnostic technique, allows the visualization of the capillary patterns of the superficial sub-mucosal layer. This device uses narrowed band width filters in a red/green/blue light illumination sequence [1, 2], with wavelengths values for each band being 415 nm and 540 nm. The 415 nm light (blue) highlights the microvasculature [3] among epithelial papillae, providing images of these subtle capillary vessels. NBI, by allowing enhanced inspection of shallow vascular structures of the superficial mucosal layers, has shown its effectiveness for detection of dysplastic/cancerous lesions of the upper aero-digestive tract: oral cavity, oro- and hypopharynx, larynx, esophagus [1–8]. In a recent meta-analysis [9] assessing NBI capability to detect head & neck squamous cell carcinoma (HNSCC), the calculated specificity, sensitivity, negative likelihood rate, positive likelihood rate, and diagnostic odds ratio (OR) of NBI were 95.6, 88.5%, 0.11, 12.33, and 121.26, respectively. Different systems for classifying patterns of intraepithelial capillary vessels (intraepithelial papillary capillary loop, IPCL) have been identified, related to increasing grades of dysplasia/neoplasia of oral cavity [1–4, 6, 8]. In a recent systematic review [10], the four pattern system [2] is considered the most effective in oral cavity, being the all types: type I (physiological arborization of IPCL), type II (circuitous or dilated IPCL), type III (convoluted/winding and/or elongated IPCL) and type IV (complete loss of organization/annihilation of IPCL). A more recent classification has been proposed for oral cavity [11], but it cannot be taken into account as the authors do not show any statistical analysis to corroborate their results. Data from the literature have shown that oral lesions with NBI pattern III and IV have increased chances of anatomopathological diagnosis of High Grade Dysplasia (HGD), oral SCC (OSCC) and OSCC in situ (Cis), when compared to those with the NBI pattern I and II [10, 12, 13]. Furthermore, NBI inspection showed more effective results in predicting HGD/Cis/OSCC (these lesions are usually grouped

together in NBI studies on oral mucosa) if compared to use of regular broad-band white light (BWL) and traditional clinical criteria (Fig. 1); the same authors suggested that best results were achieved combining NBI with BWL [12, 13]. NBI has thus found its strong rationale in the follow-up of OSCC patients [14] and in the evaluation of resection margins [15].

Despite these excellent results, routine clinical use in the inspection of oral cavity may present some difficulties. Many studies often exclude Oral Potentially Malignant Disorders (OPMDs), as they are considered confounding factors [9], especially in case of patients with Oral Lichen Planus (OLP) [9–11] due to the dishomogeneous/ulcerated aspect of the lesions and the correlation with high-grade NBI patterns. The site of the lesion is sometimes considered as bias too, due to different types of epithelium found in oral cavity; usually, epithelium of the oral cavity is classified into four categories, namely: lining epithelium (non-keratinized; e.g.: cheek and floor of mouth), masticatory epithelium (keratinized; e.g.: gum), tongue epithelium (keratinized epithelium of the lateral borders of the tongue) and specialized epithelium (on the dorsal tongue) [16]. It has been hypothesized that thicker (e.g.: tongue and masticatory) types of epithelium may obstruct IPCL visualization in the submucosa, but literature is not concordant on this aspect [10, 11]. Furthermore, history of head & neck radiotherapy has been investigated to understand a possible alteration of NBI visualization of the larynx/pharynx [17], but there are no data about oral cavity; the same happens for smoking habits.

On the basis of the aforementioned findings, we performed a retrospective observational study on patients routinely examined with NBI, in order to understand efficacy of NBI in routine oral inspections, investigating also the possible confounding factors and conditions that may limit its applicability.

Material and methods

This retrospective study was approved by Institutional Scientific Committee and accepted by Ethical Committee (n°



Fig. 1 Example of detection of OSCC through NBI. This lesion (not from a patient from the present study), a homogenous leukoplakia at BWL (left image), showed anomalous vascularization at NBI visualization (highlighted spot, middle image). According to IPCL classification criteria, it was classified as an IPCL pattern IV (upper and lower [2] - right images) and the lesion revealed itself a Cis at histopathological examination

DSC-1398/18) of National Tumor Institute INT-IRCCS “Fondazione G. Pascale” (Naples, Italy). From November 2014 to July 2018, all patients necessitating oral cavity inspection presenting at the Outpatient Clinic of Maxillofacial-ENT Surgery Unit of National Tumor Institute INT-IRCCS “Fondazione G. Pascale” (Naples, Italy) underwent intraoral flexible endoscopy with BWL and NBI. Patients’ anamnesis and data were routinely carefully recorded. The examinations were conducted using ENF type VQ flexible endoscope plugged to a CLV-S40Pro light source and a OTV-S7Pro central video system (all items by VISERA Pro – Olympus Medical Systems Corp., Tokyo, Japan). Switch from BWL to NBI view was possible through pressing a button on the flexible endoscope. Oral inspections were first conducted using BWL illumination, for a wide and complete view of all oral mucosa, searching for areas with suspect/pathological clinical appearance, both through the flexible endoscope and direct observation. The same procedure was followed for NBI examinations, carefully inspecting all of oral mucosa; imaging analysis of the IPCLs characteristics at NBI view was performed by analyzing the intraepithelial capillary vessels patterns of oral mucosa. Images and videos were acquired with a digital recorder (Mediacapture Medicap USB200) and stored in a hard drive for eventual further analysis. All NBI oral inspections and pattern assessment were performed by the same operator (AG). When a lesion/area showed different IPCL patterns at NBI, the most advanced one was considered. Incisional/excisional biopsies were performed according to BWL appearance of the lesions or when a NBI pattern III and IV was detected (even without particular BWL clinical suspect/pathological appearance). Biopsies were performed in general or local anesthesia after obtaining informed consent. Histopathological examinations were considered as the diagnostic gold standard and they were performed on paraffin-embedded specimens by the Anatomical Pathology Unit of Our Institute, by a single dedicated pathologist, blinded to the NBI appearance of the lesion; diagnoses were obtained with every necessary coloration and immunohistochemical analysis as per World Health Organization (WHO) 2017 standards [18] for OPMDs and OSCC; specimens analyzed before 2017 were re-evaluated according to the new criteria. The frequency of visits was set for each patient according to their condition/anamnesis and National Cancer Comprehensive Network (NCCN) guidelines.

Patients with lesions appearing white, non-ulcerated, homogeneous, not augmented in consistency, not surrounded by erythematous areas nor protruding from surrounding tissues, with NBI pattern I and II, were considered as “frictional keratosis” (FK - comprehending morsicatio, frictional lesions) [19]. When it was possible to remove causative factors (e.g.: selective grinding of sharp edges of neighboring teeth or prosthetic sharp edges), the patient was re-evaluated in two-weeks; if the lesion did not disappear, biopsy was performed after informed consent was administered to the patient. If the

anatomopathological examination confirmed absence of dysplasia/neoplasia, the lesion was then classified as FK. When it was not possible to remove causative factors (e.g. food impaction, bruxism in patient refusing to wear mouth guard), patients were followed-up regularly, on a two-week interval for the first 3 months. These patients were excluded without at least 24 months follow-up.

Statistical analysis

All statistical analyses were performed with the Statistical Package for Social Science (SPSS) statistical software version 23 (SPSS inc., Chicago IL, USA). In every statistical test performed, *P*-values less than 0.05–95% confidence interval (CI) - were considered significant. Pearson’s Chi-squared test of independence (2-tailed) was used to assess the relationship between categorical variables; sex, age, smoking, use of dentures, history of OSCC, history of Head & Neck radiotherapy, site of the lesion, type of epithelium from which the tumor arose and type of lesion were statistically evaluated to understand their role in influencing NBI patterns. Similarly, relationship between use of dentures and FK presence was assessed. NBI reliability in detecting HGD/Cis/OSCC, using the histopathologic findings as the final diagnostic gold standard to set the status of “true” or “false” positive and negative, was thus evaluated through multivariate logistic regression models -built by exclusively including those factors testing at the univariate analysis- with subsequent OR calculation; Positive Predictive Value (PPV), Negative Predictive Value (NPV), sensitivity, specificity, Positive Likelihood Ratio (PLR), Negative Likelihood Ratio (NLR) and accuracy were calculated. Statistical significance for sensitivity, specificity, and accuracy was assessed with “exact” Clopper-Pearson test; log method was used for the likelihood ratios; standard logit confidence intervals was used for predictive values. OR, PPV, NPV, sensitivity, specificity, PLR, NLR and accuracy were calculated with and without OLP patients, in order to understand OLP role as bias influencing NBI reliability in detecting HGD/Cis/OSCC.

Results

Overall clinical-pathological features of patients are summarized in Table 1. One hundred and forty-nine (149) consecutive patients underwent oral cavity inspections in the considered period with NBI/BWL flexible fiberscope. Fifty-one patients were discarded: 18 required biopsy for diagnosis but they refused or withdrew, 33 had non-biopsied FKs not reaching 24-months follow-up. One hundred and six (106) lesions from 98 patients were thus finally considered for this study (median age 62 years – range 19–90; mean age 61 ± 13.7 years). During the period considered for this retrospective study, they underwent visits every 1, 3, 4 or 6 months

according their condition/anamnesis, for a total of 556 BWL/NBI inspections, with mean follow-up of 21 ± 13 months. No lesion arisen from specialized epithelium (tongue dorsum) was detected.

Detected lesions included: OSCC/Cis ($n = 19$), HGD ($n = 4$), low grade dysplasia (LGD, $n = 20$), proliferative verrucous leukoplakia (PVL, $n = 3$), OLP ($n = 30$) and FK ($n = 30$). The distribution of statistically significant values according to NBI IPCL pattern -expressed in percentage- is summarized in Table 2. Influence of Head & Neck radiotherapy history was not assessed, as statistical sample was considered inadequate - only 1 patient had undergone such treatment. Age, sex, smoking, use of dentures and anamnesis of OSCC was not found significantly associated to NBI patterns ($p > 0.5$); similarly, no statistical significance was found between use of dentures and FK. On the other hand, site of the lesion and type of epithelium were found significantly associated ($p = 0.014$, $p = 0.002$ respectively) with NBI patterns. Tongue was the anatomical site/type of epithelium most strongly associated with pattern IV (62.5%). Type of lesion was also found significantly associated to NBI pattern ($p < 0.001$), with OSCC/Cis being the lesions most strongly associated to pattern IV. Lesions were then grouped in OSCC/Cis/HGD -with PVL adjunct to this group, due to its high malignant transformation potential [18], non-OSCC/Cis/HGD (benign lesions), non-OSCC/Cis/HGD without OLP (benign lesions without OLP). These groups were found to be statistically significantly associated to NBI patterns ($p < 0.001$): when a pattern IV was shown, histological analysis revealed OSCC/Cis/HGD in 91.7% cases and LGD in 8.3%; pattern III revealed OSCC/Cis/HGD in 12.5% of total cases and in 27.2% when OLP patients were excluded; pattern I and II were strongly associated to benign lesions both with and without OLP patients. Pattern IV was never associated to FK or OLP.

Our data thus revealed a significant association only of pattern IV with the OSCC/Cis/HGD group, but literature usually group pattern III and IV [10, 12, 13] to evaluate NBI efficacy in detecting OSCC/Cis/HGD; thus multivariate analysis/OR, PPV, NPV, sensitivity, specificity, PLR, NLR and accuracy were calculated with and without OLP patients for pattern IV alone and for aggregate pattern III and IV. Results are summarized in Tables 3 and 4.

Multivariate analysis/OR was also calculated for a Non-OSCC/Cis/HGD population of OLP patients only; the assessment was possible for pattern IV only, as no OLP showed NBI pattern III. All these statistical evaluations were found to be significant ($p < 0.05$ /CI = 95%). The presence of OLP patients in our cohort did not influence sensitivity and NLR both for pattern III and IV grouped and pattern IV alone (96.2%-0.05 and 84.6%-0.16, respectively). Pattern III and IV grouped showed the highest sensitivity in the search of OSCC/Cis/HGD but also the lowest specificity, both with and without OLP patients (71.3 and 80.0%, respectively), due

Table 1 Clinicopathological features of patients

Characteristics	Case no. (%)
Gender	
Male	58 (59.1)
Female	40 (40.9)
Total	98 (100.0)
Age in years (mean \pm standard deviation)	61 \pm 13.7
Smoking	
Yes	38 (38.7)
No	43 (43.8)
Ex-smoker	17 (17.5)
Presence of removable dentures	
Yes	53 (54.0)
No	45 (46.0)
Anamnesis of radiotherapy	
Yes	5 (5.1)
No	93 (94.9)
Anamnesis of OSCC	
Yes	26 (24.5)
No	80 (75.5)
Type of epithelium	
Tongue epithelium	30 (28.3)
Specialized epithelium	0(0)
Masticatory epithelium	25 (23.6)
Lining epithelium	51 (48.1)
Topographic location of lesions	
Tongue	30 (28.4)
Buccal Mucosa	47 (44.3)
Hard Palate	11 (10.4)
Soft Palate	3 (2.8)
Gum	10 (9.4)
Floor of mouth	5 (4.7)
Total	106 (100.0)
IPCL pattern by NBI	
Pattern I	18 (16.9)
Pattern II	40 (37.7)
Pattern III	24 (22.7)
Pattern IV	24 (22.7)
Diagnoses	
OSCC/Cis	19 (17.9)
HGD	4 (3.8)
PVL	3 (2.8)
LGD	20 (18.9)
OLP	30 (28.3)
FK	30 (28.3)

OSCC/Cis oral squamous cell carcinoma/ carcinoma in situ, HGD high grade dysplasia, PVL proliferative verrucous leukoplakia, LGD low grade dysplasia, OLP oral lichen planus, FK frictional keratosis

Table 2 Prevalence of statistically significant values according to NBI IPCL pattern

Value (statistical significance)	Pattern I(%)	Pattern II(%)	Pattern III(%)	Pattern IV (%)	Total
Type of lesion ($p < 0.001$)					
OSCC/Cis	0	1(2.5)	1(4.2)	17(70.8)	19(17.9)
HGD	0	0	1(4.2)	3(12.5)	4(3.8)
PVL	0	0	1(4.2)	2(8.3)	3(18.9)
LGD	4 (22.2)	7(17.5)	7(29.2)	2(8.3)	20(2.8)
OLP	3 (16.7)	14(35)	13(54.2)	0	30(28.3)
K	11(61.1)	18(45)	1(4.2)	0	30(28.3)
Total	18(100)	40(100)	24(100)	24(100)	106(100)
Malignant lesions vs benign lesions comprehending OLP ($p < 0.001$)					
OSCC/Cis/HGD ^a	0	1(2.5)	3(12.5)	22(91.7)	26(24.5)
Benign lesions	18(100)	39(97.5)	21(87.5)	2(8.3)	80(75.5)
Total	18(100)	40(100)	24(100)	24(100)	106(100)
Malignant lesions vs benign lesions not-comprehending OLP ($p < 0.001$)					
OSCC/Cis/HGD ^a	0	1(3.8)	3(27.2)	22(91.7)	26(34.2)
Benign lesions without OLP	15(100)	25(96.2)	8(72.8)	2(8.3)	50(65.8)
Total	15(100)	26(100)	11(100)	24(100)	76(100)
Site of lesions ($p = 0.014$)					
Tongue	3(16.7)	6(15)	6(25)	15(62.5)	30(28.3)
Buccal mucosa	8(44.4)	23(57.5)	13(54.2)	3(12.5)	47(44.3)
Hard palate	4(22.2)	4(10)	1(4.2)	2(8.3)	11(10.4)
Soft palate	1(5.6)	1(2.5)	0	1(4.2)	3(2.8)
Gum	2(11.1)	5(12.5)	2(8.3)	1(4.2)	10(9.4)
Floor of mouth	0	1(2.5)	2(8.3)	2(8.3)	5(4.7)
Total	18(100)	40(100)	24(100)	24(100)	106(100)
Type of epithelium ($p = 0.002$)					
Tongue	3(16.7)	6(15)	6(25)	15(62.5)	30(28.3)
Masticatory	6(33.3)	11(27.5)	4(16.7)	4(16.7)	25(23.6)
Lining	9(50)	23(57.5)	14(58.3)	5(20.8)	51(48.1)
Total	18(100)	40(100)	24(100)	24(100)	106(100)

OSCC/Cis oral squamous cell carcinoma/ carcinoma in situ, HGD high grade dysplasia, PVL proliferative verrucous leukoplakia, LGD low grade dysplasia, OLP oral lichen planus, FK Frictional Keratosis

^aPVL was adjunct to this group due to its high malignant transformation potential

to a high number of false positive. The best value of specificity was reached when the pattern IV was considered singularly associated to OSCC/Cis/HGD, higher in presence rather than in absence of OLP patients (97.5 and 96.0%, respectively) due to a higher number of true negative. PPV was dramatically increased by considering pattern IV alone (91.7%), and did not suffer of any reduction by the presence of OLP patients. PPV of pattern III and IV grouped was low (more numerous false positive cases), remarkably reduced in the OLP cohort (from 71.4 to 52.1%). Similar values of NPV were reached between pattern IV alone and pattern III and IV grouped; presence of OLP patients affected NPV slightly (from 98.3 to 97.6% for pattern III-IV, from 95.1 to 92.3% for pattern IV). Finally, global accuracy was higher when pattern IV was considered alone, minimally influenced by the

presence/absence of OLP patients (94.3 and 92.1%, respectively). Presence of OLP patients in the cohort did reduce the significance (OR) at multivariate analysis for pattern III-IV, while increased significance of pattern IV alone (OR: 261.7; CI 37.7–1815.5). Multivariate analysis also showed significance for pattern IV when the cohort included OSCC/Cis/HGD and OLP patients only.

With descriptive purposes, we report that in one patient with no denture, a lesion from buccal mucosa of the posterior cheek with clinical characteristics (linear white patch, homogeneous, not augmented in consistency) of FK showed NBI pattern III; despite selective grinding of sharp edges of neighboring teeth, the lesion showed the same characteristics after 2 weeks. After obtaining informed consent from the patient, the lesion was biopsied

Table 3 Evaluation of NBI pattern III-IV and pattern IV alone as a diagnostic test for OSCC/Cis/HGD, with and without OLP patients

Diagnostic test	Pattern III-IV (95% CI)	Pattern IV (95% CI)
Sensitivity		
With OLP patients	96.2% (80.4–99.9%)	84.6% (65.1–95.6%)
Without OLP patients	96.2% (80.4–99.9%)	84.6% (65.1–95.6%)
Specificity		
With OLP patients	71.3% (60.0–80.8%)	97.5% (91.2–99.7%)
Without OLP patients	80.0% (66.3–89.9%)	96.0% (86.3–99.5%)
PLR		
With OLP patients	3.34 (2.35–4.76)	33.85 (8.53–134.30)
Without OLP patients	4.81 (2.75–8.41)	21.15 (5.39–83.06)
NLR		
With OLP patients	0.05 (0.01–0.37)	0.16 (0.06–0.39)
Without OLP patients	0.05 (0.01–0.33)	0.16 (0.06–0.40)
PPV		
With OLP patients	52.1% (43.3–60.7%)	91.7% (73.5–97.7%)
Without OLP patients	71.4% (58.8–81.4%)	91.7% (73.7–97.7%)
NPV		
With OLP patients	98.3% (89.2–99.7%)	95.1% (88.8–97.9%)
Without OLP patients	97.6% (85.3–99.6%)	92.3% (82.9–96.7%)
Accuracy		
With OLP patients	77.4% (68.2–84.9%)	94.3% (88.1–97.9%)
Without OLP patients	85.5% (75.6–92.5%)	92.1% (83.6–97.1%)

PLR positive likelihood ratio, NLR negative likelihood ratio, PPV positive predictive value, NPV negative predictive value, CI confidence interval

and its non-dysplastic nature was confirmed histologically; the lesion has been thus inserted in the FK group. On the other hand, in two patients being followed-up for previously treated OSCC, the inspection showed no areas with classical suspicious clinical aspect at BWL but one pattern IV NBI spot was revealed (Fig. 2). Local biopsies were performed, after informed consent was obtained, and in both cases OSCC recurrence was early diagnosed. In another patient, in follow-up for an erosive LP, which had steadily shown NBI patterns II – III for 16 months, OSCC was early diagnosed with a biopsy performed consequently to a NBI pattern switch to IV (Fig. 3).

Discussion

Several authors [20] have highlighted that OSCC remains a lethal disease in more than 50% of cases; such low rates of survival are mainly linked to the fact that most cases are diagnosed in advanced stages, despite accessibility of the mouth for regular examination. Thus, the common objective for both patients and physicians must be early detection. Specialists need to be trained to detect early signs/symptoms in order to facilitate treatment, increasing effectiveness and reducing morbidity [21, 22]. Clinical features of OSCC include:

- Red, white, mixed red/white (speckled) or irregular-white lesion (erythroplakia, leukoplakia, erythroleukoplakia and verrucous leukoplakia, respectively)
- Ulcer, eventually with fissuring or raised exophytic margins
- Mass, with or without ulcerations
- Pain/ loss of sensitivity (numbness) to any region of the lower third of the face
- Tooth/teeth with high-grade mobility or extraction socket not healing after tooth/teeth extraction(s)

As apparent, clinicians' view of the lesion may be biased by multiple factors when relying to these criteria only [21–23]. Among the numerous attempts in searching for help to overcome limits of clinical criteria, including vital staining [24] and other optical techniques [25–27], literature has shown that NBI endoscopy has a great potential of improving clinicians' possibility of performing early diagnosis. Despite excellent results, its routinary use in the inspection of oral cavity may present some difficulties at the present stage of scientific literature. History of head & neck radiotherapy is considered to be a major bias in the NBI visualization of the larynx/pharynx [17], but there are no data about oral cavity. In our retrospective study, unfortunately, we were unable to evaluate the influence of Head & Neck radiotherapy on NBI patterns, due to an insufficient sample. On the other hand, smoking habit and presence of dentures were not found statistically associated to NBI patterns. Another major bias in the NBI visualization of the larynx/pharynx is the site of the lesion, due to different epithelium thickness from site to site, but literature is

Table 4 Multivariate analysis, adjusted for terms of gender, age, smoking habits, of NBI patterns related to histopathologic diagnosis

Non- HGD/Cis/OSCC	HGD/Cis/OSCC detected by NBI pattern III-IV	HGD/Cis/OSCC detected by NBI pattern IV
With OLP patients	OR:79.04 (95%CI:9.5–652.4)	OR:261.7 (95%CI:37.7–1815.5)
Without OLP patients	OR:103.1 (95%CI:19.8–897.4)	OR:161.7 (95%CI:22.1–1180.2)
OLP patient only	OR: not evaluable	OR:53.1 (95%CI:5.06–556.1)

OSCC/Cis oral squamous cell carcinoma/ carcinoma in situ, HGD high grade dysplasia, OR odds ratio, CI confidence interval

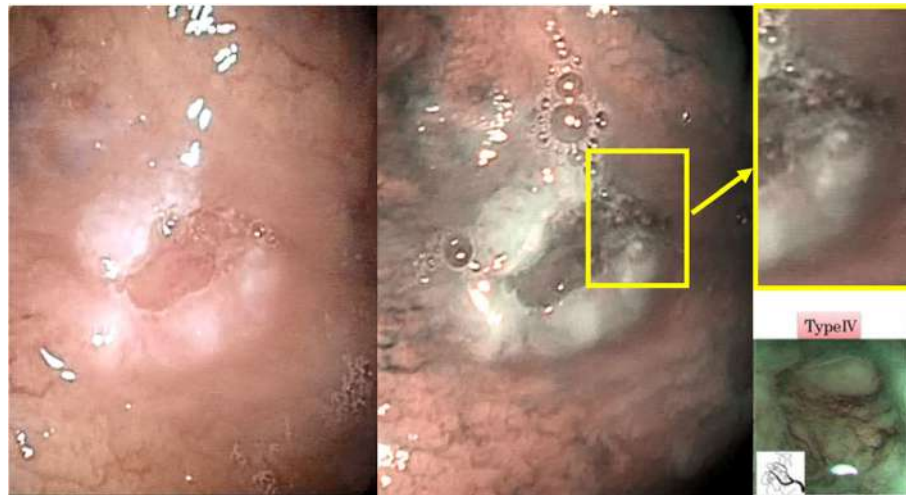


Fig. 2 Early diagnosis of OSCC recurrence through NBI. The inspection of this asymptomatic surgical scar (outcome of a second-intention healing), from a patient who had previously had surgery for OSCC, did not reveal suspicious areas – such as ulcers, lumps, red and/or white lesions – at BWL (left image). Still, it was biopsied due to an anomalous vascularization at NBI visualization (highlighted spot, middle image) which was classified as IPCL pattern IV (upper and lower [2] - right images). Histopathological examination showed a recurrence of OSCC

not concordant on this aspect [10, 11] in oral cavity. In our study, anatomical site and type of epithelium were assessed as statistically significant, with most of NBI pattern IV located on the keratinized epithelium of tongue lateral borders. Furthermore, we found that the distribution of NBI patterns in the thin non-keratinized lining epithelium was similar to the thicker masticatory epithelium. Thus in our study thicker epithelium does not seem to hide IPCLs, but wider studies are needed to understand correlation between pattern IV and tongue lateral borders, maybe influenced but the higher rate of OSCCs compared to other sites [16].

NBI has proved remarkably positive results: when IPCL pattern III and IV are detected, literature showed a high correlation to OSCC/Cis/HGD [9, 10, 12, 13]. Yet, studies generally exclude OPMDs, especially OLP, as they are considered major bias [9–11]. These lesions

often have dishomogeneous/ulcerated aspects and show high-grade NBI patterns. In our retrospective study, we assessed NBI efficacy in routine clinical use, on a cohort of patients affected by oral lesions, not normalized for possible bias suggested by present literature. This led to differences respect to data shown by literature, in which the specificity is usually higher than the sensitivity and, in general, oral cavity lesions are often grouped with oropharynx lesions and sometimes with laryngeal/nasopharyngeal lesions too [9, 10]. In order to acknowledge the OLP influence as a possible bias, we performed every statistical calculation with and without OLP patients. Our results showed that the presence of OLP patients in our cohort did not influence sensitivity and NLR. This means that, in terms of routine use of NBI, the possibility that a patient has OLP does not impair NBI reliability in detecting lesions positive for OSCC/Cis/HGD; our



Fig. 3 Early diagnosis of OSCC in OPMD patients through NBI. In a patient with multiple ulcers and erosions due to erosive LP, a biopsy was performed on this ulcer (left image) among the various lesions, as it showed an anomalous vascularization at NBI visualization (highlighted spot, middle image), which was classified as IPCL pattern IV (upper and lower [2] - right images). Histopathological examination confirmed that an occurred malignant transformation (OSCC) was intercepted

results show that both pattern III and IV (highest sensitivity when grouped) should be taken into account for biopsy, as advised by literature. On the other hand, OLP may lead to false positive cases when considering pattern III and IV as at risk (low specificity due to high rates of OLP showing pattern III), but it does not seem to impair pattern IV reliability, as confirmed by multivariate analysis. This could pave the way to future perspectives, meaning that patients with multiple/single OLP lesion(s), after initial diagnostic biopsy, could be followed up with NBI, performing a new biopsy (in addition to cases in which clinical appearance changes/becomes suspicious) when pattern IV is detected, as a sign of occurred malignant transformation - as happened once in our cohort of patients. Furthermore, both global accuracy and OR reached best results when pattern IV was considered alone; further studies are needed with the aim to interpret such result, which could highlight pattern IV as a clinical marker of OSCC/Cis/HGD presence. Another possible factor that influenced statistical outcome is the wide sample of FK. The diagnosis of FK is considered to be clinical and, being completely benign lesions, no treatment is required [19]. Even if there is no evidence that minor continuative trauma has carcinogenic potential, the removal of irritant factors is advised but sometimes not possible (e.g.: teeth malposition/absence). Yet, it is a common possibility that a patient may be affected by multiple/single FK(s), leaving the clinician with doubts about the necessity of a biopsy, especially in presence of risk factors (e.g.: smoking habit). Data from our study show that FKs are associated with NBI pattern I and II; this could be of great help for the clinician in the follow-up of patients with single/multiple FK(s), especially in presence of risk factors (e.g.: smoking habit, which from our study does not seem to alter NBI inspection result).

As a matter of fact, the present study has some limitations which need to be underlined. First, in order to perform a diagnosis of OLP, just a small part of the lesion(s) was (were) excised, and this may have resulted in sampling mistakes. Second, this study is retrospective on a relatively small cohort of patients. Bigger prospective multicentric studies should be performed to confirm obtained data. Another limitation that needs to be stressed is the lack of a widely accepted definition of “expert” and “experienced” in NBI procedures – especially in the field of oral cavity. This is a considerable criticism of present NBI literature [9] and potentially a major bias. In our experience it may require a period of several months/1 year to become expert. Classical gastrointestinal endoscopy criteria [28] state that at least 130–140 endoscopic evaluations are necessary to achieve competence. In our case, the operator (AG) had performed at least 140 procedures (NBI oral exams) per year for 5 years. General consensus should be achieved to define the status of “experienced” and “expert”. Possibly, application to NBI of

classical gastrointestinal endoscopy criteria of 130–140 procedures to set the status of “experienced” operator could be suitable, but further studies on operators’ learning curve are needed to avoid the risk of major bias when evaluating NBI reliability. Furthermore, as diagnostic percentage standards are extensively shown in literature, self-evaluation, comparing operator’s own NBI pattern evaluation with histopathological analysis, could be easily achievable.

Conclusion

- NBI has showed high sensitivity and NPV in detection of OSCC/Cis/HGD also in a cohort of patients with oral cavity lesions non-normalized for possible confounding factors, confirming its high impact in anticipating first diagnosis of malignancies.
- Presence of OLP patients in a cohort do not lead to false negatives but may raise false positive rate; this must be kept in mind e.g. during follow-up.
- NBI could help in the follow-up of patients with multiple chronic lesions, both in case of no need for treatment (e.g. FK) both for help the diagnosis of occurred malignant transformation (e.g. OLP) through detection of IPCL pattern IV;
- IPCL pattern IV does seem to be the most significantly associated to OSCC/Cis/HGD, as confirmed by the highest value of accuracy and OR;
- The results obtained from this study may function as a pilot for prospective multicentric studies with bigger samples, to confirm such findings.

Abbreviations

BWL: Broad white light; CI: Confidence interval; Cis: Carcinoma in situ; FK: Frictional keratosis; HGD: High-grade dysplasia; HNSCC: Head & neck squamous cell carcinoma; IPCL: Intrapapillary capillary loops; LGD: Low-grade dysplasia; NBI: Narrow band imaging; NCCN: National cancer comprehensive network; NLR: Negative likelihood ratio; NPV: Negative predictive value; OLP: Oral lichen planus; OPMD: Oral potentially malignant disorder; OR: Odds ratio; OSCC: Oral squamous cell carcinoma; PLR: Positive likelihood ratio; PPV: Positive predictive value; SPSS: Statistical package for social science; WHO: World health organization

Acknowledgements

Not applicable.

Funding

Authors received no funding source nor financial support/grants by any institutional, private or corporate entity.

Availability of data and materials

The datasets used and/or analysed during the current study are available from the corresponding author upon reasonable request.

Authors’ contributions

AG & MM: study design; AC: conception of statistical evaluations and data analysis; FP, GB, FI: final scientific revision; FF: anatomopathological supervision/coordination; SV, EP: data retrieving; CA, FL: bibliographical research/selection. All authors were involved in drafting the manuscript or revising it critically for important intellectual content. All authors read and approved the final manuscript. All authors agreed to be accountable for all

aspects of the work in ensuring that questions related to the accuracy or integrity of any part of the work are appropriately investigated and resolved.

Ethics approval and consent to participate

This retrospective study was approved by Institutional Scientific Committee and accepted by Ethical Committee (n° DSC-1398/18) of National Tumor Institute INT-IRCCS "Fondazione G. Pascale" (Naples, Italy). Every surgical procedure was performed after obtaining written informed consent, signed by the patient.

Consent for publication

Not applicable.

Competing interests

The authors performed all the work by themselves. The authors declare they have no competing interests nor conflicts of interests.

Publisher's Note

Springer Nature remains neutral with regard to jurisdictional claims in published maps and institutional affiliations.

Author details

¹Maxillofacial and ENT Surgery Department, Istituto Nazionale Tumori – IRCCS "Fondazione G. Pascale", via M. Semmola, Naples, Italy. ²Epidemiology and Biostatistics Unit, Istituto Nazionale Tumori – IRCCS "Fondazione G. Pascale", via M. Semmola, Naples, Italy. ³Head & Neck Medical Oncology Unit, Istituto Nazionale Tumori – IRCCS "Fondazione G. Pascale", via M. Semmola, Naples, Italy. ⁴Pathological Anatomy and Cytopathology Unit, Istituto Nazionale Tumori – IRCCS "Fondazione G. Pascale", via M. Semmola, Naples, Italy.

Received: 6 November 2018 Accepted: 12 April 2019

Published online: 30 April 2019

References

- Shih-Wei Y, Yun-Shien L, Liang-Che C, Tsan-Yu H, Tai-An C. Implications of morphologic patterns of intraepithelial microvasculature observed by narrow-band imaging system in cases of oral squamous cell carcinoma. *Oral Oncol.* 2013;49:86–92.
- Takano JH, Yakushiji T, Kamiyama I, Nomura T, Katakura A, Takano N, et al. Detecting early oral cancer: narrowband imaging system observation of the oral mucosa microvasculature. *Int J Oral Maxillofac Surg.* 2010;39(3):208–13.
- Ishihara R, Inoue T, Uedo N, Yamamoto S, Kawada N, Tsujii Y, et al. Significance of each narrow-band imaging finding in diagnosing squamous mucosal highgrade neoplasia of the esophagus. *J Gastroenterol Hepatol.* 2010;25(8):1410–5.
- Sakai A, Okami K, Ebisumoto K, Sugimoto R, Maki D, Iida M. New techniques to detect unknown primaries in cervical lymph node metastasis. *Laryngoscope.* 2010;120(9):1779–83.
- Ni XG, He S, Xu ZG, Gao L, Lu N, Yuan Z, et al. Endoscopic diagnosis of laryngeal cancer and precancerous lesions by narrow band imaging. *J Laryngol Otol.* 2010;125(3):288–96.
- Chu PY, Tsai TL, Tai SK, Chang SY. Effectiveness of narrow band imaging in patients with oral squamous cell carcinoma after treatment. *Head Neck.* 2012;34(2):155–61.
- Muto M, Satake H, Yano T, Minashi K, Hayashi R, Fujii S, et al. Long-term outcome of transoral organ-preserving pharyngeal endoscopic resection for superficial pharyngeal cancer. *Gastrointest Endosc.* 2011;74(3):477–84.
- Watanabe A, Taniguchi M, Tsujie H, Hosokawa M, Fujita M, Sasaki S. The value of narrow band imaging endoscope for early head and neck cancers. *Otolaryngol Head Neck Surg.* 2008;138(4):446–51.
- Hui Z, Jing Z, Linghong G, Ji N, Chenjing Z, Xuelei M. The value of narrow band imaging in diagnosis of head and neck cancer: a meta-analysis. *Sci Rep.* 2018;8:515.
- Vu AN, Farah CS. Efficacy of narrow band imaging for detection and surveillance of potentially malignant and malignant lesions in the oral cavity and oropharynx: a systematic review. *Oral Oncol.* 2014;50(5):413–20.
- Tirelli G, Marcuzzo AV, Boscolo Nata F. Narrow-band imaging pattern classification in oral cavity. *Oral Dis.* 2018;24(8):1458–67.
- Yang SW, Lee YS, Chang LC, Chien HP, Chen TA. Light sources used in evaluating oral leukoplakia: broadband white light versus narrowband imaging. *Int J Oral Maxillofac Surg.* 2013;42:693–701.
- Yang SW, Lee YS, Chang LC, Hwang CC, Luo CM, Chen TA. Clinical characteristics of narrow-band imaging of oral erythroplakia and its correlation with pathology. *BMC Cancer.* 2015;15:406.
- Tirelli G, Piovesana M, Bonini P, Gatto A, Azzarello G, Boscolo Nata F. Follow-up of oral and oropharyngeal cancer using narrow-band imaging and high-definition television with rigid endoscope to obtain an early diagnosis of second primary tumors: a prospective study. *Eur Arch Otorhinolaryngol.* 2017;274(6):2529–36.
- Farah CS. Narrow band imaging-guided resection of oral cavity cancer decreases local recurrence and increases survival. *Oral Dis.* 2018;24(1–2):89–97.
- Rautava J, Luukka M, Heikinheimo K, Alin J, Grenman R, Happonen RP. Squamous cell carcinomas arising from different types of oral epithelia differ in their tumor and patient characteristics and survival. *Oral Oncol.* 2007;43(9):911–9.
- Lin YC, Watanabe A, Chen WC, Lee KF, Lee IL, Wang WH. Narrowband imaging for early detection of malignant tumors and radiation effect after treatment of head and neck cancer. *Arch Otolaryngol Head Neck Surg.* 2010;136(3):234–9.
- El-Naggar AK, Chan J, Takata T, Grandis J, Blookweg P, editors. WHO classification of tumours. Pathology and genetics of head and neck tumours. 4th ed. Lyon: IARC Press; 2017.
- Scully C, editor. Oral and maxillofacial medicine: the basis of diagnosis and treatment. 2nd ed. Edinburgh: Churchill Livingstone; 2008. p. 223.
- Warnakulasuriya S. Global epidemiology of oral and oropharyngeal cancer. *Oral Oncol.* 2009;45(4–5):309–16.
- Scully C, Bagan JV. Oral squamous cell carcinoma: overview of current understanding of aetiopathogenesis and clinical implications. *Oral Dis.* 2009; 15:388–99.
- Scully C, Jose Bagan JV. Oral squamous cell carcinoma overview. *Oral Oncol.* 2009;45:301–8.
- Lumerman H, Freedman P, Kerpel S. Oral epithelial dysplasia and the development of invasive squamous cell carcinoma. *Oral Surg Oral Med Oral Pathol Oral Radiol Endod.* 1995;79(3):321–9.
- Rosenberg D, Cretin S. Use of meta-analysis to evaluate toloum chloride in oral cancer screening. *Oral Surg Oral Med Oral Pathol.* 1989;67(5):621–7.
- Swinson B, Jerjes W, El-Maaytah M, Norris P, Hopper C. Optical techniques in diagnosis of head and neck malignancy. *Oral Oncol.* 2006;42(3):221–8.
- Suhr MA, Hopper C, Jones L, George JG, Bown SG, MacRobert AJ. Optical biopsy systems for the diagnosis and monitoring of superficial cancer and precancer. *Int J Oral Maxillofac Surg.* 2000;29(6):453–7.
- Burian E, Schulz C, Probst F, Palla B, Tröltzsch M, Maglito F, et al. Fluorescence based characterization of early oral squamous cell carcinoma using the visually enhanced light scope technique. *J Craniomaxillofac Surg.* 2017;45(9):1526–30.
- Vennes JA, Ament M, Boyce HW Jr, Cotton PB, Jensen DM, Ravich WJ, et al. Principles of training in gastrointestinal endoscopy. American Society for Gastrointestinal Endoscopy. Standards of Training Committees. 1989-1990. *Gastrointest Endosc.* 1992;38(6):743–6.

Ready to submit your research? Choose BMC and benefit from:

- fast, convenient online submission
- thorough peer review by experienced researchers in your field
- rapid publication on acceptance
- support for research data, including large and complex data types
- gold Open Access which fosters wider collaboration and increased citations
- maximum visibility for your research: over 100M website views per year

At BMC, research is always in progress.

Learn more biomedcentral.com/submissions



RESEARCH ARTICLE

Open Access



Trueness and precision of 5 intraoral scanners in the impressions of single and multiple implants: a comparative in vitro study

Francesco Guido Mangano^{1*} , Uli Hauschild², Giovanni Veronesi³, Mario Imburgia⁴, Carlo Mangano⁵ and Oleg Admakin⁶

Abstract

Background: Until now, a few studies have addressed the accuracy of intraoral scanners (IOSs) in implantology. Hence, the aim of this in vitro study was to assess the accuracy of 5 different IOSs in the impressions of single and multiple implants, and to compare them.

Methods: Plaster models were prepared, representative of a partially edentulous maxilla (PEM) to be restored with a single crown (SC) and a partial prosthesis (PP), and a totally edentulous maxilla (TEM) to be restored with a full-arch (FA). These models were scanned with a desktop scanner, to capture reference models (RMs), and with 5 IOSs (CS 3600°, Trios3°, Omnicam°, DWIO°, Emerald°); 10 scans were taken for each model, using each IOS. All IOS datasets were loaded into a reverse-engineering software where they were superimposed on the corresponding RMs, to evaluate trueness, and superimposed on each other within groups, to determine precision. A statistical analysis was performed.

Results: In the SC, CS 3600° had the best trueness ($15.2 \pm 0.8 \mu\text{m}$), followed by Trios3° ($22.3 \pm 0.5 \mu\text{m}$), DWIO° ($27.8 \pm 3.2 \mu\text{m}$), Omnicam° ($28.4 \pm 4.5 \mu\text{m}$), Emerald° ($43.1 \pm 11.5 \mu\text{m}$). In the PP, CS 3600° had the best trueness ($23 \pm 1.1 \mu\text{m}$), followed by Trios3° ($28.5 \pm 0.5 \mu\text{m}$), Omnicam° ($38.1 \pm 8.8 \mu\text{m}$), Emerald° ($49.3 \pm 5.5 \mu\text{m}$), DWIO° ($49.8 \pm 5 \mu\text{m}$). In the FA, CS 3600° had the best trueness ($44.9 \pm 8.9 \mu\text{m}$), followed by Trios3° ($46.3 \pm 4.9 \mu\text{m}$), Emerald° ($66.3 \pm 5.6 \mu\text{m}$), Omnicam° ($70.4 \pm 11.9 \mu\text{m}$), DWIO° ($92.1 \pm 24.1 \mu\text{m}$). Significant differences were found between the IOSs; a significant difference in trueness was found between the contexts (SC vs. PP vs. FA). In the SC, CS 3600° had the best precision ($11.3 \pm 1.1 \mu\text{m}$), followed by Trios3° ($15.2 \pm 0.8 \mu\text{m}$), DWIO° ($27.1 \pm 10.7 \mu\text{m}$), Omnicam° ($30.6 \pm 3.3 \mu\text{m}$), Emerald° ($32.8 \pm 10.7 \mu\text{m}$). In the PP, CS 3600° had the best precision ($17 \pm 2.3 \mu\text{m}$), followed by Trios3° ($21 \pm 1.9 \mu\text{m}$), Emerald° ($29.9 \pm 8.9 \mu\text{m}$), DWIO° ($34.8 \pm 10.8 \mu\text{m}$), Omnicam° ($43.2 \pm 9.4 \mu\text{m}$). In the FA, Trios3° had the best precision ($35.6 \pm 3.4 \mu\text{m}$), followed by CS 3600° ($35.7 \pm 4.3 \mu\text{m}$), Emerald° ($61.5 \pm 18.1 \mu\text{m}$), Omnicam° ($89.3 \pm 14 \mu\text{m}$), DWIO° ($111 \pm 24.8 \mu\text{m}$). Significant differences were found between the IOSs; a significant difference in precision was found between the contexts (SC vs. PP vs. FA).

Conclusions: The IOSs showed significant differences between them, both in trueness and in precision. The mathematical error increased in the transition from SC to PP up to FA, both in trueness than in precision.

Keywords: Intraoral scanners, Oral implantology, Trueness, Precision

* Correspondence: francescoguidomangano@gmail.com

This Manuscript is to be considered as part of – “The Digital Dentistry Society II Consensus Conference on Digital Technologies – Marrakech” thematic series.

¹Department of Prevention and Communal Dentistry, Sechenov First Moscow State Medical University, Moscow, Russia

Full list of author information is available at the end of the article



© The Author(s). 2019 **Open Access** This article is distributed under the terms of the Creative Commons Attribution 4.0 International License (<http://creativecommons.org/licenses/by/4.0/>), which permits unrestricted use, distribution, and reproduction in any medium, provided you give appropriate credit to the original author(s) and the source, provide a link to the Creative Commons license, and indicate if changes were made. The Creative Commons Public Domain Dedication waiver (<http://creativecommons.org/publicdomain/zero/1.0/>) applies to the data made available in this article, unless otherwise stated.

Background

Intraoral scanners (IOSs) are powerful devices for acquiring an optical impression of dental arches, able to replace the conventional techniques with trays and materials (alginate, polyvinylsiloxane, polyether) that have always been unwelcome to patients [1–3]. IOSs, for this reason and for their different possible applications—diagnosis and acquisition of study models [4], fixed prostheses [2, 3], guided implant surgery [5], orthodontics [6]—are spreading in the dental world and an increasing number of dentists purchase such machines and adopt this technology [1–3, 6, 7]. IOSs project a light source (generally a structured light grid with a known geometry; or a laser beam) on the surface of the teeth and capture its deformation with powerful cameras; this data is reworked by the acquisition software that generates a point cloud, which is then triangulated to produce a mesh [1–3]. This mesh represents the direct reconstruction of the surface of the object [1–3]. With IOSs, the dentate models are directly captured; there is no need to pour a plaster cast from a negative impression, as with the conventional alginate, polyvinylsiloxane, or polyether impressions. This is theoretically an advantage, because all the possible errors related to the transition from negative to positive are eliminated; also, the virtual model can be quickly emailed to the dental laboratory, at no cost [1–3, 6, 7].

Even though the clinicians often focus their attention on speed and ease of use, as well as on practical features such as the absence of powder, the color, and the possibility of exporting files without having to pay any release fee, it must be noted that the mathematical quality of the files derived from the IOS is more important [1]. The main mathematical features an IOS should possess are accuracy [1, 7–11] and resolution [12].

Accuracy is key in all clinical applications in prosthesis, whether with natural teeth or with implants—an IOS should be able to detect an accurate impression [8–11]. In metrics and engineering, accuracy is defined as the “closeness of agreement between a measured quantity value and a true quantity value of a measurand” (JCGM 200:2012; ISO 5725–1, 1994). Ultimately, accuracy is the sum of trueness and precision [8–11]. Trueness, usually expressed in terms of bias, is the “closeness of agreement between the expectation of a test result or a measurement result and a true value” [9, 10]. Precision is defined as the “closeness of agreement between indications or measured quantity values obtained by replicate measurements on the same objects under specified conditions” [9, 10]. In other words, the ideal IOS should be able to reconstruct and therefore reproduce as faithfully as possible the surface of the scanned object, i.e., it should possess high trueness; and it should have high precision, giving consistent and repeatable results without any deviations when scanning the same object [10, 11].

It is rather simple to measure, *in vivo*, the precision of an IOS: it is sufficient to capture different scans of the same arch, one after the other, save these 3D models, and, via reverse-engineering software, overlap them. In this context, minimal deviations between the models indicate high precision of the IOS. Calculating the trueness *in vivo* instead is more difficult; in order to do it, via reverse engineering software, we need in fact a reference model (RM), onto which we can superimpose our intraoral scans [9, 10]. To date, a RM can be captured only by means of sophisticated machines such as articulated arms or coordinate measuring machines (CMMs), i.e., devices that physically probe the surface of the object for detailed 3D information; alternatively, powerful industrial or desktop optical scanners can be used for this purpose [10]. Since it is not possible to detach the patient's dental arches and place them inside a CMM or an industrial optical scanner to get a RM, it is impossible to calculate the trueness of an IOS *in vivo*.

Finally, in IOS, the resolution is given by the density of the point cloud and therefore by the number of triangles that constitutes the mesh [12]. This resolution is essential for the visualization of details such as the margin or preparation line of a natural tooth [12], but it is of lesser importance in the case of implants, where the impression captures only a position and the scanbody is then replaced by pre-formed components from a library, on which the computer assisted design (CAD) modeling takes place [13, 14]. Therefore, there are important differences between scanning of natural teeth and scanning of implants, and the latter could be defined as easier.

However, only a few clinical studies have been published so far in the literature on the full-digital workflow, starting from intraoral scanning, for implant-supported rehabilitations [1–3, 7, 13–17]. Most of these studies reported good results with single implants [3, 7, 13–17], while few have focused on the restoration of multiple implants [18, 19]. It seems that the IOSs have difficulty in capturing, *in vivo*, accurate impressions for the design and manufacture of long-span restorations [20, 21]. To date, in particular, the scientific literature does not support the use of IOSs for impression capture on multiple implants, aimed at the manufacture of extended implant-supported restorations as full arches (FAs) [20, 21]. This limitation is determined by the acquisition methods of IOS and therefore the difficulty of reconstructing extended surfaces [22].

Since the IOSs that are currently on the market have different characteristics (acquisition methods and reconstruction algorithms) and today few studies have addressed their accuracy [12, 23–28], particularly in implantology [9–11, 26–28], the aim of the present *in vitro* study was to assess the trueness and precision of 5 different IOSs in the impressions of single and multiple implants, and to compare them.

Methods

Study casts

The dental laboratory prepared two different plaster models, representing three different situations/contexts in the maxilla. The first model was a partially edentulous maxilla (PEM), with an implant analog in position #23 (left upper canine) to simulate the situation of an implant-supported single crown (SC), and with two implant analogs in position #14 and #16 (respectively right first premolar and first molar) to simulate the situation of an implant-supported partial prosthesis (PP) (Fig. 1a). The second model was instead a totally edentulous maxilla (TEM), with implant analogs in position #11, #14, #16, #21, #24, and #26 (right and left central incisors, first premolars and first molars), to simulate the situation of an implant-supported fixed FA prosthesis (Fig. 1b). All models presented pink gums in the areas of implant analogs. High-precision non-reflective polyether-ether-ketone (PEEK) scanbodies (Megagen®, Daegu, South Korea) were screwed on the implant analogs; PEEK was selected because it does not reflect light and therefore facilitates acquisition with three-dimensional (3D) scanners [29].

Design of the study

The present in vitro study compared 5 different IOSs that are currently available on the market (CS 3600®, Carestream Dental, Atlanta, Georgia USA; Trios3®, 3Shape, Copenhagen, Denmark; CEREC Omnicam®, Dentsply-Sirona, York, Pennsylvania, USA; DWIO®, Dentalwings, Montreal, Quebec, Canada; and Emerald®, Planmeca, Helsinki, Finland), with the aim of investigating their trueness and precision, and therefore their accuracy, within oral implantology.

The design of the study was the following: the two models with the scanbodies in position were acquired with a desktop scanner of industrial derivation (Freedom UHD®, Dof Inc., Seogdong-gu, Seoul), and three scans were captured for each of the models. These scans were subsequently imported and cut into a reverse-engineering software (Geomagic Studio 2012®, Geomagic, Morrisville, North Carolina, USA), using a preconfigured cutting tool (in order to always reproduce the same cuts). The resulting three preconfigured cuts corresponded respectively to: (1) the single implant (to be restored with a SC) in conjunction with the two adjacent teeth; (2) the two implants (to be restored with a PP) in conjunction with their two adjacent teeth; and (3) the six implants (to be restored with a fixed FA). These surface meshes (nine in all, three per type) were saved as standard triangulation language (.STL) files, and overlapped each other, within each group (single on single, partial on partial, total on total) inside the reverse-engineering software. These superimpositions were performed to validate the reference tool, evaluating the deviations between the different files acquired, and thus to select the virtual RM, one by type, to be used later as a basis for the overlap of the various IOS files (trueness evaluation).

Once the reference tool was validated and the three RMs were selected, a single operator expert in digital dentistry began to scan the plaster models with each of the IOSs available. In all, 10 scans were captured for each of the three situations (SC, PP, FA) with each of the IOSs. In the case of the PEM, therefore, the operator did not perform a complete scan of the model, but only captured the area of the pink gingiva, of the scanbody, and

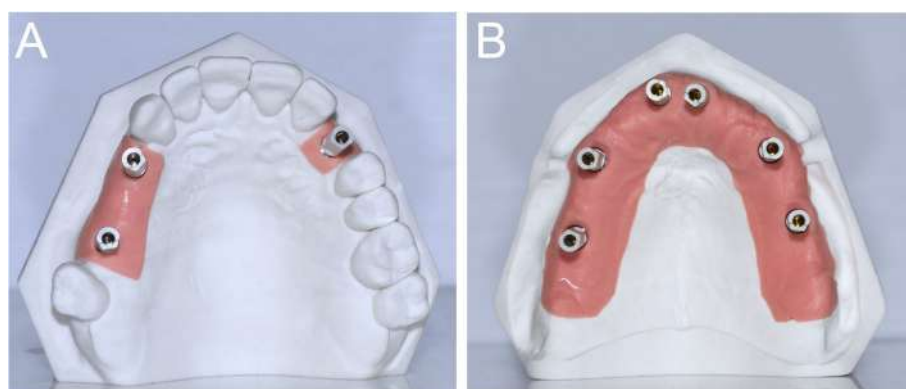


Fig. 1 Two different plaster models were prepared, representing three different situations in the maxilla. The first model (a) was a partially edentulous maxilla (PEM), with an implant analog in position #23 (left upper canine), to simulate the situation of an implant-supported single crown (SC), and with two implant analogs in position #14 and #16 (respectively right first premolar and first molar), to simulate the situation of an implant-supported partial prosthesis (PP). The second model (b) was a totally edentulous maxilla (TEM), with implant analogs in position #11, #14, #16, #21, #24 and #26 (right and left central incisors, first premolars and first molars), to simulate a situation of an implant-supported fixed full-arch (FA) prosthesis. All models presented pink gums in the areas of implant analogs, with high-precision non-reflective polyether-ether-ketone (PEEK) scanbodies (Megagen®, Daegu, South Korea) screwed on the implant analogs

of the adjacent teeth (single implant); and the area of the pink gingiva, the two scanbodies, and the adjacent teeth (two implants). In the case of the TEM, the operator captured the whole area of the pink gingiva and the scanbodies (six implants). To avoid the effects of operator fatigue, the sequence of scans was randomized and the scans were captured sequentially, one after the other, with the different machines, at intervals of 5 min from each other. In all cases, and for all IOSs, the operator used a zig-zag technique: he started from the buccal side, carried occlusal and then palatal, and then returned to the occlusal, progressing constantly. The movement described by the tip of the scanner was therefore an arc, moving slowly to fly over the teeth and scanbodies, capturing all details possible but only in the area of interest. All IOSs were used under the same environmental conditions—in a room with a temperature of 22°C (humidity at 45%, air pressure around 750 ± 5 mm).

The scanners

The main characteristics of all IOSs were summarized in Table 1. A reference scanner (Freedom UHD®, Dof Inc., Seogdong-gu, Seoul, Korea) of industrial derivation was used for the acquisition of the RMs in this study. Freedom UHD uses structured light (white LED light) and acquires thanks to two 5.0 MegaPixel cameras, using the patented stable scan stage (SSS) technology. The SSS system allows the cameras to move above and around the model to be scanned. The cameras and lights rotate around the center of the scan plate, while the model remains stationary; this allows one to capture all the details of the model effectively and quickly (in less than 50 s). The scanner has a certified accuracy of 5 µm and generates STL files immediately usable by any CAD. The scanner weighs 15 kg, has dimensions of 330 × 495 × 430 mm, is powered at 110–240 V, 50–60 Hz, and works with Windows operating systems 7, 8, and 10 (64-bit).

CS 3600®, launched in 2016, is a structured LED light scanner. CS 3600® is fast thanks to the Intelligent Matching System™, which allows the software to connect the scanned images very quickly and build the mesh continuously, without interruption. CS 3600® is equipped with interchangeable and autoclavable tips, of different sizes and with different orientations, to facilitate scanning even in the most difficult areas. The IOS easily connects to the computer through a USB port, does not require the use of powder, and is able to provide HD full-color images in 3D, which are a valuable marketing tool from the patient's perspective and at the same time help the clinician in identifying the margin line (when used in scanning on natural teeth). Finally, CS 3600® is an open IOS, which produces proprietary files (.CSZ) with color information, which can be opened in the simplified Carestream CAD (CS Restore®) for design and the subsequent manufacture of a whole series of simple restorations (inlays, onlays, veneers, single crowns), but also open files (.PLY, .STL) that can be processed by any dental CAD. One of these formats in particular (.PLY), although usable by any CAD, allows one to keep the color information. CS 3600® does not require the payment of any annual or monthly fee for use or for the unlocking of proprietary files. There are no restrictions for laboratories in the use of color (.PLY) or monochromatic (.STL) files of CS 3600®. The IOS is suitable for the acquisition of images for the design of a wide range of prosthetic restorations (inlays, onlays, veneers, single crowns, and bridges up to bars) and for the acquisition of the dento-gingival information to be combined with the bone, obtained with the cone-beam computed tomographies (CBCTs) produced by Carestream (CS 9300®, CS 8100®, and others) in the workflow in guided surgery. Finally, CS 3600® is used for the diagnosis and design of orthodontic devices. In the present study, the release V3.0 (09–2017) of the acquisition software was used.

Table 1 The five intraoral scanners used in this study

	Producer	Technology of acquisition	Powder	Colour	System
CS 3600®	Carestream Dental, Atlanta, Georgia, USA	Structured light-Active Speed 3D Video™	No	Yes	Proprietary files (.CSZ), but also open formats (.PLY,.STL) immediately available
Trios3®	3-Shape, Copenhagen, Denmark	Structured light –Confocal microscopy and Ultrafast Optical Scanning™	No	Yes	Proprietary files (.DCM) available, but possibility to export .STL files via the new Trios on Dental Desktop®
Omniscam®	Dentsply-Sirona, York, Pennsylvania, USA	Structured light -Optical triangulation and confocal microscopy	No	Yes	Proprietary files (.CS3,.SDT,.CDT,.IDT) are available, but possibility to export .STL files via the Cerec Connect®
DWIO®	Dentalwings, Montreal, Quebec, Canada	Blue laser-Multiscan Imaging™ technology	No	No	Proprietary files (.XORDER), but also open Formats (.STL) immediately available
Emerald®	Planmeca, Helsinki, Finland	Red, green and blue lasers-Projected Pattern Triangulation™	No	Yes	Open formats (.PLY,.STL) immediately available

Trios3° has been released by the 3Shape Company in 2015. Available in different versions (trolley with touch screen, built-in version in dental unit, and version connected to a laptop via USB) with a straight pen-grip handle or with a pistol-shaped handle (320 × 56 × 16 mm); since 2017 it implements a wireless version, in which the scanner is connected to a laptop via WiFi, eliminating the need for connection cables. Trios3° is a structured light scanner that uses confocal microscopy and Ultra-fast Optical Scanning™ technology to capture more than 3000 two-dimensional images per second. It then combines up to 1000 3D digital pictures. It is powder-free and produces high-quality color images implementing Real Color Scan™, HD Photo Function™, and Digital Shade Determination™ technologies. With Trios3°, the colour scanning can help to differentiate the natural tooth structure and the gingival tissues, and therefore it may help dentists to identify the margin lines; in addition, it represents a valuable marketing tool with patients. Trios3° has a big wand, but this is not a limitation because this tip can be used to avoid scanning of unwanted tissues (tongue, cheeks, lips). Trios3° is still considered to be a closed system; in fact, it generates proprietary files (.DCM) which can be opened by the 3Shape CAD software (3Shape Dental System®), one of the most widespread design platforms available on the market, via the proprietary cloud-based platform (Trios Inbox®) or setting up a direct connection via Direct Connect®, through which data are fed into the dental system and read out from there. However, in the present study, the software version 1.6.4 (Trios on Dental Desktop®) has been used. Trios on Dental Desktop® is the new 3Shape unified platform that integrates all digital workflows into an intuitive user interface, with integrated HD intraoral camera, patient monitoring, smile design, treatment simulator, shade measurement, and, for the first time, STL scan export. The CAD software from 3Shape allows design of all kinds of prosthetic restorations and frameworks (inlays, onlays, veneers, crowns, bridges, bars); in addition, modules for implant (3Shape Implant Studio®) and orthodontic planning (3Shape Ortho Analyzer®) are available. However, 3Shape still has no dedicated milling machines for in-office, chairside restorations.

CEREC Omnicam® has long been the most sophisticated IOS of the Dentsply-Sirona, at least until the recent presentation, at the annual fair in Dubai in 2019, of the company's new product, Primescan®. Omnicam® represents the development and technological evolution of the previous IOSs produced by the German Sirona (CEREC Bluecam®, available since 2009, and Apollo DI®), the first company to introduce intraoral scanning in the world, and therefore long monopolising the market. Introduced in 2012 and available in two different versions (trolley, Omnicam AC®, and tabletop, Omnicam AF®)

Omnicam® is a structured light scanner that uses a white LED and works under the principle of optical triangulation and confocal microscopy. Extremely fast, it does not require the use of powder and incorporates the color inside the reconstructed 3D model. The scanner is of medium size (228 × 16 × 16 mm), but the tip is not too large and this makes scanning even easier in the posterior areas (maxillary or mandibular third molars). The acquisition software is as powerful as the dedicated CAD, and the workflow can be done directly at the chairside, using the proprietary CAD software or the cloud-based platform (CEREC Connect®). CEREC Omnicam® is theoretically a closed system, because it produces proprietary files (.CS3, .SDT, .CDT, .IDT) that can only be opened by CAD software of the same company; however, with the introduction of CEREC Connect® the system has been partially opened, giving the user the possibility to transform the proprietary files into. STL, which can be used by any other CAD software. In this study, we have used the software CEREC Connect 4.4.4°, and all proprietary files have been converted into. STL via Inlab software (16.0). Sirona has always had cutting-edge chairside solutions, such as the Chairside software 4.4° in combination with the 3 + 1-axis CEREC MC° milling unit (X / XL); however, the company also has powerful laboratory tools such as the inLAB15° CAD software and the MC X5° milling machine. The computer assisted design/ computer assisted manufacturing (CAD/ CAM) system by Sirona allows the clinician and the laboratory to design and mill a series of prosthetic restorations and frameworks (inlays, onlays, veneers, crowns, bridges, bars). In addition, Omnicam® has a software for guided surgery (CEREC Guide®), enabling the chairside manufacture of surgical templates, and a software for orthodontic applications (CEREC Ortho®).

DWIO®, presented in its first version during the Chicago Midwinter Meeting of 2015, is a laser scanner that uses a Multiscan Imaging™ technology and integrates five pairs of miniaturized 3D scanners into the tip of the handpiece. The main feature of this IOS is that the handpiece is really thin and light and it has about the same dimensions as a common implant handpiece; it therefore allows one to capture even difficult preparation areas, without effort and without causing any discomfort to the patient. The scanner, which initially required the use of powder, is, in the latest version (used in this study, the version 2.1.0.421) powder-free and as output has proprietary files (.XORDER) and free. STL files that can be open from any CAD and do not require payment of fees for unlocking. The scanner is very fast (< 60 s per arcade) but does not rebuild the object in color. It is available in two versions, both of which feature an innovative voice and gesture control system, to allow the clinicians to control the computer without having to

remove their gloves during the scan. The DWIO® is integrated into the powerful CAD system from Dentalwings, one of the best known and used worldwide. DWIO® is indicated for the capture of models for the fabrication of several prosthetic restorations (inlays, onlays, veneers, crowns, bridges) and for the guided surgery as well, thanks to the CoDiagnostiX® software, one of the most important on the market, always developed by Dentalwings.

The latest addition to the Planmeca family, and launched in 2017, Emerald® is a laser scanner (red, green, and blue lasers) that uses Projected Pattern Triangulation™ technology to quickly capture 3D images of dental arches. This IOS reconstructs the models in color and does not require the use of powder. In addition, it is rather small in size (41 × 45 × 249 mm) and light (235 g with the tip mounted) and has autoclavable tips of different sizes to allow the operator to scan even the most difficult areas (posterior sectors, third molars). The scanner easily connects to the computer via USB-3 / USB-C port but can even be integrated into the dental unit, with foot control. The scanner exports free files (.PLY / . STL) that, whether integrating the color information or not, can be opened by the software of the company (Planmeca Romexis® and Planmeca PlanCAD® Easy software suites) as well as freely from any CAD software available on the market. Since Planmeca is a renowned and well-known home for the production of high quality X-ray and CBCT devices (such as ProMax3D®), the Emerald® scanner represents not only the access door for digital prosthetics, with the possibility of designing a whole series of restorations (inlays, onlays, veneers, crowns, bridges, bars), but also the ideal tool to acquire dento-gingival models for guided surgery. 3D models acquired with Emerald® are easily combined with 3D acquisitions of bone volumes using CBCT for planning and making templates for guided implant surgery. In this study we used Planmeca Romexis 5.1.0 software for scanning.

Trueness and precision

The evaluation of the trueness and precision of the models acquired through the different IOSs studied was as previously reported [9, 10]. In short, all the models acquired with the different IOSs, and their corresponding three RMs, were imported into a reverse-engineering software (Geomagic Studio 2012). The models were then cut/trimmed using dedicated templates through the function “cut with planes” in order to make them uniform. These uniform models were then saved in specific folders and were ready for superimposition. The power of the superimposition algorithms of the reverse-engineering software in use had already been validated in a previous study [9] through the duplication of an identical model, moved in space and then superimposed

on itself; these tests had confirmed the absolute reliability of the aforementioned algorithms [9]. For the evaluation of trueness, each of the IOS scans was superimposed onto the corresponding RM, obtained with the desktop scanner. The process basically consisted of three steps. First, a rough alignment was manually performed by means of three fixed points that were identified on the surface of the implant scanbodies in the IOS and RM models. Once this manual phase had been completed, we proceeded to the surface alignment through the “best fit” superposition algorithm of the reverse-engineering software. This algorithm made the final superimposition of the various. STL files derived from IOS on the corresponding RMs. The parameters set for this superimposition were a minimum of 100 iterations per case, for the registration that occurred thanks to a RICP (“robust-iterative-closest-point”) algorithm. The distances between the IOS models and the corresponding RMs were minimized using a point-to-plane method; congruence between specific corresponding structures was calculated. Thanks to these superimposing algorithms, the mean ± standard deviation (SD) of the distances between the two superimposed models was calculated by the software. Finally, the software allowed the generation of a colorimetric map for the immediate visualization, in 3D, of the distances between the models. This was done through the “3D deviation” function and the colorimetric map quantified the distances between specific points, globally and in all space planes. The color maps indicated inward (blue) or outward (red) displacement between overlaid structures, whereas a minimal change was indicated by green color. The same setting of the colorimetric map was set, for all three models (SC, PP, FA); the color scale ranged from a maximum deviation of + 100 and – 100 µm, with the best result given by the deviations between + 30 and – 30 µm (green color). For the precision evaluation, the working method was identical: a first superimposition by points followed the overlap for surfaces and the generation of the colorimetric map. However, IOS-derived models were overlapped on each other, within each group, and not on the corresponding RM (which was not used). The choice of the IOS models to be superimposed was based on a randomized design, which led to a total of 10 overlaps within each group; the precision of each IOS could therefore be obtained, and expressed as a mean (±SD).

Statistical analysis

A careful statistical analysis was performed, for mean and absolute deviations. Trueness was defined from the superimposition of each scan (10 scans per each IOS group) on the corresponding RM, captured with the desktop scanner. The analysis was first stratified by the context (SC, PP, and FA). For each scanner, the mean

trueness and its SD were calculated from analysis of variance, and all possible pairwise comparisons between IOSs were tested, using the Tukey investigation for multiple comparisons. In the footnotes to the tables, the minimum significant mean differences after the Tukey's correction were reported. Bartlett's test was used for the assumption of homoscedasticity of variances across groups. The same analyses were replicated for precision, defined from the superimposition between different scans made with the same IOS. For this analysis, 10 comparisons for each scanner were available per each IOS type. Finally, we compared mean trueness and precision of any given scanner, by context (SC vs. PP vs. FA), using separate *t*-tests, with Satterthwaite approximation for the variance. All statistical analyses were conducted using a powerful statistical package (SAS software release 9.4°, SAS Institute, Cary, NC).

Results

The trueness results are summarized in Table 2 and in Figs. 2, 3, 4, 5 and 6. In brief, in the SC, CS 3600° had the best trueness ($15.2 \pm 0.8 \mu\text{m}$), followed by Trios3° ($22.3 \pm 0.5 \mu\text{m}$), DWIO° ($27.8 \pm 3.2 \mu\text{m}$), Omnicam° ($28.4 \pm 4.5 \mu\text{m}$), and Emerald° ($43.1 \pm 11.5 \mu\text{m}$). CS 3600° was statistically truer than DWIO°, Omnicam°, and Emerald°; while Trios3°, DWIO°, and Omnicam° were statistically truer than Emerald°. In the PP, CS 3600° had the best trueness ($23 \pm 1.1 \mu\text{m}$), followed by Trios3° ($28.5 \pm 0.5 \mu\text{m}$), Omnicam° ($38.1 \pm 8.8 \mu\text{m}$), Emerald° ($49.3 \pm 5.5 \mu\text{m}$), and DWIO° ($49.8 \pm 5.0 \mu\text{m}$). CS 3600° and Trios3° were statistically truer than Omnicam°, Emerald°, and DWIO°; while Omnicam° was statistically truer than Emerald° and DWIO°. Finally, in the FA, CS 3600° had the best trueness ($44.9 \pm 8.9 \mu\text{m}$), followed by Trios3° ($46.3 \pm 4.9 \mu\text{m}$), Emerald° ($66.3 \pm 5.6 \mu\text{m}$), Omnicam° ($70.4 \pm 11.9 \mu\text{m}$), and DWIO° ($92.1 \pm 24.1 \mu\text{m}$). CS 3600° and Trios3° were statistically truer than Emerald°, Omnicam°, and DWIO°; while Emerald° and Omnicam° were statistically truer than DWIO°. A statistically significant

difference in trueness was found, for each scanner, between the different contexts (SC vs. PP vs. FA).

The precision results are summarized in Tab. 3 and in Figs. 7 and 8. In brief, in the SC, CS 3600° had the best precision ($11.3 \pm 1.1 \mu\text{m}$), followed by Trios3° ($15.2 \pm 0.8 \mu\text{m}$), DWIO° ($27.1 \pm 10.7 \mu\text{m}$), Omnicam° ($30.6 \pm 3.3 \mu\text{m}$), and Emerald° ($32.8 \pm 10.7 \mu\text{m}$). CS 3600° and Trios3° were statistically more precise than DWIO°, Omnicam°, and Emerald°. In the PP, CS 3600° had the best precision ($17 \pm 2.3 \mu\text{m}$), followed by Trios3° ($21 \pm 1.9 \mu\text{m}$), Emerald° ($29.9 \pm 8.9 \mu\text{m}$), DWIO° ($34.8 \pm 10.8 \mu\text{m}$), and Omnicam° ($43.2 \pm 9.4 \mu\text{m}$). CS 3600° was statistically more precise than Emerald°, DWIO°, and Omnicam°; while Trios3° was statistically more precise than DWIO° and Omnicam°; and Emerald° was statistically more precise than Omnicam°. Finally, in the FA, Trios3° had the best precision ($35.6 \pm 3.4 \mu\text{m}$), followed by CS 3600° ($35.7 \pm 4.3 \mu\text{m}$), Emerald° ($61.5 \pm 18.1 \mu\text{m}$), Omnicam° ($89.3 \pm 14 \mu\text{m}$), and DWIO° ($111 \pm 24.8 \mu\text{m}$). CS 3600° and Trios3° were statistically more precise than Emerald°, Omnicam°, and DWIO°; while Emerald° was statistically more precise than Omnicam° and DWIO°; and Omnicam° was statistically more precise than DWIO°. A statistically significant difference in precision was found, for each scanner, between the different contexts (SC vs. PP vs. FA).

Discussion

To date, only a few studies have compared the accuracy of different IOSs in implantology [9–11, 26–28].

Van der Meer and colleagues compared three different IOSs (CEREC AC Bluecam°, iTero°, and Lava COS°) in a partially edentulous model with 3 implants [27]. The implants were connected with PEEK scanbodies, 10 scans were taken for each IOS, and all of these were loaded into reverse-engineering software, where the distances and angles between the different cylinders were calculated [27]. These values were compared with reference measurements obtained with an industrial 3D scanner. Considering the linear distances, Lava COS° showed the

Table 2 Mean trueness and its standard deviation (SD) in micrometers (μm) with single crown (SC), partial prosthesis (PP) and full-arch (FA), and *p* values testing the scanner by context interaction. *N* = 10 scans for each scanner and implant type

Scanner	Single Crown (SC) Mean \pm SD	Partial prosthesis (PP) Mean \pm SD	Full arch (FA) Mean \pm SD	<i>p</i> -value ¹
Trios 3°	22.3 \pm 0.5†	28.5 \pm 0.5†,‡,•	46.3 \pm 4.9†,‡,•	< 0.0001
CS 3600°	15.2 \pm 0.8‡,‡,§	23.0 \pm 1.1^,§,‡	44.9 \pm 8.9^,§,‡	< 0.0001
Emerald°	43.1 \pm 11.5†,‡,•,^	49.3 \pm 5.5†,^,°	66.3 \pm 5.6†,^,°	< 0.0001
DWIO°	27.8 \pm 3.2‡,•	49.8 \pm 5.0†,§,•	92.1 \pm 24.1†,§,°,*	< 0.0001
Omnicam°	28.4 \pm 4.5§,^	38.1 \pm 8.8•,‡,°,•	70.4 \pm 11.9•,‡,°,•	< 0.0001

The same symbol after SD indicates differences in trueness between scanner pairs (Tukey-adjustment for multiple comparison). Minimum significant difference across scanners: 7.3 μm , 6.6 μm , 16.8 μm for single crown (SC), partial prosthesis (PP) and full arch (FA), respectively. ¹*p*-value testing the interaction between scanner and context (SC vs. PP vs. FA) from non-parametric, Kruskal-Wallis test. A *p*-value > 0.05 indicates no difference in scanner trueness according to the context

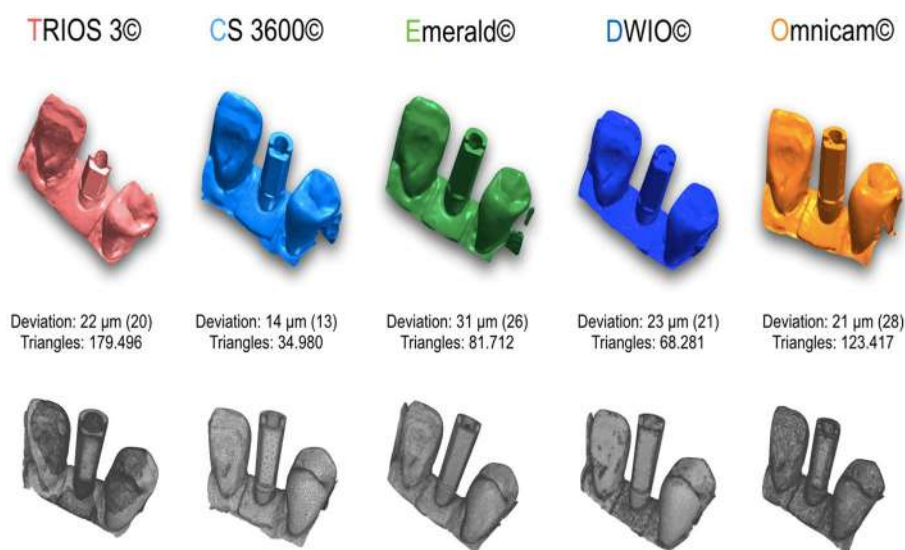


Fig. 2 Single crown (SC): best result in trueness (standard deviation), in μm , for the 5 examined scanners, and the number of triangles composing each mesh

minor deviations, CEREC® the major [27]. Angular deviations were minimal in all IOSs [27]. The authors concluded that an increase in linear and angular errors is to be expected with all IOSs, over the length of the arch as well as on the accumulation of patched 3D surfaces [27].

In another in vitro study, two representative models of a PEM and TEM were prepared, with three and six PEEK scanbodies, respectively [10]. These models were scanned with four different IOSs (Trios2®, CS 3500®, Zfx Intrascan®, and Planscan®), five scans for each of the scanners; the models were then superimposed via reverse-engineering software to the RMs, captured with

a powerful industrial scanner, in order to evaluate the general trueness [10]. In addition, the distance and angles between simulated implants were measured in each group and compared to those of the RM, to evaluate local trueness [10]. Finally, the precision was calculated by overlapping the scans captured with the different IOSs, within each group. General trueness and precision of any IOSs were compared by model type, through an ANOVA model including scanner, model, and their interaction [10]. At the end of the study, CS 3500® had the best general trueness ($47.8 \mu\text{m}$) and precision ($40.8 \mu\text{m}$) in the PEM, followed by Trios2® (trueness

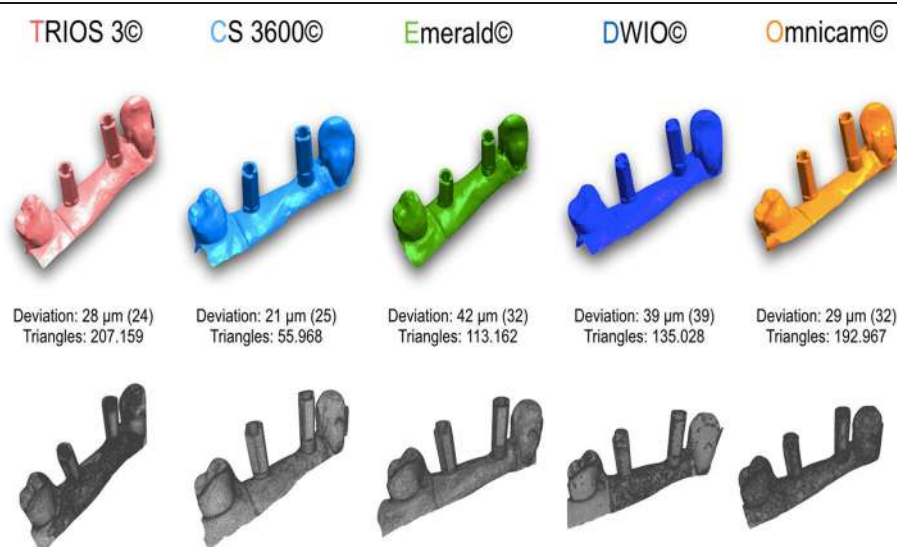
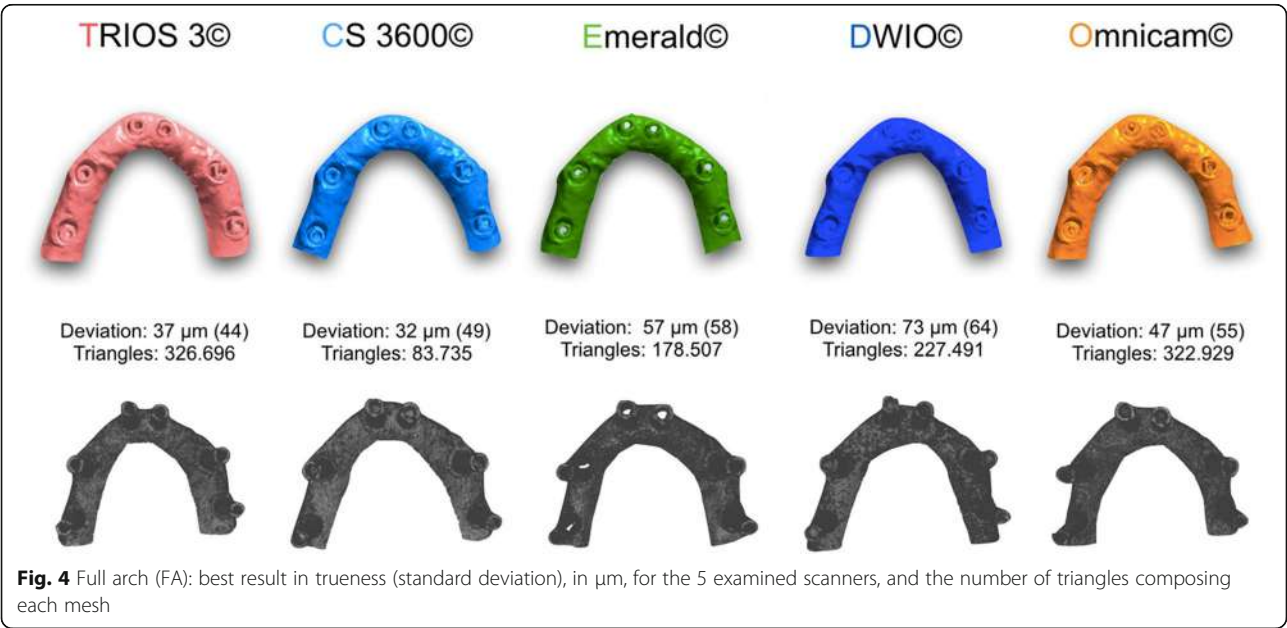
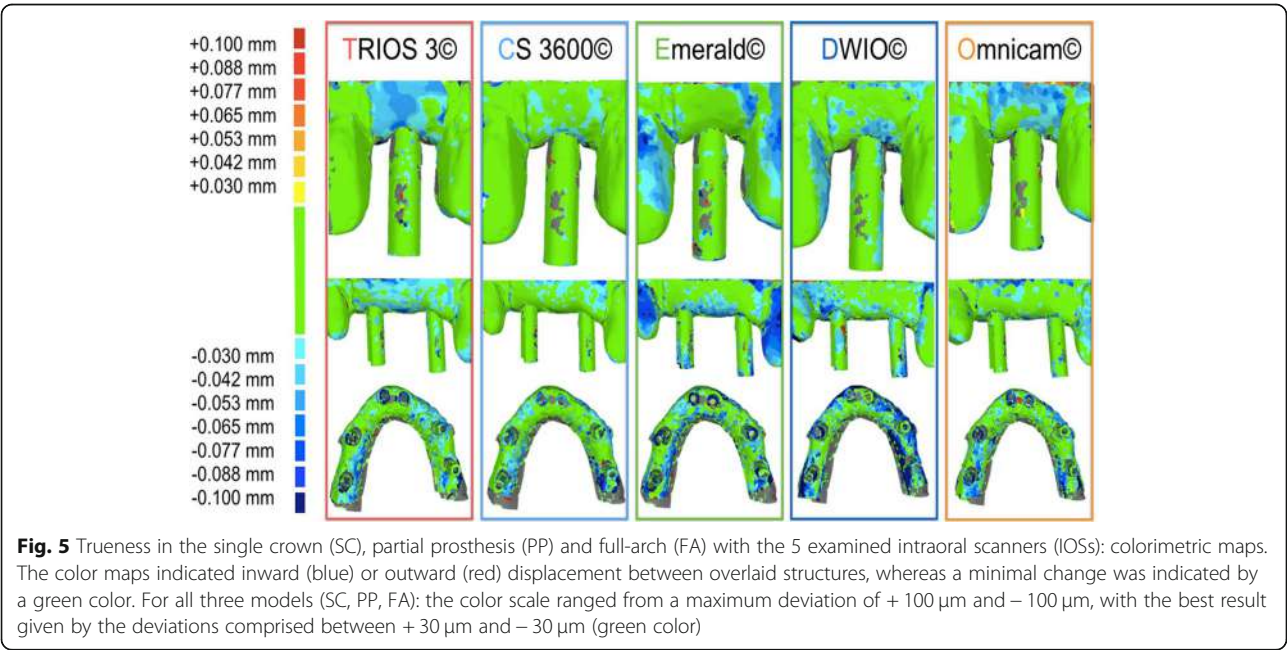


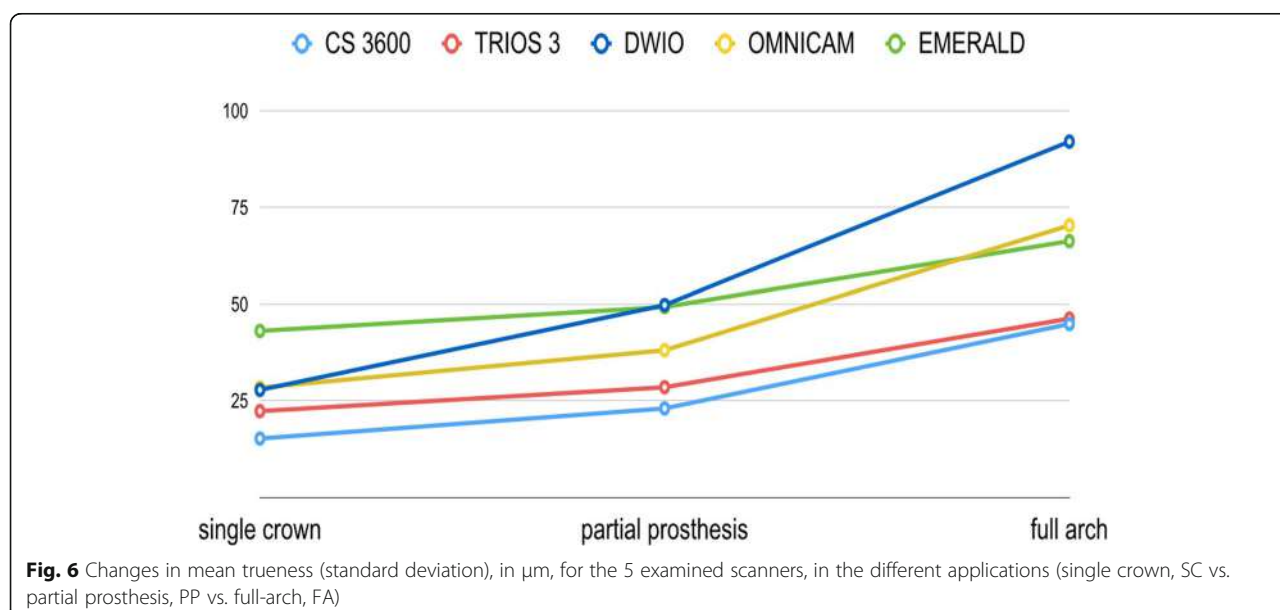
Fig. 3 Partial prosthesis (PP): best result in trueness (standard deviation), in μm , for the 5 examined scanners, and the number of triangles composing each mesh



71.2 μm ; precision 51.0 μm), Zfx Intrascan[®] (trueness 117.0 μm ; precision 126.2 μm), and Planscan[®] (trueness 233.4 μm ; precision 219.8 μm) [10]. The study highlighted statistically significant differences between the different IOSs in the PEM, as well as in the TEM [10]. In the TEM, CS 3500[®] had the best performance in terms of general trueness (63.2 μm) and precision (55.2 μm), followed by Trios2[®] (trueness 71.6 μm ; precision 67.0 μm), Zfx Intrascan[®] (trueness 103.0 μm ; precision 112.4 μm), and Planscan[®] (trueness 253.4 μm ; precision 204.2 μm) [10].

More recently, Imburgia and colleagues have published another in vitro study with a similar structure and setting [9], comparing four different and modern IOSs (CS 3600[®], Trios3[®], Omnicam[®], and TrueDefinition[®]). The authors prepared models with (respectively) three (partially edentulous model, PEM) and six implant analogs (totally edentulous model, TEM), on which PEEK scanbodies were screwed. Once again, the models were scanned with an industrial scanner to obtain. STL files of reference, onto which the individual intraoral scans captured with the different IOSs were superimposed, in





order to evaluate trueness [9]; finally, the IOS models were superimposed on each other within groups, to determine precision. At the end of the study, CS3600° had the best trueness ($45.8 \pm 1.6 \mu\text{m}$) in the PEM, followed by Trios3° ($50.2 \pm 2.5 \mu\text{m}$), Omnicam° ($58.8 \pm 1.6 \mu\text{m}$), and TrueDefinition° ($61.4 \pm 3.0 \mu\text{m}$) [9]. In the TEM, CS 3600° had the best trueness ($60.6 \pm 11.7 \mu\text{m}$), followed by Omnicam° ($66.4 \pm 3.9 \mu\text{m}$), Trios3° ($67.2 \pm 6.9 \mu\text{m}$), and TrueDefinition° ($106.4 \pm 23.1 \mu\text{m}$) [9]. With regard to precision, TrueDefinition° had the best precision ($19.5 \pm 3.1 \mu\text{m}$) in the PEM, followed by Trios3° ($24.5 \pm 3.7 \mu\text{m}$), CS 3600° ($24.8 \pm 4.6 \mu\text{m}$), and Omnicam° ($26.3 \pm 1.5 \mu\text{m}$); conversely, in the TEM, Trios3° had the best precision ($31.5 \pm 9.8 \mu\text{m}$), followed by Omnicam° ($57.2 \pm 9.1 \mu\text{m}$), CS 3600° ($65.5 \pm 16.7 \mu\text{m}$), and TrueDefinition° ($75.3 \pm 43.8 \mu\text{m}$) [9]. The study revealed statistically significant differences between the various IOSs examined, both in terms of trueness and precision; moreover, differences were found among the different applications, with the best results obtained for the PEM when compared to the TEM. This confirms the evidence emerging from

previous studies in the literature [11, 26–28] that have shown how the error in the intraoral scan increases progressively with the increase of the scanned area.

In our present in vitro study, which represents the evolution of the aforementioned studies [9, 10], all IOSs showed high trueness, and a rather small deviation from the RM, in the single implant scan. In fact, four out of five scanners (CS 3600°, Trios3°, DWIO°, and Omnicam°) showed an error below the critical threshold, set at $30 \mu\text{m}$. In particular, CS 3600° had a mean error of $15.2 \mu\text{m}$ (± 0.8), followed by Trios3° ($22.3 \pm 0.5 \mu\text{m}$), DWIO° ($27.8 \pm 3.2 \mu\text{m}$), and Omnicam° ($28.4 \pm 4.5 \mu\text{m}$). Furthermore, the SDs or variations within each of the groups were very small, confirming a high reliability and repeatability of results, in the single implant scan. In this specific application, only the Emerald° scanner had a mean error of more than $30 \mu\text{m}$, with an average truth value of $43.1 \mu\text{m}$ and a rather high SD (11.5). However, this error is in any case compatible with the design (and thus the manufacture and clinical application) of an implant-supported SC. In any case, already from the SC,

Table 3 Mean precision and its standard deviation (SD) in micrometers (μm) with single crown (SC), partial prosthesis (PP) and full-arch (FA), and p values testing the scanner by context interaction. $N = 10$ scans for each scanner and implant type

Scanner	Single Crown (SC) Mean \pm SD	Partial prosthesis (PP) Mean \pm SD	Full arch (FA) Mean \pm SD	p -value ¹
Trios 3°	$15.2 \pm 0.8 \dagger, \ddagger, \bullet$	$21.0 \pm 1.9 \ddagger, \bullet$	$35.6 \pm 3.4 \dagger, \ddagger, \bullet$	<.0001
CS 3600°	$11.3 \pm 1.1 \wedge, \S, \#$	$17.0 \pm 2.3 \wedge, \S, \#$	$35.7 \pm 4.3 \wedge, \S, \#$	<.0001
Emerald°	$32.8 \pm 10.7 \dagger, \wedge$	$29.9 \pm 8.9 \wedge, ^\circ$	$61.5 \pm 18.1 \dagger, \wedge, ^\circ, *$	0.0007
DWIO°	$27.1 \pm 10.7 \ddagger, \S$	$34.8 \pm 10.8 \ddagger, \S$	$111.0 \pm 24.8 \ddagger, \S, ^\circ, \S$	<.0001
Omnicam°	$30.6 \pm 3.3 \bullet, \#$	$43.2 \pm 9.4 \bullet, \#, ^\circ$	$89.3 \pm 14.0 \bullet, \#, *, ^\circ, \S$	<.0001

The same symbol after SD indicates differences in precision between scanner pairs (Tukey-adjustment for multiple comparison). Minimum significant difference across scanners: $8.8 \mu\text{m}$, $9.8 \mu\text{m}$, $19.4 \mu\text{m}$ for single crown (SC), partial prosthesis (PP) and full arch (FA), respectively. ¹ p -value testing the interaction between scanner and context (SC vs. PP vs. FA) from non-parametric, Kruskal-Wallis test. A p -value > 0.05 indicates no difference in scanner precision according to the context

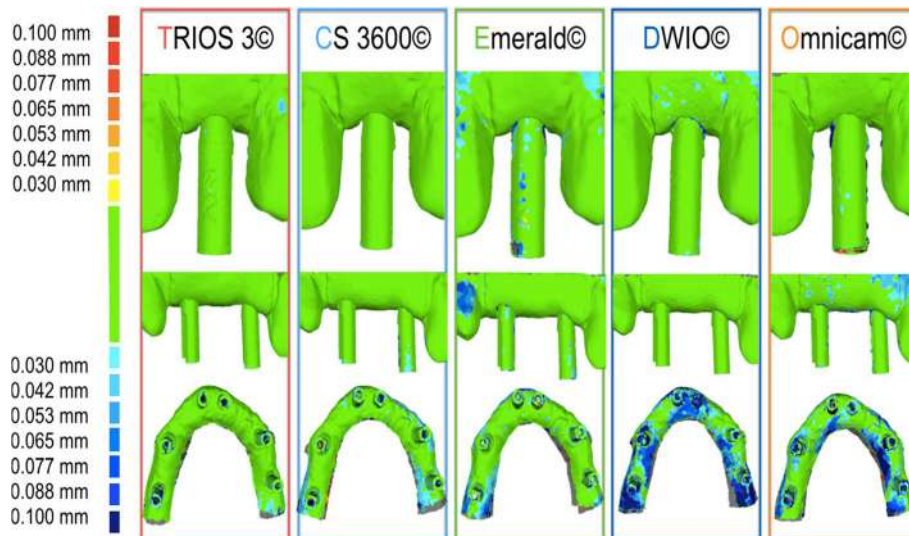


Fig. 7 Precision in the single crown (SC), partial prosthesis (PP) and full-arch (FA) with the 5 examined intraoral scanners (IOs): colorimetric maps. The color maps indicated inward (blue) or outward (red) displacement between overlaid structures, whereas a minimal change was indicated by a green color. For all three models (SC, PP, FA): the color scale ranged from a maximum deviation of + 100 μ m and – 100 μ m, with the best result given by the deviations comprised between + 30 μ m and – 30 μ m (green color)

statistically significant differences were found between the different scanners. In particular CS 3600® was statistically truer than DWIO®, Omnicam®, and Emerald®; moreover Trios3®, DWIO®, and Omnicam® were statistically truer than Emerald. The primacy of CS 3600® and Trios3® was also confirmed by the results obtained in the scan on two implants, for the design of a bridge of three elements (PP). In fact, in trueness, CS 3600® had a mean error of 23.0 μ m (± 1.1), with Trios3® showing a slightly higher error (28.5 ± 0.5 μ m). The stability of the result within the 10 measurements for each of these two scanners was remarkable; both, among other things,

presented for this specific application an error lower than the critical threshold of 30 μ m. Omnicam® followed, with an error of 38.1 μ m (± 8.8), while Emerald® (49.3 ± 5.5 μ m) and DWIO® (49.8 ± 5.0 μ m), practically paired, were more distant. From the statistical point of view, once again, there were clear differences between the scanners analyzed. In particular, CS 3600® and Trios3® were statistically truer than Omnicam®, Emerald®, and DWIO®; moreover, Omnicam® was statistically truer than Emerald® and DWIO®. Globally, in any case, these results were, for all the scanners, compatible at least in theory (and without prejudice to the subsequent error in the

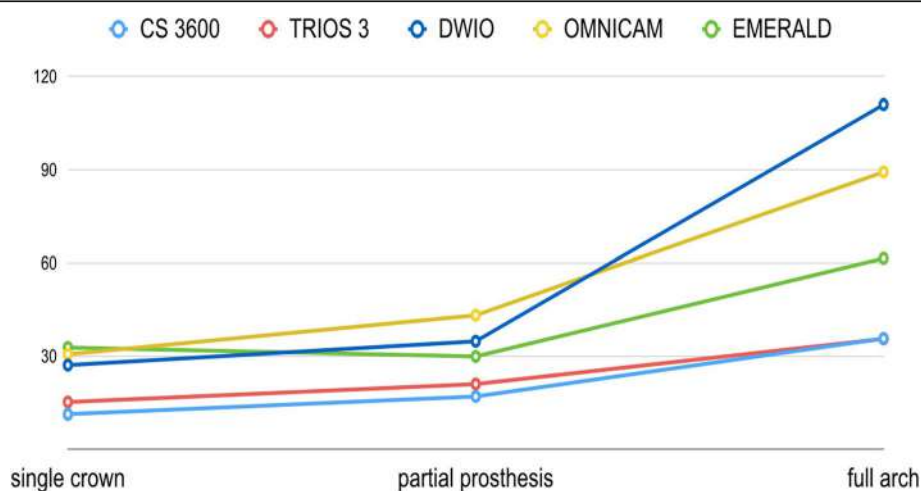


Fig. 8 Changes in mean precision (standard deviation), in μ m, for the 5 examined scanners, in the different applications (single crown, SC vs. partial prosthesis, PP vs. full-arch, FA)

CAM phase) with the fabrication of a bridge of three elements. It was rather interesting to evaluate how, in all the IOSs, the error grew with the passage from a single implant scan to a scan of two implants. The average error growth was $6.2\ \mu\text{m}$ (Trios 3° and Emerald°), $7.8\ \mu\text{m}$ (CS 3600°), $9.7\ \mu\text{m}$ (Omnicam°), and $22\ \mu\text{m}$ (DWIO°), respectively. Evidently, all the IOSs showed a good stability of result, in terms of trueness, in the transition from a single implant scan to a scan of two implants; the only scanner that seemed to present more difficulties in this sense was DWIO, with a greater gap than all the others. From the statistical point of view, anyway, there was a significant difference between a single implant and two implants, for all the scanners. Finally, in the scan of six implants for the design and manufacture of a fixed FA prosthesis, the best result in trueness was that of the CS 3600° ($44.9 \pm 8.9\ \mu\text{m}$), which was confirmed as the best scanner for this application, followed very closely by Trios3° ($46.3 \pm 4.9\ \mu\text{m}$). Surprising, then (although detached from the first two), was the result of Emerald°, with a trueness in the acquisition of six implants in the completely edentulous patient of $66.3\ \mu\text{m}$ (± 5.6). Omnicam° ($70.4 \pm 11.8\ \mu\text{m}$) and DWIO° ($92.1 \pm 24.1\ \mu\text{m}$) followed that; due to the greater error and the poor repeatability of results, these two scanners appeared the most difficult to use for the manufacture of a FA prosthesis. In light of all this, from a statistical point of view, CS 3600° and Trios3° were statistically truer than Emerald°, Omnicam°, and DWIO°; while Emerald° and Omnicam° were statistically truer than DWIO°. Once again, it was also interesting to evaluate the difference between the scan on two implants (for the design of a three-unit bridge) and the scan on six implants (for the design of a FA fixed prosthesis). In this sense, the average error in all IOSs increased (respectively) by $17\ \mu\text{m}$ (Emerald°), $17.8\ \mu\text{m}$ (Trios3°), $21.9\ \mu\text{m}$ (CS 3600°), $32.3\ \mu\text{m}$ (Omnicam°), and $42.3\ \mu\text{m}$ (DWIO°). With regard to this, the best result was achieved by Emerald°, which confirmed a pattern of high stability in the comparison between quality of different scans (single implant vs. two implants vs. six implants), closely followed by Trios3°. In any event, there was a significant difference between two and six implants, for all the scanners.

What, then, are the main evidences that emerge from this study, at the level of trueness? First of all is the exceptional performance of all IOSs investigated in scanning for SCs and short-span restorations on implants. The results obtained in the present study are in fact fully compatible with the realization, through a careful digital workflow in the subsequent CAD and CAM phases, of high-quality restorations with satisfactory marginal gaps. Only in the TEM model did the results seem not yet fully compatible with the realization of a FA, as also reported in the literature [20, 21]. However, if we compare

the trueness of CS 3600° and Trios3° in the FA, in the present study, with the results obtained in the previous work of Imburgia and colleagues [9], we note how the improvements introduced by the new versions of the acquisition software of these scanners are substantial: the error is reduced from $60\ \mu\text{m}$ to $44\ \mu\text{m}$ for CS 3600° and from $67\ \mu\text{m}$ to $46\ \mu\text{m}$ for Trios3°. Conversely, from the comparative analysis of the results obtained in the present study with those reported by Imburgia and colleagues [9], it emerges that the results obtained by Omnicam are stable; this is obvious since the version of the acquisition software used is identical in the two studies. Planmeca, instead, made a decisive leap forward with the new hardware (Emerald°) compared to the previous scanner (Planscan°). Finally, a last interesting element that emerges from the present study is how the accuracy does not seem to be related in any way to the resolution of acquisition. In fact, the CS 3600° was the most accurate scanner, but also the one with the lowest acquisition resolution (fewer triangles making up the meshes, in all applications). In implantology the number of triangles that make up the mesh seems to be of lesser importance than accuracy: the optical impression aims to capture a position [13]. With natural teeth is different: in that context, a higher resolution of acquisition contributes to making visible the margin of the prosthetic preparation [12].

From the point of view of precision, the results were excellent for all IOSs, at least for SC and PP, with minimal errors, and were contained within the $30\text{-}\mu\text{m}$ range. Only Omnicam° ($30.6 \pm 3.3\ \mu\text{m}$) and Emerald° ($32.8 \pm 10.7\ \mu\text{m}$) showed deviations slightly higher than $30\ \mu\text{m}$ in the SC; in the PP, they were DWIO° ($34.8 \pm 10.8\ \mu\text{m}$) and Omnicam° ($43.2 \pm 9.4\ \mu\text{m}$) to deviate beyond the $30\text{-}\mu\text{m}$ threshold. Deviations grew, of course, in the FA, where all the IOSs showed errors of more than $30\ \mu\text{m}$. These errors were contained for Trios3° ($35.6 \pm 3.4\ \mu\text{m}$) and CS 3600° ($35.7 \pm 4.3\ \mu\text{m}$), more marked for Emerald° ($61.5 \pm 18.1\ \mu\text{m}$), Omnicam° ($89.3 \pm 14\ \mu\text{m}$), and DWIO° ($111 \pm 24.8\ \mu\text{m}$). Even in precision, statistically significant differences emerged between the different machines examined.

Our study has limits. First of all, it is an *in vitro* study. Although it is not possible, to date, to determine the trueness and therefore the accuracy of an IOS *in vivo*, it should not be forgotten that there are important factors that can differentiate the quality of a scan on a plaster model from that of a scan in the patient's mouth. Variations in measurements between *in vitro* and *in vivo* may be important and depend not only on the presence of blood and saliva, but above all on the technical difficulty of the intraoral acquisition, as well as on the patient's movements and the peculiar optical behavior of dental tissues [30–32]. The teeth, being made of enamel and

dentin, have a different optical behavior from that of gypsum models; this does not help the IOS in reading and rebuilding the mesh. In a recent study, Albdour et al. [33] cautioned that the trueness of the IOS in vivo may be less than that shown in vitro (on plaster models). Although these considerations are probably of greater importance when capturing the impression on the natural tooth (with implants we mainly capture the position of scanbodies, made of PEEK), we must not forget that the presence of adequate contact points is key in prosthetic rehabilitation with implant-supported SCs or fixed PP. Another limitation of the present study is our having used an optical desktop scanner as a tool for capturing RMs. This desktop scanner, although of an industrial derivation and with a certified accuracy of 5 µm, does not have the same accuracy as a probe. Furthermore, another limit of the present study could be the scanning strategy. The scanning method used (zig-zag) could be more suitable for some of the IOSs analyzed in this study, while penalizing others; however, since neither the literature [11, 34] nor the companies themselves provide details on the ideal scanning strategy, in this paper we have extended the same protocol to all IOSs analyzed. Finally, an inherent limitation of all comparative studies on IOSs is the fact that a new acquisition software release is sufficient to improve (or worsen) the accuracy of a machine considerably. As companies continue to improve their products and release new software, it is possible that our current study may not reflect the accuracy of the most up-to-date machines currently on the market. To overcome this problem, however, we have specified in the text (under Methods) the version of the acquisition software used for each scanner. Moreover, in our present work, only 5 IOSs have been evaluated, while new machines are introduced on the market every month, with more than 20 scanners already available today. Ideally, a comprehensive study should include as many IOSs already on the market as possible. However, for reasons of time, and given the great amount of data to be processed, in this work we limited ourselves to 5 IOSs that we considered modern, deliberately excluding the older devices that used powder to capture the mesh. This was a precise choice, due to the fact that powder represents a major limitation in terms of accuracy and clinical use [35]; nevertheless, we are aware of the fact that new machines recently introduced on the market—for example the Primescan® from Dentsply-Sirona, the Trios4® from 3-Shape, the CS 3700® from Carestream, the Virtuo-Vivo® from Dentalwings or the Korean scanner Medit i500®—must necessarily be studied, in order to understand the real mathematical reliability and whether they can ensure further technological advancement to digital dentistry. The analysis of the new machines introduced to the market can and should be the subject of the next comparative studies of IOSs.

Conclusions

Since only a few studies have compared the accuracy of different IOSs in implantology, the aim of our present in vitro work was to compare the trueness and precision of 5 different scanners in the impressions of single and multiple implants. Hence, two plaster models were prepared, representative of three clinical situations: a single crown (SC), a partial prosthesis (PP), and a full-arch (FA). These models were scanned with a desktop scanner, to capture reference models (RMs), and then with different 5 IOSs (CS 3600®, Trios3®, Omnicam®, DWIO®, Emerald®); 10 scans were taken for each model, using each IOS. All IOS datasets were loaded into reverse-engineering software where they were superimposed on the corresponding RMs, to evaluate trueness, and superimposed on each other within groups, to determine precision. At the end of the study, the five IOSs examined showed significant differences between them; in addition, the mathematical error increased in the transition from SC to PP up to FA. Both these data seem to confirm what reported in the literature, and this has relevant clinical implications because from this study we can draw indications for the use of different IOSs, in different clinical contexts. However, we must not forget that this is an in vitro study, and the evidence emerging from this work must be confirmed in the clinics.

Abbreviations

CAD: Computer-assisted-design; CAM: Computer-assisted-manufacturing; CBCT: Cone beam computer tomography; CMM: Coordinate measuring machine; FA: Full-arch; IOS: Intraoral scanner; PEEK: Polyether-ether-ketone; PEM: Partially edentulous model; PP: Partial prosthesis; RCP: Robust-iterative-closest-point; RM: Reference model; SC: Single crown; SD: Standard deviation; SSS: Stable scan stage; STL: Standard triangulation language; TEM: Totally edentulous model

Acknowledgements

The authors are grateful to Megagen implants, for having provided free of charge to authors the PEEK scanbodies and implant analogs and used in the present study.

Authors' contributions

All authors made substantial contributions to the present study. In details, UH prepared and provided the two stone cast models (a partially and a totally edentulous maxilla, respectively). FM contributed to conception and design of the study, acquisition of data (he acquired all data with the different IOSs), analysis and interpretation of data; he was, moreover, involved in writing and editing the manuscript. GV made the statistical evaluation, therefore he analyzed and interpreted all data. MI acquired the data with the reference desktop scanner. CM and OA revised the manuscript before submission. All authors read and approved the final manuscript.

Funding

The present in vitro study was not funded, nor supported by any grant. All the scanners and materials used here belonged to the authors, and nothing was provided by third-parts or private Companies: therefore, the authors have no conflict of interest related to the present work.

Availability of data and materials

The .STL files and the 3D surface models obtained in this study with the different five IOS as well as the reference files obtained with the desktop scanner belong to the authors, and are therefore available only upon reasonable request, after approval by all the authors.

Ethics approval and consent to participate

No patient data was used here, and no patients did contribute in any way to the present in vitro study; therefore, not Ethics Committee approval nor consent to participate was requested for this research.

Consent for publication

Not applicable.

Competing interests

The authors declare that they have no competing interests in relation to the present study. Francesco Mangano is a Section Editor for BMC Oral Health.

Author details

¹Department of Prevention and Communal Dentistry, Sechenov First Moscow State Medical University, Moscow, Russia. ²Department of Post-graduate Education, Faculty of Oral and Dental Medicine, J.W. Goethe University, Frankfurt, Germany. ³Department of Medicine and Surgery, Research Center in Epidemiology and Preventive Medicine, University of Varese, Varese, Italy. ⁴Private Practice, Palermo, Italy. ⁵Department of Dental Sciences, Vita and Salute University San Raffaele, Milan, Italy. ⁶Department of Prevention and Communal Dentistry, Sechenov First Moscow State Medical University, Moscow, Russia.

Received: 11 March 2019 Accepted: 20 May 2019

Published online: 06 June 2019

References

- Mangano F, Gandolfi A, Luongo G, Logozzo S. Intraoral scanners in dentistry: a review of the current literature. *BMC Oral Health*. 2017;17(1):149.
- Joda T, Zarone F, Ferrari M. The complete digital workflow in fixed prosthodontics: a systematic review. *BMC Oral Health*. 2017;17(1):124.
- Mangano F, Veronesi G. Digital versus Analog Procedures for the Prosthetic Restoration of Single Implants: A Randomized Controlled Trial with 1 Year of Follow-Up. *Biomed Res Int*. 2018;2018:5325032.
- Porter JL, Carrico CK, Lindauer SJ, Tüfekçi E. Comparison of intraoral and extraoral scanners on the accuracy of digital model articulation. *J Orthod*. 2018;45(4):275–82.
- Mangano FG, Hauschild U, Admakin O. Full in-Office Guided Surgery with Open Selective Tooth-Supported Templates: A Prospective Clinical Study on 20 Patients. *Int J Environ Res Public Health*. 2018;15(11).
- Lee H, Cha J, Chun YS, Kim M. Comparison of the occlusal contact area of virtual models and actual models: a comparative in vitro study on Class I and Class II malocclusion models. *BMC Oral Health*. 2018;18(1):109.
- Mühlemann S, Kraus RD, Hämmerle CHF, Thoma DS. Is the use of digital technologies for the fabrication of implant-supported reconstructions more efficient and/or more effective than conventional techniques: A systematic review. *Clin Oral Implants Res*. 2018;29(Suppl 18):184–95.
- Abduo J, Elseyoufi M. Accuracy of Intraoral Scanners: A Systematic Review of Influencing Factors. *Eur J Prosthodont Restor Dent*. 2018;26(3):101–21.
- Imburgia M, Logozzo S, Hauschild U, Veronesi G, Mangano C, Mangano FG. Accuracy of four intraoral scanners in oral implantology: a comparative in vitro study. *BMC Oral Health*. 2017;17(1):92.
- Mangano FG, Veronesi G, Hauschild U, Mijiritsky E, Mangano C. Trueness and precision of four intraoral scanners in Oral Implantology: a comparative in vitro study. *PLoS One*. 2016;11(9):e0163107.
- Medina-Sotomayor P, Pascual MA, Camps AI. Accuracy of four digital scanners according to scanning strategy in complete-arch impressions. *PLoS One*. 2018;13(9):e0202916.
- Nedelcu R, Olsson P, Nyström I, Thor A. Finish line distinctness and accuracy in 7 intraoral scanners versus conventional impression: an in vitro descriptive comparison. *BMC Oral Health*. 2018;18(1):27.
- Mangano F, Margiani B, Admakin O. A Novel Full-Digital Protocol (SCAN-PLAN-MAKE-DONE) for the Design and Fabrication of Implant-Supported Monolithic Translucent Zirconia Crowns Cemented on Customized Hybrid Abutments: A Retrospective Clinical Study on 25 Patients. *Int J Environ Res Public Health*. 2019;16(3).
- Joda T, Ferrari M, Bragger U, Zitzmann NU. Patient Reported Outcome Measures (PROMs) of posterior single-implant crowns using digital workflows: A randomized controlled trial with a three-year follow-up. *Clin Oral Implants Res*. 2018;29(9):954–61.
- Joda T, Ferrari M, Bragger U. Monolithic implant-supported lithium disilicate (LS2) crowns in a complete digital workflow: a prospective clinical trial with a 2-year follow-up. *Clin Implant Dent Relat Res*. 2017;19(3):505–11.
- Joda T, Bragger U, Zitzmann NU. CAD/CAM implant crowns in a digital workflow: five-year follow-up of a prospective clinical trial. *Clin Implant Dent Relat Res*. 2019;21(1):169–74.
- Spies BC, Pieralli S, Vach K, Kohal RJ. CAD/CAM-fabricated ceramic implant-supported single crowns made from lithium disilicate: final results of a 5-year prospective cohort study. *Clin Implant Dent Relat Res*. 2017;19(5):876–83.
- Ferrini F, Capparé P, Vinci R, Gherlone EF, Sannino G. Digital versus traditional workflow for posterior maxillary rehabilitations supported by one straight and one tilted implant: a 3-year prospective comparative study. *Biomed Res Int*. 2018;2018:4149107.
- Gherlone EF, Ferrini F, Crespi R, Gastaldi G, Capparé P. Digital impressions for fabrication of definitive “all-on-four” restorations. *Implant Dent*. 2015;24(1):125–9.
- Alikhasi M, Alsharbaty MHM, Moharrami M. Digital implant impression technique accuracy: a systematic review. *Implant Dent*. 2017;26(6):929–35.
- Khraishi H, Duane B. Evidence for use of intraoral scanners under clinical conditions for obtaining full-arch digital impressions is insufficient. *Evid Based Dent*. 2017;18(1):24–5.
- Ahlholm P, Sipilä K, Vallittu P, Jakonen M, Kotiranta U. Digital versus conventional impressions in fixed prosthodontics: a review. *J Prosthodont*. 2018;27(1):35–41.
- Güth JF, Runkel C, Beuer F, Stimmelmayer M, Edelhoff D, Keul C. Accuracy of five intraoral scanners compared to indirect digitalization. *Clin Oral Investig*. 2017;21(5):1445–55.
- Nedelcu R, Olsson P, Nyström I, Rydén J, Thor A. Accuracy and precision of 3 intraoral scanners and accuracy of conventional impressions: A novel in vivo analysis method. *J Dent*. 2018;69:110–8.
- Patzelt SB, Emmanouilidi A, Stampf S, Strub JR, Att W. Accuracy of full-arch scans using intraoral scanners. *Clin Oral Investig*. 2014;18(6):1687–94.
- Ajioka H, Kihara H, Odaira C, Kobayashi T, Kondo H. Examination of the position accuracy of implant abutments reproduced by intra-Oral optical impression. *PLoS One*. 2016;11(10):e0164048.
- van der Meer WJ, Andriessen FS, Wismeijer D, Ren Y. Application of intra-oral dental scanners in the digital workflow of implantology. *PLoS One*. 2012;7(8):e43312.
- Chew AA, Esguerra RJ, Teoh KH, Wong KM, Ng SD, Tan KB. Three-dimensional accuracy of digital implant impressions: effects of different scanners and implant level. *Int J Oral Maxillofac Implants*. 2017;32(1):70–80.
- Najeeb S, Zafar MS, Khurshid Z, Siddiqui F. Applications of polyetheretherketone (PEEK) in oral implantology and prosthodontics. *J Prosthodont Res*. 2016;60(1):12–9.
- Logozzo S, Zanetti EM, Franceschini G, Kilpela A, Makynen A. Recent advances in dental optics – part I: 3D intraoral scanners for restorative dentistry. *Optic Lasers Eng*. 2014;54(3):203–21.
- Elgendy H, Maia RR, Skiff F, Denehy G, Qian F. Comparison of light propagation in dental tissues and nano-filled resin-based composite. *Clin Oral Investig*. 2019;23(1):423–33.
- Volpato CAM, Pereira MRC, Silva FS. Fluorescence of natural teeth and restorative materials, methods for analysis and quantification: A literature review. *J Esthet Restor Dent*. 2018;30(5):397–407.
- Albdour EA, Shaheen E, Vranckx M, Mangano FG, Politis C, Jacobs R. A novel in vivo method to evaluate trueness of digital impressions. *BMC Oral Health*. 2018;18(1):117.
- Kim RJ, Park JM, Shim JS. Accuracy of 9 intraoral scanners for complete-arch image acquisition: A qualitative and quantitative evaluation. *J Prosthet Dent*. 2018;120(6):895–903.e1.
- Prudente MS, Davi LR, Nabbout KO, Prado CJ, Pereira LM, Zancopé K, Neves FD. Influence of scanner, powder application, and adjustments on CAD-CAM crown misfit. *J Prosthet Dent*. 2018;119(3):377–83.

Publisher's Note

Springer Nature remains neutral with regard to jurisdictional claims in published maps and institutional affiliations.

RESEARCH ARTICLE

Open Access



An in vitro evaluation of marginal fit zirconia crowns fabricated by a CAD-CAM dental laboratory and a milling center

Avi Meirowitz^{1†}, Yoli Bitterman^{2*†}, Sharon Levy¹, Eitan Mijiritsky³ and Eran Dolev¹

Abstract

Background: Marginal fit is critical for the success and longevity of a dental restoration. Zirconia crowns can be fabricated either chair-side, in a dental laboratory or in a milling center; each can give different marginal fits results. However, discussion of the marginal fit of zirconia crowns when different fabrication methods are compared is lacking in the literature.

Purpose: To compare the marginal discrepancy (MD) and absolute marginal discrepancy (AMD) of computer-aided design, and computer-aided manufacturing (CAD-CAM) used in a dental laboratory and a milling center for producing monolithic zirconia crowns.

Methods: The marginal fit of 30 zirconia crowns cemented to typodont teeth was evaluated by means of a sectioning technique. Fifteen crowns were fabricated with a CEREC inLAB MC X5 from IPS e.max ZirCAD blocks. Fifteen crowns were fabricated using a LAVA milling center from LAVA Plus Zirconia Blocks. The 30 crowns were sectioned with a precision saw, and MD and AMD were subsequently measured using a light microscope. Data were analyzed using the one-way ANOVA technique to investigate significant differences in the marginal fit between the two fabrication systems ($\alpha = .05$).

Results: The AMD dimension of the CEREC inLAB system was significantly smaller ($P < .05$). Mean AMD values for zirconia crowns fabricated by the CEREC inLAB were 85 μm , and for the LAVA milling center 133 μm . There was no significant difference between the two systems regarding the MD dimensions. The MD values for zirconia crowns fabricated by the CEREC inLAB were 53 μm and for the LAVA milling center 61 μm .

Conclusions: The CEREC inLAB system demonstrated significantly better marginal fit in relation to the AMD. However, no difference between the systems was found in the MD. Monolithic zirconia crowns fabricated by the CAD-CAM CEREC inLAB system and the LAVA system milling center showed MD values of less than 120 μm , which is within the clinically acceptable range.

Keywords: CAD-CAM, Zirconia, Crown, Marginal fit, CEREC, LAVA

Background

In recent decades, increasing demand from patients for natural-appearing dental restorations has led to the development of all-ceramic materials with improved mechanical characteristics that ensure suitable longevity. These are now replacing traditional metal-ceramic restorations

[1–3]. The introduction of CAD-CAM technology allows for the use of materials such as zirconia, which is free of metal, in dental restorations [1].

Zirconia is a polycrystalline ceramic without a glassy phase and exists in several temperature-dependent forms. At room temperature, it exists in a monoclinic crystalline form, changing to a tetragonal and cubic crystalline form when sintered [4]. The cooling from cubic to tetragonal results in an expansion of 2.3% and from tetragonal to monoclinic of 4.2%. These expansions are the cause of cracks and hence there is a need to stabilize

* Correspondence: Dr.bitterman@gmail.com; dr.bitterman@gmail.com

[†]Avi Meirowitz and Yoli Bitterman contributed equally to this work.

²Department of Orthodontics, Goldschleger School of Dental Medicine, The Sackler Faculty of Medicine, Tel Aviv University, 69978 Tel – Aviv, Israel

Full list of author information is available at the end of the article



© The Author(s). 2019 **Open Access** This article is distributed under the terms of the Creative Commons Attribution 4.0 International License (<http://creativecommons.org/licenses/by/4.0/>), which permits unrestricted use, distribution, and reproduction in any medium, provided you give appropriate credit to the original author(s) and the source, provide a link to the Creative Commons license, and indicate if changes were made. The Creative Commons Public Domain Dedication waiver (<http://creativecommons.org/publicdomain/zero/1.0/>) applies to the data made available in this article, unless otherwise stated.

the tetragonal form. The most common method of stabilizing the tetragonal phase and maintaining zirconia in a metastable condition at room temperature is achieved via the addition of a small amount of yttria to the zirconia [3–5]. Such treatment produces a stronger material than other available ceramics. The zirconia is a biocompatible material with high mechanical properties of 1200 HV hardness, 900–1200 MPa flexural strength and fracture toughness of 6–8 MPa m^{1/2} [6, 7].

Zirconia restorations fabricated by CAD-CAM technology can be produced chair-side, in a laboratory or in a milling center. The restorations are processed either by soft machining of pre-sintered blanks with enlarged contours followed by sintering at high temperature during which they shrink to their desired and final size, or by hard machining of fully sintered blocks [8].

Superior marginal fit is an important characteristic for the success and longevity of dental restorations. Poor marginal fit results in plaque retention and microleakage; this can lead to secondary dental caries, pulpal lesions, periodontal disease, and bone loss [9, 10]. Although dental literature includes significant investigation of the accuracy of marginal fit, there is no consensus on the maximum acceptable marginal discrepancy. Marginal discrepancies of between 50 and 120 µm are considered clinically acceptable as regards longevity of the restoration, while more restrictive studies proposed marginal discrepancies of less than 100 µm [11, 12]. An in vivo study of more than 1000 crowns found a greater association between a marginal discrepancy of less than 120 µm and higher longevity [13]. Studies on the marginal fit of zirconia copings fabricated by CAD-CAM have reported measured marginal discrepancies of as low as 10 µm and as high as 160 µm, with most being less than 80 µm [14–16]. With regard to full zirconia crown, the studies show marginal discrepancies between 11 µm to 58 µm [17, 18].

The definition of marginal fit can differ and depends on the gap measured in the studies. Holmes et al. defined the marginal discrepancy (MD) as the perpendicular measurement from the cervical margin of the restoration to the preparation margin, while the AMD is measured from the cervical margin of the restoration to the cavosurface of the preparation [19]. The MD represents the surface of the cement that is exposed to the oral environment and can be dissolved, resulting in microleakage. The AMD is indicative of the under- or over-extension of the restoration margins relative to the margins of the preparation and plays a significant role in plaque accumulation (Fig. 1) [19].

Studies that have compared the marginal fit of zirconia copings to other ceramic restorations show higher accuracy for zirconia [20]. The marginal fit of zirconia copings produced using different CAD-CAM

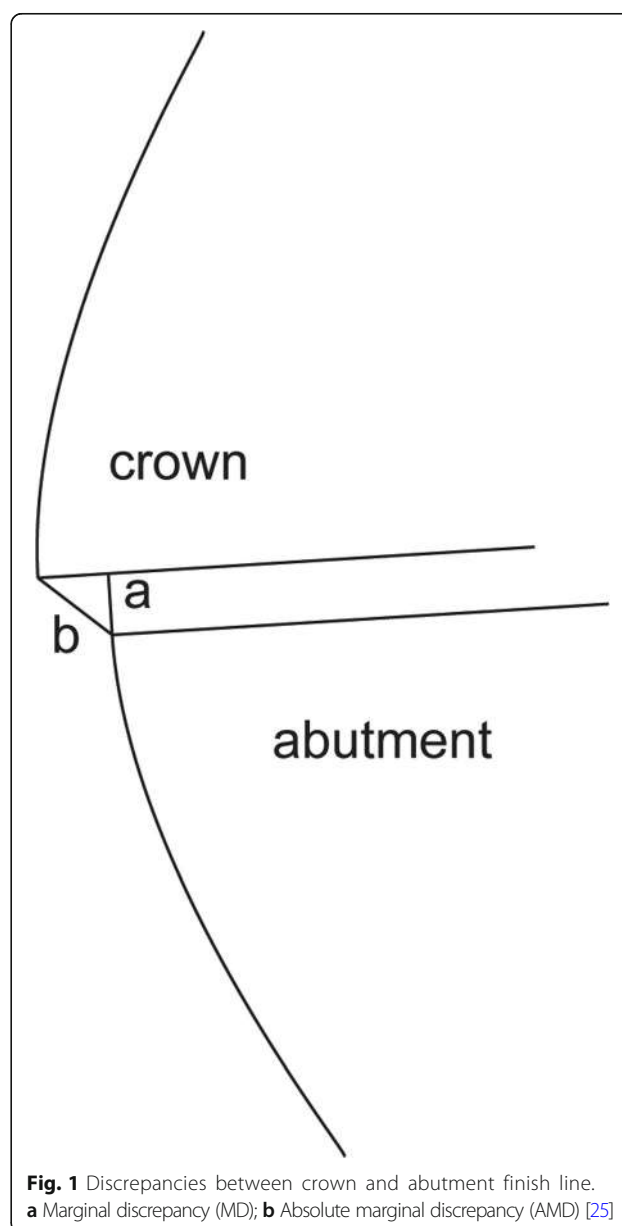


Fig. 1 Discrepancies between crown and abutment finish line. **a** Marginal discrepancy (MD); **b** Absolute marginal discrepancy (AMD) [25]

system has also been investigated [15, 16, 21, 22]. The marginal fit of monolithic zirconia crown was studied with regard to different preparation designs and sintering techniques [17, 18]. However, no studies investigate the effect of different CAD-CAM fabrication methods on the marginal fit of monolithic zirconia crowns; the use of monolithic zirconia crowns is increasing, and therefore a comparison of fabrication methods is justified. The purpose of this in vitro study was thus to compare the marginal fit of monolithic zirconia crowns produced using two fabrication methods: dental laboratory and milling center. The null hypothesis was that no difference would be found in the marginal fit of the fabrication methods.

Many methods exist for the evaluation of marginal fit using non-disruptive methods like silicone paste technique [12], micro-CT scan [20, 23], and disruptive methods, which include sectioning with a disk [21, 24]. In this in vitro study, the sectioning method was used on typodont teeth to investigate the two parameters of marginal fit, AMD and MD.

Material and methods

The following method is the same as that previously published by Dolev et al. and will be described here only briefly [25]. Mandibular left first molar, typodont teeth (FLUX 8634; Columbia Dentoform) were used as abutment. For the CEREC inLAB system group, 15 typodont teeth were scanned with an intraoral scanner (CEREC SW 4.52, CEREC Omnicam scanner; Dentsply Sirona) by dentists with experience using CAD-CAM systems, who also marked the finish line using CAD system (CEREC Connect SW 4.1 software; Dentsply Sirona). The 15 crowns were prepared in a dental laboratory (TOTALI - AMIR LIFF LTD, Tel Aviv, Israel) by master dental technician (MDT). They were formed from partially sintered zirconia blocks (IPS e.max ZirCAD; Ivoclar Vivadent) using a CAM milling unit (CEREC inLAB MC X5; Dentsply Sirona), followed by sintering (Ceramill Therm 1; Amann Girrbach) to produce completely sintered crowns (Fig. 2). The CAD-CAM parameters were as followed: Spacer (radial) – 90 μ m, Spacer occlusal – 100 μ m, Proximal contacts strength – 25 μ m, Minimal thickness (radial) – 700 μ m, Minimal thickness (occlusal) – 1500 μ m, Marginal thickness – 50 μ m, Marginal ramp width – 150 μ m, Marginal ramp angle – 45°. Fifteen typodont teeth were sent to a milling center (LAVA; 3 M ESPE) for scanning (Lava Scan ST; 3 M ESPE) and design (LAVA Design 5; 3 M ESPE). The zirconia crowns were fabricated by partially sintered zirconia blocks (LAVA Plus Zirconia Blocks; 3 M ESPE) using

a CAM milling machine (LAVA Form; 3 M ESPE) followed by sintering (LAVA Furnace 200; 3 M ESPE) for production of the final crowns. The parameters of both the CAD-CAM systems were identical.

The crowns were cemented with self-adhesive resin cement (Rely X U-200; 3 M ESPE) and then sectioned with a cutting machine (Izomet Plus precision saw; Buehler), creating four specimens from each crown: Mesio-Buccal (MB), Disto-Buccal (DB), Disto-Lingual (DL), and Mesio-Lingual (ML). In each specimen, the AMD and MD were measured in two locations (Fig. 3) using a light microscope (Axioplan 2; Zeiss) at $\times 110$ magnification [21].

Repeat measurements using the one-way ANOVA statistical test were carried out ($\alpha = .05$) to examine significant differences between the groups.

Results

Figures 4 and 5 show the mean values with standard errors for the AMD and MD dimensions as measured in 8 locations for crowns fabricated by the CEREC inLAB and LAVA milling center. The CEREC inLAB presented smaller AMD values than the LAVA milling center (Fig. 4). The MD values of CEREC inLAB crowns were smaller than those produced in the LAVA milling center, except for Mid-L/ML, Mid-L/DL, and Mid-M/ML locations (Fig. 5).

The overall mean \pm standard error (SE) value for AMD and MD of the CEREC inLAB and LAVA milling center fabrication methods are presented in Table 1. The statistical outcome showed significant differences for AMD ($df = 1$, $F = 35.081$; $P = .000$) whereas MD yielded no significant differences ($df = 1$, $F = 1.799$; $P = .191$) between CEREC inLAB and the LAVA milling center. The MD 95% confidence intervals are presented in Table 1.



Fig. 2 Lower left first molar typodont tooth and corresponding CEREC inLAB zirconia crown

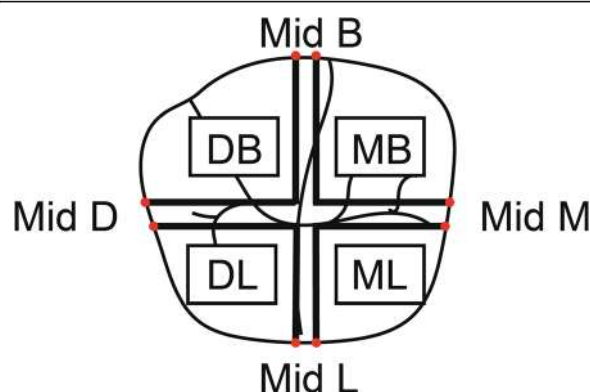


Fig. 3 Illustration of sectioned mandibular left first molar. Colored points demonstrate eight measurement locations of finish line discrepancies

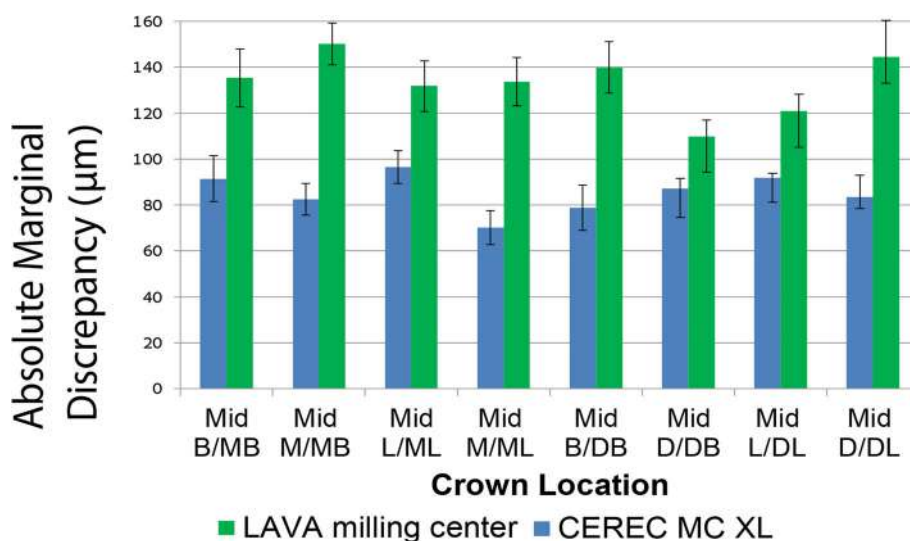


Fig. 4 Comparison of mean values and standard errors of AMD at different marginal area locations for CEREC inLAB system and LAVA milling center crowns

Discussion

In accordance with the study results, the null hypothesis regarding the AMD parameter was rejected, with the dental laboratory using the CEREC inLAB CAD-CAM displaying a significantly lower gap ($85 \pm 2 \mu\text{m}$) compared to the LAVA milling center ($133 \pm 4 \mu\text{m}$). For the MD parameter, the null hypothesis was not rejected since no statistically significant differences were found between the two systems.

Beuer et al. identified significant differences when examining the MD of 3-unit zirconia frameworks [21]. They found a smaller mean MD value in the milling center ($29.1 \mu\text{m}$) than in frameworks produced by CEREC inLAB ($56.6 \mu\text{m}$). However, this study made use of an Etkon milling center and a traditional silicone impression technique rather than an intraoral scanner. Studies that compared marginal fit of zirconia coping found that the CEREC inLAB system showed smaller

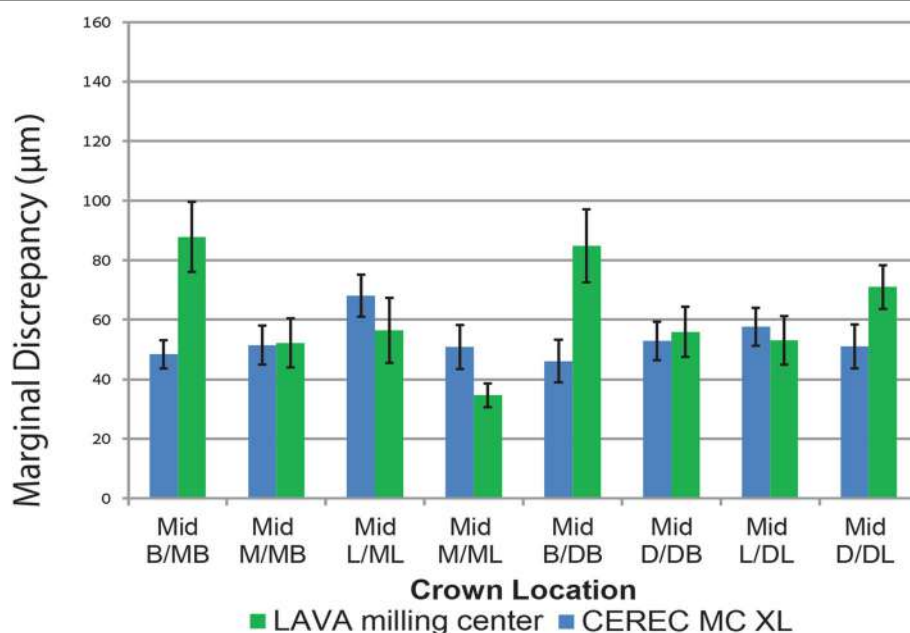


Fig. 5 Comparison of mean values and standard errors of MD at different marginal area locations for CEREC inLAB system and LAVA milling center crowns

Table 1 Overall mean \pm standard error (SE) and 95% confidence intervals of the fabrication methods

	AMD mean \pm SE	MD mean \pm SE	MD 95% confidence intervals-Lower bound	MD 95% confidence intervals-upper bound
CEREC inLAB	85 \pm 2 μm^*	53 \pm 2 μm	43 μm	62 μm
LAVA milling center	133 \pm 4 μm^*	61 \pm 3 μm	52 μm	71 μm

*significant difference

MD values compared to other CAD-CAM systems [15, 16, 22]. Rajan et al. compared the marginal fit of zirconia coping produced by CEREC inLAB with that of the CERAMILL system and found significant differences, whereby CEREC inLAB copings had better adaptation than CERAMILL. For both CAD-CAM systems, a digital scanner was used [22]. Marginal fit for CERAMILL was 83 μm and for the CEREC InLAB MC XL was 68 μm [22]. Saab et al. compared marginal fit of zirconia coping with four different CAD-CAM systems: CEREC inLAB, CERCON, CERAMILL, and LAVA milling unit. They used a specific intraoral scanning device for each of the CAD-CAM systems. CEREC inLAB showed significant lower mean value of MD, 37.68 μm [16]. ArRejaie et al. compared marginal fit of zirconia coping with 3 different CAD-CAM systems: DeguDent, KaVo Everest, and Lava Ultimate. They also digitized their model with an intraoral scanner of the specific CAD-CAM unit. Lava Ultimate showed a significantly lower MD mean value of 112.5, (statistically significant compared to KaVo Everest) [15], this MD value is relatively high compared to previous mentioned studies. Another study by Beuer et al. examined the marginal gap of 3-unit zirconia framework using two different fabrication concepts. One was fabricated by a laboratory system (Circon Brain, DeguDent) and the other in a milling center (Compartis Integrated Systems, DeguDent). In their study, both fabrication systems used a polyether impression technique, the same CAD-CAM system and porous zirconia, but a different milling unit. They found no significant differences between the two fabrication methods regarding the marginal gap [26].

In their systematic review of the fit of zirconia restorations, Abduo et al. [27]. indicated the difficulty in comparing the many studies existing on the marginal gap of zirconia given the different methodology used in each study [27], including the sectioning technique [17, 20], use of microcomputed tomography [20, 23], and silicone paste technique [12]. Additionally, each study examined and compared different parameters of marginal fit, MD and AMD being a few of the many that were described by Holmes et al. [19]. Hence there is a need for standardization.

Crown cementation has been used in the present study to reproduce the clinical conditions of the crown-abutment relationship. Earlier publications have found that crown cementation has a negative effect on the marginal fit, which increases after cementation [23, 28].

McLean and Fraunhofer showed that crown marginal discrepancies ranging up to 120 μm were clinically acceptable [13]. According to the 95% confidence interval, the present study yielded MD values within the clinically acceptable range.

This study examined MD and AMD in four surfaces: buccal, lingual, mesial, and distal. It did not compare those parameters between the different surfaces because this is clinically irrelevant given that this study used model teeth with a constant finish line, in an in-vitro setting.

Several limitations were identified in the study, as follows: The study was conducted in vitro with typodont teeth used as abutments instead of natural teeth, and finger pressure was used to lute the crowns. These characteristics differ from those of the intraoral environment. The cemented crowns were cut with a disk, a destructive method, which can have negative effects on the quality of specimens and the reading of marginal fit. Additionally, the cement thickness in the occlusal area that affects the internal marginal fit and the seating quality of the crowns was not measured, and could therefore have influenced the MD. One other limitation is the fact that the two CAD-CAM systems used zirconia blocks manufactured by different companies, which may also have affected the results.

The study revealed that when using a well-known, established CAD-CAM system, zirconia monolithic crowns are a good treatment option as regards marginal fit during tooth restoration. This is of relevance given the popularity of zirconia monolithic crowns as a treatment option. Because these systems are constantly developing with the arrival of new manufacturers, further in vitro and in vivo studies are needed to substantiate these results.

Conclusions

Within the limitations of this study, the following conclusions were drawn:

1. The CEREC inLAB system shows a significantly smaller AMD than the LAVA milling center.
2. No significant difference was found in MD between the systems.
3. Monolithic zirconia crowns fabricated by the CEREC inLAB system and the LAVA milling center produced MD values within the clinically acceptable standard (120 μm).

4. There is a need for standard rules and guidance when comparing marginal fit between different CAD-CAM systems.

Abbreviations

AMD: Absolute marginal discrepancy; CAD-CAM: computer-aided design and computer-aided manufacturing; DB: Disto Buccal; DL: Disto Lingual; MB: Mesio Buccal; MD: Marginal discrepancy; ML: Mesio Lingual; SE: Standard error

Acknowledgements

Not applicable.

Authors' contributions

All the authors made substantial contributions to the present study. AM designed the study, and wrote, reviewed, and edited the report. YB analyzed and interpreted the results and was a major contributor in writing the manuscript. SL performed the experiment. EM performed critical revisions of the paper. ED contributed to conceptualization, methodology, supervision, and writing, review, editing. All authors read and approved the final manuscript.

Funding

The authors have no funding to report.

Availability of data and materials

The datasets used and/or analysed during the current study are available from the corresponding author upon reasonable request.

Ethics approval and consent to participate

Not applicable.

Consent for publication

Not applicable.

Competing interests

The authors declare that they have no competing interests.

Author details

¹Department of Oral Rehabilitation, Goldschleger School of Dental Medicine, The Sackler Faculty of Medicine, Tel Aviv University, Tel Aviv, Israel.

²Department of Orthodontics, Goldschleger School of Dental Medicine, The Sackler Faculty of Medicine, Tel Aviv University, 69978 Tel – Aviv, Israel.

³Sackler Faculty of Medicine, Department of Otolaryngology Head and Neck and Maxillofacial Surgery, Tel-Aviv Sourasky Medical Center, Tel-Aviv University, Tel Aviv, Israel.

Received: 13 February 2019 Accepted: 31 May 2019

Published online: 13 June 2019

References

- Raigrodski AJ, Hillstead MB, Meng GK, Chung KH. Survival and complications of zirconia-based fixed dental prosthesis: a systematic review. *J Prosthet Dent*. 2012;107:170–7 Review.
- Biscaro L, Bonfiglioli R, Soattin M, Vigolo P. An in vivo evaluation of fit of zirconium-oxide based ceramic single crowns, generated with two CAD/CAM systems, in comparison to metal ceramic single crowns. *J Prosthodont*. 2013;22:36–41.
- Zarone F, Russo S, Sorrentino R. From porcelain-fused-to-metal to zirconia: clinical and experimental considerations. *Dent Mater*. 2011;27:83–96.
- Denry I, Kelly JR. State of the art of zirconia for dental applications. *Dent Mater*. 2008;24:299–307.
- Christel P, Meunier A, Heller M, Torre JP, Peille CN. Mechanical properties and short-term in-vivo evaluation of yttrium-oxide-partially-stabilized zirconia. *J Biomed Mater Res*. 1989;23:45–61.
- Piconi C, Maccauro G. Zirconia as a ceramic biomaterial. *Biomaterials*. 1999; 20:1–25.
- Kosmac T, Oblak C, Jevnikar P, Funduk N, Marion L. The effect of surface grinding and sandblasting on flexural strength and reliability of Y-TZP zirconia ceramic. *Dent Mater*. 1999;15:426–33.
- Filser F, Kocher P, Gauckler LJ. Net-shaping of ceramic components by direct ceramic machining. *Assembly Autom*. 2003;23:382–90.
- Sorensen JA. A rationale for comparison of plaque-retaining properties of crown systems. *J Prosthet Dent*. 1989;62:264–9.
- Kashani HG, Khera SC, Gulker IA. The effects of bevel angulation on marginal integrity. *J Am Dent Assoc*. 1981;103:882–5.
- Suárez MJ, González de Villambrosia P, Pradiés G, Lozano JF. Comparison of the marginal fit of procera AllCeram crowns with two finish lines. *Int J Prosthodont*. 2003;16:229–32.
- Coli P, Karlsson S. Fit of a new pressure-sintered zirconium dioxide coping. *Int J Prosthodont*. 2004;17:59–64.
- McLean JW, von Fraunhofer JA. The estimation of cement film thickness by an in vivo technique. *Br Dent J*. 1971;131:107–11.
- Boitelle P, Mawussi B, Tapie L, Fromentin O. A systematic review of CAD/CAM fit restoration evaluations. *J Oral Rehabil*. 2014;41:853–74.
- ArRejaie A, Alalawi H, Al-Harbi FA, Abulsaud R, Al-Thobity AM. Internal fit and marginal gap evaluation of zirconia copings using microcomputed tomography: an in vitro analysis. *Int J Periodontics Restorative Dent*. 2018; 38:57–63.
- Saab RC, da Cunha LF, Gonzaga CC, Mushashe AM, Correr GM. Micro-CT analysis of Y-TZP copings made by different CAD/CAM Systems: marginal and internal fit. *Int J Dent*. 2018;2018:5189767.
- Ahmed WM, Abdallah MN, McCullagh AP, Wyatt CCL, Troczynski T, Carvalho RM. Marginal discrepancies of monolithic zirconia crowns: the influence of preparation designs and sintering techniques. *J Prosthodont*. 2019;28:288–98.
- Carbajal Mejia JB, Yatani H, Wakabayashi K, Nakamura T. Marginal and internal fit of CAD/CAM crowns fabricated over reverse tapered preparations. *J Prosthodont*. 2019;28:477–84.
- Holmes JR, Bayne SC, Holland GA, Sulik WD. Considerations in measurement of marginal fit. *J Prosthet Dent*. 1989;62:405–8.
- Ricciardiello F, Amato M, Leone R, Spagnuolo G, Sorrentino R. In vitro evaluation of the marginal fit and internal adaptation of zirconia and Lithium Disilicate single crowns: micro-CT comparison between different manufacturing procedures. *Open Dent J*. 2018;12:160–72.
- Beuer F, Aggstadler H, Edelhoff D, Gernert W, Sorensen J. Marginal and internal fits of fixed dental prostheses zirconia retainers. *Dent Mater J*. 2009; 25:94–102.
- Rajan BN, Jayaraman S, Kandhasamy B, Rajakumaran I. Evaluation of marginal fit and internal adaptation of zirconia copings fabricated by two CAD-CAM systems: an in vitro study. *The Journal of the Indian Prosthodontic Society*. 2015;15:173–8.
- Demir N, Ozturk AN, Malkoc MA. Evaluation of the marginal fit of full ceramic crowns by the microcomputed tomography (micro-CT) technique. *Eur J Dent*. 2014;8:437–44.
- Sulaiman F, Chai J, Jameson LM, Wozniak WT. A comparison of the marginal fit of in-Ceram, IPS empress, and procera crowns. *Int J Prosthodont*. 1997;10: 478–84.
- Dolev E, Bitterman Y, Meirowitz A. Comparison of marginal fit between CAD-CAM and hot-press lithium disilicate crowns. *J Prosthet Dent*. 2019;121: 124–128.26.
- Beuer F, Korczynski N, Rezac A, Naumann M, Gernert W, Sorensen JA. Marginal and internal fit of zirconia based fixed dental prostheses fabricated with different concepts. *Clin Cosmet Investig Dent*. 2010;25:5–11.
- Abduo J, Lyons K, Swain M. Fit of zirconia fixed partial denture: a systematic review. *J Oral Rehabil*. 2010;37:866–76.
- Borges GA, Faria JS, Agarwal P, Spohr AM, Correr-Sobrinho L, Miranzi BA. In vitro marginal fit of three all-ceramic crown systems before and after cementation. *Oper Dent*. 2012;37:641–9.

Publisher's Note

Springer Nature remains neutral with regard to jurisdictional claims in published maps and institutional affiliations.

RESEARCH ARTICLE

Open Access



Influence of margin location and luting material on the amount of undetected cement excess on CAD/CAM implant abutments and cement-retained zirconia crowns: an in-vitro study

Peter Gehrke^{1,2*} , Konstantin Bleuel³, Carsten Fischer⁴ and Robert Sader⁵

Abstract

Background: The flexibility in designing the submucosal part of CAD/CAM customized implant abutments and the individual positioning of its shoulder line has been suggested to reduce the risk of leaving undetected cement residues, thus preventing adverse effects on peri-implant tissues. A high correlation between excess cement left in the soft tissues and the occurrence of increased biofilm accumulation with sulcular bleeding and/ or suppuration has been reported. This in turn may cause peri-implant inflammation and peri-implant marginal bone loss. The aim of this study was to assess the frequency of cement remnants after the luting of zirconia crowns on CAD/CAM custom molar abutments with different margin levels and to evaluate the impact of the luting material.

Material and methods: A total of 20 titanium molar CAD/CAM implant abutments (BEGO Medical GmbH) with internal taper connection/ internal hex anti-rotation protection, and a convex emergence profile with different margin positions (0, 1, 2 and 3 mm below the mucosa), were virtually designed (Implant Studio, 3Shape) and manufactured. A master cast was scanned, duplicated by a 3D printer and individual gingival masks were produced to simulate peri-implant soft tissues. 20 corresponding zirconia crowns were designed (Cerec 3D, Dentsply Sirona), produced and cemented to the abutments with two different luting materials; a zinc oxide non-eugenol cement (Temp Bond NE) or a methacrylate cement (Panavia V5). To ensure retrievability of the crown/abutment connection, occlusal openings providing access to the abutment screws were designed. Excess cement was thoroughly removed and the crown/abutment units were unscrewed to evaluate the occurrence of cement residues. All the quadrants of each specimen were evaluated for calculation of the ratio between the cement remnant area and the total specimen area using Adobe Photoshop. Spearman analysis was performed to detect correlations between different variables. A two-sided t-test, ANOVA, Mann–Whitney, and Kruskal–Wallis tests were applied to detect differences between the groups.

(Continued on next page)

* Correspondence: dr-gehrke@prof-dhom.de

¹Private Practice for Oral surgery and Implant Dentsity, Bismarckstraße 27, 67059 Ludwigshafen, Germany

²Department of Postgraduate Education, Oral and Dental Medicine, Johann Wolfgang Goethe-University, Frankfurt, Germany

Full list of author information is available at the end of the article



© The Author(s). 2019 **Open Access** This article is distributed under the terms of the Creative Commons Attribution 4.0 International License (<http://creativecommons.org/licenses/by/4.0/>), which permits unrestricted use, distribution, and reproduction in any medium, provided you give appropriate credit to the original author(s) and the source, provide a link to the Creative Commons license, and indicate if changes were made. The Creative Commons Public Domain Dedication waiver (<http://creativecommons.org/publicdomain/zero/1.0/>) applies to the data made available in this article, unless otherwise stated.

(Continued from previous page)

Results: Cement remnants were found in every depth of the crown abutment complex and in almost every area investigated. The amount of cement residues increased as the crown-abutment margin was located more submucosally. Lingual areas were more prone to cement remnants than other surface areas ($p = 0.0291$). Excess cement was not only found at the margins of the crown-abutment complex, but also underneath (basal) the abutment itself, where cleaning was impossible. No statistical difference in the effect of zinc oxide non-eugenol- and methacrylate cement on the frequency of excess material at the lateral abutment surfaces could be demonstrated in vitro. The proportion of basal abutment aspects covered with cement residues was, however, significantly smaller in Panavia V5 samples with an average of $4.9 \pm 3.7\%$ compared to Temp Bond samples with an average of $8.6 \pm 5.5\%$.

Conclusions: Given the results obtained in the present investigation the margin of CAD/CAM molar abutments should be located as coronally as possible to minimize the amount of cement remnants. If an epigingival or supragingival margin location is not feasible due to esthetic concerns, it cannot be recommended to place the margin of molar CAD/CAM abutments deeper than 1.5 mm in the proximal and oral regions.

Keywords: CAD/CAM implant abutments, Cement excess, Cement cleaning, Cement-retained implant restorations, Subgingival margins, Zirconia crowns

Background

An abutment serves as the extension of a dental implant into the oral cavity and thus as basis for the subsequent restoration. Its biological function is to shape and support the peri-implant soft tissues while at the same time functioning as a sufficient barrier for bacterial colonization [1, 2]. Implant abutments are selected according to the bone level, mucosal thickness, angulation, shape and size of the reconstruction. The shoulder margin can be set both sub- and supra-mucosal, depending on soft-tissue architecture and esthetic requirements. Implants can be restored with either screw-retained or cement-retained restorations. The latter is a commonly utilized prosthetic technique since it allows for a tolerance with respect to the implant axis and position and it is familiar to the majority of practitioners [3]. Cemented restorations, however, have a

number of disadvantages, including the challenge of completely removing cement remnants around the restoration [4–9]. As undetected cement excess of fixed implant-supported restorations has been associated with clinical and radiographic signs of peri-implant inflammation, there is an essential need to reduce this risk. Agar et al. [10] examined the removal of excess cement around implant crowns with stock abutment margins placed at various levels below an artificial mucosal margin. Even after careful removal attempts, cement remnants could always be detected, independent of the examiners experience or instruments used. Additional aspects, such as the vertical position of the crown-abutment interface or the type of luting material appeared to be influential. These findings are supported by in vitro and in vivo studies demonstrating that the depth of the crown-abutment interface of

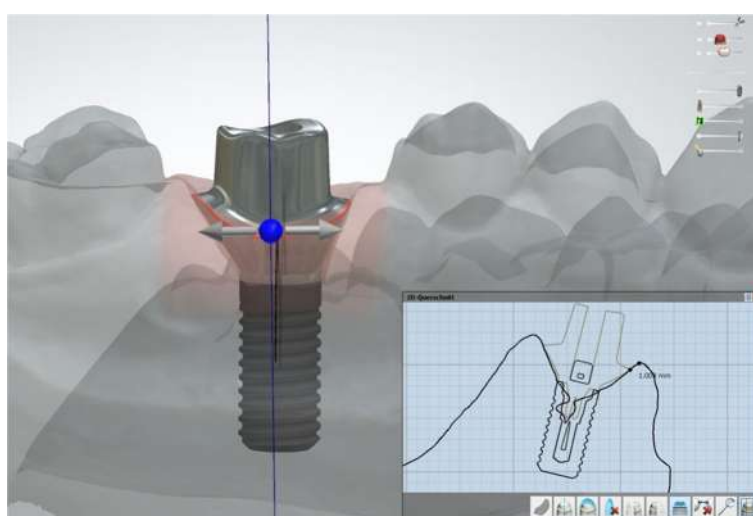


Fig. 1 Digital design of abutment emergence profile



Fig. 2 Sample abutments with their corresponding zirconium crowns from left to right: 3 mm–0 mm subgingival

stock abutments negatively influences the practitioner's ability to remove cement excess [8, 11, 12]. Another weakness of cement retained restorations is the difficulty or impossibility of removing the restoration in case of complications, without damaging or destroying it. In contrast, the major benefit of screw-retained reconstructions is their retrievability [4, 7]. While the majority of available data refers to prefabricated stock abutments, little is known about the incidence of undetected cement residues of computer-aided designed and manufactured (CAD/CAM) custom abutments in the molar region. The flexibility in designing the sub-mucosal part of custom abutments and the individual positioning of its shoulder line has been suggested to reduce the risk of leaving undetected cement residues, thus preventing adverse effects on peri-implant tissues [13, 14]. However, so far there is little data available to support this hypothesis. Consequently, the aim of the present in vitro study was to assess the frequency of cement remnants after luting of zirconia crowns

on convex emergence profile molar CAD/CAM abutments with different margin levels (0, 1, 2 and 3 mm below the mucosa), and to evaluate the impact of two different luting materials.

Methods

A total of 20 titanium CAD/CAM implant abutments with a convex emergence profile and different margin positions (0, 1, 2 and 3 mm below the mucosa), were virtually designed (Implant Studio, 3Shape, Copenhagen, Denmark) (Fig. 1) and manufactured (BEGO Medical GmbH, Bremen, Germany). The master cast of a clinical case in which the left maxillary first molar had been replaced by an implant restoration served as the origin of the model. The case was restored using a regular platform two-piece implant with an internal taper connection and internal hex anti-rotation protection (BEGO Semados® RSX D 4.1/L 11.5, BEGO Implant Systems GmbH & Co. KG, Bremen, Germany). The emergence profile of the peri-implant mucosa had been pre-conditioned by means of a temporary implant-supported single crown. The original master cast with the implant analog (PS IMPA 4.1, BEGO Implant Systems GmbH & Co. KG, Bremen, Germany) was duplicated in type IV plaster (Quadro-Rock Plus, Picodent, Wipperfurth, Germany). All abutment specimens were cleansed three times in an ultrasonic bath at 30 °C for 5 min each, as previously described by the authors [15, 16]. In addition, 20 corresponding monolithic zirconia crowns (Zirlux, Henry Schein, Langen, Germany) were CAD/CAM designed and produced (Cerec 3D, Dentsply Sirona, Bensheim, Germany) (Fig. 2). The master cast with the implant analog was scanned with a 3D scanner (3Shape, Copenhagen, Denmark), duplicated by a 3D printer (Formlabs, Boston, USA) and

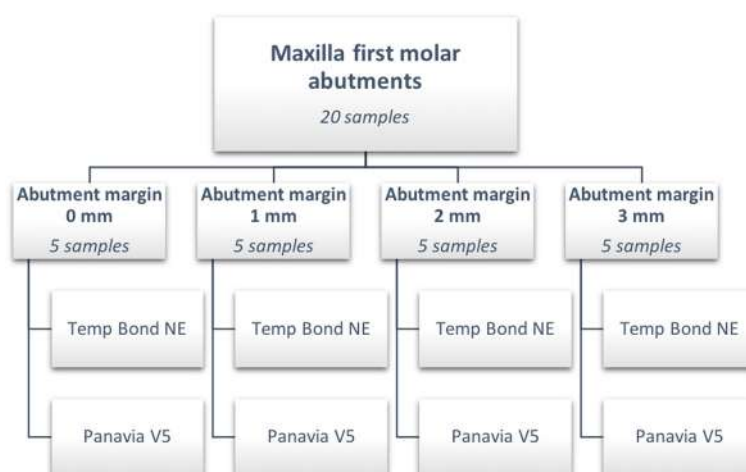


Fig. 3 Sample distribution of abutment margin designs and luting materials



Fig. 4 Cementation process on mounted titanium abutment with gingival mask and mixing tip into crown

individual gingival masks were confectioned to simulate the peri-implant mucosal tissues. The light body polyvinyl siloxane gingival mask (Gingifast, Zermak, Marl, Germany) was replicated four times and altered for each depth of the crown-abutment distance. Occlusal openings were designed in the zirconia crowns in order to have access to the occlusal abutment screw after cementation. Before cementation, the top of each prosthetic abutment was covered with a cotton pellet in order to protect the abutment screw. The occlusal crown openings were closed with a dual cured flexible composite Telio CS Link (Ivoclar Vivadent, Liechtenstein) to obturate the screw access and to allow for retrieval of the abutment-crown complex after cementation. The cement was mixed according to the manufacturer's instructions. A thin uniform layer was applied to all internal surfaces of the crowns by using the mixing tips of the cartridges and

seated onto the abutment with constant finger pressure. The exact amount of cement was not quantified as the cementation protocol tried to imitate a real clinical scenario. The cementation process was performed by one experienced clinician (PG). In the first trial, a zinc oxide non-eugenol cement (Temp Bond NE, Kerr Dental, Germany) was used for luting the crowns. After the cleaning and evaluation process, the crown was separated from the abutment and all parts were thoroughly cleaned. For this purpose, the luting area of the CAD/CAM abutments and the inner surfaces of the zirconia crowns were first cleaned from the remaining zinc oxide non-eugenol cement remnants with an acrylic scaler (Hu Friedy Mfg. Co., LLC, Frankfurt, Germany). The inner surfaces of the zirconia crowns were additionally treated with 100- μ m aluminum oxide particles at 1.0 bars pressure for 20 s at a distance of 10 mm. Afterwards all crowns and abutments were cleansed three times in an ultrasonic bath at 30 °C for 5 min each [15]. The first bath contained an antibacterial cleansing solution (FINEVO 01, Bredent GmbH & Co. KG, Senden, Germany), the second bath contained 80% ethylalcohol, and the third bath contained medically pure water (aqua dest.). In the second trial, a methacrylate cement (Panavia V5, Kuraray, Japan) was used for the cementation (Fig. 3). A second investigator (KB) not involved in the cementing process attempted to remove any cement residues. After setting of the zinc oxide non-eugenol cement or light curing of the resin cement, the excess was removed with a steel scaler (Hu Friedy Co., LLC, Tuttlingen, Germany) and super-floss (Procter & Gamble, Surrey, UK) until the investigator was convinced it had been completely cleaned. Once cleaned,

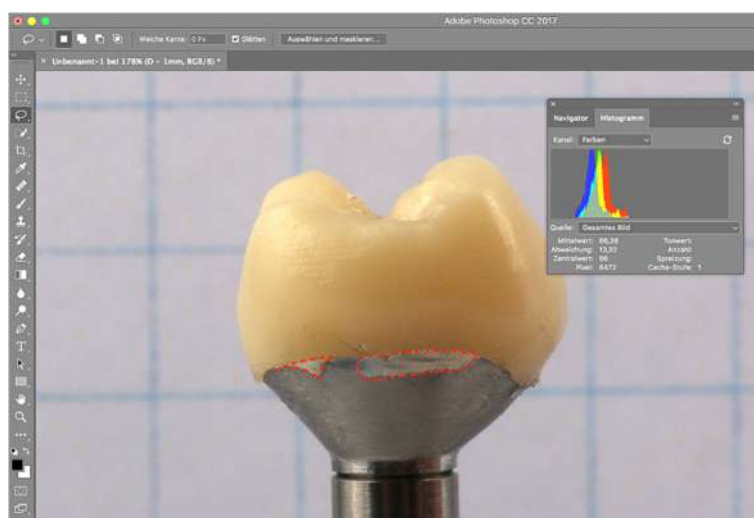


Fig. 5 Evaluation of the area covered with cement remnants and the total surface of the specimen in Adobe Photoshop

Table 1 Total cement residues on lateral aspects: Temp Bond (%)

Total Temp Bond cement residues on lateral aspects (%) (mesial, buccal, distal and lingual) (%)						
Margin depth	N	Mean	Median	Min	Max	SD
0	5	1.08	0.63	0.51	2.34	0.77
1	5	1.85	1.59	0.43	4.95	1.81
2	5	2.91	3.03	1.07	4.32	1.17
3	5	2.49	2.26	0.62	4.79	1.50

constant vertical pressure on the crown was kept until the cement had fully set. Subsequently, the occlusal closing materials were removed, the abutment screw was unscrewed and the superstructure complex was dismantled for assessment (Fig. 4). A computerized planimetric method of cement assessment described by Linkevicius et al. was utilized [11]. All measurements were obtained by a single calibrated examiner (CF). Calibration was tested by double analysis of standardized digital photographs from 10 CAD/CAM abutments, with a one-week interval. The agreement coefficient was of 0.96, with a mean difference of 0.03 ± 0.92 (values ≥ 0.75 are considered excellent). The specimens were fixed on a custom-made device, to keep a standardized distance between the camera (Canon EOS D80, Tokyo, Japan) and the specimen. Digital photographs were taken from all four quadrants (mesial, buccal, distal and lingual) using a 100 mm macro objective lens. The images were imported and analyzed using Adobe Photoshop (Adobe Systems Ltd., Europe, Uxbridge, UK). For each image obtained from each quadrant, the

circumference of the total crown-abutment surface was marked using a free line tool (lasso-tool) of the software. The number of pixels was recorded from the histogram option (Fig. 5). The same procedure was applied to the area covered with cement remnants following the contours of the excess cement. The ratio between the area covered with cement and the total surface area of the specimen was calculated. A surface of the specimen was considered as a statistical unit, therefore each specimen had four measurements, resulting in a sample size of 20 for each group. Statistical analyses were carried out using the program packages STATISTICA (STATSOFT, Tulsa, USA, version 9.1) and BiAS (Epsilon-Verlag, Frankfurt, version 11.02). Frequency distributions were used to characterize categorical variables. The Mann-Whitney-U-Test and the Kruskal-Wallis H-Test were used to compare independent groups for continuous variables. Significance was set at $p < 0.05$.

Results

Cement remnants were found in almost every abutment area investigated. The amount of the remnants varied according to the depth of the crown-abutment margin. Excess cement was not only found at the margins of the crown-abutment complex, but also underneath (basal) the molar abutment itself, where no cleaning was possible due to its prominent emergence profile. The two types of cement were separately investigated and statistically analyzed. The summary of the total Temp Bond cement residues on the lateral aspects (mesial, buccal, distal and lingual) is shown in Table 1. Comparing the different margin

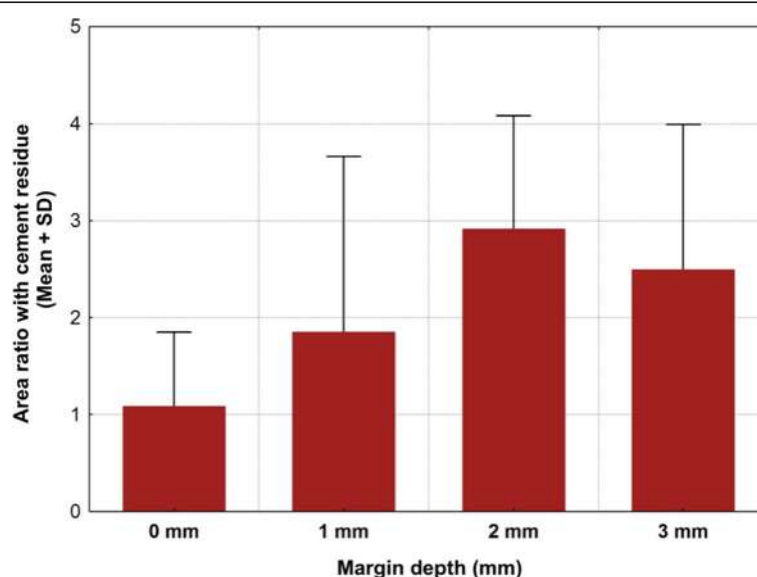
**Fig. 6** Total cement residues on lateral aspects: Temp Bond (Mean + SD).

Table 2 Total cement residues on lateral aspects: Temp Bond (%)

Kruskal-Wallis-Test: H (3, N = 20) = 5.285714 p = 0.1520			
Margin depth	N	Rank total	Mean rank
0	5	32.00000	6.40000
1	5	46.00000	9.20000
2	5	73.00000	14.60000
3	5	59.00000	11.80000

levels, there was a clear tendency to increase the proportion of undetected Temp Bond residues on the lateral abutment surfaces with increasing margin depth from 0 to 2 mm (Fig. 6). Positioning the abutment shoulder from 2 to 3 mm depth, however, showed a slight decrease in excess cement. No statistical significance was found between the depth of margin and the frequency of remnants (total $p = 0.1520$) (Table 2). The Kruskal-Wallis-Tests for the individual surfaces revealed the following values: mesial $p = 0.1106$, distal $p = 0.0581$, buccal $p = 0.061$, lingual $p = 0.1312$. Although notable excess of Temp Bond could be identified at the basal surface of all investigated CAM/CAM molar abutments, their presence in relation to the individual abutment shoulder was not statistically significant ($p = 0.336$) (Tables 3 and 4) (Fig. 7). Comparing the four margin depths (0–3 mm subgingival) in the Panavia V 5 sample group, the buccal ($p = 0.0860$), mesial ($p = 0.0922$), distal ($p = 0.9679$), and basal surfaces ($p = 0.9846$) showed no statistical significance. The total cement residues of Panavia V 5 on the lateral abutment aspects are shown in Tables 5 and 6 and Fig. 8. However, the lingual surface demonstrated a statistical significance ($p = 0.0291$) at a margin depth of 3 mm subgingivally (Tables 7 and 8) (Fig. 9). Tables 9 and 10 show, separated by the cement type, the individual aspect, the sum of lateral aspects, and the amount of excess cement in percent irrespective of the gap depth. Table 11 displays the results for the comparison the two cement types utilized. The proportion of basal abutment aspects covered with cement residues was significantly smaller in the methacrylate cement samples (Panavia V5) with an average of $4.9 \pm 3.7\%$ compared to the temporary zinc oxide non-eugenol

Table 3 Basal cement residues: Temp Bond (%)

Basal Temp Bond cement residues (%)						
Margin depth	N	Mean	Median	Min	Max	SD
0	5	7.11	7.58	3.49	11.82	3.24
1	5	7.32	5.56	3.11	14.30	4.28
2	5	13.52	13.25	3.33	25.16	7.88
3	5	6.51	6.15	2.55	11.60	3.36

Table 4 Basal cement residues: Temp Bond (%)

Kruskal-Wallis-Test: H (3, N = 20) = 3.388571 p = 0.3355			
Margin depth	N	Rank total	Mean rank
0	5	48.00000	9.60000
1	5	48.00000	9.60000
2	5	73.00000	14.60000
3	5	41.00000	8.20000

cement samples (Temp Bond) with an average of $8.6 \pm 5.5\%$ ($p = 0.007$) (Fig. 10). The difference in the mean sum of the lateral abutment surfaces affected by cement residues was not statistically significant ($p = 0.398$) (Table 11).

Discussion

Biological properties of the interface between implant abutment and surrounding tissues are of critical importance for long-term success [17]. Cement remnants of fixed implant-supported restorations have been associated with clinical and radiographic signs of peri-implantitis [6, 13, 18]. Numerous in vitro and in vivo studies demonstrated that the depth of the crown-abutment interface of stock abutments negatively influence the practitioner's ability to remove cement remnants [8, 10–12]. It has been claimed that the application of computer-aided design and computer-aided manufacturing (CAD/CAM) facilitates the formation of an anatomical abutment design with a natural emergence profile and a proper spatial outline at the cervical margin [19]. The flexibility in designing the submucosal part of the custom abutment and the positioning of the shoulder finish line has been suggested to reduce the challenges of undetected excess cement [20]. Unlike most previous studies [6, 10–12], the present investigation analyzed the quantity and depth of remnants around custom CAD/CAM abutments with a convex emergence profile at different regions of a molar crown-abutment complex. The results revealed cement remnants in every depth of the crown-abutment complex and in almost every investigated area. The amount of cement left was influenced by the location of the crown-abutment margin. Although no statistical significance was found between the depth of margin and the presence of remnants, an increase in remnants was detected when the crown-abutment margin was located more submucosally. Deep crown-abutment margin positions (deeper than 1 mm below mucosa) increased the risk of residual cement. Excess cement was more difficult to remove utilizing a scaler and super-floss at oral and approximal surfaces than other surface areas. It could be demonstrated, that cement remnants were not only found at the margins of the crown-abutment

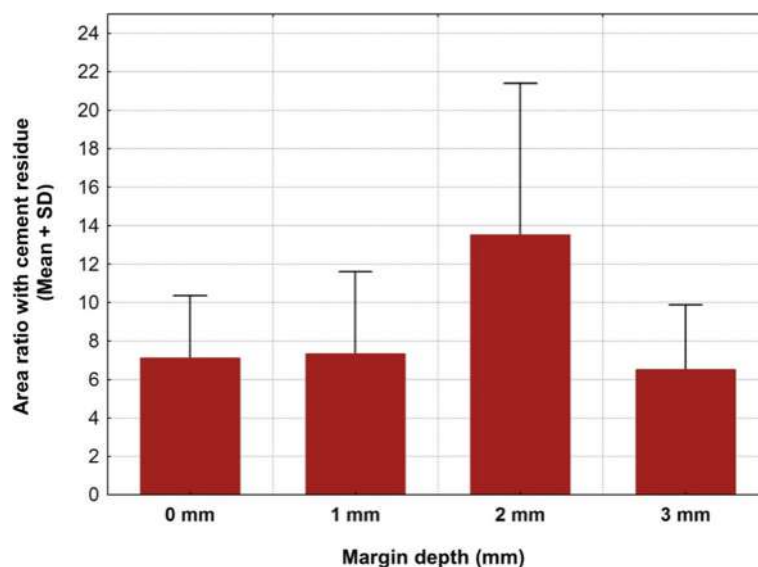


Fig. 7 Basal cement residues: Temp Bond (Mean + SD)

complex, but also at the basal surface of the abutment. Therefore, it is essential to exercise the utmost care when cementing crowns to CAD/CAM molar abutments with a prominent convex emergence profile. These findings are in concordance with recent research and clinically relevant as they uncover the critical areas where cement remains even after careful removal attempts [8, 11, 12, 14, 21, 22].

In the clinical context, a mismatch between the digitally planned margin of a CAD/CAM-customized abutment, and its intraoral position after delivery and functioning can be found [23, 24]. The use of standard impression copings or implant scan bodies with a circular diameter produces inconsistency within the emergence profile. It may begin with a collapse of the supra-implant mucosa during intra-oral optical or conventional impression taking and then result in computer-generated mismatch of the position and contour of the abutment shoulder. Hence, there is a risk of discrepancy between the position of the free mucosal margin in a digital image and its actual position. In a recent clinical study Pietruski et al. [25]

examined the concordance between the virtual planned and the clinical position of an abutment shoulder against the mucosal margin and their actual position. Although for the majority of all cases (a total of 257 abutments) soft tissue stability or growth could be confirmed favouring the use of CAD/CAM abutments, in 20% of cases, soft tissue height reduction was demonstrated with unfavorable abutment shoulder display. In order to avoid the risk of soft tissue deficiency, the authors recommended to set the abutment shoulder slightly deeper submucosally than the CAD software routinely recommends.

There are several limitations associated with this in vitro study. Therefore, the results obtained can not be directly translated into the clinical context. Beside its in vitro nature, the small sample size, although balanced using proper statistical analysis, might limit the generalization of the study outcomes. The statistically significant result for an increased presence of methacrylate cement ($p = 0.0291$) at the lingual abutment surface must be regarded with caution. Even though the cementation and subsequent cleaning procedures were kept as close as possible to clinical reality, the

Table 5 Total cement residues on lateral aspects: Panavia V5 (%)

Total Panavia V 5 cement residues on lateral aspects (mesial, buccal, distal and lingual) (%)						
Margin depth	N	Mean	Median	Min	Max	SD
0	5	1.23	0.68	0.42	3.47	1.28
1	5	1.21	1.33	0.42	1.66	0.48
2	5	1.57	1.13	0.91	3.46	1.07
3	5	2.39	2.31	1.26	3.78	1.09

Table 6 Total cement residues on lateral aspects: Panavia V5 (%)

Kruskal-Wallis-Test: H (3, N = 20) = 5.194286 $p = 0.1581$			
Margin depth	N	Rank total	Mean rank
0	5	34.00000	6.80000
1	5	51.00000	10.20000
2	5	49.00000	9.80000
3	5	76.00000	15.20000

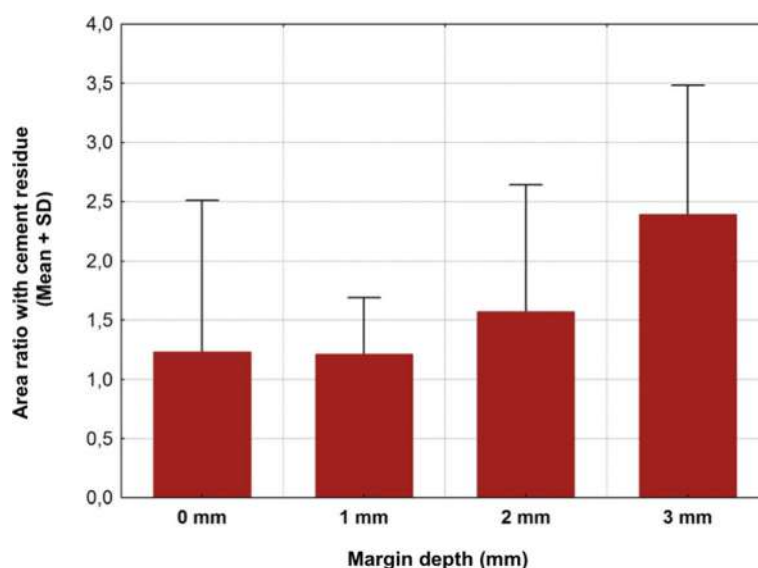


Fig. 8 Total cement residues on lateral aspects: Panavia V5 (Mean + SD)

in vitro nature of the study setup might limit a clinical generalization of the outcomes. A master cast with a silicone gingiva mask cannot entirely replicate the nature of the peri-implant sulcus and its interaction with the submucosal anatomy of a convex abutment configuration. In addition, clinical data suggest that temporary cements such as zinc oxide non-eugenol materials are more likely to be washed out by sulcus fluids than resin based cements [26, 27]. Further clinical research is needed to confirm or disprove these results. One of the major difficulties in cementing the crowns was the standardization of the amount of cement. Alternatively, a micro brush should have been considered to apply a uniform layer of cement or automatic pipettes to avoid initial disparities between the groups. Another drawback relates to the surface measurement of cement residues. Since cement volume and weight were not assessed, data analysis was more complex. In some cases, after the attempt of cement removal, small amounts of cement could be spread over a larger area, compromising the reliability of the results. In order to be able to compare the results of the present study with those of earlier in vitro and clinical trials [11, 12], it was

decided to use digital photography for evaluation. Instead of using digital photographs to analyze cement excess, scanning electron microscopy (SEM), with significantly higher image resolution, would have enabled a more objective assessment of cement residue. A SEM assessment might have detected higher cement volumes and therefore altered the results. Although the current results cannot be directly extrapolated to the clinical situation, the potential occurrence of adverse effects caused by excess cement should be considered when making clinical decisions.

The impact of cement remnants in the development of peri-implantitis is still discussed controversially. Excess cement in subgingival areas is described as an “artificial calculus” and may have a similar irritating effect as calculus on periodontally involved teeth [28]. A multicenter 3-year prospective study reported that peri-implant soft tissues reacted more favorably to screw-retained crowns when compared with cement-retained restorations [29]. A recent clinical trial compared cemented versus screw-retained single implant-supported ceramic crowns in terms of histological, microbiological and radiological outcome measures 6 months after insertion [30]. Although both types of

Table 7 Lingual cement residues: Panavia V5 (%)

Panavia V 5 cement lingual residues (%)						
Margin depth	N	Mean	Median	Minimum	Maximum	SD
0	5	0.71	0.28	0.13	1.77	0.74
1	5	0.44	0.00	0.00	1.42	0.64
2	5	0.53	0.46	0.13	1.12	0.38
3	5	1.74	1.68	1.15	2.59	0.54

Table 8 Lingual cement residues: Panavia V5 (%)

Kruskal-Wallis-Test: H (3, N = 20) = 9.015686 $p = 0.0291$			
Margin depth	N	Rank total	Mean rank
0	5	50.00000	10.00000
1	5	32.00000	6.40000
2	5	43.00000	8.60000
3	5	85.00000	17.00000

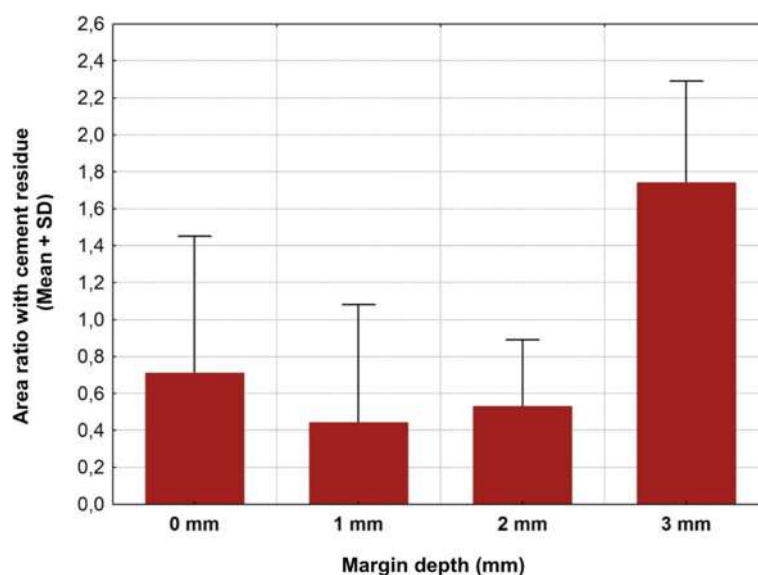


Fig. 9 Lingual cement residues: Panavia V5 (Mean + SD)

reconstructions resulted in a similar radiological and clinical outcome, the results displayed that cemented restorations were associated with more inflammatory cells and more patients were diagnosed with periodontal pathogens. In contrast Blanes et al. [31] showed that peri-implant tissues around cemented restorations were not more inflamed when compared to tissues around screw-retained prostheses.

It should be emphasized, however, that the excess of cement is just one of several potential factors causing tissue inflammation and the development of peri-implantitis. While peri-implantitis represents a predominantly plaque-induced inflammatory condition [32], certain local factors may be associated with this biologic complication, as they involve plaque retention. Recent longitudinal and cross-sectional trials have investigated additional parameters that could promote the onset of adverse conditions and encourage the transformation of physiologic bone loss to peri-implant disease [33–35]. As the patient's compliance in supportive peri-implant maintenance plays an important factor in determining the chance of

developing peri-implant disease [36], smoking and alcohol consumption are supposed to be potential contributing factors [32, 37]. Foreign body reactions to alloplastic grafting materials [35], varying soft and hard tissue composition [38], or improper three-dimensional implant positioning [39], might also predispose to the presence of disease. Regardless of the implant positioning and placement protocol, vertical and horizontal bone remodeling has been described [40, 41] which in some cases may result in minimal thread exposure followed by the adherence of pathogenic bacteria, which in turn promote bone resorption. Implant surface morphology [42], contamination of the inner part of the implant connection [43] and contamination due to the laboratory workflow [15, 16] might represent other pathogenic pathways for peri-implant disease.

Canullo et al. [44] demonstrated in a recent cross-sectional clinical study that although symptoms of peri-implantitis are always a plaque-induced inflammatory entity, certain prosthetic (eg, inadequate superstructure design, incorrect distribution of

Table 9 Comparison of the two types of cement: Panavia V5

Panavia V5	N	Mean	Median	Min	Max	SD
Basal: Cement residues (%)	20	4.91	3.53	0.05	13.19	3.69
Buccal: Cement residues (%)	20	0.94	0.73	0.00	3.23	0.83
Mesial: Cement residues (%)	20	2.05	1.65	0.00	6.97	1.96
Lingual: Cement residues (%)	20	0.85	0.70	0.00	2.59	0.76
Distal: Cement residues (%)	20	2.58	2.08	0.00	6.97	1.66
Sum of lateral aspects: Cement residues (%)	20	1.60	1.30	0.42	3.78	1.06

Table 10 Comparison of the two types of cement: Temp Bond

Temp Bond	N	Mean	Median	Min	Max	SD
Basal: Cement residues (%)	20	8.61	7.49	2.55	25.16	5.48
Buccal: Cement residues (%)	20	1.41	1.09	0.04	4.20	1.27
Mesial: Cement residues (%)	20	2.40	2.11	0.00	6.23	1.89
Lingual: Cement residues (%)	20	1.03	0.89	0.00	4.22	0.96
Distal: Cement residues (%)	20	3.60	3.24	0.58	8.95	2.49
Sum of lateral aspects: Cement residues (%)	20	2.08	1.88	0.43	4.95	1.44

Table 11 Summary of the comparison of the two types of cement (%)

Mann-Whitney U-Test						
	Rank total Temp Bond	Rank total Panavia V5	U	N Temp Bond	N Panavia V5	2*incl. exact p
Basal: Cement residues (%)	508.0000	312.0000	102.0000	20	20	0.007331
Buccal: Cement residues (%)	449.0000	371.0000	161.0000	20	20	0.301253
Mesial: Cement residues (%)	439.0000	381.0000	171.0000	20	20	0.444964
Lingual: Cement residues (%)	430.5000	389.5000	179.5000	20	20	0.583114
Distal: Cement residues (%)	453.0000	367.0000	157.0000	20	20	0.253380
Sum of lateral aspects: Cement residues (%)	442.0000	378.0000	168.0000	20	20	0.398302

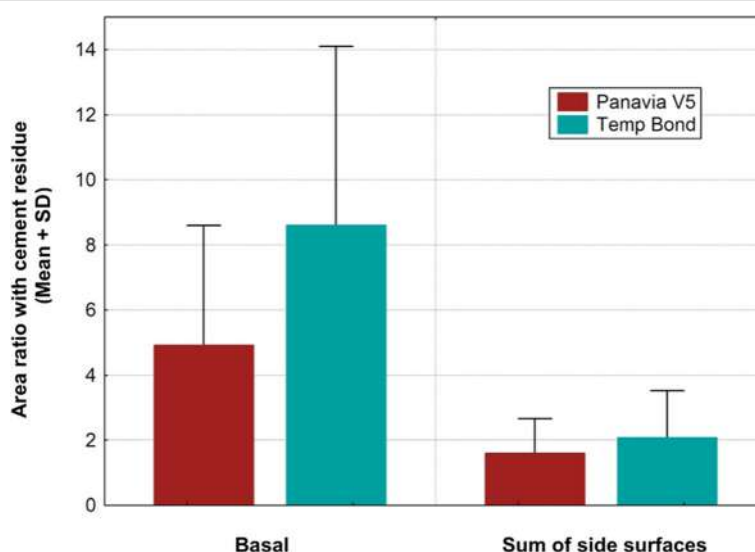
prosthetic loading), surgical (eg, implant malpositioning, failed bone reconstruction), or biomechanical (eg, overloading) factors might be associated with this clinical phenomenon. Interestingly, in the aforementioned clinical trial involving 554 patients and 1507 dental implants, the second most common determinant of peri-implantitis was implant width. The authors assumed that bone grafting and/ or higher compression force created during the drilling sequence for wider implant placement might inject another contributing factor for developing peri-implantitis.

Until now, a fixed implant supported restoration could either be cemented or screw-retained. Recently, a cone-in-cone morse taper connection between the abutment and the crown has been alternatively introduced to retain implant-retained definitive fixed dentures (FDPs). The frictional connection eliminates the use of cements or screws, allowing for easy retrieval of the restorations with regular maintenance. This restorative approach,

named the “Acuris™ Conometric Concept” (Dentsply Sir-ona Implants, Bensheim, Germany), has been used to retain hybrid acrylic-composite [45], monolithic lithium disilicate [46, 47] and monolithic zirconia [48] implant restorations in the posterior region. The authors reported favorable mid-term results with high implant survival, stable hard and soft tissues, and few prosthetic complications.

Conclusions

Given the results obtained in the present in vitro investigation, the margin of CAD/CAM molar abutments should be located as coronally as possible to minimize the amount of cement remnants. If this ideal margin location is not feasible due to esthetic concerns, it cannot be recommended to place the margin of molar abutments deeper than 1.5 mm in the approximal and oral regions.

**Fig. 10** Summary of the comparison of the two cement types (%)

Acknowledgements

The authors gratefully acknowledge Dr. Wolfgang Reimers for his contribution to data analysis and statistical support.

Authors' contributions

PG and KB contributed to the design of the study. PG, KB and CF contributed to study selection and data extraction. RS contributed to the drafting of the paper and revising it critically. All authors read, revised, and approved the final manuscript.

Funding

This study was not financially supported by a third party.

Availability of data and materials

The datasets used and/or analysed during the current study are available from the corresponding author on reasonable request.

Ethics approval and consent to participate

This article does not contain any studies with human participants or animals performed by any of the authors.

Consent for publication

Not applicable.

Competing interests

The authors declare that they have no competing interests. BEGO Medical GmbH (Bremen, Germany) provided the CAD/CAM abutments for the experimental investigation. The design, documentation and analyses of this study were completed entirely independent of BEGO Medical GmbH.

Author details

¹Private Practice for Oral surgery and Implant Dentsity, Bismarckstraße 27, 67059 Ludwigshafen, Germany. ²Department of Postgraduate Education, Oral and Dental Medicine, Johann Wolfgang Goethe-University, Frankfurt, Germany. ³Private Practice, Aschaffenburg, Germany. ⁴Sirius Ceramics Laboratory, Frankfurt, Germany. ⁵Department for Oral, Cranio-Maxillofacial and Facial Plastic Surgery, Medical Center of the Goethe University Frankfurt, Frankfurt, Germany.

Received: 23 April 2019 Accepted: 31 May 2019

Published online: 14 June 2019

References

- Welander M, Abrahamsson I, Berglund T. The mucosal barrier at implant abutments of different materials. *Clin Oral Implants Res.* 2008;19:635–41.
- Huh JB, Rhee GB, Kim YS, Jeong CM, Lee JY, Shin SW, et al. Influence of implant transmucosal design on early peri-implant tissue response in beagle dogs. *Clin Oral Implants Res.* 2014;25:962–8.
- Jung RE, Pjetursson BE, Glauser R, Zembic A, Zwahlen M, Lang NP. A systematic review of the 5-year survival and complication rates of implant-supported single crowns. *Clin Oral Implants Res.* 2008;19:119–30.
- Chee W, Felton DA, Johnson PF, Sullivan DY. Cemented versus screw-retained implant prostheses: which is better? *Int J Oral Maxillofac Implants.* 1998;14:137–41.
- Gapski R, Neugeboren N, Pomeranz AZ, Reissner MW. Endosseous implant failure influenced by crown cementation: a clinical case report. *Int J Oral Maxillofac Implants.* 2008;23:943–6.
- Wilson T Jr. The positive relationship between excess cement and peri-implant disease: a prospective clinical endoscopic study. *J Periodontol.* 2009;80:1388–92.
- Sailer I, Muhlemann BE, Zwahlen M, Hammerle CH, Schneider D. Cemented and screw-retained implant reconstructions: a systematic review of the survival and complication rates. *Clin Oral Implants Res.* 2012;23(Suppl 6):163–201.
- Linkevicius T, Puisys A, Vindasiute E, Linkeviciene L, Apse P. Does residual cement around implant-supported restorations cause peri-implant disease? A retrospective case analysis. *Clin Oral Implants Res.* 2013;24:1179–84.
- Renvert S, Quirynen M. Risk indicators for peri-implantitis. A narrative review. *Clin Oral Implants Res.* 2015;26 Suppl 11:15–44.
- Agar JR, Cameron SM, Hughbanks JC, Parker MH. Cement removal from restorations luted to titanium abutments with simulated subgingival margins. *J Prosthetic Dent.* 1997;78:43–7.
- Linkevicius T, Vindasiute E, Puisys A, Peculienė V. The influence of margin location on the amount of undetected cement excess after delivery of cement-retained implant restorations. *Clin Oral Implants Res.* 2011;22:1379–84.
- Linkevicius T, Vindasiute E, Puisys A, Linkeviciene L, Maslova N, Puriene A. The influence of the cementation margin position on the amount of undetected cement. A prospective clinical study. *Clin Oral Implants Res.* 2013;24:71–6.
- Wasiluk G, Chomik E, Gehrke P, Pietruska M, Skurska A, Pietruski J. Incidence of undetected cement on CAD/CAM monolithic zirconia crowns and customized CAD/CAM implant abutments. A prospective case series. *Clin Oral Implants Res.* 2017;28:774–8.
- Sancho-Puchades, et al. The influence of the emergence profile on the amount of undetected cement excess after delivery of cement-retained implant reconstructions. *Clin Oral Implants Res.* 2017;28:1515–22.
- Gehrke P, Smeets R, Gosau M, Friedrich RE, Madani E, Duddeck D, Fischer C, Tebbel F, Sader R, Hartjen P. The influence of an ultrasonic cleaning protocol for CAD/CAM abutment surfaces on cell viability and inflammatory response in vitro. *In Vivo.* 2019;33:689–98.
- Gehrke P, Tabellion A, Fischer C. Microscopical and chemical surface characterization of CAD/CAM zirconia abutments after different cleaning procedures. A qualitative analysis. *J Adv Prosthodont.* 2015;7:151–9.
- Esposito M, Hirsch JM, Lekholm U, Thomsen P. Biological factors contributing to failures of osseointegrated oral implants. (ii). Etiopathogenesis. *Eur J Oral Sci.* 1998;3(7):21–64.
- Korsch M, Obst U, Walther W. Cement-associated peri-implantitis: a retrospective clinical observational study of fixed implant-supported restorations using a methacrylate cement. *Clin Oral Implants Res.* 2014;25:797–802.
- Priest G. Virtual-designed and computer-milled implant abutments. *J Oral Maxillofac Surg.* 2005;63(Suppl 2):22–32.
- Gehrke P, Sing T, Fischer C, Spintzyk S, Geis-Gerstorfer J. Marginal and internal adaptation of hybrid abutment assemblies after central and local manufacturing, respectively. *Int J Oral Maxillofac Implants.* 2018;33:808–14.
- Wadhvani C, et al. Cement application techniques in luting implant-supported crowns: a quantitative and qualitative survey. *Int J Oral Maxillofac Implants.* 2012;27:859–64.
- Canullo L, et al. Clinical evaluation of an improved cementation technique for implant-supported restorations: a randomized controlled trial. *Clin Oral Implants Res.* 2016;27:1492–9.
- Shah K, Yilmaz B. A technique to transfer the emergence profile contours of a provisional implant crown to the definitive impression. *Int J Oral Maxillofac Implants.* 2016;31(2):e15–7.
- Lops D, Bressan E, Cea N, Sbricoli L, Guazzo R, Scanferla M, Romeo E. Reproducibility of buccal gingival profile using a custom pick-up impression technique: a 2-year prospective multicenter study. *J Esthet Restor Dent.* 2016;28:43–55.
- Pietruski JK, Skurska A, Bernaczyk A, Milewski R, Pietruska MJ, Gehrke P, Pietruska MD. Evaluation of concordance between CAD/CAM and clinical positions of abutment shoulder against mucosal margin: an observational study. *BMC Oral Health.* 2018;18:73.
- Yanikoglu N, Duymus Y. Evaluation of the solubility of dental cements in artificial saliva of different pH values. *Dent Mater.* 2007;26:62–7.
- Korsch M, Marten SM, Dötsch A, Jauregui R, Pieper DH, Obst U. Effect of dental cements on peri-implant microbial community: comparison of the microbial communities inhabiting the peri-implant tissue when using different luting cements. *Clin Oral Implants Res.* 2016;27:161–6.
- White DJ. Dental calculus: recent insights into occurrence, formation, prevention, removal and oral health effects of supragingival and subgingival deposits. *Eur J Oral Sci.* 1997;105:508–22.
- Weber HP, Kim DM, Ng MW, Hwang JW, Fiorelli JP. Peri-implant soft-tissue health surrounding cement- and screw-retained implant restorations: a multi-center, 3-year prospective study. *Clin Oral Implants Res.* 2006;17:375–9.
- Thoma DS, Wolleb K, Bienz SP, Wiedemeier D, Hammerle CHF, Sailer I. Early histological, microbiological, radiological, and clinical response to cemented and screw-retained all-ceramic single crowns. *Clin Oral Implants Res.* 2018 Oct;29:996–1006.
- Blanes RJ, Bernard JP, Blanes ZM, Belser UC. A 10-year prospective study of ITI dental implants placed in the posterior region. II: influence of the crown-

- to-implant ratio and different prosthetic treatment modalities on crestal bone loss. *Clin Oral Implants Res.* 2007;18:707–14.
32. Heitz-Mayfield LJ. Peri-implant diseases: diagnosis and risk indicators. *J Clin Periodontol.* 2008 Sep;35(Suppl 8):292–304.
 33. Sgolastra F, Petrucci A, Severino M, Gatto R, Monaco A. Periodontitis, implant loss and peri-implantitis. A meta-analysis. *Clin Oral Implants Res.* 2015;26:8–16.
 34. Armitage GC. Development of a classification system for periodontal diseases and conditions. *Ann Periodontol.* 1999;4:1–6.
 35. Albrektsson T, Dahlin C, Jemt T, Sennerby L, Turri A, Wennerberg A. Is marginal bone loss around oral implants the result of a provoked foreign body reaction? *Clin Implant Dent Relat Res.* 2014;16:15565.
 36. Costa FO, Takenaka-Martinez S, Cota LO, Ferreira SD, Silva GL, Costa JE. Peri-implant disease in subjects with and without preventive maintenance: a 5-year follow-up. *J Clin Periodontol.* 2012;39:173–81.
 37. Sgolastra F, Petrucci A, Severino M, Gatto R, Monaco A. Smoking and the risk of peri-implantitis. A systematic review and meta-analysis. *Clin Oral Implants Res.* 2015;26:62–7.
 38. Berglundh T, Lindhe J, Ericsson I, Marinello CP, Liljenberg B, Thomsen P. The soft tissue barrier at implants and teeth. *Clin Oral Implants Res.* 1991;2:81–90.
 39. Chen ST, Buser D. Clinical and esthetic outcomes of implants placed in postextraction sites. *Int J Oral Maxillofac Implants.* 2009;24 Suppl:186–217.
 40. Botticelli D, Berglundh T, Lindhe J. Hard-tissue alterations following immediate implant placement in extraction sites. *J Clin Periodontol.* 2004;31:820–8.
 41. Covani U, Bortolaia C, Barone A, Sbordone L. Bucco-lingual crestal bone changes after immediate and delayed implant placement. *J Periodontol.* 2004;75:1605–12.
 42. Doornewaard R, Christiaens V, De Bruyn H, Jacobsson M, Cosyn J, Vervaeke S, Jacquet W. Long-term effect of surface roughness and Patients' factors on Crestal bone loss at dental implants. A systematic review and Meta-analysis. *Clin Implant Dent Relat Res.* 2017;19:372–99.
 43. Canullo L, Radovanović S, Delibasic B, Blaya JA, Penarrocha D, Rakic M. The predictive value of microbiological findings on teeth, internal and external implant portions in clinical decision making. *Clin Oral Implants Res.* 2017;28:512–9.
 44. Canullo L, Peñarrocha M, Monje A, Catena A, Wang HL, Peñarrocha D. Association between clinical and microbiologic cluster profiles and peri-implantitis. *Int J Oral Maxillofac Implants.* 2017;32:1054–64.
 45. Degidi M, Nardi D, Piattelli A. The Conometric Concept: Coupling Connection for Immediately Loaded Titanium-Reinforced Provisional Fixed Partial Dentures- A Case Series. *Int J Periodontics Restorative Dent.* 2016;36(3):347–54.
 46. Degidi M, Nardi D, Sighinolfi G, Piattelli A. The Conometric concept: definitive fixed lithium disilicate restorations supported by conical abutments. *J Prosthodont.* 2018;27:605–10.
 47. Degidi M, Nardi D, Sighinolfi G, Degidi D, Piattelli A. The conometric concept: a two-year follow-up of fixed partial CEREC restorations supported by cone-in-cone. *J Prosthodont.* 2019;28:780–7.
 48. Degidi M, Nardi D, Sighinolfi G, Piattelli A. The Conometric concept: a five-year follow-up of fixed partial monolithic zirconia restorations supported by cone in cone abutments. *Int J Periodontics Restorative Dent.* 2018;38:363–71.

Publisher's Note

Springer Nature remains neutral with regard to jurisdictional claims in published maps and institutional affiliations.

Ready to submit your research? Choose BMC and benefit from:

- fast, convenient online submission
- thorough peer review by experienced researchers in your field
- rapid publication on acceptance
- support for research data, including large and complex data types
- gold Open Access which fosters wider collaboration and increased citations
- maximum visibility for your research: over 100M website views per year

At BMC, research is always in progress.

Learn more biomedcentral.com/submissions



RESEARCH ARTICLE

Open Access



Current status on lithium disilicate and zirconia: a narrative review

Fernando Zarone¹, Maria Irene Di Mauro^{*}, Pietro Ausiello, Gennaro Ruggiero and Roberto Sorrentino

Abstract

Background: The introduction of the new generation of particle-filled and high strength ceramics, hybrid composites and technopolymers in the last decade has offered an extensive palette of dental materials broadening the clinical indications in fixed prosthodontics, in the light of minimally invasive dentistry dictates. Moreover, last years have seen a dramatic increase in the patients' demand for non-metallic materials, sometimes induced by metal-phobia or alleged allergies. Therefore, the attention of scientific research has been progressively focusing on such materials, particularly on lithium disilicate and zirconia, in order to shed light on properties, indications and limitations of the new protagonists of the prosthetic scene.

Methods: This article is aimed at providing a narrative review regarding the state-of-the-art in the field of these popular ceramic materials, as to their physical-chemical, mechanical and optical properties, as well as to the proper dental applications, by means of scientific literature analysis and with reference to the authors' clinical experience.

Results: A huge amount of data, sometimes conflicting, is available today. Both in vitro and in vivo studies pointed out the outstanding peculiarities of lithium disilicate and zirconia: unparalleled optical and esthetic properties, together with high biocompatibility, high mechanical resistance, reduced thickness and favorable wear behavior have been increasingly orientating the clinicians' choice toward such ceramics.

Conclusions: The noticeable properties and versatility make lithium disilicate and zirconia materials of choice for modern prosthetic dentistry, requiring high esthetic and mechanical performances combined with a minimal invasive approach, so that the utilization of such metal-free ceramics has become more and more widespread over time.

Keywords: Lithium disilicate, Zirconia, ZLS, Ceramic, Minimally invasive, E.max, MDP, Aging, Translucent cubic zirconia

Background

At "The Digital Dentistry Society II Consensus Conference on Digital Technologies – Marrakech 2018" the main topics of digital interest were thoroughly discussed, in order to draw clinical recommendations based on scientific evidence and, when missing, on the clinical experience shared by the scientific community. The present narrative review is focused on the technical and clinical profile of the two most popular metal-free materials, lithium disilicate and zirconia, in order to briefly

shed light on their different indications, advantages and shortcomings.

Methods

An extensive research has been carried out in the literature available on the subject, worldwide, limiting itself exclusively to articles in english, available on the main search engines (Pubmed, Embase, Scopus) and published in the most important indexed journals of the Materials and Dental sector, with and without impact factor. The results highlighted in this narrative review were extrapolated from this literature search, with reference to the authors' clinical experience.

* Correspondence: mariadimauro94@gmail.com

This Manuscript is considered to be as part of – "The Digital Dentistry Society II Consensus Conference on Digital Technologies – Marrakech" thematic series.

Department of Neurosciences, Reproductive and Odontostomatological Sciences, University "Federico II" of Naples, Viale Pansini, 5 -, 80131 Naples, Italy



© The Author(s). 2019 **Open Access** This article is distributed under the terms of the Creative Commons Attribution 4.0 International License (<http://creativecommons.org/licenses/by/4.0/>), which permits unrestricted use, distribution, and reproduction in any medium, provided you give appropriate credit to the original author(s) and the source, provide a link to the Creative Commons license, and indicate if changes were made. The Creative Commons Public Domain Dedication waiver (<http://creativecommons.org/publicdomain/zero/1.0/>) applies to the data made available in this article, unless otherwise stated.

Results

Lithium disilicate

Physico-chemical features, optical and mechanical properties

Lithium disilicate (LS₂) is classified as a glass-ceramic, in the class of particle-filled glass materials. Introduced on the market in the 90s with the commercial formulation named “IPS Empress 2” (Ivoclar Vivadent, Schaan, Liechtenstein), it was composed of 65 vol% lithium disilicate, small needle-shaped crystals (3–6 μm × 0.8 μm) embedded in a glass matrix, with a 1 vol% porosity [1–3], showing valuable mechanical characteristics (flexural strength: 350 MPa; fracture toughness (KIC): 3.3 MPa√m; heat extrusion temperature: 920 °C; thermal expansion coefficient (CTE): 10.6 ± 0.25 ppm/°C). At first, this material was made commercially available as ingots, to be utilized according to the “heat-pressing” fabrication procedure, similar to the classic “lost wax” technique for metal-alloy casts, aimed at producing cores, hot pressed into a mold. In order to get an appealing reproduction of the optical characteristics of natural teeth, the cores are lately veneered with a very translucent fluorapatite ceramic, containing 19–23% of fluorapatite crystals (Ca₅(PO₄)₃F) embedded in a glassy matrix [4].

Thanks to an optimization of the processing parameters, allowing the formation of smaller and more uniformly distributed crystals, in 2005 a new formulation of LS₂ was marketed as “IPS e.max Press” (Ivoclar Vivadent), exhibiting improved mechanical properties and optical features (flexural strength: 370–460 MPa; fracture toughness (KIC): 2.8–3.5 MPa√m), much higher than the older glass-ceramics. The high mechanical performance of this material is due, on one side, to a layered, tightly interlocked distribution of the elongated disilicate crystals, hindering crack propagation across the planes and, on the other side, to a mismatch between the thermal expansion coefficients of LS₂ crystals and the glassy matrix, so that the latter induces a tangential, compressive stress around the crystals [2]. Besides the production of ceramic cores for bilayered crowns, the increase of strength and toughness of IPS e.max Press has allowed to extend its clinical indication to monolithic restorations, without veneering ceramic, anatomically shaped, colored by surface stains and characterized by a higher fatigue resistance than the bilayered ones.

Besides the heat-pressed technique, the widespread, increasing implementation of computer-aided design/computer-aided manufacturing (CAD-CAM) technologies has led to the introduction of ceramic blocks aimed at the production of restorations by milling devices (IPS e.max CAD), also suitable for chairside production of restorations. Partially, pre-crystallized blocks are manufactured in a “blue state”, containing 40% of metasilicates (Li₂SiO₃) in addition to lithium disilicate crystal nuclei

(Li₂Si₂O₅). Such blocks are characterized by moderate flexural strength of ~130 MPa, resulting in higher cutting efficiency, easier and faster workability and lower wear of the milling tools [2, 3, 5]. The milling procedure is performed in this pre-crystallized state and, after its completion, it is followed by a heating cycle (840°–850 °C for 10 min) that turns metasilicate crystals into lithium disilicate (~70%), increasing the flexural strength up to values of 262 ± 88 MPa, together with a fracture toughness of 2.5 MPa·m^{1/2}. The blocks are available in different colors, obtained by dispersing staining ions in the glassy matrix [6] and in different degrees of translucency, on the basis of the size and distribution of the crystals in the glassy matrix [4]. The variability of flexural strength of lithium disilicate among heat-pressed and CAD-CAM blocks with different translucency is still under debate [7, 8]. Particularly, the flexural strength of IPS e.max Press and IPS e.max CAD was reported to be similar and the manufacturing process did not seem to affect the mechanical characteristics of lithium disilicate ceramics; moreover, the flexural strength was significantly influenced by translucency only for CAD-processed materials [7].

In vitro fully anatomical e.max CAD crowns have been shown to exhibit fracture resistance that is suitable for posterior, monolithic restorations [9] and to be more resistant to fatigue in cyclic loading than veneered zirconia, that is more prone to chipping [10]. For the high interest generated by its clinical versatility, further developments are expected on this material, being it influenced by different production processes, like thermal gradients, times and rates, that affect its microstructure and mechanical properties. It has been shown, for instance, that extending temperature range (750–840 °C, compared to the standard 820–840 °C) or prolonging holding time (14 min vs 7 min at 840 °C) increase elastic modulus and hardness properties, without affecting flexural strength and fracture toughness [11]. Moreover, new technologies, as spark plasma sintering, can induce a refinement and a densification of the nano-crystalline microstructure, increasing lithium disilicate and metasilicate phases and reducing lithium orthophosphate and cristobalite/quartz phases [12, 13].

As regards mechanical resistance, it has been clearly demonstrated that, in vitro, veneered LS₂ crowns exhibit significantly lower fracture load values (1431.1 ± 404.3 N) compared to monolithic ones (2665.4 ± 759.2 N), the main failure mechanism being bulk fracture initiating from the occlusal surface [14]. To date, there is strong evidence from in vitro studies that, differently from bilayered restorations, monolithic ones show fracture strength and fatigue resistance suitable for use in the posterior areas, both in tooth- and implant-supported single crowns (SC) and 3-unit fixed dental prostheses (FDPs) [15–22].

Monolithic LS₂, as well as Zirconia reinforced-Lithium Silicate ceramics (ZLS), offers higher fracture resistance than bilayered, hand-veneered zirconia [20], while a recent in vitro research has shown that load-to-fracture values of monolithic zirconia are higher than those of LS₂; the latter, in turn, are higher than those of ZLS [23].

It has to be pointed out, however, that, particularly as regards LS₂, fatigue resistance is strongly influenced by many experimental variables, like amount of cyclic loading, abutment and antagonist design and material, thermocycling parameters and test environment; for this reason, the heterogeneity and lack of standardization in research designs, tested materials and experimental conditions make a comparison of data not easily feasible [24].

Abrasiveness and wear

As to wear and abrasiveness, LS₂ shows quite favourable properties, that are highly depending on the surface characteristics of the restoration. When accurately polished at its surface, the material exhibits convenient tribological behaviour in vitro, in terms of friction and wear of restorations, being its abrasiveness quite close to enamel, although more aggressive when compared to type III gold [25] or to polished monolithic zirconia in in vitro simulations [26–28]. Such favourable wear behaviour and durability have been also confirmed by some in vivo evidence [15].

On the other hand, it has been reported that grinding, glaze coating and fluorapatite ceramic veneering can increase wear, both of the antagonist teeth and of the restoration itself; at the same time, surface roughness can also be increased, besides a reduction of gloss, in the presence of basic pH environment and after toothbrushing with abrasive toothpaste [29–33]. For these reasons, when it is not crucially needed for esthetic reasons, glazing of monolithic restorations should be avoided on the occlusal surfaces in posterior sites and only limited to the esthetically relevant zones; moreover, careful polishing procedures should always follow any occlusal grinding or esthetic refinement of disilicate restorations, although in vitro evidences at scanning electron microscope (SEM) have shown that LS₂ is one of the most critical materials to adjust intraorally, due to significant chip accumulation in the diamond burs, requiring higher machining forces and energy, with likely onset of intergranular and transgranular fractures, besides risks of thermal damage to tissues and restorations [32].

Biocompatibility

One of the strongest points of LS₂ is the excellent quality of soft tissue response. In vitro, this material exhibits high levels of biocompatibility, not only due to low plaque retention, but also to adhesion and proliferation of human epithelial cells [34] and human gingival

fibroblasts [35], particularly when its surface is polished. In vivo, in the presence of LS₂ restorations no inflammatory reactions were detected, analyzing the concentration of inflammation indicators in the gingival crevicular fluid; the same results were found with zirconia restorations [36]. Such favourable tissue responses have also been confirmed by tissue culture data [34]. In clinical experience, LS₂ restorations are likely to yield very natural and sound aspect of soft tissues when in contact with marginal gingiva or peri-implant mucosa, in the presence of subgingival margins.

Surface treatment and cementation

In addition to excellent biocompatibility and high mechanical properties, LS₂ exhibits very good esthetic features, especially as regards translucency, that is about 30% higher than conventional zirconia [37]. Moreover, for the presence of silica, LS₂ is an acid-sensitive ceramics, so that high strength of adhesion to the substrate is expected, due to both micromechanical and chemical bonding mechanisms. Micromechanical interlocking between ceramics and resin cement at the intaglio surface is based on the creation of surface microirregularities, pits and roughness by means of acid etching and/or physical treatments like alumina particles sandblasting or diamond bur grinding. For the glass-ceramic class, to date hydrofluoric acid (HF) etching is the best-established procedure, to be performed according to validated protocols taking into account both acid concentration and etching time. For LS₂, 20 s HF etching (at 5% concentration) is suggested, that is a shorter time than requested for feldspathic and leucite-based ceramics (generally 60 s). Higher HF concentrations (9–10%) and longer etching times have been shown to be too aggressive and can introduce relevant damages, not only to the surface but also to the internal microstructure of the material, negatively influencing mechanical performance (reduction of flexure strength), adhesion potential and long-term success of ceramic restorations, particularly when thickness is low [38–41]. Another system to create surface microirregularities is sandblasting LS₂ with aluminum oxide particles. Nevertheless, it has been shown that this procedure, as well as laser etching, can determine excessive loss of material, with surface modifications that are less uniformly distributed than after HF etching and that can significantly reduce flexural strength [42, 43]. In addition to micromechanical interlocking, as for all silica-based materials, adhesive bonding of LS₂ is efficiently increased by silane, ensuring a chemical interaction between the resin-based agent and the ceramics, obtained forming strong siloxane linkages [44–50].

Recently, it has been shown that the use of silane combined to a phosphate functional monomer, the 10-Methacroyloxydecyl-Dihydrogen-Phosphate (10-MDP),

creating an acidic environment further improves the bond strength of resin-based luting cement to lithium disilicate ceramics [51].

Clinical indications and performances

As regards clinical indications of LS₂, it has to be pointed out that this is one of the most versatile metal-free materials for its high esthetic potential, good mechanical properties and favourable bonding strength to dental tissues, thanks to its silica content. Lithium disilicate ceramics can be utilized both for tooth- and implant-supported restorations, ranging from SCs to FDPs, from anterior veneers to posterior inlays, onlays and overlays [4, 7].

To date, due to its relatively recent market introduction, there is still a lack of data about long-term outcomes of LS₂ restorations, particularly as regards CAD-CAM production. Prospective, medium-term studies reported good cumulative survival rates, both for tooth-supported crowns (94.8% after 8 years [52]) and implant-supported crowns, made by CAD-CAM procedure following conventional impression (100% after 5 years [53]). A recent prospective study on implant-supported, single-unit monolithic restorations made of LS₂ in a complete digital workflow has demonstrated survival rates of 100%, without any technical or biological complications, after 2 years of service [54]. Similarly, retrospective studies have shown that LS₂ can yield satisfactory clinical performance with favourable survival rates and low incidence of mechanical failures, like debonding, fractures and chipping [15, 55–58].

As regards chairside procedures, monolithic LS₂ crowns revealed a survival rate of 83.5% after 10 years of follow-up; the main complications were loss of retention, secondary caries and hypersensitivity [59].

In the last decade, LS₂ has been proposed for producing full-contoured, monolithic SCs to be bonded to CAD-CAM zirconia full-arch frameworks supported by implants. In a mid-term study, such a restorative solution exhibited 100% survival rate, after 5 years of follow-up [60]. Recently, an in vitro study has suggested that LS₂ crowns supported by ceramic-reinforced polyether ether ketone (PEEK) implant abutments may be an alternative to zirconia abutments with a titanium base for single-implant restorations in the anterior region [61].

Thanks to the high reliability of resin bond to glass-ceramics, LS₂ clinical indications also include adhesively retained, tooth-supported restorations. In the anterior sites, in the authors' and in other clinicians' clinical experience, laminate veneers made of bilayered, hand-veneered LS₂ are a likely choice, particularly when clinical performance and high esthetic results are expected [62]. Clinical and in vitro studies demonstrated that, in the presence of long teeth, margins positioned beyond the cemento-enamel junction (CEJ), large areas

of exposed dentin or flexural tensile stresses due to high functional loads, laminate veneers are exposed to higher failure risks, being maximum enamel preservation and veneer mechanical resistance paramount success factors [63, 64]. Due to its mechanical properties, lithium disilicate can be considered a viable option to fabricate ceramic veneers in the presence of unfavorable biomechanical conditions; in fact, it was reported that more rigid ceramic materials exert a kind of shield effect onto underlying tooth structures, strengthening the restorative complex [65].

Since their introduction in 1991, all-ceramic, resin-bonded fixed dental prostheses (RBFDPs) have been increasingly utilized as minimally invasive restorations aimed at replacing one missing tooth in the anterior arch [66]. Although recording a high rate of early (1-year), unilateral retainer fractures in conventional, two retainers all-ceramic adhesive bridges, the authors noticed that the fractured, unilaterally supported restorations stayed in situ for 5 to 10 years [67–69]; for that reason, since 1997 cantilevered all-ceramic RBFDPs were proposed as a new conservative treatment modality for replacement of single anterior missing teeth, with minimal tooth preparation on the lingual side, just aimed at achieving a correct positioning during cementation [70]. Different materials have been proposed over the years, mainly, for their high strength, glass-infiltrated alumina ceramics [71] and densely sintered, bilayered zirconia, treated with a combination of moderate pressure air-abrasion and MDP, with promising medium-term outcomes [72–75]. Thanks to its advantageous optical properties and to its HF etching/silane bonding option, LS₂ has also been proposed as an alternative material for such cantilevered restorations, showing comparably promising clinical results [76–78]. In a systematic review, cantilevered RBFDPs showed a lower failure rate than conventional, two-retainer, “Maryland bridge-style” ones, in which higher biomechanical stress arises for the different directions of forces acting on the adjacent supporting teeth during anterior guidance in protrusive and lateral mandibular movements [79]. In another recent review, an estimated 91.2% survival rate at 5 years was reported for all-ceramic RBFDPs, exhibiting higher debonding rate with zirconia resin-bonded restorations than with glass-ceramic ones; conversely a higher fracture rate was reported with glass-ceramics [80], even though higher level of evidence will be necessary to draw final long-term evaluations of all-ceramic RBFDPs clinical performances. RBFDPs are a suitable prosthetic solution as an alternative to implant-supported SCs, in the presence of anatomical impairment requiring costly and invasive surgical procedures, financial problems, young age of patients with congenitally or post-traumatically missing incisors; in any case, to limit the risks of mechanical failure or debonding, after an extensive esthetic, occlusal

and technical evaluation of the case, a very careful treatment planning has to be defined prior to proceed with the operative phases.

In the posterior sites, LS₂ can be successfully employed for resin-bonded single restorations, like inlays, onlays, non-retentive partial crowns and full coverage table-tops, in the monolithic form. The material offers undisputable advantages, like high fracture resistance, showed by high load-at-fracture values in table-tops/occlusal veneers, allowing reduced thickness of the restorations (1–1.5 mm), low wear and abrasive potential, adhesive bonding strength and high biocompatibility, properties that are very favourable when teeth are severely abraded or a heavy occlusal correction is needed (like in lateral post-orthodontic open bite) [10, 81–85]. These restorative solutions have shown favourable clinical outcomes in the most recent literature, even though with limited follow-up [86, 87]. A recent 3-years randomized, controlled prospective trial has shown that LS₂ partial crowns can be used as successful restorative solutions for endodontically treated posterior teeth, with no significant differences between premolar or molars and with or without the use of fiber posts [88].

The utilization of LS₂ for FDPs is a controversial topic: literature data is quite scant and not homogeneous, with a high variability of reported survival and success rates, ranging from rather poor clinical results [89–92] to acceptable long-term serviceability both in anterior and posterior sites, similar to metal-ceramics [93]. In the opinion of the authors, from a strictly clinical point of view, taking into account the cost/benefit ratio in terms of esthetic needs and structural resistance, the material of choice for 3- or 4-unit FDPs is still zirconia, in all of its different typologies.

Marginal accuracy and internal fit

Several studies evaluated the adaptation of lithium disilicate restorations, fabricated in both conventional and digital workflow. According to the most recent literature, there is no significant difference in terms of marginal accuracy between conventional and full-digital procedures for the fabrication of monolithic lithium disilicate crowns [94–96]. Moreover, some authors reported that hot-pressed LS₂ crowns made from conventional impressions with polyvinylsiloxanes exhibit better fit than CAD-CAM digitally produced ones [97].

Furthermore, centralized milling production has been reported to result in better fit compared to chairside system; in the same study, occlusal internal adaptation was better in the conventionally manufactured crowns than in the digitally fabricated ones [95]. Conversely, other studies reported that marginal and internal fit of LS₂ crowns were more accurate when using digital impression technique; in any case, whatever the workflow

used, the adaptation was shown to be within clinical acceptability range [98–101].

To date, drawing univocal conclusions about adaptation accuracy of lithium disilicate restorations is not easy, due to the high number of variables involved in the final prosthetic fit, like digital impression system and technique, used material and fabrication procedure, so there is still a noticeable amount of controversial debate [3, 102]. As regards fabrication techniques, hot-pressed lithium disilicate is reported to offer better internal fit and mechanical performances compared to CAD-CAM pre-crystallized blocks, even if, also about this topic, further data will be necessary to definitely shed light on these aspects, due to the constant evolution and increasing quality of milling procedures and devices [103–108].

Zirconia reinforced-Lithium silicate ceramics (ZLS)

In the last years, the continuous research and progress in prosthetic material field for dental CAD-CAM applications has led to the introduction on the market of promising materials, the ZLS, thanks to an alternative strategy to enhance translucency: a glassy matrix, containing a homogeneous crystalline structure made of lithium silicate crystals, is reinforced with tetragonal zirconia fillers (about 10% by weight) allowing higher strength values than LS₂ [109]. The higher mean translucency, together with proper biaxial flexural strength values, make such material a proper choice for minimally invasive, single tooth esthetic restorations, like inlays, onlays, partial crowns, veneers, anterior and posterior crowns, both tooth- and implant-supported [109, 110], also fulfilling the “no-prep, table-top” strategy [85]. The restorations show higher translucency and ease of intraoral polishing than both feldspathic and disilicate blocks, but, at the same time, exhibit high brittleness [110–112]. In case of a dark substrate, moreover, it has to be considered that the high translucency of the material requires adequate thickness (1.5–2.0 mm) in order to get a proper chromatic masking [113].

To date, as regards mechanical properties and clinical performances of ZLS, data are still limited, often controversial and short-term; these highly promising ceramics need further studies, both in vitro and in vivo, in order to precisely define physical-mechanical properties, clinical indications, limits and long-term performance of such restorations [114–117].

Zirconia

Physico-chemical features

In the ceramic classification, zirconia (ZrO₂) is a heterogenous, highly-resistant, polycrystalline ceramic, characterized by favourable mechanical properties (toughness: 5–10 MPa√m, flexural strength: 500–1200 MPa, Young's modulus: 210 GPa) and good optical characteristics [118–121]; however, differently from

glass-ceramics, it is not susceptible to conventional acid etching techniques and, consequently, does not take advantage of conventional adhesive bonding procedures [122].

Both in vitro and in vivo, it shows excellent biocompatibility, lower plaque retention than titanium and good radiopacity; moreover, it is not soluble in water and its susceptibility to corrosion in the oral environment is negligible [118–121]. Among the various metal-free, ceramic materials, after conventional finishing and polishing, monolithic zirconia exhibits the lowest wear behaviour towards opponent teeth [123].

Phase transformation toughening (PTT)

In dentistry, zirconia is usually considered an all-ceramic material but, from the physical-chemical point of view, it is a metal oxide with ceramic properties characterized by polymorphism and allotropy. In fact, it is present in nature with three different crystalline configurations at different temperatures: cubic (from the melting point at 2680 °C to 2370 °C), tetragonal (from 2370 °C to 1170 °C) and monoclinic (from 1170 °C to room temperature). These different allotropic states present with distinct mechanical and optical properties that can be exploited differently in Prosthodontics [118–121, 124].

Conventionally, zirconia is mainly used in its partially yttria-stabilized tetragonal phase (Y-TZP) as a prosthetic material for indirect restorations. Under the effect of mechanical, thermal and/or combined stresses, the adsorbed energy can break part of the atomic bonds of its polycrystalline structure turning such tetragonal crystals to a stabler monoclinic shape. This spontaneous and irreversible transformation is known as Phase Transformation Toughening (PTT) and shows a contemporary 4–5% increase in crystals volume, creating significant compressive stresses within the material [118–121, 124].

From the technological and prosthetic sides, the PTT has been advertised as a paramount advantage, since it allows a kind of self-repairability of zirconia; indeed, it permits to block or at least to hinder the propagation of micro-cracks and fractures within the material. In fact, the subsequent volumetric increment of the crystals generates compresses within the material at the fracture tip, limiting crack propagation [118–121, 124–126]. It is worth noticing that at room temperature such transformation is irreversible and localized, centered at the stress bearing area (i.e. occlusal load area, traumatic impact zone, etc.): once the limiting action of the fracture propagation has occurred, in its monoclinic configuration zirconia is no longer able to limit cracks any further [119, 124, 126]. On the contrary, heating monoclinic zirconia again up to 900–1000 °C (for limited time according to manufacturers' instructions), the PTT becomes reversible: by means of a process called

“regeneration” or “annealing”, monoclinic crystals can be moved back to the tetragonal phase, causing the relaxation of compressive stresses within the material [125, 126]. After annealing, however, zirconia toughness tends to be reduced and, as regards the optical properties, a chromatic oversaturation can occur; consequently, thermal treatments at high temperature should be used carefully and only after potentially aggressive mechanical procedures (i.e. relevant occlusal grinding, polishing, etc.) [126–128].

In order to profit from the positive features of the PTT intraorally, during industrial manufacturing cubic and tetragonal zirconia are stabilized with metal oxides, just like yttrium, magnesium, cerium and lanthanum; the percentage of such dopants can vary according to manufacturing techniques and clinical use. These stabilizing oxides contribute to keep zirconia in its crystalline tetragonal phase also at room temperature in a thermodynamically metastable state, preventing the spontaneous transformation in the more stable monoclinic crystals. However, such dopant oxides can get lost after traumatic events, surface modifications (i.e. occlusal adjustments, grinding, polishing, etc.) and material aging [118–121, 124–127].

Low temperature degradation (LTD) and aging

In turn, the PTT is closely related to a negative phenomenon, the so-called “Low Temperature Degradation (LTD)”, responsible for zirconia aging. At room temperature, the material can undergo a spontaneous and irreversible transformation to the monoclinic phase, even in the absence of any mechanical stress. This phenomenon causes a worsening of mechanical properties, till the possible occurrence of spontaneous fractures [118–121, 124–127, 129, 130]. The LTD is a multifactorial phenomenon affected by several variables, such as crystals dimension, temperature, surface defects, manufacturing techniques, percentage and distribution of stabilizing oxides, mechanical stress and wetness; particularly, the last two factors can significantly accelerate zirconia aging. Although aging is considered a risk factor for mechanical failure, to date no univocal correlation has been evidenced between this phenomenon and the failures affecting zirconia during clinical service. Nonetheless, the LTD is known to cause a worsening of zirconia characteristics, contributing to the onset of micro-cracks, toughness reduction, increased wear, roughening and plaque accumulation, till a severe surface degradation, affecting both mechanical and optical properties [118–121, 125–127, 129, 130].

As reported in a recent in vitro study, monolithic tetragonal zirconia restorations can undergo hydrothermal degradation (i.e. aging) also after short observation times; however, such phenomenon does not reduce significantly the mechanical properties of tetragonal zirconia even in

the presence of wide monoclinic transformed areas [126]. In the same research, the glassy layer used for glazing effect can act as a protective barrier against hydrothermal degradation; nonetheless, some restoration areas, particularly at the margins, can show absence of glazing protection and subsequently can be more susceptible to aging [126].

In vitro studies have clearly demonstrated that mechanical properties of zirconia, expressed by parameters like load-to-fracture values, are higher than those of LS₂, which, from their part, are higher than those of ZLS; the number of fatigue loading cycles does not seem to affect the load-to-fracture of zirconia restorations [23].

Optical and mechanical properties

Laboratory investigations reported that monolithic zirconia restorations showed higher resistance to fracture than bilayered ones, even after mechanical cycling and aging [131–136]. Surface finishing techniques did not influence mechanical performance [132], neither did cementation techniques, particularly onto implants [137]; on the contrary, fracture resistance has been reported to be significantly influenced by preparation design [138, 139] and low temperature degradation [138], so it can be inferred that material and geometrical characteristics are crucial to optimize longevity of monolithic zirconia restorations [140]. The high mechanical reliability of zirconia has been confirmed by recent in vitro analyses, demonstrating that monolithic zirconia crowns with occlusal thickness of 0.5 mm exhibit sufficient fracture resistance to withstand occlusal loads in the molar regions [134, 135]. Moreover, increasing the content of yttrium oxide to improve the optical properties of zirconia can reduce mechanical properties after aging, although fracture resistance was reported to be higher than masticatory loads (3000 N) [141].

Zirconia is usually considered as an opaque restorative material with optical and esthetic properties less attractive than glassy ceramics, particularly in terms of translucency. By means of transillumination, it has been shown that tetragonal zirconia allows only about 25% of incident light to pass through; this characteristic can be advantageously used to mask dark substrates (i.e. metal posts/abutments, dark teeth, etc.) [126, 127, 142–144].

Recently, in order to enhance the esthetic properties of the material, translucent zirconia has been introduced in the market, characterized by the presence of 30–35% of cubic crystals. Besides the improved optical characteristics, in the presence of such cubic phase no hydrothermal degradation (i.e. aging) of this allotropic component is evidenced. However, apart from the better optical properties, the toughness of translucent zirconia is reduced, compared to tetragonal one, with values of flexural strength ranging between 500 and 900 MPa; as a consequence, translucent zirconia represents a suitable

esthetic and mechanical compromise to be preferred in anterior areas up to the first premolars in its monolithic configuration [126, 142, 143]. As demonstrated by a recent investigation, the reduced mechanical properties of translucent zirconia are due to the dimensions and distribution of the crystals: in fact, cubic grains present with wider dimensions than tetragonal ones and segregate a higher amount of stabilizing oxides, making the tetragonal phase more prone to aging [126].

Manufacturing procedures

Although new additive technologies are emerging from the research on dental materials, to date, zirconia is still fabricated by CAD-CAM milling, according to two different production techniques: either soft machining of pre-sintered zirconia or hard machining of fully-sintered zirconia. Both procedures can be accomplished in industrial milling centers, in dental laboratories or by chair-side devices [118–121, 124, 127].

Soft machining represents the most popular manufacturing technique and is based on milling of pre-sintered zirconia blanks fabricated by cold-isostatic pressing a mixture of zirconia powder, stabilizing oxides and binding agents (the latter removed during the pre-sintering process). With this technique, zirconia is highly homogenous and easier to mill, reducing production times, machinery wear and surface flaws; furthermore, soft machining generates negligible internal porosities (about 20–30 nm). The downside is that this process requires a 25% oversizing of the framework to be milled, since following sintering a linear shrinkage of the final volume occurs; as a consequence, although milling procedures are easier, soft machining requires a precise matching of CAD oversizing and material shrinking in order to avoid dimensional inaccuracies, particularly in the presence of complex framework geometry [118–121, 125, 127].

Viceversa, hard machining requires milling of fully-sintered zirconia blanks generally produced with hot isostatic pressing (HIP) at 1400°–1500 °C. This approach eliminates the problem of post-milling shrinkage, since neither oversizing nor sintering are necessary; however, hard machining needs longer milling times and more complex manufacturing, involving higher costs due to accelerated wear of production machinery and increased risks of attrition flaws. In addition, right after hard machining, zirconia frameworks can undergo a certain amount of monoclinic transformation phase due to mechanical stress, working burs friction and overheating subsequent to machining of the hard material [118–121, 125, 127].

Literature data are still controversial about which technique is the best, being the choice mainly guided by the operator preference, according to considerations related

to shape, volume and complexity of the prosthetic geometry as well as time and cost of the milling procedures [118–121, 127].

High temperature and prolonged sintering time generate bigger zirconia crystals and the dimension of such grains significantly influences the mechanical properties of the material. In fact, the critical crystal dimension is about 1 mm: above this diameter, zirconia becomes spontaneously more susceptible to PTT, while under 0.2 mm such phenomenon does not occur and the toughness of the material decreases. Consequently, fabrication procedures (particularly sintering) significantly affect mechanical properties and stability of zirconia and have to be carefully checked during the whole manufacturing process [126, 127, 129, 130, 142].

In order to get a proper color of the restorations, specific metal oxides can be used as stains within the pre-sintering zirconia powder mixture or metallic salts can be infiltrated after milling; moreover, zirconia blanks are also available in multilayered color configurations. It has been clearly demonstrated that the coloring process does not influence mechanical properties of tetragonal zirconia, whilst uncertainty still remains regarding translucent cubic crystals [118–121, 125, 127, 129, 130].

Zirconia can be fabricated in monolithic or layered configurations. The monolithic material, not veneered with any ceramic layer, shows a less attractive esthetic appearance, but is not affected by the frequent cohesive fractures of the layering ceramics, known as “chipping” [134, 145].

To date, scientific evidences support the use of monolithic zirconia in posterior regions and in not esthetically relevant areas of the anterior arch (i.e. lingual tooth surfaces), while the use of layered restorations should be mainly addressed in highly esthetic zones [134, 145–149]. The minimum thickness suitable for monolithic Y-TZP restorations is 0.5 mm [134]; as regards layered prostheses, the total thickness ranges between 1.0 and 1.5 mm [134, 145–149]. In order to optimize mechanical resistance of layered restorations, it is paramount that veneering ceramics exhibit zirconia-compatible CTE [128, 150].

Marginal accuracy and internal fit

The accuracy of zirconia prostheses can be influenced by several factors, such as manufacturing, complexity of framework geometry (i.e. marginal finish line, span length, connectors dimension, etc.) and aging. The comparison of data regarding internal precision and marginal fit of zirconia is quite difficult, as literature data are heterogeneous and study designs are different for both laboratory and clinical investigations [119, 120, 127]. To date, it is possible to state that marginal precision of zirconia restorations is better than internal fit

(probably because of the shape/size of the CAD-CAM milling burs) and that, in any case, precision values are well within the range of clinical acceptability reported in the specifications of the American Dental Association (ADA). Marginal gap values have been reported between 0 and 75 µm for SCs [151, 152] and 140 µm for FDPs, the latter showing an increasing proportional to framework span [119, 120, 127, 153].

As regards preparation geometry, the high stability and structural resistance of zirconia are compatible with both vertical and horizontal finish lines [124, 153].

Surface treatment and cementation

Due to the absence of any glassy matrix, zirconia is free from silica and, consequently, cannot be conditioned with conventional acid etching techniques, differently from glass-ceramics [119, 122]. Several surface treatments aimed at getting a reliable bond to the substrate have been reported in the literature but to date this topic is still controversial [154–163]. Aggressive sandblasting (i.e. 250 µm alumina particles at 0.4 MPa) can cause loss of the stabilizing oxides with a subsequent increased risk of accelerated PTT and aging of the material; as a consequence, it would be advisable to treat zirconia surfaces with milder sandblasting, using 110 µm alumina particles at 0.2 MPa. Such treatment can be advantageous for partially stabilized zirconia (PSZ) while it seems to weaken the fully stabilized material (FSZ) [155, 156, 158, 159, 163].

The use of coupling agents like silane can be adopted only after a tribochemical conditioning with silica-coated alumina particles or after infiltrating the zirconia surface with a thin layer of glassy ceramics [154, 155, 161]; however, the latter approach can determine the creation of excessive ceramic thickness and the effectiveness of adhesion between the glassy matrix and the polycrystalline network still remains unclear [154, 155, 158, 161].

The combination of mechanical and chemical treatments of zirconia surface was proved to offer the best results; particularly, the use of primers and adhesion promoting agents containing acidic monomers (10-MDP) can have a synergic effect with silane, improving the effectiveness of simplified adhesive techniques [155, 160–163].

On the basis of the physical-chemical properties of zirconia, in the presence of retentive preparation geometries and full coverage prostheses, conventional water-based luting agents (i.e. glass-ionomer and zinc phosphate cements) and hybrid cements (i.e. resin-modified glass-ionomer cements) can be considered a good choice for cementation. Otherwise, in the presence of partial coverage restorations, scarcely retentive preparation geometries (e.g. abutment teeth with reduced occluso-cervical dimension) and/or high masticatory loads, besides the above mentioned conditioning treatments of zirconia surface, it is possible to use

conventional resin cement or simplified self-adhesive luting agents, so as to allow resin better adsorb, distribute occlusal forces and withstand possible micro-cracks on the inner surface of the restorations [155, 158, 162].

Clinical indication and performances

From a clinical point of view, in the last decades zirconia has more and more gained ground in the realm of metal-free, mainly utilized to restore both natural teeth and osseointegrated implants with SCs and short- and medium-span FDPs up to 5 elements [134, 145, 146, 148, 149, 164, 165]. As regards FDPs, besides the high mechanical properties of the material, fracture resistance and clinical performance are also strongly related to a proper framework architecture. In case of bilayered FDPs, in particular, an “anatomic” design has to be performed, ensuring proper support and thickness to the veneering; moreover, connectors are to be designed with adequate dimensions (minimum area of section: 9, 15 and 25 mm² for 3-, 4- and 5-unit FDPs respectively) and with rounded interdental embrasures, in order to avoid sharp angles that can contribute to generate risky stress concentration [146]. The presence of an adequate occlusal support is a relevant factor in maintaining an efficient chewing [166]; consequently, due to the absence of veneering ceramics that could be subjected to wear over time, monolithic restorations could be helpful in keeping occlusal stability during clinical service, particularly in the presence of discrepancies in occlusal contact patterns that could influence the onset of temporo-mandibular disorders [167].

Recently, clinical investigations regarding tooth- and implant-supported full-arch restorations have been published [165]. Although short- and medium-term results were encouraging with 94.8% success rate after 3 years of clinical service for monolithic full-arch bridges [145], it is worth noticing that a systematic review of the literature has reported 5-year complication rates of 27.6 and 30.5%, respectively for tooth-supported and implant-supported full-arch restorations [168]. Moreover, layered restorations showed 5-year success rates significantly lower than monolithic prostheses (i.e. 60.4% vs 90.9%) [169]. Consequently, the use of full-arch, extended zirconia restorations should always be carefully evaluated and further long-term clinical studies are necessary to validate the effectiveness of their serviceability.

As regards zirconia implants, the literature reports controversial, short-term and mainly anecdotal data [165, 170–174]. A recent systematic review with meta-analysis has evidenced similar potentialities of hard- and soft-tissue integration between zirconia and titanium implants, although with a slower initial osseointegration process detected in zirconia ones. In any case, the use of the latter should be cautiously evaluated, until more

light is shed on long term outcomes and, particularly, on the possible mechanical complications. Viceversa, zirconia abutments are to be considered widely validated today in the esthetic sites, where the clear color of zirconia contributes to achieve a natural aspect of peri-implant soft tissues, particularly when they are quite thin [127, 148, 165, 172, 173]. A retrospective clinical study on a relevant number of ceramic abutments reported that internal zirconia implant connections are much more prone to mechanical complications (i.e. unscrewing, fractures, etc.) than hybrid connections with zirconia abutments cemented onto titanium bases; moreover, the same investigation reported that the distance between the implant/abutment connection and the occlusal plane can significantly influence the onset of bending moments that can be detrimental for the long-term prognosis of metal-free restorations [172].

Conclusions

At the moment, it can be stated that silicate- and zirconia-based ceramics are amongst the most versatile metal-free materials available for the “digital prosthodontic environment”. In the last years, an increasing amount of available in vitro and in vivo data is shedding precious light on the outline of guidelines for a restorative rational use, focused on specific materials advantages and limitations, taking into account mechanical, optical and biological properties in the light of a widespread clinical experience (Table 1). In the meanwhile, the world of industry is intensively

Table 1 Lithium disilicate and zirconia: pros and cons

Lithium disilicate	
Pros	Cons
<ul style="list-style-type: none"> • excellent optical characteristics and good mechanical properties • clinical versatility • biocompatibility • favourable abrasiveness • marginal accuracy and internal fit • high strength of adhesion to the substrate • monolithic and layered 	<ul style="list-style-type: none"> • glaze coating and fluorapatite ceramic veneering can increase wear • critical to adjust intraorally • chipping of the veneering ceramics
Zirconia	
Pros	Cons
<ul style="list-style-type: none"> • excellent mechanical characteristics and good optical properties • excellent biocompatibility and low plaque retention • favourable wear behaviour • implant abutments for esthetic sites • crack-hindering potential (through PTT) • marginal accuracy and internal fit • monolithic and layered 	<ul style="list-style-type: none"> • opacity • unetchable with conventional methods • low temperature degradation and aging • critical to adjust intraorally • glaze coating and fluorapatite ceramic veneering can increase wear • chipping of the veneering ceramics

working on new strategies aimed at further enhancing microstructural characteristics of these materials, together with the introduction of new production technologies, mainly based on additive processes.

Abbreviations

10-MDP: 10-Methacryloyloxydecyl-Dihydrogen-Phosphate; ADA: American Dental Association; $\text{Ca}_5(\text{PO}_4)_3\text{F}$: Fluorapatite crystals; CAD-CAM: Computer-aided design/computer-aided manufacturing; CEJ: Cemento-enamel junction; CTE: Coefficient of thermal expansion; FDPs: Fixed dental prostheses; FSZ: Fully stabilized zirconia; HF: Hydrofluoric acid; HIP: Hot isostatic pressing; KIC: Fracture toughness; $\text{Li}_2\text{Si}_2\text{O}_5$: Lithium disilicate crystal nuclei; Li_2SiO_3 : Metasilicates; LS_2 : Lithium disilicate; LTD: Low Temperature Degradation; PEEK: Polyether ether ketone; PSZ: Partially stabilized zirconia; PTT: Phase Transformation Toughening; RBFDPs: Resin-bonded fixed dental prostheses; SCs: Single crowns; SEM: Scanning electron microscope; Y-TZP: Yttria stabilized tetragonal zirconia; ZLS: Zirconia reinforced-Lithium Silicate ceramics; ZrO_2 : Zirconia

Publisher's Note

Springer Nature remains neutral with regard to jurisdictional claims in published maps and institutional affiliations.

Acknowledgements

Not applicable.

Authors' contributions

MIDM and GR acquired and analyzed all the papers included in the present review and performed the preparation of the manuscript; FZ, PA and RS revised the work and approved the submitted version. All authors read and approved the final manuscript.

Funding

Not applicable.

Availability of data and materials

Not applicable.

Ethics approval and consent to participate

Not applicable.

Consent for publication

The authors give their consent for publication.

Competing interests

The authors declare that they have no competing interests.

Received: 24 April 2019 Accepted: 27 June 2019

Published online: 04 July 2019

References

- Albakry M, Guazzato M, Swain MV. Influence of hot pressing on the microstructure and fracture toughness of two pressable dental glass-ceramics. *J Biomed Mater Res B Appl Biomater*. 2004;71(1):99–107.
- Denry I, Holloway JA. Ceramics for dental applications: a review. *Materials*. 2010;3:351–68.
- Zarone F, Ferrari M, Mangano FG, Leone R, Sorrentino R. "Digitally oriented materials": focus on lithium disilicate ceramics. *Int J Dent*. 2016;2016:9840594.
- Fischer K, Bühler-Zemp P, Völkel T. Scientific Documentation IPS e.max CAD. Schaan, Liechtenstein: Ivoclar Vivadent; 2005. p. 1–30.
- Willard A, Gabriel Chu TM. The science and application of IPS e. max dental ceramic. *Kaohsiung J Med Sci*. 2018;34(4):238–42.
- Vivadent I. IPS e. max lithium disilicate: the future of all- ceramic dentistry material science, practical applications, keys to success. Amherst, NY: Ivoclar Vivadent; 2009. p. 1e15.
- Fabian Fonzar R, Carrabba M, Sedda M, Ferrari M, Goracci C, Vichi A. Flexural resistance of heat-pressed and CAD-CAM lithium disilicate with different translucencies. *Dent Mater*. 2017;33(1):63–70.
- Belli R, Geinzer E, Muschweck A, Petschelt A, Lohbauer U. Mechanical fatigue degradation of ceramics versus resin composites for dental restorations. *Dent Mater*. 2014;30(4):424–32.
- Furtado de Mendonça A, Shahmoradi M, Gouvêa CVD, De Souza GM, Ellakwa A. Microstructural and mechanical characterization of CAD/CAM materials for monolithic dental restorations. *J Prosthodont*. 2019;28(2):e587–94.
- Guess PC, Zavanelli RA, Silva NR, Bonfante EA, Coelho PG, Thompson VP. Monolithic CAD/CAM lithium disilicate versus veneered Y-TZP crowns: comparison of failure modes and reliability after fatigue. *Int J Prosthodont*. 2010;23(5):434–42.
- Lien W, Roberts HW, Platt JA, Vandewalle KS, Hill TJ, Chu TM. Microstructural evolution and physical behavior of a lithium disilicate glass-ceramic. *Dent Mater*. 2015;31:928–40.
- Al Mansour F, Karpukhina N, Grasso S, Wilson RM, Reece MJ, Cattell MJ. The effect of spark plasma sintering on lithium disilicate glass-ceramics. *Dent Mater*. 2015;31(10):e226–35.
- Kubatík TF, Lukáč F, Mušálek R, Brožek V, Stehliková K, Chrástka T. Compaction of lithium-silicate ceramics using spark plasma sintering. *Ceramics-Silikáty*. 2017;61(1):40–4.
- Zhao K, Wei YR, Pan Y, Zhang XP, Swain MV, Guess PC. Influence of veneer and cyclic loading on failure behavior of lithium disilicate glass-ceramic molar crowns. *Dent Mater*. 2014;30(2):164–71.
- Silva NR, Thompson VP, Valverde GB, Coelho PG, Powers JM, Farah JW, Esquivel-Upshaw J. Comparative reliability analyses of zirconium oxide and lithium disilicate restorations in vitro and in vivo. *J Am Dent Assoc*. 2011;142(Suppl 2):45–9S.
- Schultheis S, Strub JR, Gerds TA, Guess PC. Monolithic and bi-layer CAD/CAM lithium disilicate versus metalceramic fixed dental prostheses: comparison of fracture loads and failure modes after fatigue. *Clin Oral Investig*. 2013;17(5):1407–13.
- Kim JH, Lee SJ, Park JS, Ryu JJ. Fracture load of monolithic CAD/CAM lithium disilicate ceramic crowns and veneered zirconia crowns as a posterior implant restoration. *Implant Dent*. 2013;22(1):66–70.
- Monaco C, Rosentritt M, Llukacej A, Baldissara P, Scotti R. Marginal adaptation, gap width, and fracture strength of teeth restored with different all-ceramic vs metal ceramic crown systems: an in vitro study. *Eur J Prosthodont Restor Dent*. 2016;24(3):130–7.
- Dogan DO, Gorler O, Mutaf B, Ozcan M, Eyuboglu GB, Ulgey M. Fracture resistance of molar crowns fabricated with monolithic all-ceramic CAD/CAM materials cemented on titanium abutments: an in vitro study. *J Prosthodont*. 2017;26(4):309–14.
- Hamza TA, Sherif RM. Fracture resistance of monolithic glass-ceramics versus bilayered zirconia-based restorations. *J Prosthodont*. 2019;28(1):e259–64.
- Choi JW, Kim SY, Bae JH, Bae EB, Huh JB. In vitro study of the fracture resistance of monolithic lithium disilicate, monolithic zirconia, and lithium disilicate pressed on zirconia for three-unit fixed dental prostheses. *J Adv Prosthodont*. 2017;9(4):244–51.
- Alsarani M, Souza G, Rizkalla A, El-Mowafy O. Influence of crown design and material on chipping-resistance of all-ceramic molar crowns: an in vitro study. *Dent Med Probl*. 2018;55(1):35–42.
- Kashkari A, Yilmaz B, Brantley WA, Schricker SR, Johnston WM. Fracture analysis of monolithic CAD-CAM crowns. *J Esthet Restor Dent*. 2019. <https://doi.org/10.1111/jerd.12462>.
- Nawafleh N, Hatamleh M, Elshiyab S, Mack F. Lithium disilicate restorations fatigue testing parameters: a systematic review. *J Prosthodont*. 2016;25(2):116–26.
- Lee A, Swain M, He L, Lyons K. Wear behavior of human enamel against lithium disilicate glass ceramic and type III gold. *J Prosthet Dent*. 2014;112:1399–405.
- Kim MJ, Oh SH, Kim JH, Ju SW, Seo DG, Jun SH, Ahn JS, Ryu JJ. Wear evaluation of the human enamel opposing different Y-TZP dental ceramics and other porcelains. *J Dent*. 2012;40(11):979–88.
- Amer R, Kürklü D, Kateeb E, Seghi RR. Three-body wear potential of dental yttrium-stabilized zirconia ceramic after grinding, polishing, and glazing treatments. *J Prosthet Dent*. 2014;112(5):1151–5.
- Zurek AD, Alfaro MF, Wee AG, Yuan JC, Barao VA, Mathew MT, Sukotjo C. Wear characteristics and volume loss of CAD/CAM ceramic materials. *J Prosthodont*. 2019;28(2):e510–8.
- Preis V, Weiser F, Handel G, Rosentritt M. Wear performance of monolithic dental ceramics with different surface treatments. *Quintessence Int*. 2013;44:393–405.

30. Mörmann WH, Stawarczyk B, Ender A, Sener B, Attin T, Mehl A. Wear characteristics of current aesthetic dental restorative CAD/CAM materials: two-body wear, gloss retention, roughness and martens hardness. *J Mech Behav Biomed Mater.* 2013;20:113–25.
31. Peng Z, Izzat Abdul Rahman M, Zhang Y, Yin L. Wear behavior of pressable lithium disilicate glass ceramic. *J Biomed Mater Res B Appl Biomater.* 2016; 104(5):968–78.
32. Song XF, Ren HT, Yin L. Machinability of lithium disilicate glass ceramic in vitro dental diamond bur adjusting process. *J Mech Behav Biomed Mater.* 2016;53:78–92.
33. Figueiredo-Pina CG, Patas N, Canhoto J, Cláudio R, Olhero SM, Serro AP, Ferro AC, Guedes M. Tribological behaviour of unveneered and veneered lithium disilicate dental material. *J Mech Behav Biomed Mater.* 2016;53:226–38.
34. Forster A, Ungvári K, Györgyey Á, Kukovecz Á, Turzó K, Nagy K. Human epithelial tissue culture study on restorative materials. *J Dent.* 2014; 42(1):7–14.
35. Tetè S, Zizzari VL, Borelli B, De Colli M, Zara S, Sorrentino R, Scarano A, Gherlone E, Cataldi A, Zarone F. Proliferation and adhesion capability of human gingival fibroblasts onto zirconia, lithium disilicate and feldspathic veneering ceramic in vitro. *Dent Mater J.* 2014;33(1):7–15.
36. Ariaans K, Heussen N, Schiffer H, Wienert AL, Plümackers B, Rink L, Wolfart S. Use of molecular indicators of inflammation to assess the biocompatibility of all-ceramic restorations. *J Clin Periodontol.* 2016;43(2):173–9.
37. Baldissara P, Llukacej A, Ciocca L, Valandro FL, Scotti R. Translucency of zirconia copings made with different CAD/CAM systems. *J Prosthet Dent.* 2010;104(1):6–12.
38. Murillo-Gómez F, Palma-Dibb RG, De Goes MF. Effect of acid etching on tridimensional microstructure of etchable CAD/CAM materials. *Dent Mater.* 2018;34(6):944–55.
39. Bajraktarova-Valjakova E, Grozdanov A, Guguvcevski L, Korunoska-Stevkovska V, Kapusevska B, Gigovski N, Mijoska A, Bajraktarova-Misevska C. Acid etching as surface treatment method for luting of glass-ceramic restorations, part 1: acids, application protocol and etching effectiveness. *Open Access Maced J Med Sci.* 2018;6(3):568–73.
40. Prochnow C, Venturini AB, Guillard LF, Pereira GKR, Burgo TAL, Bottino MC, Kleverlaan CJ, Valandro LF. Hydrofluoric acid concentrations: effect on the cyclic load-to-failure of machined lithium disilicate restorations. *Dent Mater.* 2018;34(9):e255–63.
41. Sundfeld D, Paliolol ARM, Fugolin APP, Ambrosano GMB, Correr-Sobrinho L, Martins LRM, Pfeifer CS. The effect of hydrofluoric acid and resin cement formulation on the bond strength to lithium disilicate ceramic. *Braz Oral Res.* 2018;32:e43.
42. Ataol AS, Ergun G. Repair bond strength of resin composite to bilayer dental ceramics. *J Adv Prosthodont.* 2018;10(2):101–12.
43. Menees TS, Lawson NC, Beck PR, Burgess JO. Influence of particle abrasion or hydrofluoric acid etching on lithium disilicate flexural strength. *J Prosthet Dent.* 2014;112(5):1164–70.
44. Blatz MB, Sadan A, Kern M. Resin-ceramic bonding: a review of the literature. *J Prosthet Dent.* 2003;89(3):268–74.
45. Carvalho AO, Bruzi G, Giannini M, Magne P. Fatigue resistance of CAD/CAM complete crowns with a simplified cementation process. *J Prosthet Dent.* 2014;111:310–7.
46. Fabbri G, Sorrentino R, Brennan M, Cerutti A. A novel approach to implant screw-retained restorations: adhesive combination between zirconia frameworks and monolithic lithium disilicate. *Int J Esthet Dent.* 2014;9:490–505.
47. Frankenberger R, Hartmann VE, Krech M, Krämer N, Reich S, Braun A, Roggendorf M. Adhesive luting of new CAD/CAM materials. *Int J Comput Dent.* 2015;18:9–20.
48. Neis CA, Albuquerque NL, Albuquerque Ide S, Gomes EA, Souza-Filho CB, Feitosa VP, Spazzini AO, Bacchi A. Surface treatments for repair of feldspathic, leucite - and lithium disilicate-reinforced glass ceramics using composite resin. *Braz Dent J.* 2015;26(2):152–5.
49. Carvalho AO, Bruzi G, Anderson RE, Maia HP, Giannini M, Magne P. Influence of adhesive core buildup designs on the resistance of endodontically treated molars restored with lithium disilicate CAD/CAM crowns. *Oper Dent.* 2016;41:76–82.
50. Swank HM, Motyka NC, Bailey CW, Vandewalle KS. Bond strength of resin cement to ceramic with simplified primers and pretreatment solutions. *Gen Dent.* 2018;66(5):33–7.
51. Taguchi S, Komine F, Kubochi K, Fushiki R, Kimura F, Matsumura H. Effect of a silane and phosphate functional monomer on shear bond strength of a resin-based luting agent to lithium disilicate ceramic and quartz materials. *J Oral Sci.* 2018;60(3):360–6.
52. Gehrt M, Wolfart S, Rafai N, Reich S, Edelhoff D. Clinical results of lithium-disilicate crowns after up to 9 years of service. *Clin Oral Investig.* 2013;17(1):275–84.
53. Spies BC, Pieralli S, Vach K, Kohal RJ. CAD/CAM-fabricated ceramic implant-supported single crowns made from lithium disilicate: final results of a 5-year prospective cohort study. *Clin Implant Dent Relat Res.* 2017;19(5):876–83.
54. Joda T, Ferrari M, Brägger U. Monolithic implant-supported lithium disilicate (LS2) crowns in a complete digital workflow: a prospective clinical trial with a 2-year follow-up. *Clin Implant Dent Relat Res.* 2017;19(3):505–11.
55. Fabbri G, Zarone F, Dellificorelli G, Cannistraro G, De Lorenzi M, Mosca A, Sorrentino R. Clinical evaluation of 860 anterior and posterior lithium disilicate restorations: retrospective study with a mean follow-up of 3 years and a maximum observational period of 6 years. *Int J Periodontics Restorative Dent.* 2014;34(2):165–77.
56. Simeone P, Gracis S. Eleven-year retrospective survival study of 275 veneered lithium disilicate single crowns. *Int J Periodontics Restorative Dent.* 2015; 35(5):685–94.
57. Valenti M, Valenti A. Retrospective survival analysis of 110 lithium disilicate crowns with feather-edge marginal preparation. *Int J Esthet Dent.* 2015; 10(2):246–57.
58. van den Breemer CR, Vinkenborg C, van Pelt H, Edelhoff D, Cune MS. The clinical performance of monolithic lithium disilicate posterior restorations after 5, 10, and 15 years: a retrospective case series. *Int J Prosthodont.* 2017; 30(1):62–5.
59. Rauch A, Reich S, Dalchau L, Schierz O. Clinical survival of chair-side generated monolithic lithium disilicate crowns: 10-year results. *Clin Oral Investig.* 2018;22(4):1763–9.
60. Pozzi A, Tallarico M, Barlattani A. Monolithic lithium disilicate full-contour crowns bonded on CAD/CAM zirconia complete-arch implant bridges with 3 to 5 years of follow-up. *J Oral Implantol.* 2015;41(4): 450–8.
61. Atsü SS, Aksan ME, Bulut AC. Fracture resistance of titanium, zirconia, and ceramic-reinforced polyetheretherketone implant abutments supporting CAD/CAM monolithic lithium disilicate ceramic crowns after aging. *Int J Oral Maxillofac Implants.* 2019;34(3):622–30.
62. Radz GM. Minimum thickness anterior porcelain restorations. *Dent Clin N Am.* 2011;55(2):353–70 ix.
63. Ge C, Green CC, Sederstrom D, McLaren EA, White SN. Effect of porcelain and enamel thickness on porcelain veneer failure loads in vitro. *J Prosthet Dent.* 2014;111(5):380–7.
64. Ge C, Green CC, Sederstrom DA, McLaren EA, Chalfant JA, White SN. Effect of tooth substrate and porcelain thickness on porcelain veneer failure loads in vitro. *J Prosthet Dent.* 2018;120(1):85–91.
65. Sorrentino R, Apicella D, Riccio C, Gherlone E, Zarone F, Aversa R, Garcia-Godoy F, Ferrari M, Apicella A. Nonlinear visco-elastic finite element analysis of different porcelain veneers configuration. *J Biomed Mater Res B Appl Biomater.* 2009;91(2):727–36.
66. Kern M, Knöde H, Strub JR. The all-porcelain, resin-bonded bridge. *Quintessence Int.* 1991;22(4):257–62.
67. Kern M, Strub JR. Bonding to alumina ceramic in restorative dentistry: clinical results over up to 5 years. *J Dent.* 1998;26(3):245–9.
68. Kern M. Clinical long-term survival of two-retainer and single-retainer all-ceramic resin-bonded fixed partial dentures. *Quintessence Int.* 2005; 36(2):141–7.
69. Kern M, Sasse M. Ten-year survival of anterior all-ceramic resin-bonded fixed dental prostheses. *J Adhes Dent.* 2011;13(5):407–10.
70. Kern M, Gläser R. Cantilevered all-ceramic, resin-bonded fixed partial dentures: a new treatment modality. *J Esthet Dent.* 1997;9(5):255–64.
71. Kern M. Fifteen-year survival of anterior all-ceramic cantilever resin-bonded fixed dental prostheses. *J Dent.* 2017;56:133–5.
72. Sasse M, Kern M. CAD/CAM single retainer zirconia-ceramic resin-bonded fixed dental prostheses: clinical outcome after 5 years. *Int J Comput Dent.* 2013;16(2):109–18.
73. Sailer I, Hämmeler CH. Zirconia ceramic single-retainer resin-bonded fixed dental prostheses (RBFDPs) after 4 years of clinical service: a retrospective

- clinical and volumetric study. *Int J Periodontics Restorative Dent*. 2014;34(3):333–43.
74. Sasse M, Kern M. Survival of anterior cantilevered all-ceramic resin-bonded fixed dental prostheses made from zirconia ceramic. *J Dent*. 2014;42(6):660–3.
 75. Klink A, Hüttig F. Zirconia-based anterior resin-bonded single-retainer cantilever fixed dental prostheses: a 15- to 61-month follow-up. *Int J Prosthodont*. 2016;29(3):284–6.
 76. Sun Q, Chen L, Tian L, Xu B. Single-tooth replacement in the anterior arch by means of a cantilevered IPS e.max press veneer-retained fixed partial denture: case series of 35 patients. *Int J Prosthodont*. 2013;26:181–7.
 77. Sailer I, Bonani T, Brodbeck U, Hämmerle CH. Retrospective clinical study of single-retainer cantilever anterior and posterior glass-ceramic resin-bonded fixed dental prostheses at a mean follow-up of 6 years. *Int J Prosthodont*. 2013;26(5):443–50.
 78. Zhou T, Wang X, Zhang G. All-ceramic resin bonded fixed partial denture made of IPS hot-pressed casting porcelain restore anterior missing teeth: a three years clinical observation. *Beijing Da Xue Xue Bao*. 2011;43(1):77–80.
 79. Wei YR, Wang XD, Zhang Q, Li XX, Blatz MB, Jian YT, Zhao K. Clinical performance of anterior resin-bonded fixed dental prostheses with different framework designs: a systematic review and meta-analysis. *J Dent*. 2016;47:1–7.
 80. Chen J, Cai H, Ren X, Suo L, Pei X, Wan Q. A systematic review of the survival and complication rates of all-ceramic resin-bonded fixed dental prostheses. *J Prosthodont*. 2018;27(6):535–43.
 81. Dhima M, Carr AB, Salinas TJ, Lohse C, Berglund L, Nan KA. Evaluation of fracture resistance in aqueous environment under dynamic loading of lithium disilicate restorative systems for posterior applications. Part 2. *J Prosthodont*. 2014;23(5):353–7.
 82. Seydler B, Rues S, Muller D, Schmitter M. In vitro fracture load of monolithic lithium disilicate ceramic molar crowns with different wall thicknesses. *Clin Oral Investig*. 2014;18:1165–71.
 83. Sasse M, Krummel A, Klosa K, Kern M. Influence of restoration thickness and dental bonding surface on the fracture resistance of full-coverage occlusal veneers made from lithium disilicate ceramic. *Dent Mater*. 2015;31(8):907–15.
 84. Vianna ALSV, Prado CJD, Bicalho AA, Pereira RADS, Neves FDD, Soares CJ. Effect of cavity preparation design and ceramic type on the stress distribution, strain and fracture resistance of CAD/CAM onlays in molars. *J Appl Oral Sci*. 2018;26:e20180004.
 85. von Maltzahn NF, E Meniawy OI, Breitenbuecher N, Kohorst P, Stiesch M, Eisenburger M. Fracture strength of ceramic posterior occlusal veneers for functional rehabilitation of an abrasive dentition. *Int J Prosthodont*. 2018;31(5):451–2.
 86. Mobilio N, Fasiol A, Catapano S. Survival rates of lithium disilicate single restorations: a retrospective study. *Int J Prosthodont*. 2018;31(3):283–6.
 87. Politano G, Van Meerbeek B, Peumans M. Nonretentive bonded ceramic partial crowns: concept and simplified protocol for long-lasting dental restorations. *J Adhes Dent*. 2018;20(6):495–510.
 88. Ferrari M, Ferrari Cagidiaco E, Goracci C, Sorrentino R, Zarone F, Grandini S, Joda T. Posterior partial crowns out of lithium disilicate (LS2) with or without posts: a randomized controlled prospective clinical trial with a 3-year follow up. *J Dent*. 2019;83:12–7.
 89. Makarouna M, Ullmann K, Lazarek K, Boening KW. Six-year clinical performance of lithium disilicate fixed partial dentures. *Int J Prosthodont*. 2011;24:204–6.
 90. Taskonak B, Sertgöz A. Two-year clinical evaluation of lithia-disilicate-based all-ceramic crowns and fixed partial dentures. *Dent Mater*. 2006;22:1008–13.
 91. Solá-Ruiz MF, Lagos-Flores E, Román-Rodríguez JL, Highsmith Jdel R, Fons-Font A, Granell-Ruiz M. Survival rates of a lithium disilicate-based core ceramic for three-unit esthetic fixed partial dentures: a 10-year prospective study. *Int J Prosthodont*. 2013;26(2):175–80.
 92. Teichmann M, Göckler F, Weber V, Yildirim M, Wolfart S, Edelhoff D. Ten-year survival and complication rates of lithium-disilicate (empress 2) tooth-supported crowns, implant-supported crowns, and fixed dental prostheses. *J Dent*. 2017;56:65–77.
 93. Kern M, Sasse M, Wolfart S. Ten-year outcome of three-unit fixed dental prostheses made from monolithic lithium disilicate ceramic. *J Am Dent Assoc*. 2012;143:234–40.
 94. Abdel-Aziz T, Rogers K, Elathamna E, Zandinejad A, Metz M, Morton D. Comparison of the marginal fit of lithium disilicate crowns fabricated with CAD/CAM technology by using conventional impressions and two intraoral digital scanners. *J Prosthet Dent*. 2015;114(4):554–9.
 95. Zeltner M, Sailer I, Mühlemann S, Özcan M, Hämmerle CH, Benic GL. Randomized controlled within-subject evaluation of digital and conventional workflows for the fabrication of lithium disilicate single crowns. Part III: marginal and internal fit. *J Prosthet Dent*. 2017;117(3):354–62.
 96. Haddadi Y, Bahrami G, Isidor F. Accuracy of crowns based on digital intraoral scanning compared to conventional impression-a split-mouth randomised clinical study. *Clin Oral Investig*. 2019. <https://doi.org/10.1007/s00784-019-02840-0>.
 97. Anadioti E, Aquilino SA, Gratton DG, Holloway JA, Denry I, Thomas GW, Qian F. 3D and 2D marginal fit of pressed and CAD/CAM lithium disilicate crowns made from digital and conventional impressions. *J Prosthodont*. 2014;23(8):610–7.
 98. Memari Y, Mohajerfar M, Armin A, Kamalian F, Rezayani V, Beyabanaki E. Marginal adaptation of CAD/CAM all-ceramic crowns made by different impression methods: a literature review. *J Prosthodont*. 2019;28(2):e536–44.
 99. Mostafa NZ, Ruse ND, Ford NL, Carvalho RM, Wyatt CCL. Marginal fit of lithium disilicate crowns fabricated using conventional and digital methodology: a three-dimensional analysis. *J Prosthodont*. 2018;27(2):145–52.
 100. Ng J, Ruse D, Wyatt C. A comparison of the marginal fit of crowns fabricated with digital and conventional methods. *J Prosthet Dent*. 2014;112(3):555–60.
 101. Alfaro DP, Ruse ND, Carvalho RM, Wyatt CC. Assessment of the internal fit of lithium disilicate crowns using micro-CT. *J Prosthodont*. 2015;24:381–6.
 102. Schaefer O, Decker M, Wittstock F, Kuepper H, Guentsch A. Impact of digital impression techniques on the adaption of ceramic partial crowns in vitro. *J Dent*. 2014;42(6):677–83.
 103. Mously HA, Finkelman M, Zandparsa R, Hirayama H. Marginal and internal adaptation of ceramic crown restorations fabricated with CAD/CAM technology and the heat-press technique. *J Prosthet Dent*. 2014;112:249–56.
 104. Guess PC, Vagkopoulou T, Zhang Y, Wolkewitz M, Strub JR. Marginal and internal fit of heat pressed versus CAD/CAM fabricated all-ceramic onlays after exposure to thermo-mechanical fatigue. *J Dent*. 2014;42(2):199–209.
 105. Azar B, Eckert S, Kunkela J, Ingr T, Mounajjed R. The marginal fit of lithium disilicate crowns: press vs. CAD/CAM. *Braz Oral Res*. 2018;32:e001.
 106. Neves FD, Prado CJ, Prudente MS, Carneiro TA, Zancopé K, Davi LR, Mendonça G, Cooper LF, Soares CJ. Micro-computed tomography evaluation of marginal fit of lithium disilicate crowns fabricated by using chairside CAD/CAM systems or the heat-pressing technique. *J Prosthet Dent*. 2014;112(5):134–40.
 107. Homsy F, Bottin M, Özcan M, Majzoub Z. Fit accuracy of pressed and milled lithium disilicate inlays fabricated from conventional impressions or a laboratory-based digital workflow. *Eur J Prosthodont Restor Dent*. 2019;27(1):18–25.
 108. Revilla-León M, Olea-Vielba M, Estes-Saiz A, Martínez-Klemm I, Özcan M. Marginal and internal gap of handmade, milled and 3D printed additive manufactured patterns for pressed lithium disilicate onlay restorations. *Eur J Prosthodont Restor Dent*. 2018;26(1):31–8.
 109. Elsaka SE, Elnaghy AM. Mechanical properties of zirconia reinforced lithium silicate glass-ceramic. *Dent Mater*. 2016;32(7):908–14.
 110. Sen N, Us YO. Mechanical and optical properties of monolithic CAD-CAM restorative materials. *J Prosthet Dent*. 2018;119(4):593–9.
 111. Lauvahanon S, Takahashi H, Shiozawa M, Iwasaki N, Asakawa Y, Oki M, Finger WJ, Arksornnukit M. Mechanical properties of composite resin blocks for CAD/CAM. *Dent Mater J*. 2014;33(5):705–10.
 112. Vichi A, Fonzar RF, Goracci C, Carrabba M, Ferrari M. Effect of finishing and polishing on roughness and gloss of lithium disilicate and lithium silicate zirconia reinforced glass ceramic for CAD/CAM systems. *Oper Dent*. 2018;43(1):90–100.
 113. Passos L, Linke B, Street A, Torrealba Y. Effect of thickness, translucency, and firing protocol on the masking ability of a CAD/CAM zirconia-reinforced lithium silicate for different backgrounds. *Int J Comput Dent*. 2019;22(1):29–38.
 114. Ramos Nde C, Campos TM, Paz IS, Machado JP, Bottino MA, Cesar PF, Melo RM. Microstructure characterization and SCG of newly engineered dental ceramics. *Dent Mater*. 2016;32(7):870–8.
 115. Fathy SM, Swain MV. In-vitro wear of natural tooth surface opposed with zirconia reinforced lithium silicate glass ceramic after accelerated ageing. *Dent Mater*. 2018;34(3):551–9.

116. Zimmermann M, Koller C, Mehl A, Hickel R. Indirect zirconia-reinforced lithium silicate ceramic CAD/CAM restorations: preliminary clinical results after 12 months. *Quintessence Int.* 2017;48(1):19–25.
117. Saavedra GSFA, Rodrigues FP, Bottino MA. Zirconia-reinforced lithium silicate ceramic - a 2-year follow-up of a clinical experience with anterior crowns. *Eur J Prosthodont Restor Dent.* 2017;25(1):57–63.
118. Denry I, Kelly JR. State of the art of zirconia for dental applications. *Dent Mater.* 2008;24:299–307.
119. Zarone F, Russo S, Sorrentino R. From porcelain-fused-to-metal to zirconia: clinical and experimental considerations. *Dent Mater.* 2011;27(1):83–96.
120. Miyazaki T, Nakamura T, Matsumura H, Ban S, Kobayashi T. Current status of zirconia restoration. *J Prosthodont Res.* 2013;57(4):236–61.
121. Chen YW, Moussi J, Drury JL, Wataha JC. Zirconia in biomedical applications. *Expert Rev Med Devices.* 2016;13(10):945–63.
122. Zarone F, Sorrentino R, Vaccaro F, Traini T, Russo S, Ferrari M. Acid etching surface treatment of feldspathic, alumina and zirconia ceramics: a micromorphological SEM analysis. *Int Dent South Afr.* 2006;8:50–6.
123. Nakashima J, Taira Y, Sawase T. In vitro wear of four ceramic materials and human enamel on enamel antagonist. *Eur J Oral Sci.* 2016;124:295–300.
124. Sorrentino R, Navarra CO, Di Lenarda R, Breschi L, Zarone F, Cadenaro M, Spagnuolo G. Effects of finish line design and fatigue cyclic loading on phase transformation of zirconia dental ceramics: a qualitative micro-Raman spectroscopic analysis. *Materials.* 2019;12:6. <https://doi.org/10.3390/ma12060863>.
125. Lugh V, Sergio V. Low temperature degradation -aging- of zirconia: a critical review of the relevant aspects in dentistry. *Dent Mater.* 2010;26(8):807–20.
126. Camposilvan E, Leone R, Gremillard L, Sorrentino R, Zarone F, Ferrari M, Chevalier J. Aging resistance, mechanical properties and translucency of different yttria-stabilized zirconia ceramics for monolithic dental crown applications. *Dent Mater.* 2018;34(6):879–90.
127. Ferrari M, Vichi A, Zarone F. Zirconia abutments and restorations: from laboratory to clinical investigations. *Dent Mater.* 2015;31:e63–76.
128. Rodrigues CDS, Aurélio IL, Kaizer MDR, Zhang Y, May LG. Do thermal treatments affect the mechanical behavior of porcelain-veneered zirconia? A systematic review and meta-analysis. *Dent Mater.* 2019;35(3):807–17.
129. Mota YA, Cotes C, Carvalho RF, Machado JPB, Leite FPP, Souza ROA, Özcan M. Monoclinic phase transformation and mechanical durability of zirconia ceramic after fatigue and autoclave aging. *J Biomed Mater Res B Appl Biomater.* 2017;105(7):1972–7.
130. Wille S, Zumstrull P, Kaidas V, Jessen LK, Kern M. Low temperature degradation of single layers of multilayered zirconia in comparison to conventional unshaded zirconia: phase transformation and flexural strength. *J Mech Behav Biomed Mater.* 2018;77:171–5.
131. Sun T, Zhou S, Lai R, Liu R, Ma S, Zhou Z, Longquan S. Load-bearing capacity and the recommended thickness of dental monolithic zirconia single crowns. *J Mech Behav Biomed Mater.* 2014;35:93–101.
132. Lameira DP, Buarque e Silva WA, Andrade e Silva F, De Souza GM. Fracture strength of aged monolithic and bilayer zirconia-based crowns. *Biomed Res Int.* 2015;2015:418641.
133. Lan TH, Liu PH, Chou MM, Lee HE. Fracture resistance of monolithic zirconia crowns with different occlusal thicknesses in implant prostheses. *J Prosthet Dent.* 2016;115(1):76–83.
134. Sorrentino R, Triulzio C, Tricarico MG, Bonadeo G, Gherlone EF, Ferrari M. In vitro analysis of the fracture resistance of CAD-CAM monolithic zirconia molar crowns with different occlusal thickness. *J Mech Behav Biomed Mater.* 2016;61:328–33.
135. Nakamura K, Harada A, Inagaki R, Kanno T, Niwano Y, Milleding P, Örtengren U. Fracture resistance of monolithic zirconia molar crowns with reduced thickness. *Acta Odontol Scand.* 2015;73(8):602–8.
136. Ramos GF, Monteiro EB, Bottino MA, Zhang Y, Marques de Melo R. Failure probability of three designs of zirconia crowns. *Int J Periodontics Restorative Dent.* 2015;35(6):843–9.
137. Weyhrauch M, Iglie C, Scheller H, Weibrich G, Lehmann KM. Fracture strength of monolithic all-ceramic crowns on titanium implant abutments. *Int J Oral Maxillofac Implants.* 2016;31(2):304–9.
138. Mitov G, Anastassova-Yoshida Y, Nothdurft FP, von See C, Pospiech P. Influence of the preparation design and artificial aging on the fracture resistance of monolithic zirconia crowns. *J Adv Prosthodont.* 2016;8(1):30–6.
139. Øilo M, Kvam K, Gjerdet NR. Load at fracture of monolithic and bilayered zirconia crowns with and without a cervical zirconia collar. *J Prosthet Dent.* 2016;115(5):630–6.
140. Zhang Y, Mai Z, Barani A, Bush M, Lawn B. Fracture-resistant monolithic dental crowns. *Dent Mater.* 2016;32(3):442–9.
141. Elsayed A, Meyer G, Wille S, Kern M. Influence of the yttrium content on the fracture strength of monolithic zirconia crowns after artificial aging. *Quintessence Int.* 2019. <https://doi.org/10.3290/jqia42097>.
142. Vichi A, Sedda M, Fabian Fonzar R, Carrabba M, Ferrari M. Comparison of contrast ratio, translucency parameter, and flexural strength of traditional and “augmented translucency” zirconia for CEREC CAD/CAM system. *J Esthet Restor Dent.* 2016;28(Suppl 1):S32–9.
143. Shahmiri R, Standard OC, Hart JN, Sorrell CC. Optical properties of zirconia ceramics for esthetic dental restorations: a systematic review. *J Prosthet Dent.* 2018;119(1):36–46.
144. Bacchi A, Boccardi S, Alessandretti R, Pereira GKR. Substrate masking ability of bilayer and monolithic ceramics used for complete crowns and the effect of association with an opaque resin-based luting agent. *J Prosthodont Res.* 2019. <https://doi.org/10.1016/j.jpor.2019.01.005>.
145. Venezia P, Torsello F, Cavalcanti R, D’Amato S. Retrospective analysis of 26 complete-arch implant supported monolithic zirconia prostheses with feldspathic porcelain veneering limited to the facial surface. *J Prosthet Dent.* 2015;114:506–12.
146. Sorrentino R, De Simone G, Tetè S, Russo S, Zarone F. Five-year prospective clinical study of posterior three-unit zirconia-based fixed dental prostheses. *Clin Oral Investig.* 2012;16(3):977–85.
147. Borelli B, Sorrentino R, Goracci C, Amato M, Zarone F, Ferrari M. Evaluating residual dentin thickness following various mandibular anterior tooth preparations for zirconia full-coverage single crowns: an in vitro analysis. *Int J Periodontics Restorative Dent.* 2015;35(1):41–7.
148. Ferrari M, Sorrentino R, Cagidiaco C, Goracci C, Vichi A, Gherlone E, Zarone F. Short-term clinical performance of zirconia single crowns with different framework designs: 3-year clinical trial. *Am J Dent.* 2015;28(4):235–40.
149. Fuzzi M, Tricarico MG, Ferrari Cagidiaco E, et al. Nanoleakage and internal adaptation of zirconia and lithium disilicate single crowns with knife edge preparation. *J Oss Periodont Prosthodont.* 2017;9:262–74.
150. Vichi A, Sedda M, Bonadeo G, Bosco M, Barbiera A, Tsintsadze N, Carrabba M, Ferrari M. Effect of repeated firings on flexural strength of veneered zirconia. *Dent Mater.* 2015;31(8):e151–6.
151. Lee B, Oh KC, Haam D, Lee JH, Moon HS. Evaluation of the fit of zirconia copings fabricated by direct and indirect digital scanning procedures. *J Prosthet Dent.* 2018;120(2):225–31.
152. Pilo R, Folkman M, Arieli A, Levartovsky S. Marginal fit and retention strength of zirconia crowns cemented by self-adhesive resin cements. *Oper Dent.* 2018;43(2):151–61.
153. Riccitiello F, Amato M, Leone R, Spagnuolo G, Sorrentino R. In vitro evaluation of the marginal fit and internal adaptation of zirconia and lithium disilicate single crowns: micro-CT comparison between different manufacturing procedures. *Open Dent J.* 2018;12:160–72.
154. Pagniano RP, Seghi RR, Rosenstiel SF, Wang R, Katsube N. The effect of a layer of resin luting agent on the biaxial flexure strength of two all-ceramic systems. *J Prosthet Dent.* 2005;93(5):459–66.
155. Papia E, Larsson C, du Toit M, Vult von Steyern P. Bonding between oxide ceramics and adhesive cement systems: a systematic review. *J Biomed Mater Res B Appl Biomater.* 2014;102:395–413.
156. Özcan M, Bernasconi M. Adhesion to zirconia used for dental restorations: a systematic review and meta-analysis. *J Adhes Dent.* 2015;17(1):7–26.
157. Srikanth R, Kosmac T, Della Bona A, Yin L, Zhang Y. Effects of cementation surface modifications on fracture resistance of zirconia. *Dent Mater.* 2015;31(4):435–42.
158. Luthra R, Kaur P. An insight into current concepts and techniques in resin bonding to high strength ceramics. *Aust Dent J.* 2016;61:163–73.
159. Sulaiman TA, Abdulmajeed AA, Shahramian K, Lassila L. Effect of different treatments on the flexural strength of fully versus partially stabilized monolithic zirconia. *J Prosthet Dent.* 2017;118:216–20.
160. Ebeid K, Wille S, Salah T, Wahsh M, Zohdy M, Kern M. Evaluation of surface treatments of monolithic zirconia in different sintering stages. *J Prosthodont Res.* 2018;62(2):210–7.
161. Dal Piva AMO, Carvalho RLA, Lima AL, Bottino MA, Melo RM, Valandro LF. Silica coating followed by heat-treatment of MDP-primer for resin bond stability to yttria-stabilized zirconia polycrystals. *J Biomed Mater Res B Appl Biomater.* 2019;107(1):104–11.
162. Pilo R, Dimitriadis M, Palaghia A, Eliades G. Effect of tribochemical treatments and silane reactivity on resin bonding to zirconia. *Dent Mater.* 2018;34(2):306–16.

163. Schünemann FH, Galárraga-Vinueza ME, Magini R, Fredel M, Silva F, Souza JCM, Zhang Y, Henriques B. Zirconia surface modifications for implant dentistry. *Mater Sci Eng C Mater Biol Appl*. 2019;98:1294–305.
164. Poggio CE, Ercoli C, Rispoli L, Maiorana C, Esposito M. Metal-free materials for fixed prosthodontic restorations. *Cochrane Database Syst Rev*. 2017. <https://doi.org/10.1002/14651858.CD009606.pub2>.
165. Bagegni A, Abou-Ayash S, Rücker G, Algarni A, Att W. The influence of prosthetic material on implant and prosthetic survival of implant-supported fixed complete dentures: a systematic review and meta-analysis. *J Prosthodont Res*. 2019. <https://doi.org/10.1016/j.jpor.2019.02.001>.
166. Ciancaglini R, Gherlone EF, Radaelli G. Association between loss of occlusal support and symptoms of functional disturbances of the masticatory system. *J Oral Rehabil*. 1999;26(3):248–53.
167. Ciancaglini R, Gherlone EF, Radaelli S, Radaelli G. The distribution of occlusal contacts in the intercuspal position and temporomandibular disorder. *J Oral Rehabil*. 2002;29(11):1082–90.
168. Le M, Papia E, Larsson C. The clinical success of tooth- and implant-supported zirconia-based fixed dental prostheses. A systematic review. *J Oral Rehabil*. 2015;42(6):467–80.
169. Wong CKK, Narvekar U, Petridis H. Prosthodontic complications of metal-ceramic and all-ceramic, complete-arch fixed implant prostheses with minimum 5 years mean follow-up period. A systematic review and meta-analysis. *J Prosthodont*. 2019;28(2):e722–35.
170. Ferrari M, Tricarico MG, Cagidiaco MC, Vichi A, Gherlone EF, Zarone F, Sorrentino R. 3-year randomized controlled prospective clinical trial on different CAD-CAM implant abutments. *Clin Implant Dent Relat Res*. 2016;18(6):1134–41.
171. Abdulmajeed AA, Donovan TE, Cooper LF, Walter R, Sulaiman TA. Fracture of layered zirconia restorations at 5 years: a dental laboratory survey. *J Prosthet Dent*. 2017;118(3):353–6.
172. Fabbri G, Fradeani M, Dellificorelli G, De Lorenzi M, Zarone F, Sorrentino R. Clinical evaluation of the influence of connection type and restoration height on the reliability of zirconia abutments: a retrospective study on 965 abutments with a mean 6-year follow-up. *Int J Periodontics Restorative Dent*. 2017;37(1):19–31.
173. Sailer I, Balmer M, Hüsler J, Hämmerle CHF, Känel S, Thoma DS. Comparison of fixed dental prostheses with zirconia and metal frameworks: five-year results of a randomized controlled clinical trial. *Int J Prosthodont*. 2017;30(5):426–8.
174. Roehling S, Schlegel KA, Woelfler H, Gahlert M. Zirconia compared to titanium dental implants in preclinical studies - a systematic review and meta-analysis. *Clin Oral Implants Res*. 2019;30(5):365–95.

Ready to submit your research? Choose BMC and benefit from:

- fast, convenient online submission
- thorough peer review by experienced researchers in your field
- rapid publication on acceptance
- support for research data, including large and complex data types
- gold Open Access which fosters wider collaboration and increased citations
- maximum visibility for your research: over 100M website views per year

At BMC, research is always in progress.

Learn more biomedcentral.com/submissions




RESEARCH ARTICLE

Open Access



Current state of the art in the use of augmented reality in dentistry: a systematic review of the literature

Marco Farronato^{1*} , Cinzia Maspero¹, Valentina Lanteri¹, Andrea Fama¹, Francesco Ferrati²,
Alessandro Pettenuzzo³ and Davide Farronato⁴

Abstract

Background: The aim of the present systematic review was to screen the literature and to describe current applications of augmented reality.

Materials and methods: The protocol design was structured according to PRISMA-P guidelines and registered in PROSPERO. A review of the following databases was carried out: Medline, Ovid, Embase, Cochrane Library, Google Scholar and the Gray literature. Data was extracted, summarized and collected for qualitative analysis and evaluated for individual risk of bias (R.O.B.) assessment, by two independent examiners. Collected data included: year of publishing, journal with reviewing system and impact factor, study design, sample size, target of the study, hardware(s) and software(s) used or custom developed, primary outcomes, field of interest and quantification of the displacement error and timing measurements, when available. Qualitative evidence synthesis refers to SPIDER.

Results: From a primary research of 17,652 articles, 33 were considered in the review for qualitative synthesis. 16 among selected articles were eligible for quantitative synthesis of heterogenous data, 12 out of 13 judged the precision at least as acceptable, while 3 out of 6 described an increase in operation timing of about 1 h. 60% ($n = 20$) of selected studies refers to a camera-display augmented reality system while 21% ($n = 7$) refers to a head-mounted system. The software proposed in the articles were self-developed by 7 authors while the majority proposed commercially available ones. The applications proposed for augmented reality are: Oral and maxillo-facial surgery (OMS) in 21 studies, restorative dentistry in 5 studies, educational purposes in 4 studies and orthodontics in 1 study. The majority of the studies were carried on phantoms (51%) and those on patients were 11 (33%).

Conclusions: On the base of literature the current development is still insufficient for full validation process, however independent sources of customized software for augmented reality seems promising to help routinely procedures, complicate or specific interventions, education and learning. Oral and maxillofacial area is predominant, the results in precision are promising, while timing is still very controversial since some authors describe longer preparation time when using augmented reality up to 60 min while others describe a reduced operating time of 50/100%.

Trial registration: The following systematic review was registered in PROSPERO with RN: CRD42019120058.

Keywords: Augmented reality, Virtual reality, Digital dentistry, Orthodontics, Maxillofacial surgery, Implantology, Systematic review, Education, Dental training

* Correspondence: marcofarronato@msn.com

¹Department of Orthodontics, Fondazione IRCCS Ca' Granda, Ospedale Maggiore Policlinico, University of Milan, via Francesco Sforza 35, 20122 Milano, MI, Italy
Full list of author information is available at the end of the article



© The Author(s). 2019 **Open Access** This article is distributed under the terms of the Creative Commons Attribution 4.0 International License (<http://creativecommons.org/licenses/by/4.0/>), which permits unrestricted use, distribution, and reproduction in any medium, provided you give appropriate credit to the original author(s) and the source, provide a link to the Creative Commons license, and indicate if changes were made. The Creative Commons Public Domain Dedication waiver (<http://creativecommons.org/publicdomain/zero/1.0/>) applies to the data made available in this article, unless otherwise stated.

Background

The first application of augmented reality was developed by Ivan Edward Sunderland in 1968 with a binocular system “kinetic depth effect” made of two cathode ray tubes. It wasn’t until 1991 that the definition of “augmented reality” was first described by Tom Caudell of the Boeing Company [1–3].

Since then, the popularity explosion of augmented reality has reached high levels in the last lustrium. Its applications are also easier since many existing devices are compatible with this technology while other are being developed in order to maximize its performances [1]. The gaming industry is predominant in the augmented reality area because of the expertise brought by virtual reality development [4]. The inherence from this specific field provided tools which are being used by some researchers, for example, virtual reality headset [5, 6].

The definition of augmented reality refers to: “a technology that superimposes a computer-generated image on a user’s view of the real world, thus providing a composite view”. Augmented reality, however is commonly confused with virtual reality since both have many aspects in common, even though the outcomes are completely different. Virtual reality, as the name suggests, is a virtual immersive environment where the user’s senses are stimulated with computer-generated sensations and feedbacks generating an “interaction”. Augmented reality, instead, generates an interaction between the real environment and virtual objects. For example a virtual reality system would be a head worn helmet which simulates navigation inside human body and permits the user to explore it on the base of a virtual three-dimensional reconstruction. A similar example with the augmented reality would permit to directly observe a human body and to see virtual objects on it, or through it as the anatomy of the body was superimposed [1, 2, 7].

Immersive reality is similar to augmented reality but the user is interacting with a digital 3d world recreated through 360° real records. The user can navigate recordings which replace the real world in a convincing way. The 360 records recreate the continuity of the surrounding with no interruptions. There also might be physical interaction with the environment and physical feedback given by haptic response when interacting with an object. Other features can be added as 3D audio direction, freedom of movement in the environment and conformance to human vision, which permits correct sizing of object in distance [6].

Its application in dentistry begun with the development of new visualization system for anatomic exploration from the use of virtual-reality based software [5].

The growth in popularity has brought the use of augmented reality to the attention of the medical researchers and of the digital centers who are following two different

methods: using already available systems or developing their own, customized combination of hardware and software.

However, substituting virtual reality with augmented reality means to superimpose virtual objects to the reality in a precise and reproducible way considering the three dimensions of space as well as the user’s and patient’s movements. This is still a controversial topic since it is highly affected by the system used. Most authors propose a handmade pre-operative calibration, instead of an automatic one. However the use of markers simplifies this tracking process. The most commonly used systems are head mounted displays and half, silvered mirror projections, both of them are valid systems for augmented reality and have a multitude of different setting as described by Azuma et al. [1].

The superimposed virtual objects are usually obtained with 3-dimensional X-rays as CT dental scans which are then manipulated with commercially available software for CBCT manipulation. Also MRI, angiography or any other three-dimensional data could be used in the same way. The most commonly used software is Mimics (Materialise, Leuven). The object is exported in a widely recognisable format (.stl for example) using “mask” function set with thresholding on the area of interest and 3D reconstruction function [8–11].

The revolutionary scope of developing an augmented reality based system is to solve one of the biggest issue in the structure of most digital dentistry commonly available systematics; in fact, the use digital technologies like the scanners is structured in a 3-step procedure which can be summarized as follows: the digital image is acquired by a scanning device, the changes are performed digitally from T0 to T1, the new information is transferred back to solid state. The use of augmented reality permits direct visualization bypassing the last transfer step, which means, on a large scale, to avoid data and time loss. Visualization of digital data directly on the patient means the possibility of achieving great advantages in digital procedures [12, 13].

The aim of this systematic review was to collect and to describe available literature about the use of augmented reality in different fields of dentistry and maxillofacial surgery. Collected data will be used to describe the current combinations of hardware and software proposed by the authors, with a focus on self-development, the field of interest where augmented reality is being used, the primary outcomes which are being obtained by the use of different systems and the precision and timing of the procedures performed. Data about sample considered in the different studies and the designs of the protocol proposed will be also described.

Materials and methods

A prior research was made before the beginning of the study design. Manuscripts from 1968, the year when

augmented reality was first described, to the end of 2018 were considered. A protocol for the research was structured by the authors after screening the titles and the abstracts of the articles found. After full accordance among the authors it was registered in PROSPERO with nr:CRD42019120058. The search strategy included the databases to be screened and the search query. The articles found were selected with the application of inclusion and exclusion criteria. The resulting full texts were analyzed by the authors for data extraction. Full text access has been granted by “Università Degli Studi di Milano” - University of Milan, Orthodontics department for the research.

Search strategy

The review was researched using the following electronic databases: Medline, Ovid, Pubmed, Embase, Cochrane Library and Google Scholar. The research refers to the Preferred Reporting Items for Systematic Reviews and Meta-Analyses (PRISMA-P) 2015 [14].

The search query used is available in (Fig. 1) MeSH terms.

Grey literature was also screened according to Pisa declaration on Policy Development for Grey Literature Resources.

Inclusion criteria

Articles describing new or already existing applications or frameworks for augmented reality methodologies and relevant informations include: type of intervention, field of interest, clinical outcomes, precision and timing efficiency of the proposed system and combination of software and hardware used were considered. Articles in English referring to Dentistry, oral and maxillofacial surgery were included. No limit for study design was applied, the target of the studies considered are: humans, human parts (extracted teeth), phantoms, animals. Studies from 1968 were considered.

Exclusion criteria

All the articles describing virtual reality systems were discarded, like anatomical explorations, improper use or any concept which doesn't refer to the exact definition of augmented reality as described in the introduction section.

All the articles lacking methodology description with at least less than 3 of the following were discarded: study design, sample size, hardware utilized, software installed.

All the descriptive methodologies, conference papers, patents, and all the publications in general not identified as “Articles” were discarded.

All the application areas not related to dentistry, oral surgery or cranio-facial district where discarded.

Qualitative analysis and quantitative synthesis

The research outcomes synthesis refers to SPIDER (Sample, Phenomenon of Interest, Design, Evaluation, Research type) tool [15].

Data regarding precision measurements and times of the procedure were collected. The data regarding precision described the error in millimeters or percentage between the markers and the digital image, the error between the real object and the superposed digital image [8, 16–30] and the degree of the orientation error [18, 30–44]. Time measurements were taken regarding the additional time required to fit the digital models or the gain in the operative procedures [8, 22, 26, 27, 29, 30]. The high number of variables made the data inconsistent for meta-analysis. The variables considered for qualitative synthesis were: the type of procedure and field of interest, primary outcome and results obtained, study design, software used and if custom made or already existing, type of hardware, sample size and target of the study: animal/human or phantom.

Risk of bias in individual studies

Due to the high heterogeneity of the studies design, which is common for new technologies independently developed with different features, common tools for risk of bias assessment were not applicable. In general, risk of bias was considered and judged by the authors low or null for data description but very high for analyzing effectiveness of such methodologies. All the studies found in literature presented high or unknown selection bias and reference standards. Also none of the studies refers to a specific protocol.

Results

The primary research gave a total of 17,652 records after duplicates removal, 17,603 results were excluded on the base of full title and abstract, 45 out of 49 studies were

MeSh research strategy for systematic review on the use of augmented reality since it was first described for interventions or diagnosis on humans:

augmented[All Fields] OR mixed[All Fields] OR virtual[All Fields] AND reality[All Fields] AND ("dentistry"[MeSH Terms] OR "dentistry"[All Fields]) AND (("1968/01/01"[PDAT] : "3000/12/31"[PDAT]) AND "humans"[MeSH Terms])

Fig. 1 MeSH research strategy

considered eligible. After full text reading by two among the authors, 33 articles were selected after application of exclusion and inclusion criteria (Fig. 2). Variables regarding the sample size and target of the study: animal/human or phantom, type of hardware, software used, field of interest of the proposed procedure and study design, were then extracted from the text, collected and discussed among all the authors. Out of the 33 articles 16 contained at least one quantitative description of the following variables regarding timing of the procedure and precision of the proposed system.

Data extraction

Sample

Out of the selected studies we found that the 51% ($n = 17$) is performed on phantoms, with 2 of those performed also in one single volunteer: for video see-through on maxillofacial surgery and for the overlaying of computed tomography on the surgical area. Studies referring to experiments carried out on real human patients are 33% ($n = 11$) considering the two with a single volunteer [8, 21].

Out of in vivo studies on humans the ones referring to actual interventions carried out on patients with the use of augmented reality systems are: intra-oral distractor

positioning on 10 cases with 10 controls (OMS/maxillofacial surgery F.O.I), 16 class III patients for waferless maxillary positioning (OMS/maxillofacial surgery F.O.I), one subject for orthodontic positioning of brackets (Orthodontics F.O.I), MASO on 15 patients (OMS/maxillofacial surgery F.O.I), maxillary positioning on 5 patients (OMS/maxillofacial surgery F.O.I), and on 148 patients for multiple operations (OMS F.O.I). All the interventions carried out on humans outcomes are positively described by the authors, with no exception [20, 22, 24, 26, 27, 30].

Other samples considered refer to animal with the studies in 2017 for MASO on dogs, in 2015 for vascular landmarks on one porcine tongue and in 2015 for dental implants on a pig corpse [19, 37, 39].

Other studies have been carried out in vitro on 126 human teeth for Endodontics F.O.I in 2013 (Table 1) [25].

Phenomenon of interest: hardware used

Out of the studies considered the majority (60% $n = 20$) refers to camera-display based systems although the most classical use of augmented reality refers to systems which are head-mounted used in 21% of the studies considered ($n = 7$). Other systems described are glass silvered mirrors or mirror based systems ($n = 3$) with 3

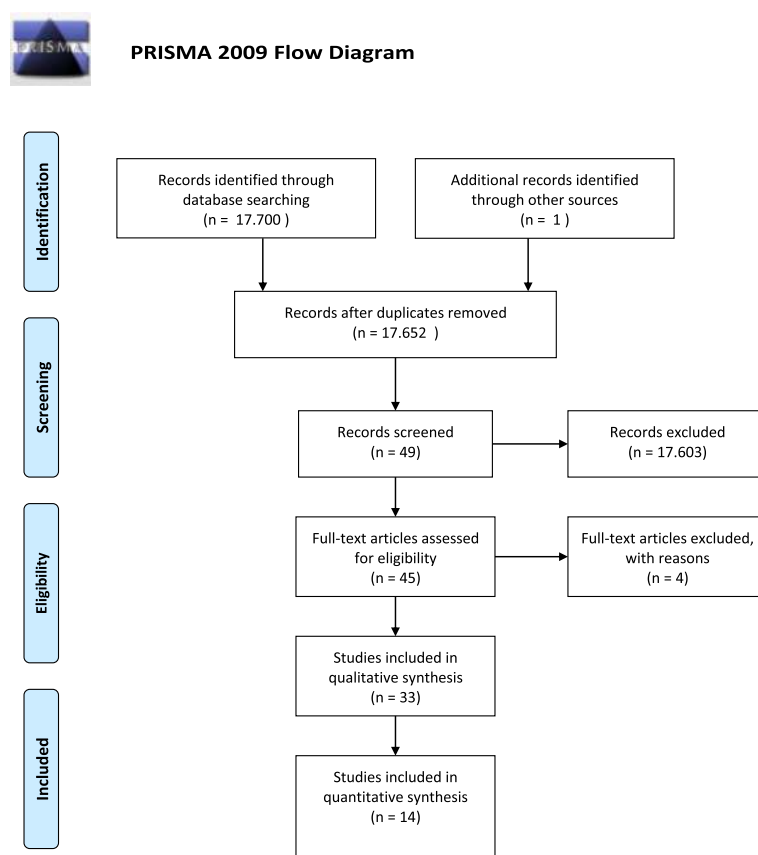


Fig. 2 PRISMA flow chart

Table 1 Overview

Author	Year	Study Design	sample size	Humans/ Phantom	Primary Endpoint	Field of Interest
Jiang W.	2018	case-control clinical trial	12	12 rapid prototyping mandibular models 3D printed	better accuracy, applicability and efficiency	implantology
Murugesan YP.	2018	experimental study	age 15 to 70; 6 categories of dental groups	humans	improved algorithm provides overall acceptable range of accuracy with a shorter operating time	dental surgery (operazioni su dente)
Pulijala Y.	2018	Randomized control trial	95 novice surgical residents	virtual phantoms	iVR experiences improve the knowledge and self-confidence of the surgical residents. a framework is needed. Tech is not available	maxillofacial surgery (leftofrl)
Schreurs R.	2018	pilot experimental study	1 skull model	3d printed hard tissue model	a novel navigation concept for orbital reconstruction that provides real-time intuitive feedback during insertion of an orbital implant has been presented	maxillofacial, orbital implant placement
Won JY.	2017	method description	1 model	phantom	simple method description (already existing software)	inferior nerve block anesthesia
Zhou C.	2017	clinical trial	4 osteotomies on two samples	dogs	In this study, the robot system based on AR promises a precise osteotomy plane even when operated by inexperienced plastic surgeons	Mandibular angle split osteotomy (MASO)
Plessas A.	2017	review	16 articles included	students	combining and alternating the traditional and pioneering simulation methods and feedback may be of benefit to the learners. However, there is insufficient evidence to advise for or against the use	educational and preclinic
Llena C.	2018	case/control	41 two groups	students on models	The AR techniques favoured the gaining of knowledge and skills	Cavity preparation
Zhu M.	2017	clinical trial	20 patients	on printed models of human patients	easy manipulation and high accuracy	maxillofacial surgery/reconstruction - nerve position
Wang J.	2017	clinical trial	1 subject 1 phantom	mandible and maxillar phantoms (3d printed) and a volunteer	simple method and can be integrated with OMS	New method in oral and maxillofacial surgery (OMS)
Liu WP	2015	experimental clinical trial	1 porcine tongue	computed tomography (CBCTA) and magnetic resonance (MR), Ex vivo (EV) porcine tongue phantoms	The 5 mm (mean) tool tracking error is not acceptable for clinical use and can be improved through intraoperative fluoroscopy. Experimental results show the feasibility and advantages	vascular landmarks for the resection of base of tongue neoplasm for transoral robotic surgery
Suenaga H.	2015	experimental clinical trial	1 subject	human	displayed 3D-CT images in real space with high accuracy.	stereo vision in oral and maxillofacial surgery
Espejo-Trung LC.	2015	blinded clinical trial with questionnaires	dental students (n = 28), professors and postgraduate students in dentistry and prosthodontics (n = 30), and dentists participating in a continuing education or remedial course in	resin teeth scanned (XCadCam, Brazil);	This study's methodology enabled the development of a learning object with a high index of acceptance among all groups, regardless of their ability with computers, gender, and age.	education

Table 1 Overview (Continued)

Author	Year	Study Design	sample size	Humans/ Phantom	Primary Endpoint	Field of Interest
Qu M.	2015	randomized clinical trial	dentistry and/or prosthetics (n = 19), total: 77 20 patients with hemifacial microsomia 10 randomized and 10 control	humans	useful approach in mandibular distraction osteogenesis	transfer surgical planning to the surgical site in hemifacial microsomia elongment
Wang J.	2014	experimental clinical study	1 phantom	A phantom experiment simulating oral and maxillofacial surgery was also performed to evaluate the proposed AR overlay device in terms of the image registration accuracy, 3D image overlay accuracy, and the visual effects of the overlay.	The experimental results show satisfactory image registration and image overlay accuracy, and confirm the system usability. Compensating 3D image distortion	a novel AR device for 3D image surgical overlay is presented
Badiali G.	2014	experimental phantom trial	physical replica of a human skull	phantom	Our results suggest that the WARM device would be accurate when used to assist in waferless maxillary repositioning during the LeFort 1 orthognathic procedure. Further, our data suggest that the method can be extended to aid the performance of many surgical procedures on the facial skeleton. Also, in vivo testing should be performed to assess system accuracy under real clinical conditions.	Le Fort I, OMS
Katić D.	2015	experimental animal study	1 pig	pig corpse	The system made the surgery easier and showed ergonomical benefits, as assessed by a questionnaire.	augmented reality (AR) system for dental implant surgery
Wang J.	2014	experimental phantom study	1 phantom	patient phantom	The application innovation of this paper is a 3-D image overlay-based AR navigation system for dental surgery.	Computer-assisted oral and maxillofacial surgery (OMS) matches dental edge
Zinser MJ	2013	clinical in vivo trial	sixteen adults class 3 humans	humans	the maxilla can be positioned independently and no intermediate intermaxillary splints are required. The surgeon gets a better feeling for the 3-dimensional nature of the maxilla, although he must adapt to the new technique	3-dimensional contours of the virtually-planned and real-time maxillary positions can be superimposed to augment the surgeon's perception to 3dimensional cephalometric landmarks
Lin YK	2013	in vitro study	40 osteotomy sites on 4 maxillar and 4 mandibular sites	in vitro stereolitho	Deviation of implant placement from planned position was significantly reduced by integrating surgical template and augmented reality technology.	implant placement
Suenaga H.	2013	experimental clinical study	1 volunteer and 1 plastic model	human/phantom	an accurate AR system for use in oral and maxillofacial dentistry that provides a real-time, in situ, stereo- scopic	overlaying a three-dimensional computed tomography image on a patient's surgical area,

Table 1 Overview (Continued)

Author	Year	Study Design	sample size	Humans/ Phantom	Primary Endpoint	Field of Interest
Aichert A.	2012	experimental clinical study	1 subject	human	visualization of 3D-CT IV images overlaid on the surgical site with the naked eye.	guided bracket placement in orthodontic correction
Bruellmann DD.	2013	experimental in vitro study	126 human teeth	human teeth in vitro	a novel application of augmented reality in an orthodontics routine procedure. The realized software shows that observations made in anatomical studies can be exploited to automate real-time detection of root canal orifices and tooth classification	reliable detection of root canals
Zhu M.	2011	clinical in vivo trial	15 patients	humans	This study has reported a new and effective way for mandibular angle oblique split osteotomy, and using occlusal splint might be a powerful option for the registration of augmented reality.	mandibular angle oblique split osteotomy (MASO) with occlusal splint
Bogdan CM.	2011	descriptive	virtual models	virtual models	project, is to increase the quality of the educational process in dental faculties, by assisting students in learning how to prepare teeth for all-ceramic restorations.	e-learning virtual reality-based software system that will be used for the developing skills in grinding teeth, needed in all-ceramic restorations. Virtual laboratory for the students of the dental medicine faculty
Suebunukam S.	2010	descriptive	thirty-two sixth-year dental students	virtual models	the augmented kinematic feedback can enhance the performance earlier in the skill acquisition and retention sessions	haptic VR training system
Wierinck ER.	2007	experimental phantom study	Eighteen right-handed volunteers: operative dentists (EXP), the peri-odontologists (PER), and the naive (NAV) group	simulated patient or manikin with head and dentoform.	The VR simulator is a valid and reliable screening device to capture expert performance even after brief training to familiarize the subject with the new environment	tooth preparation, manual dexterity training
Mischkowski RA	2006	clinical trial	5 patients	humans	Augmented reality tools like X-Scope® may be helpful for controlling maxillary translocation in orthognathic surgery.	maxillary positioning in orthognathic surgery
Wierinck ER.	2006	experimental in vitro trial	36 dental students first year divide in 3 groups of 12	phantoms	VR feedback enhances acquisition and retention of a cavity preparation task on a simulation unit	Cavity preparation simulators
Ewers R.	2005	retrospective review of clinical trials	50 telemedically supported treatments. 20 videosequences of arthroscopies of the temporomandibular joint are transmitted via UMTS cellular phones and independently evaluated by 3 experts.	humans	In many applications telecommunication technology can contribute to a quality improvement in crano- and maxillofacial surgery because of the global availability of specialized knowledge.	computer-assisted navigation technology in augmented reality environments with telecommunication is used for execution of interactive stereotaxic teleconsultation. Arthroscopic videos of the temporomandibular joint and other craniomaxillofacial structures. Orbitozygomatic osteotomies,

Table 1 Overview (Continued)

Author	Year	Study Design	sample size	Humans/ Phantom	Primary Endpoint	Field of Interest
Nijmeh AD	2005	review of the literature	n/a	CT, MRI, PET	guidance systems are useful tools for navigation of the surgical scene but not a substitute for sound surgical principles and a good knowledge of human anatomy.	positioning of the mandibular condyle in orthognathic surgery, insertion of implants, positioning of the maxilla in orthognathic surgery, distraction osteogenesis, arthroscopies of the temporomandibular joint, and operation simulations on stereolithographic models oral surgery
Wierinck ER	2005	clinical trial on students	42 dental students	models	DentSimTM navigation system, was not suitable for manual skill learning in novice dental students.	manual dexterity training drilling a geometrical class 1 cavity
Ewers R	2005	review	One hundred and fifty-eight operations from 1995 to 2003	humans	Our results indicate that the medical benefit is likely to outweigh the expenditure of technology with few exceptions	positioning of dental implants; arthroscopies of the temporomandibular joint and intraoperative optoelectrical axiography osteotomies of the facial skeleton removal of foreign bodies, image guided biopsies, punctures of the trigeminal ganglion; resection of the temporal bone, tumor resection and reconstruction with calvarial transplant, reconstruction of the orbital floor, positioning of positioning-screws

Table 2 Software and Hardware

Author	Year	Hardware	Software
Jiang W.	2018	N/A	probably custom
Murugesan YP.	2018	2 stereo cameras and a translucent mirror	new rotation matrix and translation vector (RMaTV) algorithm custom made by the authors
Pulijala Y.	2018	oculus rift	leap motion (gaming industry)
Schreurs R.	2018	Kolibri navigation system, external laptop, 15 cilindrs polyjet printer (Objet30 Prime; Stratasys Ltd., Eden Prairie, MN, USA).	self made C++ using the Open Inventor toolkit n Microsoft Visual Studio 2008.
Won JY.	2017	photocamera, laptop	Mimics software to export STL; Rapidform Explorer, free software; Actual Transparent Window
Zhou C.	2017	robot system, ar visualization system, glasses, code,nVisor ST60, Micron Tracker system,	AR Toolkits
Plessas A.	2017	N/A	N/A
Llena C.	2018	computer and mobiles, scanners	Aumentaty Viewer software .aty
Zhu M.	2017	semi transparent glass. Laser scanner (Konica Minolta Vivid 910)	mimics - materialise; Autodesk 3ds Max (version 9)
Wang J.	2017	4 k camera and a computer	self developed string codes
Liu WP	2015	da Vinci si robot	ITK-Snap (for manipulating cbcta)
Suenaga H.	2015	2 charge-coupled device stereo camera (Edmund Optics Inc., Barrington, NJ, USA) Rexcan DS2 3D scanner, cbct HALF SILVERED MIRROR	Mimics® Version 16 (Materialise, Leuven, Belgium) and Geomagic Control (Geomagic, Cary, NC, USA) AlarisTM 30 U RP technology (Objet Geometries, Rehovot, Israel); HALCON software Version 11 (MVTec Software GmbH, Munich, Germany)
Espejo-Trung LC.	2015	laptop and camera, scanner (XCadCam, Brazil)	3D-modeling program (HITLabNZ
Qu M.	2015	head-mounted display (HMD)	Mimics CAD/CAM software (Materialise, Ann Arbor, Michigan, USA); software AR Toolkits
Wang J.	2014	3D display, an AR window, a stereo camera for 3D measurement, and a workstation for information processing. Mirror/ar window	self developed
Badiali G.	2014	“wearable augmented reality for medicine” (WARM) devicelight. Weight, stereoscopic head-mounted display (HMD) Z800 instrument of eMagine (Bellevue, WA, USA); 3D printer (Stratasys Elite; Eden Prairie, MN, USA)	Augmented reality is provided by software that runs on conventional personal computers; Maya (Autodesk; Toronto, Canada)
Katić D.	2015	head-mounted display	NDI Polaris tracking system and self developed
Wang J.	2014	customized stereo camera with real-time 3-D contour matching marker free. Half-silvered mirror. A marker is attached directly to the tool. Stereo cameras	All of the algorithms were implemented using C++. The machine vision library HALCON was used for camera calibration and image processing
Zinser MJ	2013	interactive portable custom display navigational unit (BrainLab®, Vector Vision2)	3-dimensional planning software (I-plan CMF®, BrainLab) to manipulate cbct
Lin YK	2013	head mounted display	ImplantSmart, Changhua, Taiwan
Suenaga H.	2013	tracking system Polaris Spectra optical tracking system (Northern Digital Inc., Waterloo, Ontario, Canada) mirror, cameras, tracking marker.	image pro- cessing software (Mimics; Materialise, Leuven, Belgium). superimposed 3D images of the surgical instrument (SUCCESS-40MV; OSADA, Tokyo, Japan)
Aichert A.	2012	monocular AR system	n/a
Bruehlmann DD.	2013	standard intra-oral or microscope cameras connected to a standard computer.	The new software was implemented using C++, Qt, and the image processing library OpenCV; UI-Toolkit
Zhu M.	2011	computer	ARToolKit recognises the marker; Rapidform matches the marker with the mandible image. (Materialise, Ann Arbor, MI). Mimics. virtual image's position and orientation were adjusted through 3D Max (Van Nuys, CA)
Bogdan CM.	2011	Sensable's PHANTOM® OmniTM haptic feedback	VirDenT, programming language, such as C++ or Java.

Table 2 Software and Hardware (Continued)

Author	Year	Hardware	Software
Suebnuksarn S.	2010	PHANTOM Omni (SensAble Inc., Woburn, MA, USA).	
Wierinck ER.	2007	infrared camera, and two computers	DentSim™ computerized training system (DenX, Jerusalem, Israel)
Mischkowski RA	2006	portable LCD screen with a digital camera behind	X-Scope®
Wierinck ER.	2006	haptic simulators	DentSim™; DenX, Jerusalem, Israel)
Ewers R.	2005	UMTS (universal mobile telecommunication system) Apple PowerMac G3 and G4 workstations. Optoelectronic tracking systems ProReflex Motion-Capture MCU240 (Qualisys Inc., Gothenburg, Sweden), Polaris (NDI Northern Digital Inc., Waterloo, Ontario, Canada), and FlashPoint 5000 3D Localizer (Image Guided Technologies Inc., Boulder, CO). semitransparent head-mounted displays. UMTS cell-phone handset (Siemens U10; Siemens, Erlangen, Germany)	VirtualPatient System and MedScanII software (both from MedLibre Inc., Munich, Germany) are used for intraoperative navigation.
Nijmeh AD	2005	multiple	multiple
Wierinck ER.	2005	DentSim™ (DenX, Jerusalem, Israel)	virtual reality (VR) system (DentSim™)
Ewers R	2005	optoelectronic tracking systems: ProReflex™ Motion-Capture MCU240 (Qualisys Inc., Sweden), Polaris™ (NDI Northern Digital Inc., Canada), FlashPoint 5000™ 3D Localizer (Image Guided Technologies Inc., USA). Electromagnetic systems (since 1999 only used for research purposes): Polhemus Isotrak II™ (by Polhemus Inc., USA) and Aurora™ (NDI Inc., Ont., Canada), Fastrak™.	various types of navigation software (Virtual Vision™, MedScanII™, Virtual Implant™, Artma Medical Technologies, Vienna)

selected studies using other specific systems. One system described consists in an interactive portable display unit which can be defined as camera-display based, portable as the H.M.S. but not wearable (Table 2) [22].

Phenomenon of interest: software used

Extracted data about software used in the studies brings that 7 authors describe new custom-made software for a total of 9 studies. The authors involved into the development of the customized new software are describe using C++ programming language to develop the new software while Bogdan describes using C++ and Java language [16–18, 21, 25, 31, 39, 40, 45].

The majority of studies presents a variety of commercially available softwares as well as: Leap Motion® [5], Ar Toolkits® [37], ITK Snap® [19], Hitlab NZ® [32], Aumentaty® [33], Maya® [34], Iplan® [22], Implant Smart® [23], Dentsim® [29], Xscope® [27], Medscan® [30] and multiple software [43].

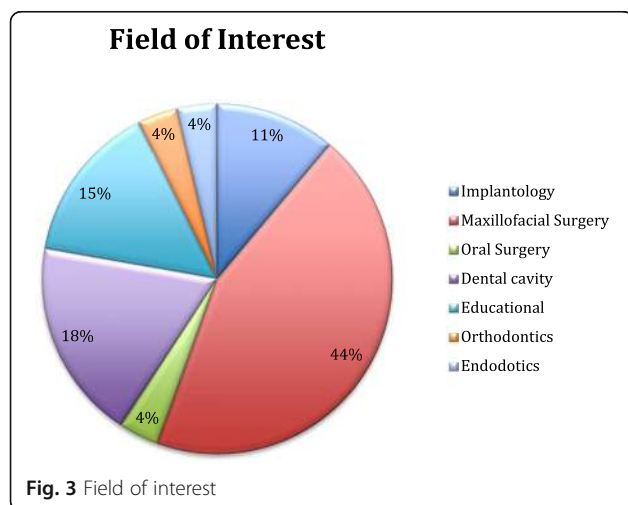
The only software used by a multitude of authors is Mimics® from 4 authors for a total of 6 manuscripts [8, 20, 26, 36] (Table 2).

Field of interest: F.O.I

Out of 33 selected studies the majority refers to the OMS (Oral and Maxillofacial Surgery) area which can be divided into three specific areas: implantology, maxillofacial surgery and oral surgery; the following area were restorative dentistry, educational and learning and orthodontics.

Respectively OMS included 21 studies divided into 17 for maxillo-facial, 3 for implantology and 1 for oral surgery; Restorative dentistry included 5 studies; educational and learning 4 studies and orthodontics 1 study (Fig. 3).

The studies considered applied augmented reality technology for the following operations: Implant placing performed on 3D printed mandibular models with better better accuracy applicability and efficiency as outcome: < 1.5 mm as linear deviation and < 5.5 degree of angular deviation by Jiang et al. [16] Lefort 1 has been performed on models by surgical residents with more self-confidence and knowledge as overall resulting experience [5]. A very specific operation like orbital implant placement has been tested out on 3D printed mode which is very useful for the instant feedback and with a translation error of 1.12–1.15 mm and rotational of < 3° [18]. Inferior block nerve anesthesia have been tested on one phantom model with good results using just a camera and a laptop [36]. MASO have been carried on by two different authors, coauthors in one of the manuscripts [26, 37]; they described an increase of time needed of about 1 h of preparation before the surgery on human in their first study. In the second study they don't report such data on MASO performed on dog mandibles, even by unexperienced operators, both of them landed good results and were judged helpful. Othe authors proposed the use of augmented reality with one of the most sophisticated hardware found in literature which is the Da Vinci si robot in 2015, their experiment involved the resection of a neoplasm on a porcine



tongue using vascular landmarks. This is one of the only articles referring a clear failure of the experiment with a mean error of more than 5 mm [19]. Other authors proposed the positioning of distractors for hemifacial microsomia with the use of augmented reality in 2015, for their study they enrolled 10 randomized cases and 10 controls presenting microsomia. The aim was to transfer the surgical planning to the surgical site in hemifacial microsomia elongment using a Head Mounted Display predisposed with the use of Mimics and of the software AR Toolkits. They found the technology useful with difference between the vertical distances from the coronoid to the plane CP1 (AA') and CP2 (AA'') of 1.43 ± 0.13 mm in the AR group and 2.53 ± 0.39 mm in the control group [20]. Another interesting study proposed the use of NDI Polaris tracking system to solve the positioning issues related with the use of augmented reality. NDI Polaris is a tracking device which use spherical markers capture by a set of two rapid movement camera. The systems was implemented with self developed software with the use of a head-mounted device as described by the authors and it was used for implant placing in a pig corpse. The outcomes were evaluated through questionnaires which assessed ergonomic benefits and easier procedures, linear and angular error in the positioning were not assessed [39].

Outcomes

13 studies quantified the errors in the superposition of the virtual objects with reality or compared the outcomes with traditional set up, while 6 studies evaluated the changes in time needed for the intervention, a total of 16 studies considered at least one of the two variables as described in (Table 3). All the studies considered the results satisfactory for the quantification of the error/precision except for one but not many considered satisfactory the timing comparisons.

Authors considered the mean error of the tracking tool for vascular landmarks of the base of the tongue for neoplasm resection by using the Da Vinci robot of 5 mm not acceptable [19].

Other authors evaluated the maxillary reposition with X-scope prolonged by approximately 1 h, while others considered MASO with computer aided tools needs approximately 1 h of registration before the start but they suggest that it can be improved with experience in the future [26, 27]. some authors in 2013 considered maxillary repositioning using a custom portable device 60 min longer than a conventional operation [22]. All the outcomes are collected in (Table 3).

Research types/design

The design proposed for the selected studies is experimental randomized clinical trial in one of the studies proposed [20], there are 3 Cohort studies [16, 33, 41] and three review studies [30, 38, 43].

Discussion

The first studies taken into account were published in 2005, 38 years after the publishing of the first head-mounted augmented reality system by Sunderland. Even though augmented reality is a specifically visual immersive system, most of the authors are proposing non-wearable display-camera systems. This reduces the efforts related to stabilization of overlapping two different dynamic systems, which is preponderant in head-mounted and portable systems but also reduces the scope of "augmenting" the perception of the operator [32].

The studies considered are rapidly growing from 2013 as can be seen by (Fig. 4) and the most productive state are China and Japan, which also collaborated between each other in different studies, followed by Germany, UK and Belgium.

The majority of the systems refer to OMS area specifically to maxillofacial surgery. Implantology and oral surgery, the two other subgroups, include just 4 studies out of 21 in the OMS, which means that 84% of OMS studies refers specifically to maxillofacial surgery. Educational and learning studies are almost equivalent to restorative dentistry respectively they include 5 and 4 studies. Orthodontics and endodontics are represented with one study each. There is lack of a system studied in different fields, this could be explained with the high customization and knowledge required for every system to adapt to a specific field. Even though some systems share the same hardware [22, 34].

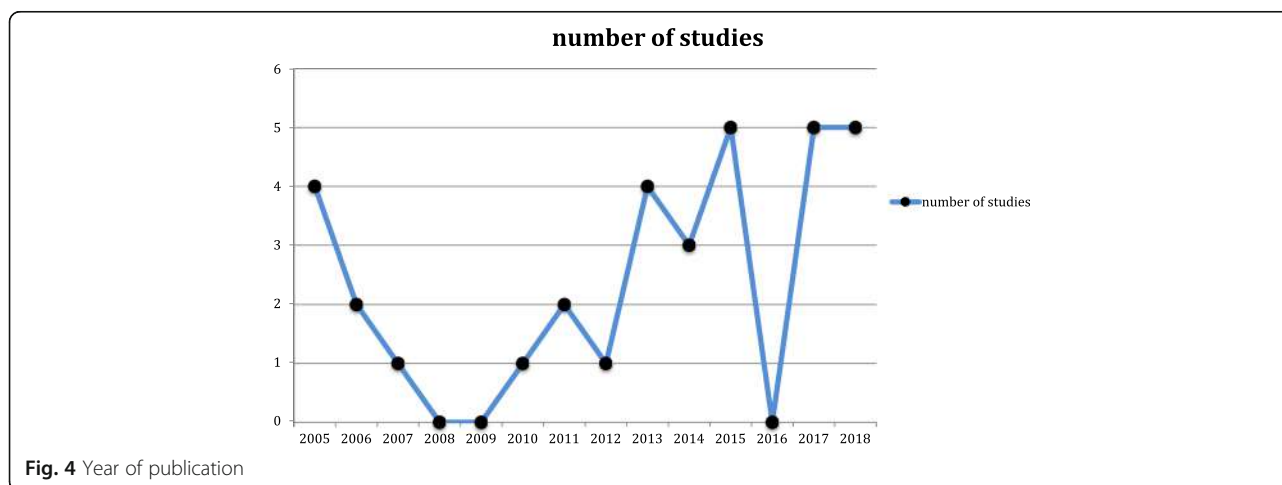
The prevalence of studies in the maxillofacial area can be associated with the extension of the area of intervention. The larger is the subject to be seen in augmented reality the more applicability finds the system. This fact can be associated with contemporary availability of

Table 3 Error and timing

	Field of interest	Error	Timing
Jiang W.	OMS	< 1.5-mm mean linear deviation and < 5.5-degree angular deviation	
Murugesan YP	Dental cavity	new algorithm improves the video accuracy by 0.30–0.40 mm. processing rate to 10–13 frames/s compared to 7–10 frames/s in existing systems	
Schreurs R.	OMS	translation error of 1.12–1.15 mm rotational < 3°.	
Liu WP	OMS	5 mm (mean) tool tracking error	
Qu M.	OMS	difference between the vertical distances from the coronoid to the plane CP1 (AA') and CP2 (AA'') was (1.43 ± 0.13) mm in the exp. group and (2.53 ± 0.39) mm in the ctrl. Group. The average angle between the two planes was 9.39° ± 0.75° in the exp. group	
Wang J.	OMS	The mean overall error of the 3-D image overlay was 0.71 mm	
Zinser MJ	OMS	Clinically acceptable precision for the surgical planning transfer of the maxilla (< 0.35 mm) was seen in the anteroposterior and mediolateral angles, and in relation to the skull base (< 0.35°),	60 min longer than a conventional operation.
Lin YK	OMS	0.50 ± 0.33 mm, 0.96 ± 0.36 mm, 2.70 ± 1.55°, 0.33 ± 0.27 mm, and 0.86 ± 0.34 mm, respectively, for the fully edentulous mandible, and 0.46 ± 0.20 mm, 1.23 ± 0.42 mm, 3.33 ± 1.42°, 0.48 ± 0.37 mm, and 1.1 ± 0.39 mm	
Suenaga H.	OMS	The positional error and angular error calculated in this study were 0.77 mm and 0.686, respectively, which is almost negligible.	time required for preparing the 3D models within Mimics and/or Slicer was 5–10 min.
Aichert A.	Orthodontics	correct alignment is recovered in about 75% of the cases	
Bruellmann DD	Endodontics	The overall sensitivity was about 94%. Classification accuracy for molars ranged from 65.0 to 81.2% and from 85.7 to 96.7% for premolars.	
Zhu M.	OMS		additional time required for manufacture of the splints. 2 to 5 min to check the result of navigation registration process cost approximately 1 h before operation. With the increasing experience, this significant extra time related to technical issues may be reduced.
Mischkowski RA	OMS	mean value of 0.97 cm for average deviation between real and virtual objects using the headset as referencing method	surgery time was prolonged by approximately 1 h
Ewers R.	OMS	48 of 60 UMTS transmissions were finished without any interruptions in constant quality, slight interruptions were observed in 8 tests, and a complete breakdown was observed during 4 streamings that required a restart of the transmission. Resolution was sufficient to diagnose even tiny anatomic structures inside the temporomandibular joint, but orientation was hardly recognizable.	
Wierinck E.	Dental cavity		students realised 50–100% more preparations in artificial teeth (depending on the type of preparation) per hour
Ewers R	OMS		reduces time

already existing hardware and components used for customized systems. High precision cameras with efficient stabilization and the possibility to zoom in a small area are still very expensive and big in size. Also the landmark of reference are highly influencing the

predominant interest in the OMS area, in fact trials carried on using vascular references, even with high precision hardwares, obtained result where the outcomes were considered not satisfactory (mean error more than 5 mm) [19].



This could be a major limitation of this new technology in operations carried on exclusively on soft tissues since the lack of stability represents an obstacle to stabilization of the overlapping images.

Primary endpoints of the studies show general positivity for improvement, usefulness and even good outcomes in the precision of the proposed systems (higher than usual standards in some cases). Educational systems were evaluated through questionnaires and brought great response in the students. While other fields of interest might appear as they are making their first step on the augmented technologies, education seems already available for wider studies since navigation systems were already available with the use of virtual reality, having a low cost [7]. Also a good response is to be expected from young generations which are more prominent to adapt to new technologies. The

use of this technology could simplify digital procedures with direct visualization of virtual informations (Fig. 5).

Timing, although, is more controversial and highly depends on the structure of the system proposed. The timing outcomes are very different between each other, in fact some relates to the setting and calibration time, some other refers to the duration of the intervention and the educational studies refer to the time needed for gaining a given skill in dental training and manual dexterity [17].

The positivity in the outcomes and primary endpoints of the studies considered (31/33) should be taken with caution since many of the systems described are self-developed by the same institutions of the authors.

Custom made software were not used by other authors except the first describing them, which is a major flaw

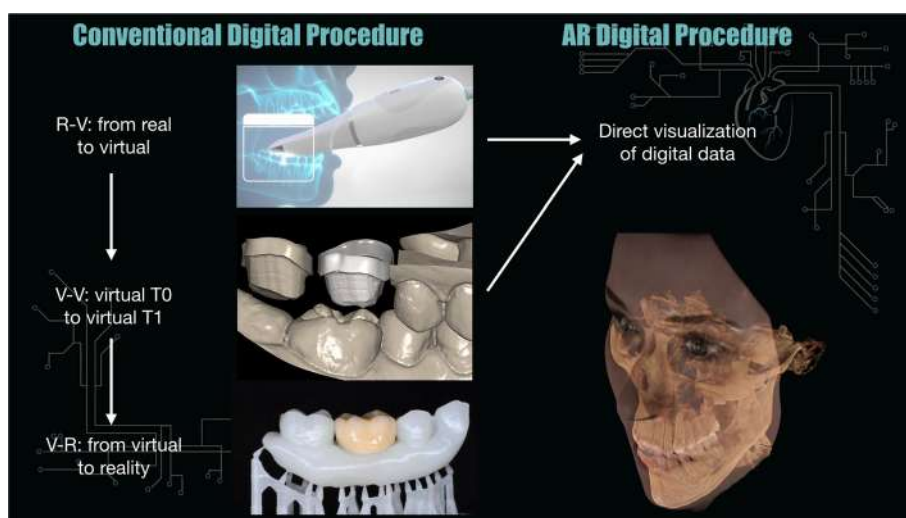


Fig. 5 Digital dentistry procedures, conventional vs augmented reality

and could represent conflict of interest in validating a new proposed system. Also, there is a lack of randomized clinical trials with a proper sample size calculation and other effort to avoid major bias.

Conclusions

Most recent technologies are being developed with custom software: 7 out of 9 were self-developed by the authors in the last 5 years. More efforts is needed to implement the hardware support. From what is known a simple, portable and accessible tool is needed. Timing is a controversial topic in different fields of interest since half of the authors (3 out of 6) report an increase of at least one hour while precision is judged satisfactory by most authors (12 out of 13).

Although the technologies proposed are not validated by external teams, customized augmented reality systems seems to provide great results in simple experimental models since most of the studies were carried on phantoms (51% $n = 17$). OMS area is referee of great advantages in interventions carried on medium sized surgical areas and its gaining the most benefits from this technology since superposition of digital images is easier on bony structures. Most of the studies were carried on this augmented reality field of application (21 out of 33).

Abbreviations

F.O.I: Field of interest; H.M.S: Head Mounted System; O.M.S: Oral and Maxillofacial Surgery

Acknowledgements

Prof. Giampietro Farronato, Dean, University of Milan, Orthodontic Department.
Prof. Moreno Muffatto, Department of Industrial Engineering, University of Padova, Padua, Italy.

Authors' contributions

MF; DF: substantial contributions to the conception and design of the work. CM; AF; VL; FF; AP: the acquisition, analysis and interpretation of data. MF; DF; AF: have drafted the work or substantively revised it. MF; CM; VL; AF; FF; AP; DF: have approved the submitted version (and any substantially modified version that involves the author's contribution to the study); MF; CM; VL; AF; FF; AP; DF: have agreed both to be personally accountable for the author's own contributions and to ensure that questions related to the accuracy or integrity of any part of the work, even ones in which the author was not personally involved, are appropriately investigated, resolved, and the resolution documented in the literature.

Authors' information

The authors MF; DF; FF; are working on a new augmented reality system.

Funding

The authors declare self funding for the research.

Availability of data and materials

The datasets used and/or analysed during the current study are available from the corresponding author on reasonable request. Other resources are available under the dataset at: https://www.crd.york.ac.uk/prospero/display_record.php?RecordID=120058

Ethics approval and consent to participate

Not applicable.

Consent for publication

Not applicable.

Competing interests

The authors declare that they have no competing interests.

Author details

¹Department of Orthodontics, Fondazione IRCCS Ca' Granda, Ospedale Maggiore Policlinico, University of Milan, via Francesco Sforza 35, 20122 Milano, MI, Italy. ²Department of Industrial Engineering, University of Padova, via Venezia 1, 35131 Padua, Italy. ³Department of Informatics and Computational Sciences, University of Milan, Milano, Italy. ⁴School of Medicine and Surgery, University of Insubria, Via G. Piatti 10, 21100 Varese, Italy.

Received: 2 April 2019 Accepted: 31 May 2019

Published online: 08 July 2019

References

- Azuma RT. A survey of augmented reality. *Presence Teleoperators Virtual Environ.* 1997;6(4):355–85.
- Bimber O, Raskar R. *Spatial augmented reality: merging real and virtual worlds.* Wellesley: AK Peters/CRC Press; 2005.
- Van Krevelen D, Poelman R. Augmented reality: technologies, applications, and limitations. *Vrije Univ Amsterdam Dep Comput Sci.* 2007;9(2):1–20.
- Ausburn LJ, Ausburn FB. Desktop virtual reality: a powerful new technology for teaching and research in industrial teacher education. *J Ind Teach Educ.* 2004;41(4):1–16.
- Pulijala Y, Ma M, Pears M, Peebles D, Ayoub A. Effectiveness of immersive virtual reality in surgical training—a randomized control trial. *J Oral Maxillofac Surg.* 2018;76(5):1065–72.
- Joda T, Gallucci GO, Wismeijer D, Zitzmann NU. Augmented and virtual reality in dental medicine: a systematic review. *Comput Biol Med.* 2019;108:93–100.
- Satava RM, Jones SB. Current and future applications of virtual reality for medicine. *Proc IEEE.* 1998;86(3):484–9.
- Suenaga H, Tran HH, Liao H, Masamune K, Dohi T, Hoshi K, et al. Real-time in situ three-dimensional integral videography and surgical navigation using augmented reality: a pilot study. *Int J Oral Sci.* 2013;5(2):98.
- Jayaram S, Connacher HI, Lyons KW. Virtual assembly using virtual reality techniques. *Comput Aided Des.* 1997;29(8):575–84.
- Farronato G, Santamaria G, Cressoni P, Falzone D, Colombo M. The digital-titanium Herbst. *J Clin Orthod.* 2011;45(5):263–7. quiz 287–8.
- Farronato G, Galbiati G, Esposito L, Mortellaro C, Zanoni F, Maspero C. Three-dimensional virtual treatment planning: Presurgical evaluation. *J Craniofac Surg.* 2018;29(5):e433–7.
- Caudell TP, Mizell DW. Augmented reality: an application of heads-up display technology to manual manufacturing processes. In: *Proceedings of the twenty-fifth Hawaii international conference on system sciences*, vol. 2. Kauai: IEEE; 1992. p. 659–69.
- Mangano F, Shibli JA, Fortin T. Digital dentistry: new materials and techniques. *Int J Dent.* 2016;2016:5261247.
- Moher D, Shamseer L, Clarke M, Ghersi D, Liberati A, Petticrew M, et al. Preferred reporting items for systematic review and meta-analysis protocols (PRISMA-P) 2015 statement. *Syst Rev.* 2015;4(1):1.
- Cooke A, Smith D, Booth A. Beyond PICO: the SPIDER tool for qualitative evidence synthesis. *Qual Health Res.* 2012;22(10):1435–43.
- Jiang W, Ma L, Zhang B, Fan Y, Qu X, Zhang X, Liao H. Evaluation of the 3D augmented reality-guided intraoperative posit ioning of dental implants in edentulous mandibular models. *Int J Oral Maxillofac Implants.* 2018;33(6):1219–28.
- Murugesan YP, Alsadoon A, Manoranjan P, Prasad PWC. A novel rotational matrix and translation vector algorithm: geometric accuracy for augmented reality in oral and maxillofacial surgeries. *Int J Med Robot Comput Assist Surg.* 2018;14(3):e1889.
- Schreurs R, Dubois L, Becking AG, Maal TJJ. Implant-oriented navigation in orbital reconstruction. Part 1: technique and accuracy study. *Int J Oral Maxillofac Surg.* 2018;47(3):395–402.
- Liu WP, Richmon JD, Sorger JM, Azizian M, Taylor RH. Augmented reality and cone beam CT guidance for transoral robotic surgery. *J Robot Surg.* 2015;9(3):223–33.

20. Qu M, Hou Y, Xu Y, Shen C, Zhu M, Xie L, et al. Precise positioning of an intraoral distractor using augmented reality in patients with hemifacial microsomia. *J Cranio-Maxillofac Surg.* 2015;43(1):106–12.
21. Wang J, Suenaga H, Yang L, Kobayashi E, Sakuma I. Video see-through augmented reality for oral and maxillofacial surgery. *Int J Med Robot Comput Assist Surg.* 2017;13(2):e1754.
22. Zinser MJ, Mischkowski RA, Dreiseidler T, Thamm OC, Rothamel D, Zöller JE. Computer-assisted orthognathic surgery: waferless maxillary positioning, versatility, and accuracy of an image-guided visualisation display. *Br J Oral Maxillofac Surg.* 2013;51(8):827–33.
23. Lin YK, Yau HT, Wang IC, Zheng C, Chung KH. A novel dental implant guided surgery based on integration of surgical template and augmented reality. *Clin Implant Dent Relat Res.* 2015;17(3):543–53.
24. Aichert A, Wein W, Ladikos A, Reichl T, Navab N. Image-based tracking of the teeth for orthodontic augmented reality. In: International conference on medical image computing and computer-assisted intervention. Berlin, Heidelberg: Springer; 2012. p. 601–8.
25. Bruellmann DD, Tjaden H, Schwanecke U, Barth P. An optimized video system for augmented reality in endodontics: a feasibility study. *Clin Oral Investig.* 2013;17(2):441–8.
26. Zhu M, Chai G, Zhang Y, Ma X, Gan J. Registration strategy using occlusal splint based on augmented reality for mandibular angle oblique split osteotomy. *J Craniofac Surg.* 2011;22(5):1806–9.
27. Mischkowski RA, Zinser MJ, Kübler AC, Krug B, Seifert U, Zöller JE. Application of an augmented reality tool for maxillary positioning in orthognathic surgery—a feasibility study. *J Cranio-Maxillofac Surg.* 2006;34(8):478–83.
28. Ewers R, Schicho K, Undt G, Wanschitz F, Truppe M, Seemann R, Wagner A. Basic research and 12 years of clinical experience in computer-assisted navigation technology: a review. *Int J Oral Maxillofac Surg.* 2005;34(1):1–8.
29. Wierinck E, Puttemans V, Van Steenberghe D. Effect of tutorial input in addition to augmented feedback on manual dexterity training and its retention. *Eur J Dent Educ.* 2006;10(1):24–31.
30. Ewers R, Schicho K, Wagner A, Undt G, Seemann R, Figl M, Truppe M. Seven years of clinical experience with teleconsultation in craniomaxillofacial surgery. *J Oral Maxillofac Surg.* 2005;63(10):1447–54.
31. Bogdan CM, Popovici DM. Information system analysis of an e-learning system used for dental restorations simulation. *Comput Methods Prog Biomed.* 2012;107(3):357–66.
32. Espejo-Trung LC, Elian SN, Luz MAADC. Development and application of a new learning object for teaching operative dentistry using augmented reality. *J Dent Educ.* 2015;79(11):1356–62.
33. Llena C, Folguera S, Forner L, Rodríguez-Lozano FJ. Implementation of augmented reality in operative dentistry learning. *Eur J Dent Educ.* 2018;22(1):e122–30.
34. Badiali G, Ferrari V, Cutolo F, Freschi C, Caramella D, Bianchi A, Marchetti C. Augmented reality as an aid in maxillofacial surgery: validation of a wearable system allowing maxillary repositioning. *J Cranio-Maxillofac Surg.* 2014;42(8):1970–6.
35. Farronato M, Lucchina AG, Mortellaro C, Fama A, Galbiati G, Farronato G, Maspero C. Bilateral hyperplasia of the coronoid process in pediatric patients: what is the gold standard for treatment? *J Craniofac Surg.* 2019;30(4):1058–63.
36. Won YJ, Kang SH. Application of augmented reality for inferior alveolar nerve block anesthesia: a technical note. *J Dent Anesth Pain Med.* 2017;17(2):129–34.
37. Zhou C, Zhu M, Shi Y, Lin L, Chai G, Zhang Y, Xie L. Robot-assisted surgery for mandibular angle split osteotomy using augmented reality: preliminary results on clinical animal experiment. *Aesthet Plast Surg.* 2017;41(5):1228–36.
38. Plessas A. Computerized virtual reality simulation in preclinical dentistry: can a computerized simulator replace the conventional phantom heads and human instruction? *Simul Healthc.* 2017;12(5):332–8.
39. Katić D, Spengler P, Bodenstedt S, Castrillon-Oberndorfer G, Seeberger R, Hoffmann J, et al. A system for context-aware intraoperative augmented reality in dental implant surgery. *Int J Comput Assist Radiol Surg.* 2015;10(1):101–8.
40. Wang J, Suenaga H, Hoshi K, Yang L, Kobayashi E, Sakuma I, Liao H. Augmented reality navigation with automatic marker-free image registration using 3-D image overlay for dental surgery. *IEEE Trans Biomed Eng.* 2014;61(4):1295–304.
41. Wierinck ER, Puttemans V, Swinnen SP, van Steenberghe D. Expert performance on a virtual reality simulation system. *J Dent Educ.* 2007;71(6):759–66.
42. Wierinck E, Puttemans V, Swinnen S, van Steenberghe D. Effect of augmented visual feedback from a virtual reality simulation system on manual dexterity training. *Eur J Dent Educ.* 2005;9(1):10–6.
43. Nijmeh AD, Goodger NM, Hawkes D, Edwards PJ, McGurk M. Image-guided navigation in oral and maxillofacial surgery. *Br J Oral Maxillofac Surg.* 2005;43(4):294–302.
44. Shahrbanian S, Ma X, Aghaei N, Korner-Bitensky N, Moshiri K, Simmonds MJ. Use of virtual reality (immersive vs. non immersive) for pain management in children and adults: a systematic review of evidence from randomized controlled trials. *Eur J Exp Biol.* 2012;2(5):1408–22.
45. Wang J, Suenaga H, Liao H, Hoshi K, Yang L, Kobayashi E, Sakuma I. Real-time computer-generated integral imaging and 3D image calibration for augmented reality surgical navigation. *Comput Med Imaging Graphics.* 2015;40:147–59.

Publisher's Note

Springer Nature remains neutral with regard to jurisdictional claims in published maps and institutional affiliations.

Ready to submit your research? Choose BMC and benefit from:

- fast, convenient online submission
- thorough peer review by experienced researchers in your field
- rapid publication on acceptance
- support for research data, including large and complex data types
- gold Open Access which fosters wider collaboration and increased citations
- maximum visibility for your research: over 100M website views per year

At BMC, research is always in progress.

Learn more biomedcentral.com/submissions



RESEARCH ARTICLE

Open Access



The accuracy and reliability of digital measurements of gingival recession versus conventional methods

Hytham N. Fageeh^{*} , Abdullah A. Meshni, Hassan A. Jamal, Reghunathan S. Preethanath and Esam Halboub

Abstract

Background: An apical shift in the position of the gingiva beyond the cemento-enamel junction leads to gingival recession. This study aimed to evaluate the reproducibility of digital measurements of gingival recession when compared to conventional measurements taken clinically using periodontal probes.

Methods: Gingival recession was measured at 97 sites in the oral cavity by four examiners using the following methods: CP, direct measurement of gingival recession using William's periodontal probe intraorally; CC, measurements on cast models using a caliper; DP, digital measurement on virtual models obtained by intraoral scanning, and DC, digital measurements on virtual models of dental casts. Intra-class and inter-rater correlations were analyzed. Bland Altman plots were drawn to visually determine the magnitude of differences in any given pair-wise measurements.

Results: In this study, good inter-methods reliability was observed for almost all the examiners ranging from 0.907 to 0.918, except for one examiner (0.837). The greatest disagreements between the raters were observed for methods; CP (0.631) followed by CC (0.85), while the best agreements were observed for methods DP (0.9) followed by DC (0.872).

Conclusion: Variations in measurements between examiners can be reduced by using digital technologies when compared to conventional methods. Improved reproducibility of measurements obtained via intraoral scanning will increase the validity and reliability of future studies that compare different treatment modalities for root coverage.

Keywords: Gingival recession, Intraoral scanning, Cast model, Intra-class coefficient

Background

Gingival recession refers to the exposure of the surface of the root following an apical shift in the position of the gingiva beyond the cemento-enamel junction (CEJ) [1, 2]. It is generally seen in adults, and may be localized or generalized, involving one or more teeth. The gingiva comprises epithelial and connective tissues and forms a collar around the neck of the tooth [3]. The parts of the gingival epithelium include the oral gingival epithelium, the sulcular gingival epithelium, which lines the gingival sulcus, and the junctional epithelium, which attaches the gingiva to the tooth [3, 4].

Gingival recession is caused by several factors such as anatomical abnormalities (thin alveolar bone or gingival

tissue, deficient keratinized mucosa, tooth malposition, high frenal attachment), trauma (tooth brushing), inflammation (due to presence of plaque or calculus) and from iatrogenic factors such as improper denture design, placement of orthodontic appliances or restorations [1, 5, 6]. In a healthy periodontium, the gingiva is positioned 0.5 to 2.0 mm coronal to the CEJ, and a shift from its normal position beyond the CEJ results in gingival recession [7]. Clinically, gingival recession is measured in millimeters from the gingival crest to the CEJ, using a dental probe; however, this method is thought to be semi-quantitative and inaccurate [8]. Plaster models may prove useful in cases where it is difficult to measure recession intraorally, as they provide a three-dimensional (3D) view allowing for detailed assessments of the impressions obtained during clinical examination without interference from soft tissues within the confines of the oral cavity [9]. However,

* Correspondence: hfageeh@jazanu.edu.sa

Division of Periodontics, College of Dentistry, Jazan University, P.O.Box 114, Jazan 45142, Saudi Arabia



© The Author(s). 2019, corrected publication 2019. **Open Access** This article is distributed under the terms of the Creative Commons Attribution 4.0 International License (<http://creativecommons.org/licenses/by/4.0/>), which permits unrestricted use, distribution, and reproduction in any medium, provided you give appropriate credit to the original author(s) and the source, provide a link to the Creative Commons license, and indicate if changes were made. The Creative Commons Public Domain Dedication waiver (<http://creativecommons.org/publicdomain/zero/1.0/>) applies to the data made available in this article, unless otherwise stated.

the disadvantages of study casts include, physical and chemical damage, wear and tear, and distortion [10]. In addition, the use of plaster models is neither time- nor cost-effective. Thus, digital models were introduced in the late 1990s. The advantages of using digital models include ease of handling and storage, time-effectiveness, and reduced manual errors since data can be electronically transferred and stored. Digital models may be obtained via scanning of the intraoral tissues (creating virtual models) or study casts (creating digital cast models). Intraoral scanners are devices used for capturing direct optical impressions in dentistry [11, 12]. The dental arches are scanned, images of the oral tissues are captured and processed, and a 3D virtual model is finally created [12]. Similarly, plaster models are scanned using 3D scanners to create digital images. These advances in technology have proved extremely useful as diagnostic tools in dentistry.

In the present study, we aimed to investigate the reproducibility and reliability of digital measurements of gingival recession when compared with the conventional methods (dental probe, study casts).

Methods

This study was performed at the College of Dentistry, Jazan University, from September 2017 to February 2018. Fifteen volunteers exhibiting a gingival recession of at least 2 mm were enrolled in this study. The participants aged between 20 and 50 years were screened clinically to exclude those with systemic illnesses. The following exclusion criteria were used: use of any type of medication over the past two or more weeks; presence of any chronic medical condition, including diabetes or viral, fungal or bacterial infections; history of physical trauma during the previous 2 weeks; presence of aggressive periodontitis, periodontal abscess, or necrotizing ulcerative gingivitis/ periodontitis; any periodontal treatment and/or antibiotic therapy received during the preceding 3 months; any type of dental work or tooth extraction(s) performed over the last 2 weeks; and refusal to sign the consent form.

Ethical approval was obtained by the ethical committee of the scientific research unit, College of Dentistry, Jazan University under the reference number: CODJU-1709I and a written informed consent was obtained from all participants.

Gingival recession was measured as the distance from the CEJ to the gingival margin (GM), parallel to the long axis of the tooth starting from the most apical point of recession. The height of the mesial papilla was measured from a line connecting the cusp tips or incisal edges of the adjacent teeth to the tip of the papilla parallel to the long axis of the tooth. The mesial papilla was chosen due to better visual accessibility. Consistency in measurements

between recession and papilla height was obtained by this method.

A total of 97 sites were evaluated via direct clinical and digital measurements.

The two conventional methods used for the direct clinical measurements were as follows:

- Measurements in the oral cavity using a calibrated William's periodontal probe (CP) (Fig. 1)
- Measurements on cast models using a caliper (CC) (Fig. 2). Polyether impressions were taken using customized impression trays, and cast models were fabricated. A caliper with a 10-mm scale was used for the linear measurements.

Digital measurements were obtained using the following two methods:

- Measurements on virtual models obtained from intraoral optical impressions using Trios 3 shape software program (DP) (Fig. 3).
- Measurements on virtual models obtained from optical impressions of cast models using Trios 3 shape software (DC) (Fig. 4).

All measurements were performed by four examiners (3 faculty members and 1 intern at the school where the study was conducted) in random order using a computer-generated randomization list. The obtained data from the measurements were entered into a data extraction table, which was not accessible to the examiners.

Statistical analysis

Statistical analysis of the data was performed using SPSS Version 22 (Armonk, New York: IBM Corp.) and MedCalc for Windows, version 15.0 (MedCalc Software, Ostend, Belgium). The means, standard deviations (SD),



Fig. 1 Direct measurement of gingival recession using a William's periodontal probe (CP)



Fig. 2 Measurement of gingival recession on cast models using a caliper (CC)

and standard errors (SE) of the measured recessions were presented. Intra-class correlation coefficients (ICC), along with their 95% confidence intervals (CI) were used to evaluate the inter-method and inter-examiner reliabilities of gingival recession measurements obtained from the 97 sites in the oral cavity. Based on the study by Landis and Koch (1997), the ICC scale was interpreted as follows: poor to fair (below 0.4), moderate (0.41–0.60), excellent (0.61–0.80), and almost perfect (0.81–1) [13].

In order to depict the pair-wise variations between each pair of methods/examiners, Bland and Altman Plots were drawn displaying the mean values for each pair against the difference, and demonstrating the degree of agreement between the examiners or methods. The difference for each point, the mean difference, and the confidence limits are illustrated on the vertical axis, while the average of two measurements are depicted along the horizontal axis [14]. Of the four horizontal lines in the graph, the middle blue line represents the observed difference in mean values, and dotted red line in the middle indicates the expected mean difference



Fig. 3 Measurements on virtual models obtained from intraoral optical impressions using 3 shape software program (DP)

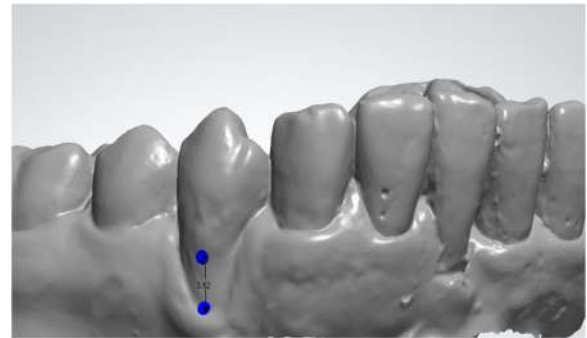


Fig. 4 Measurements on virtual models obtained from optical impressions of cast models using the 3 shape software (DC)

(zero). The two lines on the top and bottom indicate the 95% confidence limits within which about 95% of the differences between the measurements of each examiner or method should lie [15]. The within-examiners and within-methods biases along with their 95% upper and lower limits were calculated.

Results

Table 1 shows the mean and SD values of gingival recession measured by the four examiners using the four different methods. The highest mean was reported by examiner B using the conventional probe model (CP; 2.24 ± 0.97 mm), while the lowest was reported by examiner D using DC (1.64 ± 0.74 mm). The method with the highest mean value obtained by combining the measurements taken by all four examiners was CP (2.11 ± 1 mm), and the one with lowest mean value was CC (1.91 ± 0.7 mm). The highest score for all methods combined was measured by examiner B (2.16 ± 0.85 mm), and the lowest by examiner D (1.79 ± 0.8 mm).

Table 2 shows the values of the intra-class correlation coefficients (ICCs) for the inter-method, inter-examiner, all methods, and all examiners. The ICCs for all methods combined, irrespective of the examiners, and for all examiners combined, irrespective of the methods, were almost perfect 0.933 and 0.912, respectively.

Differences between examiners, irrespective of the methods used, are illustrated in the Bland and Altman plots in Fig. 5 and presented in Table 3. The least differences were found between examiners A and C (-0.004 mm), A and B (0.055 mm), followed by B and C (-0.056 mm). In spite of the low differences (biases) between values, the 95% confidence interval limits were fairly wide, particularly for examiner D when compared with the other three examiners (Fig. 5 and Table 3).

Differences between methods, irrespective of the examiners, are illustrated in the Bland and Altman plots in Fig. 6 and presented in Table 3. The least differences were observed between CP and DP (-0.013 mm), DP and

Table 1 Means, standard deviations (SD) and standard errors (SE) of the recession measurements by individual examiners and methods, and for all methods and all examiners combined

Examiner	Method	Recession Measurement ^a		
		Mean	SD	SE
A	CP	2.23	1.38	0.14
	CC	1.95	0.84	0.09
	DP	2.19	0.8	0.08
	DC	2.16	0.79	0.08
B	CP	2.24	0.97	0.1
	CC	2.06	0.86	0.09
	DP	2.17	0.80	0.08
	DC	2.17	0.77	0.08
C	CP	2.14	1.12	0.11
	CC	1.98	0.97	0.1
	DP	2.16	0.85	0.08
	DC	2.12	0.82	0.08
D	CP	1.91	0.94	0.1
	CC	1.64	0.74	0.07
	DP	1.85	0.83	0.08
	DC	1.77	0.65	0.07
CP all (N = 392)		2.11	1	0.05
CC all (N = 392)		1.91	0.87	0.04
DP all (N = 392)		2.09	0.83	0.04
DC all (N = 392)		2.06	0.78	0.04
A all (N = 392)		2.11	0.85	0.04
B all (N = 392)		2.16	0.85	0.04
C all (N = 392)		2.1	0.95	0.05
D all (N = 392)		1.79	0.8	0.04

^a: N = 98 unless stated otherwise. A, B, C, and D: the four examiners in the study. CP, conventional method using periodontal probe; CC, conventional method of taking measurements on cast model using caliper; DP, digital measurements of intraoral scans; and DC, digital measurements of digitized cast models

DC (− 0.036 mm,) followed by CP and DC (− 0.049 mm). Although these differences (biases) were very low, their 95% confidence interval limits were fairly broad, except for the difference between methods DP and DC. The discrepancy was more obvious for CC when compared with the other methods (Fig. 6 and Table 3).

Discussion

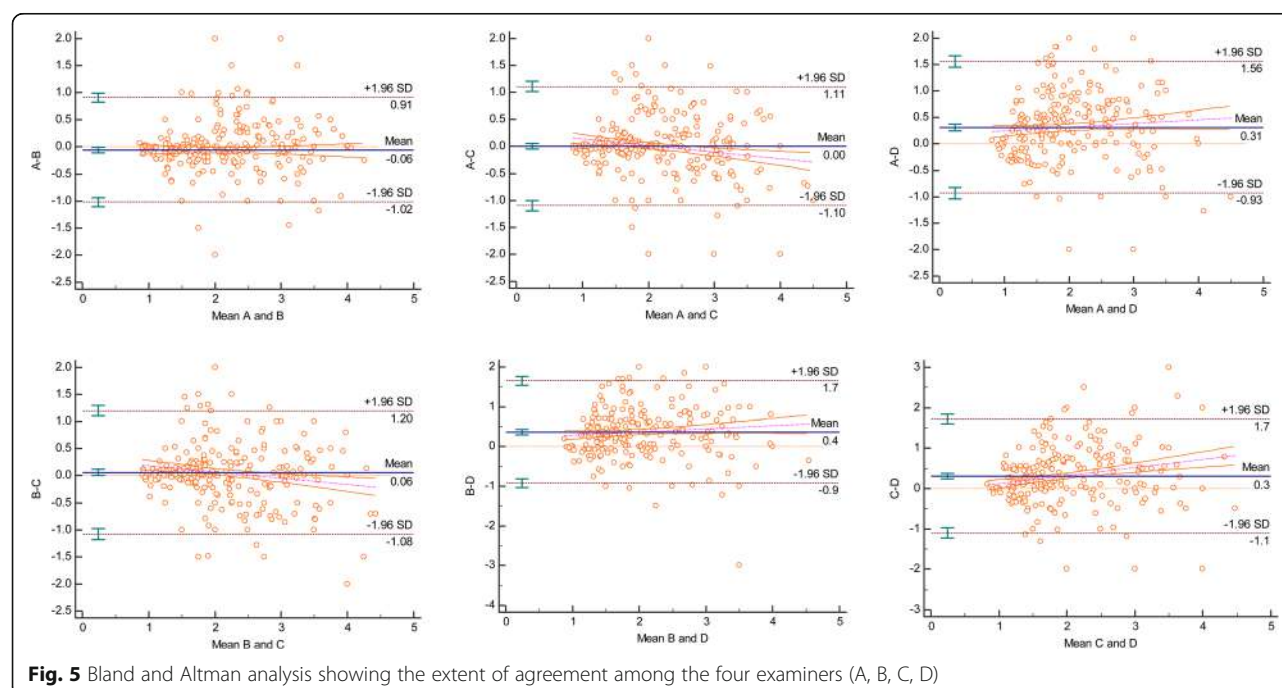
In the present study, the reliability and reproducibility of digital measurements of gingival recession (DP, DC) compared with the conventional methods using dental probe and cast models (CP, CC) were assessed. Digital measurements proved to be more accurate when compared to the clinical measurements with regard to reproducibility between examiners.

Table 2 Intraclass correlation coefficients (ICC) for inter-methods, inter-examiners, and all methods and all examiners combined

Examiner	Method	ICC	95% ICC
A	CP	0.911	0.869–0.940
	CC		
	DP		
	DC		
B	CP	0.907	0.867–0.936
	CC		
	DP		
	DC		
C	CP	0.918	0.886–0.943
	CC		
	DP		
	DC		
D	CP	0.837	0.759–0.891
	CC		
	DP		
	DC		
Method	Examiner	ICC	95% ICC
CP	A	0.631	0.495–0.737
	B		
	C		
	D		
CC	A	0.850	0.765–0.903
	B		
	C		
	D		
DP	A	0.900	0.849–0.933
	B		
	C		
	D		
DC	A	0.872	0.788–0.920
	B		
	C		
	D		
Agreement between		ICC	95% CI
All Methods		0.933	0.920–0.944
All examiners		0.912	0.887–0.931

A, B, C, and D: the four examiners in the study. CP, conventional method using periodontal probe; CC, conventional method of taking measurements on cast model using caliper; DP, digital measurements of intraoral scans; and DC, digital measurements of digitized cast models

In the present study, significant differences were observed in the measurements obtained by CP and CC when compared with those obtained by DP and DC. The highest measurements of gingival recession were achieved



using the conventional dental probe method (CP) when compared with the other three methods in the current study. This is in accordance with the findings of the study by Schneider et al. [16], who reported discrepancy in measurements taken by (CP) and attributed this phenomenon to the color difference between the exposed root surface

Table 3 Bias of measurements between different examiners and different methods

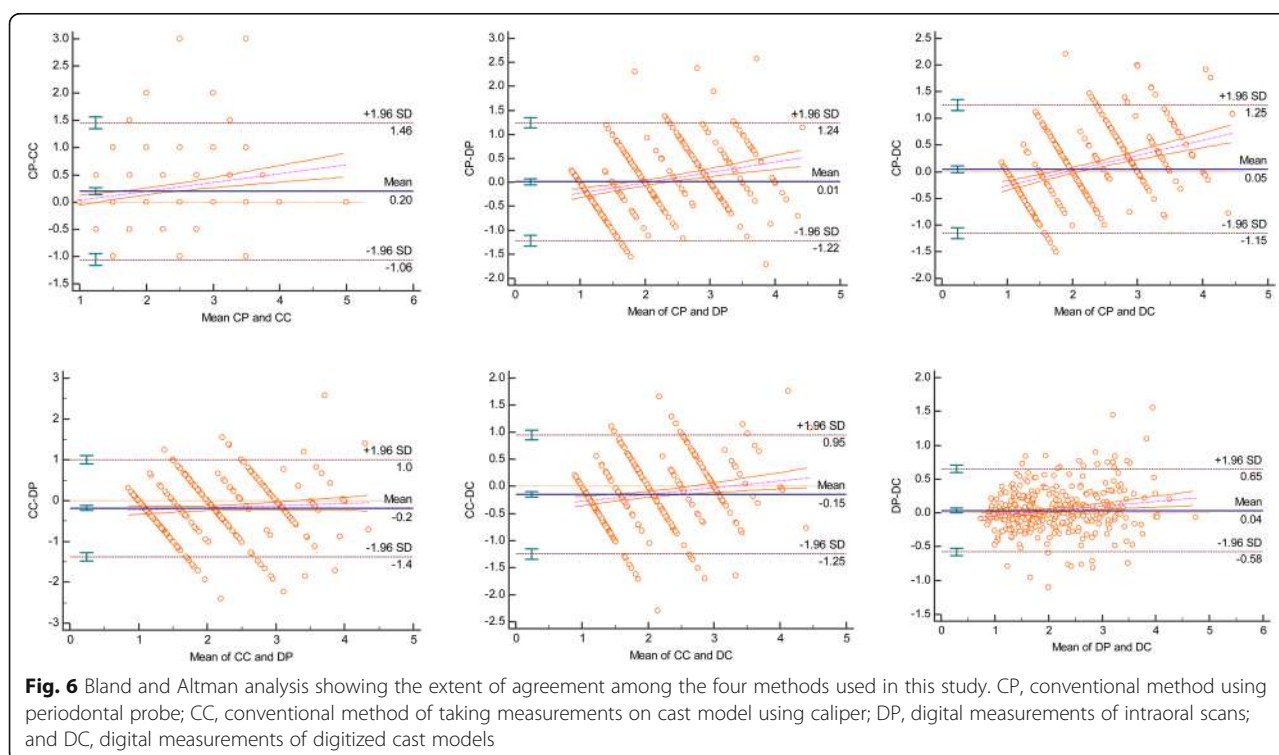
	95% Lower Limit	95% Upper Limit	Bias
Examiners			
A to B	-0.912	1.023	0.055
A to C	-1.107	1.099	-0.004
A to D	-1.559	0.934	-0.313
B to C	-1.199	1.080	-0.056
B to D	-1.656	0.919	-0.369
C to D	-1.717	0.718	-0.309
Methods			
CP to CC	-1.455	1.060	-0.198
CP to DP	-1.244	1.219	-0.013
CP to DC	-1.249	1.152	-0.049
CC to DP	-1.012	1.382	0.185
CC to DC	-0.952	1.250	0.149
DP to DC	-0.652	0.580	-0.036

A, B, C, and D: the four examiners in the study. CP, conventional method using periodontal probe; CC, conventional method of taking measurements on cast model using caliper; DP, digital measurements of intraoral scans; and DC, digital measurements of digitalized cast models

and the enamel, which is more distinctly visible intraorally when compared to the cast or digital models.

Inter-examiner variability was higher between CC and CP methods when compared to methods DP and DC indicating superior reproducibility of measurements when digital methods were used. Similar findings have been reported in previous studies comparing measurements in the oral cavity using conventional and digital methods [16, 17]. Moreover, the lowest inter-examiner agreement was noted with method CP and the highest with method DP. One of the main advantages of using digital technology is that the images can be magnified and viewed from various angles. In addition, the possibility of taking repeated measurements with superior reproducibility will greatly improve the quality of the data collected. In a recent study, the reproducibility of a digital method aimed at evaluating the apico-coronal migration of free gingival margin was validated [18]. Furthermore, the use of a digital model is patient-friendly, as it can reduce both anxiety and discomfort for the patient.

Failure in obtaining accurate measurements of gingival recession can lead to false results and affect the credibility of research studies. Often conventional methods used for these measurements are cost-effective, but have an increased potential for errors due to various factors, such as limited accessibility, manual errors, and variations in the angle of approach. Cast models offer better visual accessibility and the opportunity for repeated measurements. However, additional steps such as impression taking and fabrication of casts may lead to inaccuracies in measurement [16]. Digital measurements



have been shown to be more accurate than those obtained using direct oral and cast model methods [16, 17, 19].

Bland and Altman [15] plots aid in calculating the mean of the differences between two measurements. The confidence limits around the mean can be used to assess the extent of variation, which might influence the measurements; mean values closer to zero indicate better agreement between the examiners. On the basis of biases shown in Table 3, it can be implied that the differences in measurement (between examiners and to lesser extent between methods) are not clinically significant; the maximum difference did not exceed half a millimeter. However, these differences have somewhat broad 95% confidence intervals extending up to 2 mm which is known to be clinically paramount and may violate the reliability of the used methods. According to McCoy et al. [14], if the ratings of one examiner are consistently higher than the other, the mean will be far from zero, but the confidence interval will be narrow; alternatively, if the disagreement between examiners demonstrates an inconsistent pattern, the mean may be closer to zero but the confidence interval will be wide. In the present study, the means between examiners A and B, A and C, and B and C were closer to zero (0.055, 0.004, and 0.056, respectively) with narrow 95% CIs (Table 3 and Fig. 5). As seen in inter-method (Table 2), intra-examiner agreement was nearly similar for examiners A, B, and C (ICC, > 90), while the ICC for examiner D was 0.837 (95% CI, 0.759–0.891). These findings indicate

the need for further studies to assess the reliability of measurements among dentists.

Intraoral scanning involves the creation of a 3D image of the structures in the oral cavity using various optical technologies. Computer-aided design/computer-aided manufacturing (CAD/CAM) was introduced by Dr. Francois Duret in 1973 [20]. This system can be used to take direct images from the oral cavity or from models created after impressions are taken from the patients [21]. Recently, this technique was successfully used for volumetric analyses after gingival recession treatment [22]. In another study, Wiranto et al. [19] reported that intraoral scanning is a valid and reliable method with high reproducibility for diagnostic measurements in the field of dentistry. Chalmers et al., [17] reported that the reliability of measurements of dental arch relationships using intraoral 3D scans was superior to that using plaster models. Similar to the findings of their study, the inter-examiner reliability of intraoral scans (DP) was superior to the digital cast models (DC), which in turn were superior to the conventional methods (CP, CC) used in the current study. The present study was not able to identify the method with the most accurate measurements of gingival recession. Nevertheless, the use of digital methods and intraoral scanning for measuring gingival recession has not been explored extensively. The current study corroborates the findings of Schneider et al. [16], and endorses the use of digital technology to assess the outcome of various root coverage procedures.

The limitations for the current study include: First, the lack of repeated measures for the same examiners using the same methods which is essential in assessing intra-examiner reliability. Second, the number of the recession sites was comparatively small. With a larger sample size, more reliable results can be obtained. Finally using a William's periodontal probe does not allow measurements to be recorded to the tenths of millimeter owing to the fact that it is marked in absolute mm. This can significantly alter the readings of gingival recession as the examiner is obliged to round the measurement to the nearest mm.

Conclusions

Although mostly minor, there was variability in measurements observed for almost all examiners. Inter-examiner variability was higher for methods CC and CP when compared to DP and DC methods indicating superior reproducibility of measurements using digital technology. Variations between examiners or methods can be reduced considerably using digital methods when compared with the conventional methods. In addition, improved reproducibility of measurements obtained via intraoral scanning will increase the validity of the data and enhance the quality of the study.

Additional file

Additional file 1: Gingival recession measurements for all methods. (XLSX 19 kb)

Abbreviations

3D: Three dimensional; CAD/CAM: Computer-aided design/computer-aided manufacturing; CC: Measurements on cast models using a caliper; CEJ: Cemento-enamel junction; CI: Confidence intervals; CP: Direct measurement of gingival recession using William's periodontal probe intraorally; DC: Digital measurements on virtual models of dental casts; DP: Digital measurement on virtual models obtained by intraoral scanning; GM: Gingival margin; ICC: Intra-class correlation coefficients; SD: Standard deviations; SE: Standard errors of the measured recessions

Acknowledgments

We would like to thank Mr. Mahmoud Al Muhaimed at MINA Lab for assisting us with exporting the digital files and to Dr. Hashim Bajawi for allowing us to use the digital intra-oral scanner at the University Staff Clinic at Jazan University.

Authors' contributions

HF has made a substantial contribution to the conceptualization and execution of this study; AM, HJ and RP has contributed to the acquisition of clinical and digital data; The statistical analysis and interpretation of the data was performed by EH. The drafting of the article was performed by HJ. HF was a major contributor in writing the manuscript and RP and EH revised and edited the manuscript. All authors read and approve the manuscript.

Funding

No funding was obtained for this study.

Availability of data and materials

The data sets used and/or analyzed during the current study are included in this published article (and its Additional file 1).

Ethics approval and consent to participate

This study has been performed in accordance with the declaration of Helsinki and was approved by the ethical committee of the scientific research unit, College of Dentistry, Jazan University under the reference number: CODJU-1709L.

Consent for publication

Not applicable.

Competing interests

The authors declare that they have no competing interests.

Received: 28 March 2019 Accepted: 9 July 2019

Published online: 16 July 2019

References

- Joss-Vassalli I, Grebenstein C, Topouzelis N, Sculean A, Katsaros C. Orthodontic therapy and gingival recession: a systematic review. *Orthod Craniofac Res*. 2010;13(3):127–41.
- Kassab MM, Cohen RE. The etiology and prevalence of gingival recession. *J Am Dent Assoc*. 2003;134(2):220–5.
- Schroeder HE, Listgarten MA. The gingival tissues: the architecture of periodontal protection. *Periodontol*. 2000. 1997;13:91–120.
- Bosshardt DD, Lang NP. The junctional epithelium: from health to disease. *J Dent Res*. 2005;84(1):9–20.
- Mythri S, Arunkumar SM, Hegde S, Rajesh SK, Munaz M, Ashwin D. Etiology and occurrence of gingival recession - an epidemiological study. *J Indian Soc Periodontol*. 2015;19(6):671–5.
- Chrysanthakopoulos NA. Prevalence and associated factors of gingival recession in Greek adults. *J Investig Clin Dent*. 2013;4(3):178–85.
- Loe H, Anerud A, Boysen H. The natural history of periodontal disease in man: prevalence, severity, and extent of gingival recession. *J Periodontol*. 1992;63(6):489–95.
- Handelman CS, Eltink AP, BeGole E. Quantitative measures of gingival recession and the influence of gender, race, and attrition. *Prog Orthod*. 2018;19(1):5.
- Correia GD, Habib FA, Vogel CJ. Tooth-size discrepancy: a comparison between manual and digital methods. *Dental Press J Orthod*. 2014; 19(4):107–13.
- Sweeney WT, Taylor DF. Dimensional changes in dental stone and plaster. *J Dent Res*. 1950;29(6):749–55.
- Ting-Shu S, Jian S. Intraoral digital impression technique: a review. *J Prosthodont*. 2015;24(4):313–21.
- Mangano F, Gandolfi A, Luongo G, Logozzo S. Intraoral scanners in dentistry: a review of the current literature. *BMC Oral Health*. 2017;17(1):149.
- Landis JR, Koch GG. The measurement of observer agreement for categorical data. *Biometrics*. 1977;33(1):159–74.
- McCoy M, Campbell I, Stone P, Fedorchuk C, Wijayawardana S, Easley K. Intra-examiner and inter-examiner reproducibility of paraspinal thermography. *PLoS One*. 2011;6(2):e16535.
- Bland JM, Altman DG. Applying the right statistics: analyses of measurement studies. *Ultrasound Obstet Gynecol*. 2003;22(1):85–93.
- Schneider D, Ender A, Truninger T, Leutert C, Sahrman P, Roos M, Schmidlin P. Comparison between clinical and digital soft tissue measurements. *J Esthet Restor Dent*. 2014;26(3):191–9.
- Chalmers EV, McIntyre GT, Wang W, Gillgrass T, Martin CB, Mossey PA. Intraoral 3D scanning or dental impressions for the assessment of dental arch relationships in cleft care: which is superior? *Cleft Palate-Craniofac J*. 2016;53(5):568–77.
- Rancitelli D, Ciccio M, Lini F, Fumagalli D, Frigo AC, Maiorana C. Reproducibility of a digital method to evaluate soft tissue modifications: a study of inter and intra-operative measurement concordance. *Open Dent J*. 2017;11:171–80.
- Wiranto MG, Engelbrecht WP, Tutein Nolthenius HE, van der Meer WJ, Ren Y. Validity, reliability, and reproducibility of linear measurements on digital models obtained from intraoral and cone-beam computed tomography scans of alginate impressions. *Am J Orthod Dentofacial Orthop*. 2013;143(1):140–7.
- Logozzo S, Franceschini G, Kilpelä A, Caponi M, Governi L, Blois L. A comparative analysis of intraoral 3D digital scanners for restorative dentistry. *Internet J Med Technol*. 2011;5(1):1–12.

21. Strebel J, Ender A, Paque F, Krahenmann M, Attin T, Schmidlin PR. In vivo validation of a three-dimensional optical method to document volumetric soft tissue changes of the interdental papilla. *J Periodontol*. 2009;80(1):56–61.
22. Aydinyurt HS, Ertugrul AS. A novel volumetric analysis using CAD/CAM scanners in gingival recession treatment. *Med Sci Discov*. 2017;4(10):72–9.

Publisher's Note

Springer Nature remains neutral with regard to jurisdictional claims in published maps and institutional affiliations.

Ready to submit your research? Choose BMC and benefit from:

- fast, convenient online submission
- thorough peer review by experienced researchers in your field
- rapid publication on acceptance
- support for research data, including large and complex data types
- gold Open Access which fosters wider collaboration and increased citations
- maximum visibility for your research: over 100M website views per year

At BMC, research is always in progress.

Learn more biomedcentral.com/submissions



CASE REPORT

Open Access



Augmented reality for dental implantology: a pilot clinical report of two cases

Gerardo Pellegrino^{1*}, Carlo Mangano², Roberto Mangano³, Agnese Ferri¹, Valerio Taraschi⁴ and Claudio Marchetti⁵

Abstract

Background: Despite the limited number of articles dedicated to its use, augmented reality (AR) is an emerging technology that has shown to have increasing applications in multiple different medical sectors. These include, but are not limited to, the Maxillo-facial and Dentistry disciplines of medicine. In these medical specialties, the focus of AR technology is to achieve a more visible surgical field during an operation. Currently, this goal is brought about by an accurate display of either static or dynamic diagnostic images via the use of a visor or specific glasses. The objective of this study is to evaluate the feasibility of using a virtual display for dynamic navigation via AR. The secondary outcome is to evaluate if the use of this technology could affect the accuracy of dynamic navigation.

Case presentation: Two patients, both needing implant rehabilitation in the upper premolar area, were treated with flapless surgery. Prior to the procedure itself, the position of the implant was virtually planned and placed for each of the patients using their previous scans. This placement preparation contributed to a dynamic navigation system that was displayed on AR glasses. This, in turn, allowed for the use of a computer-aided/image-guided procedure to occur. Dedicated software for surface superimposition was then used to match the planned position of the implant and the real one obtained from the postoperative scan. Accuracies, using this procedure were evaluated by way of measuring the deviation between real and planned positions of the implants. For both surgeries it was possible to proceed using the AR technology as planned. The deviations for the first implant were 0.53 mm at the entry point and 0.50 mm at the apical point and for the second implant were 0.46 mm at the entry point and 0.48 mm at the apical point. The angular deviations were respectively 3.05° and 2.19°.

Conclusions: From the results of this pilot study, it seems that AR can be useful in dental implantology for displaying dynamic navigation systems. While this technology did not seem to noticeably affect the accuracy of the procedure, specific software applications should further optimize the results.

Keywords: Computer-assisted surgery, Image-guided surgery, Implantology, Navigation system, Real-time tracking, Implant placement accuracy

Background

Computer-assisted procedures are becoming more and more integrated into different fields of dentistry [1]. This is particularly evident in the increasing use of processes such as 3D printing and CAD-CAM methods in the manufacturing of dental implantology. This has not only allowed for a more accurate and diverse manufacturing capability but also dramatically expands on the production surgical templates often made in-house.

Currently, the examination of static guided surgery as a means of creating surgical templates to accurately position implants is ample. The conclusion drawn from this research is that should the implant be inserted with a margin of error of approximately 1 mm, the implant rehabilitation process will be mostly successful [2]. However, the working time for planning and producing the surgical template do not encourage or justify an ordinary use of this method [3]. Another method for computer-assisted surgery in dental implantology is image-guided surgery through dynamic navigation. Such surgical techniques are already largely used in major Neurosurgery, Maxillo-facial surgery, ORL, and Orthopedic surgeries and is quickly becoming popular in Implantology. Some

* Correspondence: gerardo.pellegrino2@unibo.it

¹Oral and Maxillofacial Surgery Unit, DIBINEM, University of Bologna, 125, Via San Vitale 59, 40125 Bologna, Italy

Full list of author information is available at the end of the article



© The Author(s). 2019 **Open Access** This article is distributed under the terms of the Creative Commons Attribution 4.0 International License (<http://creativecommons.org/licenses/by/4.0/>), which permits unrestricted use, distribution, and reproduction in any medium, provided you give appropriate credit to the original author(s) and the source, provide a link to the Creative Commons license, and indicate if changes were made. The Creative Commons Public Domain Dedication waiver (<http://creativecommons.org/publicdomain/zero/1.0/>) applies to the data made available in this article, unless otherwise stated.

papers published in past years report on the comparable accuracy between dynamic and static surgical navigation [4–6]. It was shown that dynamic navigation could overcome some of the disadvantages associated with static guided surgery. These included reducing costs and time needed for the impression and laboratory procedures of a static guided system. Another advantage of a dynamic guided system could be the ability to have a direct view of the surgical field as well as the possibility to use standard drills which is optimal in a case of mouth opening reduction [7]. In addition to this, dynamic navigation allows for changes in implant planning to be made at the time of surgery. This level of flexibility is not offered by statically derived surgical guides as they are fixed and cannot be altered once they are planned and manufactured. Also, tight single-tooth edentulous ridge areas can be fully guided using dynamic guidance as a dynamic guide is not restricted by drill tube size (i.e. in the anterior mandibular incisor sites). Furthermore, implant size is not limited with dynamically guided systems, as they are with static guides and CBCT, planning and surgery can be achieved in a single day [1, 8, 9].

However, a possibly problematic disadvantage of a dynamic guided system is the need to simultaneously pay attention to the patient as well as the output from the navigation system display. This unfavourable feature is exacerbated in systems where the tracking device is positioned on the same mobile carriage as the navigation system display. This could cause difficulties in following the virtual procedure while also keeping sight of the surgical site itself [10]. Systems that use a mobile screen fixed near the patient's head on the dental chair may address this issue as they limit the movement of the surgeon's head and, therefore, their loss of sight of the surgical site [11].

The use of AR through specific glasses and an integrated screen is a fairly new trend in the field of medicine. This technology can allow the surgeon to visualize, in real-time, patient parameters, relevant x-rays, 3D reconstruction or a navigation system screen [12, 13]. This last item could significantly increase the use of dynamic navigation a process that has already been readily adopted in other major surgical disciplines. The use of these devices is currently under validation and only few publications are present in literature to date and even fewer papers investigate this technology in dentistry [10, 14]. The aim of our pilot study is to evaluate the feasibility of adopting AR as a means of facilitating the use of dynamic navigation for dental implantology. The secondary objective was to evaluate if the accuracy obtained with this innovative display device was maintained in the range already described in literature regarding dynamic navigation.

Case presentation

Two patients were referred to the Oral and Maxillo-facial Unit of the Department of Biomedical and Neuromotor Sciences for implant supported prosthetic rehabilitation. Both patients were to be treated in the upper premolar area and were in good general health conditions and had no contra-indications to the implant surgery. The clinical procedures were carried out in accordance with national guidelines as well as with the Declaration of Helsinki.

Navigation system setting

After the filling of the appropriate consent documentation, both patients undertook a CBCT scan with the markers plate from the navigation system. These markers were positioned in situ as per protocol of using the navigation system ImplaNav (BresMedical, Sydney, Australia) which requires that the markers plate is fixed with a hard impression material (Ramitec, 3 M Espe, USA). After the scan, the markers plate was removed and replaced in the same position on the day of the surgery. The CBCT data was analyzed through the navigation system planning software and the position of two implants were virtually planned. At the time of the surgery the patient reference tool for the navigation system was fixed on the same support of the markers plate. Another reference tool was positioned and rigidly fixed on the implant drill handle. Then the calibration tool was connected to the handle and the drill axis was identified by the navigation system. The first lance drill was successively used to touch the fiducial markers on the markers plate to verify the patient position. After the calibration procedures, the navigation system was directly interfaced with the virtual reality glasses (Hololens, Microsoft, USA) through a wifi connection using a dedicated software created by Fiftithingenium (Milan, Italy) (Fig. 1).



Fig. 1 Overview of the Hololens glasses and navigation system reference tools during the surgery

Augmented reality glasses setting

Microsoft HoloLens is an augmented reality headset which can be used to expand the limits of interaction between the virtual and the physical world. HoloLens runs a custom Windows 10 version as its operating system. It also features Bluetooth and Wi-Fi connectivity and is powered by a Holographic Processing Unit HPU 1.0, 2GB RAM and 64GB of Solid State storage. It is also equipped with an Inertial Measurement Unit, four environment understanding cameras, mixed reality capture, four microphones, an ambient light sensor and two HD displays capable of automatic pupillary distance calibration.

The plethora of applications of the HoloLens in industry is mainly attributed to its ability to create, manipulate and display holograms or virtual objects in the field of the user. Combined with the ability to recognize objects, rooms and environments through the use of AI and markers, the capabilities of the HoloLens allows it to be useful in many industries including the Healthcare and Dental sector.

An application to use HoloLens in the dental field was developed in order to visualize 2D/3D data (CBCTs, face scans, oral scans) while at the dental chair without forcing the practitioner to look at a specific monitor/computer. By controlling the device via only voice commands or simple gestures, the surgeon is able to maintain visual of the physical surgical site and avoiding contamination.

A system capable of mirroring the desktop of a computer on the HoloLens was developed and coupled with the navigation system used for the surgery. Such system allows the doctor to avoid looking at the computer screen to receive guidance for the surgery. Instead, the doctor can visualize the system data, info, targets and positions by placing a virtual desktop near the patient's face without being forced to look away from the patient's mouth.

Clinical procedure

Using the HoloLens glasses, the surgeon can contemporarily visualize the surgical field (Fig. 2) and the output of the navigation system screen. The virtual position and the trajectory of the drill into the bone, the implant planned position and the bone anatomy around the implant site were checked in real-time during the whole surgical procedure (Fig. 3). The navigation system software input can also be managed with HoloLens through hand movements. Two implants were placed, one for each patient following the drill sequences provided by the implant company protocol. In one case a 3.8 × 9 mm (TTi, WinSix, Ancona, Italy) was positioned. In the other case a 4.1 × 11 mm (BL, Straumann, Switzerland). In both cases, a flapless surgery was carried out (Fig. 4). A postoperative radiograph was taken to evaluate the correct positioning of the implants (Fig. 5a, b). The



Fig. 2 The external view of the surgeon during the surgical procedure

healing abutments were fixed without any suture. In one case the implant position had been planned to be close to the maxillary sinus (Fig. 6) and postoperative CBCT was taken to verify if the goal had been reached (Fig. 7). After about 3 months, the contra-torque test was manually performed to verify the osseointegration status of the implants. Then through a scan of the abutment and the use of the intra-oral scanner, the implant position was digitally recorded concurrently with the bordering teeth. The virtual planned position of the implant and the adjacent teeth were exported from the planning module in the ImplaNav software. The two surfaces comprehending the teeth and the implants were compared via an N-point surface alignment of the teeth using Materialise 3-Matic (Materialise, Leuven, Belgium) (Fig. 8). The deviation between the planned implant position and the real one obtained by the scan were evaluated (Fig. 9). Both patients were rehabilitated with screw-retained crowns (Fig. 10).

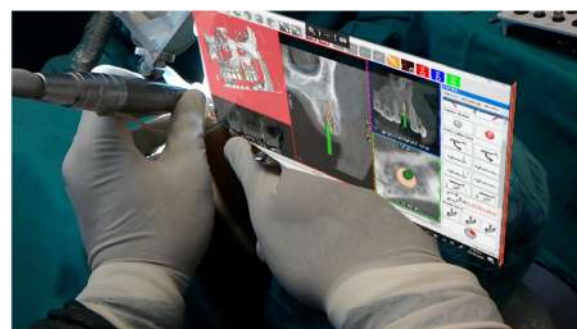


Fig. 3 The view of the surgeon during the surgery wearing HoloLens glasses

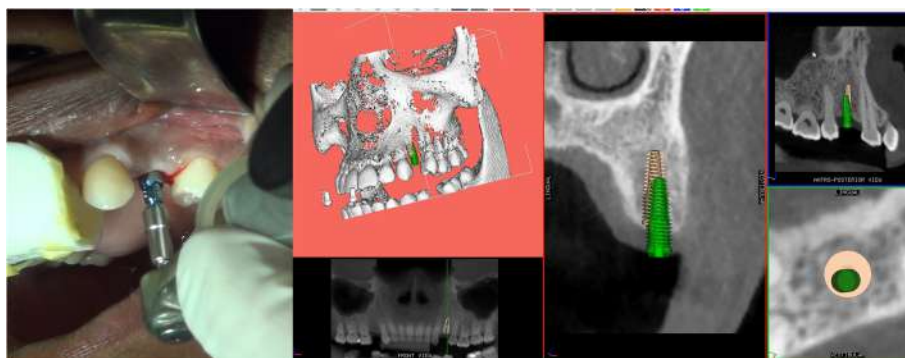


Fig. 4 The real and the virtual implant position on the navigation system screen

Results

In both cases it was possible to proceed with the navigation-aided implant placement with the Augmented Reality (AR) displaying in real-time a combination of surgical planning, real anatomy and the output from the navigation system (Fig. 3). The deviation between the planned and the real position of the implants resulted 0.53 mm at the entry point and 0.50 mm at the apical point for the first implant and 0.46 mm at the entry point and 0.48 mm at the apical point for the second one. The angular deviations were respectively 3.05° and 2.19° and the depth deviations were 0.26 mm and 0.37 mm.

Discussion

Dynamic navigation is one of the two computer-guided surgery techniques used in implantology. Many authors reported relatively good results in terms of implant placement accuracy using different navigation systems [1, 15–17]. Block et al. [16] reported on the implant placement accuracy obtained by 3 surgeons using dynamic navigation to treat 100 partially edentulous patients. They reported a mean error of 0.87 ± 0.42 mm at the entry point, 1.56 ± 0.69 mm at the apex and $3.62^\circ \pm 2.73^\circ$ for angle deviations using dynamic navigation. Non-dynamically guided entry point deviations, apex deviations and angle discrepancies had corresponding mean values of 1.15 ± 0.59 mm, 2.51 ± 0.86 mm and $7.69^\circ \pm 4.92^\circ$. Stefanelli et al. [17], in a retrospective study on 231 implants reported an error of 0.71 ± 0.40 mm at coronal point, 1 ± 0.49 mm at apex and a mean angular error of $2.26 \pm 1.62^\circ$. Although there are reported advantages using dynamic navigation, this method requires the surgeon to coordinate his view of the screen with the movements of his hands. The look out of the implant site with the rotation of the head for looking at the navigation system screen could represent a risk in case of accidental surgical instrument shifting or unexpected patient movement, especially in advanced implantology. The use of the augmented reality

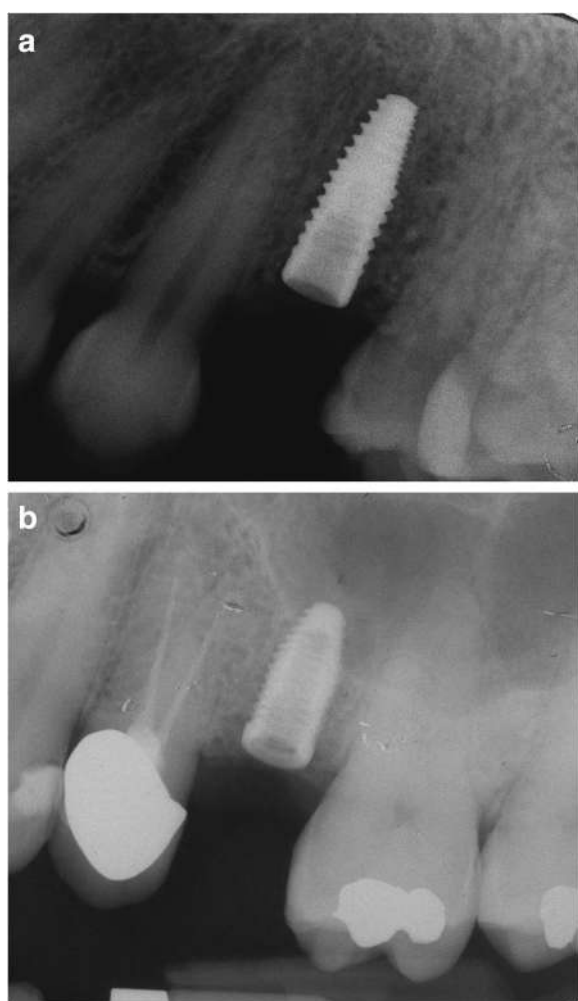


Fig. 5 a, b: Postoperative radiographs

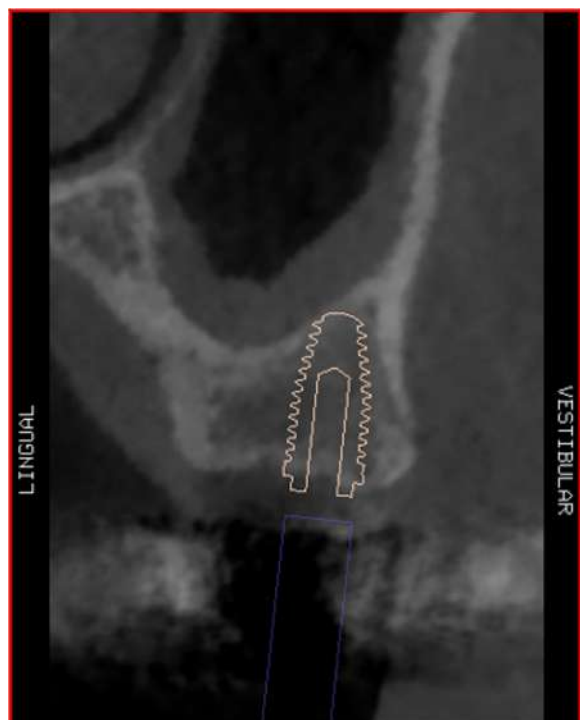


Fig. 6 Implant position planned to be close to the maxillary sinus

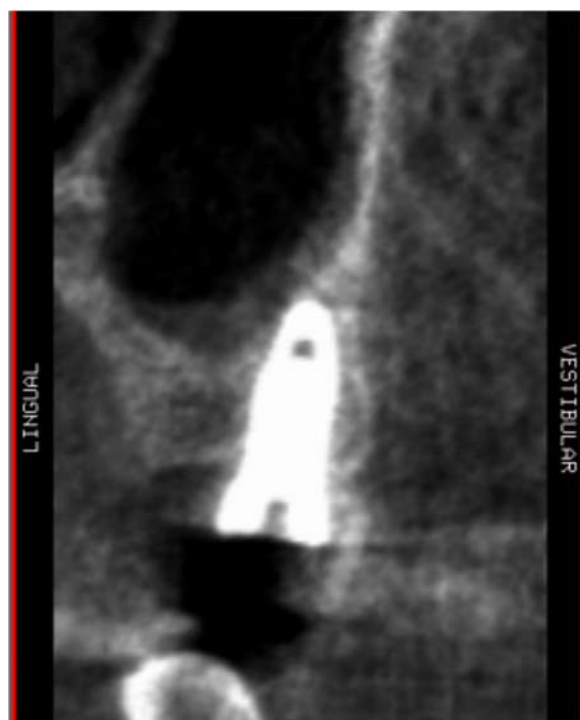


Fig. 7 Postoperative implant position on CBCT

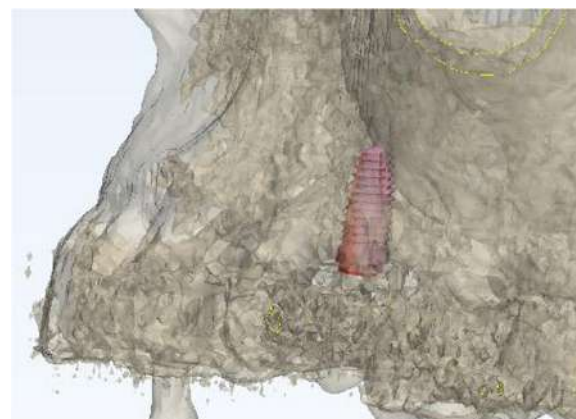


Fig. 8 The two surfaces comprehending the teeth and the implants were compared via an N-point surface alignment of the teeth

can overcome this drawback and also reduce operating time [10].

The categories of AR-guided surgery are grouped as follows: type I, involving the use of glasses or head-sets [12, 13]; type II, with digital data being projected on a half-silvered mirror [18]; type III, where the images are shown directly onto the patients; type IV, with the use of an external monitor [11]. In this study glasses have been used, allowing the contemporary projection of the patient's anatomy and the virtual instruments near the surgical field. However, when a 3D virtual layer is displayed and laid over the real environment, there is often a discrepancy between the real image and the virtual image due to an overlay or positional error.

Augmented reality is employed in neurosurgery, laparoscopic digestive, laparoscopic thoracic, vascular, urological and gynecological laparoscopic and cardiac surgery. As per its application in maxillofacial surgery, most of the publications refer to its use in orthognathic surgery [13, 19, 20],

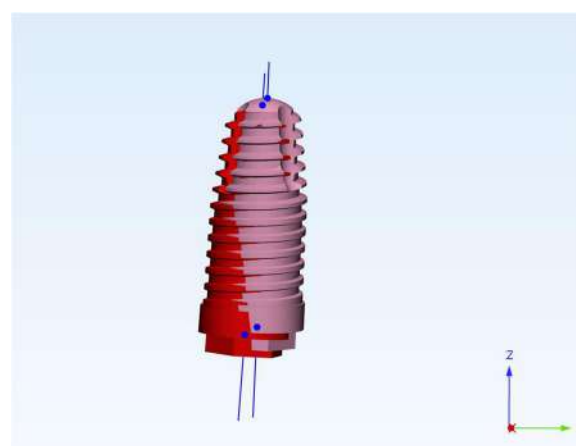


Fig. 9 Superimposed view showing the correspondence between the planned and the real implant position



Fig. 10 The prosthetic rehabilitation of one implant with a screw-retained crown

traumatic surgery and reconstructive surgery [21–23]. In dentistry, AR is applied in orthodontics for guided bracket placement [24]. In endodontics it is applied to detect root canals and for educational and training purposes [25–27].

In implantology, few studies regarding the use of dynamic navigation, especially in vitro, have been published. Ewers et al. [14] reported a significant medical benefit for the patients when navigation and AR are used for implant placement. In an in-vitro study, Jiang et al. [10] demonstrated a smaller error in incisive and canine regions implant placement using AR associated with dynamic navigation as opposed to the use of 2D navigation methods. The surgery time was significantly shorter by using a combination of the two technologies. In the present study, a dynamic navigation system associated with the augmented reality was deployed. This technique allowed the surgeon to simultaneously having a view of the surgical field as well as the navigation system monitor displaying implant planning and virtual burs. By wearing glasses where the virtual image is projected near the surgical field, the surgeon could see the implant site without interference and without the risk of overlay errors.

The main limit of this technology, currently, is emanated by the sometimes inconvenient virtual window positioning and orientation together with the working distance of the glasses which could force the surgeon to operate in an uncomfortable position. Nevertheless, the cases reported were simple and these limitations did not affect the results. Despite this, a comfortable work position might become mandatory in advanced clinical cases

[28, 29] in which this technology would prove to be beneficial. Other disadvantages could be considered the cost of the device, the time spent to set-up and the need to manage additional software for the AR. Possible setbacks could also occur from the device wireless connection and the battery charge although there were not reported in the present study. These problems could be solved by developing a dedicated software application for implantology and by upgrading the associated hardware.

As per the application in maxillofacial surgery of an AR technique displaying 3D images without the use of glasses, Suenaga et al. [30] reported a positional error of 0.77 ± 0.19 mm (range 0.45–1.34) and an angular error of 2° . Zhu et al. [12], however, reported a discrepancy of 0.96 ± 0.51 mm (range 0.55–2 mm). Most of the maximum overlay errors reported in literature are lower than 3 mm [11] with an exception for the research performed by Lin et al. [31], who reported a maximum error of 6.56 mm. The increase of accuracy, in addition to the lack of depth perception, is a problem the authors of these studies are working to address [32].

An in-vitro study by Lin et al. [31] showed good results in terms of implant placement accuracy using the drill-guides technique combined to AR. Katić et al. [33], by using an AR system in a pig cadaver experiment, reported a deviation of 1.1 mm and 2° between the planned implant and the positioned one. In the present case report, a less than 1 mm accuracy was achieved, comparable with the one reported in literature by only using the navigation system [1, 34]. This seems to indicate that AR does not affect the accuracy of the navigation procedure.

A touch-less interface for the navigation system software could also promote the use of this technology in the surgical theatre. By simplifying the procedures and reducing operative time, AR can prove to be an exceptional resource in dental implantology. This kind of technology could increase the use of dynamic navigation as it solves the problem of monitoring the screen and the patient simultaneously. The further development of AR could allow matching of the virtual with the real anatomy of the patient, a concept that is already under investigation for major surgery. At the moment, this is made difficult due to the need to follow the patient movement during the intervention usually carried out under local anesthesia.

Conclusions

AR resulted to be quite useful in displaying dynamic navigation despite some software and hardware limits. The presence of the two environments in the AR does not seem to affect the accuracy of the surgical procedure. Specific software applications for navigation systems can further contribute to optimizing the results. Additional in vitro and clinical trials are required to validate the use of this new promising technology for dental implantology.

Abbreviations

AI: Artificial Intelligence; AR: Augmented Reality; CBCT: Cone-beam computerized tomography; mm: Millimeters

Acknowledgements

We thank BresMedical (Sydney, Australia) for the collaboration, Fiftithingenium (Milan, Italy) for providing Hololens glasses and the Dental Radiology Division (Prof. Paolo Pisi), University of Bologna, Italy for assisting with the tomographic scanning facilities.

Authors' contributions

GP was the surgeon, conceived the ideas and wrote the manuscript; CM (author 2) conceived the ideas, RM managed the augmented reality glasses procedures, AF was the accuracy outcome assessor and wrote the manuscript, VT gave the support for the navigation system, CM (author 6) supervised the protocol. All Authors read and approved the manuscript.

Funding

No funding was obtained for this study.

Availability of data and materials

All data generated or analyzed during this study are included in this published article.

Ethics approval and consent to participate

This pilot case report was performed in accordance with the Declaration of Helsinki.

The present study was carried out following standard clinical procedures and the Authors confirm that this complies with national guidelines.

(reference: http://www.salute.gov.it/imgs/C_17_pubblicazioni_2128_allegato.pdf) Every patient gave his consent to the treatment.

Consent for publication

The identifying images and other personal or clinical details of participants are presented without compromise anonymity. The patients signed the consent form for publication.

Competing interests

The authors declare that they have no competing interests. The Author RM and VT, which have a relationship with the Companies providing the devices, gave only technical support in the device use.

Author details

¹Oral and Maxillofacial Surgery Unit, DIBINEM, University of Bologna, 125, Via San Vitale 59, 40125 Bologna, Italy. ²Digital Dentistry Section, University San Raffaele, Milan, Italy. ³Fiftithingenium, Milan, Italy. ⁴University of Technology - Sydney, School of Life Sciences, Sydney, Australia. ⁵Chief of Oral and Maxillofacial Surgery Unit, DIBINEM, University of Bologna, Bologna, Italy.

Received: 18 April 2019 Accepted: 11 July 2019

Published online: 19 July 2019

References

- Block MS, Emery RW. Static or dynamic navigation for implant placement—choosing the method of guidance. *J Oral Maxillofac Surg.* 2016;74:269–77. <https://doi.org/10.1016/j.joms.2015.09.022>.
- Bover-Ramos F, Viña-Almunia J, Cervera-Ballester J, Peñarocha-Diogo M, García-Mira B. Accuracy of implant placement with computer-guided surgery: a systematic review and meta-analysis comparing cadaver, clinical, and in vitro studies. *Int J Oral Maxillofac Implants.* 2018;33(1):101–15. <https://doi.org/10.11607/jomi.5556>.
- D'haese J, Van De Velde T, Komiyama A, Hultin M, De Bruyn H. Accuracy and complications using computer designed stereolithographic surgical guides for oral rehabilitation by means of dental implants: a review of the literature. *Clin Implant Dent Relat Res.* 2012;14(3):321–35. <https://doi.org/10.1111/j.1708-8208.2010.00275.x>.
- Ruppin J, Popovic A, Strauss M, Spüntrup E, Steiner A, Stoll C. Evaluation of the accuracy of three different computer-aided surgery systems in dental implantology: optical tracking vs. stereolithographic splint systems. *Clin Oral Implants Res.* 2008;19(7):709–16. <https://doi.org/10.1111/j.1600-0501.2007.01430.x>.
- Somogyi-Ganss E, Holmes HI, Jokstad A. Accuracy of a novel prototype dynamic computer-assisted surgery system. *Clin Oral Implants Res.* 2015; 26(8):882–90. <https://doi.org/10.1111/clr.12414>.
- Kang SH, Lee JW, Lim SH, Kim YH, Kim MK. Verification of the usability of a navigation method in dental implant surgery: in vitro comparison with the stereolithographic surgical guide template method. *J Craniomaxillofac Surg.* 2014;42(7):1530–5. <https://doi.org/10.1016/j.jcms.2014>.
- Cassetta M, Stefanelli LV, Giansanti M, Di Mambro A, Calasso S. Depth deviation and occurrence of early surgical complications or unexpected events using a single stereolithographic surgi-guide. *Int J Oral Maxillofac Surg.* 2011;40(12):1377–87. <https://doi.org/10.1016/j.ijom.2011.09.009>.
- D'haese J, Ackhurst J, Wismeijer D, De Bruyn H, Tahmaseb A. Current state of the art of computer-guided implant surgery. *Periodontol.* 2000. 2017; 73(1):121–33. <https://doi.org/10.1111/prd.12175>.
- Mandelaris GA, Stefanelli LV, DeGroot BS. Dynamic navigation for surgical implant placement: overview of technology, key concepts, and a case ReportDynamic navigation for surgical implant placement: overview of technology, key concepts, and a case report. *Compend Contin Educ Dent.* 2018;39(9):614–21.
- Jiang W, Ma L, Zhang B, Fan Y, Qu X, Zhang X, Liao H. Evaluation of the 3D Augmented Reality-Guided Intraoperative Positioning of Dental Implants in Edentulous Mandibular Models. *Int J Oral Maxillofac Implants.* 2018;33(6): 1219–28. <https://doi.org/10.11607/jomi.6638>.
- Bosc R, Fitoussi A, Hersant B, Dao TH, Meningaud JP. Intraoperative augmented reality with heads-up displays in maxillofacial surgery: a systematic review of the literature and a classification of relevant technologies. *Int J Oral Maxillofac Surg.* 2019;48(1):132–9. <https://doi.org/10.1016/j.ijom.2018.09.010>.
- Zhu M, Liu F, Chai G, Pan JJ, Jiang T, Lin L, Xin Y, Zhang Y, Li Q. A novel augmented reality system for displaying inferior alveolar nerve bundles in maxillofacial surgery. *Sci Rep.* 2017;15(7):42365. <https://doi.org/10.1038/srep42365>.
- Badiali G, Ferrari V, Cutolo F, Freschi C, Caramella D, Bianchi A, Marchetti C. Augmented reality as an aid in maxillofacial surgery: validation of a wearable system allowing maxillary repositioning. *J Craniomaxillofac Surg.* 2014;42(8):1970–6. <https://doi.org/10.1016/j.jcms.2014.09.001>.
- Ewers R, Schicho K, Undt G, Wanschitz F, Truppe M, Seemann R, Wagner A. Basic research and 12 years of clinical experience in computer-assisted navigation technology: a review. *Int J Oral Maxillofac Surg.* 2005;34(1):1–8. <https://doi.org/10.1016/j.ijom.2004.03.018>.
- Wittwer G, Adeyemo WL, Schicho K, Birkfellner W, Enislidis G. Prospective randomized clinical comparison of 2 dental implant navigation systems. *Int J Oral Maxillofac Implants.* 2007;22(5):785–90.
- Block MS, Emery RW, Lank K, Ryan J. Implant placement accuracy using dynamic navigation. *Int J Oral Maxillofac Implants.* 2017;32(1):92–9. <https://doi.org/10.11607/jomi.5004>.
- Stefanelli LV, DeGroot BS, Lipton DI, Mandelaris GA. Accuracy of a dynamic dental implant navigation system in a private practice. *Int J Oral Maxillofac Implants.* 2019;34(1):205–13. <https://doi.org/10.11607/jomi.6966>.
- Wang J, Suenaga H, Hoshi K, Yang L, Kobayashi E, Sakuma I, Liao H. Augmented reality navigation with automatic marker-free image registration using 3-D image overlay for dental surgery. *IEEE Trans Biomed Eng.* 2014;61(4):1295–304. <https://doi.org/10.1109/TBME.2014.2301191>.
- Pulijala Y, Ma M, Pears M, Peebles D, Ayoub A. Effectiveness of Immersive Virtual Reality in Surgical Training-A Randomized Control Trial. *J Oral Maxillofac Surg.* 2018;76(5):1065–72. <https://doi.org/10.1016/j.joms.2017.10.002>.
- Mischkowski RA, Zinser MJ, Kübler AC, Krug B, Seifert U, Zöller JE. Application of an augmented reality tool for maxillary positioning in orthognathic surgery - a feasibility study. *J Craniomaxillofac Surg.* 2006;34(8): 478–83. <https://doi.org/10.1016/j.jcms.2006.07.862>.
- Nijmeh AD, Goodger NM, Hawkes D, Edwards PJ, McGurk M. Image-guided navigation in oral and maxillofacial surgery. *Br J Oral Maxillofac Surg.* 2005;43(4):294–302. <https://doi.org/10.1016/j.bjoms.2004.11.018>.
- Marmulla R, Hoppe H, Mühling J, Eggers G. An augmented reality system for image-guided surgery. *Int J Oral Maxillofac Surg.* 2005;34(6):594–6. <https://doi.org/10.1016/j.ijom.2005.05.004>.
- Qu M, Hou Y, Xu Y, Shen C, Zhu M, Xie L, Wang H, Zhang Y, Chai G. Precise positioning of an intraoral distractor using augmented reality in patients with hemifacial microsomia. *J Craniomaxillofac Surg.* 2015;43(1):106–12. <https://doi.org/10.1016/j.jcms.2014.10.019>.
- Aichert A, Wein W, Ladikos A, Reichl T, Navab N. Image-based tracking of the teeth for orthodontic augmented reality. *Med Image Comput Assist Interv.* 2012;15(Pt 2):601–8.

25. Llana C, Folguera S, Forner L, Rodríguez-Lozano FJ. Implementation of augmented reality in operative dentistry learning. *Eur J Dent Educ*. 2018; 22(1):e122–30. <https://doi.org/10.1111/eje.12269>.
26. Huang TK, Yang CH, Hsieh YH, Wang JC, Hung CC. Augmented reality (AR) and virtual reality (VR) applied in dentistry. *Kaohsiung J Med Sci*. 2018;34(4): 243–8. <https://doi.org/10.1016/j.kjms.2018.01.009>.
27. Yu H, Shen SG, Wang X, Zhang L, Zhang S. The indication and application of computer-assisted navigation in oral and maxillofacial surgery-Shanghai's experience based on 104 cases. *J Craniomaxillofac Surg*. 2013;41(8):770–4. <https://doi.org/10.1016/j.jcms.2013.01.016>.
28. Pellegrino G, Tarsitano A, Taraschi V, Vercellotti T, Marchetti C. Simplifying Zygomatic Implant Site Preparation Using Ultrasonic Navigation: A Technical Note. *Int J Oral Maxillofac Implants*. 2018;33(3): e67–71. <https://doi.org/10.11607/jomi.6270>.
29. Wang F, Bornstein MM, Hung K, Fan S, Chen X, Huang W, Wu Y. Application of Real-Time Surgical Navigation for Zygomatic Implant Insertion in Patients With Severely Atrophic Maxilla. *J Oral Maxillofac Surg*. 2018;76(1):80–7. <https://doi.org/10.1016/j.joms.2017.08.021>.
30. Suenaga H, Hoang Tran H, Liao H, Masamune K, Dohi T, Hoshi K, Mori Y, Takato T. Real-time in situ three-dimensional integral videography and surgical navigation using augmented reality: a pilot study. *Int J Oral Sci*. 2013;5(2):98–102. <https://doi.org/10.1038/ijos.2013.26>.
31. Lin YK, Yau HT, Wang IC, Zheng C, Chung KH. A novel dental implant guided surgery based on integration of surgical template and augmented reality. *Clin Implant Dent Relat Res*. 2015;17(3):543–53. <https://doi.org/10.1111/cid.12119>.
32. Murugesan YP, Alsadoon A, Manoranjan P, Prasad PWC. A novel rotational matrix and translation vector algorithm: geometric accuracy for augmented reality in oral and maxillofacial surgeries. *Int J Med Robot*. 2018;14(3):e1889. <https://doi.org/10.1002/rcs.1889>.
33. Katić D, Spengler P, Bodenstedt S, Castrillon-Oberndorfer G, Seeberger R, Hoffmann J, Dillmann R, Speidel S. A system for context-aware intraoperative augmented reality in dental implant surgery. *Int J Comput Assist Radiol Surg*. 2015;10(1):101–8. <https://doi.org/10.1007/s11548-014-1005-0>.
34. Pellegrino G, Taraschi V, Vercellotti T, Ben-Nissan B, Marchetti C. Three-Dimensional Implant Positioning with a Piezosurgery Implant Site Preparation Technique and an Intraoral Surgical Navigation System: Case Report. *Int J Oral Maxillofac Implants*. 2017;32(3):e163–5. <https://doi.org/10.11607/jomi.5800>.

Publisher's Note

Springer Nature remains neutral with regard to jurisdictional claims in published maps and institutional affiliations.

Ready to submit your research? Choose BMC and benefit from:

- fast, convenient online submission
- thorough peer review by experienced researchers in your field
- rapid publication on acceptance
- support for research data, including large and complex data types
- gold Open Access which fosters wider collaboration and increased citations
- maximum visibility for your research: over 100M website views per year

At BMC, research is always in progress.

Learn more biomedcentral.com/submissions




RESEARCH ARTICLE

Open Access



Impact of molar teeth distalization with clear aligners on occlusal vertical dimension: a retrospective study

Silvia Caruso^{1†}, Alessandro Nota^{1,2*†}, Shideh Ehsani², Elena Maddalone², Kenji Ojima³ and Simona Tecco² 

Abstract

Background: A common strategy in the non-extraction treatment of Class II molar relationship is maxillary molar distalization, which could increase lower face height and cause clockwise mandibular rotation. The aim of this retrospective study was to analyse the effects on vertical dentoskeletal dimension of young adults treated with sequential distalization with orthodontic aligners.

Methods: Lateral cephalometric radiographs of 10 subjects (8 females 2 males; mean age 22.7 ± 5.3 years) treated with upper molars sequential distalization with orthodontic aligners (Invisalign, Align Technology, San José, California, USA) were analyzed.

Results: No statistically significant difference was observed for the primary outcome SN-GoGn between T0 and T1 and it was recorded a mean variation of 0.1 ± 2.0 degrees. Statistically significant differences were found in the linear position of the upper molars (6-PP, 7-PP) the molar class relationship parameter (MR) and the upper incisive inclination (1° PP) with at least $p < 0.01$.

Conclusions: Upper molar distalization with orthodontic aligners guarantee an excellent control of the vertical dimension representing an ideal solution for the treatment of hyperdivergent or openbite subjects. It also allows an excellent control of the incisal torque without loss of anchorage during the orthodontic procedure.

Keywords: Malocclusion, angle class II, Vertical dimension, Tooth movement techniques, Orthodontic appliances, removable

Background

One of the most common strategies applied in the non-extraction treatment of Class II molar relationship is maxillary molar distalization. The major indication are patients with maxillary dentoalveolar protrusion or minor skeletal discrepancies [1, 2].

Since 1950's headgear has been the most frequently used appliance for maxillary molar distalization. Unfortunately this appliance requires considerable patient compliance [3, 4] so several alternative intraoral methods had been proposed to reduce or cut out patient's co-operation [5, 6]. Despite the effectiveness of many of

these appliances clinicians must consider many side-effects: increase in lower face height, clockwise mandibular rotation, extrusion of first premolars, undesirable tipping of the maxillary molars and loss of anterior anchorage during distalization [1, 7–10]. Most of these side effects involve an increase of the vertical dimension of the treated subjects, keeping this treatment procedure generally contraindicated in hyperdivergents [2, 11].

In the last decades, the orthodontic treatment with removable clear aligners has become an increasingly common choice because of the growing number of adult patients that ask for aesthetic and comfortable alternatives to conventional fixed appliances [12, 13]. Clear aligners are based on computer aided design procedures. The orthodontic treatment with the Invisalign (Align Technology, San José, California, USA) system

* Correspondence: dr.alessandro.nota@gmail.com

¹Department of Life, Health and Environmental Sciences, University of L'Aquila, Piazzale Salvatore Tommasi 1, 67100 L'Aquila, Coppito, Italy

²Dental School, Vita-Salute University and IRCCS San Raffaele Hospital, Via Olgettina, 58, 20132 Milan, Italy

Full list of author information is available at the end of the article



© The Author(s). 2019 **Open Access** This article is distributed under the terms of the Creative Commons Attribution 4.0 International License (<http://creativecommons.org/licenses/by/4.0/>), which permits unrestricted use, distribution, and reproduction in any medium, provided you give appropriate credit to the original author(s) and the source, provide a link to the Creative Commons license, and indicate if changes were made. The Creative Commons Public Domain Dedication waiver (<http://creativecommons.org/publicdomain/zero/1.0/>) applies to the data made available in this article, unless otherwise stated.

is a digitized process that starts from the acquisition of a 3D model of the dental arches allowing the planning of teeth movements with a proper software. The aligner allows the control of 3D movements by holding teeth on all the surfaces (vestibular, palatal-lingual and occlusal) and applying proper forces thanks to attachments of different size and shape and other specific features.

Aligners can also provide a class II correction by a sequential maxillary molar distalization [14, 15] with a high predictability (88%) of the distalization movement of upper molars if supported by the presence of attachments on the tooth surface assessed by Simon et al. [16, 17]. Ravera et al. [15] showed that clear aligners are suitable for distalizing maxillary up to 2–3 mm without significant mesiodistal tipping movement, and it seems that this result could be improved if combined with photobiomodulation or other acceleration tooth movement systems [18–20].

The aim of this retrospective study was to analyze the effects of class II treatment by sequential distalization with orthodontic aligners on vertical dentoskeletal dimension.

Methods

Subjects and procedure

This retrospective study analysed lateral cephalometric radiographs of a sample of 10 subjects (8 females 2 males; mean age 22.7 ± 5.3 years) treated with sequential distalization with orthodontic aligners (Invisalign, Align Technology, San José, California, USA). Figure 1 shows the lateral cephalometric radiographs of a patient included in this study. The retrospective study was ethically approved by the Institution, the procedures were in accordance with the declaration of Helsinki and all the subjects signed a consent form. Bilateral molar class II or end-to-end molar relationship, absence of mesial rotation of the upper first molars, mild or light crowding

in the upper arch, absence of periodontal disease, absence of previous prosthodontic treatments of the upper molars, good compliance during the treatment, good quality and definition of the radiographs were the study inclusion criteria. All the subjects that satisfied the inclusion criteria were included in the study and were successfully treated even if the treatment success wasn't an inclusion criterion. The mean treatment time was of 1.9 ± 0.5 years. Four subjects were excluded from the initial study sample of 14 subjects because they didn't match with the inclusion criteria.

Lateral cephalograms in habitual occlusion were considered for the study. Cephalometric head films were collected at the beginning (T0) at the end of treatment (T1) with orthodontic aligners.

The treatment of sequential upper arch distalization (Fig. 2) was performed by the same expert operator (K.O.) as proposed by Align Technology and described by Ravera et al. [15] using II class elastics and rectangular vertical attachments on the upper molars and premolars.

Radiographs were manually traced by the same expert operator (S.E.) blinded about the study. A total of fourteen cephalometric parameters (5 linear, 9 angular) were measured and recorded for each cephalogram, afterwards the relationship between the posterior facial height and the anterior facial height were calculated.

SN-GoGn ($^{\circ}$) was considered as primary outcome. [21] It shows the impact of the orthodontic procedure on the sagittal vertical dimension of the samples.

Intra-observer method error

In order to verify the method error, ten lateral cephalometric radiographs underwent to the same cephalometric analysis two times by the same operator, at a distance of about 2 weeks. Applying the Dahlberg's formula, the method error resulted lower than the standard deviation observed in the whole sample for the variable. For the primary outcome the measured method error was 0.98° .

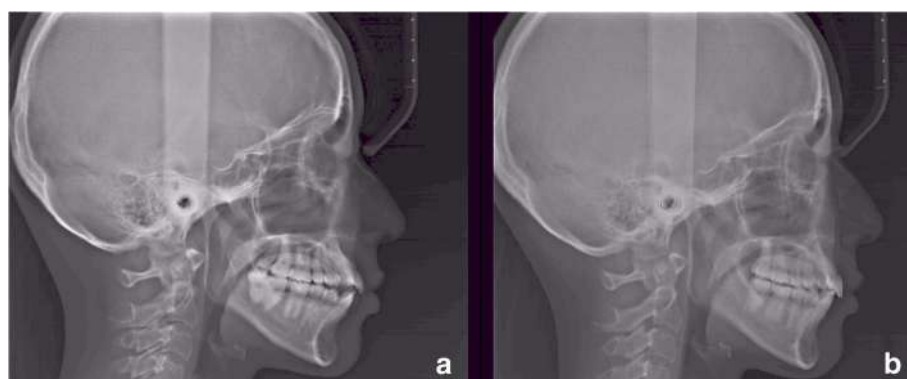


Fig. 1 a-b: Lateral cephalometric radiographs of a patient, before the orthodontic treatment with sequential distalization (a) and after treatment (b)

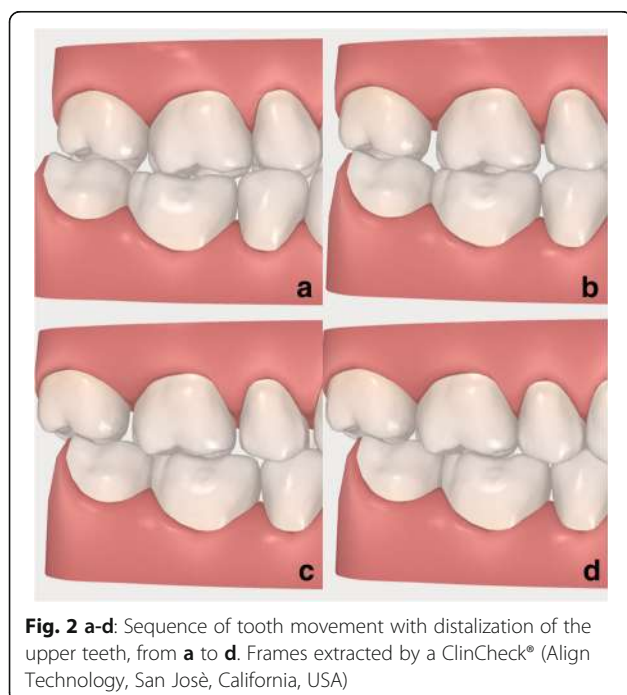


Fig. 2 a-d: Sequence of tooth movement with distalization of the upper teeth, from **a** to **d**. Frames extracted by a ClinCheck® (Align Technology, San José, California, USA)

The intraclass correlation coefficient (ICC) was also calculated, for the primary outcome, obtaining a value of 0.99.

Statistical analysis

Descriptive statistics were calculated for each variable of recorded data.

The normality assumption of the data was confirmed by the Shapiro-Wilk test. Thus, the differences between before (T0) and after treatment (T1) were compared with the paired-t test. The level of significance was set at $P < 0.05$.

Results

Descriptive data, means and standard deviation (SD), of the recorded parameters are reported in Table 1. Figure 3 shows a lateral intra-oral view of one of the treated patients, before and after treatment.

No statistically significant difference was observed for the primary outcome SN-GoGn between T0 and T1 and it was recorded a mean variation of 0.1 ± 2.0 degrees. Similarly no statistically significant difference was observed for the linear measurements of vertical dimension (S-Go;N-Me).

Statistically significant differences were found for the linear position of the upper molars (6-PP, 7-PP) the MR parameter and the upper incisor inclination (1[^]PP) with at least $p < 0.01$.

No significant variations were observed for the other cephalometric parameters analysed.

Table 1 Descriptive data and statistical analysis of the differences between T0 and T1

	T0		T1		Student T Test Sig.
	MEAN	SD	MEAN	SD	
SNA (°)	82.4	4.7	83.0	4.9	0.559
SNB (°)	79.0	4.9	78.7	4.9	0.403
ANB (°)	3.4	3.3	4.3	3.2	0.195
SN [^] GoGn (°)	35.6	6.9	35.4	8.4	0.445
SN [^] FOP (°)	18.9	4.1	20.6	6.3	0.122
SN [^] PP (°)	7.3	6.1	6.3	5.7	0.309
6-PP (mm)	25.0	3.0	23.0	3.0	0.000****
6 [^] PP (°)	81.2	3.5	79.9	4.4	0.220
7-PP (mm)	16.0	3.0	13.0	3.0	0.000****
7 [^] PP (°)	81.7	5.6	82.3	4.3	0.352
1 [^] PP (°)	118.3	6.6	104.8	10.9	0.006***
MR (mm)	3.1	1.4	1.2	0.6	0.000****
S-Go (mm)	68.0	6.1	68.0	6.8	0.476
N-Me (mm)	109.0	6.0	108.9	6.2	0.438
S-Go/N-Me	0.62	0.05	0.63	0.06	0.421

* = $P < 0.05$; ** = $P < 0.01$; *** = $P < 0.001$; **** = $P < 0.0001$

Discussion

In literature it was observed that different orthodontic appliances caused undesired effects on the upper molars distalization procedure and on the sagittal vertical pattern as clockwise rotation of the mandibular plane and increase in the anterior facial height [22–26]. This finding implied a contraindication of the upper molar distalization in hyperdivergent subjects.

The present retrospective study analysed the sagittal vertical dimension changes associated with successful orthodontic treatment of subjects with second molar class by sequential upper molar distalization performed with clear aligners. A previous study showed a high predictability of clear aligners in performing the upper molars distalization movement with absence of distal tipping [15].

Results indicated that there were no changes in the subject divergence by observing variations of the SN-GoGn angle lower than 1°. The present findings suggest that clear aligners allow a good control of mandibular divergence during molar distalization. These results are in accordance with what reported by Ravera et al. [15] as a secondary outcome of their study.

Similarly, it was observed a significant distal movement of the upper molars (and the related correction in molar relationship) with absence of distal tipping, confirming the capability of performing a distal body movement of the upper molars by clear aligners with a control of the vertical dimensions the opposite of what reported by previous authors [22–26] with other orthodontic appliances.



Fig. 3 a-b: Lateral intra-oral view of a patient, before the orthodontic treatment (a) and after treatment (b)

No significant rotations of the maxillary and functional occlusal plane were observed. No significant changes were observed in the sagittal position of mandible and maxilla, in contrast to what reported by Ravera et al. [15] that showed a significant reduction of the ANB angle.

Previous studies showed a control of the vertical dimension during distalization with pendulum appliance properly activated by expert operators [2, 22, 24]. Recent review indicates a molar distal tipping that range between 8.4° and 14.5°, much higher than what reported by the present study (mean tipping of 1.3°), furthermore a trend to an anterior anchorage loss was observed with pendulum appliance if bone anchorage was not applied [25, 26].

No anchorage loss was observed on upper incisors that had a significant mean reduction of their inclination of 13.2° showing a torque control much higher than what reported by Ravera et al. [15].

Looking at the results of this study, the upper molar distalization performed with clear aligners seems to overcome various side effects related with this orthodontic procedure typically observed with other appliances in previous studies [1, 7–10] and seems to allow a predictable distal body movement of upper molars [15–17] with a control of the vertical dimension and of the incisal torque. This could be related with the aligner design, that allows the control of 3D movements by holding teeth on all the surfaces (vestibular, palatal-lingual and occlusal) and applying proper forces thanks to properly digitally planned attachments.

Consequently, orthodontic aligners could represent an effective alternative for upper molar distalization especially in hyperdivergent or openbite subjects at least for distal molar movements up to 2–3 mm. Further studies should be conducted on distal molar movements higher than 2–3 mm and on hyperdivergent subjects.

At the authors' knowledge this is the first study that analysed as a primary outcome the effects of the upper molar distalization orthodontic technique with clear

aligners on the vertical dimension of subjects with molar class II malocclusion.

Limitations of the study

Limitations of this study are the low sample size and the limited mean amount of distal movement that should be increased in future studies to confirm the control of the vertical dimension. Furthermore, the retrospective design should be replaced by a longitudinal design in order to reduce the risk of bias.

Conclusions

Upper molar distalization with orthodontic aligners properly digitally planned by the orthodontist seems to allow a good control of the vertical dimension. A satisfactory control of the incisal torque without loss of anchorage during the orthodontic procedure was also observed.

Further studies should be performed to confirm the results of the present study and analyse if the upper distalization with orthodontic aligners could represent an effective alternative for the treatment of class II subjects even with hyperdivergent or openbite skeletal patterns.

Abbreviation

MR: Molar Relationship

Acknowledgements

The authors acknowledge dr. Atanaz Darvizeh for her contribution to English language revision.

Authors' contributions

SC concept, data collection, manuscript revision, accountability for research integrity and accuracy, approval of the article. AN concept, design, writing of the article, methodology, data analysis, data interpretation, critical revisions, approval of the article. SE data collection, data analysis, manuscript writing, approval of the article. EM manuscript writing, data collection, critical revisions, approval of the article. KO data collection, clinical procedures, critical revisions, approval of the article. ST concept, design, writing of the article, methodology, data analysis, data interpretation, critical revisions, approval of the article. All authors read and approved the final manuscript.

Funding

This research did not receive any specific grant from funding agencies in the public, commercial, or not-for-profit sectors.

Availability of data and materials

The data that support the findings of this study are available from the archive of the University of L'Aquila, but restrictions apply to the availability of these data, which were used under permission and consent for the current study, and so are not publicly available. Data are however available from the authors upon reasonable request and with permission of the patients and the Ethic Committee of the University of L'Aquila.

Ethics approval and consent to participate

The study was ethically approved by the Ethic Committee of the University of L'Aquila, Italy (Document DR206/2013). The treated subjects gave the consent to the analysis of their documentation for research purposes. The retrospective study was ethically approved by the Institution, the procedures were in accordance with the declaration of Helsinki and all the subjects signed a consent form.

Consent for publication

Not applicable.

Competing interests

The authors declare that they have no competing interests.

Author details

¹Department of Life, Health and Environmental Sciences, University of L'Aquila, Piazzale Salvatore Tommasi 1, 67100 L'Aquila, Coppito, Italy. ²Dental School, Vita-Salute University and IRCCS San Raffaele Hospital, Via Olgettina, 58, 20132 Milan, Italy. ³Private Practice of Orthodontics, Tokyo, Japan.

Received: 6 April 2019 Accepted: 7 August 2019

Published online: 13 August 2019

References

- Bolla E, Muratore F, Carano A, Bowman SJ. Evaluation of maxillary molar distalization with the distal jet: a comparison with other contemporary methods. *Angle Orthod*. 2002;72:481–94.
- Lione R, Franchi L, Laganà G, Cozza P. Effects of cervical headgear and pendulum appliance on vertical dimension in growing subjects: a retrospective controlled clinical trial. *Eur J Orthod*. 2015;37:338–44.
- Baldini A, Nota A, Santariello C, Assi V, Ballanti F, Cozza P. Influence of activation protocol on perceived pain during rapid maxillary expansion. *Angle Orthod*. 2015;85:1015–20.
- Clemmer EJ, Hayes EW. Patient cooperation in wearing orthodontic headgear. *Am J Orthod*. 1979;75:517–24.
- Fuziy A, Rodrigues de Almeida R, Janson G, Angelieri F, Pinzan A. Sagittal, vertical, and transverse changes consequent to maxillary molar distalization with the pendulum appliance. *Am J Orthod Dentofac Orthop*. 2006;130:502–10.
- Fontana M, Cozzani M, Caprioglio A. Non-compliance maxillary molar distalizing appliances: an overview of the last decade. *Prog Orthod*. 2012;13:173–84.
- Byloff FK, Darendeliler MA, Clar E, Darendeliler A. Distal molar movement using the pendulum appliance. Part 2: the effects of maxillary molar root uprighting bends. *Angle Orthod*. 1997;67:261–70.
- Bussick TJ, McNamara JA. Dentoalveolar and skeletal changes associated with the pendulum appliance. *Am J Orthod Dentofac Orthop*. 2000;117:333–43.
- Lima Filho RMA, Lima AL, de Oliveira Ruellas AC. Longitudinal study of anteroposterior and vertical maxillary changes in skeletal class II patients treated with Kloehe cervical headgear. *Angle Orthod*. 2003;73:187–93.
- Mariani L, Maino G, Caprioglio A. Skeletal versus conventional intraoral anchorage for the treatment of class II malocclusion: dentoalveolar and skeletal effects. *Prog Orthod*. 2014;15:43.
- Saccucci M, Polimeni A, Festa F, Tecco S. Do skeletal cephalometric characteristics correlate with condylar volume, surface and shape? A 3D analysis. *Head Face Med*. 2012;8:15.
- Giancotti A, Mampieri G, Greco M. Correction of deep bite in adults using the Invisalign system. *J Clin Orthod*. 2008;42:719–26 quiz 728.
- Miller DB. Invisalign in TMD treatment. *Int J Orthod Milwaukee*. 2009;20:15–9.
- Fischer K. Invisalign treatment of dental class II malocclusions without auxiliaries. *J Clin Orthod*. 2010;44:665–72 quiz 687.
- Ravera S, Castroflorio T, Garino F, Daher S, Cugliari G, Deregibus A. Maxillary molar distalization with aligners in adult patients: a multicenter retrospective study. *Prog Orthod*. 2016;17:12.
- Simon M, Keilig L, Schwarze J, Jung BA, Bourauel C. Forces and moments generated by removable thermoplastic aligners: incisor torque, premolar derotation, and molar distalization. *Am J Orthod Dentofac Orthop*. 2014;145:728–36.
- Rossini G, Parrini S, Castroflorio T, Deregibus A, Debernardi CL. Efficacy of clear aligners in controlling orthodontic tooth movement: a systematic review. *Angle Orthod*. 2015;85:881–9.
- Ojima K, Dan C, Watanabe H, Kumagai Y. Upper molar distalization with Invisalign treatment accelerated by photobiomodulation. *J Clin Orthod*. 2018;52:675–83.
- Cassetta M, Altieri F, Barbato E. The combined use of corticotomy and clear aligners: a case report. *Angle Orthod*. 2016;86:862–70.
- Long H, Pyakurel U, Wang Y, Liao L, Zhou Y, Lai W. Interventions for accelerating orthodontic tooth movement: a systematic review. *Angle Orthod*. 2013;83:164–71.
- Ahmed M, Shaikh A, Fida M. Diagnostic performance of various cephalometric parameters for the assessment of vertical growth pattern. *Dental Press J Orthod*. 2016;21:41–9.
- Angelieri F, de Almeida RR, Janson G, Castanha Henriques JF, Pinzan A. Comparison of the effects produced by headgear and pendulum appliances followed by fixed orthodontic treatment. *Eur J Orthod*. 2008;30:572–9.
- Kirjavainen M, Kirjavainen T, Hurmerinta K, Haavikko K. Orthopedic cervical headgear with an expanded inner bow in class II correction. *Angle Orthod*. 2000;70:317–25.
- Mossaz CF, Byloff FK, Kiliaridis S. Cervical headgear vs pendulum appliance for the treatment of moderate skeletal class II malocclusion. *Am J Orthod Dentofac Orthop*. 2007;132:616–23.
- Caprioglio A, Fontana M, Longoni E, Cozzani M. Long-term evaluation of the molar movements following pendulum and fixed appliances. *Angle Orthod*. 2013;83:447–54.
- Al-Thomali Y, Basha S, Mohamed RN. Pendulum and modified pendulum appliances for maxillary molar distalization in class II malocclusion - a systematic review. *Acta Odontol Scand*. 2017;75:394–401.

Publisher's Note

Springer Nature remains neutral with regard to jurisdictional claims in published maps and institutional affiliations.

Ready to submit your research? Choose BMC and benefit from:

- fast, convenient online submission
- thorough peer review by experienced researchers in your field
- rapid publication on acceptance
- support for research data, including large and complex data types
- gold Open Access which fosters wider collaboration and increased citations
- maximum visibility for your research: over 100M website views per year

At BMC, research is always in progress.

Learn more biomedcentral.com/submissions



RESEARCH ARTICLE

Open Access



Three-dimensional photographic analysis of the face in European adults from southern Spain with normal occlusion: reference anthropometric measurements

M. L. Menéndez López-Mateos¹, J. Carreño-Carreño², J. C. Palma³, J. A. Alarcón^{1*}, C. Menéndez López-Mateos³ and M. Menéndez-Núñez¹

Abstract

Background: Recent non-invasive 3D photography method has been applied to facial analysis, offering numerous advantages in orthodontic. The purpose of this study was to analyze the faces of a sample of healthy European adults from southern Spain with normal occlusion in order to establish reference facial soft tissue anthropometric parameters in this specific geographic-ethnic population, as well as to analyze sexual dimorphism.

Methods: A sample of 100 healthy adult volunteers consisting of 50 women (mean age, 22.92 ± 1.56 years) and 50 men (mean age, 22.37 ± 2.12 years) were enrolled in this study. All participants had normal occlusion, skeletal Class I, mesofacial pattern, and healthy body mass index. Three-dimensional photographs of the faces were captured non-invasively using Planmeca ProMax 3D ProFace[®]. Thirty landmarks related to the face, eyes, nose, and orolabial and chin areas were identified.

Results: Male displayed higher values in all vertical and transversal dimensions, with the exception of the lower lip height. Larger differences between sexes were observed in face, mandible, and nose. Male also had higher values in the angular measurements which referred to the nose. No sex differences were found in transverse upper lip prominence or transverse mandibular prominence. No differences were found in the ratio measurements, with the exception of intercantal width/nasal width, which was higher in women than in men.

Conclusions: Reference anthropometric measurements of facial soft tissues have been established in European adults from southern Spain with normal occlusion. Significant sexual dimorphism was found, with remarkable differences in size between sexes

Keywords: 3D photography, Face, Soft tissues, Anthropometry, Morphometrics, Reference values

Background

Analysis of both hard and soft facial tissues is used in orthodontic diagnoses. Until recently, classical orthodontics considered the study of hard tissues and cephalometric measurements of upper and lower jaws and the teeth as more relevant. These measurements have thus been the most used diagnostic tools in orthodontics [1, 2]. Nevertheless, facial soft tissue morphology has gained increasing

interest among clinicians. In fact, currently, orthodontic and maxillofacial surgery diagnoses are not made without the inclusion of specific soft tissue measurements. In addition, lay people (patients and their friends and relatives) assess the success of orthodontic and orthognathic surgery treatments based on perceived visual facial changes [3]. Therefore, a complete three-dimensional (3D) assessment of facial soft tissue shape, size, and proportions should be included as a fundamental step in orthodontic diagnoses, assessment of facial deformities, maxillofacial surgery planning, and evaluation of treatment results [4].

* Correspondence: jalardon@ugr.es

¹Department of Stomatology, Faculty of Odontology, Campus Universitario de Cartuja, University of Granada, 18071 Granada, Spain

Full list of author information is available at the end of the article



© The Author(s). 2019 **Open Access** This article is distributed under the terms of the Creative Commons Attribution 4.0 International License (<http://creativecommons.org/licenses/by/4.0/>), which permits unrestricted use, distribution, and reproduction in any medium, provided you give appropriate credit to the original author(s) and the source, provide a link to the Creative Commons license, and indicate if changes were made. The Creative Commons Public Domain Dedication waiver (<http://creativecommons.org/publicdomain/zero/1.0/>) applies to the data made available in this article, unless otherwise stated.

Currently, detailed facial soft tissue examinations can be carried out using 3D radiographic techniques, such as computed tomography, or cone-beam computed tomography (CBCT), which is preferable due to the use of lower radiation doses [5]. Anthropometric facial features can also be analyzed using non-invasive 3D X-ray-free systems, such as laser surface scanning, multi-image photogrammetry, stereo-photogrammetry, or recent 3D facial photography techniques. These new methods offer numerous advantages, including speed of data collection, feasibility of data storage and handling, accuracy, and reliability [6–11].

Reference normative values for specific races and ethnic groups have thus become absolutely necessary [12], as there are remarkable variations between different populations and groups [13]. Some studies have provided reference anthropometric facial data acquired using stereo-photogrammetry or photography from Chinese [4], Korean [14], Malay [15], and Turkish [16] adults. No 3D facial data are available from southern European adult populations.

We used a recent non-invasive 3D photography method to analyze the faces of a sample of healthy European adults from southern Spain with normal occlusion. The main aims were to establish standards for facial soft tissue anthropometric parameters in this specific geographic-ethnic population, as well as to analyze sexual dimorphism. We also compared our findings to morphological features of other similarly studied populations.

Methods

A sample of 100 healthy adult volunteers consisting of 50 women (mean age, 22.92 ± 1.56 years) and 50 men (mean age, 22.37 ± 2.12 years) were enrolled in this study. The inclusion criteria were as follows: 1) European ethnicity, specifically that from Granada in southern Spain. Information regarding ethnicity and geographic origin was obtained using a self-administered questionnaire, which included questions regarding the participants and their parents and grandparents; 2) age between 20 and 30 years; 3) normal occlusion classified as skeletal Class I (based on ANB angle: $0-4^\circ$, as measured on a lateral cephalogram), mesofacial growth pattern (according to the Frankfort horizontal-to-mandibular plane angle: $20-28^\circ$ on a lateral cephalogram), and dental angle Class I; 4) lip competence; and 5) healthy body mass index ($18-25 \text{ kg/m}^2$). The exclusion criteria were 1) craniofacial anomalies; 2) previous or current orthopedic, orthodontic, maxillofacial, or aesthetic surgery treatment; 3) nasal or facial disfigurement, deformity, asymmetry, or surgery; 4) history of facial trauma; and 5) any type of cosmetic facial aesthetic procedure. The sample size was determined using the 3.1.2 version of PS: Power and Sample Size Calculation[®] according to previously described methods [4, 17].

Participants volunteered for the study after a detailed explanation of the protocol and agreed to participate by signing an ethics committee-approved informed consent form.

Three-dimensional image capture, methods, and measurements

Three-dimensional photography of the faces was carried out using Planmeca ProMax 3D ProFace[®] (Planmeca USA, Inc.; Roselle, IL, USA), which produces a realistic 3D picture of the face (Fig. 1). Photographs were recorded using the ProFace option, which requires no radiation. The system is based on lasers that scan facial geometry and a few digital cameras, which capture texture and color. The sensor components consist of two lights, a laser, two digital cameras, and two light-emitting diodes. The spatial accuracy of this device is 0.03 mm (as reported by the manufacturer). The 3D photographs were processed using Planmeca Romexis[®] software, which facilitated accurate and detailed operation.

Subjects were instructed not to wear heavy makeup 2 days prior to the scan. They were also instructed to shave and remove their glasses at least 2 h prior to 3D photography. During the image capture, the participant was with the head in a natural position, a neutral facial expression, the mandible in a resting position, and the lips lightly opposed without undue muscular effort.



Fig. 1 Three-dimensional photography device

Thirty soft tissue anthropometric landmarks related to the face, eyes, nose, and orolabial and chin areas (Fig. 2), based on those suggested by Farkas [18] and Mulliken et al. [19], were identified. The points were recorded manually using Nemotec Arnetts FAB Software[®], version 10.0 (Software Nemotec SL; Madrid, Spain).

Nineteen linear and 7 angular measurements were used to assess facial anthropometric morphological features, and 12 facial ratios were derived from the linear measurements (Table 1).

Statistical analysis

Statistical analyses were performed using Statistical Package for the Social Sciences version 22.0 (Chicago, IL, USA). Descriptive statistics (mean, standard deviation, and standard error of the mean) for each measurement were computed for each sex. Sex differences were tested using Student's *t* tests. Mann-Whitney U tests were used for measurements with non-normal data. Additional file 1: Table S1 includes all data generated or analyzed during this study (Additional file 1).

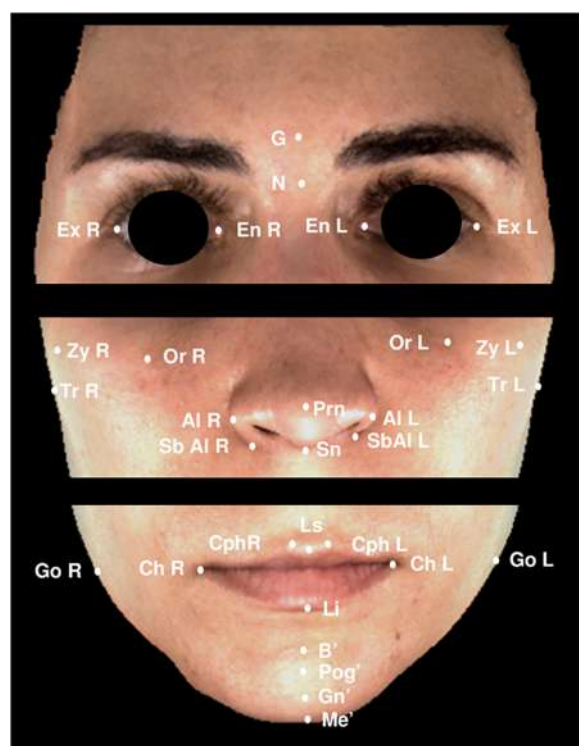


Fig. 2 Soft tissue landmarks. N (soft-tissue nasion); G (glabella); Prn (pronasale); Sn (subnasale); Ls (labrale superius); Li (labrale inferius); B (soft-tissue B point); Pg (soft-tissue pogonion); Me (soft-tissue menton); En (endocanthion, R-Right and L-Left); Ex (exocanthion; R-Right and L-Left); Or (orbitale, R-Right and L-Left); Al (alare, R-Right and L-Left); SbAl (subalare, R-Right and L-Left); Cph (chista philtri, R-Right and L-Left) Ch (cheilion, R-Right and L-Left); Zy (zygomatic point, R-Right and L-Left); Go (soft-tissue gonion, R-Right and L-Left); and Tr (tragus, R-Right and L-Left)

Table 1 Facial soft tissue anthropometric measurements

Measurements	
Face (mm)	
Face height	N-Me
Lower face height	Sn-Me
Middle facial width	Tr R- TrL
Facial width	ZyR- ZyL
Mandible width	GoR- GoL
Right mandibular body length	GoR-Me
Left mandibular body length	GoL-Me
Nose (mm)	
Nose height	N-Sn
Nasal bridge length	N-Prn
Nasal width	AlR- AlL
Alar base root width	SbAlR- SbAl L
Ocular (mm)	
Biocular width	ExR- ExL
Intercantal width	EnR- EnL
Biorbitale width	OrR- OrL
Orolabial (mm)	
Vermillion height	Ls-Li
Mouth width	ChR-ChL
Philtrum width	CphR-CphL
lower lip height	Li-B
Chin (mm)	
Chin height	Li-Me
	B-Pg
	Pg-Me
Angular measurements (°)	
Nasolabial angle	G-N-Prn
Nasomental angle	N-Prn-Pg
Transverse nasal prominence	Zy R-Prn-ZyL
Transverse upper lip prominence	ChR-Ls-Ch
Transverse mandibular prominence	GoR-Pg-GoL
Ratio measurements	
Upper face height/mandibular width	N-Sn / GoR-GoL
Lower face height/mandibular width	Sn-Me / GoR-GoL
Anterior face height/mandibular width	N-Me/ GoR-GoL
Anterior face height/facial width	N-Me / ZyR-ZyL
Intercantal width/nasal width	EnR-EnL / AlR-AIL
Vermillion height/mouth width	Ls-Li / ChR-ChL
Chin height/right mandibular body length	Li-Me / GoR-Me
Chin height/left mandibular body length	Li-Me / GoL-Me
Nose height/lower face height	N-Sn / SnMe
Nose height/facial width	N-Sn / ZyR-ZyL
Mouth width/intercantal width	ChR-ChL / EnR-EnL
Mandible width/biocular width	GoR-GoL / ExR-ExL

Reliability of measurements of the 3D imaging capture system used was tested using the method of moments [20]. Twenty linear measurements were made directly over the faces of 10 randomly selected participants (5 women and 5 men) using an electronic caliper (Ratio®). These measurements were then compared to those made indirectly over the 3D images captured from the same participants.

All images were scored by a single experienced observer (MLM). To test for intra-observer reliability, 10 randomly selected images (5 women and 5 men) were scored again after a two-week period. To test for inter-observer reliability, the same 10 randomly selected images were scored by another independent expert (MMN). Inter- and intra-rater agreements were calculated using intra-class correlation coefficients (ICCs).

Results

The reliability measurements of the 3D images captured by the system indicated a mean reproducibility of 1.04 mm, which is considered adequate for clinical applications [10]. The inter-examiner ICC value was 0.83 (IC 0.61–0.92). The intra-examiner ICC scores ranged from 0.51 (N-Me / ZyR-ZyL) to 0.99 (ChR-ChL / EnR-EnL); the mean ICC score for all of the variables included in the study was 0.84 (IC 0.67–0.99), with 79% of variables having ICC scores > 0.7, which is considered good agreement [21].

Table 2 shows the means, standard deviations, mean differences, and comparisons between male and female subjects for all of the morphological facial variables included in the study. A statistically significant difference was found between male and female subjects in 23 of our 38 measurements. The most prominent differences between the sexes were observed in the measurements obtained from the face region.

Face

The male subjects had longer and mostly wider faces than the women. The largest differences were found in the transversal plane, mainly in middle facial width (134.97 ± 5.44 mm in men vs. 128.22 ± 6.37 mm in women) and in facial width (114.42 ± 4.63 mm in men vs. 110.73 ± 5.06 mm in women) ($p < 0.001$). Mandibles were also wider in men than in women, with higher values for mandible width (mean difference, 6.91 mm), and right (mean difference, 7.74 mm) and left (mean difference, 7.12 mm) mandibular body lengths.

Nose

All measurements (nose height, nasal bridge length, nasal width, and alar base root width) for the nose were significantly larger in men than in women. Larger differences were again found in the transversal dimension

(nasal width and alar base root width), with wider noses in men than in women (mean differences, 5.23 and 3.20 mm, respectively).

Ocular region

The 3 variables used to analyze the ocular region were larger in men than in women. We observed especially large differences in biocular width (90.40 ± 4.68 mm vs. 86.58 ± 3.20 mm) and biorbitale width (76.06 ± 4.79 mm vs. 71.97 ± 4.62 mm).

Orolabial region

Vermilion height, mouth width, and philtrum width were significantly larger in men than in women. No statistically significant sex difference was found in lower lip height.

Chin

All evaluated chin measurements were significantly larger in men than in women, with a large difference in chin height (39.07 ± 7.01 mm vs. 38.14 ± 3.68 mm).

Angular measurements

Significant sex differences in angular measurements were found in the nose region (nasolabial angle, nasomental angle, and transverse nasal prominence) ($p < 0.001$). Transverse upper lip prominence and transverse mandibular prominence were similar in both sexes.

Ratio measurements

We found no significant sex differences in ratio measurements, with the exception of the intercantal width to nasal width ratio, which was higher in women than in men ($p < 0.01$).

Discussion

In spite of the recent increase in the relevance of soft tissue facial analysis, there is an absence of reference values for some races, ethnicities, and geographic population groups. These data are required to determine deviations from standard measurements. We used a recent non-invasive 3D photography method to analyze the faces of a sample of healthy European adults with normal occlusion from southern Spain. We established anthropometric facial soft tissue reference values for this specific geographic-ethnic population. We also investigated differences between the sexes in this population.

We found clear sexual dimorphism, with statistically significant differences between male and female subjects in most facial variables that were analyzed. The male subjects had higher values in all vertical and transversal dimensions, with the exception of lower lip height, which was similar in the two groups. The male subjects also had higher values in the angular measurements of

Table 2 Means, standard deviations, mean differences, and *p*-values for facial morphologic value differences between male and female subjects

Measurements	Male Mean (SD)	Female Mean (SD)	Mean difference (95% CI)	<i>p</i> value
Face (mm)				
Face height	120.40 (8.22)	119.69 (4.25)	3.48 (0.20; 6.75)	0.038*
Lower face height	66.77 (8.05)	65.99 (4.22)	2.77 (−0.46; 6.00)	0.003**
Middle facial width	134.97 (5.44)	128.22 (6.37)	9.04 (6.49; 11.60)	0.000***
Facial width	114.42 (4.63)	110.73 (5.06)	7.39 (4.23; 10.55)	0.000***
Mandible width	113.52 (6.23)	107.58 (7.51)	6.91 (2.80; 11.01)	0.001***
Right mandibular body length	92.56 (13.33)	83.48 (7.45)	7.74 (1.78; 13.70)	0.002**
Left mandibular body length	92.48 (13.96)	83.97 (6.89)	7.12 (1.05; 13.18)	0.008**
Nose (mm)				
Nose height	56.94 (4.45)	56.17 (2.83)	1.58 (0.01; 3.15)	0.049*
Nasal bridge length	48.35 (4.76)	47.56 (2.97)	1.97 (0.04; 3.52)	0.012*
Nasal width	36.62 (3.28)	31.15 (2.21)	5.23 (3.97; 6.50)	0.000***
Alar base root width	23.17 (6.07)	20.17 (3.85)	3.20 (1.25; 5.15)	0.002**
Ocular (mm)				
Biocular width	90.40 (4.68)	86.58 (3.20)	4.83 (3.14; 6.53)	0.000***
Intercantal width	32.52 (4.52)	31.38 (2.78)	2.27 (0.56; 3.98)	0.010**
Biorbitale width	76.06 (4.79)	71.97 (4.62)	4.53 (2.60; 6.45)	0.000***
Orolabial (mm)				
Vermilion height	13.07 (3.75)	11.83 (2.45)	1.52 (0.34; 2.70)	0.040*
Mouth width	51.11 (4.77)	47.34 (3.65)	4.21 (2.26; 6.17)	0.000***
Philtrum width	10.62 (2.43)	9.29 (1.95)	1.73 (0.82; 2.64)	0.000***
lower lip height	20.25 (3.20)	19.32 (3.69)	1.95 (−1.19; 2.59)	0.695
Chin (mm)				
Chin height	39.07 (7.01)	38.14 (3.68)	2.06 (−0.82; 4.95)	0.004**
B-Pg	6.61 (2.34)	5.69 (1.70)	1.57 (0.37; 2.76)	0.011*
Pg-Me	12.91 (3.22)	12.08 (2.98)	1.77 (0.42; 3.11)	0.011*
Angular measurements (°)				
Nasolabial angle	28.22 (4.32)	24.26 (4.30)	3.92 (1.89; 5.95)	0.000***
Nasomental angle	30.77 (4.00)	28.62 (3.20)	1.94 (0.54; 3.35)	0.000***
Transverse nasal prominence	43.82 (2.08)	41.64 (2.63)	2.76 (1.50; 4.01)	0.000***
Transverse upper lip prominence	35.82 (8.71)	35.53 (3.49)	0.63 (−0.86; 2.08)	0.402
Transverse mandibular prominence	50.62 (3.61)	49.91 (4.20)	1.22 (−0.41; 2.85)	0.142
Ratio measurements				
Upper face height/mandibular width	0.50 (0.05)	0.53 (0.05)	−0.02 (−0.05; 0.00)	0.081
Lower face height/mandibular width	0.59 (0.08)	0.62 (0.06)	−0.01 (−0.06; 0.03)	0.784
Anterior face height/mandibular width	1.06 (0.09)	1.12 (0.09)	−0.04 (−0.95; 0.01)	0.140
Anterior face height/facial width	1.05 (0.08)	1.08 (0.05)	−0.03 (−0.07; 0.00)	0.055
Intercantal width/nasal width	0.89 (0.13)	1.01 (0.11)	−0.08 (−0.14; −0.02)	0.008**
Vermilion height/mouth width	0.26 (0.08)	0.25 (0.06)	0.01 (−0.01; 0.03)	0.424
Chin height/right mandibular body length	0.42 (0.08)	0.45 (0.07)	−0.02 (−0.07; 0.02)	0.207
Chin height/left mandibular body length	0.43 (0.09)	0.46 (0.06)	−0.02 (−0.06; 0.03)	0.332
Nose height/lower face height	0.87 (0.18)	0.86 (0.08)	0.01 (−0.06; 0.07)	0.175

Table 2 Means, standard deviations, mean differences, and *p*-values for facial morphologic value differences between male and female subjects (*Continued*)

Measurements	Male Mean (SD)	Female Mean (SD)	Mean difference (95% CI)	<i>p</i> value
Nose height/facial width	0.50 (0.05)	0.51 (0.03)	−0.02 (−0.03; 0.00)	0.063
Mouth width/intercantal width	1.59 (0.21)	1.52 (1.18)	0.01 (−0.11; 0.12)	0.859
Mandible width/biocular width	1.26 (0.08)	1.24 (0.09)	0.15 (−0.03; 0.06)	0.541

p* < 0.05; *p* < 0.01; ****p* < 0.001

the nose. No sex differences were found in transverse upper lip prominence or transverse mandibular prominence. Only one statistically significant sex difference was found in the ratio measurements (intercantal width/nasal width, which was higher in women than in men). The rest of the measured ratios were similar in both sexes.

Planmeca ProFace™, which was used to capture facial soft tissue characteristics, generates 3D photos in one imaging session while the patient position, facial expression, and muscle position remain unchanged. This leads to the production of images that are perfectly compatible (technical information provided on the company website) (<http://www.planmeca.com/Imaging/3D-imaging/Planmeca-ProFace/>).

The reliability of the measurements produced by the 3D imaging capture system used was tested using the method of moments. Specifically, we compared the direct measurements (those made over the face of the patient using an electronic caliper) with the same measurements made indirectly (over the 3D images captured using Planmeca ProMax 3D ProFace® [Planmeca USA, Inc.; Roselle, IL, USA]) using the same randomly selected participants. The results indicated adequate reproducibility (mean, 1.04 mm) [10].

The 3D photography method offers many advantages over conventional (non-3D) photography, including accurate 3D images and reliability to perform facial analysis. Nevertheless, a more sophisticated device and software are required.

In our population, which consisted of European adults from southern Spain, prominent sex differences were observed in measurements of the face, mandible, and nose. These measurements were significantly larger in men than in women.

In our study, the male subjects had longer and wider faces than the female subjects. Similar results were found by Baik et al. in Korean adults [14] and by Ozdemir et al. in Turkish young adults [16]. Othman et al. also described longer faces in men than in women in a Malaysian population, although they did not include facial width measurements [15]. There are also differences between populations: Korean men have slightly longer faces than Europeans from southern Spain (face height, N-Me, 121.42 ± 6.03 mm vs. 120.40 ± 8.22 mm), while women from southern Spain have longer faces than Korean women (119.69 ± 6.9 mm vs. 114.41 ± 5.89 mm). Sexual dimorphism in face height was

more prominent in the Korean population [14]. Our results are not comparable with those obtained in Turkish [16] or Malaysian [15] populations. This is because, in those studies, the authors considered face height as the distance from N to Gn, although they also found higher sexual dimorphism than we did. Sexual dimorphism has also been reported in a Chinese population [4], although the different methodology used makes it difficult to compare the Chinese study to ours.

Mandible width and right and left mandibular body length were also significantly larger in men than in women in our southern European sample. Similar results were found in Turkish and Korean adults, with wider mandibles in men than in women. Inter-group differences can be observed when comparing populations: Koreans men and women have the widest mandibles (measured from right to left gonion) (127.38 ± 7.43 mm in men and 118.01 ± 7.41 mm in women). They are followed by the Turkish (116.3 ± 1.26 mm in men and 110.2 ± 1.65 mm in women) and the southern Europeans in our study, who had the smallest mandible width (113.52 ± 6.23 mm in men and 107.58 ± 7.51 mm in women). These inter and intra-population differences in face and mandible size and shape may be attributed to several factors, including genetic or environmental factors, as suggested by paleo-anthropology studies [22–26].

In our study, all the measurements of the nose had larger values in men than in women. This was especially true of nasal width, which had a mean difference of 5.23 mm. Sexual dimorphism in nose dimensions had also been described in Malaysian adults. Malaysian men have generally longer and more prominent noses. In addition, nose height and nasal bridge length are significantly in Malaysian men (mean differences of 4.93 mm and 5.73 mm, respectively) [15]. Baik et al. [14] also found longer and more prominent noses in men than in women. In contrast, Ozdemir et al. [16] did not find sexual dimorphism in the height of the nose, the length of the nasal bridge, or the nasal root width in Turkish adults. Our southern European population had narrower noses (nasal width: 36.62 ± 3.28 mm in men and 31.15 ± 2.21 mm in women) than other racial and ethnic groups [14–16, 27–29]. In contrast, the nose height was had higher values in our group (56.94 ± 4.45 mm in men and

56.17 ± 2.83 mm in women) than in Malaysian (54.13 ± 3.61 mm in men and 49.20 mm in women) [15], Chinese (50.15 ± 4.16 mm in men and 46.93 ± 3.3 mm in women) [30], Turkish (51.9 ± 0.75 mm in men and 51.7 ± 0.58 mm in women) [16], and Korean (53.26 ± 3.46 mm in men and 48.4 ± 4.52 mm in women) [14] populations. Our results were similar to those found in white northern Italians (57.43 ± 3.93 mm in men and 54.07 ± 3.68 mm in women) [27]. A proposed explanation for sexual differences in nose dimensions is that men have higher daily energy expenditure, greater respiratory air consumption, and different body composition [22, 31].

Sexual dimorphism was also found in the ocular region in our population, with significantly higher values in men than in women for all variables analyzed. Major differences were found in biocular width (mean difference, 4.83 mm) and biorbitale width (mean difference, 4.53 mm). In the study by Othman et al. [15], only biocular width (mean difference, 4.14 mm) was significantly larger in Malay men than in Malay women. Although the main differences in biocular width were quite similar in both studies, the Malaysian subjects had higher values for both men (96.19 ± 4.64 mm) and women (92.05 ± 3.22 mm) than those found in our southern European sample (90.40 ± 4.68 mm in men and 86.58 ± 3.20 mm in women). No sexual dimorphism was found in a Korean population [14], although the linear distance ExR-ExL (what is referred to as 'upper face width') was even higher (106.75 ± 6.13 mm in men and 104.98 ± 5.47 mm in women) in that population. There are thus large differences in the ocular area between races and ethnic groups.

All of the measurements in the orolabial were significantly larger in men than in women, with the remarkable exception of lower lip height, which did not display a significant sex difference. Similarly, no sexual dimorphism was found in the lower vermilion height in a Turkish population [16]. In our sample, philtrum width (10.62 ± 2.43 mm in men and 9.29 ± 1.95 mm in women) and mouth width (51.11 ± 4.77 mm in men and 47.34 ± 3.65 mm in women) values were similar to those found by Othman et al. [15] in Malaysians (11.84 ± 1.90 mm in men and 10.40 ± 1.14 mm in women, and 50.83 ± 3.75 mm in men and 48.00 ± 2.61 mm in women, respectively). The above authors, however, found smaller differences in mouth width between sexes (2.83 mm vs. 4.21 mm in our study). Turkish [16] and Korean [14] subjects have wider philtrums in both sexes. The widest mouths are found in white northern Italians [27] (55.71 ± 3.81 mm in men and 50.84 ± 3.83 mm in women). The narrowest mouths are found in Turks [16] (47.1 ± 0.54 mm in men and 44 ± 0.31 mm in women).

Angular and ratio measurements are difficult to compare among the published studies due to the different

methodologies and variables that have been considered. In our population, nasolabial, nasomental, and transverse nasal prominence angles were significantly larger in men than in women. In contrast, transverse upper lip prominence and transverse mandibular prominence did not show sexual dimorphism. Thus, there were significant sex differences in the angular measurements of the nose between the sexes. Baik et al. [14] also did not find significant sex differences in angular measurements, with the exception of the nasal frontal angle and the transverse nasal prominence, in a Korean population. Othman et al. [15] did not find clinically significant differences between the sexes in angular and ratio measurements in Malaysians.

Among the ratio measurements in our study, only the intercant width/nasal width ratio was significantly different between the sexes, with higher ratios in women (1.01 ± 0.11) than men (0.89 ± 0.13). In contrast, Baik et al. [14] found significant sex differences in the ratio of anterior facial height to the interzygomatic distance and that of forehead height to forehead width. However, the ratio of facial height to upper facial height relative to mandibular width was similar in both sexes, which is consistent with our study. These results suggest that there are larger differences in the sizes, rather than the shapes, of faces between men and women. The comparisons and differences with other populations reported in our study should be interpreted with caution due to the different systems used for facial evaluation, as well as in the different variables used to analyze anthropometric facial features.

Conclusions

Here we establish reference anthropometric measurements of facial soft tissues in European adults from southern Spain with normal occlusion using non-invasive 3D photography. Most of the parameters had significant sexual dimorphism. Men had higher values in all vertical and transversal dimensions, with the exception of lower lip height, which was similar in the two groups. The greatest differences between sexes were observed in measurements obtained from the face, mandible, and nose, which were significantly larger in men than in women. However, only one statistically significant sex difference was found in the ratio measurements (intercant width/nasal width, which was higher in women than in men).

Additional file

Additional file 1: Variables data generated or analyzed during this study. (XLSX 51 kb)

Abbreviations

3D: Three dimensional; Al: Alare; B: B point; CBCT: Cone-beam computed tomography; Ch: Cheilion; Cph: Christa philtri; En: Endocanthion; Ex: Exocanthion; G: Glabela; Go: Gonion; ICCs: Intra-class correlation

coefficients; L: Left; Li: Labrale inferius; Ls: Labrale superius; Me: Menton; N: Nasion; Or: Orbitale; Pg: Pogonion; Prn: Pronasale; R: Right; SbAl: Subalare; Sn: Subnasale; Tr: Tragus; Zy: Zygomatic point

Acknowledgments

The authors are grateful to Dr. Conchita Martín, for her contribution of the statistical analysis.

Author contributions

Conceptualization: MLMLM, JCC, JCPF, JAA, CML, and MMN. Data curation: LMLM, CML, and MMN. Formal analysis: MLMLM, JCC, JCPF, JAA, CML, and MMN. Investigation: MLMLM and MMN. Methodology: MLMLM, JCC, JCPF, JAA, CML, and MMN. Project administration: MLMLM and MMN. Resources: JCC, JCPF, JAA, and CML. Supervision: MLMLM and MMN. Validation: MLMLM, JCC, JCPF, JAA, CML, and MMN. Visualization: MLMLM, JCC, JCPF, and MMN. Writing original draft: MLMLM, JAA, and MMN. Writing review & editing: MLMLM, JCC, JCPF, JAA, CML, and MMN. All authors have read and approved the manuscript.

Funding

Not applicable.

Availability of data and materials

All data generated or analysed during this study are included in this published article and its supplementary information files.

Ethics approval and consent to participate

Approval for this cross-sectional study was obtained from the University of Granada Ethics Committee (reference number 319/CEIH/2017). The study was ethically approved by the Institution, the procedures were in accordance with the declaration of Helsinki and all the subjects signed a consent form.

Consent for publication

Written informed consent to publish individual person's data (images) were obtained.

Competing interests

The authors declare that they have no competing interests.

Author details

¹Department of Stomatology, Faculty of Odontology, Campus Universitario de Cartuja, University of Granada, 18071 Granada, Spain. ²Faculty of Odontology, European University, 28670 Madrid, Spain. ³Department of Stomatology IV, Faculty of Odontology, Complutense University, Plaza de Ramón y Cajal s/n, 28040 Madrid, Spain.

Received: 29 June 2019 Accepted: 21 August 2019

Published online: 28 August 2019

References

- Ricketts RM. Perspectives in the clinical application of cephalometrics. The first fifty years. *Angle Orthod.* 1981;51:115–50.
- Tzou CH, Frey M. Evolution of 3D surface imaging systems in facial plastic surgery. *Facial Plast Surg Clin North Am.* 2011;19:591–602 vii.
- Bishara SE, Cummins DM, Jorgensen GJ, Jakobsen JR. A computer assisted photogrammetric analysis of soft tissue changes after orthodontic treatment. Part I: methodology and reliability. *Am J Orthod Dentofac Orthop.* 1995;107:633–9.
- Dong Y, Zhao Y, Bai S, Wu G, Zhou L, Wang B. Three-dimensional anthropometric analysis of chinese faces and its application in evaluating facial deformity. *J Oral Maxillofac Surg.* 2011;69:1195–206.
- Karatas OH, Toy E. Three-dimensional imaging techniques: a literature review. *Eur J Dent.* 2014;8:132–40.
- Deli R, Gioia ED, Galantucci LM, Percoco G. Accurate facial morphologic measurements using a 3-camera photogrammetric method. *J Craniofac Surg.* 2011;22:54–9.
- Plooij JM, Maal TJ, Haers P, Borstlap WA, Kuijpers-Jagtman AM, Berge SJ. Digital three-dimensional image fusion processes for planning and evaluating orthodontics and orthognathic surgery. A systematic review. *Int J Oral Maxillofac Surg.* 2011;40:341–52.
- Gwilliam JR, Cunningham SJ, Hutton T. Reproducibility of soft tissue landmarks on three-dimensional facial scans. *Eur J Orthod.* 2006;28:408–15.
- Othman SA, Ahmad R, Mericant AF, Jamaludin M. Reproducibility of facial soft tissue landmarks on facial images captured on a 3D camera. *Aust Orthod J.* 2013;29:58–65.
- Wong JY, Oh AK, Ohta E, Hunt AT, Rogers GF, Mulliken JB, et al. Validity and reliability of craniofacial anthropometric measurement of 3D digital photogrammetric images. *Cleft Palate Craniofac J.* 2008;45:232–9.
- Brons S, van Beusichem ME, Bronkhorst EM, Draaisma J, Berge SJ, Maal TJ, et al. Methods to quantify soft-tissue based facial growth and treatment outcomes in children: a systematic review. *PLoS One.* 2012;7:e41898.
- Liu Y, Kau CH, Pan F, Zhou H, Zhang Q, Zacharopoulos GV. A 3-dimensional anthropometric evaluation of facial morphology among Chinese and Greek population. *J Craniofac Surg.* 2013;24:e353–8.
- Farkas LG, Katic MJ, Forrest CR, Alt KW, Bagic I, Baltadjiev G, et al. International anthropometric study of facial morphology in various ethnic groups/races. *J Craniofac Surg.* 2005;16:615–46.
- Baik HS, Jeon JM, Lee HJ. Facial soft-tissue analysis of Korean adults with normal occlusion using a 3-dimensional laser scanner. *Am J Orthod Dentofac Orthop.* 2007;131:759–66.
- Othman SA, Majawit LP, Wan Hassan WN, Wey MC, Mohd RR. Anthropometric study of three-dimensional facial morphology in Malay adults. *PLoS One.* 2016;11:e0164180.
- Ozdemir ST, Sigirli D, Ercan I, Cankur NS. Photographic facial soft tissue analysis of healthy Turkish young adults: anthropometric measurements. *Aesthet Plast Surg.* 2009;33:175–84.
- Kau CH, Richmond S, Zhurov A, Ovsenik M, Tawfik W, Borbely P, et al. Use of 3-dimensional surface acquisition to study facial morphology in 5 populations. *Am J Orthod Dentofacial Orthop.* 2010;137(4 Suppl):S56 e1–9 discussion S-7.
- Farkas LG. *Anthropometry of the head and face.* New York: Lippincott Raven Press; 1994.
- Mulliken JB, Burvin R, Farkas LG. Repair of bilateral complete cleft lip: intraoperative nasolabial anthropometry. *Plast Reconstr Surg.* 2001;107:307–14.
- Bowman KO, Shenton LR. Estimator: Method of Moments. *Encyclopedia of statistical sciences.* New York: Wiley; 1998. p. 2092-8.
- Landis JR, Koch GG. The measurement of observer agreement for categorical data. *Biometrics.* 1977;33:159–74.
- Bastir M, Godoy P, Rosas A. Common features of sexual dimorphism in the cranial airways of different human populations. *Am J Phys Anthropol.* 2011; 146:414–22.
- Rosas A, Bastir M, Alarcon JA, Kuroe K. Thin-plate spline analysis of the cranial base in African, Asian and European populations and its relationship with different malocclusions. *Arch Oral Biol.* 2008;53:826–34.
- Rosas A, Bastir M. Thin-plate spline analysis of allometry and sexual dimorphism in the human craniofacial complex. *Am J Phys Anthropol.* 2002;117:236–45.
- Alarcon JA, Bastir M, Rosas A. Variation of mandibular sexual dimorphism across human facial patterns. *Homo.* 2016;67:188–202.
- Coquerelle M, Bookstein FL, Braga J, Halazonetis DJ, Weber GW, Mitteroecker P. Sexual dimorphism of the human mandible and its association with dental development. *Am J Phys Anthropol.* 2011;145:192–202.
- Ferrario VF, Sforza C, Serrao G. A three-dimensional quantitative analysis of lips in normal young adults. *Cleft Palate Craniofac J.* 2000;37:48–54.
- Porter JP, Olson KL. Anthropometric facial analysis of the African American woman. *Arch Facial Plast Surg.* 2001;3:191–7.
- Porter JP. The average African American male face: an anthropometric analysis. *Arch Facial Plast Surg.* 2004;6:78–81.
- Aung SC, Foo CL, Lee ST. Three dimensional laser scan assessment of the oriental nose with a new classification of oriental nasal types. *Br J Plast Surg.* 2000;53:109–16.
- Holton NE, Yokley TR, Froehle AW, Southard TE. Ontogenetic scaling of the human nose in a longitudinal sample: implications for genus Homo facial evolution. *Am J Phys Anthropol.* 2014;153:52–60.

Publisher's Note

Springer Nature remains neutral with regard to jurisdictional claims in published maps and institutional affiliations.

RESEARCH ARTICLE

Open Access



Accuracy of in vitro mandibular volumetric measurements from CBCT of different voxel sizes with different segmentation threshold settings

Ting Dong, Lunguo Xia, Chenglin Cai, Lingjun Yuan*, Niansong Ye* and Bing Fang*

Abstract

Background: To determine the accuracy of volumetric measurements of the mandible in vitro by cone-beam computed tomography (CBCT) and to analyze the influence of voxel sizes and segmentation threshold settings on it.

Methods: The samples were obtained from pig mandibles and scanned with 4 voxel sizes: .125 mm, .20 mm, .30 mm, and .40 mm. The minimum segmentation thresholds in Hounsfield units (HU) were set as 0, 100, 200, 300, and 400, respectively, for each voxel size for 3D reconstruction. Laser scanning as the reference, the volumes of each CBCT scanning, the mean iterative distances of superimposition and total positive and negative deviations were recorded and compared.

Results: The volumes of CBCT-scan deviated from those of laser-scan by + 7.67% to – 3.05% with different HU and voxel sizes. The deviation increased with the voxel size. There was a more suitable minimum HU threshold of segmentation (HU100 for .125 mm, 200 for .20 mm, 300 for .30 mm, and 400 for .40 mm) for each voxel size.

Conclusions: Voxel sizes and Hounsfield unit thresholds influence the accuracy of volumetric measurements in CBCT scanning. The volume increase with the voxel size, and different voxel sizes correspond to different optimal Hounsfield unit thresholds.

Keywords: Cone-beam computed tomography (CBCT), Voxel size, Hounsfield unit threshold, Volumetric measurement

Background

Three-dimensional (3D) reconstruction of maxillofacial structures with cone-beam computed tomography (CBCT) has been widely applied in orthodontics [1], oral and maxillofacial surgery [2], oral implantology, and other fields. The inaccuracy of volumetric measurement in CBCT reconstruction may have important clinical influence.

First, such inaccuracy will influence diagnosis, such as 3D cephalometric analysis, which is necessary to identify cephalometric landmarks on 3D volumetric surfaces; further, the accuracy of maxillofacial reconstruction affects the precision of landmark identification and measurement

analysis [3]. Recently, many scholars focused automated 3D cephalometric landmarking on CBCT volumes, where landmarks that have been located are directly annotated in volume voxels. Montúfar et al. [4] investigated a model-based algorithm for automatic landmarking in CBCT volume and scored a 3.6-mm error for 18 landmarks. Gupta et al. [5] reported an average error of 2.01 mm for 20 landmarks, with 64.67% of the landmarks in a range of 0 to 2 mm, 82.67% from 0 to 3 mm, and 90.33% from 0 to 4 mm. The deviations in 3D-reconstructed volume will create unavoidable error in landmark positioning.

Second, the inaccuracy of volumetric measurement will influence creation of the bone-supported guide template for use in orthognathic surgery, which is indicated for the treatment of significant skeletal malocclusions and facial dysmorphism. Accurate volumetric measurements and the surface profiles of jaws play an important

* Correspondence: 38741244@qq.com; yns119@126.com; fangbing@sjtu.edu.cn

Department of Orthodontics, Ninth People's Hospital Affiliated to Shanghai Jiao Tong University, School of Medicine, No. 639 Zhizaoju Road, Shanghai, China



© The Author(s). 2019 **Open Access** This article is distributed under the terms of the Creative Commons Attribution 4.0 International License (<http://creativecommons.org/licenses/by/4.0/>), which permits unrestricted use, distribution, and reproduction in any medium, provided you give appropriate credit to the original author(s) and the source, provide a link to the Creative Commons license, and indicate if changes were made. The Creative Commons Public Domain Dedication waiver (<http://creativecommons.org/publicdomain/zero/1.0/>) applies to the data made available in this article, unless otherwise stated.

role in the design of jaw movement and contour trimming. Ye et al. [6] developed a method for a computer-image-guided surgical template for the navigation of Mandibular Angle Osteotomy. The template was obtained from the reconstructed mandibular model, so the volume of the mandibular model would doubtless affect the precision of the template. Various surgical devices have been developed to connect intact anatomic structures other than the maxillary and mandibular jaws, which are displaced during surgery. Lee et al. [7] examined the precision of a CAD/CAM facebow-based surgical guide template by comparing it with a bite wafer and found significant intergroup differences in lateral error compared with the absolute values of the 3D linear distance. Thus, it can be seen that artefacts of 3D volumetric surface can degrade the precision of orthognathic surgery design.

Third, the inaccuracy of volumetric measurement can influence superimposition and comparison before and after surgery, such as with bone augmentation and orthognathic surgery. CBCT and 3D reconstruction can be used to assess the efficiency of bone augmentation by aiding in the evaluation of the osteogenesis of grafting materials, and the accuracy of volumetric measurement plays a key role here. Lo et al. [8] investigated the relationship between soft- and hard-tissue changes after orthognathic surgery. Pre- and postoperative CBCT images were superimposed by the surface registration method, and the volumetric differences of each region were used to estimate the average movement. If the volumes of craniofacial structures before and after surgery disagree with each other, the reconstructed models cannot be precisely superimposed, especially affecting the accuracy and stability evaluation of orthognathic surgery. For a larger structure that requires more than one scan due to the limited field of view (FOV) of CBCT, the images of the two scans cannot be well-integrated, as a result of different volumetric errors.

However, there has been limited research on the volumetric error of 3D reconstruction with CBCT. As we know, the quality of images obtained by CBCT depends on many acquisition parameters, such as tube voltage, tube current, the field of view (FOV), the Hounsfield unit (HU) threshold of segmentation, and voxel size [9]. The first aim of this study was to compare the accuracy of volumetric measurement of CBCT scans. The second aim was to evaluate the effects of voxel sizes and HU thresholds on volumetric measurements and to assess optimal segment thresholds for different voxel sizes of CBCT volumetric measurement. In considering radiation, we chose pig mandibles for preliminary in vitro exploration.

Methods

For this study, we obtained pig mandibles from a butcher and removed the soft tissues, teeth, and alveolar

bone from the mandibles. This study was approved by the Institutional Review Board of Shanghai Ninth People's Hospital affiliated to Shanghai Jiao Tong University, School of Medicine (2018–87-T78). For the FOV we used, we cut the pig mandibles into several small pieces and included 24 pieces in the study. Because a laser scan is a surface scan, we filled the cavities on the mandibular surfaces with a mixture of plaster and bone meal. The samples were coated with Arti-Spray BK-285 powder (Dr Jean Bausch, Köln, Germany) to facilitate laser scanning. The laser scan was performed with a 3Shape scanner (R700, 3Shape, Copenhagen, Denmark), which can obtain surface models in the form of a “point cloud” format with an accuracy of 20 μ m and produce a stereolithography (STL) digital representation of the physical object [10]. The laser-scanned models were exported as STL format files to Geomagic Control software (Geomagic Control 2015.1.1; 3D Systems, Rock Hill, SC, USA) and were regarded as the reference.

A Hounsfield unit threshold must be calibrated before use due to variations among manufacturers. Therefore, we adopted the method described by Ye et al. [10] and scanned wax and a cup of water with the CBCT machine (KaVo Dental, Biberach, Germany) according to the manufacturer's instructions. The means and standard deviations of the thresholds of water, air, and wax were calculated in Hounsfield units with eXamVisionQ software (KaVo Dental).

All mandibular pieces were covered with double layers of boxing wax for soft-tissue simulation. CBCT acquisition was performed with a KaVo 3D exam scanner (KaVo Dental) with a field-of-view size (FOV) of 8.5 \times 8.5 cm, 120 kv, and 5 mA. A foam pad with a flute was used to stabilize pieces of the mandible in our study. Each sample was scanned 4 times with 4 voxel sizes: .125 mm, .20 mm, .30 mm, and .40 mm. The CBCT scan parameters are presented in Table 1. After scanning was completed, the CBCT data were exported as DICOM format files and imported into Mimics software (version 10.01; Materialise, Leuven, Belgium) for segmentation and 3D reconstruction. The mandibular cavities were filled by the “cavity fill” tool in the Mimics software to obtain the intact volume. The minimum segmentation thresholds in HU

Table 1 Preset CBCT scanning parameters

Group	Voxel size (mm)	FOV (mm ²)	Scan time (sec)	Tube current (mA)	Tube voltage (kV)
CS 0.125	0.125	85*85	23	5	120
CS 0.2	0.20	85*85	23	5	120
CS 0.3	0.30	85*85	8.9	5	120
CS 0.4	0.40	85*85	8.9	5	120

CS, CBCT scan; FOV, field of view

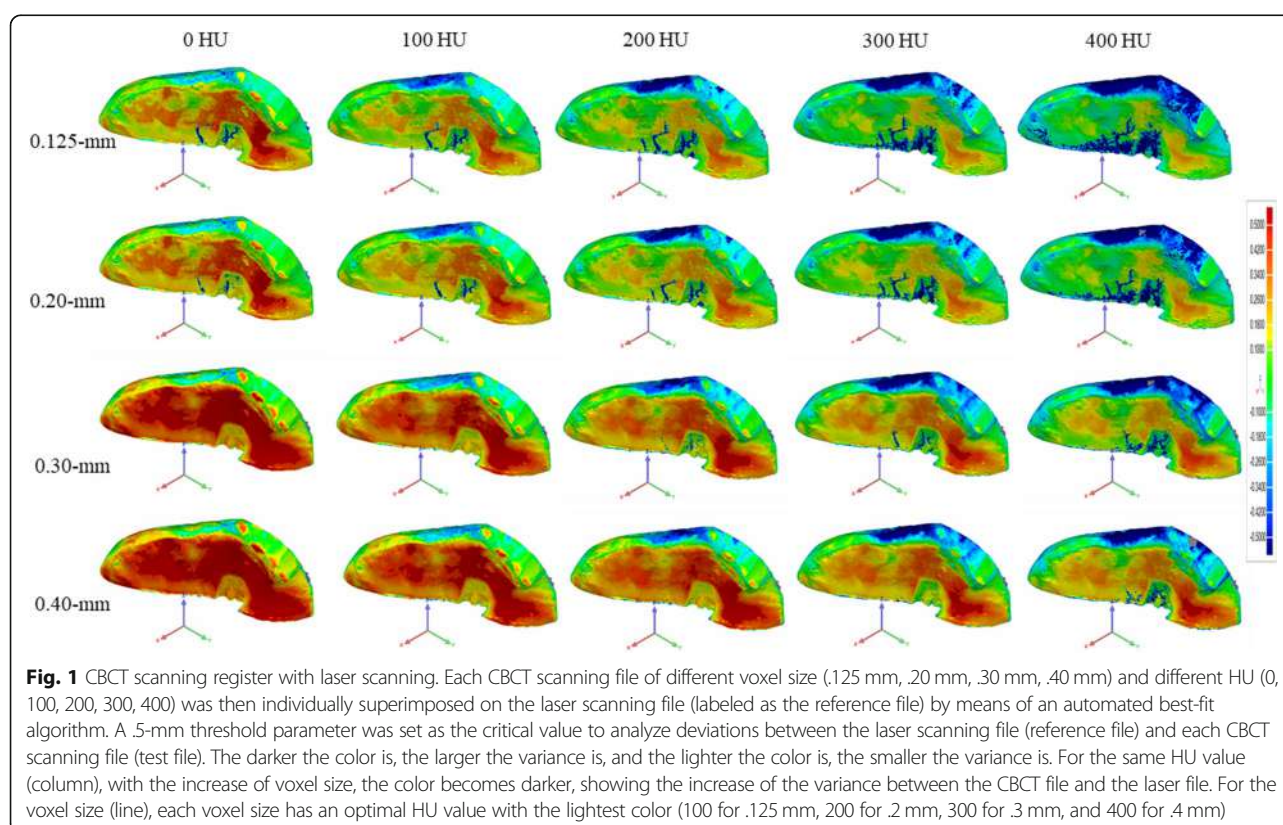
were set as 0, 100, 200, 300, and 400, respectively, for each voxel size, and the maximum segmentation thresholds remained unchanged. The 3D models of CBCT scans were then imported as STL format files into Geomagic Control software (3D Systems) for volumetric measurement and registration. Each CBCT scanning file (labeled as the test file) was then individually superimposed on the laser scanning file (labeled as the reference file) by means of an automated best-fit algorithm. A color map was made for comparison of the mean iterative distance of the CBCT scan and the laser scan (Fig. 1). A .5-mm threshold parameter was set as the critical value for the analysis of deviations between the laser scanning file (reference file) and each CBCT scanning file (test file) (Fig. 2). Any points in the test file deviating from the reference file by more than .5 mm in the positive or negative direction were considered to be beyond the upper or lower limits, accordingly. Reports were generated for separate calculation of the total positive and negative deviations (Fig. 3).

IBM SPSS Statistics 20.0 (IBM, Chicago, IL, USA) was used for statistical analysis. Due to the different sizes of the mandibular pieces, the within-group variation was the major difference; thus, we chose a paired *t* test (each test file and reference file) to analyze the effect of the Hounsfield unit threshold of segmentation with different voxel sizes.

Results

The means and standard deviations of the HU thresholds of water, air, and wax were 55.0 ± 10.8 , -980.0 ± 13.7 , and -270.0 ± 36.8 , respectively. The means of the volume measurements of laser scans and CBCT scans are presented in Table 2. The measurements of CBCT-scan volumes deviated from those of laser-scan volumes by +7.67% to -3.05%, with different HU thresholds of segmentation and voxel sizes (Table 2). The deviation increased with the voxel size. For each voxel size, there was a more suitable HU threshold of segmentation that showed no significant difference from the laser scan (minimum 100 for .125 mm, 200 for .20 mm, 300 for .30 mm, and 400 for .40 mm). The other testing HU threshold of segmentation showed a significant difference from the reference ($P < .05$).

The mean iterative distance of the superimposition of each CBCT scanning file and laser scanning file was auto-calculated by the Geomagic software, and a histogram was made to show the deviation visually (Fig. 2). For the .125-mm voxel size, the least iterative distance was achieved when we chose 100 as the minimum HU threshold of segmentation. This applied equally to 200 for the .20-mm voxel size, 300 for the .30-mm voxel size, and 400 for the .40-mm voxel size as the minimum HU threshold of segmentation. Statistical significance can be seen in the .40-mm group ($P = .07$). Seen as a whole, the



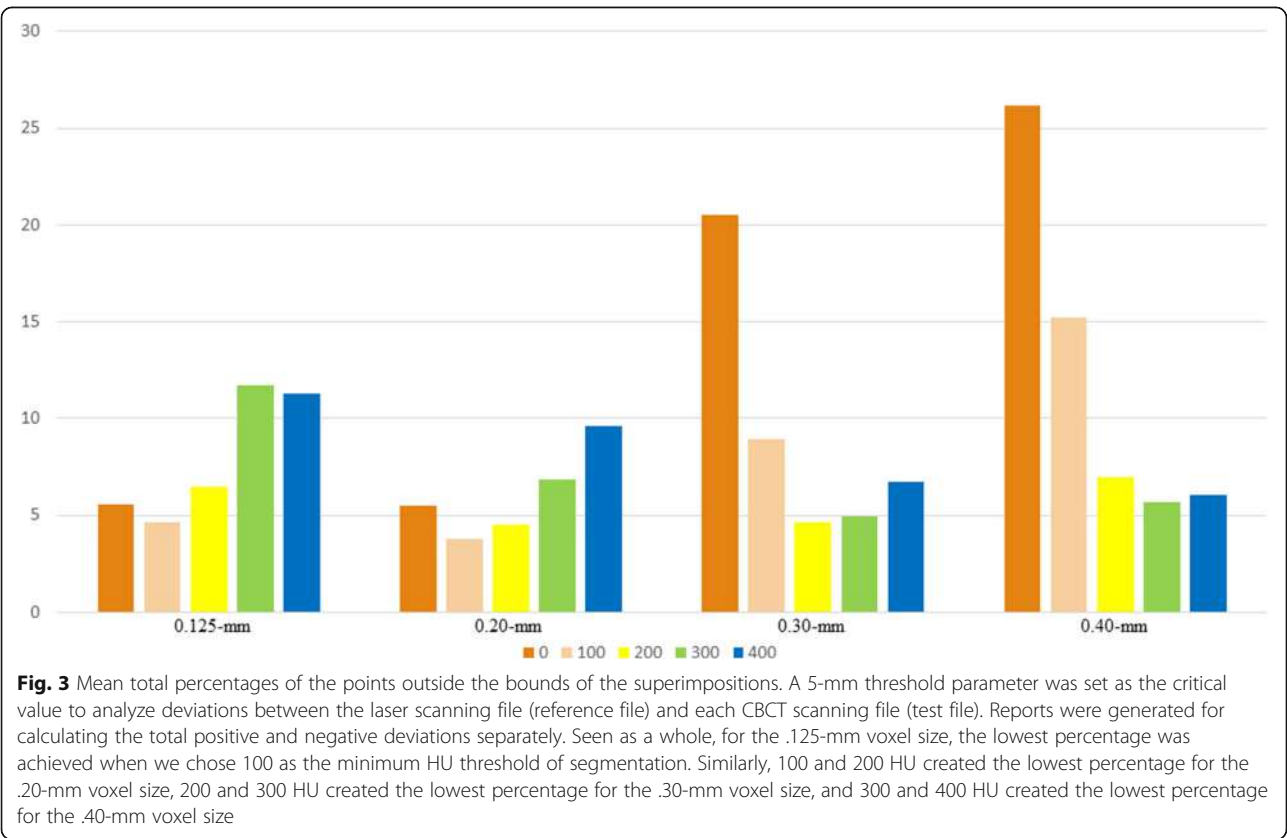
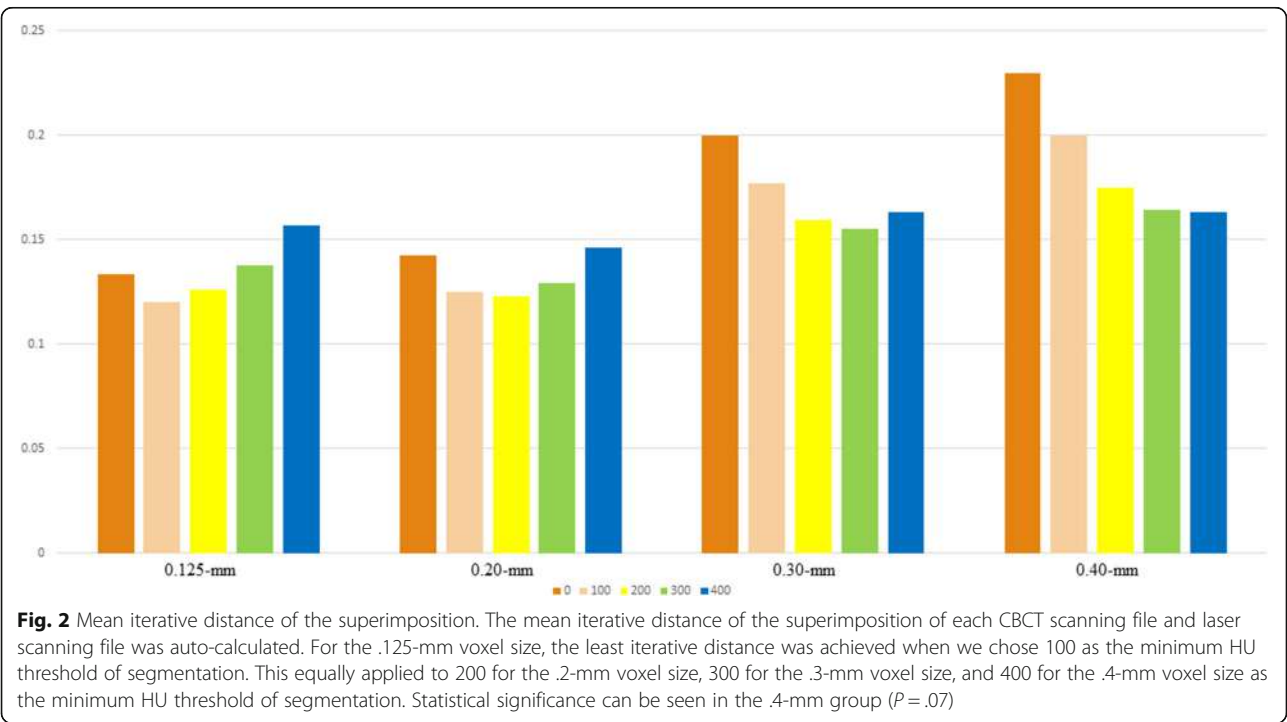


Table 2 Volumetric measurement of different CBCT voxel sizes with 5 minimum thresholds compared with laser scan

Voxel size (mm)	HU	Mean vol (mm ³)	Deviation%	P
.125	0	24,436.83	1.91	.004*
	100	24,007.69	.12	.794
	200	23,690.75	-1.2	.018*
	300	23,350.4	-2.62	.000*
	400	23,014.19	-4.02	.000*
.20	0	24,695.64	2.99	.000*
	100	24,282.46	1.27	.020*
	200	23,959.73	-.07	.855
	300	23,601.82	-1.57	.009*
	400	23,246.79	-3.05	.000*
.30	0	25,494.24	6.32	.000*
	100	24,968.95	4.13	.000*
	200	24,506.46	2.2	.002*
	300	24,018.74	.17	.757
	400	23,604.68	-1.56	.018*
.40	0	25,817.22	7.67	.000*
	100	25,275.56	5.41	.000*
	200	24,771.32	3.31	.000*
	300	24,291.91	1.31	.044*
	400	23,898.76	-.33	.52
Laser		23,978.13		

*P < 0.05

mean iterative distance increased with the voxel size. Mean total percentages of the points outside the bounds of the superimpositions were also recorded (Fig. 3). For the .125-mm voxel size, the lowest percentage was achieved when we chose 100 as the minimum HU threshold of segmentation. Similarly, 100 and 200 HU created the lowest percentages for the .20-mm voxel size, 200 and 300 HU created the lowest percentage for the .30-mm voxel size, and 300 and 400 HU created the lowest percentage for the .40-mm voxel size.

Discussion

The quality of images obtained by CBCT depends on many acquisition parameters such as tube voltage, tube current, the field of view (FOV), HU threshold of segmentation, and voxel size [9]. To control the above factors, we chose the same CBCT scanner, the same scanning tube voltage and tube current, and the same FOV. The main variables were voxel sizes (.125 mm to .40 mm) and HU threshold settings of segmentation and will be discussed below.

Voxel size is one of the critical parameters that influence the volumetric measurement of 3D-reconstructed jaws. Voxel size is the minimum unit of digital data

segmentation in three-dimensional space, similar in concept to pixels in two-dimensional space. It is of paramount importance in terms of scanning and reconstruction times, as well as quality of CBCT images [11]. Ye et al. [10] discovered that the volume measurements of teeth tended to be larger with increasing voxel sizes during scanning (with laser scanning as the gold standard). Sang et al. [12] found that increasing voxel resolution from .30 to .15 mm did not result in increased accuracy of 3D tooth reconstruction (with 3Shape optical scanning as the gold standard). Hassan et al. [13] investigated the influence of voxel size on the quality of the 3D surface models of the dental arches from CBCT and found that large voxel size reduced the visibility of the occlusal surfaces and bone in the anterior region in both the maxilla and mandible.

Meanwhile, the HU threshold is also an important parameter in 3D reconstruction. Computed tomography uses HU — a numeric value that represents tissue density by quantitative measurement of tissue absorptivity for x-rays — as its unit of measure. Computed tomography values can be calculated as $(\mu_{\text{tissue}} - \mu_{\text{water}}) * k / \mu_{\text{water}}$, where μ is the x-ray absorption coefficient of tissue, and k is the constant [10]. However, there is insufficient research on the influence of voxel size and reconstruction threshold on the accuracy of volumetric measurement of the mandible from CBCT. There is a significant difference among the HU values of CBCT obtained by different manufacturers. The CBCT in this study was calibrated based on each manufacturer's instructions as the reference, and the HU values of CBCT we obtained were close to the CT values. Therefore, the results of this study can provide some reference to guide this kind of CBCT reconstruction.

The deviation of volumetric measurement may be due to the artefacts of CBCT scanning and 3D reconstruction. Artefacts are discrepancies between the reconstructed visual image and the actual physical image which degrade the quality of CBCT images [14], including extinction artefacts, beam-hardening artefacts, partial volume effect, 'aliasing' artefacts, ring artefacts, and motion artefacts, as well as noise and scatter [15]. In this study, we found that the mandibular volume measurements from the CBCT scans were larger than those from the laser scans with the increase of voxel sizes. This result might be owing to the surface-surrounding artefacts that can be induced by the partial-volume effect and scatter, which act as halation around the mandible. The partial-volume effect [10, 16] is a common artefact in computed tomography and can produce deviation in the digital image. According to the theory of the partial-volume effect, the value of each pixel (voxel size) on the CT image represents the average CT value of the corresponding unit. It cannot reflect the CT value of the diverse structures in the unit faithfully. Therefore, when

we used a larger voxel size in our study, the volume of reconstructed bone was larger than its reality by artefacts. There is little research on the relationship of the HU threshold of segmentation and CBCT volumetric measurement.

In our study, we showed that with increased voxel size, the artefacts of CBCT scanning increased from .125 mm to .40 mm, and the volumetric measurement increased for each corresponding HU threshold of segmentation. For this reason, a smaller range of thresholds is required to diminish the increased artefacts. This explains why the optimal HU threshold of segmentation differs, to some extent, with different voxel sizes. The minimum threshold increases, the range of threshold narrows, and some artefacts may be hidden.

In this study, we chose laser scanning as the reference to compare the accuracy of CBCT volumetric measurement with different HU thresholds of segmentation and voxel sizes. Micro-computed tomography and laser scanning were often used as references in previous research. According to Teeter et al. [17], both the micro-computed tomography and laser scans produced complete reconstructions of the surfaces, and micro-computed tomography has superior repeatability compared with laser scanning (mean of 1 mm for micro-computed tomography vs 19 mm for laser scans). Micro-computed tomography requires a rather long time to scan and reconstruct, depending on the size of the object and scan resolution. Laser scanning, in contrast, requires a much shorter time, and its data are much more amenable to transmission and processing. Today, many scholars use laser scanning as the reference. Ye et al. [10] used laser scanning as the reference to study the accuracy of volumetric measurements of teeth in vitro by CBCT. Sang et al. [12] used laser scanning as the reference to assess the linear, volumetric, and geometric accuracy of 3D reconstructions from CBCT and to investigate the influence of voxel size and the CBCT system on the reconstruction results. Lemos et al. [18] evaluated the reliability of measurements made on digital cast models scanned in the 3Shape R700 scanner and found laser scanning to be reliable in producing a digital version of the physical models.

ALARA [19], the acronym used in radiation safety (“As Low As Reasonably Achievable”), requires that ionizing radiation be maintained as low as reasonably achievable, which means choosing the minimum resolution that does not affect diagnostic accuracy. Ionizing radiation (IR) is a known carcinogen and produces DNA damage directly or indirectly. A recent study reported that the dental pulp stem cells (DPSCs) exposure to CBCT induced transient DNA damage and persistent inflammatory reaction in DPSCs [20]. Images acquired in smaller voxel sizes exactly have better quality, but also increase the radiation dose to the patient. There may be

no significant difference in the diagnostic outcome compared with slightly lower resolution images within a certain range, so we must choose optimal voxel size based on the reliability and accuracy of the diagnostic outcome and radiation dose. Many of these parameters can be varied according to the diagnostic task, but no protocols have yet been established for specific diagnostic tasks in dentistry. This study paid specific attention to the optimal HU thresholds for different voxel sizes, which may provide a new avenue to a suitable protocol.

Limits

In this research we found that voxel sizes and HU thresholds indeed have significant effects on the volumetric measurement of CBCT 3D reconstruction, which deserves more attention in our clinics. Clinicians need to choose suitable voxel size to do the scanning and optimal HU thresholds to do the reconstruction in order to improve the accuracy of volumetric measurement. In consideration of radiation dose, we adopted an in vitro experiment for preliminary exploration and chose pig mandibles as samples, which may cause some unavoidable divergence due to the anatomic differences between humans and pigs. Only one CBCT machine was adapted in this study and this may be a limitation of this research. Also, an in vitro experiment cannot completely reflect true clinical conditions, so an in vivo experiment is expected in future research. Larger sample sizes are also anticipated. Also, only one CBCT machine was adapted in this study and this may influence the validity of this research.

Conclusions

Voxel sizes and Hounsfield unit thresholds influence the accuracy of volumetric measurements in CBCT scanning. The artifacts increase with the voxel size, and there exist optimal Hounsfield unit thresholds correspond to different voxel sizes. We are thus reminded to select optimal parameters to perform CBCT scanning and 3D reconstruction in clinical work.

Abbreviations

3D: Three-dimensional; CBCT: Cone-beam computed tomography; FOV: Field of view; HU: Hounsfield units

Acknowledgements

Not applicable.

Authors' contributions

DT performed the main study and drafted the manuscript. XLG and CCL helped to acquire data. YLJ analyzed and interpreted the data. YNS was a major contributor in designing the manuscript. FB designed the main scheme of the research and modified the manuscript. All authors read and approved the final manuscript.

Funding

No funding was obtained for this study.

Availability of data and materials

The datasets used and/or analysed during the current study are available from the corresponding author on reasonable request.

Ethics approval and consent to participate

This study was approved by the Institutional Review Board of Shanghai Ninth People's Hospital affiliated to Shanghai Jiao Tong University, School of Medicine (2018–87-T78).

Consent for publication

Not applicable.

Competing interests

The authors declare that they have no competing interests.

Received: 5 June 2019 Accepted: 18 August 2019

Published online: 04 September 2019

References

- Almaqrani BS, Alhammadi MS, Cao B. Three dimensional reliability analyses of currently used methods for assessment of sagittal jaw discrepancy. *J Clin Exp Dent*. 2018;10(4):e352–e60.
- Pelo S, Correria P, Gasparini G, Marianetti TM, Cervelli D, Grippaudo C, et al. Three-dimensional analysis and treatment planning of hemimandibular hyperplasia. *J Craniofac Surg*. 2011;22(6):2227–34.
- Hariharan A, Diwakar NR, Jayanthi K, et al. The reliability of cephalometric measurements in oral and maxillofacial imaging: cone beam computed tomography versus two-dimensional digital cephalograms. *Indian J Dent Res*. 2016;27(4):370–7.
- Montúfar J, Romero M, Scougall-Vilchis RJ. Automatic 3-dimensional cephalometric landmarking based on active shape models in related projections. *Am J Orthod Dentofac Orthop*. 2018;153(3):449.
- Gupta A, Kharbanda OP, Sardana V, Balachandran R, Sardana HK. A knowledge-based algorithm for automatic detection of cephalometric landmarks on CBCT images. *Int J Comput Assist Radiol Surg*. 2015;10(11):1737.
- Ye N, Long H, Zhu S, Yang Y, Lai W, Hu J. The accuracy of computer image-guided template for mandibular angle Osteotomy. *Aesthet Plast Surg*. 2015;39(1):117–23.
- Lee JW, Lim SH, Kim MK, Kang SH. Precision of a CAD/CAM-engineered surgical template based on a facebow for orthognathic surgery: an experiment with a rapid prototyping maxillary model. *Oral Surg Oral Med Oral Pathol Oral Radiol*. 2015;120(6):684.
- Lo L-J, Weng J-L, Ho C-T, Lin H-H. Three-dimensional region-based study on the relationship between soft and hard tissue changes after orthognathic surgery in patients with prognathism. *PLoS One*. 2018;13(8):e0200589.
- Kamburoglu K, Murat S, Kolsuz E, Kurt H, Yuksel S, Paksoy C. Comparative assessment of subjective image quality of cross-sectional cone-beam computed tomography scans. *J Oral Sci*. 2011;53(4):501–8.
- Ye N, Jian F, Xue J, Wang S, Liao L, Huang W, et al. Accuracy of in-vitro tooth volumetric measurements from cone-beam computed tomography. *Am J Orthod Dentofac Orthop*. 2012;142(6):879–87.
- Spin-Neto R, Gotfredsen E, Wenzel A. Impact of voxel size variation on CBCT-based diagnostic outcome in dentistry: a systematic review. *J Digit Imaging*. 2013;26(4):813–20.
- Sang YH, Hu HC, Lu SH, Wu YW, Li WR, Tang ZH. Accuracy assessment of three-dimensional surface reconstructions of in vivo teeth from cone-beam computed tomography. *Chin Med J*. 2016;129(12):1464–70.
- Hassan B, Couto Souza P, Jacobs R, de Azambuja Berti S, van der Stelt P. Influence of scanning and reconstruction parameters on quality of three-dimensional surface models of the dental arches from cone beam computed tomography. *Clin Oral Investig*. 2010;14(3):303–10.
- Nagarajappa AK, Dwivedi N, Tiwari R. Artifacts: the downturn of CBCT image. *J Int Soc Prev Community Dent*. 2015;5(6):440–5.
- Schulze R, Heil U, Gross D, Bruellmann DD, Dranischnikow E, Schwanecke U, et al. Artefacts in CBCT: a review. *Dentomaxillofac Radiol*. 2011;40(5):265–73.
- Baumgaertel S, Palomo JM, Palomo L, Hans MG. Reliability and accuracy of cone-beam computed tomography dental measurements. *Am J Orthod Dentofac Orthop*. 2009;136(1):19–25.
- Teeter MG, Brophy P, Naudie DD, Holdsworth DW. Comparison of micro-computed tomography and laser scanning for reverse engineering orthopaedic component geometries. *Proc Inst Mech Eng H*. 2012;226(3):263–7.

- Lemos LS, Rebello IM, Vogel CJ, Barbosa MC. Reliability of measurements made on scanned cast models using the 3Shape R700 scanner. *Dentomaxillofac Radiol*. 2015;44(6):20140337.
- Kaplan DJ, Patel JN, Liporace FA, Yoon RS. Intraoperative radiation safety in orthopaedics: a review of the ALARA (as low as reasonably achievable) principle. *Patient Saf Surg*. 2016;10:27.
- Virag P, Hedesiu M, Soritau O, Perde-Schrepler M, Brie I, Pall E, et al. Low-dose radiations derived from cone-beam CT induce transient DNA damage and persistent inflammatory reactions in stem cells from deciduous teeth. *Dentomaxillofac Radiol*. 2019;48(1):20170462.

Publisher's Note

Springer Nature remains neutral with regard to jurisdictional claims in published maps and institutional affiliations.

Ready to submit your research? Choose BMC and benefit from:

- fast, convenient online submission
- thorough peer review by experienced researchers in your field
- rapid publication on acceptance
- support for research data, including large and complex data types
- gold Open Access which fosters wider collaboration and increased citations
- maximum visibility for your research: over 100M website views per year

At BMC, research is always in progress.

Learn more biomedcentral.com/submissions




RESEARCH ARTICLE

Open Access



Milled versus moulded mock-ups based on the superimposition of 3D meshes from digital oral impressions: a comparative in vitro study in the aesthetic area

Francesca Cattoni^{1,2}, Giulia Teté^{2,3}, Alessandro Mauro Calloni^{1,2}, Fabio Manazza^{1,2}, Giorgio Gastaldi^{1,4} and Paolo Cappare^{1,2*} 

Abstract

Background: Aesthetic porcelain veneers proved to be a long-term reliable prosthetic solution, ensuring minimal invasiveness. The use of veneers requires an adhesive cementation technique, so maintaining as much enamel as possible is to ensure lasting success. A diagnostic mock-up is a key tool that allows a preview of the outcome of the aesthetic restoration: it is obtainable both in an analog and digital way. With the recent developments in impression technology and the ever so fast growing use of CAD-CAM technologies it is useful to understand the pros and cons of either one of these techniques (analog and digital) in order to identify the easier and more convenient workflow in aesthetic dentistry.

Methods: After taking pictures and impressions of the dental arcs of a patient in need of aesthetic rehabilitation, 52 resin models were produced and a digital drawing of the smile was outlined. Both an analog and a digital wax-up were obtained from two of the 52 models: the latter was obtained using digital impressions and a dedicated software. The analog wax-up was then used to produce 25 matrices that have later been used to mould 25 resin mock-ups using a traditional moulding protocol (Control Group - CG). The digital wax-up was used to mill 25 PMMA mock-ups. Each mock-up, both milled and moulded (total 50), was then laid on the other 50 resin models as a digital impression of it was taken. The STL files of the milled mock-ups were compared with the 3D CAD wax-up made using a specific software. The STL files of the analog printed mock-ups were compared with the traditional wax-up design. A statistical analysis was carried out to evaluate the difference between the groups.

Results: The statistical analysis showed a significant difference ($P > 0.01$) between the mean value of the distance between the points of the overlapping STL meshes in GC (0.0468 mm) and in TG (Test Group - TG) (0.0109 mm).

Conclusions: The study showed a difference in accuracy between traditional moulded and milled mock-ups compared to their original wax-up. The data analysis reports that the digital method allows for greater accuracy. Within the limitations of this study, a fully digital workflow is to be considered more reliable when it comes to creating an esthetic mockup: the digital procedure has been shown to be more accurate than the one made manually which is much more operator dependent and it brings an increase to the chance of error, and that could ultimately affect the final result.

Keywords: Digital planning, Digital smile design, Mock up, Milling mock up, Digital workflow

* Correspondence: cappare.paolo@hsr.it

¹Dental School, Vita-Salute San Raffaele University, Milan, Italy

²Department of Dentistry, IRCCS San Raffaele Hospital, Milan, Italy

Full list of author information is available at the end of the article



© The Author(s). 2019 **Open Access** This article is distributed under the terms of the Creative Commons Attribution 4.0 International License (<http://creativecommons.org/licenses/by/4.0/>), which permits unrestricted use, distribution, and reproduction in any medium, provided you give appropriate credit to the original author(s) and the source, provide a link to the Creative Commons license, and indicate if changes were made. The Creative Commons Public Domain Dedication waiver (<http://creativecommons.org/publicdomain/zero/1.0/>) applies to the data made available in this article, unless otherwise stated.

Background

In recent years, the expectations of dental patients regarding aesthetic appearance have increased greatly. Aesthetic results have already reached comparable importance to masticatory function [1, 2]. Porcelain veneers proved to be a long-term reliable solution, ensuring maximum aesthetics success and minimal invasiveness [3, 4]. It is a priority to the clinician to pursue the least invasive procedure in every prosthetic restoration, preserving as much natural tooth structure as possible and respecting surrounding soft tissues [5]. Furthermore, since the use of veneers requires an adhesive cementation technique, maintaining as much enamel as possible is to ensure lasting success [6]. A diagnostic mock-up is to be intended as a tool that allows a better understanding of the patient's aesthetic expectations previewing the outcome of the aesthetic restoration, at a stage where it is still very easy to make changes according to patient's requests. It improves the communication with the patient, allowing prosthetic restorations to be achieved more successfully ([7, 8]). Moreover, a protocol that uses a diagnostic mock-up to guide the preparation has proved to be more conservative than a classical

non-guided preparation made by the clinician [9]. As reported by Magne et Al., a veneer preparation driven by the final volume of the restoration (a diagnostic mock-up) allows for more enamel preservation, avoiding unnecessary over-preparation by only removing the structure needed to create proper prosthetic thicknesses, and more predictable outcome in terms of bonding, biomechanics and final aesthetics [10]. According to Coachman's protocol, the realization of the diagnostic wax-up is preceded and guided by the Digital Smile Design, which has proved to be a fundamental and useful tool for improving communication and patient's acceptance of the dental procedure [11–15]. This articulated workflow requires several steps that can lead to various inaccuracies. For instance, the mock-up molding phase on the existing tooth appears to be a very complex and heavily operator-dependent process. The most common problems related to the resin mock-ups are: the unevenly balanced positioning of the matrix, the inhomogeneous pressure during resin hardening, the difficulty in remove excess resin and the while finishing part to get a good final result [10]. Result that, if excessively discordant from what was promised and



UPPER ARCH

	1.3	1.2	1.1	2.1	2.2	2.3
width	6.00mm	5.64mm	8.44mm	8.67mm	6.00mm	6.04mm
height	9.44mm	9.04mm	10.54mm	10.64mm	9.57mm	9.44mm
rotation	0.00°	0.00°	0.00°	0.00°	0.00°	0.00°

LOWER ARCH

	4.3	4.2	4.1	3.1	3.2	3.3
width	6.70mm	6.14mm	5.44mm	5.44mm	6.14mm	6.70mm
height	10.87mm	10.64mm	9.60mm	9.60mm	10.64mm	10.87mm
rotation	0.00°	0.00°	0.00°	0.00°	0.00°	0.00°

Fig. 1 The DSS report. All the numeric measurements of the digital design are recorded and can be sent to the technician for a more efficient communication

evaluated with the patient through the DSS software preview, could cause communication problems, misunderstanding and disappointment, or even the need to repeat the procedure, causing a waste of time and increasing the number of appointments required. Today, in attempt to minimize the chance of error and to shorten working times, the clinician can rely on effective smile planning tools and CAD / CAM systems (3D-Lynx Srl. Varese, Italy). Such systems, as shown by McLaren et Al., have proved their reliability in the realization of adhesive restorations in aesthetic areas [16]. A dedicated digital smile planning software with both two-dimensional and three dimensional features, is able to obtain excellent results in a simple, standardized and less operator-dependent way (3D-Lynx Srl. Varese, Italy). The aim of this study is to evaluate the traditional mock-up production method, which involves mock-up molding with a silicone matrix of the wax-up, compared to an exclusively digital workflow, which consists of mock-up milling from a CAD design, based on a digital optic impression. The accuracy of the two different types of mock-ups was compared each to their specific design and diagnostic wax-up.

Methods

A patient (male) in need of an additive restoration in the anterior area was selected in the dentistry department of IRCCS San Raffaele Hospital. Diagnostic pictures were taken during the first appointment, as well as analog polyether impressions of the upper arch (Impregum Penta, 3 M ESPE, Sain Paul, Minn. USA). The virtual drawing of the final restoration was then obtained using a digital smile design software called DDS-2D (3D-Lynx Srl. Varese, Italy) (Fig. 1). Starting from two photos of the patient, a extraoral shot (Fig. 2) with a maximum smile and an intra-oral one with slightly disclosed dental arches (Fig. 3) a digital drawing of the new smile was obtained and shown to the patient. This drawing was based



Fig. 2 Extra-oral photograph with with maximum smile



Fig. 3 Intraoral photograph with slightly spaced teeth, with specific glasses

on standard dental shapes included in a library inside the 2D software (Fig. 4). The digital restoration project was then realized (Fig. 5). This study was approved by the ethical board of the IRCCS San Raffaele Hospital of Milan (9/INT/2015). The patient provided their informed consent in writing.

Traditional wax-up (control group)

Fifty-two resin models were obtained from the analog impressions: one of them was used to produce a traditional wax-up by the technician, one was scanned using a laboratory desktop scanner (Scanner S-6000, Zirkonzhan Srl, Gais BZ) finally obtaining a STL file (Fig. 6) that allowed the design of a diagnostic mock-up using the Smile Design Software 3D-CAD expansion DDS-3D (3D-Lynx s.r.l., Varese, Italy). For the analog diagnostic wax-up, the software report provided the technician with all the images (Fig. 1) and all the operations performed by the clinician, indicating, with linear measures, how lengthened or shortened each measure had been during the design process. A intra-oral scanner (Dental Wings Intraoral Scanner, Dental Wings, Montreal, Canada) was then used to generate a STL file of the wax-up itself (Fig. 7).

Twenty-five silicone matrices (Fig. 8) were produced starting from the traditional wax-up (Fig. 9) (CG - Control group) and they were then used to mould a dual curing compost resin mock-up (Protemp 4, 3 M ESPE, Saint Paul, Minn. USA) on 25 of the remaining 50 resin models. The other 25 were used as a base for the 25 milled resin mock-ups to be laid upon (TG - Test Group). Those milled resin mock-ups were obtained by the STL - CAD project. Finally a digital impression of each of the 50 mock-ups (both moulded and milled) was taken with an integral scanner (Dental Wings Intraoral Scanner, Dental Wings, Montreal, Canada) and later analyzed.



Fig. 4 The selected 3D teeth library

Digital wax-up (test group)

In order to obtain a digital wax-up, the STL files of the patient's dental arches were uploaded to DSS 3D, a software which is the direct 3D implementation of the aforementioned DSS 2D. This software is able to align the patient's photograph to the digital model and support. The CAD software allowed us to design a three-dimensional digital wax-up directly on the model. 25 resin mock-ups (PMMA - polymethyl methacrylate) were then milled from the from the digitally planned 3D wax-up. Each of these were then laid on the other 25 plaster models and as an optical digital impression was detected with the aforementioned intra-oral scanner. All the digital impressions of milled mock-ups, the moulded mock-ups, the wax-up and the STL file of the CAD design were then uploaded to a lab software (OpenText Exceed 2017-EIM-Waterloo, ON, Canada). A superimposition and segmentation of the digital files have been performed to ensure that the impressions were cut out all the same way so the comparisons could not be affected by the different extensions of the original scans. Using a comparison software by (CloudCompare, <https://www.cloudcompare.org>) (Fig. 10), the STL files of the digital impressions, of the 25 manually moulded mock-ups were compared with the digital impressions of the traditional analog diagnostic wax-up while the STL files of the milled mock-ups were compared with the CAD designed project made with CAD - DSS 3D software (3D Lynx - Varese, Italy). The Stl. Files were segmented to make sure that only the area of the wax up was taken into consideration during the comparison. This was done by overlapping the two meshes with a



Fig. 5 Diagnostic mock-up

“three point” manual alignment technique and measuring the average distance between the points of each one. This procedure represented also an index of the actual volumetric difference between them. Finally, the two methods were compared, evaluating which carried more errors and which remained more faithful to their design. Statistical analysis was carried out with SPSS-Student T-test, which allows to compare the mean values of two non-coupled data sets.

Results

Results has shown specific areas of accumulation of errors and deviations: the cervical margin and the incisal edge (Fig. 10). The reasons why these particular areas exhibited major alterations are likely to be that the area of the cervical margin is the point where the excess of resin is removed from the silicone matrix, a procedure that is understandably difficult to replicate, while the differences found at the incisal edge are plausibly associated with variations in the pressure exerted by the operator on the silicone matrix to keep it in place during the hardening phase of the resin. The incisal edge, in particular, is of great aesthetic importance since it is a focal point for the observer; excessive variations in this area between the design and mock-ups can surely upset the patient, who is able to perceive the diversity of what has been promised with what he is really trying in his mouth.

The statistical analysis showed a significant difference between the two types of mock-ups. The null hypothesis that claims that the differences between the two groups were due to chance must be therefore rejected. The result obtained thus showed a clear difference in accuracy between moulded and milled mock-ups compared to their design. In the first case, not only moulded mock-ups diverged significantly from the diagnostic wax-up, demonstrating less accuracy (how much a measure is

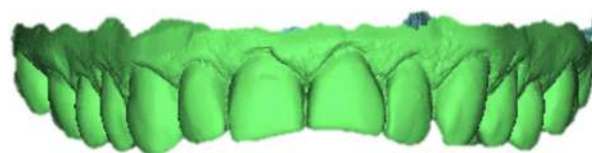


Fig. 6 STL file of the initial situation

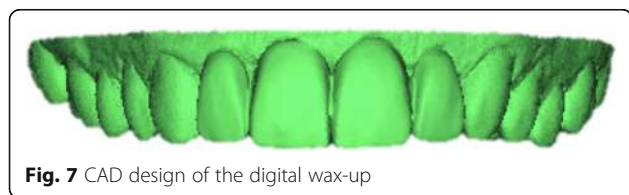


Fig. 7 CAD design of the digital wax-up

close to the true value of the size), but they also denoted a lesser degree of precision (how much measures are close to each other), indicated by the variance compared to the sample average (variance of moulded mock-ups: 0.0004). The milled mock-ups, on the contrary, were much more faithful to their CAD design, since the only error existing is that of the milling machine during the production phase, certainly negligible (variance of milled mock-ups: 0.00002) (Fig. 11). The milled mock-ups were therefore more accurate and precise. The use of the software allowed the comparison between the mean value of the distance between the points of the meshes superimposed on each other. Comparing the results obtained from the 50 evaluations performed, it was graphically very clear how the degree of overlap between moulded mock-ups and the diagnostic wax-up was significantly lower than that between milled mock-ups and the relative CAD design (Fig. 10).

From a more careful assessment, it was noted that the areas of accumulation of major deviations, which reflect errors during the realization, were consistently related to the portion of the cervical margin and the incisal edge.

The statistical analysis showed that the difference between mean value of the distance between the points of the meshes superimposed in the moulded mock-up group (0.0468 mm) compared to the milled mock-up group (0.0109 mm) was statistically significant ($P < 0.01$; $P = 0.300000000326$) (Fig. 12).

Discussion

The aim of this study is to evaluate which method allows for the closest match with the initial wax up design and to find which stage of the production is affected by the



Fig. 8 The silicon index used to mould the mock-up

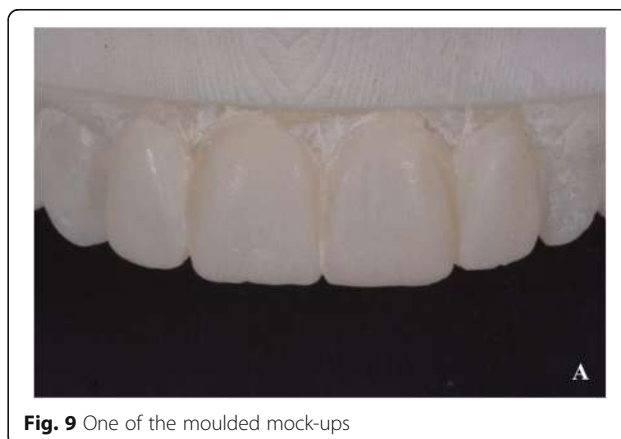


Fig. 9 One of the moulded mock-ups

greatest loss of precision, compromising the final result. In addition to the geometric and volumetric comparison between the different mock-ups and the respective wax-ups, the ease of execution for an inexperienced user has also been evaluated for each technique, since all the tests were carried out by an inexperienced operator. Many studies have shown how a mock up based approach can enable the clinician to provide patients with predictable aesthetics, since this particular kind of tool works with the psychology of patients, improving their attitude and compliance towards the treatment [10]. When starting a case, it is best for the practitioner to have in mind the end result since this has been shown to be vital in cases where the anterior teeth morphology is to be changed. A diagnostic wax-up can enhance the predictability of treatment by modeling the desired result in wax prior to treatment. It is critical to correlate the wax-up to the patient to avoid a result that appears optimal on the casts but does not correspond to the patient's smile [15–24]. Sancho-Puchades et al., point out that the use of a mock up will only be effective in an additive reconstructive case, while in subtractive cases it has to be used later in the treatment, after a minimum preparations of the natural teeth [25]. Wax ups and mock ups are reported to be extremely useful also for periodontal surgeons as tools used to perform crown lengthening procedures to enable future restorations in specific cases [13]. Results has shown specific areas of accumulation of errors and deviations; the cervical margin and the incisal edge. The reasons why these particular areas exhibited major alterations are likely to be that the area of the cervical margin is the point where the excess of resin is removed from the silicone matrix, a procedure that is understandably difficult to replicate, while the differences found at the incisal edge are plausibly associated with variations in the pressure exerted by the operator on the silicone matrix to keep it in place during the hardening phase of the resin. From the perspective of the impression techniques used in this study, the results showed that a

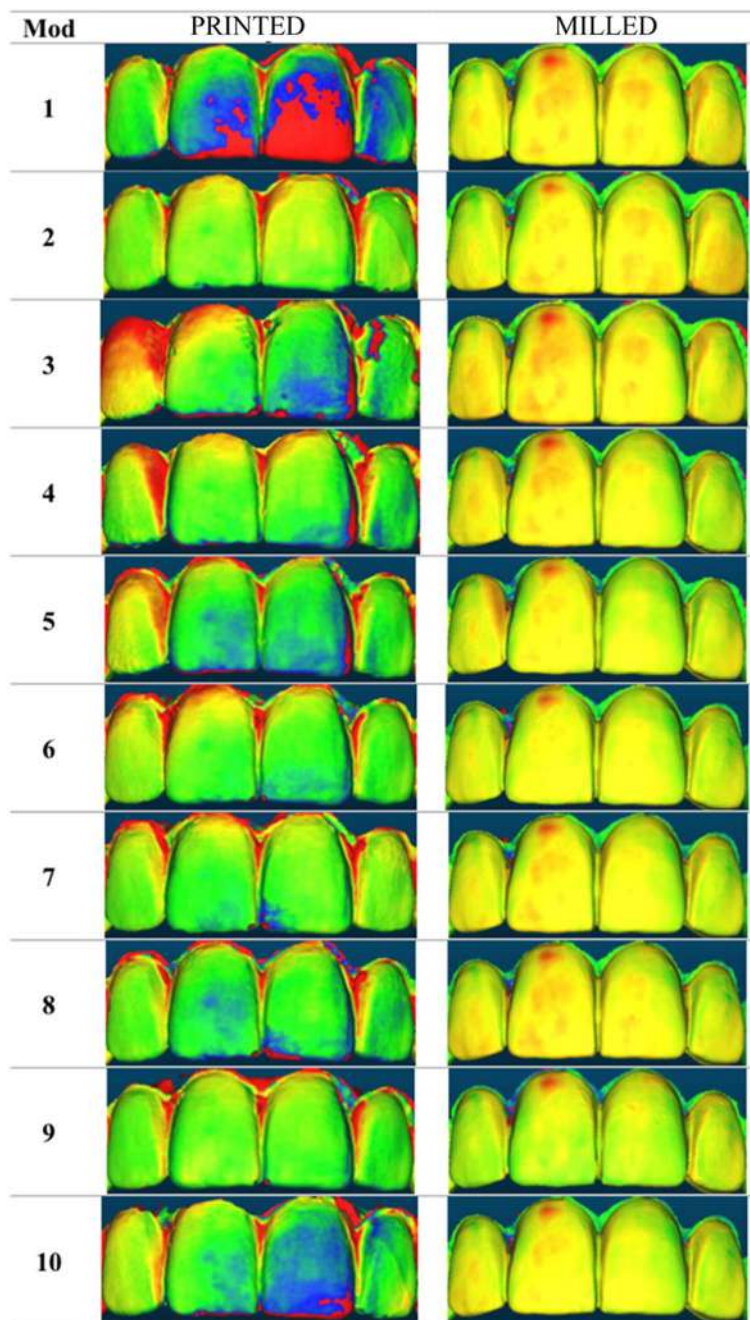


Fig. 10 Graphical evaluation of printed and milled mock-up overlays for each of the 10 respective models in occlusal view, made with CloudCompare software

digital workflow was to be considered preferable in the hands of an unexperienced operator. Studies in literature claim that even though material such as poly-vinyl siloxane present great accuracy, digital impression techniques seem to be superior in terms of time and material saving; at the same time, said techniques lack in repeatability and this aspect represents a problem in need of

solution [2]. As it was shown by the works of Gherlone et al. digital impression techniques manage to create an accurate physical model significantly improving efficiencies for the dental team and streamlining the workflow [17]. As far as the whole digital technique is concerned, a big role is played by the preview of the final result obtained through Digital Smile Design protocol. The use of

Number of samples	25	25
Mean	0,046842916	0,010395569
Variance	0,000417003	0,000016484
Standard Dev.	0,020420642	0,004059990
Student's T-Test	P = 0,000000003256218	
Difference between mean values was statistically significant per $P > 0,01$		

Fig. 11 Comparing mean values of two non-coupled data sets, with different variance

a smile designing software allows for an interdisciplinary collaboration between practitioners and this seems to improve the decision making process, ultimately decreasing the amount of intra-oral adjustments [12–28]. This tool allows the patient to preview the prosthetic result directly on a picture; it also provides the dental technician with all the necessary information on the execution of the work through a detailed report.

Conclusions

The study showed a difference in accuracy between traditional moulded and milled mock-ups compared to their original wax-up. The data analysis reports that the digital method allows for greater accuracy. Compared to the milled ones, the use of moulded mock ups would resolve in less accuracy of the mockup itself making it more difficult for the patient to visualize the final result

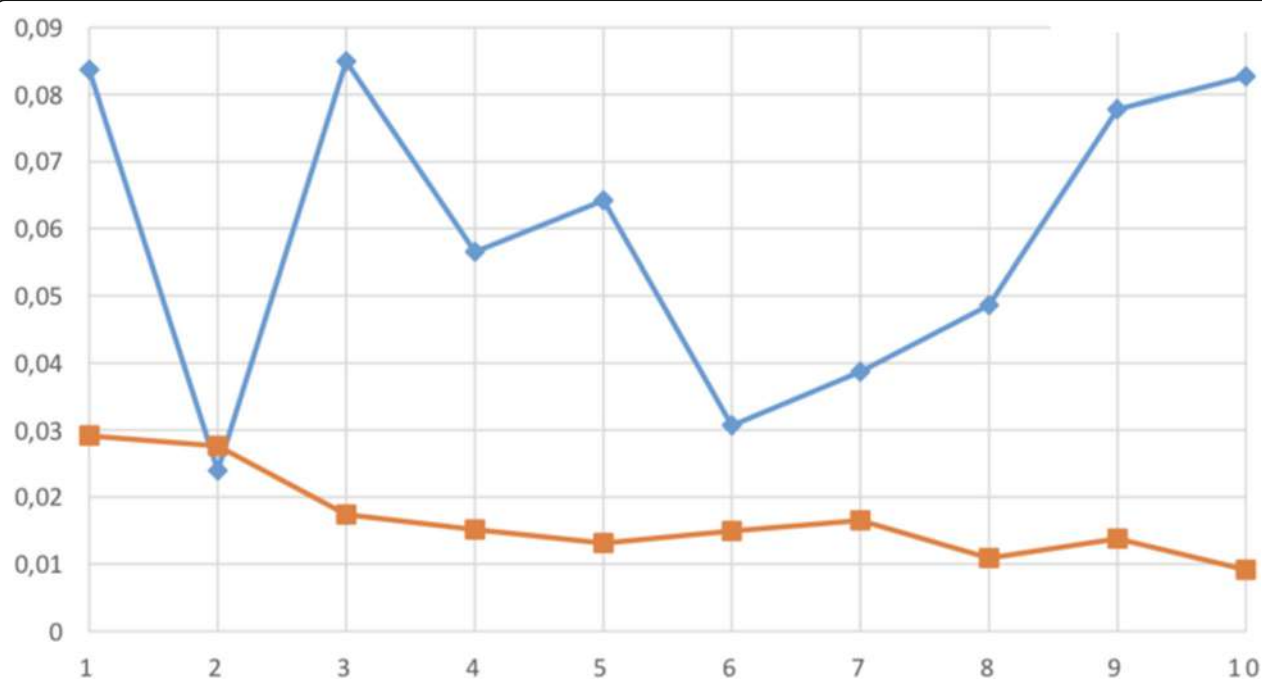


Fig. 12 Linear distribution of medium distances between points of the two meshes expressed in millimeters (blu line: average distance in the printed group, orange line average distance in the milled group). The graph points out a higher variability. In the moulded group and a higher deviation of the measurements compared to the milled group. This means that moulded mock ups tend to vary in shape and measurements from the original design of the wax up a lot more than the milled ones

while wearing it therefore compromising the validity and acceptance of the entire prosthetics treatment plan. Within the limitations of this study, a fully digital workflow consisting in digital impression, digital wax up and milling technology is to considered more reliable when it comes to creating an esthetic mockup: the manual procedure has been proven to be much more operator dependent and it brings an increase to the chance of error, and that could ultimately affect the final result.

Abbreviations

CG: Control Group; PMMA: Polymethyl methacrylate; TG: Test Group

Acknowledgements

Not applicable.

Authors' contributions

AC and FM designed the study, FC and AC did the acquisition of data and analysis, FC and PC interpreted the data, PC and GT have drafted the work or substantively revised it. The last revision by GG. All Authors read and approved the final submitted version of the manuscript (and any substantially modified version that involves the author's contribution to the study);

Funding

This study has not any funder.

Availability of data and materials

All materials described in this manuscript including all relevant raw data, will be freely available to any scientist wishing to use them for non-commercial purposes, without breaching participant confidentiality. The data of this research is available from Paolo Capparé (corresponding author).

Ethics approval and consent to participate

This study was approved by the ethical board of the Scientific Hospitalization and Care Institutes San Raffaele Hospital of Milan (IRCSS) (9/INT/2015). All patients provided their informed consent in writing.

Consent for publication

All authors agree to publish the data collected and all authors read and approve the manuscript.

Written informed consent for publication of potentially identifying information was obtained from the subject of our manuscript.

Competing interests

The authors declare that they have no competing interests.

Author details

¹Dental School, Vita-Salute San Raffaele University, Milan, Italy. ²Department of Dentistry, IRCCS San Raffaele Hospital, Milan, Italy. ³Specialisation School of Oral Surgery, Vita Salute San Raffaele University, Milan, Italy. ⁴Unit of Oral Maxillofacial Surgery, San Rocco Clinical Institute, Ome, Brescia, Italy.

Received: 26 February 2019 Accepted: 27 September 2019

Published online: 29 October 2019

References

- Dawood A, Purkayastha S, Patel S, MacKillop F, Tanner S. Microtechnologies in implant and restorative dentistry: a stroll through a digital dental landscape. *Proc Inst Mech Eng H*. 2010;224(6):789–96.
- Ting-Shu S, Jian S. Intraoral digital impression technique: a review. *J Prosthodont*. 2015;4(24):313–21.
- Joda T, Zarone F, Ferrari M. The complete digital workflow in fixed prosthodontics: a systematic review. *BMC Oral Health*. 2017;17(1):124.
- Peumans M, Van Meerbeek B, Lambrechts P, Vanherle G. Porcelain veneers: a review of the literature. *J Dent*. 2000;28(3):163–77.
- Little D. The Impact of Aesthetics in Restorative Treatment Planning. *Dent Today*. 2015;34(5):104, 106–07.
- Gurel G, Morimoto S, Calamita MA, Coachman C, Sesma N. Clinical performance of porcelain laminate veneers: outcomes of the aesthetic pre-evaluative temporary (APT) technique. *Int J Periodontics Restorative Dent*. 2012;32(6):625–35.
- Granell-Ruiz M, Fons-Font A, Labaig-Rueda C, Martinez-Gonzalez A, Roman-Rodriguez JL, Solà-Ruiz MF. A clinical longitudinal study 323 porcelain laminate veneers. Period study from 3 to 11 years. *Med Oral Patol Oral Cir Bucal*. 2010;15(3):531–7.
- Gurel G. Porcelain laminate veneers: minimal tooth preparation by design. *Dent Clin N Am*. 2007;51(2):419–31.
- Buonocore MG. A simple method of increasing the adhesion of acrylic filling materials to enamel surfaces. *J Dent Res*. 1955;34(6):849–53.
- Reshad M, Cascione D, Magne P. Diagnostic mock-ups as an objective tool for predictable outcomes with porcelain laminate veneers in esthetically demanding patients: a clinical report. *J Prosthet Dent*. 2008;99(5):333–9.
- Santos DMD, Moreno A, Vechiato-Filho AJ, Bonatto LR, Pesqueira AA, Junior MCL, de Medeiros RA, da Silva EV, Goiato MC. The importance of the lifelike esthetic appearance of all-ceramic restorations on anterior teeth. *Case Rep Dent*. 2015. <https://doi.org/10.1155/704348>.
- Veneziani M. Ceramic laminate veneers: clinical procedures with a multidisciplinary approach. *Int J Esthet Dent*. 2017;12(4):426–48.
- Gurrea J, Bruguera A. Wax-up and mock-up. A guide for anterior periodontal and restorative treatments. *Int J Esthet Dent*. 2014;9(2):146–62.
- Magne P, Belser UC. Novel porcelain laminate preparation approach driven by a diagnostic mock-up. *J Esthet Restor Dent*. 2004;16(1):7–16.
- Simon H, Magne P. Clinically based diagnostic wax-up for optimal esthetics: the diagnostic mock-up. *J Calif Dent Assoc*. 2008;36(5):355–62.
- Coachman C, Calamita MA, Sesma N. Dynamic documentation of the smile and the 2D/3D digital smile design process. *Int J Periodontics Restorative Dent*. 2017;37(2):183–93.
- Gherlone EF, Ferrini F, Crespi R, Gastaldi G, Capparé P. Digital impressions for fabrication of definitive all-on-four restorations. *Implant Dent*. 2015;24(1):125–9.
- Gherlone EF, Capparé P, Vinci R, Ferrini F, Gastaldi G, Crespi R. Conventional versus digital impressions for all-on-four restorations. *Int J Oral Maxillofac Implants*. 2016;31(2):324–30.
- Schmitter M, Seydler B. Minimally invasive lithium disilicate ceramic veneers fabricated using chairside CAD/CAM: a clinical report. *J Prosthet Dent*. 2012; 107(2):71–4.
- Gherlone EF, Mandelli F, Capparé P, Pantaleo G, Traini T, Ferrini F. A 3 years retrospective study of survival for zirconia-based single crowns fabricated from intraoral digital impressions. *J Dent*. 2014;42(9):1151–5.
- Cattoni F, Mastrangelo F, Gherlone EF, Gastaldi G. A New Total Digital Smile Planning Technique (3D-DSP) to Fabricate CAD-CAM Mockups for Esthetic Crowns and Veneers. *Int J Dent*. 2016. <https://doi.org/10.1155/6282587>.
- Seydler B, Schmitter M. Esthetic restoration of maxillary incisors using CAD/CAM chairside technology: a case report. *Quintessence Int*. 2011;42(7):533–7.
- Ercus S, Chung E, McLaren E. Esthetics with minimal tooth preparation achieved through a digital approach. *Compend Contin Educ Dent*. 2013; 34(6):428–31.
- Lin WS, Zandinejad A, Metz MJ, Harris BT, Morton D. Predictable restorative work flow for computer-aided design/computer-aided manufacture-fabricated ceramic veneers utilizing a virtual smile design principle. *Oper Dent*. 2015;40(4):357–63.
- Sancho-Puchades M, Fehmer V, Hämmerle C, Sailer I. Advanced smile diagnostics using CAD/CAM mock-ups. *Int J Esthet Dent*. 2015;10:374–91.
- Fasbinder DJ. Computerized technology for restorative dentistry. *Am J Dent*. 2013;26(3):115–20.
- Murchison DF, Burke FJ, Worthington RB. Incisal edge reattachment: indications for use and clinical technique. *Br Dent J*. 1999;186(12):614–9.
- Coachman C, Paravina RD. Digitally enhanced esthetic dentistry – from treatment planning to quality control. *J Esthet Restor Dent*. 2016;28(Suppl 1):S3–4.

Publisher's Note

Springer Nature remains neutral with regard to jurisdictional claims in published maps and institutional affiliations.

RESEARCH ARTICLE

Open Access



The application of virtual reality and augmented reality in Oral & Maxillofacial Surgery

Ashraf Ayoub* and Yeshwanth Pulijala

Abstract

Background: Virtual reality is the science of creating a virtual environment for the assessment of various anatomical regions of the body for the diagnosis, planning and surgical training. Augmented reality is the superimposition of a 3D real environment specific to individual patient onto the surgical field using semi-transparent glasses to augment the virtual scene. The aim of this study is to provide an overview of the literature on the application of virtual and augmented reality in oral & maxillofacial surgery.

Methods: We reviewed the literature and the existing database using Ovid MEDLINE search, Cochran Library and PubMed. All the studies in the English literature in the last 10 years, from 2009 to 2019 were included.

Results: We identified 101 articles related to the broad application of virtual reality in oral & maxillofacial surgery. These included the following: Eight systematic reviews, 4 expert reviews, 9 case reports, 5 retrospective surveys, 2 historical perspectives, 13 manuscripts on virtual education and training, 5 on haptic technology, 4 on augmented reality, 10 on image fusion, 41 articles on the prediction planning for orthognathic surgery and maxillofacial reconstruction. Dental implantology and orthognathic surgery are the most frequent applications of virtual reality and augmented reality. Virtual planning improved the accuracy of inserting dental implants using either a statistic guidance or dynamic navigation. In orthognathic surgery, prediction planning and intraoperative navigation are the main applications of virtual reality. Virtual reality has been utilised to improve the delivery of education and the quality of training in oral & maxillofacial surgery by creating a virtual environment of the surgical procedure. Haptic feedback provided an additional immersive reality to improve manual dexterity and improve clinical training.

Conclusion: Virtual and augmented reality have contributed to the planning of maxillofacial procedures and surgery training. Few articles highlighted the importance of this technology in improving the quality of patients' care. There are limited prospective randomized studies comparing the impact of virtual reality with the standard methods in delivering oral surgery education.

Keywords: Virtual reality, Augment reality, Haptic, Navigation, Oral surgery

* Correspondence: ashraf.ayoub@glasgow.ac.uk
Scottish Craniofacial Research Group, Glasgow University MVLS College,
School of Medicine, Dentistry and Nursing, Glasgow University Dental
School, 378 Sauchiehall Street, Glasgow G2 3JZ, UK



© The Author(s). 2019 **Open Access** This article is distributed under the terms of the Creative Commons Attribution 4.0 International License (<http://creativecommons.org/licenses/by/4.0/>), which permits unrestricted use, distribution, and reproduction in any medium, provided you give appropriate credit to the original author(s) and the source, provide a link to the Creative Commons license, and indicate if changes were made. The Creative Commons Public Domain Dedication waiver (<http://creativecommons.org/publicdomain/zero/1.0/>) applies to the data made available in this article, unless otherwise stated.

Background

Virtual reality “near reality” is the art and science of creating a virtual environment that provides a standardized, safe and flexible platforms for the assessment of various anatomical regions of the body for examination, diagnosis, planning and for the surgical training. To achieve this objective the user of this technology should be exposed to a realistic multidimensional visual stimulus. This to allow the full integration of cognitive, motor and mental functions of the operator. So, virtual reality describes a 3D computer generated environment which can be readily explored and interacted with by a person [1].

Augmented reality combines virtual reality with a 3D real environment specific to individual patient via a sophisticated registration process to achieve an integral image which augments the virtual scene with the real one. The integrated image is superimposed on the real environment using semi-transparent glass [2].

Based on the level of presence experienced by a user, virtual reality technology can be broadly classified into immersive virtual reality and non-immersive virtual reality. The basic elements of immersive reality experience include interactivity and involvement of the user within the virtual environment to create a sense of being “present” in the environment. Immersive virtual reality combines virtual reality with the added characteristics of the captured environment to provide the operator the sense of being in the scene, able to visualise the recorded image in 3D, and interact using a sophisticated wearable device that detects eye movements and track leap motions of the hands. Non-immersive virtual reality involves computer generated experiences on a desktop, while the user interacts with a mouse, in a virtual environment. Conventional surgical simulations fall under this category [3].

The advances in computing power have made simulated images much more realistic and much faster to create. The concept of virtual reality requires the development of specialised software to manipulate the recorded 3D images of the dental and oro-facial morphology. Therefore, it is important to highlight the existing methods of recording the 3D dental, skeletal and soft tissue structures of the dentofacial anatomy and be cognisant of the strength and the limitation of each method.

Different techniques have been developed for capturing dental, facial soft tissue and hard tissue data to produce 3D virtual models for the analysis and surgical planning. These techniques helped to overcome the drawbacks of the 2D photographs and radiographs. Four main types of 3D imaging systems have been used to capture dental and oro-facial structures which include cone-beam computed tomography (CBCT) Laser scanner, structured light scanner, and stereophotogrammetry [4]. These are essential for virtual planning of the

surgical correction of dento-facial deformities, maxillo-facial reconstruction after cancer resection and the simulation of facial fractures. The 3D acquisition of the various tissues of the head and neck region provides a realistic platform for maxillofacial training. The recorded images can be superimposed into the patient, using semi-transparent glasses, to allow the surgical procedure to be carried out in environment of augmented virtual reality.

CBCT is a 3D radiographic imaging of the craniofacial region; it is also known as “digital volume topography”. Even though CBCT is excellent in the imaging of hard tissue, the soft tissues are of poor contrast and the method does not produce the normal photorealistic appearance and the texture of the skin of the face. The stereophotogrammetry allows the 3D recording of facial texture which can be easily superimposed the 3D surface image of the CBCT. The time required for image acquisition is less than one millisecond, and it is highly accurate and reliable for the capture of face morphology. The capture 3D image of the skin can be accurately superimposed on the CBCT to produce a photorealistic image of the face over the captured facial skeleton [5].

Image artefacts are another limitation of CBCT, artefacts such as streaking, shading, and distortion are usually produced due to the presence of metallic restoration, fixed orthodontic appliances, or implants that are affecting the quality of the images. Therefore, the image of the defective dentition of the CBCT is usually replaced with the 3D image of the scanned dental models using either CT or laser scanner. The fusion of the images can be also achieved between the CBCT and the intra oral scans for orthognathic surgery planning, the accuracy of the method was within 0.5 mm [6].

Aim of the study

Provide an over view of the literature on the application of virtual and augmented reality in oral & maxillofacial surgery.

Methodology

We reviewed the literature and the existing database using Ovid MEDLINE search, Cochran Library and PubMed. All the studies in the English literature in the last 10 years, from 2009 to 2019, related to the application on virtual and or augmented reality in oral & maxillofacial surgery were considered. A set of key words guided the literature search including 3D, virtual reality, augmented reality, oral & maxillofacial surgery, dental and training. Key articles based on a robust methodology, adequate sample size and novel applications were retrieved for evaluation and the findings were presented in this manuscript.

Articles related to the detailed programming for virtual reality, abstracts, conference proceedings, letters to the editor, single case report, and those related to software development were excluded.

Results

We identified 101 articles related the broad application of virtual reality in dentistry and oral & maxillofacial surgery. These were subdivided as follows; Eight systematic reviews [7–13], (Table 1), 4 expert reviews, 9 case reports, 5 retrospective surveys, 2 historical perspectives, 13 manuscripts on virtual education and training, 5 on haptic technology, 4 on augmented reality, 10 on image fusion, 41 articles on the prediction planning for orthognathic surgery and maxillofacial reconstruction. The results will be presented under two main categories, clinical applications and surgical training.

Clinical application

Technological advances in virtual and augmented reality are enabling the application of the methods in dentistry, oral and maxillofacial surgery is the primary area of application, dental implantology and orthognathic surgery are the most frequent application [14]. Most of the publications were on the assessment of the accuracy of virtual planning for orthognathic surgery [15]. Three-dimensional virtual surgery and mandibular reconstruction after cancer resection and reconstruction were the main applications of virtual reality [16]. Virtual planes for mandibular and maxillary reconstruction can be achieved with an excellent match. This was demonstrated on 30 cases of complex head and neck

reconstruction including the planes of the resection, the length of the segmental defect and the distance between the transplanted segments and the remaining bone. There was excellent match between the virtual plans and the achieved results [17].

In a series of case reports the virtual surgical planning and hardware fabrication for open reduction and internal fixation of atrophic edentulous mandibular fractures were demonstrated [18–20].

In dental implantology, the accurate placement of dental implants is essential to meet the required functional and aesthetic demands [21]. Virtual reality has been extensively applied using the preoperative CBCT to determine the implant size, position, direction and proximity to vital structures. Various software packages are available for the virtual planning of dental implants [22]. The 3D virtual planning is then transferred onto the surgical field via either the static guide or the dynamic navigated approach [23]. The static transfer of the surgical plan is based on the virtual designing followed by fabrication of a surgical guide using computer-aided-design/computer-aided-manufacturing (CAD/CAM) to facilitate the insertion of dental implants. Various types of surgical guides are available based on the type of support, bony, mucosal or dental. A remarkable accuracy can be achieved with the sleeve-in-sleeve template is used in which multiple sleeves are applied and fixed to the surrounding bone to improve the precision of insertion of dental implants [24]. Various static guiding systems are available based on the CAD/CAM technology which includes EasyGuide, GPIS, Impla 3D, InVivoDental, Implant 3D, Nobel Bioguide and VIP (Implant Logic System) [25].

Table 1 Systematic reviews on the application of virtual reality and augmented reality in oral and maxillofacial surgery

Authors	Year	Scope	Main findings	Conclusion	Recommendations
Joda et al [7]	2019	Augmented and virtual reality in dental medicine	The technologies were mainly used for educational training	Virtual reality is a promising tool that could deliver predictable outcomes	Establishing technological standards and developing approved applications are essential
Maliha et al. [8]	2018	Haptic, physical and web-based simulators in maxillary surgery	Most of the studies “10” were on virtual reality haptic based simulators.	no studies with high level of evidence	Studies on the effectiveness of the surgical simulators with high level of evidence are needed.
Huang Y et al [13]	2018	Application of virtual and augmented reality in dentistry	Computerized dental simulators provide the best training system for dental students	The methods are essential tools in the future of dental OSCE	The methods should be applied more extensively in medical treatment
Chen X, Hu J [9]	2018	Virtual reality based haptic simulation in oral surgery	Virtual and tactile fusion of virtual environment is effective for surgical simulation	Haptic technology provides excellent facility to improve surgical skills	Controlled studies are needed
Azarmehr et al	2017	Treatments and outcomes of surgical navigation	The accuracy of surgical navigation was within 1–2 mm	The method is useful addition to the surgical toolkit	Training is required due to the steep learning curve
Lin H, Lo J [10]	2015	Surgical simulation and intraoperative navigation in orthognathic surgery	The method provides precise translation of the surgical plan	Navigation facilitates intraoperative manipulation of the osteotomy segments	Randomised controlled trials are essential
Jayaratne et al [12]	2010	Computer assisted oral & maxillofacial surgery	Most focused on CBCT, stereophotogrammetry and surgical planning software	Accurate diagnosis can be achieved and can be executed via surgical navigation	Technology transfer from research to clinical care

On the other hand, the dynamic navigation allows the real time adjustment of the direction of dental implant during surgery based on the virtual preoperative planning.

One of the main advantages of the dynamic navigation is the operator flexibility of changing the implant position to avoid compromised bony foundation and anatomical structures that may have not be detected during the presurgical planning phase. A high level of accuracy has been reported with the image guide implantology (IGI) system with an overall navigation error of 0.35 mm (and a mean angular deviation of less than 4 degrees [26]. However, it must be emphasised that the technology requires an expensive hard ware, significant learning curve and a rigorous intra-operative referencing and orientation process. Moreover, a disrupted surgical procedure may be encountered due to sensors being blocked during the navigation process.

No doubt, the virtual computerized implant dentistry has opened a new horizon in the management of complex cases where the anatomy of the jaw bones has been altered due to trauma or pathology. It improved the accuracy of implant placement where minimally invasive surgery is required in those who suffer from blood dyscrasias and radiation related bone damage.

Navigation within a virtual environment has been successfully used for the during orthognathic surgical [27], and for the repositioning of the maxilla to correct facial asymmetry [28]. The accuracy of the method was evaluated on 15 patients and ranged from 0.9 to 2 mm. An overview on the indication and the application of computer assisted navigation in oral and maxillofacial surgery was carried out on 104 cases, including 37 zygomatico-orbital maxillary fractures, 27 unilateral TMJ ankylosis, 29 craniofacial fibrous dysplasia, 9 mandibular hypertrophy, 3 bone tumours, two foreign body cases [29]. All the surgeries were performed under the guidance of the navigation system based on the preoperative simulation and superimposing the procedure in real time. The accuracy of the navigation system was assessed by measuring the discrepancies between the achieved results and the virtual plans. The mean error was 1.4 mm, it was concluded that navigation surgery is useful as it improved the accuracy of the performed procedure and reduced operation risks.

The application of augmented reality was mainly in dental implant placement and orthognathic surgery. A novel augmented reality system for displaying alveolar nerve bundles in maxillofacial surgery was recently developed. A novel approach based on fiducial markers within an occlusal splint was used to establish a relationship between the virtual image and the real object. The systems promise a broad clinical application [30]. The application of augmented reality system for oral and maxillofacial surgery

was investigated [31]. The three-dimensional virtual image of osseous structures was projected into the patient's body. This helped the surgeons to avoid important structure inside the bone during surgery. Surgical procedures including hole drilling, screw fixation were performed and guided by the augmented reality, the overall precision of the system was within 1 mm.

The application of augmented reality for dental implantology was recently tested in two cases [32]. The study explored the feasibility of a virtual display of the implant position, using specific glasses, on surgical field for surgical navigation in augmented reality. The two virtual environments did not affect the accuracy of the surgical procedure. However, this prove of consent study promises a wider application in maxillofacial surgery.

For an immersive virtual experience, the user wears a head-mounted displays or goggles to engage his visual senses, headphones to engage his auditory senses, and gloves to engage his tactile sense. Rapid advances in technology and research led to the introduction of commercially available high quality immersive virtual reality devices including Oculus Rift (Te 2015) [33], Google Daydream (Google 2017) [34], Gear VR (Samsung, 2015) [35], Goggle Cardboard (Goggle, 2015a) [36] and HTC Vive (Corp 2015) [37]. Among these Google Daydream, Gear VR and Google Cardboard headsets can create a portable virtual reality environment as they work with smartphones. These lead physicians to explore the potential of immersive spherical videos in medical education.

The addition of haptic technology which provides the operator with tactile feedback of the touched or held digital object on the computer screen, has augmented virtual reality and created a more realistic environment for clinical training. Most of the haptic technology applications in immersive virtual environment were carried out on experimental models [38]. A haptic-assisted craniomaxillofacial surgery planning system was applied for the restoration of skeletal anatomy in complex trauma cases [39]. A virtual model was derived from the patient CT data. The developed system combined stereo visualization with six degrees of freedom, high fidelity haptic feedback that enabled the analysis, planning, testing options for restoring bony segmental defects. The system has the potential to be a powerful tool in oral and maxillofacial surgical planning. The literature showed that most of the application of surgical navigation was in orthognathic surgery to improve the accuracy of guiding the osteotomy segment of the jaw bones according to the pre-planned position [11].

Surgical training

Virtual reality has been utilised to improve the delivery of education and the quality of training in dentistry and

in oral & maxillofacial surgery [40]. Voxel Man Simulator was used for virtual apicoectomy procedure and found that out of 53 dental students who undertook virtual apicoectomy, 51 were positive regarding the impact of virtual simulation as an additional modality in dental education. The trainees indicated that the integrated force feedback (e.g. simulation of haptic pressure), spatial 3D perception, and image resolution of the simulator were key features for virtual training of the dental surgical procedures. Trainees also developed the ability to self-assess their performance which is a valuable skill in surgery which is essential for the refinement of surgical technique. This study also proposed that application of virtual surgery using the 3D reconstruction of patient's anatomy might help surgeons to plan complex surgical procedures [41].

Recently, the impact of virtual reality as a training tool for surgical procedures was evaluated in a cross-sectional study to validate a novel virtual simulator for orbital reconstruction, and a training tool in oral and maxillofacial surgery [42]. A novel virtual reality approach based on haptic technology was introduced and validated for computer aided cephalometry. Twenty-one dental surgeons performed a range of case studies using haptic-enabled digital cephalometric analysis. They proved that by providing a sense of touch the errors in cephalometric analysis has been reduced and the landmarking became more feasible and more intuitive [43].

The applicability of using 3D visualisation in dental training was also reported where a haptic dental injection was developed for inferior alveolar nerve block injection as shown in Fig. 1, they also developed a virtual training system (VR-MFS) with advanced haptic feedback and immersive workbench [44]. In addition to drilling, this system allowed cutting and milling aspects of the bones. 3D stereoscopic visualisation on an immersive workbench provided visual, tactile and aural feedback bringing it close to reality. Le Fort 1 maxillary surgery was simulated in this system; the cutting and drilling trajectories and were compared with a preoperative plan for evaluation. The study found that expert surgeons' trajectories were close to the plan when compared to the novices. Though the experts believed that VR-MFS could be used for skill development, they pointed out that the system lacked realistic simulation that is required for effective training.

The implementation of web-based virtual patient simulation program to teach dental students oral surgery has been investigated. Virtual reality has improved students' knowledge and proved to be effective in teaching clinical reasoning and patient evaluation [45].

Recently, the use and the clinical application of virtual reality in pre-clinical dental education was reviewed. Four educational thematic areas were identified which



Fig. 1 Demonstration of haptic technology of injection of the inferior dental nerve (taken from Anderson, P., Chapman, P., Ma, M. and Rea, P. (2013) Real-time medical visualization of human head and neck anatomy and its applications for dental training and simulation. *Current Medical Imaging Reviews*, 9(4), pp. 298–308)

included the simulation hardware, the realism of virtual simulation, scoring system for the assessment of virtual reality and the validation of the emerged systems. Four types of simulators have been used for dental education which included desktop pcs, haptic desktops, and dental skill trainers and digitally enhanced phantom heads. It was clear there were no established educational standards for dental simulators. Most of the available dental simulators have not been validated [46].

On the other hand, a stereoscopic 3D videos using immersive reality was developed (Fig. 2) and its impact on improving the non-surgical skills among trainees was investigated [47]. Based on the 3D computer-generated model of the operating room the trainees can navigate, explore and interact with the digital images of the patient's data. A Leap Motion sensor tracks the trainee's hands (Fig. 2) to provide a multi-sensory interactive learning experience. The users were able to choose a specific application and zoom in on certain items within a surgical menu. Through specific gestures the trainees can interact with the anatomy of the maxillofacial region and select the most appropriate surgical instrument to perform certain surgical procedure. The developed



Fig. 2 Oculus Rift showing 3D digital data, the operating theatre, the leap motion sensor tracks the trainee's hands to select items from the menu or apply a surgical instrument (PhD thesis of Yeshwanth Pulijala The University of Huddersfield, 2017)

programme tests the trainees' knowledge through a quiz scene. The efficacy of VR Surgery in training novices was assessed. A single-blind prospective randomised controlled trial confirmed that the group of the trainees who used VR Surgery performed better than the control group.

Virtual reality has been utilised to create a learning environment for training in maxillofacial emergencies to improve knowledge and confidence of junior trainees [48]. The pilot studies showed improved in the two examined domains, further was recommended by the investigators. Following the same theme of virtual surgical simulation, the feasibility of tree-structure architectonic model to simplify virtual orthognathic surgical was explored [49]. This was tested on a group of patients who require orthognathic surgery. The operators were immersed in the virtual environment and tactile feedback was perceived which augmented the training opportunities [49].

The importance of virtual reality in standardizing clinical education to facilitate learning and practicing has been highlighted. The methods encouraged the students to learn by themselves which can reduce faculty time significantly. CDS-100 simulator, designed by EPED Inc. has been shown to be effective computerised tool as it provided 3D real time accurate feedback for endodontic and prosthetic applications. The objective structured clinical examination (OSCE) can be easily incorporated.

The authors highlighted the importance of the real time navigation technology in dentistry and emphasised the need for high quality medical images for accurate implementation of the technology [13].

It has been recently highlighted that the current customized augmented reality systems have not been fully validated by independent teams, they provide good results in simple experimental models. The superimposition of digital images is easier on bony structures, therefore, the application of this innovation in oral & maxillofacial surgery is readily achievable and prepare the way for a wider application [50].

Conclusion

In conclusion, virtual reality and augmented reality have contributed to the surgical practice and training in oral & maxillofacial surgery. Few articles highlighted the importance of this imaging innovation in improving the quality of care delivered to patients. The main application of virtual reality is in implantology and orthognathic surgical. Virtual reality facilitated the restoration of orbital floor following blow out fracture and the planning of mandibular reconstruction following cancer resection. There are limited prospective randomized studies to assess the impact of virtual reality with the standard methods of delivering education or carrying out oral surgical procedures. Most of the existing models of simulation focused on the technical skills of the

surgical trainees. Non-technical skills including cognitive development, interpersonal communication, teamwork, and emergency management are hardly touched upon except in few studies. The technical skills learnt by the trainees on the virtual surgery simulators are limited but expected to transfer into a stressful environment of operating theatre. However, as a surgical procedure is a combination of expert anatomical knowledge, spatial visualisation, judgment and inter-professional teamwork, it is essential to give a holistic learning experience to the trainees. Hence, there is a gap in the modern simulators developed for dentistry and oral and maxillofacial surgery, which needs to be met adequately. Researchers attempted the use of serious games and gamification of simulations to overcome these training obstacles. Further studies are required to compare the impact of augmented reality in improving the quality of care delivered to patients with the standard approaches.

Acknowledgements

Not applicable.

Authors' contributions

The first author (AA) designed the study, reviewed the literature, and edited the manuscript. The second author (YP) conducted the original study on virtual and immersive reality, provided an insight on the relevant studies in the literature and offered some of the illustrations in the manuscript. Both authors read and approved the final manuscript.

Funding

Not funding was required.

Availability of data and materials

Existing literature in Ovid & PubMed. The data sheets generated during the current study area available by contacting the first author (AA) via his email address.

Ethics approval and consent to participate

Not required.

Consent for publication

Not applicable.

Competing interests

The authors declare that they have no competing interests.

Received: 1 April 2019 Accepted: 24 October 2019

References

- Freina L, Ott M. A literature review on immersive virtual reality in education: state of the art and perspectives; 2015.
- Bartella AK, Kamal M, Scholl I, Steegmann J, Ketelsen D, Holzle F, et al. Virtual reality in preoperative imaging in maxillofacial surgery: implementation of "the next level". *Br J Oral Maxillofac Surg*. 2019;57(7):644–8.
- Kim Y, Kim H, Kim YO. Virtual reality and augmented reality in plastic surgery: a review. *Arch Plast Surg*. 2017;44(3):179–87.
- Ayoub A, Xiao Y, Khambay B, Siebert P, Hadley D. Toward building a virtual human face. *Int J Oral Maxillofac Surg*. 2007;36(5):423–8.
- Naudi K, Benramdan R, Brocklebank L, Khambay B, Ayoub A. The virtual human face - superimposing the simultaneously captured 3D photorealistic skin surface of the face on the untextured skin image of the CBCT scan. *Int J Oral Maxillofac Surg*. 2013;42(3):393–400.
- de Waard O, Baan F, Verhamme L, Breuing H, Kuijpers-Jagtman AM, Maal T. A novel method for fusion of intra-oral scans and cone-beam computed tomography scans for orthognathic surgery planning. *Craniomaxillofac Surg*. 2016;44(2):160–6.
- Joda T, Gallucci GD, Wismeijer D, Zizmann NU. Augmented and virtual reality in dental medicine: a systematic review. *Comput Biol Med*. 2019; 108:93–100.
- Maliha SG, Diaz-Siso JR, Plana NM, Torrie A, Flores RL. Haptic, physical and web-based simulators: are they underused in maxillary surgery training. *J Oral Maxillofac Surg*. 2018;76(11):2424.e1–2424.e11.
- Chen X, Hu J. A review of haptic simulator for oral and maxillofacial surgery based on virtual reality. *Expert Rev Med devices*. 2018;15(6):435–44.
- Azarmehr I, Stokbro K, Bell RB, Thygesen T. Surgical navigation: a systematic review on indications, treatments, and outcomes in oral and maxillofacial surgery. *J Oral Maxillofac Surg*. 2017;75(9):1987–2005.
- Lin HH, Lo LJ. Three-dimensional computer assisted surgical simulation and intraoperative navigation in orthognathic surgery: a literature review. *J Formosan Med Assoc*. 2015;114(4):300–7.
- Jayarathne YS, Zwehlen RA, Lo J, Tam SC, Cheung LK. Computer aided maxillofacial surgery: an update. *Surg Innov*. 2010;17(3):217–25.
- Huang TK, Yang HS, Hsieh YH, Wang JC, Hung CC. Augmented reality (Ar) and virtual reality (VR) applied in dentistry. *Kaohsiung J Med Scie*. 2018; 34(2):243–8.
- Kwon HB, Park YS, Han JS. Augmented reality in dentistry; a current perspective. *Acta Odontol Scand*. 2018;76(7):497–503.
- Holzinger D, Juergens P, Shahim K, Reyes M, Schicho K, Milesi G, Perisanidis C, Zeilhofer HF, Seemann R. Accuracy of soft tissue prediction in surgery-first concept in orthognathic surgery: a prospective study. *J Cranio-maxillofac-Surg*. 2018;46(9):1455–60.
- Metzeir P, Geiger EJ, Alcon A, Ma X, Steinbacher DM. Three-dimensional virtual surgery for free fibula mandibular reconstruction: planned versus actual results. *J Oral Maxillofac Surg*. 2014;72(12):2601–12.
- Hanken H, Schablowsky C, Smeets R, Heiland M, Riecke B, Nourwali I, Vorwig O, Grobe A, Al-Dam A. Virtual planning complex head and neck reconstruction results in satisfactory match between real outcomes and virtual models. *Clin Oral Investig*. 2015;19(3):647–56.
- Maloney KD, Rutner T. Virtual surgical planning and hardware fabrication prior to open reduction and internal fixation of atrophic edentulous mandible fractures. *Craniomaxillofac Traum Reconstr*. 2019;12(2):156–62.
- Nguyen A, Vanderbeek C, Herford AS, Thakker JS. Use of virtual planning and virtual database with intraoperative navigation to guide revision of complex facial fractures. *J Oral Maxillofac Surg*. 2019;77(4):790e1–790e17.
- Drake VE, Rizzi CJ, Greywoode JD, Vakharia KT. Midface fracture simulation and repair: a computer-based algorithm. *Craniomaxillofac Trauma Reconstr*. 2019;12(1):14–9.
- Jemt T. A retro-prospective effectiveness study on 3448 implant operations at one referral clinic: A multifactorial analysis. Part II: Clinical factors associated to peri-implantitis surgery and late implant failures. *Clin Implant Dent Res*. 2017;19(6):972–9.
- D'souza KM, Aras MA. Types of implant surgical guides in dentistry: a review. *J Oral Implantol*. 2012;38(5):643–52.
- Gulati M, Anand V, Salaria SK, Jain N, Gupta S. Computerized implant-dentistry: advances toward automation. *J Indian Soc Periodontol*. 2015;19(1):5–10.
- Holst S, Blatz MB, Eitner S. Precision for computer-guided implant placement: using 3D planning software and fixed intraoral reference points. *J Oral Maxillofac Surg*. 2007;65(3):393–9.
- Sengul SV. Computer assisted implant dentistry: possibilities and limitations. In: Dibart S, Dibart JP, editors. *Text Book of Practical Osseous Surgery in Periodontics and Implant Dentistry*. 1st ed. UK: Wiley; 2011. p. 205–26.
- Elian N, Jalbout ZN, Classi AJ, Wexler A, Sarment D, Tarnow DP. Precision of flapless implant placement using real-time surgical navigation: a case series. *Int J Oral Maxillofac Implants*. 2008;23(6):1123–7.
- Chang HW, Lin HH, Chortrakarnkij P, Kim SG, Lo LJ. Intraoperative navigation for single splint two-jaw orthognathic surgery. From model to actual surgery. *J Craniomaxillofac Surg*. 2015;43(7):1119–26.
- Badiali G, Roncani A, Bianchi A, Taddei F, Marchetti C, Schileo E. Navigation in orthognathic surgery: 3D accuracy. *Facial Plast Surg*. 2015;31(5):463–73.
- Yu H, Shen SG, Wang X, Zhang L, Zhang S. The indication and application of computer-assisted navigation in oral and maxillofacial surgery- Shanghai's experience based on 104 cases. *J Craniomaxillofac Surg*. 2013;41(8):770–4.
- Zhu M, Liu F, Chai G, Pan JJ, Jiang T, Linh L, Xin Y, Zhang Y, Li Q. A novel augmented reality system for displaying alveolar nerve bundles in maxillofacial surgery. *Sci Rep*. 2017;7(42365):1–10.

31. Tran H, Suenaga H, Kuwana K, Dohi T, Nakajama S, Liao H. Augmented reality system for oral surgery using 3D auto stereoscopic visualization. *Med Image Comput Comput Assist Interv*. 2011;14(Pt 1):81–8.
32. Pellegrino G, Mangano C, Mangano R, Ferri A, Taraschi V, Marchetti C. Augmented reality for dental implantology: a pilot clinical report of two cases. *BMC Oral Health*. 2019;19(158):1–8.
33. TE Z. 2015 Oculus Rift vs. Morpheus vs Vive VR; 2015.
34. GOOGLE. 2017. Daydream vr. Available: <https://vr.google.com/daydream/> , Project Tango . Google. Available: <https://get.google.com/tango/>
35. SAMSUNG 2015 Samsung Gear VR. 2015.
36. GOOGLE 2015. Google cardboard.
37. CORP, H. T. C. 2015 HTC RE vive VR. 2015.
38. Lin Y, Chen H, Yu D, Zhang Y, Yuan W. A predictive bone drilling force model of haptic rendering with experimental validation using fresh cadaveric bone. *Int J Comput Assist Radiol Surg*. 2017;12(1):91–8.
39. Olsson P, Nysjo F, Hirsch JM, Carlbom IB. A haptic assisted cranio-maxillofacial surgery planning system for restoring skeletal anatomy in complex Rauma cases. *Int J Comput Assist Radiol Surg*. 2013;8(6):887–94.
40. Wu F, Chen X, Lin Y, Wanf C, Wang X, Shen G, Qin J, Heng PAS. A virtual training system for maxillofacial surgery using advanced haptic feedback and immersive workbench. *Int J Med Robot*. 2014;10(1):78–87.
41. Pohlenz P, Grobe A, Petersik A, Von Sternberg N, Pflesser B, Pommert A, Hohne K-H, Tiede U, Springer I, Heiland M. Virtual dental surgery as a new educational tool in dental school. *J Craniomaxillofac Surg*. 2010;38(8):560–4.
42. Khelemsky R, Hill B, Buchbinder D. Validation of a novel cognitive simulator for orbital floor reconstruction. *J Oral Maxillofac Surg*. 2017;75(4):775–85.
43. Medellin-Castillo HI, Govea-Valladares EH, Perez-Guerrero CN, Gil-Valladares J, Lim T, Richie JM. The evaluation on a novel haptic-enabled virtual reality approach for computer aided cephalometry. *Comput Methods Prog Biomed*. 2016;130:46–53.
44. Anderson P, Chapman P, Ma M, Rea P. Real-time medical visualization of human head and neck anatomy and its applications for dental training and simulation. *Current Med Imag*. 2013;9(4):298–308.
45. Weiner CK, Skalen M, Harju-Jeanty D, Heymann R, Rosen A, Fors U, Lund B. Implementation of a web-based patient simulation program to teach dental students in oral surgery. *J Dent Edu*. 2016;80(2):133–40.
46. Towers A, Field J, Stokes C, Maddock S, Martin N. A review of the use and application of virtual reality in pre-clinical dental education. *Br Dent J*. 2019;226(5):358–66.
47. Pulijala Y, Minhua E, Pears M, Peebles D, Ayoub A. Effectiveness of immersive virtual reality in surgical training - a randomized control trial. *J Oral Maxillofac Surg*. 2018;76(5):1065–72.
48. Elledge R, McAleer S, Thakar M, Begum F, Singhota S, Grew N. Use of a virtual learning environment for training maxillofacial emergencies: impact on the knowledge and attitudes of staff in accident and emergency department. *Brit J Oral Maxillofac Surg*. 2016;54(2):166–9.
49. Yu H, Cheng G, Cheng A, Shen G. Preliminary study of virtual orthognathic surgical simulation and training. *J Craniofac Surg*. 2011;22(2):648–51.
50. Farronato M, Maspero C, Lanteri V, Fama A, Ferrati F, Pettenuzzo A, Farronato D. Current state of the art in the use of augmented reality in dentistry: a systematic review of the literature. *BMC Oral Health*. 2019;19(1):135.

Publisher's Note

Springer Nature remains neutral with regard to jurisdictional claims in published maps and institutional affiliations.

Ready to submit your research? Choose BMC and benefit from:

- fast, convenient online submission
- thorough peer review by experienced researchers in your field
- rapid publication on acceptance
- support for research data, including large and complex data types
- gold Open Access which fosters wider collaboration and increased citations
- maximum visibility for your research: over 100M website views per year

At BMC, research is always in progress.

Learn more biomedcentral.com/submissions



RESEARCH ARTICLE

Open Access



Comparison of the abrasive properties of two different systems for interproximal enamel reduction: oscillating versus manual strips

Francesca Gazzani^{1*} , Roberta Lione^{1,2}, Chiara Pavoni^{1,2}, Gianluca Mampieri¹ and Paola Cozza^{1,3}

Abstract

Background: The aim of the present investigation was to evaluate enamel reduction efficiency, abrasive property decay, and enamel effects between oscillating mechanical and manual systems for interproximal enamel reduction (IPR).

Methods: Three oscillating strips and three manual strips were tested on twelve freshly extracted premolars blocked in an acrylic cylinder pot by means of a material testing machine. Each strip underwent one test of 8 cycles (30 s each). Both abrasive tracks and teeth surfaces were qualitative evaluated before and after IPR by means of SEM analysis. Efficiency and abrasive property decay of both IPR systems were investigated by the amount of enamel reduction within the eight-cycle testing. *Independent t-test* was used to evaluate differences in variables between the two systems.

Results: Mechanical IPR system showed higher efficiency in terms of enamel reduction ($p < 0.005$) when compared with manual IPR system (0.16 mm and 0.09 mm, respectively). Quantity of removed enamel decreased throughout the 8 cycles for both systems. Less presence of enamel debris and detachment of abrasive grains were observed on mechanical strips rather than manual strips. SEM analysis revealed more regular surface of teeth undergone mechanical IPR procedures.

Conclusion: Oscillating diamond strips showed more controlled efficiency when compared with the manual IPR system leading to a more regular enamel surface.

Keywords: Interproximal enamel reduction, Mechanical strips, Manual strips, SEM analysis

Background

Interproximal reduction (IPR) is a common procedure used in orthodontic treatment [1] in several clinical cases. Main clinical indications include correction of Bolton tooth-size discrepancies, mild or moderate crowding, morphologic dental anomalies, prevention of relapse, and reduction of interdental gingival papilla retraction [1–5]. It is frequently used as part of treatment in combination with clear aligners [6]. Sheridan [1] described Air-rotor stripping (ARS) technique more than 20 years ago as an alternative to extraction borderline cases. Several IPR systems have been developed [6–8] and progressively modified over the years. Recently, many powered IPR systems such as mechanical oscillating

abrasive strips or diamond-coated segmented discs have gained in popularity [6–8]. Since these IPR procedures have become more frequent in orthodontic practice, several studies analyzed their effects on enamel surface [9, 10]. Qualitative SEM evaluations [6, 9, 10] showed that IPR systems can affect enamel morphology leaving furrows and scratches. The use of medium and fine manual metallic strips followed by polishing and topical fluoride application were introduced in 1956 by Hudson [11] in order to reduce enamel irregularities produced [12, 13]. Bonetti et al. [14] suggested topical applications of casein phosphopeptide-amorphous calcium phosphate to enhance enamel remineralization after IPR. However, only fewer studies [8, 15–17] analyzed the efficiency of various existing IPR systems. In a recent literature review, Lapenaite et al. [7] compared different IPR systems highlighting their indications, contraindications, and complications. Even if all

* Correspondence: francescagazzani@hotmail.it

¹Department of Clinical Sciences and Translational Medicine, University of Rome 'Tor Vergata', Viale Oxford 81, 00133 Rome, Italy

Full list of author information is available at the end of the article



© The Author(s). 2019 **Open Access** This article is distributed under the terms of the Creative Commons Attribution 4.0 International License (<http://creativecommons.org/licenses/by/4.0/>), which permits unrestricted use, distribution, and reproduction in any medium, provided you give appropriate credit to the original author(s) and the source, provide a link to the Creative Commons license, and indicate if changes were made. The Creative Commons Public Domain Dedication waiver (<http://creativecommons.org/publicdomain/zero/1.0/>) applies to the data made available in this article, unless otherwise stated.

instruments are effective in reducing interproximal enamel, there are evident differences in terms of efficiency, effects on enamel surface roughness, and technical aspects such as abrasive grain size, application speed, and intensity of use. Moreover, it is important to quantify the amount of enamel that can be removed to prevent residue excessive space, persisting misaligned teeth, or inter-arch discrepancies. High accuracy is required to achieve treatment objectives especially during 3D digitally treatment plans. In regard to this issue, one aim of the present study was to evaluate the efficiency in terms of enamel reduction of two most commonly used IPR systems by means of Instron Universal Testing Machine. A qualitative evaluation of strips and enamel surfaces before and after application of the two different IPR systems was also performed by means of SEM analysis.

Methods

Three oscillating strips (Intensiv Ortho-Strips L-OS80XC-R/3, Intensiv SA, Montagnola, Switzerland) and three manual strips (Horico Stahlcarbo 304 Medium, Hopf Ringleb & Company, Berlin, Germany) were collected and tested. Twelve teeth were selected from a collection available and obtained over the years from patients who had an extraction therapy at the Department of Orthodontics, University of Rome “Tor Vergata”. Informed consent agreement was signed by all patients for orthodontic treatment and to allow their teeth to be used for research purposes. All extracted teeth were thoroughly cleaned of debris and soft tissue, then conserved and fixed in 4% glutaraldehyde in 0.2-M sodium cacodylate buffer solution at 48 °C. Each tooth root was blocked by acrylic resin (Leocryl, Leone S.p.A. Ortodonzia e Implantologia, Sesto Fiorentino, Florence, Italy) in a cylinder pot, designed and manufactured by a 3D printer (Object Eden260V, Stratasys, Commerce Way Eden Prairie, Minnesota, USA). Each cylinder pot was placed and fixed with screws inside a metallic support designed and manufactured by Leone company (Leone S.p.A. Ortodonzia e Implantologia, Sesto Fiorentino, Florence, Italy).

Evaluation of enamel reduction efficiency

Initially, the amount of enamel reduction achieved in a fixed amount of time by two IPR systems was compared. The experimental analysis was performed by means of an Instron Universal Testing Machine (Model 3365, Instron, Industrial Product Group, Grove City, PA. USA) (Fig. 1). A displacement-controlled method was implemented using Bluehill Software. In the experimental set-up, the reciprocating movement was obtained by means of a contra-angle with 2:1 reduction (Intensiv Swingle, Intensiv SA, Montagnola, Switzerland). Manual strips were also adapted on the oscillating strips framework in order to be applied into designed experimental set up setting the



Fig. 1 Oscillating diamond strip and contra-angle adapted on the Instron Universal Testing Machine for the experimental analysis

contra-angle at lower oscillations per minute. Before starting the test, a conditioning phase was performed for each strip to correct the lashes of the experimental set-up. The contra-angle with 2:1 reduction was set at the revolutions per minute (RPM) required by the method (40,000 RPM for the mechanical IPR system, resulting in 20,000 oscillations per minute as suggested by the manufacture, and 40 RPM for the manual IPR system, resulting in 20 oscillations per minute simulating manual usage and speed). An adequate water spray (50 ml/s) was activated during the entire test with the mechanical IPR system, as suggested by the manufacturer.

Description of cycle test setting

Each strip, both oscillating and manual, underwent one test consisting of 8 cycles. Therefore, a total of 24 cycles were performed for 3 oscillating strips and a total of 24 cycles for 3 manual strips. One cycle (30 s) was set according to the following steps:

1. For both systems, contra-angle reciprocating movement started before the data acquisition in order to eliminate any load dissipations (T0, no contact between the strip and tooth surface);
2. With the contra-angle activated, the movable rig of the Instron machine moved down at 0.1 mm/s till the load of 0.1 N (T1, first contact between the strip and the tooth surface);
3. The movable rig moved down of a further 0.8 mm to deflect the strip of 0.8 mm, corresponding to a load of 1 N applied on tooth surface. The strip worked for 30 s (T2, working contact between the strip and tooth surface);

4. At the end of 30 s, the handpiece returned to the starting point (T0);
5. The contra-angle reciprocating movement was stopped and the movable rig of the Instron machine moved down again till the load of 0.1 N (T3, contact between the strip and the tooth surface after stripping).

Each cycle was performed on two untreated tooth surfaces rotating of 90° around the cylinder pot in the metallic clamp support. The down displacement of the movable rig from T0 to T1 position was recorded at the end of each cycle and calculated by Bluehill software. The displacement difference recorded at T3 and T1 was reasonably the dimension of the reduced enamel.

Evaluation of abrasive property decay of the strips

The effects on strips' surface structure were analyzed by means of SEM. In particular, both abrasive tracks were analyzed in order to qualitatively evaluate the abrasive grain distribution on the metallic strip matrix, and the presence of enamel debris before and after their use. SEM analysis was performed with a FEI Quanta 200 (Hillsboro, USA) in High Vacuum at 30.00 kV. Images were acquired at 50X, 100X and 200X of magnification. Abrasive property decay for both IPR systems was investigated by evaluating the enamel reduction data described within the 8- cycle testing.

Evaluation of effects on enamel surface

Also, enamel surface condition was qualitatively evaluated before and after IPR with SEM analysis (Low Vacuum at 10.00 kV) at 30X, 140X, and 300X of magnification. A modified version of a scoring scale previously used by Nucci et al. [18, 19] was adopted to describe enamel surface, and the integrity level of the enamel surface was evaluated as follows:

Score 0: Enamel surface free of scratches and grooves;

Score 1: Scratches and grooves not very accentuated and covering a portion of the surface;

Score 2: Deep furrows with rounded edges evident over the entire surface, without debris;

Score 3: Evident and deep-edged furrows visible on the whole surface and presence of debris on the enamel.

Statistical analysis

For a standardized effect size of 1 (a clinically relevant change of 0.20 mm with a combined SD of 0.05 derived from a primary pilot test) for the outcome variable enamel reduction in mm, a sample size of 3 strips per group was required for a significance level of 0.05 and test power of 80% [20]. Exploratory statistics revealed that the variable was normally distributed (Kolmogorov-Smirnov test) with equality of variances (Levene's test). The independent *t*-test was used to evaluate differences in variables between the two systems. Data were analyzed using a statistical software (MS Excel, Micros). Significance level was set at $p < 0.05$.

Results

Mean and standard deviation (SD) of reduced enamel underwent the cyclic test for 8 times are shown in Table 1. Enamel reduction efficiency of two systems throughout the 8 IPR cycles is shown in Fig. 2. Mechanical strips showed higher enamel reduction efficiency in comparison with the manual system. Concerning abrasive property decay, the quantity of removed enamel decreased throughout the 8 cycles for both IPR systems (Fig. 2). Normalization for the two IPR systems was performed according to their respective maximum value of removed enamel: first cycle with mechanical IPR system (0.23 mm of removed enamel) and first cycle with manual IPR system (0.15 mm of removed enamel). The decrease in abrasive properties was significantly less considerable for mechanical IPR system. Before testing, both mechanical and manual strip surfaces showed a metallic substrate with the arrangement of abrasive grains at SEM observation (Fig. 3). Diamond abrasive grains of mechanical strip had a mean dimension of about 80 μ m with variable quantity and homogeneous distribution on the metallic substrate. In addition, the abrasive track was characterized by a perforated structure. Manual strip presented aluminum oxide abrasive grains of variable dimension. The surface was continuous without holes. SEM analysis at different magnification (50X, 100X and 200X) showed the presence of enamel debris and the detachment of abrasive grains on both abrasive strips after 8 cycle-tests (Figs. 4 and 5). These two phenomena were less evident on mechanical strips. SEM evaluation (30X, 140 X and 300X) of enamel surface before and after the test is shown in Figs. 6 and 7. All tested

Table 1 Descriptive statistics and statistical comparisons (independent-samples *t* tests) of the enamel reduction efficiency in mm of removed enamel. Mean values obtained from 24 cycles performed for 3 oscillating strips and 24 cycles performed for 3 manual strips

Variable	Oscillating mechanical system (3 strips)		Manual system (3 strips)		Diff.	<i>P</i> value	95% CI of the difference	
	Mean	SD	Mean	SD			Lower	Upper
Enamel reduction (mm)	0.16	0.04	0.09	0.04	0.07	0.004*	0.025	0.110

SD Standard Deviations, Diff. Differences, CI Confidence interval

* $p < 0.005$

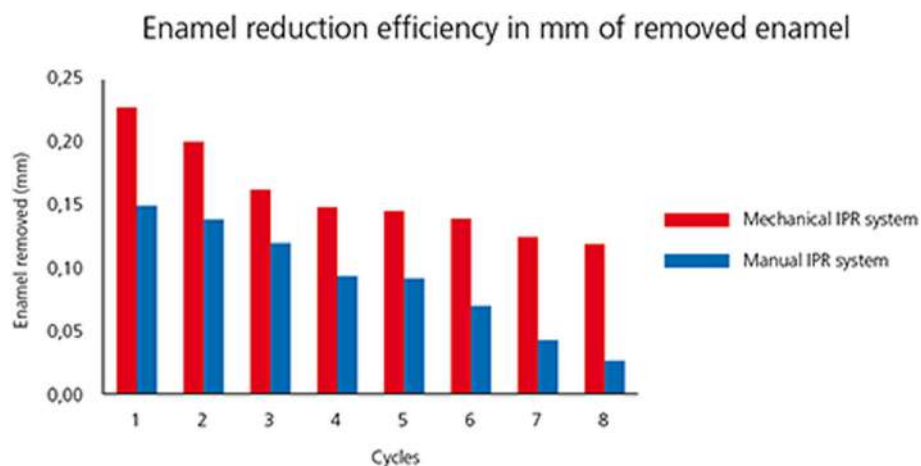


Fig. 2 Enamel reduction efficiency (mm) comparing two IPR systems during one cycle test

surfaces showed scratches and grooves when compared to non-tested surfaces. In particular, SEM analysis revealed different shapes and dimensions of the incisions produced by two different IPR systems. Mechanical IPR system produced more regular surface with a series of light parallel lines with some minor grooves of 1–3 μm and a more uniform enamel coating (Score 1). Manual IPR system revealed a more irregular surface characterized by extended grooves, alternated with enamel ridges and irregular fragment. This configuration corresponds to a Score 2 according to Nucci's enamel surface classification.

Discussion

Increasing demand of alternative procedures to extraction treatments promoted the introduction of several IPR systems [1–8]. Most common ones are manual abrasive strips, mechanical oscillating abrasive

strips, diamond-coated segmented discs and rotating diamond burs [1, 6–8, 13]. The effects that IPR can have on the enamel surface have been well documented in literature [9–14]. However, comparative data on the efficiency of different IPR systems are not so common [7, 8, 15–17, 21]. Recently, mechanical oscillating abrasive strips have gained in popularity [7, 22, 23]. Some authors highlighted various advantages of this system in comparison with more traditional ones: avoiding risk of cutting into the soft tissue, possibility of more regular enamel surface, and more predictable results [14, 16, 24, 25]. Several studies [6, 7] concluded that mechanical IPR systems reduce chair-side time compared to manual strips. In contrast, manual abrasive strips are particularly indicated for anterior teeth, rotated elements, and recontouring procedures [1, 2]. However, they can result impractical, unproductive, and time-consuming when used for

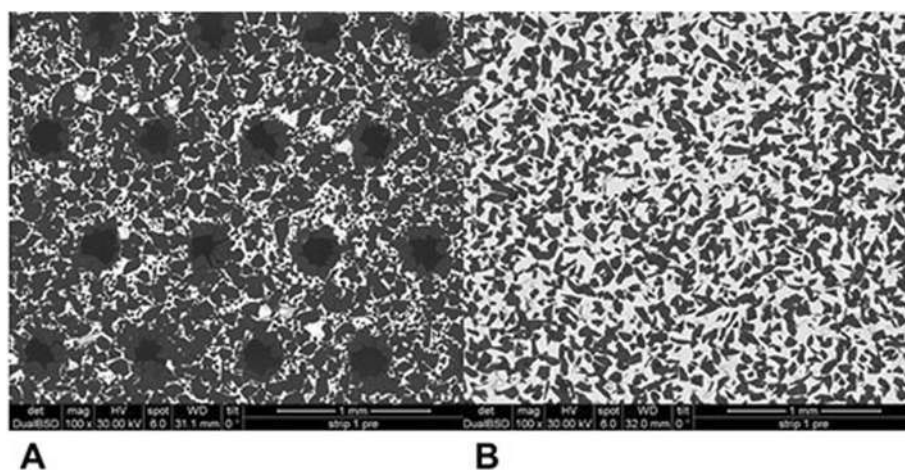


Fig. 3 SEM analysis (100X) of non-used mechanical and manual IPR systems

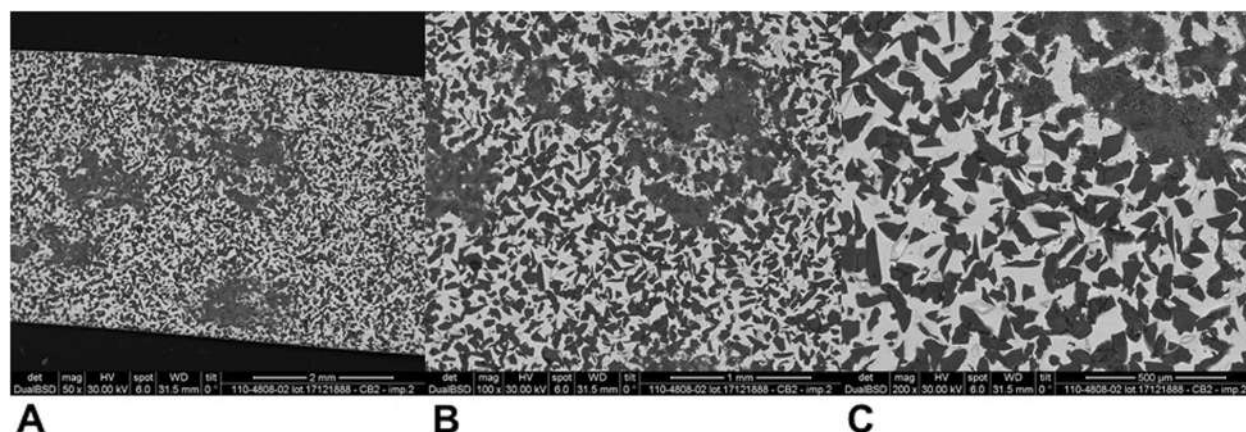


Fig. 4 SEM analysis of manual IPR system surface after 8 IPR test cycles. **a** 50X. **b** 100X. **c** 200X

posterior teeth [1–7]. In the present study, both effects on enamel surface and enamel reduction efficiency were investigated. In terms of superficial effects, Arman et al. and Bonetti et al. [9, 14] concluded that all stripping methods significantly roughened the enamel surfaces. According to the recent investigation of Kaaouara Y et al. [26], our results revealed that mechanical oscillating diamond strips produced more regular surface, with light parallel lines and minor grooves than manual abrasive strips. After manual IPR procedures enamel presented a more irregular surface with extended grooves, enamel ridges and irregular fragments suggesting some irregularities of manual abrasive track (Figs. 6 and 7). The most considerable presence of enamel imperfections was due to the reduced accuracy and high variability of the abrasive grain size and distribution. Abrasive particle grain size significantly affects the efficiency of dental abrasives, as well as the attainable enamel surface quality [27]. The SEM evaluation revealed

some differences in terms of abrasive particle grain sizes between the two strips. Mechanical oscillating diamond strips presented diamonds grain sizes with mean dimension close to 80 μm , while manual abrasive strips were characterized by the presence of grains with variable dimensions. As for enamel reduction efficiency, mechanical oscillating IPR system reduced the inaccuracy of manual IPR systems satisfying precision potentially down to 0.1 mm required by 3D treatment plans such as clear aligners. Enamel removed by mechanical IPR system was of 0.16 mm, whereas the mean value obtained with manual IPR system was of 0.09 mm (Table 1). The higher efficiency of oscillating systems was observed all throughout the 8 cycles (Fig. 2). These findings were correlated with different characteristics and design of abrasive track [7, 15–17]. The perforated structure of the mechanical strips and compulsory water rinsing facilitated the removal of enamel debris enhancing the overall efficiency in

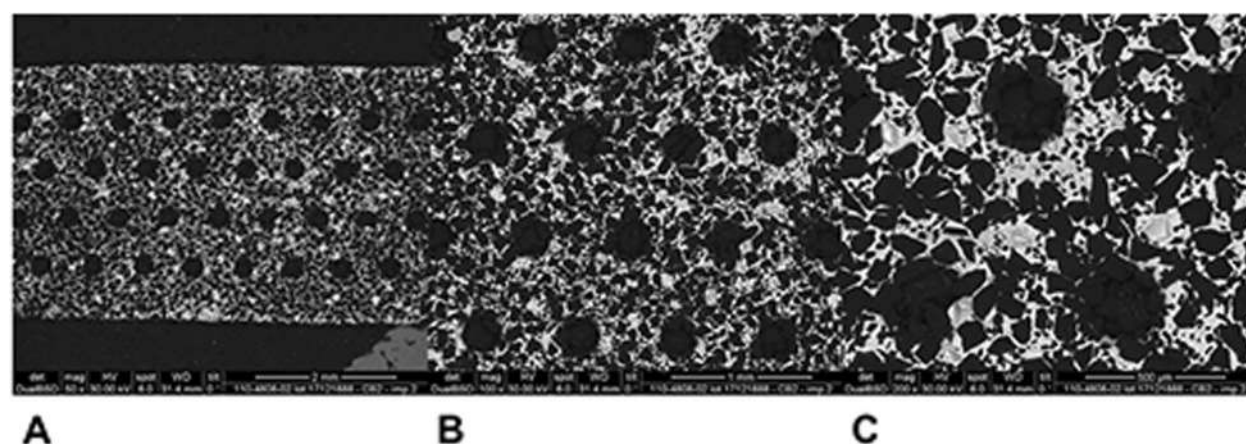


Fig. 5 SEM analysis of mechanical IPR system surface after 8 IPR test cycles. **a** 50X. **b** 100X. **c** 200X

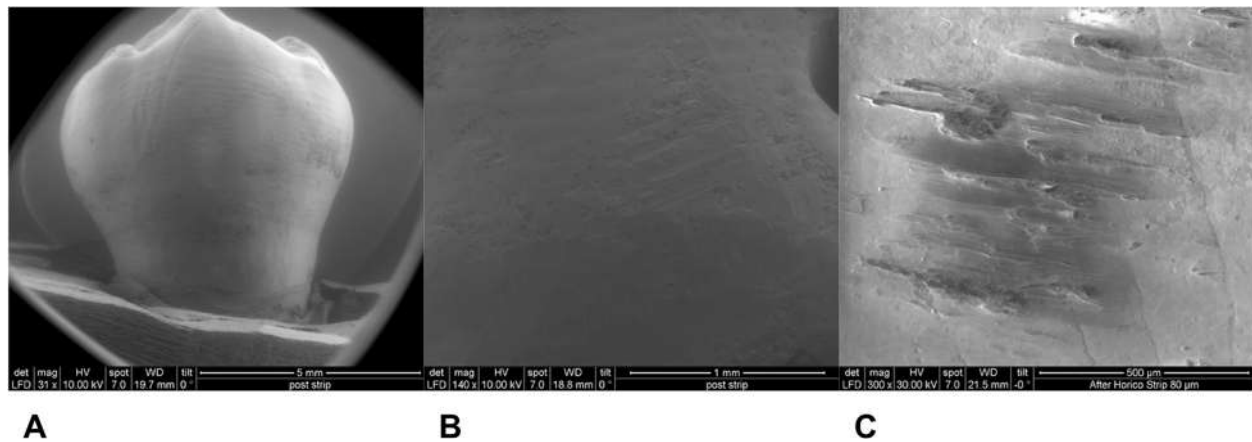


Fig. 6 SEM analysis of enamel surface after 8 IPR cycles by means of manual IPR system. **a** 30X. **b** 140X. **c** 300X

combination with higher velocity of the system. On the contrary, the absence of a perforated structure on the manual strips, and the consequent higher enamel deposition on its abrasive track, reduced the abrasive potential and thus its efficiency [23]. As for the abrasive property decay, the percentage of decrease in enamel reduction throughout the 8 cycles was significantly lower for mechanical strips, although a constant decrease was observed for both systems. According to a previous study [23], the progressive loss of abrasive properties is due to the presence of enamel debris on the strip surface and the detachment of some abrasive grains. These two phenomena resulted less evident on mechanical strips according to the qualitative characterization of the abrasive surfaces after the test cycles (Figs. 4 and 5). As for enamel structure, both manual and mechanical IPR systems produce furrows and grooves on the enamel surface [9, 10, 27]. Baumgartner et al. [22] concluded that grinding with mechanical oscillating systems resulted in rougher enamel

surfaces in comparison to untreated ones. In the present investigation, enamel surface appeared rougher than the untreated control after both IPR procedures. However, mechanical IPR system produced a more regular enamel surface in comparison with the manual IPR system of manual strips. Considering existing literature [6, 14, 16] and the results obtained on the necessity of an adequate polishing after IPR to guarantee a good long-term prognosis, enamel surfaces should be polished after all IPR procedures. A limitation of the present study design was the likelihood of spurious inferences that could affect the results, such as the access to the interproximal point, the severity of crowding, variability in tooth morphology and the bias related to operator ability.

Conclusions

Mechanical oscillating diamond strips showed more efficiency in enamel reduction and shorter chair-time compared to manual strips. SEM analysis confirmed a more

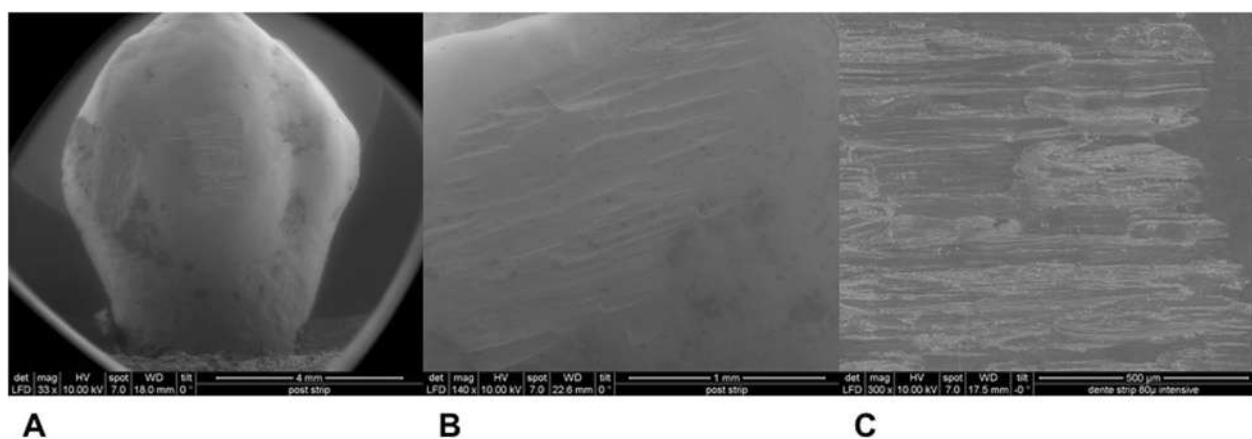


Fig. 7 SEM analysis of enamel surface after 8 IPR cycles by means of mechanical IPR system. **a** 30X. **b** 140X. **c** 300X

homogeneous abrasive grain-size distribution on the mechanical systems than manual systems. Moreover, the perforated structure and the water rinsing of the oscillating diamond strips facilitated the removal of enamel debris. Mechanical IPR system defined more regular enamel surfaces when compared with the manual IPR system.

Abbreviations

3D: Three dimensional; ARS: Air-rotor stripping; IPR: Interproximal reduction; N: Newton; RPM: Revolution per minute; SEM: Scanning electron microscopy

Acknowledgements

Not applicable.

Authors' contributions

FG, RL performed the experimental analysis and analyzed the data. CP and GM contributed in writing the manuscript. PC supervised the project and contributed in writing the manuscript. All authors have read and approved the manuscript.

Funding

No funding was provided.

Availability of data and materials

The datasets used and/or analyzed during the current study are available from the corresponding author on reasonable request.

Ethics approval and consent to participate

All patients signed an informed consent agreement for orthodontic extraction treatment and to allow their teeth to be used for research purposes. However, ethical approval was not mandatory for the retrospective design of the present in-vitro research (F. Suna Kıraç. Is Ethics Approval Necessary for all Trials? A Clear But Not Certain Process. *Mol Imaging Radionucl Ther.* 2013 Dec; 22 (3): 73–75).

Consent for publication

Not applicable.

Competing interests

The authors declare that they have no competing interests.

Author details

¹Department of Clinical Sciences and Translational Medicine, University of Rome 'Tor Vergata', Viale Oxford 81, 00133 Rome, Italy. ²Department of Dentistry UNSBC, Tirana, Albania. ³Head of the Department of Dentistry UNSBC, Tirana, Albania.

Received: 18 July 2019 Accepted: 21 October 2019

Published online: 14 November 2019

References

- Sheridan JJ. Guidelines for contemporary air-rotor stripping. *J Clin Orthod.* 2007;41:315–20.
- Bolton A. Disharmony in tooth size and its relation to the analysis and treatment of malocclusion. *Angle Orthod.* 1958;28:113–30.
- Rossouw PE, Tortorella A. Enamel reduction procedures in orthodontic treatment. *J Can Dent Assoc.* 2003;69:378–83.
- Zachrisson BU, Nyøygard L, Mobarak K. Dental health assessed more than 10 years after interproximal enamel reduction of mandibular anterior teeth. *AJODO.* 2007;131:162–9.
- Zachrisson BU. Interdental papilla reconstruction in adult orthodontics. *World J Orthod.* 2004;5:67–73.
- Lombardo L, Guarneri MP, D'Amico P, Molinari C, Meddis V, Carlucci A, Siciliani G. Orthofile(R): a new approach for mechanical interproximal reduction: a scanning electron micro- scopic enamel evaluation. *J Orofac Orthop.* 2014;75(3):203–12.
- Lapenaite E, Lopatiene K. Interproximal enamel reduction as a part of orthodontic treatment. *Stomatologija.* 2014;16(1):19–24.
- Livas C, Jongsma AC, Ren Y. Enamel reduction techniques in orthodontics: a literature review. *Open Dent J.* 2013;7:146–51.

- Arman A, Cehreli SB, Ozel E, Arhun N, Cetinsahin A, Soyman M. Qualitative and quantitative evaluation of enamel after various stripping methods. *AJODO.* 2006;130:131.
- Danesh G, Hellak A, Lippold C, Ziebur T, Schafer E. Enamel surfaces following interproximal reduction with different methods. *Angle Orthod.* 2007;77:1004–10.
- Hudson AL. A study of the effects of mesiodistal reduction of mandibular anterior teeth. *AJODO.* 1956;42:615–24.
- Stecksén-Blicks C, Renfors G, Oscarson ND, Bergstrand F, Twetman S. Caries-preventive effectiveness of a fluoride varnish: a randomized controlled trial in adolescents with fixed orthodontic appliances. *Caries Res.* 2007;41(6):455–9.
- Kirschneck C, Christl J-J, Reicheneder C, Proff P. Efficacy of fluoride varnish for preventing white spot lesions and gingivitis during orthodontic treatment with fixed appliances-a prospective randomized controlled trial. *Clin Oral Investig.* 2016;20(9):2371–8.
- Bonetti G, Zanarini M, Incerti Parenti S, Marchionni S, Checchi L. In vitro evaluation of casein phosphopeptide- amorphous calcium phosphate (CPP-ACP) effect on stripped enamel surfaces. A SEM investigation. *J Dent.* 2009;37:228–32.
- Grippaudo C, Cancellieri D, Grecolini ME, Deli R. Comparison between different interdental stripping methods and evaluation of abrasive strips: SEM analysis. *Prog Orthod.* 2010;11:127–37.
- Zingler S, Sommer A, Sen S, Saure D, Langer J, Guillon O, Lux CJ. Efficiency of powered systems for interproximal enamel reduction (IER) and enamel roughness before and after polishing: an in vitro study. *Clin Oral Invest.* 2016;20(5):933–42.
- Johner AM, Pandis N, Dudic A, Kiliaridis S. Quantitative comparison of 3 enamel-stripping devices in vitro: how precisely can we strip teeth? *AJODO.* 2013;143(4):S168–72.
- Nucci C, Marchionni S, Piana G, Mazzoni A, Prati C. Morphological evaluation of enamel surface after application of two “home” whitening products. *Oral Health Prev Dent.* 2004;2:221–9.
- Paganelli C, Zanarini M, Pazzi E, Marchionni S, Visconti L, Bonetti G. Interproximal enamel reduction: an in vivo study. *Scanning.* 2015;37(1):73–81.
- Lerman J. Study design in clinical research: sample size estimation and power analysis. *Can J Anaesth.* 1996;43(2):84–91.
- Zhong M, Jost-Brinkmann PG, Zellman M, Zellmann S, Radlanski RJ. Clinical evaluation of a new technique for interdental enamel reduction. *J Orofac Orthop.* 2000;61:432.
- Baumgartner S, Iliadi A, Eliades T, Eliades G. An in vitro study on the effect of an oscillating stripping method on enamel roughness. *Prog Orthod.* 2015; 10; 16:1.
- Lione R, Gazzani F, Pavoni C, Guarino S, Tagliaferri V, Cozza P. In vitro and in vivo evaluation of diamond-coated strips. *Angle Orthod.* 2017;87(3):455–9.
- Piacentini C, Sfondrini G. A scanning electron microscopy comparison of enamel polishing methods after air-rotor stripping. *AJODO.* 1996;109:57–63.
- Ballard ML. Asymmetry in tooth size: a factor in the etiology, diagnosis and treatment of malocclusion. *Angle Orthod.* 1944;14:67–70.
- Kaouara Y, Mohind HB, Azaroual MF, Zaoui F, Bahije L, Benyahia H. In vivo enamel stripping: a macroscopic and microscopic analytical study. *Int Orthod.* 2019;17(2):235–42.
- Joseph VP, Rossouw PE, Basson NJ. Orthodontic microabrasive reproximation. *AJODO.* 1992;102:351–9.

Publisher's Note

Springer Nature remains neutral with regard to jurisdictional claims in published maps and institutional affiliations.

Ready to submit your research? Choose BMC and benefit from:

- fast, convenient online submission
- thorough peer review by experienced researchers in your field
- rapid publication on acceptance
- support for research data, including large and complex data types
- gold Open Access which fosters wider collaboration and increased citations
- maximum visibility for your research: over 100M website views per year

At BMC, research is always in progress.

Learn more biomedcentral.com/submissions



RESEARCH ARTICLE

Open Access



Evaluation of free and total fluoride concentration in mouthwashes via measurement with ion-selective electrode

Vladimir Yu. Reshetnyak¹, Olga V. Nesterova¹, Oleg I. Admakin², Denis A. Dobrokhoto¹, Irina N. Avertseva¹, Samira A. Dostdar³ and Dinara F. Khakimova^{2*}

Abstract

Background: The aim of this study was to compare free fluoride concentration and total fluoride concentration in mouthwashes.

Methods: Fluorine-containing mouthwashes from various companies and manufacturers (Colgate Total Plax Classic Mint®, Colgate-Palmolive, New York, USA; Colgate Total Plax Gentle Mint®, Colgate-Palmolive, New York, USA; Colgate Total Plax Fresh Mint®, Colgate-Palmolive, New York, USA; Oral B Advantage®, Procter&Gamble, Cincinnati, USA; Reach Fresh Mint®, Johnson&Johnson, New Brunswick, USA; Foramen®, Laboratorios Foramen, Guarnizo, Spain; Lacalut Sensitive®, Dr. THEISS, Homburg, Germany; Sensodyne®, GlaxoSmithKline, London, UK; Vesna F®, Vita, Saint Petersburg, Russia; Lacalut Fresh®, Dr. THEISS, Homburg, Germany) were selected as study objects. Fluoride measurements were carried out using the fluoride selective electrode.

Results: Free fluoride:total fluoride ratio was more than 80% for six samples (Colgate Total Plax Gentle Mint® - 88%, Colgate Total Plax Fresh Mint® - 99%, Oral B Advantage® - 92%, Reach Fresh Mint® - 92 and 89% for the mouthwash of another batch, Lacalut Sensitive® - 94%) and less than 63% for three samples (Colgate Total Plax Classic Mint® - 56%, Foramen® - 62%, Vesna F® - 61%). Two samples had more than 70% and less than 80% of unbound fluoride, respectively (Sensodyne® - 77%, another batch of Oral B Advantage® mouthwash - 74%). Rinse containing sodium monofluorophosphate (Na₂PO₃F) (Vesna F®) had more than 50% of free fluoride, while the rinse containing amine fluoride (AmF) (Lacalut Sensitive®) had 94%. The difference in the free fluoride:total fluoride ratio can be explained by binding of fluoride ions by components contained in mouthwashes, such as coloring agents and polymeric compounds. The lowest concentration of free fluoride ions (0.000093 mol/L) was observed for aluminum fluoride (AlF₃) rinse (Lacalut Fresh®), while the total fluoride amount was not determined due to possible generation of strong fluoride complexes. This implies that fluoride ions will not be uptaken by tooth tissue and may even be washed away from it, compromising the efficacy of mouthwashes.

Conclusions: The differences in free fluoride: total fluoride ratio between analyzed mouthwashes reveal a need to develop a method for evaluation of free fluorides in mouthwashes for proper updating of national and international guidelines.

Keywords: Fluorides, Mouthwashes, Potentiometry, Ion-selective electrode

* Correspondence: dr.khakimova@gmail.com

²Department of Prevention and Communal Dentistry, Institute of Dentistry, Sechenov University, Moscow, Russia

Full list of author information is available at the end of the article



© The Author(s). 2019 **Open Access** This article is distributed under the terms of the Creative Commons Attribution 4.0 International License (<http://creativecommons.org/licenses/by/4.0/>), which permits unrestricted use, distribution, and reproduction in any medium, provided you give appropriate credit to the original author(s) and the source, provide a link to the Creative Commons license, and indicate if changes were made. The Creative Commons Public Domain Dedication waiver (<http://creativecommons.org/publicdomain/zero/1.0/>) applies to the data made available in this article, unless otherwise stated.

Background

According to the World Health Organization, dental caries is a disease prevalent among 60–90% of school-age children and almost 100% of adults worldwide [1]. There are numerous reports regarding the influence of comprehensive prevention programs on the prevalence of caries, including topical fluoridation provided by the application of fluoride-containing toothpastes, mouthwashes, gels, foams, and varnishes [2–8].

In addition to the fluorides, other inorganic elements are essential to mineralize hard tooth tissues and increase their resistance to caries. Toothpastes and mouthwashes containing sodium phosphate, calcium glycerophosphate, and zinc oxide exhibit a pronounced anticaries action [9–11].

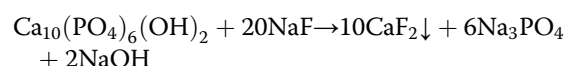
Mouthwashes are additional products for oral hygiene. Most of the currently available mouthwashes can be divided into four groups, depending on their therapeutic action: (1) mouthwashes reducing oral malodor; (2) mouthwashes decreasing dental plaque formation due to antibacterial action; (3) mouthwashes containing various concentrations of fluorine compounds and able to affect the mineralization of dental hard tissue; and (4) mouthwashes preventing or reducing gingivitis [12–17].

Various fluorine and phosphorus compounds are included as active components in the mouthwashes of the second and the third groups. Basic organic and inorganic fluorine compounds, contained in products for prophylaxis of oral cavity diseases, are sodium fluoride (NaF), sodium monofluorophosphate ($\text{Na}_2\text{PO}_3\text{F}$), amine fluoride (AmF), aluminum fluoride (AlF_3), and stannous fluoride (SnF_2) [18, 19]. The active mineral supplements could be phosphate salts, for instance, nano-sized sodium hexametaphosphate and sodium trimetaphosphate, which are capable of changing the solubility of enamel after adsorption on its surface [20, 21].

Mouthwashes containing fluorine compounds are divided into groups, depending on fluoride ion concentration: 0.05% sodium fluoride solutions can be used daily; and 0.2% sodium fluoride solutions are recommended for weekly or fortnightly application [22].

Rošin-Grget et al. reviewed various theories of the cariostatic action of fluorine. According to one of these theories, fluoride ions penetrate into the lattice of hydroxyapatite, $\text{Ca}_{10}(\text{PO}_4)_6(\text{OH})_2$, resulting in the formation of fluorohydroxyapatite, $\text{Ca}_{10}(\text{PO}_4)_6(\text{OH})\text{F}$, which is more resistant to acids [23].

According to another theory, during the exposure of the tooth surface to NaF, the reaction with hydroxyapatite results in the formation of poorly soluble crystals of calcium fluoride [23]:



It should be noted that the equilibrium shift in both chemical processes is determined by the activity of fluoride ions in the oral fluid, which in turn depends on the concentration of free fluoride ions in the applied prophylactic and therapeutic preparations. Various ingredients of mouthwashes, such as colourants, flavouring agents, sweeteners, preservatives, and surfactants, can chemically bind fluoride ions. Such bound fluoride is not effective in preventing and reducing dental caries. Thus, the control and the determination of «active» fluoride can determine the quality and, hence, the therapeutic efficacy of mouthwashes.

Fluorine-containing mouthwashes currently used in dental practice can be divided into three types: (1) therapeutic mouthwashes that can be purchased over-the-counter or prescribed only under the supervision of a doctor; (2) cosmetic mouthwashes mainly aimed at freshening breath; and (3) mouthwashes that are a combination of these two types [24].

Since the first type consists of therapeutic agents, the content of biologically active compounds is controlled by the corresponding normative and technical documentation and by appropriate methods of quantitative analysis of total fluoride.

The quality of the second type of preparations is in many cases determined only by the technical specifications in manufacturing and may not provide for the quantitative determination of the active substances in the final product.

The aim of this study was to compare active-fluoride and total-fluoride concentrations in 10 mouthwashes commercially available in Russian Federation.

Methods

Fluoride products

Fluorine-containing mouthwashes were purchased from local markets of Moscow (Russian Federation) and selected as study objects (Table 1). Colgate Total Plax Classic Mint® (0.025% NaF), Colgate Total Plax Gentle Mint® (0.025% NaF), and Colgate Total Plax Fresh Mint® (0.025% NaF) are produced by Colgate-Palmolive (New York, USA). Each of the products exhibits antibacterial activity and prevents dental plaque formation and oral malodor. Procter&Gamble (Cincinnati, USA) produces Oral B Advantage® (0.05% NaF) mouthwashes aimed at providing tooth and gum care. The company producing Reach Fresh Mint® is Johnson&Johnson (New Brunswick, USA). In addition to NaF (the content was not declared), Reach Fresh Mint® contains another active component – cetylpyridinium chloride. Laboratorios Foramen (Guarnizo, Spain) produces Foramen® (0.05% NaF), which strengthens tooth enamel. Dr. THEISS (Homburg,

Table 1 Composition of fluoride-containing mouthwashes.

Brand	Composition		Et	Glyc	Sorb	Other ingredients
	Active ingredients					
	Fluorides	Phosphates				
Colgate Total Plax Classic mint®	NaF	Disodium hydrogen phosphate	+	+	+	Sodium lauryl sulfate, sodium methyl cocoyl taurate, menthol, saccharin, aqua, flavourings, colourants
Colgate Total Plax Gentle mint®	NaF	Disodium hydrogen phosphate	+	+	+	Sodium lauryl sulfate, sodium methyl cocoyl taurate, menthol, saccharin, aqua, flavourings, colourants
Colgate Total Plax Fresh mint®	NaF	Disodium hydrogen phosphate	+	+	+	Sodium lauryl sulfate, sodium methyl cocoyl taurate, menthol, saccharin, aqua, flavouring agents, colourants
Oral B Advantage®	NaF	–	+	+	–	Methylparaben, propylparaben, poloxamer 407, cetylpyridine chloride, sodium saccharin, aqua, flavouring agents, colourants
Reach Fresh mint®	NaF	Disodium hydrogen phosphate, sodium dihydrogen phosphate	+	+	+	copolymer POE, sodium benzoate, polyphenylene oxide, POE (20) sorbitan monooleate, perfume, cetylpyridinium chloride, aqua, colourants
Foramen®	NaF	–	–	+	+	Potassium nitrate, PEG-40, allantoin, flavour additive, sodium methylparaben, sodium propylparaben, lemon acid, sodium benzoate, cetylpyridine chloride, aqua, sodium saccharinate
Lacalut sensitive®	AmF	–	–	+	–	Cocamidopropyl betaine, chlorhexidine bigluconate, aqua, aluminum lactate, propylene glycol, PEG-40, flavouring agent
Sensodyne®	NaF	Disodium hydrogen phosphate, sodium dihydrogen phosphate	–	+	+	Sodium benzoate, poloxamer 338, potassium chloride, PEG-60, aqua, cetylpyridine chloride, sodium saccharinate, sodium chloride, methylparaben, flavoring agent
Vesna F®	Na ₂ PO ₃ F	–	–	–	–	Aqua, xylitol, calcium glycerophosphate, polyoxyethylene sorbitan monooleate, sodium benzoate, citric acid, food flavour, colourants
Lacalut Fresh®	AlF ₃	–	–	–	–	Aqua, isopropyl alcohol, PEG-40 hydrogenated castor oil, flavors, peppermint extract, aluminum lactate, chlorhexidine bigluconate, sodium saccharinate, allantoin, bisabolol

Et ethanol, Glyc glycerol, Sorb sorbitol

Germany) produces Lacalut Sensitive® (0.33% AmF) and Lacalut Fresh® (0.2% AlF₃). Lacalut Sensitive® decreases sensitivity of teeth to thermal stimuli. Lacalut Fresh® prevents parodontitis due to astringent properties of aluminum lactate. GlaxoSmithKline (London, UK) is manufacturer of Sensodyne® (0.0217% NaF). Sensodyne® also reduces tooth

sensitivity. Vita (Saint Petersburg, Russia) produces Vesna F® (0.012% fluorine) mouthwash, which contains Na₂PO₃F and calcium glycerophosphate as active components. These mouthwashes are the most widely represented on Russian market and recommended by dental practitioners for the proper oral care.

Table 2 Calibration of ISE in NaF standard aqueous solutions

	Concentration of NaF, mol/L									Average
	0.5	0.1	0.05	0.01	0.005	0.001	0.0005	0.0001	0.00005	
pF	0.533	1.119	1.362	2.046	2.320	3.017	3.310	4.000	4.301	
EMF	573.0	532.0	524.2	470.0	466.9	409.0	405.5	353.0	338.0	
	573.7	531.5	524.7	471.0	467.6	407.6	406.6	350.0	344.4	
	572.8	532.3	522.0	471.0	469.2	406.7	408.0	347.6	340.0	
		534.4		478.0		410.0		340.0		
		536.0		478.0		407.0		345.5		
		539.5		473.8		404.0		348.1		
\bar{X}	573.2	534.3	523.6	473.6	467.9	407.4	406.7	347.4	340.8	
S	0.47	3.03	1.44	3.61	1.18	2.08	1.25	4.40	3.27	2.18
ΔX	0.69	3.18	2.14	3.79	1.75	2.18	1.86	4.62	4.86	2.53
E(%)	0.12	0.60	0.41	0.80	0.37	0.53	0.46	1.33	1.43	0.58

Table 3 Calibration of ISE in NaF solutions prepared with Albavit solution

pF	0	0.553	0.803	1.119	1.362	1.660	2.046	2.320	2.620	3.017	3.310
EMF (aq.)	594	573		534	520		474	467		420	406
EMF (Alba)			556			505			442		

Fluoride measurements

The method of direct potentiometry was used to determine fluoride ion activity using fluoride ion-selective electrode based on lanthanum fluoride. Standard silver chloride electrode was used as a reference electrode. Electromotive force of a galvanic cell was measured by standard laboratory ion meter I160M. The calibration of the electrode was performed every day before fluoride measurements.

To obtain calibration curves, series of NaF standard solutions ($5 \cdot 10^{-1}$ - $5 \cdot 10^{-5}$ M) were prepared using either deionized water, or Albavit solution, which does not contain fluoride ions and is similar in composition to the test mouthwashes. Calibration curve data is given in Table 2 and Table 3 and in Fig. 1. The accuracy of

measurement of fluoride ion concentrations in standard solutions of NaF is shown in Table 4. Similar measurements for NaF solution prepared with Albavit solution are represented in Table 5.

To determine total fluoride concentration in mouthwashes, the method of standard addition was applied. Samples of mouthwashes were diluted in total ionic strength adjustment buffer (TISAB), which sets constant ionic strength during measurement and which also precomplexes interfering ions (e.g., aluminium ions Al^{3+}). After the measurement of potential of each diluted sample a known amount of standard was added and the measurement was repeated again for further calculation of difference in the potentials and quantification of total fluoride. Since the results of quantitative determination of fluoride ions on

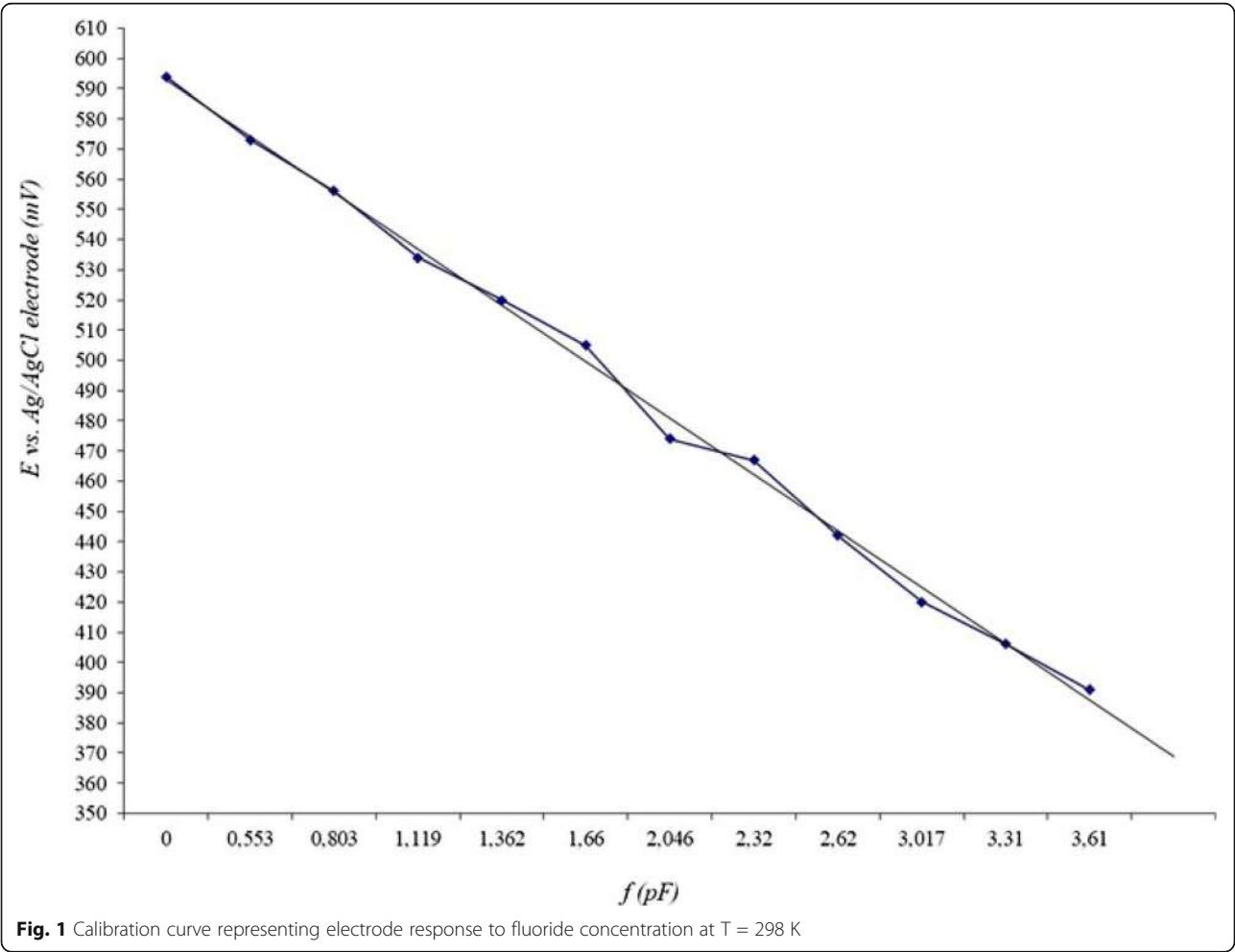


Fig. 1 Calibration curve representing electrode response to fluoride concentration at T = 298 K

Table 4 The accuracy of measurement of F^- in NaF standard aqueous solutions

NaF / TISAB	EMF	+ 10 ml TISAB	V (NaF) added, ml	ΔE	c (F^-)	%	\bar{X}	S	X	E, %
5 / 5	508.2	490.9	9.2	17.3	0.096	96	95.8	1.92	2.21	2.3
3 / 7	495.6	478.5	4.0	17.1	0.095	95				
7 / 3	518.4	498.7	19.2	19.7	0.094	94				
3 / 7	497.0	478.8	4.2	18.2	0.099	99				
5 / 5	505.0	488.0	9.1	17.0	0.095	95				

standard mixtures prepared with aqueous solution and Albavit solution were slightly differentiated (i.e., the results obtained in the first case were systematically lower compared to those obtained theoretically, whereas in the second case the results were found to be higher), we attempted to modify the procedure by using the method of double increase in concentration without preliminary dilution with TISAB solution in order to determine possible binding of fluoride ions by components contained in the mouthwashes. Every sample of the mouthwash was measured five times and the mean of the measurements was used for further statistical estimation.

Results

Results of fluoride analysis are shown in Table 6. Most of the analyzed mouthwashes contained NaF as a source of fluoride ions; other types of fluoride agents were Na_2PO_3F , AmF, and AlF_3 . Free fluoride:total fluoride ratio was more than 80% for six samples (Colgate Total Plax Gentle Mint® - 88%, Colgate Total Plax Fresh Mint® - 99%, Oral B Advantage® - 92%, Reach Fresh Mint® - 92 and 89% for the mouthwash of another batch, Lacalut Sensitive® - 94%) and less than 63% for three samples (Colgate Total Plax Classic Mint® - 56%, Foramen® - 62%, Vesna F® - 61%). Two samples had more than 70% and less than 80% of unbound fluoride, respectively (Sensodyne® - 77%, another batch of Oral B Advantage® mouthwash - 74%). Rinse containing Na_2PO_3F (Vesna F®) had more than 50% of free fluoride, while the rinse containing AmF (Lacalut Sensitive®) had 94%. The lowest concentration of free fluoride ions (0.000093 mol/L) was observed for AlF_3 rinse (Lacalut Fresh®).

Discussion

The State Standard of Russian Federation P 51577–2000 specifies only the total amount of fluoride ions in liquid oral hygiene products. We failed to find articles dedicated to the

determination of free fluoride concentration in mouthwashes; however, several authorities have been focusing on the studies aimed at free fluoride analysis in toothpaste since 2005 [25–27]. The participants of European Organization for Caries Research Workshop, which was held to discuss the issues related to the methodology for determination of potentially available fluoride in toothpastes, have emphasized the necessity of developing methods measuring fluoride bioavailability [28]. The development of techniques providing the assessment of free fluoride in mouthwashes is also required. Mouthwashes selected for fluoride measurements do not represent all the variety of brands commercially available in Russia, however even the small sample size indicates great discrepancies between the obtained data on fluoride content.

The experiment showed the results to be almost identical for the Colgate Total Plax (Gentle Mint)® and Colgate Total Plax (Fresh Mint)® solutions, with both methods.

Significant differences in concentrations determined by the method of standard addition and by the modified method of quantitative assessment were observed for such solutions as Oral B®, Reach®, and Foramen®. The fact that an increase in total fluoride content was observed with the modified method may be explained by a change in the ionic strength of the solution during the measurement; or by partial binding of fluoride ions by certain components of the mouthwashes; or possibly by polymeric compounds such as poloxamers and polyphe-nylene oxides. Analogous observations were made for the Sensodyne® solution, which does include polymeric compounds. This assumption is supported by the fact that in standard solutions prepared with Albavit solution containing polymeric compounds, the determined concentration was systematically higher than the theoretical concentration; whereas systematically lower results were obtained with model solutions in the procedure of fluoride ion determination using TISAB solution.

Table 5 The accuracy of measurement of F^- in NaF standard solutions prepared using Albavit solution (4 ml «Alba» + 1 ml NaF)

c (NaF), mol/L	EMF	+ 5 ml TISAB	+ 10 ml TISAB	V (NaF) added, ml	c (F^-) theoretical	c (F^-) actual	\bar{c} (F^-)
0.5	532.2	505.3	486.9	1.0	0.100	0.104	0.105 ± 0.002
0.5	536.7	509.7	490.8	1.0	0.100	0.106	
0.5	534.2	507.2	489.8	1.0	0.100	0.105	
0.1	501.3	469.5	450.8	1.0	0.020	0.022	0.022 ± 0.0005

Table 6 The determination of fluoride-ions concentration and activity by the method of standard addition and modified method

Label	pH	Dilution	F^- , mol/L $\times 10^{-3}$			
			Method of standard addition		Modified method	
			c (F^-)	a (F^-)	c (F^-)	a (F^-)
Colgate Total Plax Classic mint	7.15	–	9.77	5.52	9.92	5.43
		1÷10	0.75	0.89	1.11	1.06
Colgate Total Plax Gentle mint	5.70	–	9.14	8.05	8.91	8.71
		1÷10	1.22	0.75	1.19	1.20
Colgate Total Plax Fresh mint	5.95	–	9.87	9.81	9.39	8.92
		1÷10	0.63	0.47	0.70	0.43
Oral B Advantage	5.70	–	17.23	15.81	25.91	15.52
		1÷10	1.42	1.21	1.2	0.98
Oral B Advantage ^a	5.75	–	16.70	12.30	16.81	6.08
Reach Fresh mint	5.80	–	15.86	14.56	24.09	13.71
		1÷10	1.20	0.71	1.40	1.02
Reach Fresh mint ^a	5.75	–	18.15	16.10	26.90	14.20
Foramen	5.80	–	14.62	9.11	20.05	9.05
		1÷10	0.75	0.94	1.20	1.07
Lacalut sensitive	4.40	–	5.48	5.13	8.60	4.20
		1÷10	0.758	0.77	0.15	0.86
Sensodyne	5.70	–	16.25	12.53	23.59	11.12
		1÷10	2.01	1.27	–	–
Vesna F	6.05	–	4.49	2.76	5.20	2.71
Lacalut Fresh	4.20	–	–	0.093	1.30	0.095
		1÷10	–	0.012	0.14	0.012

^a mouthwash of another batch was used

In those preparations lacking polymeric compounds, results of fluoride ion determination were identical at the constant ionic strength and modified method within the error of experiment. To confirm these assumptions, we determined concentration and activity of the test solutions following 10-fold dilution. The behavior of investigated values of activity and concentration also differs in both groups of preparations: while concentration for the preparations not containing polymeric compounds showed on average a 10-fold change following dilution, the 10-fold dilution of preparations containing polymeric compounds resulted in an 18-to-20-fold change of these values.

These trends are not observed for mouthwash containing AmF (Lacalut Sensitive®) as a source of active fluorine, even though it contains polymeric compounds (polyethylene glycol) in its formulation; and the mode of change of both activity and concentration following dilution corresponds to that of mouthwashes that do not contain polymeric compounds. It is noteworthy that after each measurement of AmF mouthwash the electrode continued retaining the potential when being immersed in distilled water and even required additional

washing or mechanical cleaning of membrane surface. Therefore, one could presume that high free fluoride to total fluoride ratio (94%) could be due to adsorption of AmF on the surface of the electrode membrane.

The determinable concentrations are almost identical for the Colgate Total Plax® mouthwashes, which only vary by type of coloring agent. However, for the Colgate Total Plax (Classic Mint®) mouthwash, the decrease in the activity of fluoride ions can be explained by the difference in the type of colorant added at approximately the same concentration of total fluoride. Therefore, it is reasonable to assume that the coloring agent added to Colgate Total Plax (Classic Mint®) mouthwash could bind free fluorides.

The analysis of the results, obtained for different series of the same mouthwash, revealed differences in the content of active fluorine for the Oral B® rinses and almost identical values for the Reach Fresh mint® solutions. The comparative analysis of test solutions containing NaF or AmF as a source of fluoride ions showed that there is no significant difference between the measured values of active fluorine and those calculated theoretically, in both procedures. Thus, both

organic and inorganic sources of fluoride have similar potential against tooth decay, which can be confirmed by clinical data [29].

A particularly low activity of fluoride ions in comparison with the declared one was observed for the Lacalut Fresh® solution, in which AlF_3 served as the source of fluoride ions. The results of determination of fluoride concentration by standard method showed an abnormal increase in the activity of fluoride ions following the initial dilution with TISAB and the standard behavior following the secondary dilution. When a standard of NaF was added to the solution, a sharp reduction of the potential was observed instead of an increase. Thus, the standard procedure for this preparation turned out to be inapplicable due to a possible interaction between the components of buffer solution TISAB and the components of the test solution. Therefore, to determine the total concentration of fluoride ions, the modified method was selected. To understand the practically 700-fold fluoride ion activity decrease compared to declared values, additional studies were performed, in particular the pH determination of test solutions. The results showed that Lacalut Sensitive® and Lacalut Fresh® solutions have the lowest pH values (4.2 and 4.4, respectively). In the experiment, the pH values of these solutions were adjusted to a value of 7.00, with the electromotive force for the Lacalut Sensitive® solution changing insignificantly (within 2%), whereas for Lacalut Fresh® the change was over 16%. To elucidate the reasons for the observed behavior, we added the precise aliquot of NaF standard solution to the test sample. The addition of the known amount of NaF led to a 6.5-fold increase in the activity of fluoride ions, whereas their theoretically calculated activity should have increased 100-fold. This allows one to conclude that the obtained result is the consequence of fluoride ion binding by the solution components into a non-ionized species of the fluorine compounds (complexes or poorly dissociating dimers hydrogen fluoride H_2F_2) [30]. To evaluate the binding capacity of fluoride ions, the experiment was carried out according to the modified method by doubling the concentration of the standard. In this case, the known concentration of NaF was added to the Lacalut Fresh® solution containing the standard until the activity doubled. The result of the experiment showed that the addition of 75% of the required amount of NaF was followed by the doubling of fluoride ion activity, with the further addition of a minimal amount of fluoride ions, leading to a dramatic increase in the activity (300-fold!). This provides quantitative proof of depletion of fluoride ion binding capacity (i.e., the component binding fluoride ions has completely reacted). Interestingly, the pH value of the solution dramatically changed: from 4.2 to 6.5 (the pH value of the standard solution of NaF is 7.7). The results of the experiment may be attributable to possible generation of strong complexes due to fluoride ion binding by the components of the test solution, particularly by hexafluoroaluminate (AlF_6^{3-}), rather than to formation of non-ionized fluorine compounds due to acidic pH value (e.g., the pH shift of the Lacalut Sensitive® solution resulted in insignificant changes). Thus, a study of fluoride ion activity in the Lacalut Fresh® solution suggests that fluoride ions will not be uptaken by tooth tissue and may even be washed away from it; thus, this supplement will have no effect when applied according to the directions for use of the preparation (5–7 drops/100 ml water).

The present study has some limitations since it does not reproduce in vivo conditions, i.e. dilution by saliva and influence of saliva components on the release of fluoride ions. It is known that phosphatase, one of saliva components, hydrolyzes $\text{Na}_2\text{PO}_3\text{F}$, releasing fluoride ions [25, 32]. Thus, it may be necessary to add components reproducing artificial saliva during sample preparation in order to avoid underestimated results when measuring $\text{Na}_2\text{PO}_3\text{F}$ mouthwashes. The method of potentiometry itself does not account for the influence of mouthwash components on the work of the electrode.

The present study has some limitations since it does not reproduce in vivo conditions, i.e. dilution by saliva and influence of saliva components on the release of fluoride ions. It is known that phosphatase, one of saliva components, hydrolyzes $\text{Na}_2\text{PO}_3\text{F}$, releasing fluoride ions [25, 32]. Thus, it may be necessary to add components reproducing artificial saliva during sample preparation in order to avoid underestimated results when measuring $\text{Na}_2\text{PO}_3\text{F}$ mouthwashes. The method of potentiometry itself does not account for the influence of mouthwash components on the work of the electrode.

Conclusions

Mouthwashes are oral hygiene products aimed at enhancing the remineralization process and reducing demineralization due to the presence of fluoride ions; however, mouthwashes should also contain an appropriate amount of free fluorides to provide bioavailability. Ten different mouthwashes analyzed in the present study they revealed various free fluoride: total fluoride ratios due to binding of fluoride ions by mouthwash components or ability of fluoride source itself to form its complexes. The lower concentration of free fluoride in comparison with total one could lead to a decrease in the caries-preventive effect. However, the methods to quantify free fluoride have some disadvantages since they do not reflect in vivo conditions and, therefore, may result in distorted or underestimated values of fluoride content. Thus, there is a need to develop a method for evaluation of free fluorides in mouthwashes for proper updating of national and international guidelines.

Abbreviations

Al^{3+} : Aluminium ions; AlF_3 : Aluminum fluoride; AmF: Amine fluoride; $\text{Ca}_{10}(\text{PO}_4)_6(\text{OH})_2$: Hydroxyapatite; $\text{Ca}_{10}(\text{PO}_4)_6(\text{OH})\text{F}$: Fluorohydroxyapatite; CaF_2 : Calcium fluoride; H_2F_2 : Hydrogen fluoride; $\text{Na}_2\text{PO}_3\text{F}$: Sodium monofluorophosphate; Na_3PO_4 : Trisodium phosphate; NaF: Sodium fluoride; NaOH: Sodium hydroxide; SnF_2 : Stannous fluoride; TISAB: Total ionic strength adjustment buffer

Acknowledgements

Not applicable.

Authors' contributions

Conceptualization: VYR, OVN, OIA, DAD, INA, DFH and SAD; Data curation: VYR, OVN, OIA, DAD and INA; Formal analysis: VYR, OVN, OIA, DAD, INA, DFH and SAD; Investigation: VYR, OVN, OIA, DAD, INA, DFH and SAD; Methodology: VYR, OVN, OIA and DAD; Project administration: VYR, OVN, OIA, DAD and DFH; Resources: DAD, INA, DFH and SAD; Supervision: VYR, OVN and OIA; Validation: VYR, OVN, OIA, DAD and DFH; Visualization: VYR, OVN, OIA, DAD and INA; Writing original draft: VYR, OVN, OIA, DAD, INA, DFH

and SAD; Writing review & editing: VYR, OVN, OIA, DAD, INA, DFH and SAD; All authors have read and approved the manuscript.

Funding

There was no funding support available for this research.

Availability of data and materials

The data from this study are available upon request, which must be approved by all the authors.

Ethics approval and consent to participate

Not applicable.

Consent for publication

Not applicable.

Competing interests

The authors declare that they have no competing interests.

Author details

¹Department of Chemistry in the Institute of Pharmacy, Sechenov University, Moscow, Russia. ²Department of Prevention and Communal Dentistry, Institute of Dentistry, Sechenov University, Moscow, Russia. ³5th year undergraduate student of the Institute of Pharmacy, Sechenov University, Moscow, Russia.

Received: 3 July 2019 Accepted: 9 September 2019

Published online: 20 November 2019

References

1. Treerutkuarkul A, Gruber K. Prevention is better than treatment. *Bull World Health Organ.* 2015;93(9):594–5.
2. Walsh T, Worthington HV, Glenny AM, Appelbe P, Marinho VC, Shi X. Fluoride toothpastes of different concentrations for preventing dental caries in children and adolescents. *Cochrane Database Syst Rev.* 2010;(1):CD007868.
3. Rasines G. Fluoride toothpaste prevents caries in children and adolescents at fluoride concentrations of 1000 ppm and above. *Evid Based Dent.* 2010;11(1):6–7.
4. Marinho VC, Chong LY, Worthington HV, Walsh T. Fluoride mouthrinses for preventing dental caries in children and adolescents. *Cochrane Database Syst Rev.* 2016;7:CD002284.
5. Marinho VC, Worthington HV, Walsh T, Chong LY. Fluoride gels for preventing dental caries in children and adolescents. *Cochrane Database Syst Rev.* 2015;(6):CD002280.
6. Twetman S, Keller MK. Fluoride Rinses, Gels and Foams: An Update of Controlled Clinical Trials. *Caries Res.* 2016;50(Suppl 1):38–44.
7. Marinho VC, Worthington HV, Walsh T, Clarkson JE. Fluoride varnishes for preventing dental caries in children and adolescents. *Cochrane Database Syst Rev.* 2013;(7):CD002279.
8. Weyant RJ, Tracy SL, Anselmo TT, Beltran-Aguilar ED, Donly KJ, Frese WA, et al. Topical fluoride for caries prevention: executive summary of the updated clinical recommendations and supporting systematic review. *J Am Dent Assoc.* 2013;144(11):1279–91.
9. Sun Y, Li X, Deng Y, Sun JN, Tao D, Chen H, et al. Mode of action studies on the formation of enamel minerals from a novel toothpaste containing calcium silicate and sodium phosphate salts. *J Dent.* 2014;42(Suppl 1):S30–8.
10. Zaze AC, Dias AP, Sasaki KT, Delbem AC. The effects of low-fluoride toothpaste supplemented with calcium glycerophosphate on enamel demineralization. *Clin Oral Investig.* 2014;18(6):1619–24.
11. Takatsuka T, Tanaka K, Iijima Y. Inhibition of dentine demineralization by zinc oxide: in vitro and in situ studies. *Dent Mater.* 2005;21(12):1170–7.
12. Blom T, Slot DE, Quirynen M, Van der Weijden GA. The effect of mouthrinses on oral malodor: a systematic review. *Int J Dent Hyg.* 2012;10(3):209–22.
13. Arweiler NB, Henning G, Reich E, Netuschil L. Effect of an amine-fluoride-triclosan mouthrinse on plaque regrowth and biofilm vitality. *J Clin Periodontol.* 2002;29(4):358–63.
14. Pizzo G, La Cara M, Licata ME, Pizzo I, D'Angelo M. The effects of an essential oil and an amine fluoride/stannous fluoride mouthrinse on supragingival plaque regrowth. *J Periodontol.* 2008;79(7):1177–83.
15. Altenburger MJ, Schirmermeister JF, Wrbs KT, Hellwig E. Remineralization of artificial interproximal carious lesions using a fluoride mouthrinse. *Am J Dent.* 2007;20(6):385–9.
16. Laheij AM, van Strijp AJ, van Loveren C. In situ remineralisation of enamel and dentin after the use of an amine fluoride mouthrinse in addition to twice daily brushings with amine fluoride toothpaste. *Caries Res.* 2010;44(3):260–6.
17. Boyle P, Koechlin A, Autier P. Mouthwash use and the prevention of plaque, gingivitis and caries. *Oral Dis.* 2014;20(Suppl 1):1–68.
18. Rugg-Gunn A, Banoczy J. Fluoride toothpastes and fluoride mouthrinses for home use. *Acta Med Acad.* 2013;42(2):168–78.
19. Faller RV, Eversole SL, Saunders-Burkhardt K. Protective benefits of a stabilised stannous-containing fluoride dentifrice against erosive acid damage. *Int Dent J.* 2014;64 Suppl 1:29–34.
20. Garcia LSG, Delbem ACB, Pessan JP, Dos Passos Silva M, Neto FNS, Gorup LF, et al. Anticaries effect of toothpaste with nano-sized sodium hexametaphosphate. *Clin Oral Investig.* 2019;23(9):3535–42.
21. Emerenciano NG, Botazzo Delbem AC, Pessan JP, Nunes GP, Souza Neto FN, de Camargo ER, et al. In situ effect of fluoride toothpaste supplemented with nano-sized sodium trimetaphosphate on enamel demineralization prevention and biofilm composition. *Arch Oral Biol.* 2018;96:223–9.
22. Cheng LL. Limited evidence suggests fluoride mouthrinse may reduce dental caries in children and adolescents. *J Am Dent Assoc.* 2017;148(4):263–6.
23. Rosin-Grget K, Peros K, Sutej I, Basic K. The cariostatic mechanisms of fluoride. *Acta Med Acad.* 2013;42(2):179–88.
24. Zero DT. Dentifrices, mouthwashes, and remineralization/caries arrestment strategies. *BMC Oral Health.* 2006;6(Suppl 1):S9.
25. van Loveren C, Moorer WR, Buijs MJ, van Palenstein Helderman WH. Total and free fluoride in toothpastes from some non-established market economy countries. *Caries Res.* 2005;39(3):224–30.
26. Benzian H, Holmgren C, Buijs M, van Loveren C, van der Weijden F, van Palenstein Helderman W. Total and free available fluoride in toothpastes in Brunei, Cambodia, Laos, the Netherlands and Suriname. *Int Dent J.* 2012; 62(4):213–21.
27. Carey CM, Holahan EC, Schmuck BD. Analysis of 1-Minute Potentially Available Fluoride from Dentifrice. *J Res Natl Inst Stand Technol.* 2014;119:602–9.
28. Martinez-Mier EA, Tenuta LMA, Carey CM, Cury JA, van Loveren C, Ekstrand KR, et al. European Organization for Caries Research Workshop: Methodology for Determination of Potentially Available Fluoride in Toothpastes. *Caries Res.* 2019;53(2):119–36.
29. Ringelberg ML, Webster DB, Dixon DO, LeZotte DC. The caries-preventive effect of amine fluorides and inorganic fluorides in a mouthrinse or dentifrice after 30 months of use. *J Am Dent Assoc.* 1979;98(2):202–8.
30. Frant MS, Ross JW Jr. Electrode for sensing fluoride ion activity in solution. *Science.* 1966;154(3756):1553–5.
31. Cardiano P, Cigala RM, Crea F, Giacobello F, Giuffrè O, Irto A, et al. Sequestration of Aluminium (III) by different natural and synthetic organic and inorganic ligands in aqueous solution. *Chemosphere.* 2017;186:535–45.
32. Duckworth RM, Knoop DT, Stephen KW. Effect of mouthrinsing after toothbrushing with a fluoride dentifrice on human salivary fluoride levels. *Caries Res.* 1991;25(4):287–91.

Publisher's Note

Springer Nature remains neutral with regard to jurisdictional claims in published maps and institutional affiliations.

Ready to submit your research? Choose BMC and benefit from:

- fast, convenient online submission
- thorough peer review by experienced researchers in your field
- rapid publication on acceptance
- support for research data, including large and complex data types
- gold Open Access which fosters wider collaboration and increased citations
- maximum visibility for your research: over 100M website views per year

At BMC, research is always in progress.

Learn more biomedcentral.com/submissions



RESEARCH ARTICLE

Open Access



A novel guided surgery system with a sleeveless open frame structure: a retrospective clinical study on 38 partially edentulous patients with 1 year of follow-up

Jaafar Mouhyi^{1,2*}, Maurice Albert Salama^{3,4}, Francesco Guido Mangano⁵, Carlo Mangano⁶, Bidzina Margiani⁵ and Oleg Admakin⁵

Abstract

Background: This retrospective clinical study aims to present results of experience with a novel guided surgery system with a sleeveless, open-frame structure, in which the surgical handpiece (not the drills used for preparation) is guided.

Methods: This study was based on an evaluation of the records of partially edentulous patients who had been treated with a sleeveless open-frame guided surgery system (TWIN-Guide®, 2Ingis, Brussels, Belgium), between January 2015 and December 2017. Inclusion criteria were patients with good systemic/oral health and a minimum follow-up of 1 year. Exclusion criteria were patients who had been treated without a guide, or with a guide with sleeves, patients with systemic/oral diseases and who did not have a follow-up of 1 year. The main outcomes were surgical (fit and stability of the surgical guide, duration of the intervention, implant stability, and any intra-operative or immediate post-operative complication), biologic, and prosthetic.

Results: Thirty-eight patients (24 males, 14 females; mean age 56.5 ± 14.0 years) were included in the study. These patients had been treated with 110 implants inserted by means of 40 sleeveless, open-frame guides. With regard to fit and stability, 34 guides were excellent, 4 acceptable, and 2 inadequate for use. The mean duration of the intervention was $23.7 (\pm 6.7)$ minutes. Immediately after placement, 2 fixtures were not stable and had to be removed. Two patients experienced pain/swelling after surgery. The 108 surviving implants were restored with 36 single crowns and 32 fixed partial prostheses (24 two-unit and 8 three-unit bridges); these restorations survived until the 1-year follow-up, with a low incidence of biologic and prosthetic complications.

Conclusions: Within the limits of this study, this novel guided surgery system with sleeveless, open frame-structure guides seems to be clinically reliable; further studies on a larger sample of patients are needed to confirm these outcomes.

Keywords: Guided implant surgery, Open-frame sleeveless guides, Fit, Stability, Complications

* Correspondence: j.mouhyi@hotmail.fr

¹Casablanca Oral Rehabilitation Training & Education Center (CORTEC), Casablanca, Morocco

²Biomaterials Research Department, International University of Agadir (Universiapolis), 8143 Agadir, Morocco

Full list of author information is available at the end of the article



© The Author(s). 2019 **Open Access** This article is distributed under the terms of the Creative Commons Attribution 4.0 International License (<http://creativecommons.org/licenses/by/4.0/>), which permits unrestricted use, distribution, and reproduction in any medium, provided you give appropriate credit to the original author(s) and the source, provide a link to the Creative Commons license, and indicate if changes were made. The Creative Commons Public Domain Dedication waiver (<http://creativecommons.org/publicdomain/zero/1.0/>) applies to the data made available in this article, unless otherwise stated.

Background

Static guided oral surgery consists of the insertion of dental implants in the exact position, inclination, and depth [1, 2], through the use of customized tooth- [3], bone- [4], or mucosa-supported [4, 5] surgical guides designed with dedicated software and physically realized by three-dimensional (3D) printing [3, 6] or milling [7].

Theoretically, the insertion of dental implants through a surgical guide in an ideal position, planned in the computer, would represent an undoubted advantage for the surgeon [1–6, 8]; it would allow one to reduce the risks related to the invasion of anatomical structures (such as the inferior alveolar nerve and maxillary sinus, or the periodontal ligament and the roots of adjacent teeth, where present) and to obtain an ideal prosthetic emergence through the preparation of a virtual 3D diagnostic wax-up [8, 9]. This 3D wax-up, in fact, realized on a model captured by intraoral [10] or desktop [11] scanning within computer-assisted-design (CAD) software and imported into the guided surgery software, guides the insertion of the fixtures in the exact position and inclination, facilitating the prosthetic rehabilitation process [8, 9, 12]. Last but not least, guided surgery allows insertion without the need to raise a mucoperiosteal flap [13], which allows one to reduce the post-operative pain of the patient and the duration of the intervention [14, 15].

Despite these indisputable advantages, however, only a limited number of clinicians routinely use guided implant surgery today, and then almost exclusively for implant placement in completely edentulous patients [2, 9, 16, 17]. The causes of this are different, and only partly attributable to the costs of the design and fabrication of the surgical guide (often performed by external services). Of course, the planning process takes time, and a learning curve is necessary for the clinician to learn how to design with software [8, 18]; moreover, the costs of the required machines (cone beam computed tomography [CBCT] [19], intraoral or desktop scanner [6, 20], and, if the clinician wants to produce the guides, 3D printer [21]) can be quite high. But maybe these are not the real reasons why guided surgery has still not spread universally in the dental world, particularly, in the implant-supported restoration of partially edentulous patients [6, 18, 22].

The real reason why guided implant surgery in the partially edentulous patient has not yet spread globally could lie with the design of surgical templates [6, 23]. In fact, starting from 1992, when the concept of guided implant insertion was introduced, the design of the surgical guides proposed by the various software manufacturers or implant companies remained substantially the same and did not evolve [6, 23]. Most of the tooth-supported surgical guides currently available still remain resin bites with extended surfaces, which rest on

the adjacent teeth, completely covering the area below; the preparation of the implant site and the implant positioning are still carried out by means of a metal sleeve positioned inside the template, in which the surgeon inserts diameter reducers [2, 4, 6, 24].

This conventional approach presents various clinical problems. Firstly, in the posterior maxilla and mandible of partially dentate patients, the components necessary to insert implants in a guided manner (long preparation drills, surgical template, and sleeves) often steal too much space and thus do not allow the clinician to work [2, 6, 9, 25]. The presence of the sleeve, in fact, forces the surgeon to use long drills, available only in surgical kits specifically dedicated to guided surgery: only with these long drills, in fact, it is possible to prepare the implant site at the correct depth. Unfortunately, the limited opening of the patient's mouth and the presence of teeth in the antagonist arch do not allow the insertion *in situ* of the necessary components; hence, proceeding with the intervention is impossible [6, 25]. This obviously does not apply to completely edentulous patients [4, 5, 14, 16, 17]. There are, however, other problems such as the lack of fit and stability of the tooth-supported surgical guides, which, once positioned, often tend to move, forcing the clinician and the assistant to hold them in place with their hands [2, 3, 6, 18, 21, 22]. The lack of stability is a danger, since it can determine spatial deviations in the insertion of the implants, compared to the original planning [2, 3, 6, 18, 21, 22]. Such deviations do not necessarily lead to invasion of dangerous anatomical structures, but may result in an implant placement that is too buccal, which may lead to complications and aesthetic sequelae [3, 6, 18, 21, 22, 26], or insertion too close to other teeth or implants. All these situations can complicate the prosthetic rehabilitation, forcing the dental technician to adopt compromise solutions. The scientific literature has amply reported through systematic reviews [9, 16] that guided surgery is rather inaccurate, with deviations between the planned and the real (actual) position of the implants. The lack of stability of the template depends mainly on its design (and, obviously, the acquisition and prototyping tools used to fabricate it) [21, 24]; the material used may have a role too. In any case, the conventional templates covering the whole dentate arch do not allow the surgeon to have adequate visibility of the operative field (for example, they do not allow him to raise a flap to preserve the keratinized mucosa, which plays an important role in peri-implant health over time) [6]. Moreover, with these conventional templates it may be difficult to irrigate, with the risk of overheating the implant site [6]. Finally, the positioning of the fixture through the metallic sleeve can entail the risk of contamination of the implant surface, with possible negative consequences [27–29].

All these limitations are related to the approach conventionally used in guided surgery, which involves guiding the drills during site preparation through the use of sleeves. But today, there are alternatives to this approach.

The aim of this retrospective clinical study was to present a novel guided surgery system with a sleeveless, open-frame structure. In this system, no sleeves are used; the surgical handpiece is guided, not the drills used for preparation.

Methods

Study design; inclusion and exclusion criteria

The present retrospective study was based on the analysis and evaluation of the records of patients who underwent a guided implant surgery procedure, in two clinical centers, in the period between January 2015 and December 2017. Patient records were standardized and contained a whole range of information, such as gender and age at the time of surgery, oral and systemic health status, presence of smoking and/or alcohol use/abuse, type and number of fixtures inserted, their position and characteristics (length and diameter), and type of prosthetic restoration that was subsequently loaded on (single crowns [SC] or fixed partial prosthesis [FPP]).

The records were accompanied by medical imaging, and any complications or problems registered during the guided surgery (poor fit and lack of stability of the template; impossibility of using the template in the posterior sectors for lack of space; fracture of the template; aberrant placement of the implant with or without invasion of anatomical structures) were appropriately noted.

In addition, patient records contained additional information collected during the annual follow-up controls (1/2 per year for each patient, corresponding to planned professional oral hygiene sessions) or subsequent visits, such as the onset of complications or failures and/or the need for corrective actions.

Inclusion criteria for this study were partially edentulous patients treated with a new guided surgery system (TWIN-Guide®, 2Ingis, Brussels, Belgium) based on open-frame and sleeveless templates (where the handpiece was guided, but not the drill). These patients had to be in good oral and systemic health, and they had agreed to return to the clinical centre for control visits and annual professional hygiene sessions. Finally, in order to be included in the study, patients had to be followed for a minimum period of 1 year after surgery.

On the contrary, all patients who were treated with implant insertion without the use of surgical guide or with other conventional surgical templates that foresee the use of sleeves, patients who had oral or systemic diseases and patients who did not have a follow-up of at least 1 year were excluded from the study.

All patients had been treated after having received detailed explanations regarding the procedures to which they were to be subjected and after having accepted them by signing an informed consent; all patients were also informed about enrollment in this retrospective clinical study and consented to analysis of their medical records. Thus, this study respected the principles of the protection of patient health set forth in the Helsinki Declaration on experimentation on human subjects (2008 revision) and was endorsed by the local Ethics Committee of the Sechenov University of Moscow.

Surgical planning

For each patient, an impression with polyvinyl-siloxane material was taken with a proprietary acrylic radiotransparent tray (2Ingis® tray). This tray incorporated one or more Lego® bricks (Lego®, Copenhagen, Denmark), attached on the external surface of the tray. Before removing the impression tray, the patient underwent CBCT examination. The CBCT was immediately examined by the clinician, in order to verify the available bone volume and thus the feasibility of the surgery. The impression tray was removed and, from this, a stone cast model was poured. After the patient left the dental office, the clinician extracted from the CBCT all digital imaging and communication in dentistry (DICOM) files and sent these data to the 2Ingis® center for a second check of the quality of the CBCT. The DICOM files were imported in the SMOP® software (Swissmeda, Baar, Zurich, Switzerland), where any possible distortion that occurred during the CBCT (from movements of the patient's head) was investigated, through the superimposition of the radiographic representation of the brick on the original drawing of it (present in the software).

When the correspondence between the radiographic imaging and the original drawing of the Lego® brick was verified, and no distortions occurred, the surgical plan could proceed. The clinician used a desktop scanner to acquire the 3D anatomy of the stone cast model of the patient as well as the impression tray. Then, all these data were sent by email to the 2Ingis® center. The 2Ingis® center then imported the dentate model into the aforementioned planning software and superimposed it on the bone model derived from the CBCT; a careful superimposition was then made, first by points and then by surfaces. Once again, the Lego bricks were useful for the control of the quality of the superimposition, particularly in the presence of scattering/metallic artifacts in the CBCT (derived by the presence of metal-ceramic restorations in the patient's mouth). Inside the SMOP® planning software, a virtual wax-up was imported or created; then the implants were virtually planned in the exact position, depth, and inclination, taking into account the

amount of available bone as well as the prosthetic emergence profile. The planning took place within the SMOP®, a planning software in which the conventional sleeves are present. However, the planning started from a different concept: not from the length of the implant, but from the length of the drills available for preparation. In detail, a “zero point” was obtained, as the sum of the distance between the sleeve and the implant shoulder, plus the height of the sleeve, plus a fixed value set at 12 mm (ISO value). Therefore, a “depth value” was obtained, by the subtraction between the length of the available preparation drill(s), minus the “zero point” value. The depth value had to correspond to the planned implant length: if this correspondence was present, no spacers were needed during surgery. Conversely, if the depth value was greater than the planned implant length, the use of spacers was needed during surgery. The surgical planning was thus completed and shared between the 2Ingis® center and the clinician for final check, improvements, and approval. Once the implant planning was approved, the engineers of the TWIN-Guide® center designed the open-frame, sleeveless surgical guide, using a proprietary software (2Ingis CAD software®), according to the established plan. The peculiar characteristic of these guides was the presence of an open structure, with selective supports on the adjacent teeth. Moreover, these open templates did not have the classic holes for inserting metal sleeves and/or reducers, conventionally used for guiding the preparation drills; it was instead the surgical hand-piece to be guided, by means of a proprietary adapter characterized by two full cylinders (male), which were inserted in two hollow cylinders (female) incorporated into the guide and placed externally and internally to the residual bone crest (not at the above it). Basically, the drill was free from any interference, but the hand-piece was double-guided. These open-frame, sleeveless surgical guides were then manufactured either in metal, using an industrial laser-sintering machine (Pro-X DMP200®, 3D Systems, Rock Hill, SC, USA), or in resin, using a powerful 3D printer (Nextdent®, Vertex Dental, Soesterberg, The Netherlands). The guides were then sterilized and sent to the dental office.

Surgical and prosthetic procedures

Before starting the operation, the patients were asked to rinse with a chlorhexidine-based mouthwash 0.2% for at least 4 min. Infiltration anesthesia followed, with articaine with adrenaline (1:100,000), then the template was positioned. The fit and stability of the surgical guide were carefully checked at this stage. The support of the template was made by points (not by surfaces),

on the adjacent teeth, and fit and stability had to be sufficient to allow the surgeon to proceed with the operation. If the fit or the support were unsatisfactory, the surgeon could not proceed with the intervention and was forced to proceed in a conventional manner (not guided), through the elevation of a mucoperiosteal and manual preparation/positioning of the implants. If instead the fit and the stability were satisfactory, the intervention proceeded with the passage of a mucotome, for the removal of the mucosal operculum and for accessing the underlying bone plane (flapless technique). However, where the surgeon believed it was necessary to preserve the keratinized tissue, a small crestal incision (without releasing incisions) was performed, in order to keep the keratinized mucosa, moving it buccally to the implant site. The preparation of the surgical site then proceeded, in full accordance with the indications of the implant house, through the passage of a leveling drill, one drill for the depth and the subsequent ones with incremental diameters. All these steps took place with the surgeon having visibility of the operative field, and under abundant physiological irrigation. Once the depth and, above all, the adequate size of the preparation was reached, the implants were inserted into the prepared sites, again using the guide. The surgeon placed the implant of a length and diameter corresponding to the original 3D surgical planning. The implant was initially inserted through the hand-piece, set with a maximum insertion torque of 35 Ncm; exceeding this threshold, the surgeon proceeded manually for better control. When the implant was placed, the surgeon proceeded to remove the template and, where needed, sutured. When an immediate restoration was needed, as in the anterior areas or in the case of one-piece implants, a temporary shell in acrylic resin was relined chairside on the abutment and delivered immediately after surgery. Alternatively, a polyvinylsiloxane impression was captured, and the provisional preparation was done in the laboratory. The temporary restoration was delivered within 48 h of surgery and cemented with a zinc-oxide eugenol cement (Temp-Bond®, Kerr, Orange, CA, USA). In all cases, before cementation, the restorations were carefully polished to obtain an ideal emergence profile. The occlusion was meticulously controlled so as to avoid pre-contacts, in both protrusion and laterality. An intraoral periapical radiograph was obtained with the temporary restoration in position and, after that, the patient could be discharged with analgesics and antibiotic prescription (600 mg ibuprofen every 12 h, for 2 days, and amoxicillin + clavulanic acid, 2 g per day, for 6 days). Conversely, when a delayed prosthetic protocol was selected, the impressions for the provisional restorations were scheduled 1 or 2 months after the surgery.

In all cases, the first follow-up visit was set at 10 days after the intervention. The temporaries remained in situ for a period of 2 months; after which they were replaced with the definitive metal-ceramic or zirconia restorations. In the latter case, translucent zirconia (Katana®, Kuraray Noritake, Tokyo, Japan) was employed. In all cases, the final restorations were cemented with zinc-oxide eugenol cement. Before cementation, occlusion was carefully checked with articulating papers (Bausch Articulating Paper®, Bausch Inc., Nashua, NH, USA) in order to avoid any static/dynamic precontact. After cementation, another intraoral periapical radiograph was obtained. The patient was then enrolled in a recall program, for professional oral hygiene sessions every 6 months.

Study outcomes

Each of the patients included in the study was followed for at least 1 year after implant placement, through 1 to 2 annual check-ups for professional oral hygiene sessions. The outcomes of the present study were of a surgical nature (i.e., linked to the execution of the intervention and the 2-week period immediately after) and of a biologic and functional nature (i.e., linked to the possible biologic and prosthetic complications that could occur to the implant-supported restorations during the 1-year follow up).

In detail, the main study outcomes were as follows:

1. Surgical outcomes (related to the guided surgery procedure)

- fit of the surgical guide
- stability of the surgical guide
- duration of the intervention
- intra-operative and immediate post-operative complications
- implant stability at placement

2. Biologic outcomes

- presence/absence of peri-implant mucositis
- presence/absence of peri-implantitis

3. Prosthetic outcomes

- presence/absence of mechanical complications

- presence/absence of technical complications

Surgical outcomes

Fit of the surgical guide

The fit of the surgical guide represented one of the primary outcomes of the present study, and consisted of the template's ability to adapt perfectly to the pre-defined support points, without open spaces (gaps) and at the same time without pointing above the teeth. By definition, the fit of the template could be defined as excellent (if perfect, without any gap or interference), acceptable (if sufficient, with minimal interference that still allowed an adaptation in post-processing, in the laboratory, through polishing), or inadequate. The fit test was performed before starting the surgery and consisted of a careful inspection analysis of the adaptation of the template on the occlusal surfaces of the supporting teeth, in the different sections. The correspondence and the contact between the surface of the template and the supporting teeth had to be perfect, at the occlusal level, but the fit of the template also depended on the adaptation on the approximal (mesial and distal) surfaces of the adjacent teeth, and on the perfect adhesion to their buccal and palatal (lingual) contacts. After this careful visual inspection, the surgeon could define the fit of the template as excellent, acceptable, or inadequate. If it was excellent, the clinician could proceed to verify the stability of the template. If it was acceptable, and therefore required some retouching, the clinician could adapt the guide through polishing in the laboratory and then retest the fit in the mouth. In any case, these adaptations had to be minimal, in order not to compromise the correct insertion of the fixture, according to the position, inclination, and depth planned in the software. Finally, if the fit was completely unsatisfactory, the clinician could not proceed with the guided surgery and therefore had to insert the implants manually, according to conventional protocols; in the latter case, guided surgery was considered a failure.

Stability of the surgical guide

As for the fit, the stability of the surgical guide was verified by the clinician at the time of surgery. A surgical template was defined as stable in a case in which, besides possessing a perfect adaptation, it was immobile during all the phases of the surgery (preparation of the surgical site with drills of incremental diameter, and implant insertion). Stability was defined as excellent if the template did not move at all during the operation, exerting some resistance to insertion and removal. Stability was defined as acceptable if the template had a minimal, negligible swinging / jiggling movement during the preparation of the implant site, forcing the surgeon to keep it in place manually. But if, instead, the movement were not

Table. 1 Patient demographics

Patient characteristics	n° of patients	p value*
Gender		
Males	24	.247
Females	14	
Age at surgery		
20–35 years	2	.104
36–50 years	11	
51–65 years	15	
66–80 years	10	
Smoking habit		
No	25	.163
Yes	13	
Total	38	–

* Pearson's Chi square test

manageable, the template was defined as unstable and could not be used; the surgeon therefore had to proceed to raise a full-thickness flap and prepare the implant site manually, in a conventional manner. In the latter case the guided surgery procedure was considered a failure.

Table 2 Implant distribution

Implant features	n° of implants	p value*
Implant brand		
Megagen®	38	.014
Dentium®	53	
Others	19	
Implant site		
Maxilla	65	.175
Mandible	45	
Implant position		
Incisors	15	.075
Cuspids	22	
Premolars	34	
Molars	39	
Implant length		
< 10 mm	33	< 0.001
10–12 mm	71	
> 12 mm	6	
Implant diameter		
< 4 mm	34	< 0.001
4–5 mm	68	
> 5 mm	8	
Prosthetic restoration		
Single crown (SC)	36	.009
Fixed partial prosthesis (FPP)	74	
Total	110	–

* Pearson's Chi square test

In all cases, as was the case with the fit, the stability of the surgical guide was reported in the patient's medical record.

Duration of the intervention

The chair assistant monitored exactly the time required for surgery, from the anesthesia to the insertion of the implant and the final removal of the surgical guide. The time was measured in minutes and noted in the patient's folder. The mean time per implant was then calculated, by dividing the overall time required for the surgical procedure by the number of fixtures inserted.

Intra-operative and immediate post-operative complications

Any complications occurring during the operation were noted in the patient's file and were reported among the results of the present study. Among the intra-operative complications were: fracture of the surgical guide, inadequate opening of the mouth by the patient (which made the procedure impossible), insertion of the implant in aberrant position/ inclination/ depth, compared to the plan provided in the guided software, with perforation of one of the corticals (buccal or palatal/ lingual), invasion of noble and insurmountable anatomical structures (inferior alveolar nerve, maxillary sinus, periodontal ligament of adjacent teeth), which required the opening of a full-thickness flap and the immediate removal of the implant.

Conversely, the immediate post-operative complications were the complications that could occur in the 2 weeks following the surgery. They included pain, discomfort, exudation and suppuration, swelling, and infection of the implant.

Implant stability at placement

The stability of each fixture was checked clinically, immediately after placement, by applying a reverse torque of 20 Ncm [30].

Biologic outcomes

All the biologic complications that could affect the implants from the second week of surgery until the end of the study were marked in the patient's record. These complications included peri-implant mucositis and peri-implantitis. The threshold for defining peri-implantitis was set at a probing pocket depth ≥ 6 mm, with bleeding/ suppuration on probing and evidence of peri-implant bone loss > 3.0 mm [31].

Prosthetic outcomes

All the prosthetic complications that could affect the implants from the second week of surgery until the end of the study were marked in the patient's record. These complications included mechanical complications,

such as screw loosening and/or fracture [32], as well as technical complications, such as ceramic chipping/fractures or fractures of the metal framework of the restorations [33].

Statistical evaluation

All data were extracted from the individual patient records by an independent operator, not directly involved in the insertion of the implants and their prosthesis, at the end of the 1-year follow-up period. The descriptive statistical analysis included the description of the demographic characteristics of the patients (gender, age at the time of surgery, smoking habit) and the characteristics of the implants inserted (brand, site, position, length, and diameter) and restorations placed (SC and FPP). A Pearson Chi Square test was used to analyze homogeneity in the patient and implant distribution. Absolute and relative frequency (%) distributions were calculated for qualitative variables (fit and stability of the surgical templates, intra-operative and immediate post-operative complications, implant stability) while means, standard deviations (SD), medians, and confidence intervals (95%CI) were estimated for quantitative variables (patient's age at surgery, duration/time of the surgery). Implant stability, survival, and the incidence of complications were calculated at the restoration level.

Results

In total, 38 patients (24 males and 14 females) between 20 and 80 years of age (mean age 56.5 ± 14.0 years; median 59.5; 95%CI: 52.1–60.9) were included in the present retrospective study. A summary of the patients' characteristics is provided in Table 1. These patients had been treated with 110 fixtures (38 Megagen® Gyeongbuk, South Korea; 53 Dentium® Cypress, CA, USA; and 19 implants from other brands) inserted by means of 40 sleeveless, open-frame surgical guides. Among the guides, 25 were fabricated in metal, and 15 were in resin. A summary of the implants' features is provided in

Table 2. Among the fixtures, 55 were inserted without the elevation of any surgical flap. According to the pre-established planning, 36 implants had to be restored with SCs and 74 implants had to be restored with FPPs. Among the surgical guides, 34 (85%) had excellent fit and stability, 4 (10%) had acceptable fit and stability, and only 2 (5%) had inadequate fit and stability for clinical use. The two guides with inadequate fit and stability were made in resin. The mean duration of the intervention was 23.7 min (± 6.7 , median 22, 95%CI: 21.7–25.7) per template, which resulted in a mean time per implant of 6.5 min. No immediate intra-operative complications were reported: no fracture of the surgical guide occurred, and all patients had a sufficient mouth opening to allow the surgeon to proceed with surgery. No implants were placed in an aberrant position/inclination/depth, no perforations of the corticals was evidenced, nor invasion of any anatomical inviolable structure (inferior alveolar nerve, maxillary sinus, periodontal ligament of adjacent teeth). However, two Dentium® fixtures (1.8%) were not stable at placement and consequently had to be removed. In addition, in the immediate post-operative period, two patients (5.2%) suffered pain and swelling; these patients were prescribed additional oral analgesics. The 108 surviving implants were restored with 36 SCs and 32 FPPs (24 two-unit bridges and 8 three-units bridges, respectively). These restorations survived for the entire 1-year follow-up time, without any implant failure/removal registered. Among the biologic and prosthetic complications registered during the follow-up, however, there were two instances of peri-implant mucositis (1.8%), two abutment screw loosening (2.9%) (in two SCs), and one ceramic chipping/fracture (1.4%) (in a three-unit FPP).

In Figs. 1, 2, 3, 4, 5, 6, 7, 8, 9, 10, 11 and 12, one case of anterior implants with a metal guide is fully documented in all phases. In Figs. 13, 14, 15, 16 and 17, a complete case of posterior implants with a resin guide is documented in the main phases.



Fig. 1 Pre-operative situation. The young patient presented with an old Maryland bridge, and asked the surgeon to replace it with two fixed implant-supported restorations. **a** Right side, radiographic control. The horizontal space between the roots of the adjacent teeth was narrow. **b** The Maryland bridge in position, occlusal view; **c** Left side, radiographic control. The horizontal space between the roots of the adjacent teeth was narrow

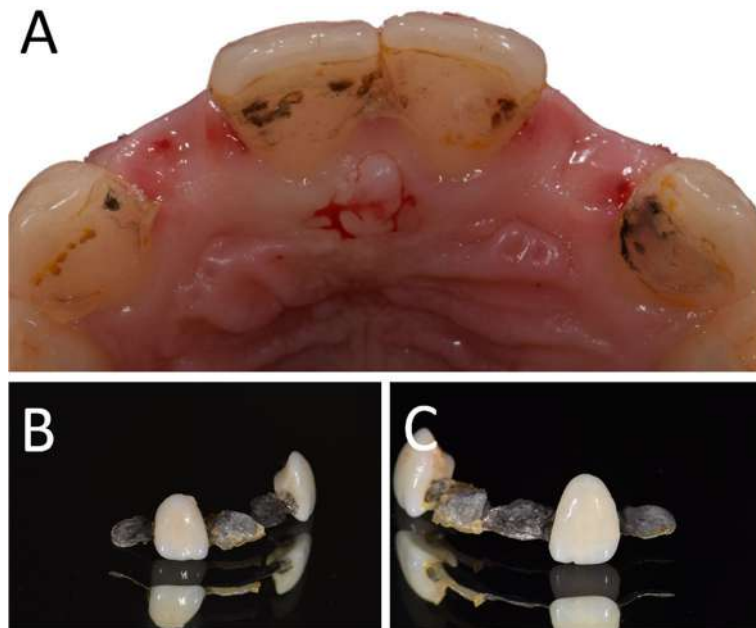


Fig. 2 Pre-operative situation. Removal of the Maryland bridge. **a** Occlusal view; **b** Details of the Maryland bridge after removal, right side; **c** Details of the Maryland bridge after removal, left side

Discussion

To our knowledge, this clinical study is today the only one that documents a large number of cases treated with the present new method of guided surgery, in which the handpiece is guided rather than the drills. In fact, in the literature, there are only two studies of this system for guided surgery [34, 35].

Schnutenhaus et al. tested this new sleeveless guided surgery system, in order to determine the accuracy of implant insertion with one-piece ceramic implants [34]. In total, 12 patients were enrolled in that study and

installed with 20 implants by means of the aforementioned sleeveless static surgical guides [34]. The accuracy of implant placement was checked using a non-invasive method, which permitted comparison of the planning data with the actual position of the fixtures after surgery [34]. All implants were placed without any clinical problem and the mean deviations were 0.52 mm (95%CI: 0.37–0.67 mm) at the implant shoulder and 0.82 mm (95%CI: 0.56–1.08 mm) at the implant apex [34]. Finally, the mean angular deviation was 2.85° (95%CI: 2.18°–3.51°) with a deviation in height/depth of 0.35 mm

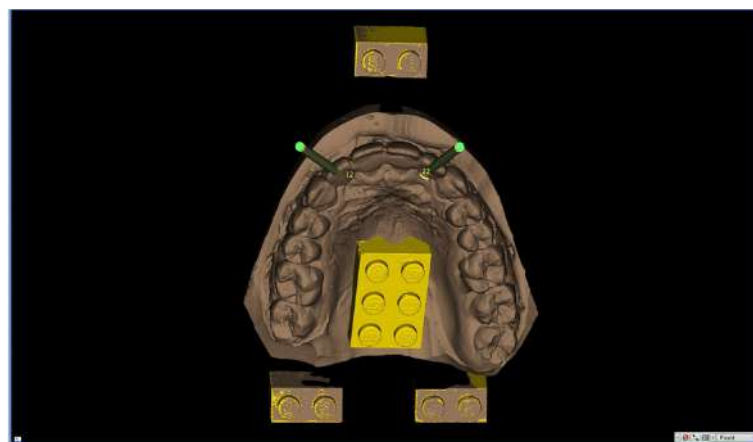


Fig. 3 The model of the teeth is imported in the guided surgery software and superimposed on the CBCT reconstruction by means of reference points (Lego bricks). These reference points are also useful to understand the quality of the CBCT, in order to highlight any possible patient movement and possible related CBCT distortion. The superimposition, by points and surfaces, is extremely accurate

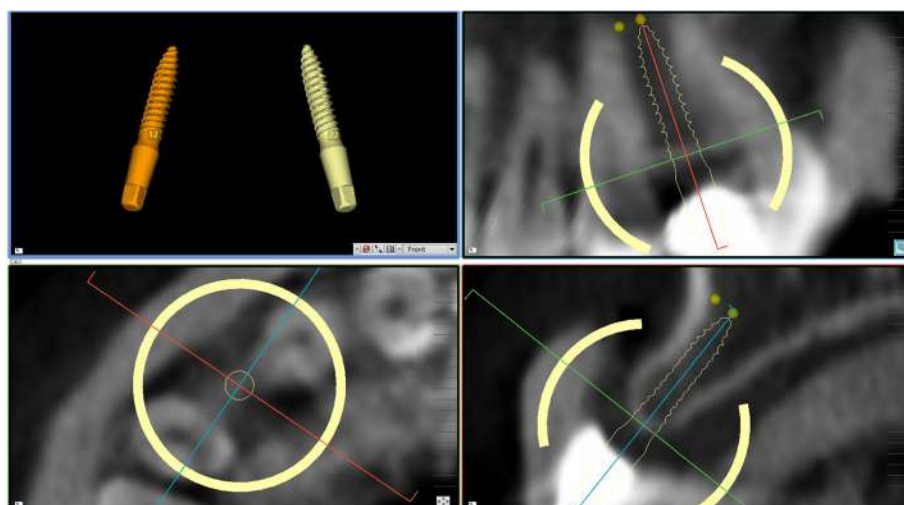


Fig. 4 Planning of implant placement with the 2Ingis® guided surgery software. The position, inclination and depth of the right maxillary incisor is carefully planned, in order not to collide with the roots of the adjacent teeth

(95%CI: 0.01–0.68 mm) [34]. The authors concluded that this sleeveless, open-frame, guided surgery system seems to be accurate, with little deviations between the planned and the actual position of the implants, and no clinical issues [34].

Fauroux et al. reported on 67 implants placed in 35 patients with this sleeveless, open-frame, guided surgery system [35]. These patients were treated with different protocols (one or two stage, flap or flapless, delayed or immediate loading). All cases revealed good implant placement with planning [35]. According to the authors, the main advantages with this system were the open-frame design, which allows irrigation and visual control of the surgical site, the ability to preserve the keratinized

gingiva where necessary, and (being a sleeveless system) the ability to insert the implant without any contact with the sleeve [35]. The authors concluded that this system represents an interesting evolution in the field of static guided surgery [35].

The clinical results of our present retrospective study have been gratifying, and seem to confirm the evidence emerging from the previous, aforementioned studies [34, 35]. In fact, in our study, 38 patients had been treated with 110 fixtures, inserted by means of 40 sleeveless, open-frame surgical guides. Among these fixtures, 55 were inserted flaplessly, i.e., without the elevation of any surgical flap. During surgery, 34 sleeveless guides (85%) had excellent fit and stability, 4 (10%) had

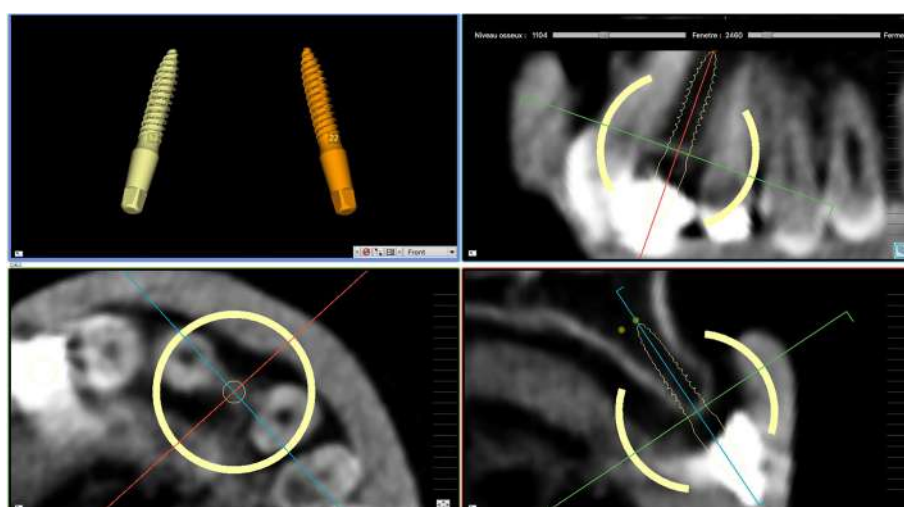


Fig. 5 Planning of implant placement with the 2Ingis® guided surgery software. The position, inclination and depth of the left maxillary incisor is carefully planned, in order not to collide with the roots of the adjacent teeth

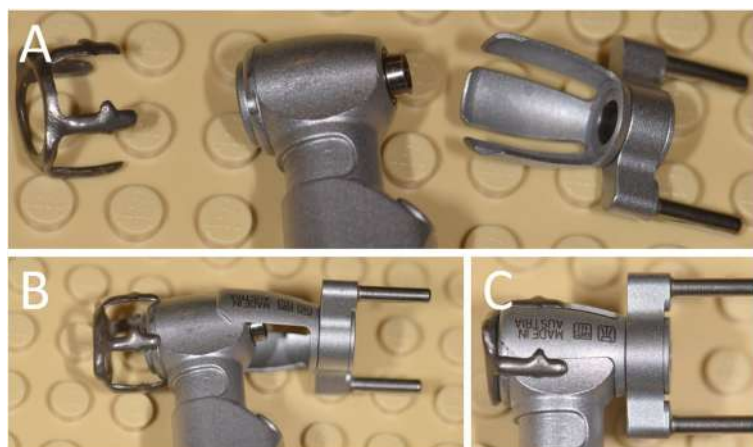


Fig. 6 In this novel guided surgery system, the handpiece – and not the drill – is guided. **a** The adapter, the handpiece and the connector. **b** The three parts are connected; **c** The handpiece is ready for the surgery

acceptable fit and stability, and only 2 (5%) had inadequate fit and stability for clinical use. It is important to point out that the two guides with inadequate fit and stability were made in resin. Resin guides have advantages, when compared with metal guides: they are cheaper and easier to print, and they can be more easily adapted to the site in case of minimal misfits. However, when working with resin guides, it is essential to avoid delays in the treatment, because the stability of these guides along time is not comparable to that of metal guides. In this study, in both cases in which the stability of the guides was inadequate, a delay in the treatment occurred, because patients cancelled the planned appointment for surgery. This delay may have contributed to the final, poor adaptation of the guides. The mean duration of the intervention was 23.7 min (\pm 6.7; median 22; 95%CI: 21.7–25.7) per template, which resulted in a mean time per implant of 6.5 min. In all patients, no immediate intra-operative complications occurred: no fractures of the surgical guides were registered, and all patients had a sufficient mouth opening to allow proceeding with surgery. Moreover, no implants were placed in an aberrant position, inclination, or depth; and no perforations of the corticals was evident nor invasion of any anatomical inviolable structure. Only a few minor immediate post-operative complications were registered, with 2 patients experiencing pain and swelling after surgery. However, 2 implants (1.8%) were not stable after placement and had to be removed. The 108 surviving implants were restored with 36 SCs and 32 FPPs (24 two-unit bridges and 8 three-units bridges, respectively), which were followed for a period of 1 year. At the end of the follow-up period, all these restorations survived without any failure, even if a few biologic and prosthetic complications occurred. Our study therefore seems to confirm that the present system for

static guided surgery is reliable and allows one to obtain clinically predictable results.

The clinical advantages of using this innovative system for guided implant surgery and this different approach to the preparation of the implant site seem to be numerous [34, 35]. First, in fact, the system presented in this study eliminates the sleeves. The use of the sleeve (metallic or not), a classic tool for guiding the drills in the vast majority of guided implant surgery systems available on the market today, has in fact some intrinsic issues [35]. The sleeve is in fact conventionally positioned above the bone site (and the overlying mucosa), which must be prepared to receive the implant; this is unavoidable if the drills are to be guided [35]. This fact, however, raises a first, intrinsic issue: it is necessary to use dedicated surgical kits with rather long drills in order to correctly prepare the surgical site [35]. In fact, the scientific literature has shown that a sleeve less than 5 mm in height is not actually able to guide the preparation of the implant site as planned (with the risk of major deviations from the original planning within the guided surgery software) [36]. If the sleeve alone “steals” at least



Fig. 7 Surgery. The laser-sintered open-frame sleeveless template is inserted in mouth, with excellent fit and stability

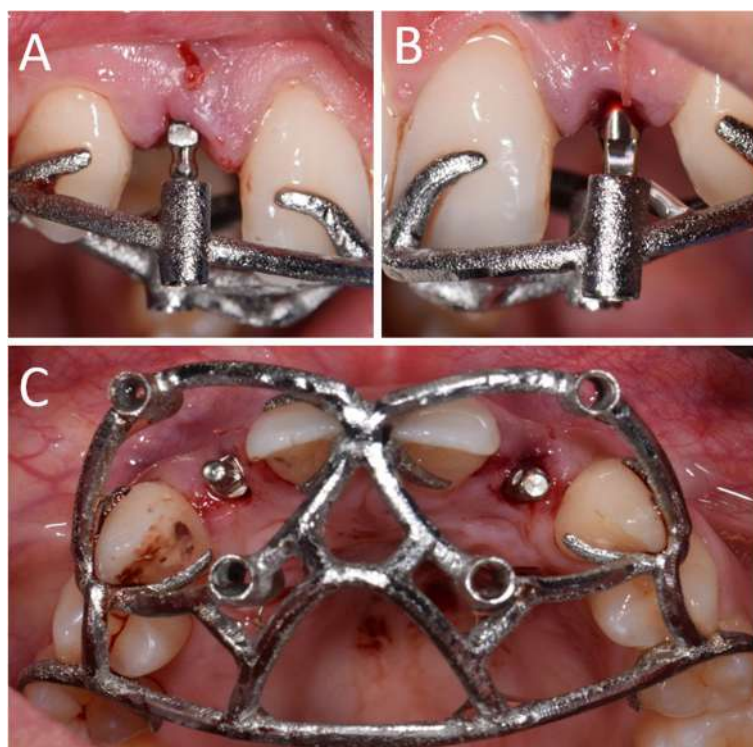


Fig. 8 Surgery. The implants are placed through the open-frame sleeveless template. **a** Placement of the right lateral incisor; **b** Placement of the left lateral incisor; **c** Both implants have been placed. Note the good visibility of the operatory field, with the guide in position

5 mm of space above the ridge, and this forces the clinician to use long preparation cutters, it may happen that in the posterior sectors (typically in the molar area, but also premolar) of a good percentage of partially edentulous patients, inserting implants through a surgical guide may be difficult (if not impossible) due to lack of space [3–6, 34, 35]. This is certainly one of the most clinically encountered problems with conventional guided surgery systems, and one that, to date, limits the use of these techniques in partially edentulous patients [3–6, 34, 35]. The presence of the teeth in the antagonist arch and the lack of space do not physically allow the long drills to be

inserted into the surgical guide, thus rendering them unworkable. Yet, the restoration of function in partially edentulous patients is today the most frequent indication in world implantology, and it is precisely the posterior sectors that most frequently require rehabilitation with implants [37]. The innovative system for guided surgery presented in this study solves the problem of the lack of vertical space, in fact it eliminates the sleeve, and moves the guides (which are two and are inserted directly on the handpiece through a dedicated adapter) lateral to the bone crest [34, 35]. This saves space and allows the clinician to work with considerably shorter drills. The direct



Fig. 9 Immediate restoration. The implants are immediately restored by means of single crowns intraorally relined on temporary abutments. **a** Right lateral incisor, radiographic control immediately after implant placement; **b** Intraoral picture, frontal view of the provisionals relined on the temporary abutments immediately after implant placement; **c** Left lateral incisor, radiographic control immediately after implant placement



Fig. 10 10-days post-surgical control, before sutures removal. **a** Right lateral incisor, radiographic control; **b** Frontal clinical view with provisional crowns in position; **c** Left lateral incisor, radiographic control

consequence of this is that it is also possible to work in the posterior areas of partially dentate patients, with teeth in the antagonist arch, and even with limited opening [34, 35].

But the sleeve, which is the basis of conventional guided surgery systems, does not only “steal” space vertically. It also removes space in a horizontal sense. In fact, in specific applications, e.g., the restoration of single mandibular teeth such as central or lateral incisors, the diameter of the sleeve can collide with the adjacent teeth. This creates problems during planning, which can

be solved by moving the sleeve away from the adjacent tooth to avoid colliding (typical planning error that may be made by non-experienced external service operators), or by moving the sleeve higher, above adjacent teeth [3–6, 34, 35]. In the first case the implant will be positioned incorrectly, with serious aesthetic consequences. In the second case, the stolen vertical space will grow further, with the need to use even longer preparation drills, and fall into all the aforementioned problems; moreover, the literature has shown that if the distance between the sleeve and the implant site grows, the

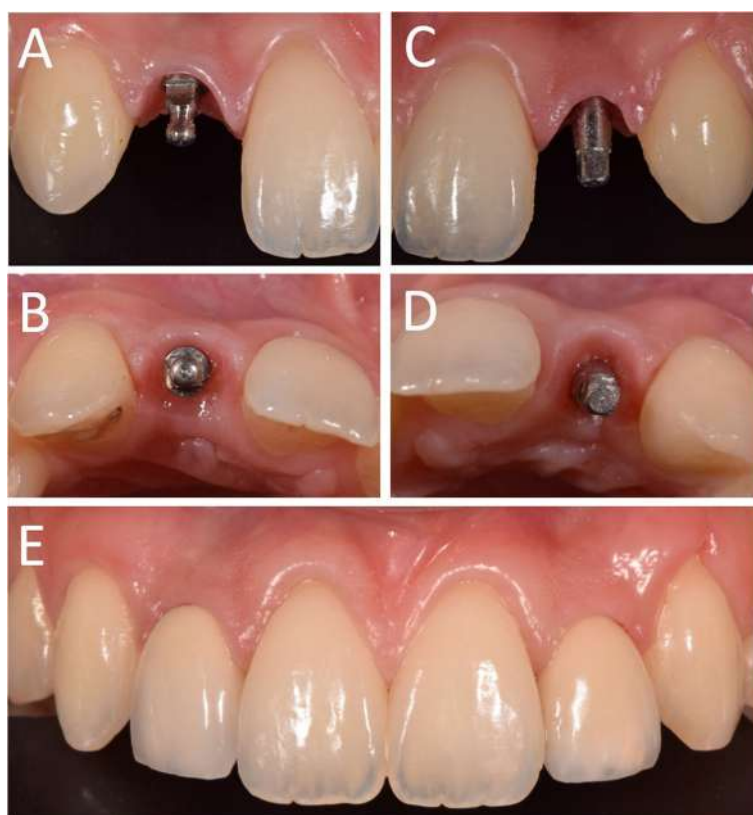


Fig. 11 Delivery of the final restorations. **a** Right lateral incisor, frontal view of the abutment in position; **b** Right lateral incisor, occlusal view of the abutment in position; **c** Left lateral incisor, frontal view of the abutment in position; **d** Left lateral incisor, occlusal view of the abutment in position; The final single crowns were delivered and cemented on the final abutments

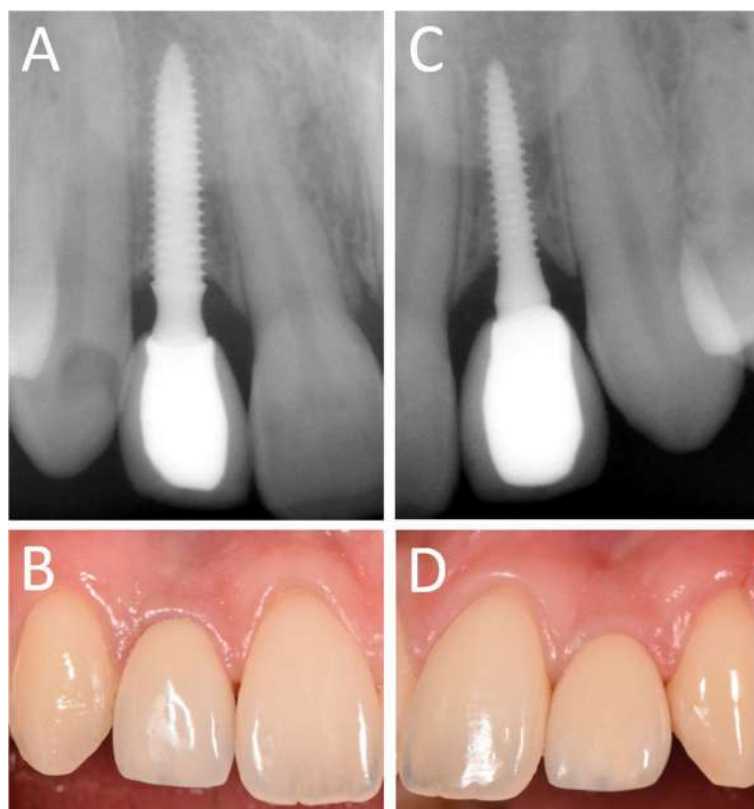


Fig. 12 1-year follow-up control. **a** Right lateral incisor, radiographic control; **b** Right lateral incisor, frontal view. Note the soft tissues maturation; **c** Left lateral incisor, radiographic control; **d** Left lateral incisor, frontal view. Note the soft tissues stability

deviations grow and therefore the accuracy in positioning the implant can drastically decrease [36]. Again, driving the handpiece instead of the drill can avoid having to incur these errors. To date, there are no clinical studies on large samples of patients, comparing, in vivo, the accuracy or correspondence between the planned position in the software and the real position of the implant after the intervention, of traditional guided surgery systems versus the present, sleeveless system. However, the fact that the guides that drive the handpiece (positioned laterally) are two, could potentially help to stabilize the

implant placement, reducing error [34, 35]. Certainly, then, in the partially edentulous patient, the design of the surgical templates plays a role in ensuring greater fit and therefore greater stability during surgery [6]. As shown in the literature, in fact, open surgical templates that rest selectively and for points, present an ideal stability [6] and potentially lower errors compared to closed templates that rest indiscriminately on the entire surface of the adjacent teeth [23]. In addition, the open templates allow you to check in section, on all the support teeth, the actual adaptation of the guide, and to intercept



Fig. 13 Planning of two implants in the posterior area with 2Ingis guided surgery software. **a** Second right premolar; **b** First right molar

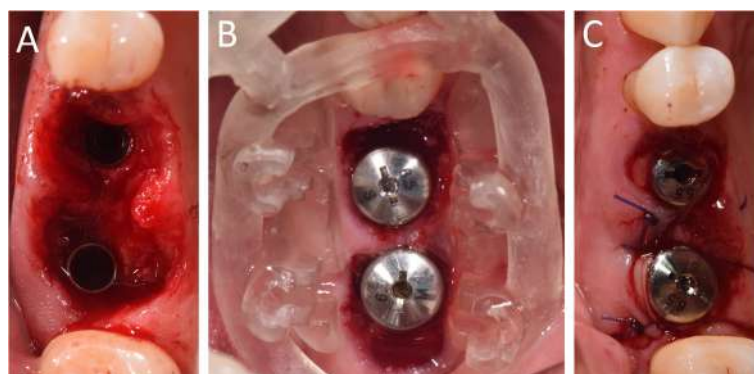


Fig. 14 Surgery on patient. **a** The implants in position; **b** The resin guide in position after implant placement, with healing abutments already positioned; **c** Sutures

such potential errors, difficult to highlight in the classic closed templates [6, 23]. This could represent an additional advantage, increasing the accuracy of guided surgery. But the advantages of this systematic are not limited to saving of space (vertical or horizontal), and to the better fit or stability of the template. Guided implant surgery is nowadays almost exclusively conceived as a tool for placing implants flaplessly, i.e., without raising a mucoperiosteal flap [4, 5, 13–17]. This approach has some advantages, shown in the literature, but there are numerous cases in which, due to the scarce quantity of keratinized gingiva and, more importantly, due to deficiency of bone tissue, the surgeon needs to raise a flap [38]. Raising a mucoperiosteal flap allows the preservation of the keratinized gingiva (which risks being sacrificed during the operculum, in the flapless approach) by managing the soft tissues in the ideal manner [38, 39]. In the same way, it is not possible today to regenerate bone (for example, to cover exposed implant threads or to increase the bone volume by means of regenerative techniques with biomaterials or membranes) if a flapless

approach is chosen. In both these scenarios, guided insertion of the implant in position, inclination, and depth remains of great utility, but it is not possible through the conventional templates for guided surgery; the sleeve (and the structure in which it is inserted) completely cover the visual and force the surgeon to work “blindly.” It is therefore not possible to manage soft tissues, nor to make small (or large) bone augmentations or perform crest splitting [40]. Once again, the sleeve creates problems for the clinician. However, if the sleeve is eliminated, and the template design is modified (open surgical guide), as happens in the system presented in this study, the surgeon can see the site on which he/she operates and consequently can better manage the soft tissues [38, 39] (for example offset the keratinized tissue, preventing it being sacrificed during the operculum) and also raise a flap with the template in place. This allows the clinician to proceed with minor and/or major bone augmentation techniques, if needed, with the guide in position.

Visibility is therefore a further, clear advantage of the method presented in this work. The presence of the

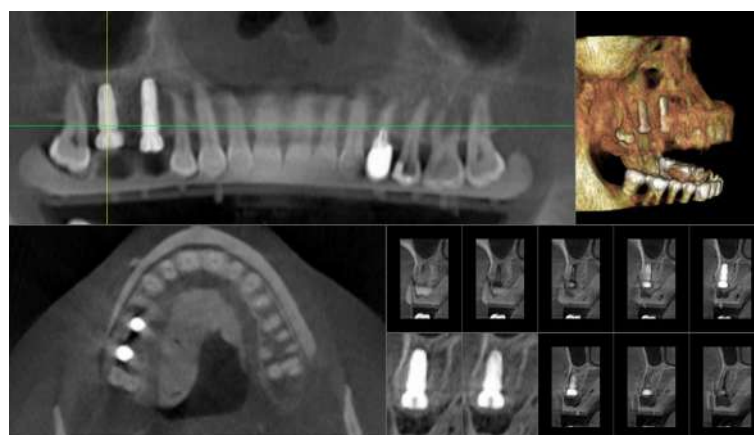


Fig. 15 Cone beam computed tomography (CBCT) for the control of implant placement



Fig. 16 Delivery of the final restoration. **a** Clinical picture; **b** Radiographic control

sleeve is not only an obstacle to the surgeon's vision, but also to the passage of the saline solution for the cooling of the operative site [2–6, 34, 35]. The drill to be guided is “engaged” in the sleeve, and there is no space to cool it properly while working. This represents a biological risk for subsequent implant integration: as described widely in the literature, it is important to avoid overheating of the bone during preparation of the implant site [41, 42]. The strategies to avoid it are a fluid movement during the preparation and, above all, the cooling through saline solution. Although several manufacturers have studied possible solutions to this problem, it remains evident even today, as, through conventional and closed surgical templates, it is very difficult to cool the drills [41, 42]. The guided system presented in this study definitively solves this problem: the drills are free and the cooling takes place in an optimal way, because it is the handpiece that is guided [34, 35]. Finally, a further aspect to consider is that linked to the positioning of the implant through the template. Inserting the implant through a sleeve, as in conventional guided surgery systems, can represent a biological risk; in fact, the implant surface can be contaminated, “crawling” on the walls of the sleeve [27, 28]. This risk is present if the sleeve is made of metal, and even greater in the case of resin sleeves. The risk is that particles of these materials are brought into the implant site, through the implant surface, and can interfere with the process of osseointegration [28, 29]. Since the literature has shown how the

implant surface represents a key factor for survival and success [29, 43], and in consideration of the efforts made by manufacturers to produce more and more performing surfaces (i.e., able to accelerate the processes of bone healing), it is unforgivable to risk compromising everything by contaminating the fixtures with external materials. The guided surgery system presented in this clinical study solves this problem, because the sleeve is eliminated and the implant is inserted through the handpiece: it is, in other words, free from contact with other, undesired surfaces [34, 35].

Despite the clinical success reported in this study and the advantages given by this modern approach to guided surgery, it should be noted that today there is insufficient data on the accuracy of the present system [34], compared to conventional systematics. In other words, we do not have sufficient mathematical data on the system; further studies will be needed in that direction. In addition to this, the present study has a retrospective design and is based on the case histories of a single, experienced operator; for this reason, this study does not allow definitive conclusions on the validity of this new system. Moreover, multiple implant systems have been used here, and the guides were printed with two different materials (25 of them in metal, 15 in resin). These can be considered as further limitations of this study. Prospective and multi-center studies, involving dental centers and operators with different levels of experience, will be necessary to dispel any doubt about the reliability of this system.



Fig. 17 1-year follow-up control. **a** Clinical picture, lateral view; **b** Clinical picture, occlusal view; **c** Radiographic control showing stable bone levels around the implants

Conclusions

This retrospective clinical study presented results with a novel guided surgery system with a sleeveless, open-frame structure, in which the surgical handpiece (not the drills used for preparation) is guided. In total, 38 patients who had been treated with 110 implants inserted by means of 40 sleeveless, open-frame guides were examined. With regard to surgery, the fit and stability of almost all open-frame sleeveless guides (36/38) was adequate, and only 2 guides were not suitable for clinical use. The mean duration of the intervention was 23.7 min (\pm 6.7). Immediately after placement, 2 fixtures were not stable and had to be removed. The 108 surviving implants were restored with 36 single crowns and 32 fixed partial prostheses, that survived until the 1-year follow-up, with a low incidence of complications. Although this clinical study has limits (limited patient sample, retrospective design, single operator, and no evaluation of the accuracy of the implant placement), the novel guided surgery system with sleeveless, open frame–structure guides presented here seems to be clinically safe and reliable. Obviously, multicenter studies on a larger sample of patients involving different operators, and evaluating the accuracy in implant position, are needed to dispel any doubt about the reliability of this system.

Abbreviations

3D: Three-dimensional; CAD: Computer-assisted-design; CBCT: Cone beam computed tomography; CI: Confidence intervals; DICOM: Digital imaging and communication in dentistry; FPP: Fixed partial prosthesis; SC: Single crown; SD: Standard deviation

Acknowledgments

The authors are grateful to Dr. Mehdi Mouhyi for help with the preparation of the present research.

Authors' contributions

Conceptualization: JM, FM; Data curation: JM, FM; Formal analysis: JM, FM; Investigation: JF, MS; Methodology: JM, MS; Project administration: JM; Resources: JM, CM; Supervision: OA; Validation: BM, OA; Visualization: JM, FM, CM; Writing original draft: JM; Writing review & editing: FM, CM. All authors read and approved the final manuscript.

Funding

The present clinical study was not funded, nor supported by any grant. All the surgical guides and implants were regularly bought by the authors, and nothing was provided by third-parts or private Companies; therefore, the authors have no conflict of interest related to the present work.

Availability of data and materials

The clinical and radiographic documentation of the patients enrolled in this study, as well as the surgical and prosthetic planning data belong to the authors, and are available only upon reasonable request, after approval by all the authors.

Ethics approval and consent to participate

The present study was approved by the Ethics Committee of the Sechenov First Moscow State Medical University.

Consent for publication

Not applicable.

Competing interests

The authors declare that they have no competing interests in relation to the present study. Francesco Mangano is the editor of the Digital Dentistry section of BMC Oral Health.

Author details

¹Casablanca Oral Rehabilitation Training & Education Center (CORTEC), Casablanca, Morocco. ²Biomaterials Research Department, International University of Agadir (Universiapolis), 8143 Agadir, Morocco. ³Department of Periodontics, University of Pennsylvania, Philadelphia, PA, USA. ⁴Department of Periodontics, Medical College of Georgia, Atlanta, GE, USA. ⁵Department of Prevention and Communal Dentistry, Sechenov First Moscow State Medical University, 119992 Moscow, Russia. ⁶Department of Dental Sciences, Vita and Salute University, San Raffaele, Milan, Italy.

Received: 5 July 2019 Accepted: 28 October 2019

Published online: 21 November 2019

References

- D'haese J, Ackhurst J, Wismeijer D, De Bruyn H, Tahmaseb A. Current state of the art of computer-guided implant surgery. *Periodontol*. 2000. 2017; 73(1):121–33.
- Vercruyssen M, Fortin T, Widmann G, Jacobs R, Quirynen M. Different techniques of static/dynamic guided implant surgery: modalities and indications. *Periodontol*. 2000. 2014;66(1):214–27.
- Bencharit S, Staffen A, Yeung M, Whitley D 3rd, Laskin DM, Deeb GR. In vivo tooth-supported implant surgical guides fabricated with desktop Stereolithographic printers: fully guided surgery is more accurate than partially guided surgery. *Oral Maxillofac Surg*. 2018;76(7):1431–9.
- Arisan V, Karabuda CZ, Ozdemir T. Implant surgery using bone- and mucosa-supported stereolithographic guides in totally edentulous jaws: surgical and post-operative outcomes of computer-aided vs. standard techniques. *Clin Oral Implants Res*. 2010;21(9):980–8.
- Cassetta M, Giansanti M, Di Mambro A, Stefanelli LV. Accuracy of positioning of implants inserted using a mucosa-supported stereolithographic surgical guide in the edentulous maxilla and mandible. *Int J Oral Maxillofac Implants*. 2014;29(5):1071–8.
- Mangano FG, Hauschild U, Admakin O. Full in-Office Guided Surgery with Open Selective Tooth-Supported Templates: A Prospective Clinical Study on 20 Patients. *Int J Environ Res Public Health*. 2018;15(11).
- Neugebauer J, Kistler F, Kistler S, Züdorf G, Freyer D, Ritter L, Dreiseidler T, Kusch J, Zöller JE. CAD/CAM-produced surgical guides: optimizing the treatment workflow. *Int J Comput Dent*. 2011;14(2):93–103.
- Ganz SD. Three-dimensional imaging and guided surgery for dental implants. *Dent Clin N Am*. 2015;59(2):265–90.
- Colombo M, Mangano C, Mijiritsky E, Krebs M, Hauschild U, Fortin T. Clinical applications and effectiveness of guided implant surgery: a critical review based on randomized controlled trials. *BMC Oral Health*. 2017;17(1):150.
- Mangano F, Gandolfi A, Luongo G, Logozzo S. Intraoral scanners in dentistry: a review of the current literature. *BMC Oral Health*. 2017;17(1):149.
- Gjelvold B, Mahmood DJH, Wennerberg A. Accuracy of surgical guides from 2 different desktop 3D printers for computed tomography-guided surgery. *J Prosthet Dent*. 2018.
- Mandelaris GA, Vlk SD. Guided implant surgery with placement of a presurgical CAD/CAM patient-specific abutment and provisional in the esthetic zone. *Compend Contin Educ Dent*. 2014;35(7):494–504.
- Berdougo M, Fortin T, Blanchet E, Isidori M, Bosson JL. Flapless implant surgery using an image-guided system. A 1- to 4-year retrospective multicenter comparative clinical study. *Clin Implant Dent Relat Res*. 2010; 12(2):142–52.
- Moraschini V, Velloso G, Luz D, Barboza EP. Implant survival rates, marginal bone level changes, and complications in full-mouth rehabilitation with flapless computer-guided surgery: a systematic review and meta-analysis. *Int J Oral Maxillofac Surg*. 2015;44(7):892–901.
- Doan NV, Du Z, Reher P, Xiao Y. Flapless dental implant surgery: a retrospective study of 1,241 consecutive implants. *Int J Oral Maxillofac Implants*. 2014;29(3):650–8.
- Marlière DAA, Demétrio MS, Picinini LS, De Oliveira RG, Chaves Netto HDM. Accuracy of computer-guided surgery for dental implant placement in fully edentulous patients: a systematic review. *Eur J Dent*. 2018;12(1):153–60.

17. Gillot L, Noharet R, Cannas B. Guided surgery and presurgical prosthesis: preliminary results of 33 fully edentulous maxillae treated in accordance with the NobelGuide protocol. *Clin Implant Dent Relat Res*. 2010;12(Suppl 1):e104–13.
18. Arunyanak SP, Harris BT, Grant GT, Morton D, Lin WS. Digital approach to planning computer-guided surgery and immediate provisionalization in a partially edentulous patient. *J Prosthet Dent*. 2016;116(1):8–14.
19. Jacobs R, Salmon B, Codari M, Hassan B, Bornstein MM. Cone beam computed tomography in implant dentistry: recommendations for clinical use. *BMC Oral Health*. 2018;18(1):88.
20. Albdour EA, Shaheen E, Vranckx M, Mangano FG, Politis C, Jacobs R. A novel in vivo method to evaluate trueness of digital impressions. *BMC Oral Health*. 2018;18(1):117.
21. Dawood A, Marti Marti B, Sauret-Jackson V, Darwood A. 3D printing in dentistry. *Br Dent J*. 2015;219(11):521–9.
22. Dolcini GA, Colombo M, Mangano C. From Guided Surgery to Final Prosthesis with a Fully Digital Procedure: A Prospective Clinical Study on 15 Partially Edentulous Patients. *Int J Dent*. 2016;2016:7358423.
23. Kern F, Benic GI, Payer M, Schär A, Müller-Gerbl M, Filippi A, Kühl S. Accuracy of three-dimensional printed templates for guided implant placement based on matching a surface scan with CBCT. *Clin Implant Dent Relat Res*. 2016;18(4):762–8.
24. Xu LW, You J, Zhang JX, Liu YF, Peng W. Impact of Surgical Template on the Accuracy of Implant Placement. *J Prosthodont*. 2016;25(8):641–6.
25. Saund DS, Pearson D, Dietrich T. Reliability and validity of self-assessment of mouth opening: a validation study. *BMC Oral Health*. 2012;12:48.
26. Peng YT, Tseng CC, Du YC, Chen YN, Chang CH. A novel conversion method for radiographic guide into surgical guide. *Clin Implant Dent Relat Res*. 2017;19(3):447–57.
27. Rupp F, Liang L, Geis-Gerstorf J, Scheideler L, Hüttig F. Surface characteristics of dental implants: A review. *Dent Mater*. 2018;34(1):40–57.
28. Mouhyi J, Sennerby L, Pireaux JJ, Dourov N, Nammour S, Van Reck J. An XPS and SEM evaluation of six chemical and physical techniques for cleaning of contaminated titanium implants. *Clin Oral Implants Res*. 1998;9(3):185–94.
29. Mouhyi J, Dohan Ehrenfest DM, Albrektsson T. The peri-implantitis: implant surfaces, microstructure, and physicochemical aspects. *Clin Implant Dent Relat Res*. 2012;14(2):170–83.
30. Andreotti AM, Goiato MC, Nobrega AS, Freitas da Silva EV, Filho HG, Pellizzer EP, Micheline Dos Santos D. Relationship between implant stability measurements obtained by two different devices: a systematic review. *J Periodontol*. 2017;88(3):281–8.
31. Saulacic N, Schaller B. Prevalence of Peri-Implantitis in Implants with Turned and Rough Surfaces: a Systematic Review. *J Oral Maxillofac Res*. 2019;10(1):e1.
32. Salvi GE, Brägger U. Mechanical and technical risks in implant therapy. *Int J Oral Maxillofac Implants*. 2009;24(Suppl):69–85.
33. Mangano F, Macchi A, Caprioglio A, Sammons RL, Piattelli A, Mangano C. Survival and complication rates of fixed restorations supported by locking-taper implants: a prospective study with 1 to 10 years of follow-up. *J Prosthodont*. 2014;23(6):434–44.
34. Schnutenhaus S, von Koenigsmarck V, Blender B, Ambrosius L, Luthardt RG, Rudolph H. Precision of sleeveless 3D drill guides for insertion of one-piece ceramic implants: a prospective clinical trial. *Int J Comput Dent*. 2018;21(2):97–105.
35. Fauroux MA, De Boutray M, Malthiéry E, Torres JH. New innovative method relating guided surgery to dental implant placement. *J Stomatol Oral Maxillofac Surg*. 2018;119(3):249–53.
36. El Kholi K, Janner SFM, Schimmel M, Buser D. The influence of guided sleeve height, drilling distance, and drilling key length on the accuracy of static computer-assisted implant surgery. *Clin Implant Dent Relat Res*. 2019;21(1):101–7.
37. Buser D, Sennerby L, De Bruyn H. Modern implant dentistry based on osseointegration: 50 years of progress, current trends and open questions. *Periodontol 2000*. 2017;73(1):7–21.
38. Moraschini V, Luz D, Velloso G, Barboza EDP. Quality assessment of systematic reviews of the significance of keratinized mucosa on implant health. *Int J Oral Maxillofac Surg*. 2017;46(6):774–81.
39. Pranskunas M, Poskevicius L, Juodzbalys G, Kubilius R, Jimbo R. Influence of Peri-Implant Soft Tissue Condition and Plaque Accumulation on Peri-Implantitis: a Systematic Review. *J Oral Maxillofac Res*. 2016;7(3):e2.
40. Elgali I, Omar O, Dahlin C, Thomsen P. Guided bone regeneration: materials and biological mechanisms revisited. *Eur J Oral Sci*. 2017;125(5):315–37.
41. Möhlhenrich SC, Modabber A, Steiner T, Mitchell DA, Hölzle F. Heat generation and drill wear during dental implant site preparation: systematic review. *Br J Oral Maxillofac Surg*. 2015;53(8):679–89.
42. Barrak I, Boa K, Joób-Fancsaly Á, Varga E, Sculean A, Piffkó J. Heat Generation During Guided and Freehand Implant Site Preparation at Drilling Speeds of 1500 and 2000 RPM at Different Irrigation Temperatures: An In Vitro Study. *Oral Health Prev Dent*. 2019;9:1–8.
43. Guglielmotti MB, Olmedo DG, Cabrini RL. Research on implants and osseointegration. *Periodontol 2000*. 2019;79(1):178–89.

Publisher's Note

Springer Nature remains neutral with regard to jurisdictional claims in published maps and institutional affiliations.

Ready to submit your research? Choose BMC and benefit from:

- fast, convenient online submission
- thorough peer review by experienced researchers in your field
- rapid publication on acceptance
- support for research data, including large and complex data types
- gold Open Access which fosters wider collaboration and increased citations
- maximum visibility for your research: over 100M website views per year

At BMC, research is always in progress.

Learn more biomedcentral.com/submissions



RESEARCH ARTICLE

Open Access



Reliability and validity of miniscrews as references in cone-beam computed tomography and intraoral scanner digital models: study on goat heads

Yiran Jiang and Gui Chen*

Abstract

Background: Miniscrews have been used to superimpose three-dimensional (3D) craniofacial images as well as explore stable structures in jaws. Our purpose was to evaluate the reliability and validity of linear and angular measurements made with miniscrews on a 3D cone-beam computed tomography (CBCT) at two voxel sizes and compared to models created by an intraoral scanner (IOS).

Methods: Altogether, 64 miniscrews were placed in 12 goat jaws. The jaws were scanned by CBCT machine at 0.12 mm and 0.3 mm voxels and by the IOS. Linear and angular measurements between miniscrews on CBCT at the two voxel settings and the IOS were compared with actual measurements and with each other.

Results: An intra- and inter-class correlation of 0.961–1.000 were obtained by each method. Linear measurements showed significant overestimations of 0.27 ± 0.24 , 0.14 ± 0.22 and 0.15 ± 0.26 mm, and angular measurements showed non-significant differences of $0.11 \pm 1.97^\circ$, $0.15 \pm 2.79^\circ$ and $0.41 \pm 2.34^\circ$ for the CBCT at 0.12-mm, 0.3-mm voxels and the IOS, respectively. Equal magnification of linear measurements was on homolateral and contralateral sides using CBCT, whereas significantly greater magnification on the homolateral side than on the opposite was observed using the IOS. There was no significant difference with angular measurements between digital CBCT models at two voxels and IOS. In addition, all angular measurements were comparable to actual measurement results.

Conclusions: Miniscrews in CBCT and IOS are reliable and clinically valid when used as a reference measuring tooth movement. However, when miniscrews are involved in high precision measurement in CBCT or IOS image, systematic error should be taken into consideration. When comparing CBCT images, using the same voxel size is recommended for miniscrew related measurements to reduce error.

Keywords: Orthodontic miniscrews, Digital dental models, CBCT, Reliability, Validity

Background

Traditional orthodontic records including plaster dental models, facial and intra-oral photos, panoramic radiographs and lateral cephalograms could be used to monitor treatment progress and outcomes. Superimposing serial cephalograms has been used widely to determine the

skeletal and dental changes that occur over time. Stable structures are the keys to a good superimposition. These structures described in Melsen's research of cranial base growth [1], Bjork and Skieler's implant research [2, 3], as well as Enlow's investigation of remodeling [4] are also suggested by American Board of Orthodontics. The locations of these natural stable structures in maxilla and mandible were best found with external metal implant references, and the superimposition of serial cephalograms on metallic implants is considered to be the best technique.

* Correspondence: chengui723@163.com

Department of Orthodontics, Peking University School and Hospital of Stomatology, National Engineering Laboratory for Digital and Material Technology of Stomatology, Beijing Key Laboratory of Digital Stomatology, 22 Zhongguancun South Street, Beijing 100081, China



© The Author(s). 2019 **Open Access** This article is distributed under the terms of the Creative Commons Attribution 4.0 International License (<http://creativecommons.org/licenses/by/4.0/>), which permits unrestricted use, distribution, and reproduction in any medium, provided you give appropriate credit to the original author(s) and the source, provide a link to the Creative Commons license, and indicate if changes were made. The Creative Commons Public Domain Dedication waiver (<http://creativecommons.org/publicdomain/zero/1.0/>) applies to the data made available in this article, unless otherwise stated.

Increasing developments in acquisition of medical images and 3D digital technologies have initiated revolutionary changes in orthodontics. Of recent, CBCT, digital dental models and 3D facial photos have become popular orthodontic records. The reliability and validity of these digital records have to be verified before they are used to make diagnosis and treatment plan. Similar to 2D cephalometric superimposition, orthodontists have tried to register serial 3D digital models to monitor treatment changes over time in three-dimensions. And a great number of studies have focused on CBCTs and digital dental models superimposition.

CBCT has been proven to be a valid 3D representation of the skull that is suitable for clinical and laboratorial usage. It is not difficult to superimpose non-growing patients' serial CBCT models because several stable craniofacial structures can be used as references [5–7]. However, it is still challenging to do so on growing patients because 3D stable structures in jaws have not been identified. Superimposing on external references will be necessary to analyze changes in jaws of growing patients [8]. Parton et al. [9] attempted to superimpose mandibular structures in growing rabbits with the aid of implants. Nguyen et al. [10] identified stable mandibular structures in three dimensions in growing patients with the aid of bone plates.

Recent decades have also witnessed remarkable advancements in digital dental model technologies, from stone dental model scanning to direct intraoral scanning. Digital software makes superimposition of serial dental models possible. Palatal rugae have historically been used to perform 2D measurements on 3D dental models [11–13]. With the aid of miniscrews, Jang et al. [14] and Chen et al. [15] evaluated the stability of the palatal region and established a 3D superimposition method for analyzing orthodontic tooth movement in maxillary dental models, respectively. However, it is still unknown how to superimpose serial digital dental models in growing patients, and again, metallic implants such as miniscrews could be identified as external references in a future study. Beforehand, the positional stability of miniscrews during orthodontic treatment should be evaluated, because only stable miniscrews could be used as references. The linear distance and angle measurements between miniscrews are two methods applied in previous studies [8, 16].

What calls for noteworthy attention is that studies showed that artifact caused by the metallic implant in CBCT will degrade image quality [17], which could bring errors into the procedure of implant superimposition. Park et al. [18] also found that the borders of metal brackets were blurred in image created by certain type of IOS. Another literature disagreed with the use of IOSs for impression capture of multiple dental implants,

aimed at the manufacture of extended implant-supported restorations as full arches [19]. Previous studies have confirmed the reliability and accuracy of digital images about anatomy on jaws bones or dentition by comparing the linear distance between landmarks on digital images with actual values [20–27]. However, no study has quantified the systematic error of digital miniscrew images.

The aim of this study is to evaluate the reliability and validity of linear and angular measurements of miniscrews in CBCT at different voxel sizes and IOS. This was the first attempt to quantify the systematic errors of miniscrew images and test the reliability of miniscrew measurements on CBCT and IOS, and we hope that the result could be served as justification for further evaluation of miniscrew stability and application of miniscrew superimposition on 3D models.

Methods

Four goat maxillae and four mandibles were obtained from the agricultural market for human daily consumption. The goats had already been sacrificed at the time of purchase. For this experiment and under these conditions, the research did not require approval from the regional ethical committee for research ethics due to national legislation. The lower jaw was dissected further into two hemi-mandibles to make direct scanning possible. Maxillae and hemi-mandibles underwent miniscrew (11 mm × 1.6 mm; Ci Bei, Zhejiang, China) implantation by two experienced orthodontists. Two miniscrews were placed on the buccal and lingual sides of each maxilla and hemi-mandible. At least one miniscrew on each hemi-mandible penetrated out of the cortical bone from one side to another (Fig. 1a, d). In all, 64 miniscrews were inserted.

CBCT and intraoral imaging

All the samples were scanned by a NewTom GIANO system (Aperio, Sarasota, FL, USA) with a field of view of 11 cm × 11 cm × 5 cm and high resolution of 0.12-mm voxels. Eight hemi-mandibles were rescanned by 0.3-mm voxels. *Invivo™ 6.0* (Anatomage, San Jose, California, USA) was used to generate 3D models by the preset threshold value of bone (Fig. 1b, e). A *3Shape TRIOS IOS* (3Shape Dental Systems, Copenhagen, Denmark) using a regular calibration procedure was applied for imaging in vitro. The imaging sequence is depicted in Fig. 2. The 3D models were imported into *RapidForm™ 2006* (INUS Technology, Seoul, Korea) for measurement.

Linear and angular measurement of miniscrews

Measurements were undertaken by a single operator thrice for each sample on three digital models and a digital caliper (*Airaj*, Tsingtao, China) on real miniscrews. They were re-measured once by another operator

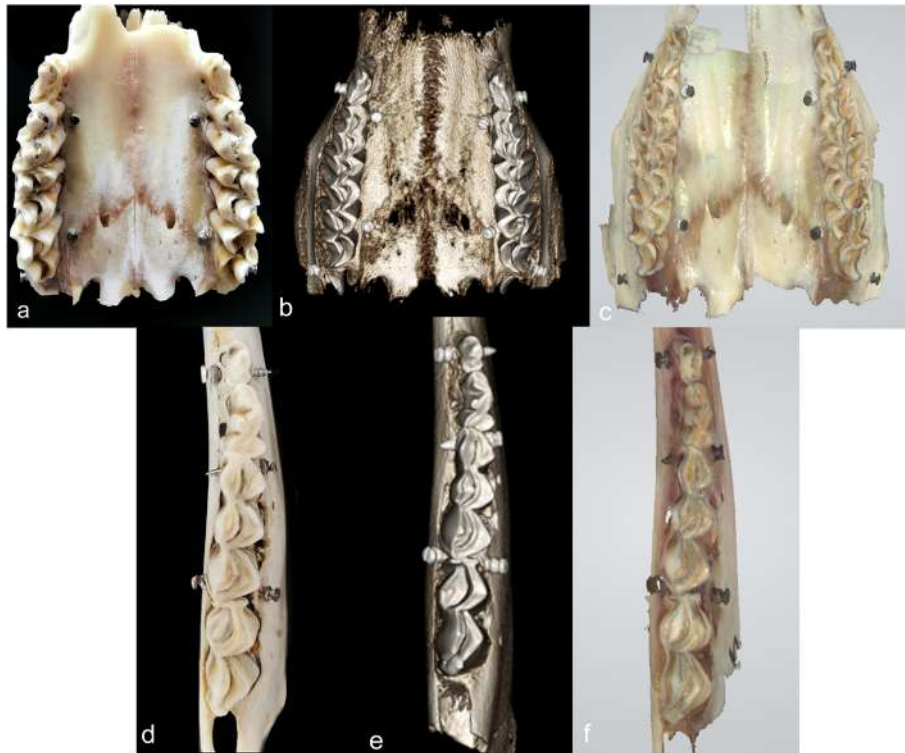


Fig. 1 **a** and **d** Two representative images among 12 samples. **b** and **e** 3D models originating from CBCT of the two actual samples on the left side. **c** and **f** 3D models of the same samples on the left scanned from the IOS

to test inter-operator reliability. The surface center of the head and apex of each miniscrew were used as reference points. The point-to-point distance along a line was used as a linear measurement value (Fig. 3a, b). A measurement was abandoned if either of the points could not

be set stably using a caliper pointer. A visual measurement system, SmartScope® MVP (OGP, Singapore), was used to measure the angle between real miniscrews (Fig. 3d). The angle had to consist of two ultimate points of one cortically penetrated miniscrew, and the third point was a

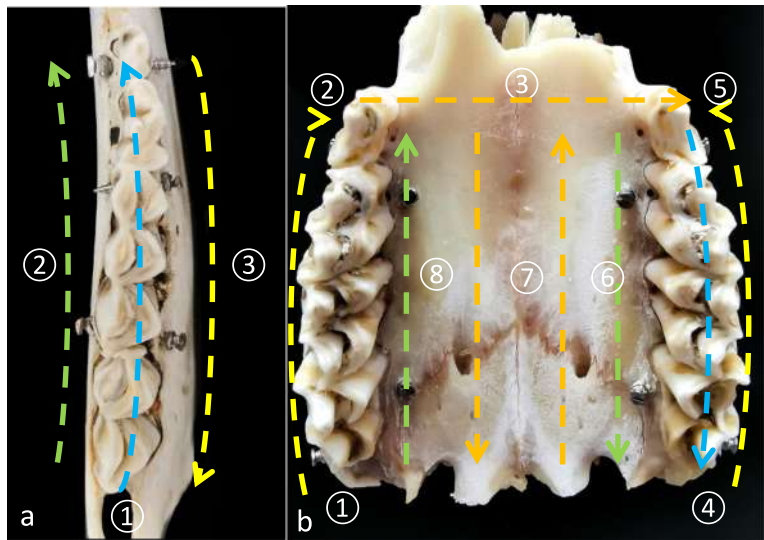


Fig. 2 The imaging sequence of the IOS. **a** Representative imaging sequence for hemimandible samples: occlusal–buccal–lingual. **b** Representative imaging sequence for maxillary samples: right occlusal–right buccal–anterior palatal–left occlusal–left buccal–left palatal–palatal–right palatal

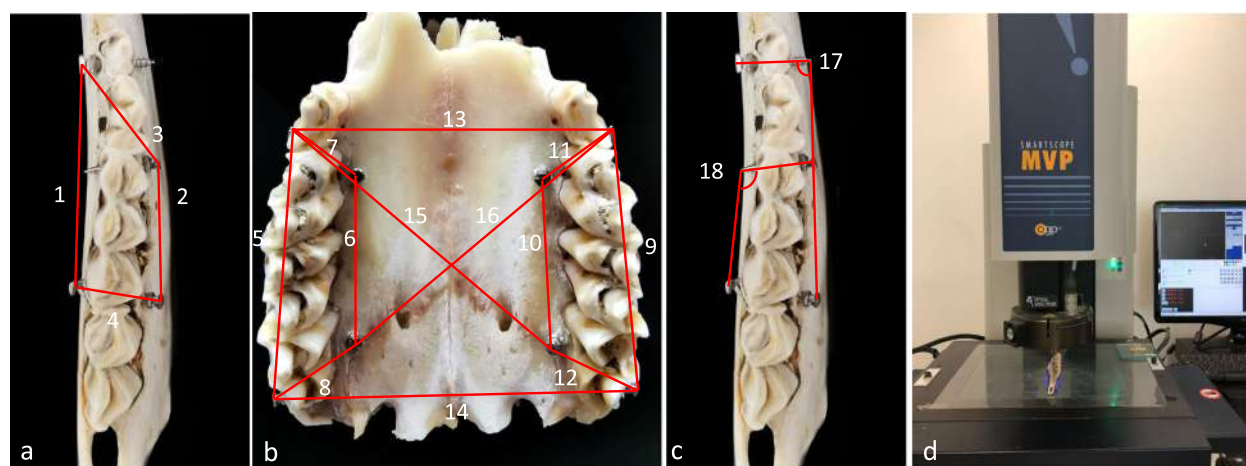


Fig. 3 **a** and **b** Sixteen linear distances measured between two miniscrew heads on hemimandibles and maxillae. **c** angles measured on the hemimandible. **d** Smartscope MVP for actual measurement of angles

surface center point of another miniscrew head or the apex of the miniscrew depending on which one was visually clear (Fig. 3c). Half of the cap of the miniscrews was ground off using a high-speed handpiece to allow better identification of reference points.

Statistical analyses

Measurements taken by the digital caliper and Smartscope MVP on real miniscrews were considered to be real values. SPSS v25 (IBM, Armonk, NY, USA) was employed for statistical analyses. Intra- and inter-operator reliabilities were tested by intra-class correlation analysis (ICC). Then, the arithmetic mean value was calculated and used as the value of each measurement. All mean data were tested to follow the normal distribution. Therefore, paired t-test was conducted to evaluate the validity of measurements of miniscrews in

CBCT and intraoral imaging. The level of significance was set at $P < 0.01$ for ICC and $P < 0.05$ for paired t-tests. An acceptable error for linear measurement for clinical application was set as $\leq \pm 0.5$ mm [28]. Also, $\leq \pm 5^\circ$ was deemed to be clinically acceptable for measuring systematic differences for angles [16].

Results

Seventy-five paired linear measurements (35 homolateral measurements and 40 contralateral measurements) at 0.12-mm voxels, 31 linear measurement (20 homolateral measurements and 11 contralateral measurements) at 0.3-mm voxels and 11 angles were evaluated. Intra- and inter-operator reliability using ICC was 0.961–1.000.

Linear measurements by 3D models from CBCT at 0.12-mm voxels (termed “CBCT1” in all Tables) and 0.3-mm voxels (CBCT2) demonstrated overestimates on

Table 1 Paired t-test for comparing linear measurement values (mm) between the three digital models with values from the digital caliper

Measurement	Mean bias	Standard deviation	95% confidence interval	t	P
Homolateral side					
CBCT1	0.31	0.20	0.24 to 0.38	9.111	< 0.001
CBCT2	0.11	0.21	0.02 to 0.21	2.450	0.024
IOS	0.25	0.20	0.18 to 0.32	7.206	< 0.001
Contralateral side					
CBCT1	0.25	0.28	0.16 to 0.34	5.637	< 0.001
CBCT2	0.19	0.26	0.02 to 0.37	2.473	0.033
IOS	0.04	0.27	−0.04 to 0.13	0.986	0.330
Total linear measurements					
CBCT1	0.27	0.24	0.22 to 0.33	9.739	< 0.001
CBCT2	0.14	0.22	0.06 to 0.22	3.505	0.001
IOS	0.15	0.26	0.09 to 0.21	5.106	< 0.001

Table 2 One sample *t*-test for comparing the differences in mean linear measurement (mm) between homolateral and contralateral sides of CBCT and IOS with measurements using the digital caliper (the test value was zero)

Measurement	Mean bias	Standard deviation	95% confidence interval	t	P
CBCT1	0.08	0.30	−0.01 to 0.19	1.714	0.093
CBCT2	−0.10	0.37	−0.35 to 0.15	−0.910	0.384
IOS	0.25	0.31	0.15 to 0.35	4.912	< 0.001

homolateral and contralateral sides compared with the paired results using the digital caliper (Table 1). The mean biases were 0.31 ± 0.20 mm and 0.25 ± 0.28 mm at 0.12-mm voxels, and 0.11 ± 0.21 mm and 0.19 ± 0.26 mm at 0.3-mm voxels. All 95% confidence intervals (CIs) were > 0 mm but < 0.5 mm. The only significant difference using the IOS relative to digital caliper pairs was observed on homo-lateral linear measurements. An equal amplification effect on sagittal and transverse directions was revealed by a one-sample *t*-test at 0.12-mm voxels and 0.3-mm voxels of CBCT with caliper measurements, whereas a significant increased enlargement was observed on the homo-lateral side using the IOS (Tables 1, 2). In total, significantly larger results were observed compared with value obtained using digital caliper pairs. Also, results at 0.12-mm voxels using CBCT were significantly larger than all other values (Table 4).

Angle measurements revealed good validity among the three digital methods compared with true values (Table 3). Values for standard deviation and ranges of 95%CIs were large. Significant differences among the three digital models were not observed (Table 4).

Discussion

Superimposing orthodontic records at different time points has been used widely to determine the cranio-facial changes. The cornerstone of superimposition is using stable structures. Identification of stable structures in jaws without having external references in growing patients is extremely challenging. In history, metal implants have been used as reference in 2D cephalograms to explore natural stable structure [2, 3]. In 3D era, implants should continually play a crucial role in CBCT [8–10] and digital dental model superimposition [14, 15]. However, metallic implants would produce artifacts both in CBCT and IOS images, which would degrade the image quality and introduce errors. In this study, the experimental

animal skulls, which are more feasible and less expensive than human skulls, were used to evaluate the reliability and validity of linear and angle measurements of 3D miniscrews on CBCT and IOS with actual values. The results of our study are applicable on human skulls as well, because the goat heads are merely platforms for miniscrew implantation. Moreover, the study is ethically impossible to be conducted on patients because of the amount of radiation exposure necessary when taking CBCT at different resolutions.

Our study showed that statistically significant overestimations of linear measurements were obtained on CBCT both at 0.12 (0.27 ± 0.24 mm) and 0.3 (0.14 ± 0.22 mm) voxels compared with actual measurements. Our results are, to some extent, consistent with several studies. Moshfeghi et al. [20] using gutta-percha, reported an enlargement by 0.10 ± 0.99 mm in axial section and 0.27 ± 1.07 mm coronal section at 0.3 voxels. However, the values for standard deviation were greater than our data. Tolentino et al. [21] used silica markers, but they did not observe statistical difference among voxels at 0.25, 0.3 or 0.4 mm. Variable materials used as references in different studies may attribute to the contradiction between studies. Schulze et al. [29] pointed that an extreme artifact could be produced by titanium implants. Instead of upgrading resolution, they suggested a more sophisticated reconstruction algorithm for meaningful reduction of artifacts. Moreover, when using linear measurement to evaluate the stability of miniscrews, the systematic error should be taken into consideration.

Secondly, miniscrews at two voxel settings presented reliable and accurate results on angle measurements when compared with actual values. Our result supported the use of angular measurements acquired through miniscrews in clinical applications, which is important on measuring the angle stability of miniscrews after orthodontic loading [16].

CBCT is limited for evaluation of short-term treatment effects due to excess radiation exposure to the

Table 3 Paired *t*-test for comparing angle measurement (°) values between the three digital models with actual measurements

Measurement	Mean bias	Standard deviation	95% confidence interval	t	P
CBCT1	0.11	1.97	−1.21 to 1.44	0.192	0.852
CBCT2	0.15	2.79	−0.88 to 1.19	0.330	0.748
IOS	0.41	2.34	−1.17 to 1.98	0.574	0.579

Table 4 Paired *t*-test for values of linear (mm) and angle (°) measurements among the three digital models

Measurement	Mean bias	Standard deviation	95% confidence interval	t	P
Linear measurements					
CBCT1–CBCT2	0.20	0.26	0.10 to 0.29	4.231	< 0.001
CBCT1–IOS	0.12	0.24	0.07 to 0.18	4.434	< 0.001
0.3-mm voxels–IOS	−0.02	0.32	−0.14 to 0.10	−0.363	0.719
Angle measurements					
CBCT1–CBCT2	−0.04	0.97	−0.69 to 0.61	−0.134	0.896
CBCT1–IOS	−0.29	2.79	−2.17 to 1.58	−0.346	0.737
CBCT2–IOS	0.49	1.20	−0.37 to 1.35	1.288	0.230

patients. Thus, chairside IOS is promising for this purpose. DeLong et al. [30] found that a smooth textured surface (such as the titanium miniscrews used in our study) could worsen the digitizing performance due to spectral reflection. However, our study confirmed the clinical reliability and validity of IOS for linear and angular measurements of miniscrews, which were consistent with other studies. However, these measurements were different with respect to systematic errors and their tendencies [22–27]. Our results supported that the evaluation of tooth movement on serial digital dental models from IOSs during growth or after orthodontic intervention is operable. In addition, we also found it quite interesting that the mean bias on the homolateral side was significantly larger than that on the opposite, implying unequal magnification in sagittal and transverse directions. Anh et al. [31] claimed that regions imaged later would generate more errors during configuration than regions imaged earlier. Thus, the scanning sequence could be one of the reasons for the unequal amplification effect observed in our study, and a modification is required when miniscrews are involved.

Above all, in accordance with results of literatures and this study, the following suggestions are proposed when miniscrews are used to superimpose 3D image: 1. The positional stability of miniscrews should be evaluated in order to ensure the reliability and clinical validity of the linear and angular measurements on 3D models. 2. The same CBCT machine with the same scanning settings is required when doing superimposition. 3. Systematic errors of miniscrew measurements on CBCT image and digital dental models acquired from IOS should be considered when stable structures are explored.

A limitation of this study is the exclusion of motion artifacts because this is an experiment on dry goat jaw bone. In addition, the study was conducted for a single experimental condition by testing systematic errors on a specific type of miniscrew, a single CBCT machine and one IOS. Whether the results of this study are suitable for other miniscrews, other CBCT machines at different voxel sizes, or other IOSs is not known.

Conclusions

1. The linear and angular measurements produced using miniscrews as a reference to measure tooth movement seem reliable and clinically valid in images generated by CBCT and IOS. However, when miniscrews are involved in high precision measurements in CBCT or IOS image, such as exploration of a stable region, systematic error should be taken into consideration.
2. Maintaining the same voxel size in CBCT images is suggested when miniscrews are set as reference to measure the changes in craniofacial structures.

Abbreviations

3D: Three-dimensional; CBCT: Cone-beam computed tomography; CI: Confidence intervals; ICC: Intra-class correlation analysis; IOS: Intraoral scanner

Acknowledgements

We would like to thank Miss Qi Guo and Miss Tiantian Wan for the assistance during all the time of the study. And the manuscript was proofread by a native English professional with science background at Elixigen Corporation.

Authors' contributions

YJ and GC designed the study together. YJ measured the data of linear distance and angles between miniscrews three digital models and a digital caliper on real miniscrews, and GC did the measurements once of inter-class consistency test. YJ analyzed and interpreted the data and was a major contributor in writing the manuscript. All authors read and approved the final manuscript.

Funding

The study is financially supported by the Emergency Management program of National Nature Science Foundation (81441036) in sample collection, CBCT and IOS images acquisition, and manuscript proof read.

Availability of data and materials

The full datasets used and analyzed during the current study are available on reasonable request from the corresponding author at chengui723@163.com.

Ethics approval and consent to participate

The goat heads were obtained from the agricultural market. They had already been sacrificed at the time of purchase. No approval from the regional committee for research ethics is required according to the national legislation.

Consent for publication

Not applicable.

Competing interests

The authors declare that they have no competing interests.

Received: 6 September 2019 Accepted: 8 November 2019

Published online: 27 November 2019

References

- Melsen B. The cranial base: The postnatal development of the cranial base studied histologically on human autopsy material: Birte Melsen. *Acta Odontol. Scand.* 32:Suppl. 62, 1974. *Am J Orthod.* 1974;66(6):689–91.
- Bjork A, Skieller V. Normal and abnormal growth of the mandible: a synthesis of longitudinal cephalometric implant studies over a period of 25 years. *Eur J Orthod.* 1983;5:1–46.
- Bjork A, Skieller V. Growth of the maxilla in three dimensions as revealed radiographically by the implant method. *Br J Orthod.* 1977;4:53–64.
- Enlow DH, Harris DB. A study of the postnatal growth of the human mandible. *Amer J Orthod.* 1964;50:25–50.
- Cevdanes LH, Bailey LJ, Tucker GR Jr, Styner MA, Mol A, Phillips CL, Proffit WR, et al. Superimposition of 3D cone-beam CT models of orthognathic surgery patients. *Dentomaxillofac Radiol.* 2005;34:369–75.
- Cevdanes LH, Motta A, Proffit WR, Ackerman JL, Styner M. Cranial base superimposition for 3-dimensional evaluation of soft-tissue changes. *Am J Orthod Dentofac Orthop.* 2010;137(4 Suppl):S120–9.
- Weissheimer A, Menezes LM, Koerich L, Pham J, Cevdanes LH. Fast three-dimensional superimposition of cone beam computed tomography for orthopaedics and orthognathic surgery evaluation. *Int J Oral Maxillofac Surg.* 2015;44:1188–96.
- Ruan MJ, Chen G, Xu TM. Comparison of orthodontic tooth movement between adolescents and adults based on implant superimposition. *PLoS One.* 2018;13:e0197281.
- Parton AL, Duncan WJ, Oliveira ME, Key O, Farella M. Implant-based three-dimensional superimposition of the growing mandible in a rabbit model. *Eur J Orthod.* 2016;38:546–52.
- Nguyen T, Cevdanes L, Franchi L, Ruellas A, Jackson T. Three-dimensional mandibular regional superimposition in growing patients. *Am J Orthod Dentofac Orthop.* 2018;153:747–54.
- Almeida MA, Phillips C, Kula K, Tulloch C. Stability of the palatal rugae as landmarks for analysis of dental models. *Angle Orthod.* 1995;65:43–8.
- Bailey LT, Esmailnejad A, Almeida MA. Stability of the palatal rugae as landmarks for analysis of dental models in extraction and nonextraction cases. *Angle Orthod.* 1996;66:73–8.
- Hoggan BR, Sadowsky C. The use of palatal rugae for the assessment of anteroposterior tooth movements. *Am J Orthod Dentofac Orthop.* 2001;119:482–8.
- Jang I, Tanaka M, Koga Y, Lijima S, Yozgatian JH, Cha BK, Yoshida N. A novel method for the assessment of three-dimensional tooth movement during orthodontic treatment. *Angle Orthod.* 2009;79:447–53.
- Chen G, Chen S, Zhang XY, Jiang RP, Liu Y, Shi FH, Xu TM. Stable region for maxillary dental model superimposition in adults, studied with the aid of stable miniscrews. *Orthod Craniofac Res.* 2011;14:70–9.
- Chen G, Chen S, Zhang XY, Jiang RP, Liu Y, Shi FH, Xu TM. A new method to evaluate the positional stability of a self-drilling miniscrew. *Orthod Craniofac Res.* 2015;18:125–33.
- Kerkfeld V, Meyer U. Higher resolution in cone beam computed tomography is accompanied by improved bone detection in peri-implant bone despite metal artifact presence. *Int J Oral Maxillofac Implants.* 2018;33:1331–8.
- Park JM, Choi SA, Myung JY, Chun YS, Kim M. Impact of orthodontic brackets on the intraoral scan data accuracy. *Biomed Res Int.* 2016;2016:5075182.
- Khraishi H, Duane B. Evidence for use of intraoral scanners under clinical conditions for obtaining full-arch digital impressions is insufficient. *Evid Based Dent.* 2017;18:24–5.
- Moshfeghi M, Tavakoli MA, Hosseini ET, Ali TH, Iman TH. Analysis of linear measurement accuracy obtained by cone beam computed tomography (CBCT-NewTom VG). *Dent Res J (Isfahan).* 2012;9(Suppl 1):S 57–62.
- Tolentino ES, Yamashita FC, de Albuquerque S, Walewski LA, Iwaki LCV, Takashita WM, Silva MC. Reliability and accuracy of linear measurements in cone-beam computed tomography using different software programs and voxel sizes. *J Conserv Dent.* 2018;21:612–07.
- Rheude B, Sadowsky PL, Ferriera A, Jacobson A. An evaluation of the use of digital study models in orthodontic diagnosis and treatment planning. *Angle Orthod.* 2005;75:300–4.
- Akyalcin S, Cozad BE, English JD, Colville CD, Laman S. Diagnostic accuracy of impression-free digital models. *Am J Orthod Dentofac Orthop.* 2013;144:916–22.
- Naidu D, Freer TJ. Validity, reliability, and reproducibility of the iOC intraoral scanner: a comparison of tooth widths and Bolton ratios. *Am J Orthod Dentofac Orthop.* 2013;144:304–10.
- Wiranto MG, Engelbrecht WP, Tutein Nolthenius HE, van der Meer WJ, Ren Y. Validity, reliability, and reproducibility of linear measurements on digital models obtained from intraoral and cone-beam computed tomography scans of alginate impressions. *Am J Orthod Dentofac Orthop.* 2013;143:140–7.
- Gruheid T, McCathy SD, Larson BE. Clinical use of a direct chairside oral scanner: an assessment of accuracy, time, and patient acceptance. *Am J Orthod Dentofac Orthop.* 2014;146:673–82.
- Mack S, Bonilla T, English JD, Cozad B, Akyalcin S. Accuracy of 3-dimensional curvilinear measurements on digital models with intraoral scanners. *Am J Orthod Dentofac Orthop.* 2017;152:420–5.
- Cassetta M, Di Giorgio R, Barbato E. Are intraoral radiographs reliable in determining peri-implant marginal bone level changes? The correlation between open surgical measurements and peri-apical radiographs. *Int J Oral Maxillofac Surg.* 2018;47:1358–64.
- Schulze RKW, Berndt D, d'Hoedt B. On cone-beam computed tomography artifacts induced by titanium implants. *Clin Oral Implants Res.* 2010;21:100–7.
- DeLong R, Pintado MR, Ko CC, Hodges JS, Douglas WH. Factors influencing optical 3D scanning of vinyl polysiloxane impression materials. *J Prosthodont.* 2001;10:78–85.
- Anh JW, Park JM, Chun YS, Kim M, Kim M. A comparison of the precision of three-dimensional images acquired by 2 digital intraoral scanners: effects of tooth irregularity and scanning direction. *Korean J Orthod.* 2016;46:3–12.

Publisher's Note

Springer Nature remains neutral with regard to jurisdictional claims in published maps and institutional affiliations.

Ready to submit your research? Choose BMC and benefit from:

- fast, convenient online submission
- thorough peer review by experienced researchers in your field
- rapid publication on acceptance
- support for research data, including large and complex data types
- gold Open Access which fosters wider collaboration and increased citations
- maximum visibility for your research: over 100M website views per year

At BMC, research is always in progress.

Learn more biomedcentral.com/submissions



RESEARCH ARTICLE

Open Access



Applying intraoral scanner to residual ridge in edentulous regions: in vitro evaluation of inter-operator validity to confirm trueness

Akinori Tasaka^{1,2*}, Yuuki Uekubo¹, Tomoharu Mitsui¹, Takao Kasahara³, Takuya Takanashi⁴, Shinya Homma⁴, Satoru Matsunaga^{2,5}, Shinichi Abe⁵, Masao Yoshinari², Yasutomo Yajima⁴, Kaoru Sakurai⁶ and Shuichiro Yamashita¹

Abstract

Background: The purpose of this study was to investigate the trueness of intraoral scanning of residual ridge in edentulous regions during in vitro evaluation of inter-operator validity.

Methods: Both edentulous maxillary and partially edentulous mandibular models were selected as a simulation model. As reference data, scanning of two models was performed using a dental laboratory scanner (D900, 3Shape A/S). Five dentists used an intraoral scanner (TRIOS 2, 3Shape A/S) five times to capture intraoral scanner data, and the “zig-zag” scanning technique was used. They did not have experience with using intraoral scanners in clinical treatment. The intraoral scanner data was overlapped with the reference data (Dental System, 3Shape A/S). Regarding differences that occurred between the reference and intraoral scanner data, the vertical maximum distance of the difference and the integral value obtained by integrating the total distance were analyzed.

Results: In terms of the maximum distances of the difference on the maxillary model, the means of five operators were as follows: premolar region, 0.30 mm; molar region, 0.18 mm; and midline region, 0.18 mm. The integral values were as follows: premolar region, 4.17 mm²; molar region, 6.82 mm²; and midline region, 4.70 mm². Significant inter-operator differences were observed with regard to the integral values of the distance in the premolar and midline regions and with regard to the maximum distance in the premolar region, respectively. The maximum distances of the difference in the free end saddles on mandibular model were as follows: right side, 0.05 mm; and left side, 0.08 mm. The areas were as follows: right side, 0.78 mm²; and left side, 1.60 mm². No significant inter-operator differences were observed in either region.

Conclusions: The present study demonstrated satisfactory trueness of intraoral scanning of the residual ridge in edentulous regions during in vitro evaluation of inter-operator validity.

Keywords: Intraoral scanner, Optical impression, Edentulous, Free end saddles, Residual ridge

Background

The recent spread of digital dentistry has seen remarkable innovation in the capture of optical impressions using intraoral scanners, with three-dimensional (3D) full-color image scanning now possible. Development of a workflow to fabricate crown restorations using the acquired imaging data is already underway [1–3].

Various systems of computer-aided design (CAD)/computer-aided manufacturing (CAM) fabrication of complete dentures have been devised [4]. CAD/CAM systems have already been applied to denture base milling and artificial tooth attachment; denture base additive manufacturing and artificial tooth attachment; and milling of discs consisting of denture base and artificial tooth. Although limited to case reports of CAD/CAM fabrication of partial dentures, satisfactory results have been published for CAD/CAM framework fabrication using intraoral scanners to capture optical impressions [5–8]. The 3D data of the oral cavity is used to create

* Correspondence: atasaka@tdc.ac

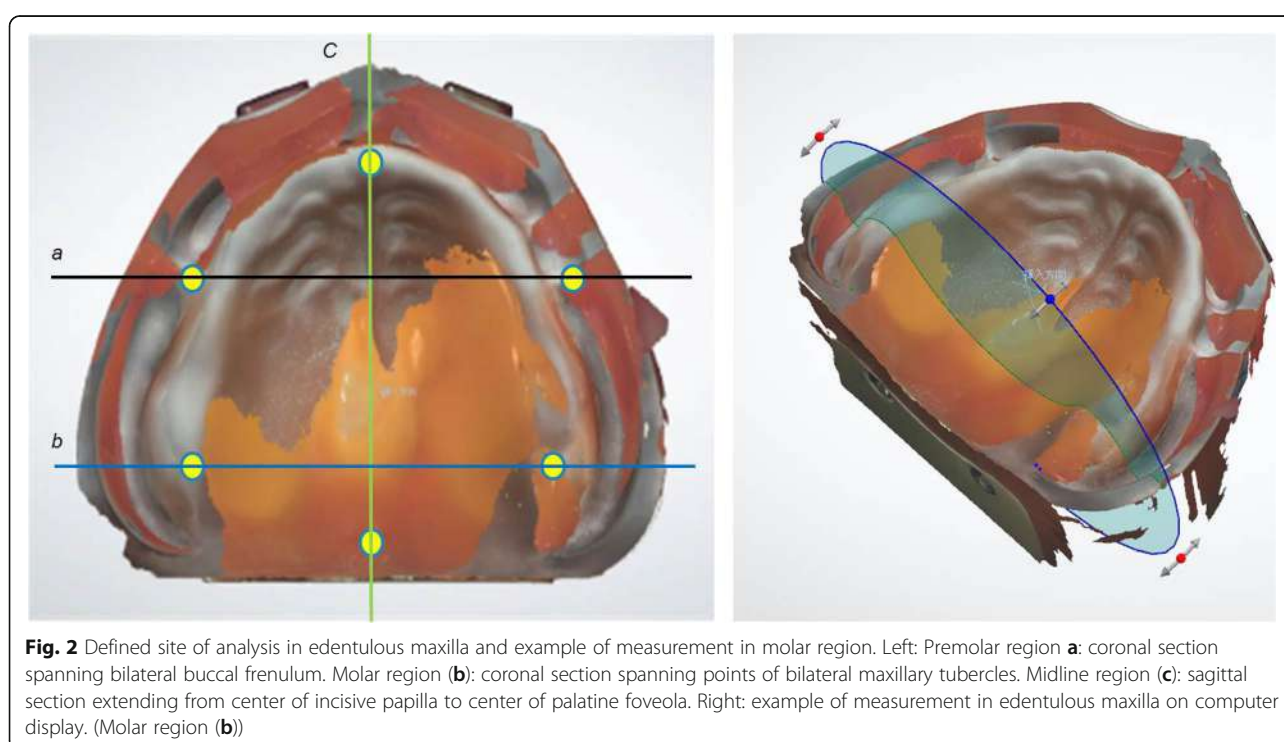
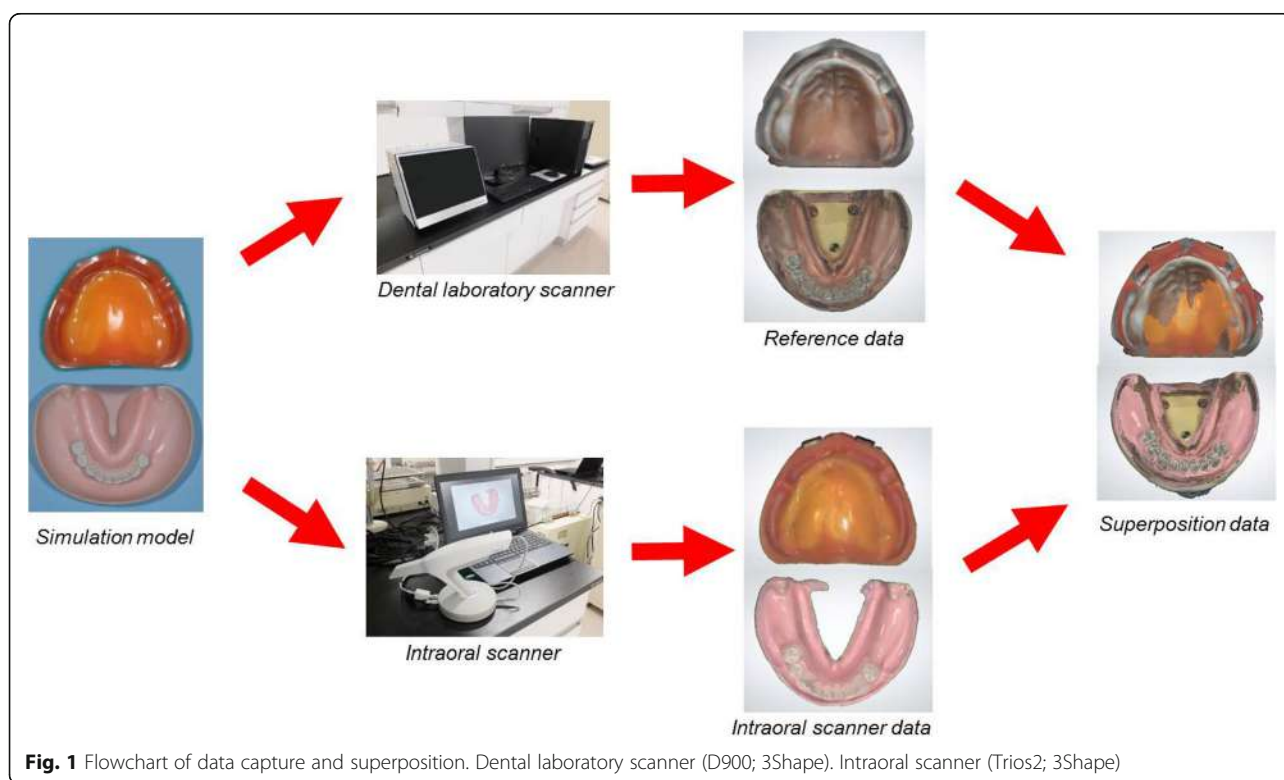
¹Department of Removable Partial Prosthodontics, Tokyo Dental College, 2-9-18 Kandasakicho Chiyoda-ku, Tokyo 101-0061, Japan

²Oral Health Science Center, Tokyo Dental College, Tokyo, Japan

Full list of author information is available at the end of the article



© The Author(s). 2019 **Open Access** This article is distributed under the terms of the Creative Commons Attribution 4.0 International License (<http://creativecommons.org/licenses/by/4.0/>), which permits unrestricted use, distribution, and reproduction in any medium, provided you give appropriate credit to the original author(s) and the source, provide a link to the Creative Commons license, and indicate if changes were made. The Creative Commons Public Domain Dedication waiver (<http://creativecommons.org/publicdomain/zero/1.0/>) applies to the data made available in this article, unless otherwise stated.



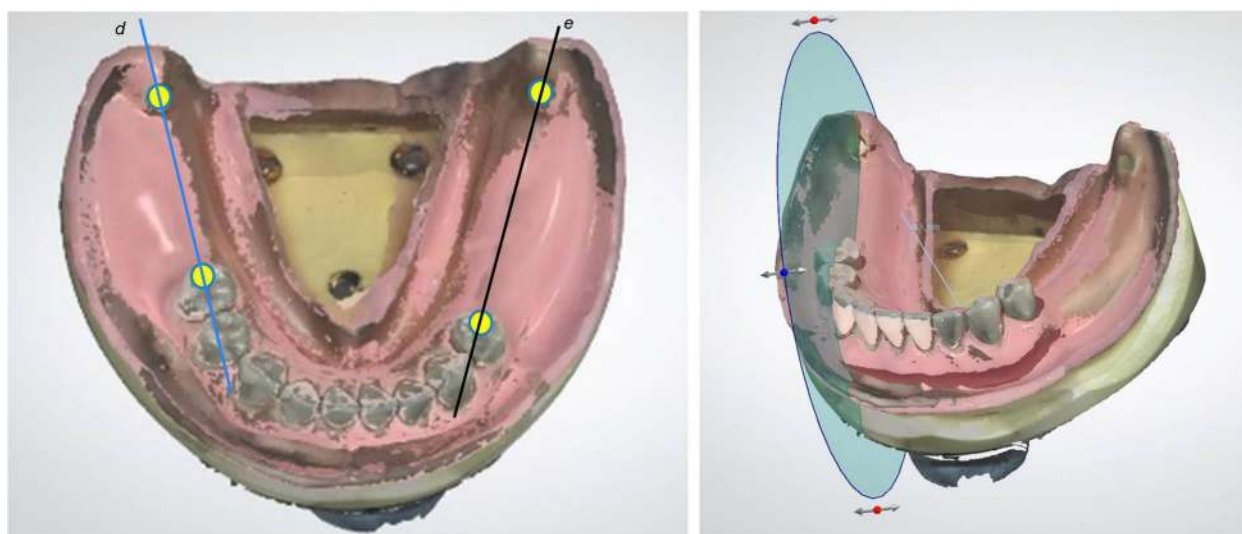


Fig. 3 Defined site of analysis in partially edentulous mandible and example of measurement in molar region. Left; Right side (d): sagittal section extending from rest seat on right second premolar to center of retromolar pad. Left side (e): sagittal section extending from rest seat on left first premolar to center of retromolar pad. Right: example of measurement in partially edentulous mandible on computer display. (Right side (d))

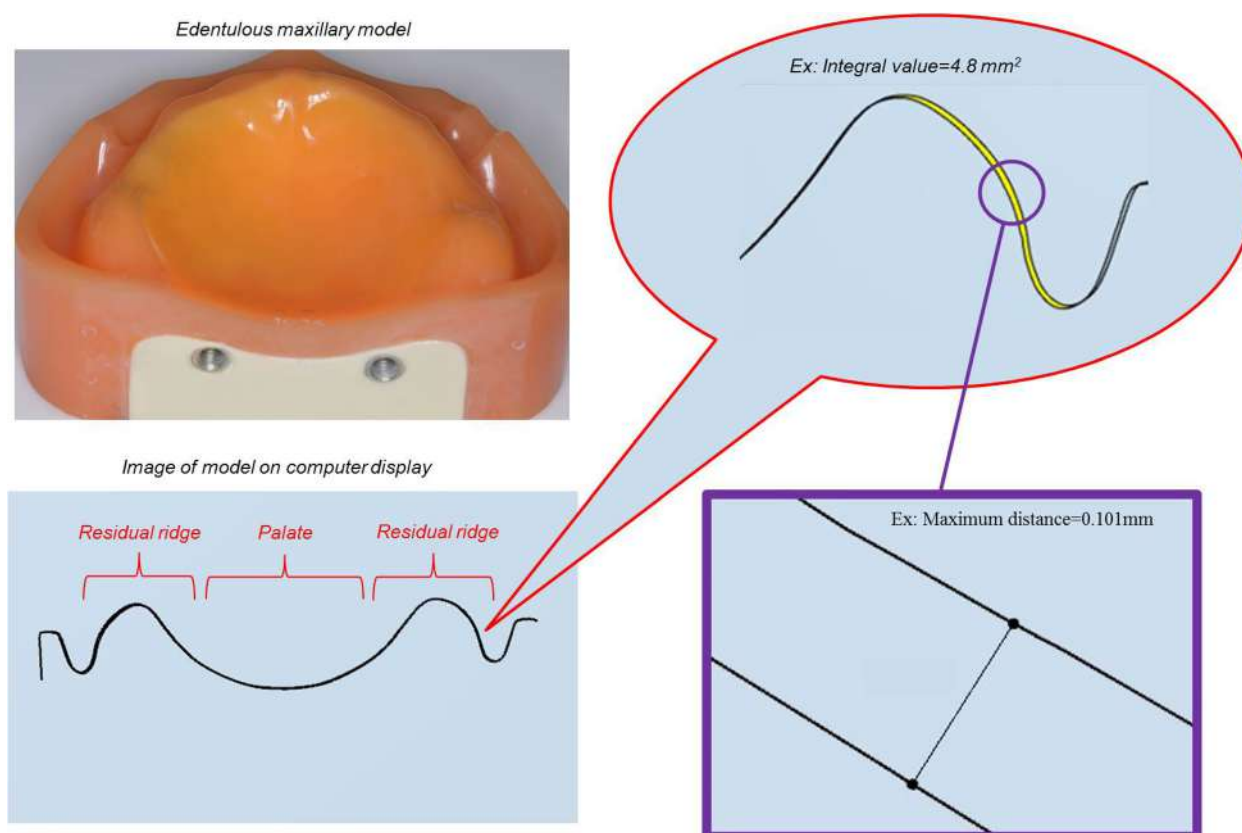


Fig. 4 Summary of analysis items in edentulous maxilla. Left: Edentulous maxilla model and computer display of coronal section spanning points of bilateral maxillary tubercles. Right: Maximum distance (point to point) and integral value (surrounded by yellow) obtained by integrating total distance were analyzed using software (Dental system; 3shape)

the CAD data of the framework for a digital wax-up. Additive manufacturing is then performed based on the framework data to create the resin pattern, after which the pattern is invested and cast [9], and the framework is molded. Another method is to mold the framework using selective laser melting [10].

However, the approaches used in all of these systems are not equivalent to creating functional impressions using conventional impression materials. The difficulty involved in capturing optical impressions of viscoelastic bodies such as mucosa required for removable dentures has delayed the spread of intraoral scanner use in this field of dentistry. It should be noted that it is difficult to obtain data regarding the amount of tissue displacement of the residual mucous membrane and the functional morphology of mobile tissues such as the oral vestibular, lips, tongue and cheeks with an intraoral scanner.

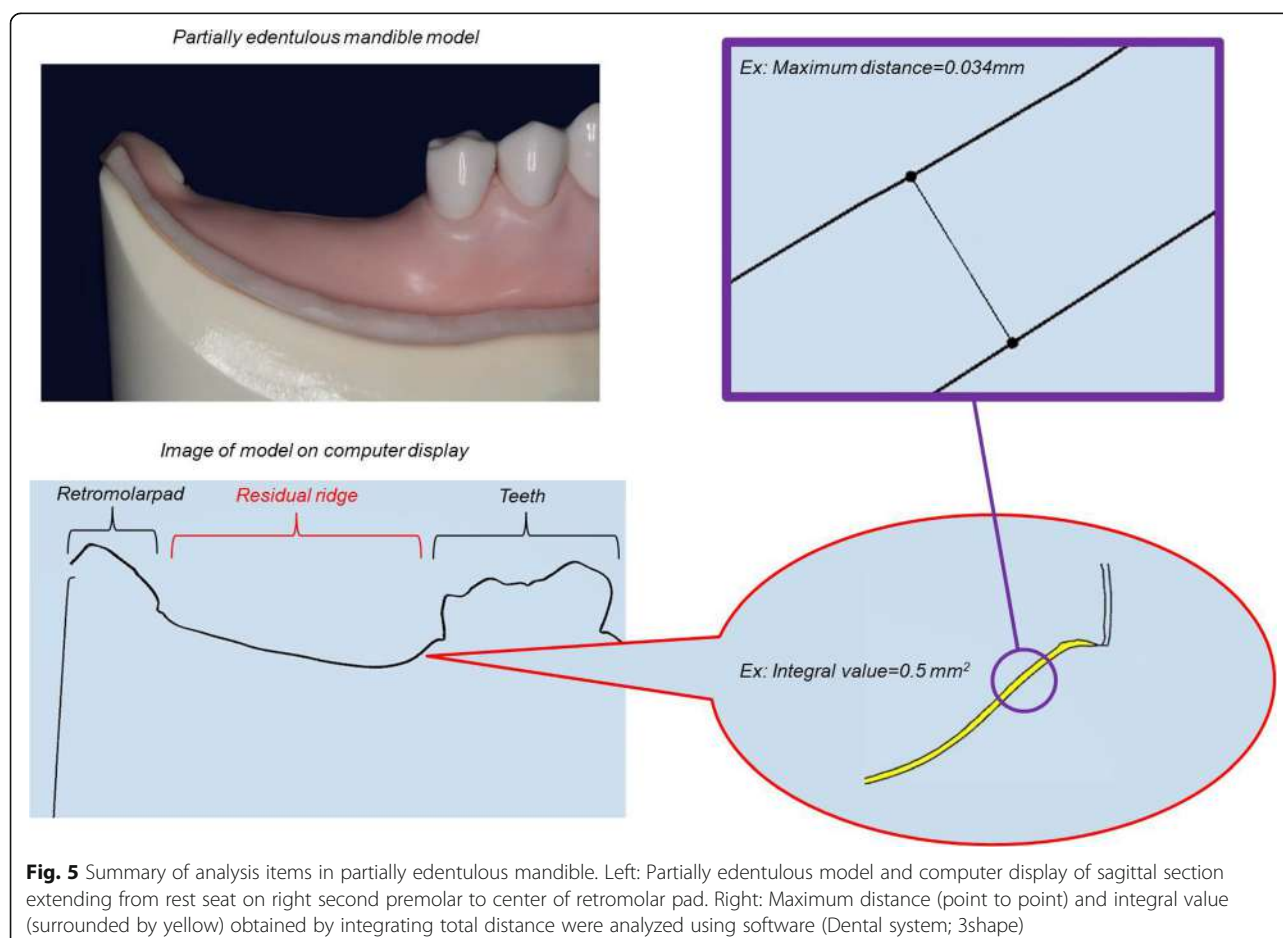
The fabrication of removable dentures using an intraoral scanner has many advantages, such as reducing patient discomfort of impression taking, eliminating rubber allergies, the distortion of impression material and storing the scan data [11]. Although many studies have verified the trueness and precision of optical impressions

captured using intraoral scanners for remaining teeth [12–15], many points remain to be clarified regarding precision for the residual ridge in edentulous regions [16–19]. In order to establish a workflow for CAD/CAM fabrication of removable dentures based on data acquired from intraoral scanners, the trueness and precision of intraoral scanning for residual ridge must be confirmed. The present study investigated the trueness of intraoral scanning regarding the residual ridge in edentulous regions for in vitro evaluation of inter-operator validity.

Methods

Simulation models

An edentulous maxillary model (G10FE-402 K, Nissin Dental Products Inc., Tokyo, Japan) and a partially edentulous mandibular model with free end saddles (P25-TP49, Nissin Dental Products Inc., Tokyo, Japan) were used as simulation models. The artificial mucosa made from silicone was attached on each simulation model. The free end saddles on mandibular model were Kennedy class I with missing bilateral molars and left second premolar. Rest seats were prepared on the distal



proximal surface of the mandibular right second and left first premolars.

Data acquisition and superimposition

A dental laboratory scanner (D900, 3Shape A/S, Copenhagen, Denmark) was used for 3D scanning of the maxillary and mandibular simulation models to acquire reference data. The D900 employs 5.0 MP cameras, and the scanner's optical system has been optimized for speckle-free capture. Four cameras and new blue light-emitting diode technology had highly accurate color scanning at $\pm 7 \mu\text{m}$.

The simulation models were fitted to the SIMPLE MANIKIN III (Nissin Dental Products Inc., Tokyo, Japan) and attached to a dental chair with the Head Rest Mount SPMIII (Nissin Dental Products Inc., Tokyo, Japan). Five dentists each used an intraoral scanner (TRIOS 2, 3Shape A/S, Copenhagen, Denmark, <https://www.3shape.com/en/support-docs>) five times to capture optical impression data. They had not used intraoral scanners in clinical treatment. The “zig-zag” scanning technique was used in this study. After scanning, unnecessary information (islands and peninsulas) was trimmed and removed using the tool function.

The captured intraoral scanner data were imported into CAD software (Dental System, 3Shape A/S, Copenhagen, Denmark). Using the double scan technique of CAD software, intraoral scanner data were superimposed onto the reference data on the basis of the incisive papilla (1 point) and the top of the bilateral maxillary tubercles (2 points) for the edentulous maxillary model and of the incisal point (1 point) and the centers of the bilateral retromolar pads (2 points) for the free end missing mandibular model (Fig. 1).

Trueness verification

Scanning data were acquired in several regions of each model in order to verify trueness. In the maxillary, these verification regions comprised a coronal section spanning the bilateral buccal frenulum (premolar region), a coronal section spanning the points of the bilateral maxillary tubercles (molar region), and a sagittal section extending from the center of the incisive papilla to the center of the palatine foveola (midline region) (Fig. 2). In the mandibular, these regions comprised a sagittal section extending from the rest seat on the right second premolar to the center of the retromolar pad (right side) and a sagittal section extending from the rest seat on the

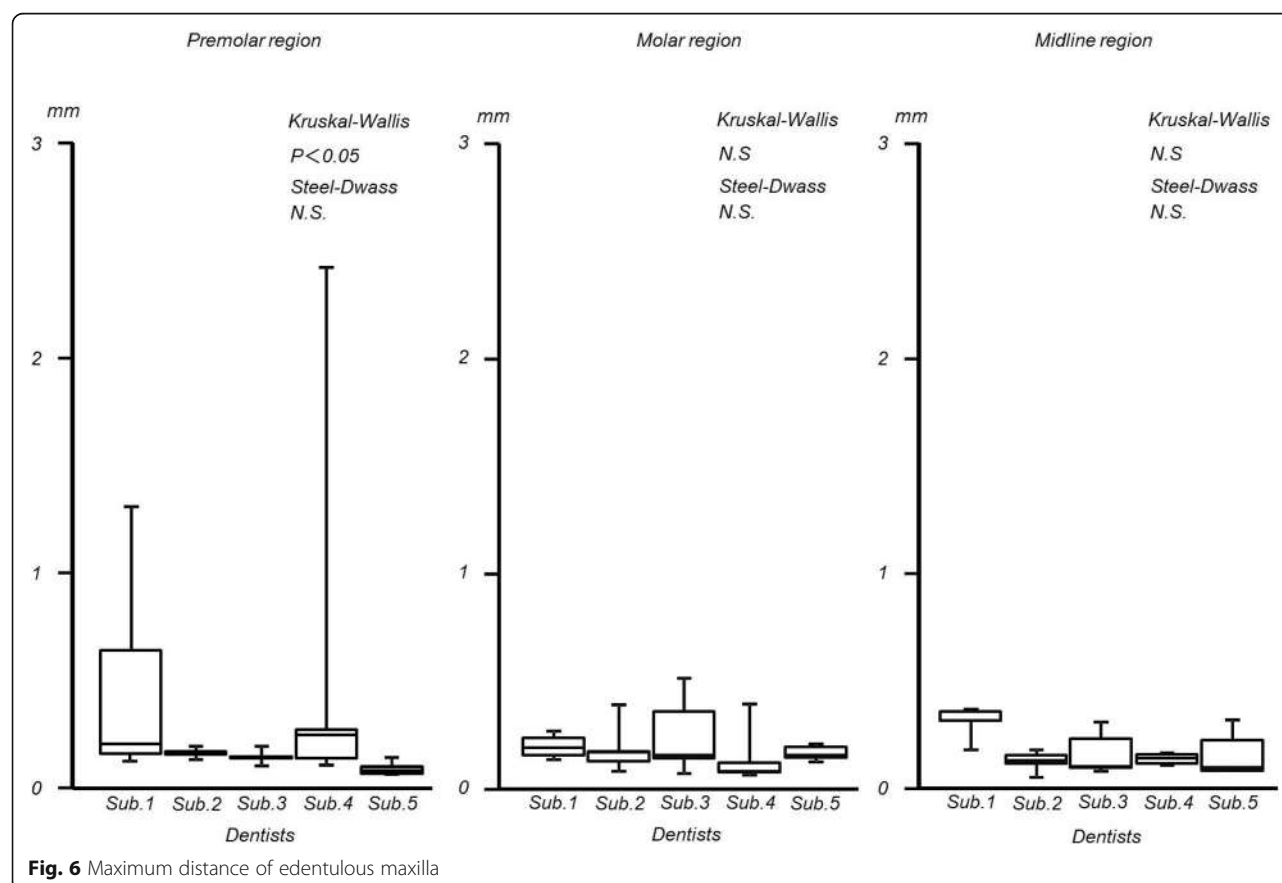


Fig. 6 Maximum distance of edentulous maxilla

left first premolar to the center of the retromolar pad (left side) (Fig. 3).

The amount of error between the reference data and intraoral scanner data in each verification region was measured, and the vertical maximum distance of the difference and the value obtained by integrating the total distance were analyzed using a two-dimensional cross section tool of the CAD software mentioned above (Figs. 4 and 5).

Statistical analysis

The vertical maximum distance of the difference and the integral value in each verification region were analyzed using the Kruskal-Wallis test, while evaluation of inter-operator validity to confirm trueness was performed with the Steel-Dwass test for multiple comparisons. Statistical analyses were performed using SPSS version 22 (IBM, New York, NY) with significance set at $p < 0.05$.

Results

In the edentulous maxillary model, the maximum distances of the difference were as follows: premolar region; 0.30 ± 0.24 (mean \pm standard deviation) mm, molar region; 0.18 ± 0.04 mm, and midline region; 0.18 ± 0.07 mm. (Interquartile range: premolar region; 0.01 to 0.481

mm, molar region; 0.04 to 0.08 mm, midline region; 0.04 to 0.14 mm). The integral values were as follows: premolar region; 4.17 ± 2.30 mm², molar region; 6.82 ± 2.48 mm², and midline region; 4.70 ± 2.30 mm² (interquartile range: premolar region; 0.1 to 3.4 mm², molar region; 1.4 to 13 mm², midline region; 0.4 to 3.8 mm²). Significant inter-operator differences were observed in the premolar and midline regions with regard to the integral values and in the premolar region with regard to the maximum distances of the difference (Figs. 6 and 7).

In the partially edentulous mandibular model, the maximum distances of the difference in the free end saddles on mandibular model were as follows: right side; 0.05 ± 0.01 mm and left side; 0.08 ± 0.05 mm (interquartile range: right side; 0.00 to 0.10 mm, left side; 0.01 to 0.35 mm). The integral values were as follows: right side; 0.78 ± 0.21 mm² and left side; 1.60 ± 0.71 mm² (interquartile range: right side; 0.2 to 0.9 mm², left side; 0.3 to 2.7 mm²). No significant inter-operator differences were observed for the maximum distances of the difference or the integral values in either region (Figs. 8 and 9).

Discussion

Many studies have verified the trueness and precision of intraoral scanners that use methods such as a confocal

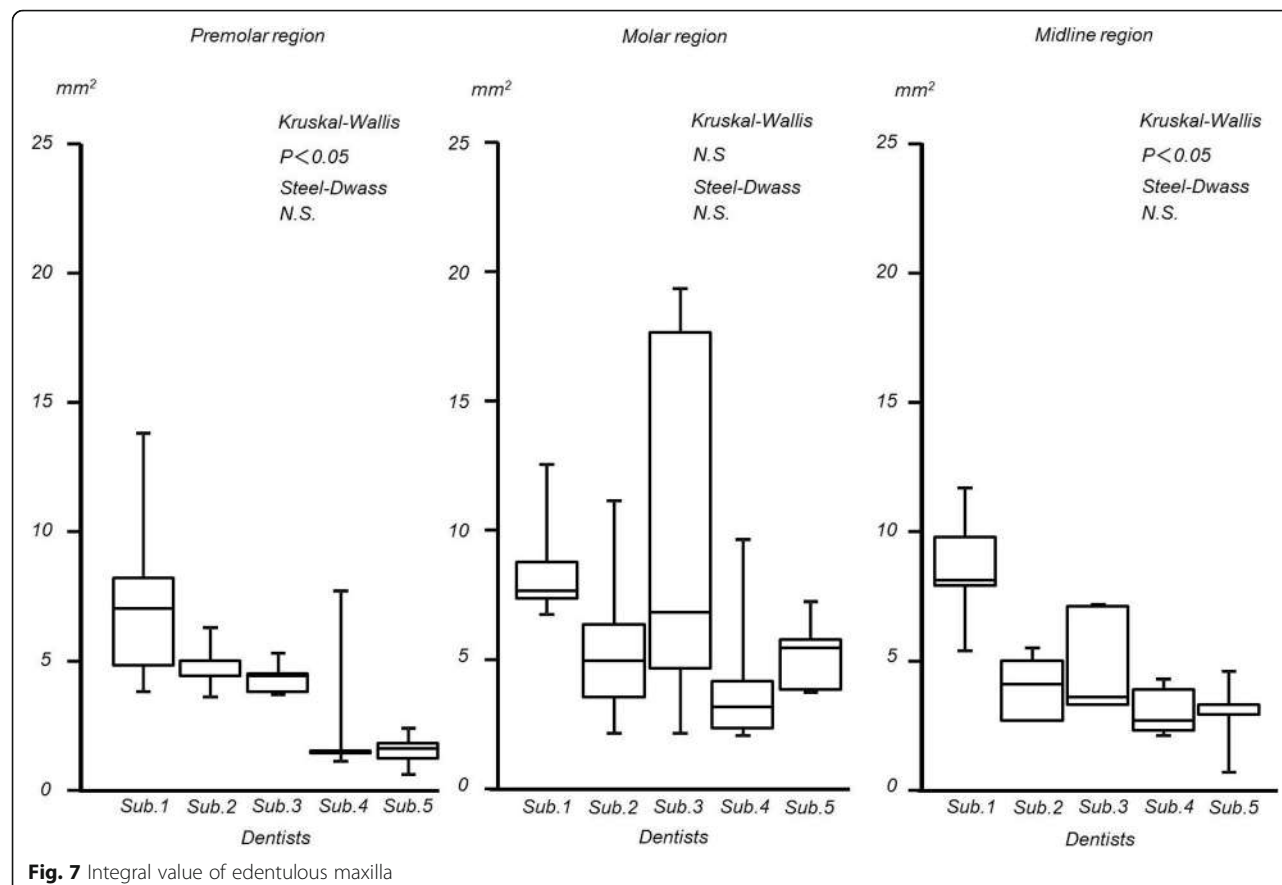
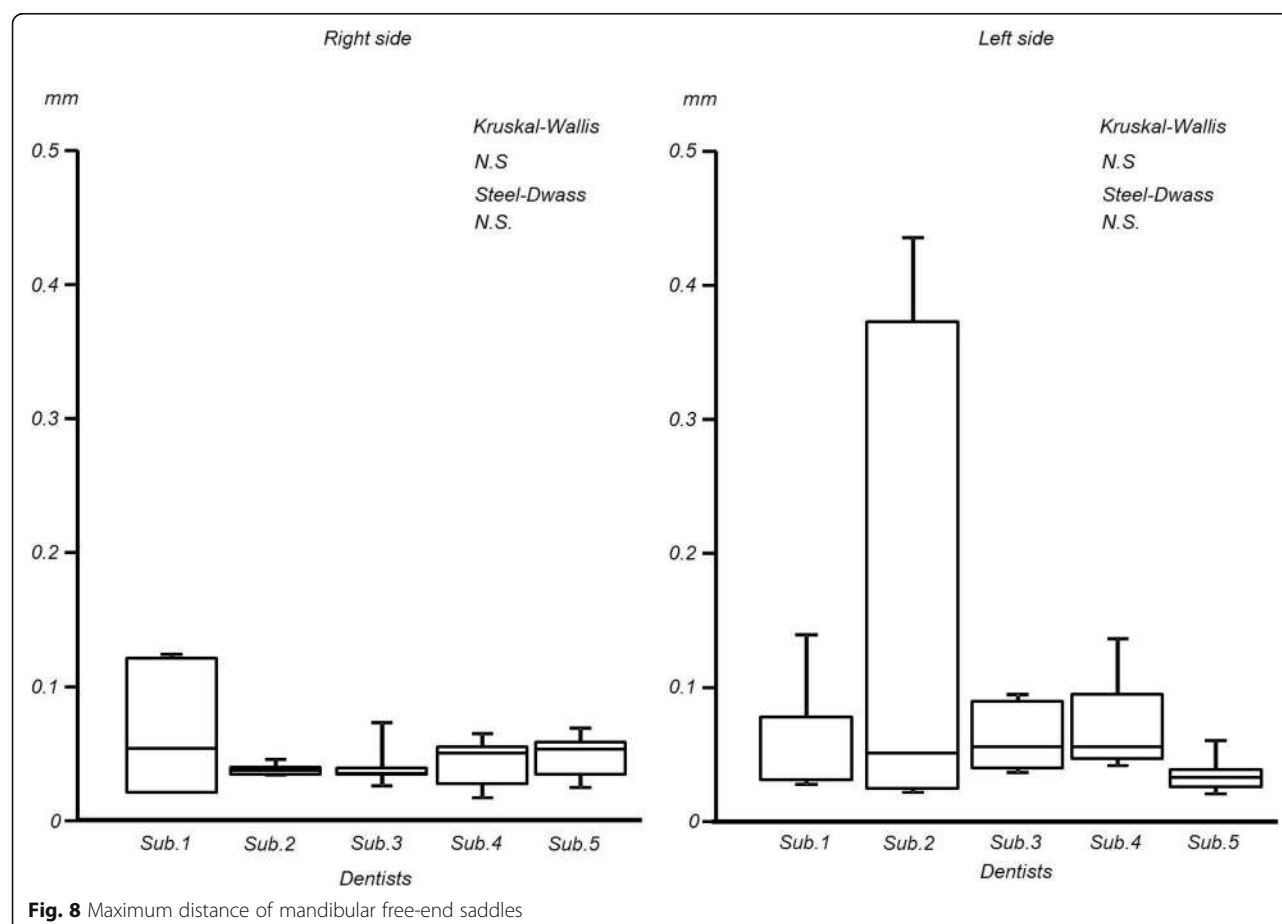


Fig. 7 Integral value of edentulous maxilla

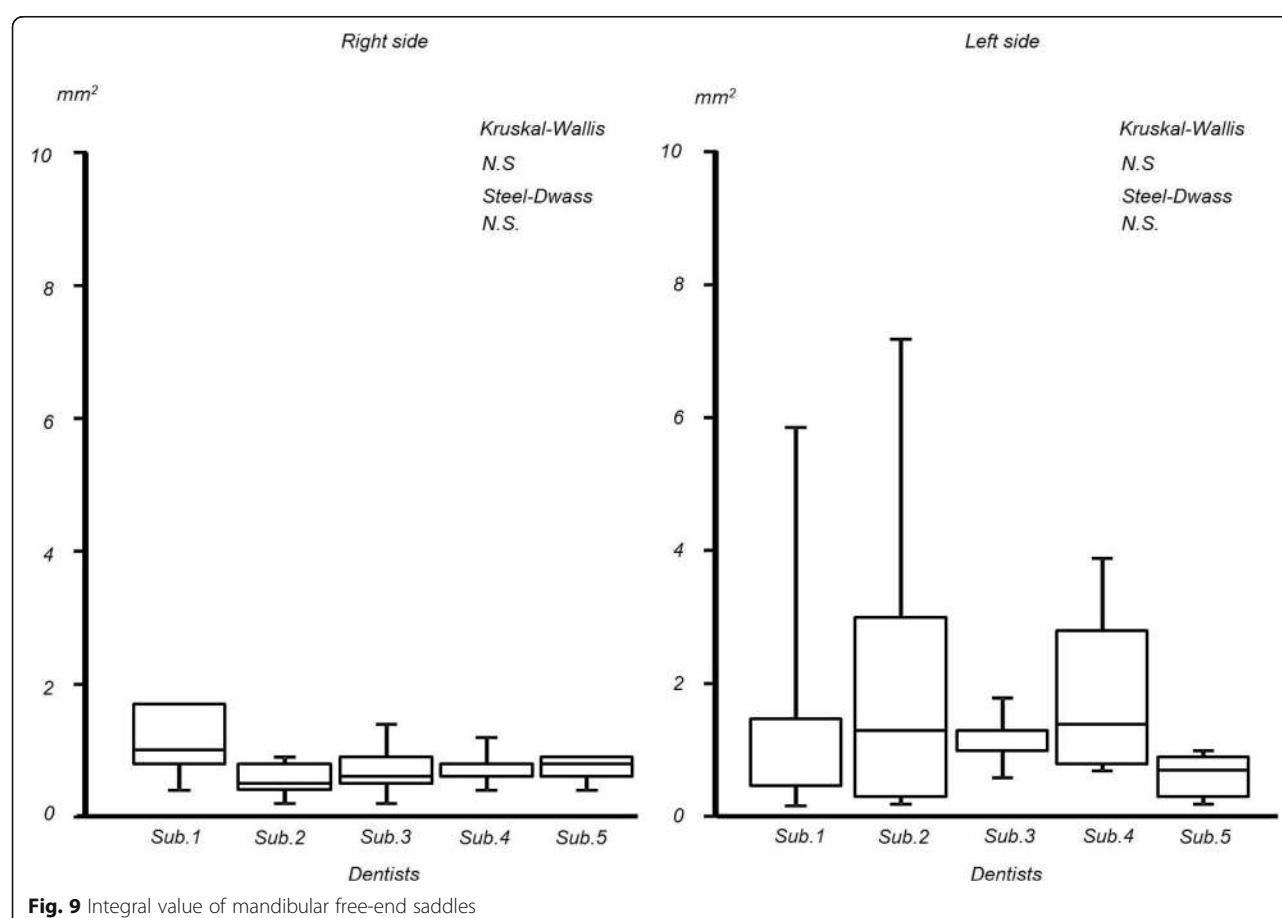


method with a light-emitting diode light source or active wavefront sampling. The intraoral scanner used in the present study applies the former system and comparatively good trueness and precision has been consistently demonstrated in previous studies [20–24].

In the present study, the maxillary and mandibular simulation models were based on an edentulous jaw and partial edentulous arch, respectively. Reference data were acquired from a dental laboratory scanner, which has greater accuracy ($\pm 7 \mu\text{m}$) than an intraoral scanner. Park et al. reported that the root mean square value of the laboratory scanner ($47.5 \pm 1.6 \mu\text{m}$) is smaller than the intraoral scanner ($343.4 \pm 56.4 \mu\text{m}$) in fully dentulous individuals [25]. This high accuracy is possible because the measurement target is fixed and natural light is blocked, enabling data to be acquired from a variety of angles with a high-performance camera [23, 26].

The regions selected for verification of precision of intraoral scanning centered on the support area in the maxillary model and on the standard area for placement of artificial tooth arrangements in the mandibular model. The method of superimposition in this study was feature based. Using the double scan technique of CAD software, the data were aligned by 3 points. The choice of

points was for the operator to decide. Three points of the characteristic anatomical structures of the edentulous maxillary and the free end missing mandibular model were selected. Significant inter-operator differences in errors in the intraoral scanning were observed in the premolar region (maximum distances of the difference and integral values) and midline region (integral values) in the edentulous maxillary model. Poorly traceable structures and a flat shape are characteristic on the palatal, suggesting that it would be difficult to stitch the image [16]. Although the edentulous maxillary model used in the present study was equivalent to the American College of Prosthodontists Type A jaw [27], factors such as residual ridge morphology, palatal depth, and the presence or absence of palatal tori may have affected the results [28, 29]. Conversely, no significant inter-operator differences were observed in errors in the intraoral scanning of either the left or right side of the free end saddles on mandibular model. This suggests that the operator effect on optical impressions in the free end saddles on mandible is small. However, the interquartile range for the maximum values of the difference and the integral values tended to be larger on the left side than on the right side of the free end saddles on



mandibular model. This is likely because the range in the free end saddles on mandibular model was mesiodistally longer on the left than the right side. Compared to teeth, the residual ridge has fewer anatomical elements, which may have affected image-stitching errors [16]. Similar results were obtained in an in vitro study of repeatability of intraoral scanner for the partially edentulous [30]. Kim et al. reported that trueness and precision of intraoral scanner were improved using an artificial landmark in the long edentulous region [31]. The intraoral scanner is affected by various conditions, and Albdour et al. suggest that different light reflections on teeth and mucous membranes affect accuracy [32]. Therefore, no significant inter-operator differences were observed, and as the maximum distances (0.04 to 0.60 mm) of the difference between the intraoral scanner data and reference data were the same or lower than the amount of tissue displacement (0.70 to 1.00 mm from results of in vivo study) [33], with practice, operators can bring these errors to within a clinically acceptable range. No significant differences were observed between conventional impression and intraoral scanner, and there were no clinically significant effects on fabrication of removable denture [11, 34, 35]. This suggests that intraoral

scanning of edentulous areas could achieve satisfactory capture by the operator.

There are two major impediments to the clinical application of optical impressions of residual mucous membrane. First, as a viscoelastic body, the residual mucous membrane is susceptible to tissue displacement. The impressions acquired of the residual mucous membrane in the present study were anatomic impressions. However, relief and pressure are possible after data digitalization. Okubo et al. reported the CAD/CAM fabrication of a mandibular complete denture in which digital relief of the mental foramen was performed [36]. In the partial edentulous arch, in order to compensate for the difference in the amount of tissue displacement between the residual teeth and the residual mucous membrane, digital pressurization of the acquired residual mucous membrane data is required. However, a simple method of acquiring data regarding the amount of tissue displacement of the residual mucous membrane has yet to be established [37]. Second, it is difficult to acquire data regarding the functional morphology of mobile tissues such as the oral vestibule, lips, tongue, and cheeks with an intraoral scanner [38]. The development of methods of border molding using intraoral scanners and devices

that can acquire data in mobile regions are awaited. Due to these issues, at present, intraoral scanners are used in edentulous patients for preliminary impressions, after which individual trays are fabricated based on those data and functional impressions are made using conventional methods [39]. In free end saddles, intraoral scanners can be used to make anatomic impressions of residual teeth and residual mucous membrane, from which data a metal framework is fabricated and functional impressions are made using the altered cast technique [40].

A limitation of this study was that the model we selected had a completely different behavior than human soft tissues. Moreover, only one type of scanner was used and the operators captured only five data sets. Imburgia et al. reported that the type of scanner affected the scanning accuracy of the missing tooth pattern [41]. For verification of trueness of intraoral scanning on specific region and limited tooth missing patterns, further study is required to investigate the use of other scanners, methods and conditions.

Conclusions

The present study demonstrated satisfactory trueness of intraoral scanning of residual ridge in edentulous regions during in vitro evaluation of inter-operator validity. The difference between the intraoral scanner data and reference data were the same or lower than the amount of tissue displacement. However, it was revealed that the lack of traceable structures and smooth surfaces, such as the palatal region, and/or long free end saddles, affected the trueness. If care is taken regarding these issues, the present study shows that optical impressions can be applied to the residual ridge of edentulous regions.

Abbreviations

3D: Three-dimensional; CAD/CAM: Computer-aided design / computer-aided manufacturing

Acknowledgements

Not applicable.

Authors' contributions

All authors made substantial contributions to the present study. AT, SY and YY contributed to conception and design, acquisition of data, analysis and interpretation of data; they were, moreover, involved in writing and editing the manuscript. YU, TM, TK, TT and SH acquired all data, and SM analyzed and interpreted all data; together, they were the major contributors in preparing and writing the manuscript. MY performed the statistical evaluation. SA and KS revised the manuscript before submission. All authors read and approved the final manuscript.

Funding

The present in vitro study was not funded or supported by any grants.

Availability of data and materials

Data are available from the corresponding author after approval by all authors.

Ethics approval and consent to participate

No Ethics Committee approval or consent to participate was requested, as the present was an in vitro study.

Consent for publication

Not applicable.

Competing interests

The authors declare that they have no competing interests.

Author details

¹Department of Removable Partial Prosthodontics, Tokyo Dental College, 2-9-18 Kandamisakicho Chiyoda-ku, Tokyo 101-0061, Japan. ²Oral Health Science Center, Tokyo Dental College, Tokyo, Japan. ³Department of Prosthodontics, Matsumoto Dental University, Shiojiri, Japan. ⁴Department of Oral and Maxillofacial Implantology, Tokyo Dental College, Tokyo, Japan. ⁵Department of Anatomy, Tokyo Dental College, Tokyo, Japan. ⁶Department of Removable Prosthodontics and Gerodontology, Tokyo Dental College, Tokyo, Japan.

Received: 16 May 2019 Accepted: 20 September 2019

Published online: 02 December 2019

References

1. Brawek PK, Wolfart S, Endres L, Kirsten A, Reich S. The clinical accuracy of single crowns exclusively fabricated by digital workflow—the comparison of two systems. *Clin Oral Investig*. 2013;17:2119–25.
2. Seelbach P, Brueckel C, Wöstmann B. Accuracy of digital and conventional impression techniques and workflow. *Clin Oral Investig*. 2013;17:1759–64.
3. Ahlholm P, Sipilä K, Vallittu P, Jakonen M, Kotiranta U. Digital versus conventional impressions in fixed prosthodontics: a review. *J Prosthodont*. 2018;27:35–41.
4. Steinmassl PA, Klauzner F, Steinmassl O, Dumfahrt H, Grunert I. Evaluation of currently available CAD/CAM denture systems. *Int J Prosthodont*. 2017;30:116–22.
5. Kattadiyil MT, Mursic Z, AlRumaih H, Goodacre CJ. Intraoral scanning of hard and soft tissues for partial removable dental prosthesis fabrication. *J Prosthet Dent*. 2014;112:444–8.
6. Mansour M, Sanchez E, Machado C. The use of digital impressions to fabricate tooth-supported partial removable dental prostheses: a clinical report. *J Prosthodont*. 2016;25:495–7.
7. Wu J, Li Y, Zhang Y. Use of intraoral scanning and 3-dimensional printing in the fabrication of a removable partial denture for a patient with limited mouth opening. *J Am Dent Assoc*. 2017;148:338–41.
8. Hu F, Pei Z, Wen Y. Using intraoral scanning Technology for Three-Dimensional Printing of Kennedy class I removable partial denture metal framework: a clinical report. *J Prosthodont*. 2019;28:e473–6.
9. Lee JW, Park JM, Park EJ, Heo SJ, Koak JY, Kim SK. Accuracy of a digital removable partial denture fabricated by casting a rapid prototyped pattern: a clinical study. *J Prosthet Dent*. 2017;118:468–74.
10. Alageel O, Abdallah MN, Alsheghri A, Song J, Caron E, Tamimi F. Removable partial denture alloys processed by laser-sintering technique. *J Biomed Mater Res B Appl Biomater*. 2018;106:1174–85.
11. Lo Russo L, Caradonna G, Troiano G, Salami A, Guida L, Ciavarella D. Three-dimensional differences between intraoral scans and conventional impressions of edentulous jaws: a clinical study. *J Prosthet Dent*. 2019. <https://doi.org/10.1016/j.prosdent.2019.04.004>.
12. Ender A, Mehl A. Accuracy of complete-arch dental impressions: a new method of measuring trueness and precision. *J Prosthet Dent*. 2013;109:121–8.
13. Patzelt SB, Emmanouilidi A, Stampf S, Strub JR, Att W. Accuracy of full-arch scans using intraoral scanners. *Clin Oral Investig*. 2014;18:1687–94.
14. Ender A, Zimmermann M, Attin T, Mehl A. In vivo precision of conventional and digital methods for obtaining quadrant dental impressions. *Clin Oral Investig*. 2016;20:1495–504.
15. Atieh MA, Ritter AV, Ko CC, Duquim I. Accuracy evaluation of intraoral optical impressions: a clinical study using a reference appliance. *J Prosthet Dent*. 2017;118:400–5.
16. Patzelt SB, Vonau S, Stampf S, Att W. Assessing the feasibility and accuracy of digitizing edentulous jaws. *J Am Dent Assoc*. 2013;144:914–20.
17. Lee JH. Improved digital impression of edentulous areas. *J Prosthet Dent*. 2017;117:448–9.
18. Goodacre BJ, Goodacre CJ, Baba NZ. Using intraoral scanning to capture complete denture impressions, tooth positions, and centric relation records. *Int J Prosthodont*. 2018;31:377–81.

19. Goodacre BJ, Goodacre CJ. Using intraoral scanning to fabricate complete dentures: first experiences. *Int J Prosthodont*. 2018;31:166–70.
20. Mangano FG, Veronesi G, Hauschild U, Mijiritsky E, Mangano C. Trueness and precision of four intraoral scanners in Oral Implantology: a comparative in vitro study. *PLoS One*. 2016;11. <https://doi.org/10.1371/journal.pone.0163107>.
21. Vandeweghe S, Vervack V, Dierens M, De Bruyn H. Accuracy of digital impressions of multiple dental implants: an in vitro study. *Clin Oral Implants Res*. 2017;28:648–53.
22. Lim JH, Park JM, Kim M, Heo SJ, Myung JY. Comparison of digital intraoral scanner reproducibility and image trueness considering repetitive experience. *J Prosthet Dent*. 2018;119:225–32.
23. Fukazawa S, Odaira C, Kondo H. Investigation of accuracy and reproducibility of abutment position by intraoral scanners. *J Prosthodont Res*. 2017;61:450–9.
24. Nedelcu R, Olsson P, Nyström I, Rydén J, Thor A. Accuracy and precision of 3 intraoral scanners and accuracy of conventional impressions: a novel in vivo analysis method. *J Dent*. 2018;69:110–8.
25. Park GH, Son K, Lee KB. Feasibility of using an intraoral scanner for a complete-arch digital scan. *J Prosthet Dent*. 2019;121:803–10.
26. Mandelli F, Gherlone E, Gastaldi G, Ferrari M. Evaluation of the accuracy of extraoral laboratory scanners with a single-tooth abutment model: a 3D analysis. *J Prosthodont Res*. 2017;61:363–70.
27. McGarry TJ, Nimmo A, Skiba JF, Ahlstrom RH, Smith CR, Koumjian JH. Classification system for complete edentulism. *Am College Prosthodont J Prosthodont*. 1999;8:27–39.
28. Gan N, Xiong Y, Jiao T. Accuracy of intraoral digital impressions for whole upper jaws, including Full Dentitions and Palatal Soft Tissues. *PLoS One*. 2016;11. <https://doi.org/10.1371/journal.pone.0158800>.
29. Deferm JT, Schreurs R, Baan F, Bruggink R, Merckx MAW, Xi T, Bergé SJ, Maal TJJ. Validation of 3D documentation of palatal soft tissue shape, color, and irregularity with intraoral scanning. *Clin Oral Investig*. 2018;22:1303–9.
30. Lee JH, Yun JH, Han JS, Yeo IL, Yoon H. Repeatability of Intraoral Scanners for Complete Arch Scan of Partially Edentulous Dentitions: An In Vitro Study. *J Clin Med*. 2019;8. <https://doi.org/10.3390/jcm8081187>.
31. Kim JE, Amelya A, Shin Y, Shim JS. Accuracy of intraoral digital impressions using an artificial landmark. *J Prosthet Dent*. 2017;117:755–61.
32. Albdour EA, Shaheen E, Vranckx M, Mangano FG, Politis C, Jacobs R. A novel in vivo method to evaluate trueness of digital impressions. *BMC Oral Health*. 2018;18:117.
33. Miyashita T. Displaceability under localized pressure in the mucous membrane and settling of the denture base caused by biting pressure. *Shikwa Gakuho*. 1970;70:38–68.
34. Chebib N, Kalberer N, Srinivasan M, Maniewicz S, Perneger T, Müller F. Edentulous jaw impression techniques: An in vivo comparison of trueness. *J Prosthet Dent*. 2019;121:623–30.
35. Jung S, Park C, Yang HS, Lim HP, Yun KD, Ying Z, Park SW. Comparison of different impression techniques for edentulous jaws using three-dimensional analysis. *J Adv Prosthodont*. 2019;11:179–86.
36. Ohkubo C, Park EJ, Kim TH, Kurtz KS. Digital relief of the mental foramen for a CAD/CAM-fabricated mandibular denture. *J Prosthodont*. 2018;27:189–92.
37. Yamashita S, Ai M, Geng Q, Sato M, Shinoda H, Ando S. Application of a newly developed 3-D deformation measurement system to prosthetic dentistry. *J Oral Rehabil*. 1996;23:849–55.
38. Fang JH, An X, Jeong SM, Choi BH. Development of complete dentures based on digital intraoral impressions-case report. *J Prosthodont Res*. 2018; 62:116–20.
39. Bonnet G, Batisse C, Bessadet M, Nicolas E, Veyrune JL. A new digital denture procedure: a first practitioners appraisal. *BMC Oral Health*. 2017;17: 155.
40. Applegate OC. The cast saddle partial denture. *J Am Dent Assoc*. 1937;27: 1280–91.
41. Imburgia M, Logozzo S, Hauschild U, Veronesi G, Mangano C, Mangano FG. Accuracy of four intraoral scanners in oral implantology: a comparative in vitro study. *BMC Oral Health*. 2017;17:92.

Publisher's Note

Springer Nature remains neutral with regard to jurisdictional claims in published maps and institutional affiliations.

Ready to submit your research? Choose BMC and benefit from:

- fast, convenient online submission
- thorough peer review by experienced researchers in your field
- rapid publication on acceptance
- support for research data, including large and complex data types
- gold Open Access which fosters wider collaboration and increased citations
- maximum visibility for your research: over 100M website views per year

At BMC, research is always in progress.

Learn more biomedcentral.com/submissions



RESEARCH ARTICLE

Open Access



A pilot trial on lithium disilicate partial crowns using a novel prosthodontic functional index for teeth (FIT)

Edoardo Ferrari Cagidiaco^{1,2,3,4*}, Simone Grandini^{2,3}, Cecilia Goracci¹ and Tim Joda⁵

Abstract

Background: Lithium disilicate is now a well accepted material for indirect restorations. The aim of this trial was to evaluate two lithium disilicate systems using a novel prosthodontic Functional Index for Teeth (FIT).

Methods: Partial adhesive crowns on natural abutment posterior teeth were made on sixty patients. Patients were divided into two groups: Group 1 IPS e.max press (Ivoclar-Vivadent, Schaan, Liechtenstein), and Group 2 Initial LiSi press (GC Co., Tokyo, Japan). The restorations were followed-up for 3 years, and the FIT evaluation was performed at last recall. The FIT is composed of seven variables (Interproximal, Occlusion, Design, Mucosa, Bone, Biology and Margins), each of them are evaluated using a 0–1–2 scoring scheme, and is investigated by an oral radiograph and occlusal and buccal pictures. More in details, three variables have the three scores made on the presence or not of major, minor or no discrepancy (for 'Interproximal', 'Occlusion' and 'Design'), presence or not of keratinized and attached gingiva ('Mucosa'), presence of bone loss > 1.5 mm, < 1.5 mm or not detectable ('Bone'), presence or not of Bleeding on Probing and or Plaque Index ('Biology'), presence of detectable gap and marginal stain or not ('Margins'). The Mann-Whitney 'U' test was used and the level of significance was set at $p < 0.05$. Also, "success" of the crowns (restoration in place without any biological or technical complication) and "survival" (restoration still in place with biological or technical complication) were evaluated.

Results: Regarding FIT scores, all partial crowns showed a stable level of the alveolar crest without detectable signs of bone loss in the radiographic analysis. All other evaluated parameters showed a high score, between 1.73 and 2. No statistically significant difference emerged between the two groups in any of the assessed variables ($p > 0.05$). All FIT scores were compatible with the outcome of clinical success and no one restoration was replaced or repaired and the success rate was 100%.

Conclusions: The results showed that it is possible to evaluate the clinical performance of partial crowns using FIT. The FIT proved to be an effective tool to monitor the performance of the restorations and their compatibility with periodontal tissues at the recall. The FIT can be really helpful for a standardized evaluation of the quality of the therapy in prosthodontic dentistry. The two lithium disilicate materials showed similar results after 3 years of clinical service.

Trial registration: The study protocol was approved by the Ethical Committee of University of Siena ([clinicaltrial.gov](https://clinicaltrials.gov/ct2/show/study/NCT01835821) # NCT 01835821), 'retrospectively registered'.

Keywords: Partial crowns, Lithium disilicate, Randomized controlled trial

* Correspondence: edoardo.ferrari.cagidiaco@gmail.com

¹Department of Prosthodontics and Dental Materials, University of Siena, Siena, Italy

²Department of Periodontics, Universidad Complutense de Madrid, Madrid, Spain

Full list of author information is available at the end of the article



© The Author(s). 2019 **Open Access** This article is distributed under the terms of the Creative Commons Attribution 4.0 International License (<http://creativecommons.org/licenses/by/4.0/>), which permits unrestricted use, distribution, and reproduction in any medium, provided you give appropriate credit to the original author(s) and the source, provide a link to the Creative Commons license, and indicate if changes were made. The Creative Commons Public Domain Dedication waiver (<http://creativecommons.org/publicdomain/zero/1.0/>) applies to the data made available in this article, unless otherwise stated.

Background

Due to the specific properties of lithium disilicate, particularly flexural strength, this restorative material is mainly indicated for single full and/or partial crowns [1–3]. Lithium disilicate provides high aesthetic results and, in comparison with porcelain and reinforced resin composites, its higher flexural strength makes it be preferable whenever the tooth defect exceeds a certain dimension [4, 5].

Lithium disilicate can be obtained using two different production processes: press technology and CAD/CAM technology. CAD/CAM technology is mainly used as chairside procedure, while the pressable technology is performed in the laboratory mainly using an analogic workflow. Pressed lithium disilicate results were very promising [6, 7] and recently the evaluation of a new lithium disilicate material (Initial LiSi press, GC) has been reported [8]. Only few clinical trials are available on lithium disilicate partial crowns, the majority of them being retrospective studies [9–11] and only one being a randomized controlled trial (RCT) [8].

Evaluation of clinical results of partial crowns on posterior teeth is usually performed following standardized parameters, such as Ryge and Snyder clinical parameters [12] or the modified FDI criteria [13]. The evaluation is usually performed after luting at baseline, and then at recalls after 1, 6, 12, 24, or 36 months. The modified FDI criteria evaluate several categories with some sub-categories [13]. Also, RCTs are done by blinded, calibrated and experienced dentists that can perform the follow-up evaluation [14, 15].

It must be pointed out that Ryge and Snyder clinical parameters and modified FDI criteria were initially defined for direct restorations, therefore there is the need to determine clinical criteria adequate to evaluate indirect restorations. Clinical criteria should reflect the patients' perception of the restorations, fulfilling teaching purposes and being easily applicable in daily practice. In order to ease the process of drafting a proper treatment plan [16, 17], some classifications and prognosis evaluations have been proposed.

Recently, a novel Functional Implant Prosthodontic Score (FIPS) was proposed [18–21]; FIPS was based on 5 clinical variables evaluated crowns placed on implants with an oral radiograph and a buccal and an occlusal picture. Its potential to serve as an objective and reliable instrument in assessing implant success and restoration and periodontal outcome as perceived by patients, as well as identifying the possible risk of failure, comparing follow-up observations, providing an effective teaching tool was demonstrated. Similarly, FIT, that is a novel index for the assessment of the prosthetic results of lithium disilicate crowns, based on seven restorative-periodontal parameters, that evaluate crowns placed on natural abutments, and want to be a reliable and

objective instrument in assessing single partial crown success and periodontal outcome as perceived by patients and dentists.

Methods

The aim of this RCT was to evaluate the clinical performance of two lithium disilicate pressed systems using a novel Functional Index for Teeth (FIT), which is made up of seven clinical variables showing, among other things, the possible correlation with the level of appreciation perceived by the patients.

Functional index for teeth (FIT)

A novel Functional Index for Teeth (FIT) was used (Table 2). Seven clinical variables have been collected and main prosthodontic and periodontal parameters were evaluated simultaneously (Interproximal Contacts and Papillae, Static and Dynamic Occlusion, Design Contour and Color, Quality and Quantity of Mucosa, Bone level in x-Ray, Biology related to Bleeding on Probing (BoP) and Plaque Index (PI) and Stain and Gap at Margins).

The FIT evaluation was performed only at last recall (3-year follow-up) by an experienced operator (Fig. 1 a-f).

The null hypothesis tested in this clinical study was that there was no statistically significant difference in the clinical performance of the two lithium disilicate systems. A sample of 60 patients in need of a single partial crown on posterior teeth (upper and lower premolars and molars), accessing the Department of Prosthodontics and Dental Materials of the University of Siena, Italy, in the time period between September 2015 and January 2016 were included in the study. Selected patients, periodontally healthy or successfully treated in need for one posterior restoration, had a mean age of 37 (± 7.5) years (between 18 and 70) (14F, 16M). Exclusion criteria were: age < 18 years, pregnancy, disabilities, prosthodontic restoration of the tooth, spontaneous sensitivity, pulpitis, non-vital or endodontically treated teeth, (chronic) periodontitis, deep defects (close to pulp, < 1 mm distance) or pulp capping, heavy occlusal contacts or history of bruxism, systemic disease or severe medical complications, allergic history concerning methacrylates, rampant caries, xerostomia, lack of compliance, language barriers, plaque index higher than 20.

Patients written consent to the trial was obtained after having provided a complete explanation of the aim of the study. The study protocol was approved by the Ethical Committee of University of Siena ([clinicaltrials.gov](https://clinicaltrials.gov/ct2/show/study/NCT01835821) # NCT 01835821). All procedures performed in this study involving human participants were in accordance with the ethical standards of the Institutional and National Research Committee and with the 1964 Helsinki



Fig. 1 **a, b** and **1c**. are related to a clinical case of Group 1 (the second premolar received a IPS e.max press restoration) while Fig. **1 d, e** and **f** of Group 2 (the first molar received a GC Initial™ LiSi Press restoration). No technical or biological complications were observed at 3-year recall

declaration and its later amendments or comparable ethical standards. This study adheres to CONSORT guidelines.

Randomization selection of the patients and masking of examiners

After recruitment, oral hygiene instructions were given to the patients and prophylaxis was performed to establish optimal plaque control and gingival health.

The clinical assessment of periodontal parameters such as probing pocket depths (PPD) [22], bleeding on probing (BoP) [23], and full-mouth plaque index (PI) [22] was performed.

All restorative procedures were carried out under local anesthesia (Articaine with 1:100,000 epinephrine) by the same experienced operator. Intraoral radiographs were also taken before starting the treatment. In order to standardize the radiographic examination, X-ray individual tray was made for each sample tooth of each patient, to be sure to have the radiogram in the same position at each recall.

Each participating patient was randomly assigned to one of the two experimental groups ($n = 30$), that were defined based on the material to be used for the restorative treatment:

Group 1: IPS e.max press (Ivoclar-Vivadent, Schaan, Lichtenstein).

Group 2: Initial LiSi press (GC Co., Tokyo, Japan).

Main characteristics of the two Lithium Disilicate materials were reported in Table 1.

Treatment assignment was noted in the registration and treatment assignment form that was kept by the study. Allocation concealment was performed by using opaque sealed, sequentially numbered envelopes. The statistician made the allocation sequence by means of a computer-generated random list and instructed a different subject to assign a sealed envelope containing the type of lithium disilicate material to be used. The opaque envelope has been opened before material selection and communicated to the operator. At the 3-year recall blinding of the examiner has been applied.

Clinical procedure

For standardization purposes, all clinical procedures were performed by the same trained operator. Following anesthesia, rubber dam was placed, all carious lesions were excavated, and any restorative material was removed. Preparation was performed using conventional diamond burs in a high-speed hand piece, with no bevel on margins. The preparation design was dictated by the extent of decay, pre-existing restorations and the preparation guidelines defined by the manufacturer of the restorative materials. The Residual Dentin Thickness (RDT) was evaluated on a periapical radiograph, and teeth with RDT thinner than 0.5 mm were excluded.

Table 1 Mechanical properties of IPS e.max press and GC Initial™ LiSi press materials.

Properties (as provided by manufacturers)	Units	IPS e.max Press	Initial LiSi Press
Manufacturer	–	Ivoclar Vivadent	GC
Components	–	lithium disilicate crystals (approx. 70%), Li ₂ Si ₂ O ₅ , embedded in a glassy matrix	lithium disilicate micro-crystals equally dispersed in a glass matrix
Crystal system	–	lithium disilicate - crystals measure 3 to 6 µm in length.	lithium disilicate - crystals measure 1.5 µm × 0.5 µm
Flexural Strength	MPa	433*	454*
Biaxial Flexural Strength	MPa	> 500	> 500
Vickers hardness		(HV10) 5900 ± 100 Mpa	600 HV
Chemical solubility	mg/cm ²	40 ± 10	5.4 µg/cm ²
Liner thermal expansion CTE	× 10 ⁻⁶ /K	Coefficient of thermal expansion (100–400 °C) 10.15 ± 0.4 10 ⁻⁶ K ⁻¹ Coefficient of thermal expansion (100–500 °C) 10.55 ± 0.35 10 ⁻⁶ K ⁻¹	Liner thermal expansion CTE (25–500 °C) 9.8 × 10 ⁻⁶ K ⁻¹
Glass transition temperature	°C	560	520
Density	g/cm ³	2.5 ± 0.1	2.4

*Internal data, University of Siena.

Cavities' preparation provided at least 0.5–1 mm space at the margin and 1.0–1.5 mm of clearance occlusally. Margins were mainly into enamel and only interproximal boxes had cervical margin below the cementum-enamel junction for no more than 1 mm. At least one cusp was covered. Teeth were kept vital.

Hybridization of dentin with adhesive material was done using Adhese Bond Ivoclar-Vivadent, Schaan, Liechtenstein, in Group 1 and G-Premio Bond, GC Co., Tokyo, Japan in Group 2, and then a thin layer of flowable has been applied on top (Tetric Flow, Ivoclar-Vivadent in Group 1 and Genial Flow, GC Co, in Group 2). After the final preparation, an impression of the prepared tooth was taken with an elastomeric material (Exa'lence, GC Co.), and poured in stone (FujiRock, GC Co.). The restoration was then waxed and pressed in lithium disilicate, strictly following the manufacturer's instructions. A temporary restoration of the prepared tooth was provided and after one week the lithium disilicate restoration was luted following manufacturer's instructions. The intaglio surface of the restoration was etched with 10% hydrofluoric acid for 1 min, silanized with Monobond Plus (Ivoclar-Vivadent, Schaan, Liechtenstein) in Group 1 and G-Multi Primer (GC Co.) in Group 2, and then luted using MultiLink Sprint (Ivoclar-Vivadent) in Group 1 and LinkForce (GC Co.) in Group 2. During cementation proper tooth isolation was provided by rubber dam.

Follow-up

All patients were enrolled in a dental hygiene program in which recalls were planned every 6 months. A clinical exam and standardized intraoral radiographs were performed immediately after the seating of the crowns

(baseline), as well as after 1, 2, and 3 years of clinical service (follow-up).

Outcome variables

"Success" was set when the restoration was in place at last recall without any biological or technical complication, whilst "Survival" when the restoration was still in place at last recall but with biological or technical complications that needed to be treated and/or the crown to be remade. "Failure" was set when the restoration was not in place anymore at last recall or, because of mechanical or biological complications, needed to be replaced.

Statistical analysis

The Mann-Whitney 'U' test was applied to verify the statistical significance of the difference between the two groups in the scores recorded for each assessed variable. The level of significance was set at $p < 0.05$. The statistical analysis was handled by the PASW Statistics 18 software (IBM, Armonk, NY, USA).

Results

The recall rate of patients was 100% and for that no loss to follow up was recorded. Survival and success rates were 100%. No technical or biological complications were observed during follow-up.

Clinical examinations of periodontal parameters showed mean scores for PI of 18.0 (SD 2.5; range: 16–21) at baseline and 17.5 (SD 1.0) (range: 16–20) at 1-year follow-up, PPD of 3.4 (SD 0.5 mm; range: 1–4) and 3.2 (SD 0.5 mm; range: 1–4), and a mean score for BoP of 18.4 (SD 2.2; range: 17–24) and 16.6 (SD 1.4; range: 16–22), respectively. At last recall, scores of periodontal parameters showed a proper maintenance of periodontal health

thanks to professional recall program and home maintenance of patients.

At the 3-year follow up, the mean total FIT score was 13.26 and 13.66 for Group 1 and 2 (range: 10–14) respectively (Table 2). All partial crowns showed a stable level of alveolar crest without signs of bone loss at the radiographic analysis. Therefore, the variable radiographic “bone level” demonstrated the most consistent result and the highest scores, with a mean value of 2 (range: 2–2) in both groups. Similarly, the mean scores recorded for the variables “static and dynamic occlusion” and “quality and quantity of mucosa” were 2 (range: 2–2) in Group 1 and 1.9 in Group 2 (range: 1–2). In contrast, mean scores for “design contour and color” were 1.86 (SD 0.7) in Group 1 (range: 1–2), and 2 (range: 2–2) in Group 2; “mucosa” 2 (range: 2–2) in Group 1 and 1.93 (SD 0.2; range 1–2) in Group 2; “interproximal contacts and papillae” 1.73 (SD 0.7; range: 1–2) in Group 1 and 2 (range: 2–2) in Group 2; “biology” scored 1.93 (SD 0.3; range 1–2) in both Groups; and “stain and gap at margins” was 1.73 (SD 0.8; range 0–2) in Group 1 and 1.86 (SD 0.7; range 1–2) in Group 2 were the most challenging to satisfy (Table 3).

No statistically significant difference emerged between the two groups in any of the assessed variables ($p > 0.05$).

Discussion

Some clinical parameters such as Ryge and Snyder criteria [12] or the modified FDI criteria [13–15, 24] are commonly used as evaluation method of clinical trials. The Ryge and Snyder parameters evaluate post-operative sensitivity, retention, marginal gap, marginal discoloration,

fracture, interproximal contacts and secondary caries, scoring each parameter in alpha, beta, charlie and delta and are the most used clinical criteria to evaluate direct restorations. The modified FDI criteria evaluate several categories such as aesthetic, functional and biological properties with four sub-categories each. Each sub-category is then divided into 5 quality scores from clinically excellent/very good to clinically poor, for a total of 16 criteria that might not be all used in the same case [13]. A calibration by e-calib system of the FDI criteria is available and its main goals were to efficiently train and calibrate clinical dental research workers using e-learning tools, to reduce the variability of the outcome of dental restorations in clinical studies using standardized assessment criteria, to better compare the results of clinical trials on dental restorations among different clinics in the world, to render clinical calibration programs more efficient, to improve daily clinical practice and to be used as a teaching tool in dental schools [15].

The FIT evaluation was proposed for the first time in the present study and is based on 7 clinical parameters: interproximal, occlusion, design, mucosa, bone, biology, margins. Although its targets resemble the ones of the modified FDI criteria, that is limited to the tooth and the restoration without evaluating the periodontal tissues, FIT can also evaluate the periodontal tissues behavior by ‘Interproximal’, ‘Mucosa’, ‘Bone’ and ‘Biology’ parameters and is a more user-friendly and straightforward method for the clinician to be applied in everyday practice.

The fact that RCTs are carried out by blinded, calibrated, and experienced dentists that perform the follow-up evaluations in specialized centers [24] might

Table 2 Functional Index for Teeth Prosthodontic (FIT)

Scoring Scheme	0	1	2
Interproximal	major discrepancy	minor discrepancy	no discrepancy
Contacts & Papillae	(2x incomplete)	(1x complete)	(2x complete)
Occlusion	major discrepancy	minor discrepancy	no discrepancy
Static & Dynamic	(supra-contact)	(infra-occlusion)	
Design	major discrepancy	minor discrepancy	no discrepancy
Contour & Color	(contour)	(color)	
Mucosa	non-keratinized	non-keratinized	keratinized
Quality & Quantity	non-attached	attached	attached
Bone	radiographic bone loss	radiographic bone loss	radiographic bone loss
X-Ray	> 1.5 mm	< 1.5 mm	not detectable
Biology	BoP and PI present	BoP present	no clinical impairment
BoP & PI			
Margins	detectable gap and visible stain	detectable gap or visible stain	no clinical impairment
Gap & Stain			
Max Score			14

Table 3 Radiographic and clinical scores based on FIT for each group

Variables	Group 1 IPS e.max (n = 30) (total) (median)	Group 2 GC Initial™ LiSi (n = 30) (total) (median)	Total Score Each Outcome
Interproximal Contacts & Papillae	26 (1.73)	30 (2)	(56)
Occlusion Static & Dynamic	30 (2)	29 (1.93)	(59)
Design Contour & Color	28 (1.86)	30 (2)	(58)
Mucosa Quality & Quantity	30 (2)	29 (1.93)	(59)
Bone X-Ray	30 (2)	30 (2)	(60)
Biology BoP -& PI	29 (1.93)	29 (1.93)	(58)
Margins Gap & Stain	26 (1.73)	28 (1.86)	(54)
Total Score Each Group	199 (13.26)	205 (13.66)	

be considered as a limit. In fact, it is still under discussion in the dental scientific community whether thus conducted RCTs accurately represent the reality of daily practice. One of the main goals of FIT is to make practitioners more familiar with the core idea of RCTs by getting them into the habit of scoring their restorations, following the evolution of clinical parameters at each recall.

The two novel proposed classifications (FIT for single crowns on natural abutments and FIPS for single crowns on fixtures) evaluate individual teeth with special regard to their periodontal conditions in order to formulate an appropriate treatment plan [16, 17]. FIT, on the other hand, was conceived for single restorations and, consequently, it can be applied to any indirect restorations.

It must be considered that the operator's experience can be a key factor when a Randomized Controlled Trial (RCT) is done and FIT is applied; However, in order to explain the high success rate found in this pilot RCT, the oral hygiene maintenance (professional and at home) of the selected patients in combination with the experience and skill of the operator must be considered.

The FIT scores recorded in this RCT were high for all parameters and no statistically significant differences were found between the two tested lithium disilicate materials. Such findings lead to acceptance of the formulated null hypothesis. The lack of differences between the two pressed lithium disilicate materials showed that the new system, which has been recently launched into the market (Initial LiSi Press), can clinically perform as well as e.max pressed system (IPS e.max press), that has instead been marketed for many years.

It must be pointed out that about IPS e.max press several clinical studies are available in the literature [25–29]. There is consensus that IPS e.max press (also with

the previous name of Empress 2) has good enough longevity when used to restore single tooth after 5 years (survival of 90%) [25, 26] and 71% after 10 years of clinical service [27, 28]. Particularly relevant is the recently published report by Malament [29] in which was found out that pressed lithium disilicate restorations (Empress 2) survived successfully over the 10.4 period studied with an overall failure rate below 0.2% per year and primarily confined to molar teeth. It can be speculated that also in this study [29] skill and knowledge of the operator and oral hygiene regime can contribute to the impressive success rate.

Regarding Initial LiSi press, only one prospective clinical study is already available and showed 100% survival after 3 years [8]. Long term RCT results are needed in order to evaluate longevity under clinical function of Initial LiSi press.

The limited number of restorations for each group and the relatively short time of observation might be considered as a shortcoming of this study, possibly affecting the power of the statistical tests. Also, it must be pointed out that, accordingly with exclusion criteria, a category of patients without any health issue were really selected. This might be considered a partial limitation of this study.

Usually RCTs are being conducted on larger samples, and they might compare Ryge and Snyder clinical parameters with the modified FDI and FIT scores. Another possible limitation of the present RCT is the reduced number of tested materials; a similar RCT comparing several restorative materials (e.g reinforced resins in different formulations) in a wider number of patients is ongoing.

Conclusions

The findings of this study showed that FIT score can be a reliable tool to rate the clinical outcome of posterior

partial crowns over time. FIT score can also be useful to monitor any possible early failure and to standardize follow-up recalls. Furthermore, the two lithium disilicate materials tested in this RCT showed comparable clinical performances, with high success rate after 3-year of service.

Abbreviations

BoP: bleeding on probing; FDI: Federation Dental International; FIPS: Functional Implant Prosthodontic Score; FIT: Functional Index for Teeth; PI: full-mouth plaque index; PPD: probing pocket depths; RCT: Randomized Controlled Trial; RTD: Residual Dentin Thickness

Acknowledgements

'Not applicable'.

Authors' contributions

All authors, EFC, TJ, SG and CG have: 1. made substantial contributions to conception and design, acquisition of data, analysis and interpretation of data; 2. been involved in drafting the manuscript and revising it critically for important intellectual content; 3. given final approval of the version to be published; 4. agreed to be accountable for all aspects of the work in ensuring that questions related to the accuracy or integrity of any part of the work are appropriately investigated and resolved. All authors read and approved the final manuscript.

Funding

No funding was received.

Availability of data and materials

The datasets used and/or analysed during the current study are available from the corresponding author on reasonable request after approval of all other authors.

Ethics approval and consent to participate

Patients written consent to the trial was obtained after having provided a complete explanation of the aim of the study. The study protocol was approved by the Ethical Committee of University of Siena ([clinicaltrials.gov](https://clinicaltrials.gov/ct2/show/study/NCT01835821) # NCT 01835821). All procedures performed in this study involving human participants were in accordance with the ethical standards of the Institutional and National Research Committee and with the 1964 Helsinki declaration and its later amendments or comparable ethical standards.

Consent for publication

'Not Applicable'.

Competing interests

The authors declare that they have no competing interests.

Author details

¹Department of Prosthodontics and Dental Materials, University of Siena, Siena, Italy. ²Department of Periodontics, Universidad Complutense de Madrid, Madrid, Spain. ³Department of Endodontics and Restorative Dentistry, University of Siena, Siena, Italy. ⁴Department of Medical Biotechnologies, Policlinico Le Scotte, Viale Bracci 1, 53100 Siena, Italy. ⁵Department of Reconstructive Dentistry, University Center for Dental Medicine, Basel, Switzerland.

Received: 29 August 2019 Accepted: 13 November 2019

Published online: 09 December 2019

References

- Monaco C, Caldari M, Scotti R. AIOF clinical research group: Clinical evaluation of 1,132 zirconia-based single crowns: a retrospective cohort study from the AIOF clinical research group. *Int J Prosthodont.* 2013;26:435–42.
- Vichi A, Sedda M, Del Siena F, Louca C, Ferrari M. Flexural resistance of Cerec CAD/CAM system ceramic blocks. Part 1: Chairside materials. *Am J Dent.* 2013;26:255–9.
- Sedda M, Vichi A, Del Siena F, Louca C, Ferrari M. Flexural resistance of Cerec CAD/CAM system ceramic blocks. Part 2: Outsourcing materials. *Am J Dent.* 2014;2:17–22.
- Manhart J, Chen H, Hamm G. Review of the clinical survival of direct and indirect restorations in posterior teeth of the permanent dentition. *Oper Dent.* 2004;29:481–508.
- Culp L, McLaren EA. Lithium disilicate: the restorative material of multiple options. *Compend Contin Educ Dent.* 2010;31:716–25.
- Ritter RG. Multifunctional uses of a novel ceramic-lithium disilicate. *J Esthet Rest Dent.* 2010;22:332–41.
- Yu J, Gao J, Guo J, Li L, Zhao Y, Zhang S. Clinical outcomes of different types of tooth-supported bilayer lithium disilicate all-ceramic restorations after functioning up to 5 years: a retrospective study. *J Dent.* 2016;51:56–61.
- Ferrari M, Cagidiaco E, Goracci C, Sorrentino R, Zarone F, Grandini S, Joda T. Posterior partial crowns with or without posts: a 3-year follow up. *J Dent.* 2019;83:12–7.
- Cortellini D, Canale A. Characteristics of Lithium Disilicate Crowns Bonded on Abutments with Knife-Edge and Large Chamfer Finish Lines after Cyclic Loading. *J Prosthodont.* 2015;24:615–9.
- Schmitz JH, Beani M. Effect of different cement types on monolithic lithium disilicate complete crowns with feather-edge preparation design in the posterior region. *J Prosthet Dent.* 2016;115:678–83.
- Schmitz JH, Cortellini D, Granata S, Valenti M. Monolithic lithium disilicate complete single crowns with feather-edge preparation design in the posterior region: A multicentric retrospective study up to 12 years. *Quintessence Int.* 2017;20:601–8.
- Ryge G, Snyder M. Evaluating the clinical quality of restorations. *J Am Dental Assoc.* 1973;87:369–77.
- Hickel R, Peschke A, Tyas M, Mjor IA, Baybe S, Peters M, Hiller KA, Randall R, Vanherle G, Heintze SD. FDI world dental federation: clinical criteria for the evaluation of direct and indirect restorations-update and clinical examples. *Clin Oral Investig.* 2010;14:349–66.
- Hickel R, Roulet JF, Bayne S, Heintze SD, Mjor IA, Peters M, Roussen V, Randall R, Schmalz G, Tyas M, Vanherle G. Recommendations for conducting controlled clinical studies of dental restorative materials. Science committee project 2/98–FDI world dental federation study design (part I) and criteria for evaluation (part II) of direct and indirect restorations including onlays and partial crowns. *J Adhes Dent.* 2007;9(Suppl):1,121–47.
- Hickel R, Peschke A, Tyas M, Mjor IA, Baybe S, Peters M, Hiller KA, Randall R, Vanherle G, Heintze SD. FDI world dental federation - clinical criteria for the evaluation of direct and indirect restorations. Update and clinical examples. *J Adhes Dent.* 2010;12:259–72.
- Kwok V, Caton J. Prognosis revisited: a system for assigning periodontal prognosis. *J Periodontol.* 2007;78:2063–71.
- Samet N, Jotkowitz A. Classification and prognosis evaluation of individual teeth-a comprehensive approach. *Quintessence Int.* 2009;40:377–87.
- Joda T, Ferrari M, Bragger U. A prospective clinical cohort study analyzing single-unit implant crowns after 3 years of loading: introduction of a novel functional implant Prosthodontic score (FIPS). *Clin Oral Implants Res.* 2017;28:1291–5.
- Joda J, Zarone F, Zitzmann NU, Ferrari M. The functional implant Prosthodontic score (FIPS): assessment of reproducibility and observer variability. *Clin Oral Investig.* 2018;22:2319–24.
- Joda T, Ferrari M, Bragger U. Monolithic implant-supported lithium disilicate (LS2) crowns in a complete digital workflow: a prospective clinical trial with a 2-year follow-up. *Clin Impl Dent Relat Res.* 2017;19:505–11.
- Joda T, Bragger U, Zitzmann NU. CAD/CAM implant crowns in a digital workflow: five-year follow-up of a prospective clinical trial. *Clin Implant Dent Relat Res.* 2019;21:169–74.
- Löe L, Silness J. Periodontal disease in pregnancy. I prevalence and severity. *Acta Odontol Scand.* 1963;21:533–51.
- Ainamo J, Bay I. Problems and proposals for recording gingivitis and plaque. *Int Dent J.* 1975;25:229–35.
- Hickel R, Roulet JF, Bayne S, Heintze SD, Mjor IA, Peters M, Roussen V, Randall R, Schmalz G, Tyas M, Vanherle G. Recommendations for conducting controlled clinical studies of dental restorative materials. *Clin Oral Investig.* 2007;11:5–33.
- Solá-Ruiz MF, Lagos-Flores E, Román-Rodríguez JL, Highsmith Jdel R, Fons-Font A, Granell-Ruiz M. Survival rates of a lithium disilicate-based core ceramic for three-unit esthetic fixed partial dentures: a 10-year prospective study. *Int J Prosthodont.* 2013;26:175–80.

26. Layton DM, Clarke M. A systematic review and meta-analysis of the survival of non-feldspathic porcelain veneers over 5 and 10 years. *Int J Prosthodont*. 2013;26:111–24.
27. Teichmann M, Göckler F, Weber V, Yildirim M, Wolfart S, Edelhoff D. Ten-year survival and complication rates of lithium-disilicate (empress 2) tooth-supported crowns, implant-supported crowns, and fixed dental prostheses. *J Dent*. 2017 Jan;56:65–77.
28. Teichmann M, Göckler F, Rückbeil M, Weber V, Edelhoff D, Wolfart S. Periodontal outcome and additional clinical quality criteria of lithium-disilicate restorations (empress 2) after 14 years. *Clin Oral Investig*. 2019;23:2153–64.
29. Malament KA, Natto ZS, Thompson V, Rekow D, Eckert S, Weber HP. Ten-year survival of pressed, acid-etched e.max lithium disilicate monolithic and bilayered complete-coverage restorations: performance and outcomes as a function of tooth position and age. *J Prosthet Dent*. 2019;121:782–90.

Publisher's Note

Springer Nature remains neutral with regard to jurisdictional claims in published maps and institutional affiliations.

Ready to submit your research? Choose BMC and benefit from:

- fast, convenient online submission
- thorough peer review by experienced researchers in your field
- rapid publication on acceptance
- support for research data, including large and complex data types
- gold Open Access which fosters wider collaboration and increased citations
- maximum visibility for your research: over 100M website views per year

At BMC, research is always in progress.

Learn more biomedcentral.com/submissions



RESEARCH ARTICLE

Open Access



Trueness of CAD/CAM digitization with a desktop scanner – an in vitro study

G. Joós-Kovács^{1*} , B. Vecsei¹, Sz. Körmendi¹, V. A. Gyarmathy^{2,3}, J. Borbély¹ and P. Hermann¹

Abstract

Background: Desktop scanners are devices for digitization of conventional impressions or gypsum casts by indirect Computer-Aided Design/Computer-Assisted Manufacturing (CAD/CAM) in dentistry. The purpose of this in vitro study was: 1, to investigate whether virtual models produced by the extraoral scanner have the same trueness as sectioned casts; and 2, to assess if digitization with an extraoral scanner influences the surface information.

Methods: A polymethyl-methacrylic acid (PMMA) cast and a reference scanner (TwoCam 3D, SCAN technology A/S, Ringsted, Denmark; field of view 200 mm, resolution 0.1 mm ± 0.025 mm) were used to create the reference data in standard tessellation format (STL). According to the extraoral CAD/CAM digitization steps, impressions, mastercasts, and sectioned casts were made, and STL files were generated with the reference scanner. The pivotal point of the study was to digitalize these sectioned casts with the extraoral scanner (Straumann CARES Scan CS2 Visual 8.0 software, InstitutStraumann AG, Basel, Switzerland) and STL files were exported. Virtual caliper measurements were performed. Absolute deviations were compared using multilevel mixed-effects linear regression. Relative distortions were calculated with mean absolute errors and reference values.

Results: Differences were observed in measurements of tooth sizes. All four prepared teeth were affected. No relationship was observed in relative deviations. Absolute differences between all the indirect digitization steps considering arch distances were: impressions, − 0.004 mm; mastercasts, 0.136 mm; sectioned casts, − 0.028 mm; and extraoral scanner, − 0.089 mm. Prepared dies on the virtual casts (extraoral scanner) were closer to each other than those on the sectioned gypsum casts. Relative deviation calculations revealed no relationship with the position of the dies in the arch.

Conclusion: The trueness of the virtual models generated by the extraoral scanner system used in this study was different from the dimensions of the sectioned casts. The digitization of gypsum casts changes both the dimensions of dies and the distances between the dies. The virtual casts had smaller distances than any distances measured at previous steps. Either bigger dies or longer distances did not result in greater distortions. We cannot, however, generalize our results to all scanners available on the market, because they might give different results.

Keywords: Digital dentistry, Desktop scanner, Indirect CAD/CAM digitization, Extraoral scanner, Gypsum cast digitization, Accuracy, Trueness, Precision

Background

Digital technology is nowadays essential in many aspects of life including industry, social life, entertainment, and health care as well. For example, digital dental technology (DDT) offers quicker, better solutions to patients: X-ray [1], CBCT [1], and digital tooth shade determination devices [2] help to improve diagnosis and treatment plan.

Extra- and intraoral scanners are also widely used to make fixed dental restorations, which promise not only better accuracy to the final rehabilitation but also better time efficiency and comfort [3–5]. DDT has also been introduced in education, and students also seem to prefer the optical impression taking method compared to the conventional one [5, 6].

Computer-Aided Design/Computer-Assisted Manufacturing (CAD/CAM) systems promise the opportunity to improve accuracy by reducing potential sources of error

* Correspondence: joos-kovacs.gellert_levente@dent.semmelweis-univ.hu

¹Department of Prosthodontics, Semmelweis University, Szentkirályi u. 47, Budapest 1088, Hungary

Full list of author information is available at the end of the article



© The Author(s). 2019 **Open Access** This article is distributed under the terms of the Creative Commons Attribution 4.0 International License (<http://creativecommons.org/licenses/by/4.0/>), which permits unrestricted use, distribution, and reproduction in any medium, provided you give appropriate credit to the original author(s) and the source, provide a link to the Creative Commons license, and indicate if changes were made. The Creative Commons Public Domain Dedication waiver (<http://creativecommons.org/publicdomain/zero/1.0/>) applies to the data made available in this article, unless otherwise stated.

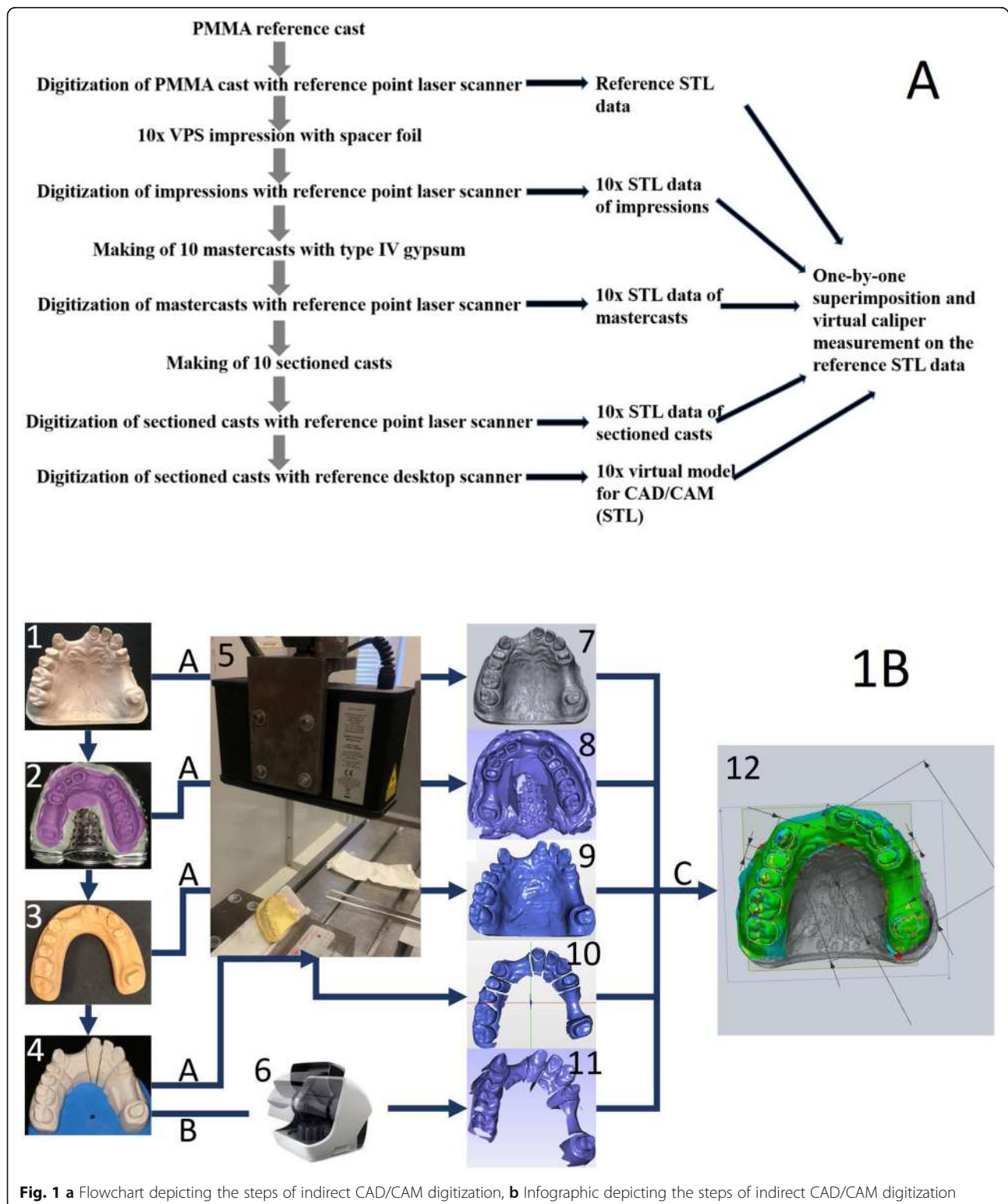


Fig. 1 **a** Flowchart depicting the steps of indirect CAD/CAM digitization, **b** Infographic depicting the steps of indirect CAD/CAM digitization

(such as, for example, the lost-wax process) [7–10]. As the first step, a scanner (either extraoral or intraoral) is utilized to transfer the information of the oral cavity into the computer. Extraorally, indirect CAD/CAM

digitization is usually performed by scanning gypsum casts, although sometimes conventional impressions may also be scanned [7, 11]. The intraoral scanning technique performs a direct scanning in the oral cavity [8,

12]. Some studies assess the patients' perception and treatment comfort, clinical outcomes, and time efficiency [5, 13], while others compare the clinical accuracy of conventional impressions with that of direct digitizers [9, 14, 15] or the accuracy of direct versus indirect digitizers [16–18].

To ensure accurate fixed dental restorations, either conventionally or digitally made, inaccuracies during the entire process should be minimized [19–22]. The distortion factors of indirect digitization are well explored according to the conventional impression techniques, impression materials, pouring techniques, gypsum materials and sectioning systems [10, 12, 23–33]. However, the last step of indirect digitization, which is performed with an extraoral laboratory scanner, still leaves lots of questions unanswered. Several studies have assessed extraoral scanners [34–37], but still little is known about their accuracy in actual clinical settings.

The accuracy measurement based on the ISO (International Organization for Standardization) standard 5725 [14, 16–18] has two components: precision and trueness. In a previous study, our research group compared the accuracy of three intraoral scanners to a desktop scanner [18]. One of the results was that the desktop scanner was less accurate compared to the intraoral scanners. This raised a question: which step or steps of the indirect CAD/CAM digitization changed the original surface information? The aim of this study, therefore, was to evaluate the trueness of virtual models produced by the extraoral scanner. Our hypothesis was that there is no significant difference between the sectioned casts and the virtual casts made by the extraoral scanner.

Methods

Study design

Figures 1a and b depict the study design. A polymethylmethacrylic acid (PMMA) cast and a reference scanner (TwoCam 3D, SCAN technology A/S, Ringsted, Denmark; field of view 200 mm, resolution $0.1\text{ mm} \pm 0.025\text{ mm}$) were used to create the reference data in standard tessellation format (STL). According to the extraoral CAD/CAM digitization steps, impressions, mastercasts, and sectioned casts were made, and STL files were generated with the reference scanner. The pivotal point of the study was to digitalize these sectioned casts with the extraoral scanner (Straumann CARES Scan CS2 Visual 8.0 software, Institut Straumann AG, Basel, Switzerland) and STL files were exported. Accordingly, in order to evaluate the information changes from the reference data through the steps of indirect digitization up to the CAD/CAM scan made by the extraoral scanner, we strictly adhered to the steps of indirect CAD/CAM digitization and compared the data of



Fig. 2 PMMA reference cast. After digitization with the reference scanner, 10 VPS impressions were taken.

impressions, mastercasts, sectioned casts, and desktop scanner digitization to the reference data.

Reference model

A PMMA cast was made from an upper arch, holding the original information of hand-prepared teeth #14, #21, #24, #27 with shoulder preparation for all-ceramic restorations. Two edentulous areas are represented on the arch, #13–21 and #24–27 (Fig. 2).

Reference scanner and reference virtual model

For the high-precision data acquisition, a point-laser scanner (635 nm wavelength, 1 mW power, Class IEC 2) was utilized (TwoCam 3D, SCAN technology A/S, Ringsted, Denmark). This scanner uses a double triangulation technique with the following parameters: field of



Fig. 3 Reference data from the PMMA cast made by the high-precision point-laser scanner

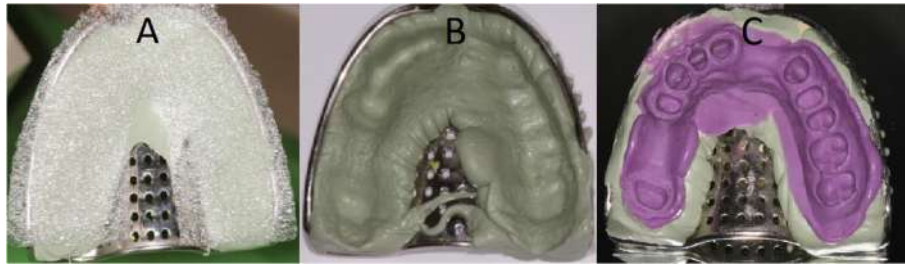


Fig. 4 VPS impression with stock metal tray: **a** Putty material with spacer foil; **b** Base impression with putty material; **c** Putty+wash material. Impressions were scanned with the reference scanner at least 1 but not more than 24 h after removing from PMMA cast

view 200 mm, resolution $0.1 \text{ mm} \pm 0.025 \text{ mm}$. The reference model was scanned by the point-laser scanner, and an STL reference virtual model was generated (Fig. 3).

Impression

Ten VPS (vinyl-polysiloxane impression material, Express XT Penta Putty, Express XT Light Body, 3 M ESPE, St. Paul, MN, USA) impressions were taken with spacer foil technique (Impression Separation Wafer, GC Corporation, Tokyo, Japan), with prefabricated perforated metal tray (Medesy 6000, MEDESY Srl, Maniago, Italy) and machine mixed (Pentamix 3 Automatic Mixing Unit, 3 M ESPE, St. Paul, MN, USA) [10, 23, 24, 31–33] (Fig. 4).

In accordance with prevailing in vitro temperature conditions, the recommended setting time (5 min and 30 s) was doubled to ensure the correct setting of the material [32, 33]. After setting, the impression was removed from the cast and washed for 5 min. Disinfection with Zeta 7 spray (Zhermack, Zhermack Spa, Badia Polesine, Italy) followed. At least 1 h but not more than 24 h after disinfection, each impression was scanned once with the reference scanner – thus, a total

of 10 impression scans were performed. The produced STL files were saved.

Mastercasts and sectioned casts

Not more than 24 h after taking the impressions, the 10 impressions were casted in the dental laboratory with type IV gypsum (GC Fujirock EP, GC Corp., Tokyo, Japan) [25, 28, 30]. The mixing of the gypsum was performed with distilled water (100 g/25 ml) first by hand, then with a vacuum mixer (20 s, BEGO Motova SL, BEGO USA Inc., Lincoln, RI, USA). A mechanical vibrator (WASSERMANN Rüttler KV-26, Wassermann Dental-Maschinen GmbH, Hamburg, Germany) was used (6000 rpm, 0.4 mm) to produce the casts. The setting time of the gypsum was always 1 h. After setting, the mastercasts were removed and finalized (Figs. 5 and 6). All 10 mastercasts were digitized with the reference scanner, and the STL files were saved. Next, the mastercasts were sawed in the laboratory (Giroform, Amann Girrbach GmbH, Pforzheim, Germany), and 10 sectioned casts were scanned with reference scanner (Fig. 7).

To perform CAD/CAM scans used in CAD/CAM technology [12], the sectioned casts were scanned 24–72 h after the casting of the impressions with an extraoral scanner (Straumann CARES Scan CS2 Visual 8.0 software,



Fig. 5 Type IV rough gypsum mastercast after removal of the impression



Fig. 6 Finalized gypsum mastercasts were scanned with the reference scanner



Fig. 7 Finalized sectioned cast. Two scanings followed: first, the sectioned casts were digitized with the reference scanner. Second, they were digitized with the desktop scanner

Institut Straumann AG, Basel, Switzerland) in line with the manufacturer's instructions (Figs. 7d - 8a). This involves a first full-arch scan of the gypsum cast followed by a second scanning of the prepared dies. The software aligns the die scans onto the full arch

scan, and this alignment will lead to higher precision of the scanned data. The STL files of 10 final virtual casts were exported and saved.

Superimposition and virtual digital caliper

For the virtual comparisons, a best-fit alignment algorithm and virtual caliper tool were used in Geomagic Verify software (3D systems, 333 Three D Systems Circle, RockHill, SC, USA). Eleven virtual caliper measurements were performed on the reference virtual model as follows: a section plane was placed on the virtual casts, and on this plane, mesial-distal points and buccal-oral points of the prepared teeth and 6 points for the measurements of abutment distances were appointed (Fig. 9). Each impression, mastercast, and sectioned cast STL file made by the reference scanner and the STL files from the sectioned casts made by the extraoral scanner were imported and aligned one after the other to the virtual reference model by best-fit alignment. The Geomagic software calculated the differences between the distances measured on the reference versus the superimposed data and output the resulting data in Excel.

The following measurements were taken

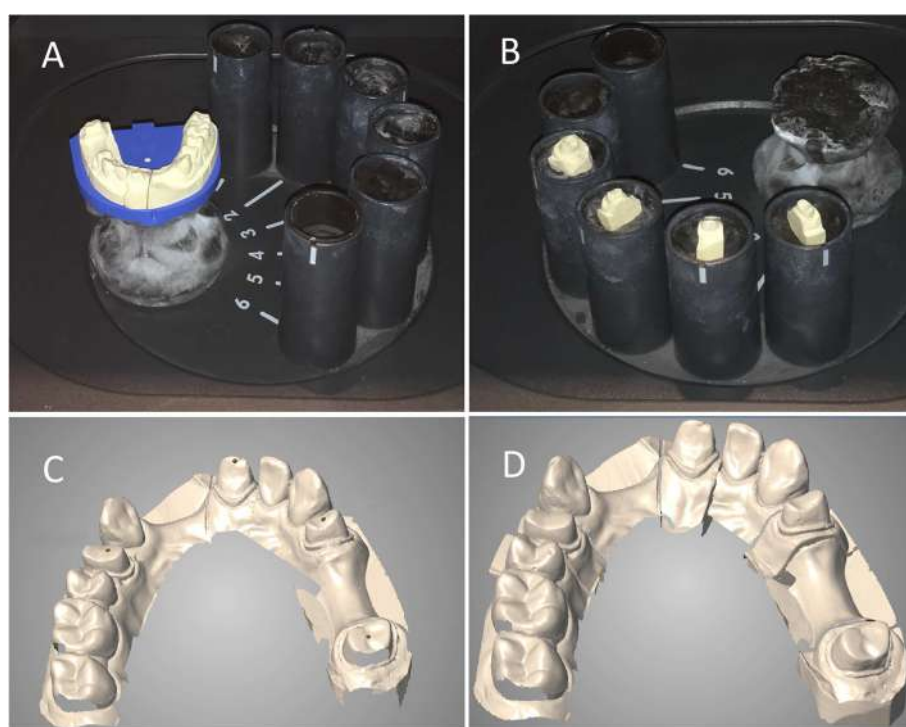


Fig. 8 Digitization of sectioned cast with desktop scanner: **a** Full arch gypsum model placed in the desktop scanner to make a whole-arch scan. **b** Removeable gypsum dies in the scanner before second scanning. **c** First scan of the full arch model with gap on the prepared 27 tooth. **d** Final virtual model with the secondary dye scans aligned

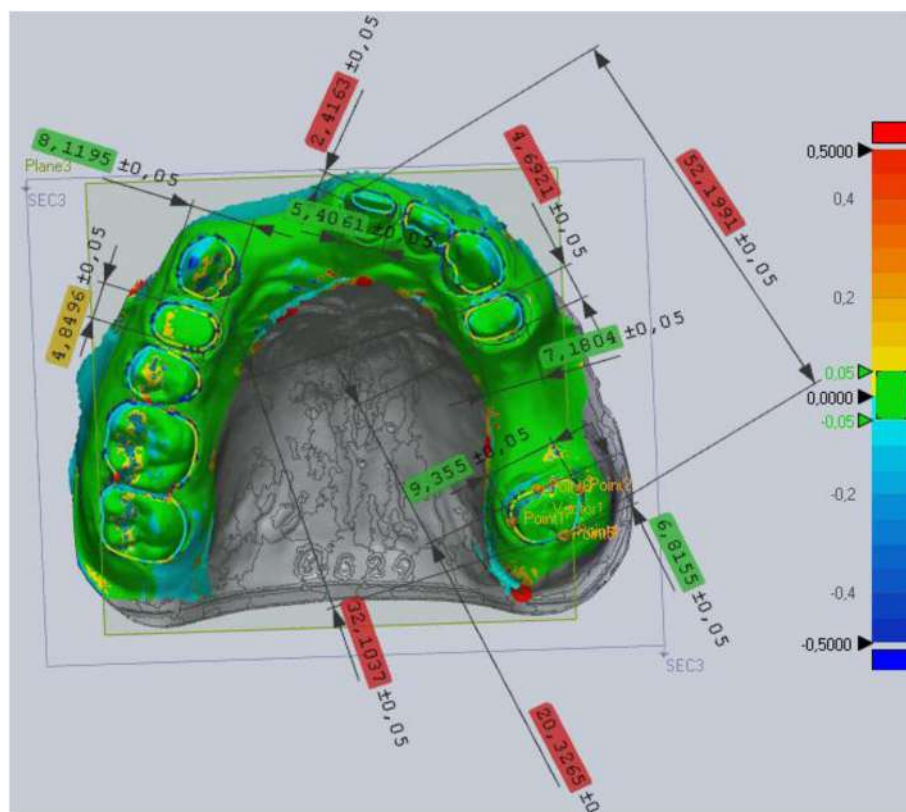


Fig. 9 Virtual digital caliper measurements on prepared teeth: between the mesio-distal and bucco-palatal points of 14, 21, 24, 27 teeth and 3 arch distances: between the closest points of 24–27, furthest points of 24–27, and furthest points of 21–27

A. Tooth sizes

1. 14 mesio-distal (14MD) and bucco-palatal (14BP) diameter,
2. 21 mesio-distal (21MD) and bucco-palatal (21BP) diameter,
3. 24 mesio-distal (24MD) and bucco-palatal (24BP) diameter,
4. 27 mesio-distal (27MD) and bucco-palatal (27BP) diameter,

B. Arch distances:

1. closest points of teeth 24–27 as “inside”,
2. furthest points of teeth 24–27 as “outside”,
3. furthest points of teeth 21–27 as “left side”.

Statistics

Observation of differences between the data points was performed in two ways. First, absolute deviations and differences were calculated (in mm). Absolute deviations were compared across CAD/CAM steps using multilevel mixed-effects linear regression and were interpreted as differences in trueness. Explanatory variables included a categorical indicator for each CAD/CAM step and a random intercept term at the observation series level. The model allowed for intragroup correlation between

observations within the same observation series. Models were fitted separately for each location. Differences between CAD/CAM steps were expressed as point estimates of the fixed effect, 95% confidence intervals (CI), and *p* values.

Second, relative distortions were calculated. To avoid misrepresentations arising from calculating the averages of positive and negative values (which can result in smaller deviations), absolute values of the observed distances were used. For each die diameter and arch distance, a mean absolute error was calculated. A relative distortion was calculated with mean absolute error and reference value registered with the reference scanner (relative distortion = mean absolute error/reference value). Median and interquartile range values were used because of skewness. Stata was used for data management and analysis (StataCorp. Stata Statistical Software: Release 15. College Station, Texas: StataCorp LLC).

Results

Differences in the measurements of tooth sizes

Significant differences were observed in the measurements of tooth diameters between the steps of indirect CAD/CAM technology performed with the Straumann

extraoral scanner at all eight locations of interest (at a minimum of one and a maximum of four per location) according to the absolute deviations (Fig. 10 and Tables 1 and 2). Overall, the highest number of differences were as follows. Between the sectioned cast and the extraoral scanner, significant differences (either higher or lower) were observed in six of the eight locations ($p < 0.01$), and the data measured on the impressions were significantly different from the data measured on the extraoral scanner at five locations ($p < 0.05$). All four prepared teeth were affected by these differences. There were differences between the steps of indirect CAD/CAM, but no relationship was observed in relative deviations (Fig. 11 and Table 3), meaning that longer diameters did not result in greater distortions.

Differences in the measurements of arch distances

Statistically significant differences were observed between all the indirect CAD/CAM digitization steps considering arch distances (Table 6). The distance between the dies became larger after the impressions (median -0.004 mm, IQR = 0.198) were poured with gypsum and the mastercasts (0.136 mm, IQR = 0.157) were made. By sectioning the mastercast, the distances became smaller and the values of the sectioned casts (-0.028 mm, IQR = 0.279) were similar to those of the impressions. Virtual casts (-0.089 mm, IQR = 0.322) made by the extraoral

scanner showed smaller distances compared to any of the previous steps' values (Fig. 12 and Table 4).

24–27 inside

Distance measurement on the closest points of 24–27 showed the following: VPS impressions had the trueness of 0.006 mm (IQR = 0.071), while mastercasts had 0.149 (IQR = 0.034) and sectioned casts had -0.023 mm (IQR = 0.073). Virtual casts made by the extraoral scanner had the trueness of -0.086 mm (IQR = 0.043).

24–27 outside

Distance measurements on the furthest points of 24–27 showed 0.038 mm (IQR = 0.051) at the VPS impressions. Mastercasts had a trueness of 0.177 mm (IQR = 0.093) and sectioned casts had 0.037 mm (IQR = 0.075). The extraoral scanner-made virtual casts had the only negative value at this distance: -0.006 mm (IQR = 0.103).

21–27 left side

Distance measurement on the furthest points of 21–27 showed the greatest distortions: the VPS impressions had the value of -0.240 mm (IQR = 0.306). The mastercasts were the closest to the reference value: -0.050 mm (IQR = 0.13). The sectioned casts were the closest to the impression value at -0.276 mm (IQR = 0.121). Virtual

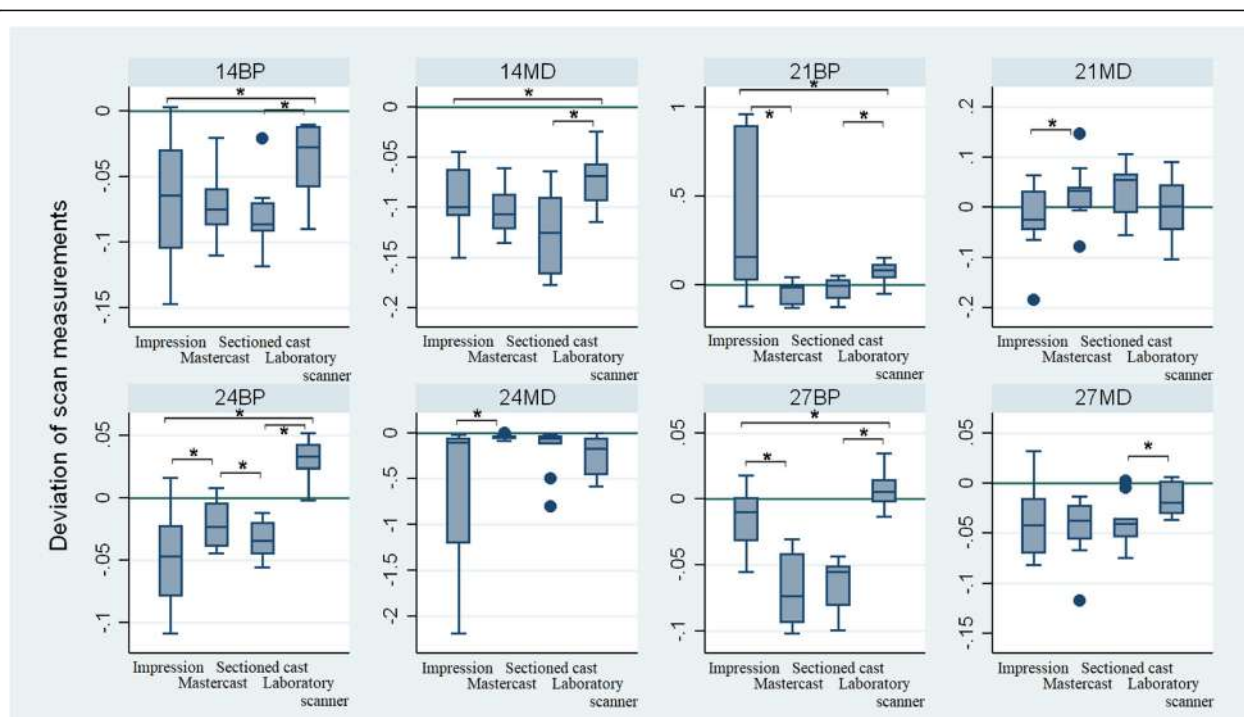


Fig. 10 – Absolute distortions of teeth registered by the virtual caliper measurement on the prepared teeth 14, 21, 24, 27. MB and BP distance (mm). Changes are shown by following the indirect CAD/CAM steps (x-axis): 1, Impression; 2, Mastercast; 3, Sectioned cast data gathered with reference scanner (Sectioned cast); 4, Sectioned cast data gathered with desktop scanner (Laboratory scanner)

Table 1 MB and BP distance (mm) changes observed by following the indirect CAD/CAM steps

	Q1	Median	Q3	IQR
14BP				
Impression	-0.115	-0.064	-0.026	0.089
Mastercast	-0.092	-0.075	-0.058	0.034
Sectioned cast	-0.095	-0.086	-0.069	0.026
Laboratory scanner	-0.058	-0.027	-0.012	0.046
14MD				
Impression	-0.118	-0.099	-0.061	0.057
Mastercast	-0.124	-0.107	-0.085	0.039
Sectioned cast	-0.168	-0.125	-0.086	0.082
Laboratory scanner	-0.095	-0.069	-0.055	0.040
21BP				
Impression	0.026	0.157	0.899	0.873
Mastercast	-0.107	-0.012	0.004	0.112
Sectioned cast	-0.082	-0.002	0.032	0.114
Laboratory scanner	0.031	0.083	0.116	0.085
21MD				
Impression	-0.049	-0.025	0.039	0.089
Mastercast	-0.002	0.033	0.049	0.051
Sectioned cast	-0.012	0.055	0.067	0.079
Laboratory scanner	-0.048	0.001	0.055	0.103
24BP				
Impression	-0.082	-0.047	-0.019	0.063
Mastercast	-0.041	-0.023	-0.004	0.036
Sectioned cast	-0.046	-0.034	-0.019	0.027
Laboratory scanner	0.021	0.033	0.043	0.022
24MD				
Impression	-1.317	-0.108	-0.065	1.253
Mastercast	-0.063	-0.044	-0.032	0.031
Sectioned cast	-0.217	-0.066	-0.035	0.183
Laboratory scanner	-0.466	-0.173	-0.056	0.410
27BP				
Impression	-0.033	-0.009	0.002	0.035
Mastercast	-0.094	-0.073	-0.039	0.055
Sectioned cast	-0.084	-0.055	-0.049	0.034
Laboratory scanner	-0.004	0.005	0.015	0.019
27MD				
Impression	-0.072	-0.042	-0.004	0.068
Mastercast	-0.058	-0.037	-0.021	0.038
Sectioned cast	-0.058	-0.041	-0.028	0.030
Laboratory scanner	-0.031	-0.019	0.002	0.033

Table 2 Significance levels of die diameters according to multilevel mixed-effect linear regression

	95%CI	p
14BP		
Impression vs Mastercast	-0.031, 0.025	0.850
Mastercast vs Sectioned cast	-0.016, 0.002	0.103
Sectioned cast vs Laboratory scanner	0.032, 0.063	< 0.001*
Impression vs Laboratory scanner	0.003, 0.071	0.032*
14MD		
Impression vs Mastercast	-0.027, 0.009	0.311
Mastercast vs Sectioned cast	-0.055, 0.009	0.152
Sectioned cast vs Laboratory scanner	0.028, 0.084	< 0.001*
Impression vs Laboratory scanner	0.008, 0.040	0.004*
21BP		
Impression vs Mastercast	-0.702, -0.168	0.001*
Mastercast vs Sectioned cast	-0.020, 0.050	0.411
Sectioned cast vs Laboratory scanner	0.066, 0.119	< 0.001*
Impression vs Laboratory scanner	-0.592, -0.063	0.015*
21MD		
Impression vs Mastercast	0.024, 0.079	< 0.001*
Mastercast vs Sectioned cast	-0.032, 0.044	0.747
Sectioned cast vs Laboratory scanner	-0.069, 0.001	0.060
Impression vs Laboratory scanner	-0.009, 0.057	0.152
24BP		
Impression vs Mastercast	0.006, 0.047	0.011*
Mastercast vs Sectioned cast	-0.019, -0.004	0.002 *
Sectioned cast vs Laboratory scanner	0.056, 0.072	< 0.001*
Impression vs Laboratory scanner	0.055, 0.103	< 0.001*
24MD		
Impression vs Mastercast	0.024, 1.024	0.040 *
Mastercast vs Sectioned cast	-0.288, 0.027	0.104
Sectioned cast vs Laboratory scanner	-0.297, 0.174	0.610
Impression vs Laboratory scanner	-0.051, 0.715	0.089
27BP		
Impression vs Mastercast	-0.064, -0.042	< 0.001*
Mastercast vs Sectioned cast	-0.007, 0.014	0.487
Sectioned cast vs Laboratory scanner	0.056, 0.083	< 0.001*
Impression vs Laboratory scanner	0.010, 0.031	< 0.001*
27MD		
Impression vs Mastercast	-0.048, 0.031	0.663
Mastercast vs Sectioned cast	-0.017, 0.024	0.735
Sectioned cast vs Laboratory scanner	0.008, 0.041	0.004*
Impression vs Laboratory scanner	-0.013, 0.051	0.248

Note: significant values are marked with *

Relative distortions of dies diameters

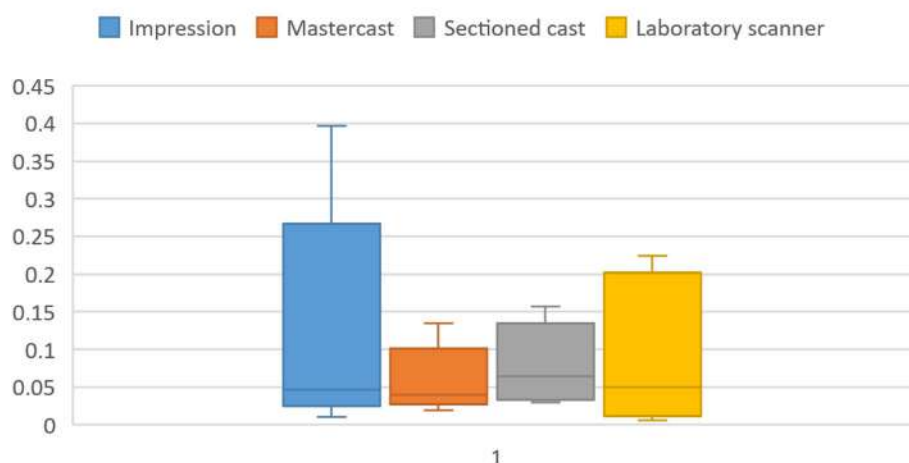


Fig. 11 Relative distortions of 8 die diameters were calculated: relative distortion = mean absolute error/reference value. There was no correlation with size. However, teeth in the impressions showed the greatest distortion

casts made by the extraoral scanner had a trueness of -0.398 mm (IQR = 0.169).

The analysis revealed significant distortion in trueness at all steps of the indirect CAD/CAM method, and significant differences were found between the impressions and virtual casts considering all three measured distances ($p < 0.01$, Table 6). The smallest values were registered on the virtual casts made by the extraoral scanner, which were significantly smaller than the values of the impressions and the sectioned casts.

Overall, absolute deviation calculations showed that the dies on the virtual casts made by the extraoral scanner were larger than those on the sectioned gypsum casts. However, prepared dies were closer to each other on the virtual casts made by the extraoral scanner compared to the sectioned casts made by the reference scanner (Fig. 13 and Table 5). Relative deviation calculations revealed no relationship with the position of dies in the arch (Fig. 14 and Table 6 and 7), meaning that further distances did not result in higher distortions.

Discussion

Little is known about the scanning step in indirect CAD/CAM digitization, and our analysis is one of the

first studies to shed more light on the entire process: not only the impression, mastercast, and sectioned cast, but also the digitization step. Our null hypothesis was rejected: our results show that there are differences between the dimensions represented by the sectioned cast and the virtual cast made by the optical extraoral scanner used in the study. We also showed that the scanning procedure influences the diameter of the dies and that there is no relationship between the distance of the dies and the distortion in the measurement of the arch.

Accurate virtual models are necessary to make accurate prostheses. Usually, indirect CAD/CAM digitization is based on conventional impression-taking and stone-cast making procedure. Residual stresses are well known as a feature of gypsum crystallization. ADA Specification #25 describes that the expansion of the dental gypsum might be as much as 0.2% [38]. This distortion caused by expansion can be compensated for by sectioning the cast. In this case, the dies must be in the correct position in the arch, and they must be able to be removed [27]. Sectioning can release stress in the gypsum so that the dies can be repositioned to the original position granted by the acrylic base [30]. The distortion of the conventional cast making steps represented in this study are similar to what has been found in other studies [25, 28, 30]. There have been studies that evaluate the trueness and precision of extraoral scanners by using solo abutments [35], silicone impression material [11], or by an easy-to-measure metric cast [34], but there is hardly any information about the factors that influence accuracy between the making of the gypsum cast and the CAD/CAM production of

Table 3 Relative calculated distortions of 8 die diameters

	Q1	Median	Q3	IQR
Impression	0.038	0.046	0.136	0.098
Mastercast	0.035	0.039	0.068	0.033
Sectioned cast	0.036	0.064	0.111	0.075
Laboratory scanner	0.018	0.049	0.178	0.160

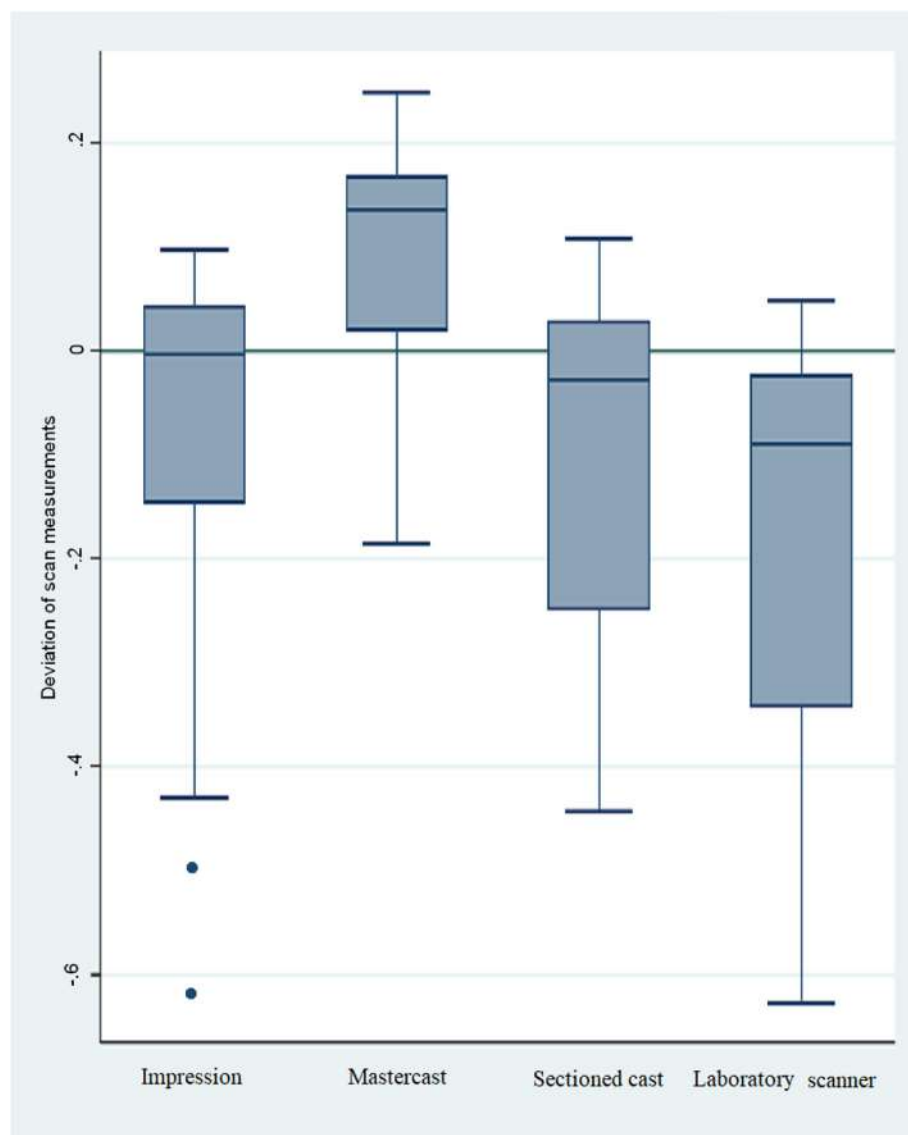


Fig. 12 – Observed absolute distortions on all three distances combined (mm) (Inside + outside + left side) The smallest values were obtained from the virtual models generated in the desktop scanner

the final prostheses using life-like samples. This current study provides information about this very important issue.

Our study aimed to assess the trueness of indirect digitization of gypsum casts using an optical extraoral

Table 4 Observed distortion on all three distances (mm) (Inside + outside + left side)

	Q1	Median	Q3	IQR
Impression	−0.156	−0.004	0.043	0.198
Mastercast	0.011	0.136	0.168	0.157
Sectioned cast	−0.250	−0.029	0.028	0.279
Laboratory scanner	−0.347	−0.089	−0.024	0.322

scanner, whereby we hypothesized that there was no difference between the sectioned casts and the virtual casts made by the extraoral scanner. However, when we explored the differences between the trueness of sectioned gypsum cast and the virtual cast made by the optical extraoral scanner, our null hypothesis was rejected. Vanderweghe et al. [34] described how gypsum casts are harder to digitize with optical scanners because of the rough surface. In their study, three out of four scanners had better trueness at scanning acrylic resin. Based on this, the sensitivity of the scanner might also play an important role during scanning. On the other hand, studies show that there is no correlation between triangle numbers (number of digital points) and accuracy, but

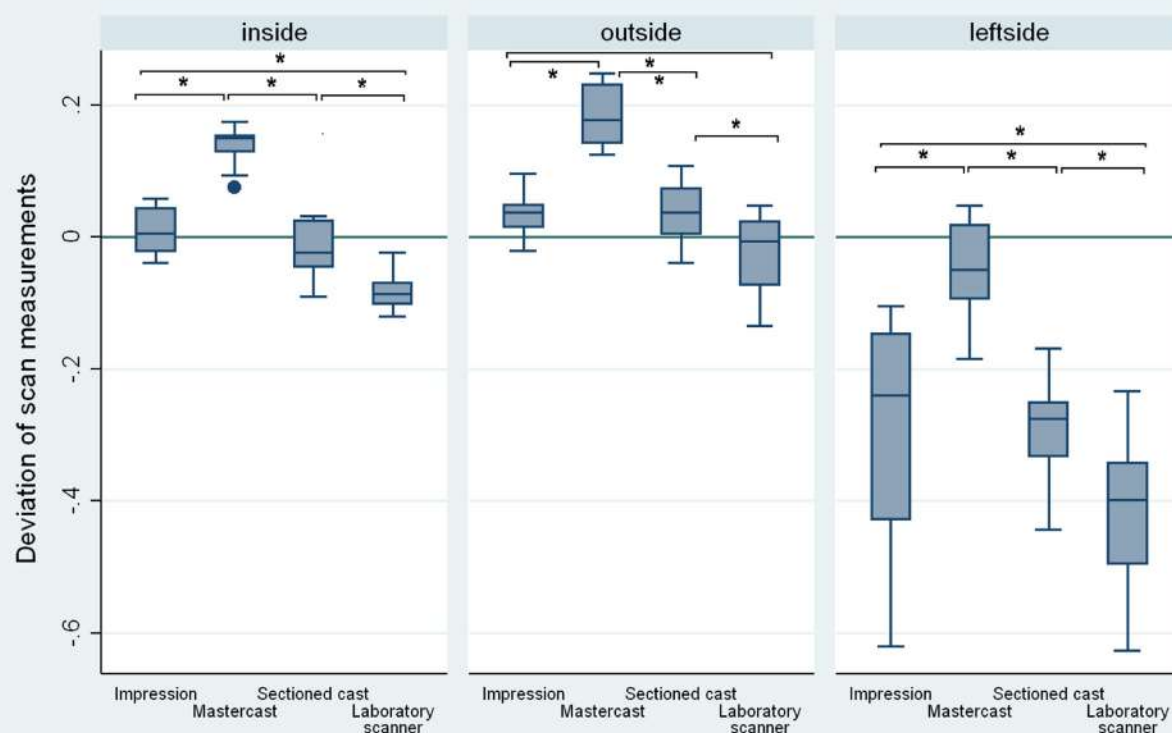


Fig. 13 Inside (closest points of 24–27 teeth), outside (furthest points of 24–27 teeth) and left side (furthest points of 21–27 teeth) absolute distance changes (mm) observed at the indirect CAD/CAM steps. The biggest distortions are represented between teeth 21 and 27

Table 5 Inside, outside and left side changes (mm) observed at the indirect CAD/CAM steps

	Q1	Median	Q3	IQR
<i>Inside</i>				
Impression	−0.023	0.006	0.048	0.071
Mastercast	0.120	0.149	0.154	0.034
Sectioned cast	−0.048	−0.023	0.026	0.073
Laboratory scanner	−0.105	−0.086	−0.062	0.043
<i>Outside</i>				
Impression	0.010	0.038	0.061	0.051
Mastercast	0.139	0.177	0.232	0.093
Sectioned cast	0.004	0.037	0.080	0.075
Laboratory scanner	−0.075	−0.006	0.029	0.103
<i>Left side</i>				
Impression	−0.447	−0.24	−0.140	0.306
Mastercast	−0.105	−0.050	0.026	0.130
Sectioned cast	−0.355	−0.276	−0.234	0.121
Laboratory scanner	−0.498	−0.398	−0.329	0.169

accuracy depends on the quality of the point cloud generated by the software algorithm [35, 39].

The diameters of the dies were influenced (distorted) by the extraoral scanner in our study. The differences observed on all four prepared teeth #11, #14, #24, #27 during the extraoral scanner scanning step indicates a necessity of caution during everyday dental practice. Our observed distortions, however, differ from those detected in other studies. Wöstmann et al. [40] compared the accuracy of four intraoral and 10 extraoral digitizers in their study, with the reference model die shaping a chamfer-prepared canine and a chamfer-prepared molar. They found differences between the accuracy of intraoral and extraoral scanners with an accuracy below 20 μm . Jeon et al. [41] measured accuracy during extraoral scanning of impressions from prepared teeth for all-ceramic restorations. Their results showed the trueness to be less than 30 μm . The reason for this difference in data could be that these studies measured single prepared teeth only, while in our study two-step scanning procedures were performed on gypsum casts to obtain the whole arch and the dies information as well. However, these differences between the results of the present study and those of other studies are not clinically significant.

Relative deviations of die distances

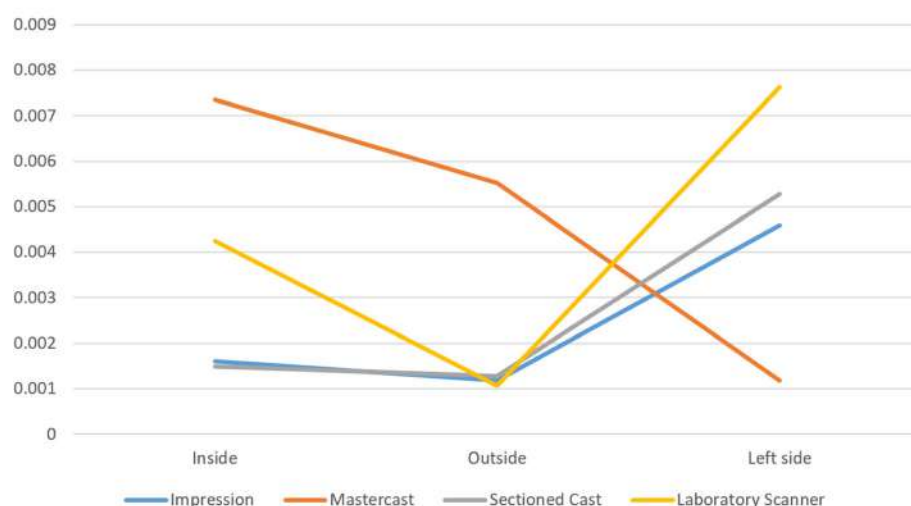


Fig. 14 Non-linear relative deviations according to the position of dies in the arch. The smallest relative distortions were observed at middle distance at 3 out of 4 steps (Impressions, sectioned casts data made by reference scanner and sectioned casts data made by desktop scanner)

The virtual casts made by the laboratory scanner that we used showed the smallest observed values in the arch distances in the whole indirect CAD/CAM digitization process in our study. The distortions observed at small and medium distances have no clinical relevance. The distortions observed at the longest distance (half arch) may have clinical relevance due to their extent (difference between the mean values of the impressions and virtual casts: -0.158 mm). The relative deviations did

Table 6 Comparison of the steps of indirect CAD/CAM method on arch distances

	95%CI	p
<i>Inside</i>		
Impression vs Mastercast	0.109, 0.141	< 0.001
Mastercast vs Sectioned cast	-0.186, -0.13	< 0.001
Sectioned cast vs Laboratory scanner	-0.083, -0.038	< 0.001
Impression vs Laboratory scanner	-0.118, -0.069	< 0.001
<i>Outside</i>		
Impression vs Mastercast	0.103, 0.159	< 0.001
Mastercast vs Sectioned cast	-0.161, -0.128	< 0.001
Sectioned cast vs Laboratory scanner	-0.075, -0.02	< 0.001
Impression vs Laboratory scanner	-0.094, -0.027	< 0.001
<i>Left side</i>		
Impression vs Mastercast	0.162, 0.312	< 0.001
Mastercast vs Sectioned cast	-0.291, -0.195	< 0.001
Sectioned cast vs Laboratory scanner	-0.173, -0.071	< 0.001
Impression vs Laboratory scanner	-0.208, -0.047	0.002

not show a relationship with the distortion of the arch. The extraoral scanner used in this study recommends a two-step digitization, and this two-step scanning and the alignment of the data might explain the observed random distortion. Vandeweghe et al. [34] evaluated the accuracy of four different extraoral scanners (Imetric D104i, Imetric 3D; KaVo Everest, KaVo Dental; Smart Optics Activity 880, Smart Optics; Lava ST,3 M ESPE). They used a geometrical model with rectangular and cylindrical shapes as a reference model, and the extraoral scanners were tested with acrylic based casts (mean trueness: 0.047 mm) and gypsum casts (mean trueness: 0.099 mm). Most of their scans met the requirements of clinical accuracy published in other studies [20–22], indicating a lack of clinically unacceptable distortion caused by indirect CAD/CAM digitization. Their results are somewhat different from the results of our present study (our mean trueness: -0.086 mm). These differences may have arisen from the fact that the two studies used different methods: in addition to us using different casts, the reference model of our study was a PMMA replica of hand-prepared anatomical teeth. As such, the

Table 7 Non-linear relative deviations according to the position of dies in the arch

	Inside	Outside	Left side
Impression	0.002	0.001	0.005
Mastercast	0.007	0.006	0.001
Sectioned cast	0.001	0.001	0.005
Laboratory scanner	0.004	0.001	0.008

anatomical arch and the prepared teeth in our study may be more difficult for the extraoral scanner to scan than the cylindrical shape in their study.

One limitation of our study is that the trueness in our study might be considered low. Mandelli et al. [35] utilized seven extraoral scanners, although not the Straumann CARES Scan CS2 that we used for scanning, and most of their scanners used only a single-step scanning procedure, while we used a two-step scanning procedure. Furthermore, their reference die was an easy-to-scan solo non-anatomical titan abutment, as opposed to an anatomical gypsum cast with hand prepared abutments used in our study. Their accuracy varied between 8 and 30 μm , depending on the scanner system while our trueness values were much higher. The two-step scanning procedure combined with a hand-prepared abutment with a more complex surface might explain the lower trueness in our study. Another limitation is that our study used only the digitization of a sectioned gypsum cast, and we did not assess the scanning of a precisional-situational impression using a laboratory extraoral scanner or intraoral scanners [7]. However, the scanning of conventional impressions is performed much less often than the scanning of sectioned gypsum casts, and therefore our study focused on the more commonly used indirect digitization. Last but not least, our study focuses only the Straumann extraoral scanner, therefore these results cannot be generalized for all extraoral desktop scanners. However, according to Holst et al. [34] who compared optical and contact scanner accuracy, there is no significant difference between the two types of scanners. A further limitation is that we measured only trueness but not precision – measuring precision might be the topic of future studies. Finally, the laboratory scanner used in this study was not pre-calibrated specifically for the purposes of this study. However, everyday dental laboratory work uses limited calibrations, and therefore our protocol followed a real-life approach.

Conclusions

Within the limitations of the present in vitro study, we can conclude that the trueness of the virtual models generated by the extraoral scanner system used by us in the study is different compared to the dimensions of the sectioned casts. The digitization of gypsum casts changes both the dimensions of the dies and distances between the dies. The differences observed on all four prepared teeth were both positive and negative at the scanning step. No relationship was observed in relative deviations, meaning that higher values of the dies did not result in higher distortions. At the last step of indirect CAD/CAM digitization, the distances of the virtual casts made by the extraoral scanner were smaller than any of the

distances measured at previous steps. No relationship was revealed with the position of dies in the arch, meaning that further distances did not result in greater distortions. Distortions observed at half arch distance may have clinical relevance. We cannot, however, generalize our results to all scanners available on the market, because they might give different results. Therefore, future studies may further explore the accuracy of other extraoral scanners in life-like samples.

Abbreviations

BP: Bucco-Palatal diameter of a measured tooth; CAD: Computer-assisted design; CAM: Computer-assisted manufacturing; CBCT: Cone beam computed tomography; DDT: Digital dental technology; MD: Mesio-distal diameter of a measured tooth; PMMA: Polimethyl-methacrylic acid; STL: Standard tessellation format

Acknowledgements

3 M provided impression material. Interdental Studio dental laboratory provided help with the casting and sectioning of the gypsum casts. Varinex Zrt. provided technical background with the reference scanner and the superimposition software (Geomagic Verify). Dr. László Kardos provided expert statistical advice.

Authors' contributions

GJ-K contributed to the design of the study, designed the analysis plan, performed data management, generated most of the figures, and wrote the paper. BV contributed to the design of the study, performed data analysis, and contributed to writing the paper. SzK contributed to the design of the analysis, performed data acquisition and data management, and contributed to writing the paper. VAG contributed to the interpretation of the data and the writing of the paper. JB contributed to the design of the study, was involved in supervising data collection, conceived the analysis plan, and contributed to writing the paper. PH contributed to the design of the study, and provided advice, was involved in supervising data collection, and contributed to writing the paper. All authors read and approved the final manuscript.

Funding

The present in vitro study was not funded by any grant.

Availability of data and materials

The datasets used and/or analyzed during the current study are available from the corresponding author on reasonable request.

Ethics approval and consent to participate

Neither approval nor consent to participate was requested because the present study is an in vitro study.

Consent for publication

Not applicable.

Competing interests

V. Anna Gyarmathy is an Associate Editor at BMC Public Health.

Author details

¹Department of Prosthodontics, Semmelweis University, Szentkirályi u. 47, Budapest 1088, Hungary. ²EpiConsult LLC, 8 The Green, STE A, Dover, DE 19901, USA. ³Johns Hopkins Bloomberg School of Public Health, Baltimore, MD, USA.

Received: 9 May 2019 Accepted: 28 November 2019

Published online: 12 December 2019

References

- Shah N, Bansal N, Logani A. Recent advances in imaging technologies in dentistry. *World J Radiol.* 2014;6(10):794–807.

2. Chu SJ, Trushkowsky RD, Paravina RD. Dental color matching instruments and systems. Review of clinical and research aspects. *J Dent*. 2010;38(SUPPL. 2):2–16.
3. Joda T, Brägger U. Digital vs. conventional implant prosthetic workflows: a cost/time analysis. *Clin Oral Implants Res*. 2014;26:1430–5.
4. Lee SJ, Gallucci GO. Digital vs. conventional implant impressions: efficiency outcomes. *Clin Oral Implants Res*. 2013;24(1):111–5.
5. Yuzbasioglu E, Kurt H, Turunc R, Bilir H. Comparison of digital and conventional impression technique: evaluation patient's perception, treatment comfort, effectiveness and clinical outcomes. *BMC Oral Health*. 2014;14(10):1–7.
6. Lee SJ, Macarthur RX IV, Gallucci GO. An evaluation of student and clinician perception of digital and conventional implant impressions. *J Prosthet Dent*. 2013;110(5):420–3.
7. Malaguti G, Rossi R, Marziali B, Esposito A, Bruno G, Dariol C, et al. In vitro evaluation of prosthodontic impression on natural dentition: a comparison between traditional and digital techniques. *ORAL Implants*. 2016;9:21–7.
8. Beuer F, Schweiger J, Edelhoff D. Digital dentistry: an overview of recent developments for CAD/CAM generated restorations. *Br Dent J*. 2008;204(9):505–11.
9. Almeida e Silva J, Erdelt K, Edelhoff D, Araújo É, Stimmelmayer M, Vieira L, et al. Marginal and internal fit of four-unit zirconia fixed dental prostheses based on digital and conventional impression techniques. *Clin Oral Investig*. 2014;18:515–23.
10. Luthardt RG, Walter MH, Quaas S, Koch R, Rudolph H. Comparison of the three-dimensional correctness of impression techniques: a randomized controlled trial. *Quintessence Int*. 2010;41(10):845–53.
11. Lee K-T, Kim H-Y, Kim W-C, Kim J-H, Jeon J-H. White light scanner-based repeatability of 3-dimensional digitizing of silicon rubber abutment teeth impressions. *J Adv Prosthodont*. 2013;5(4):452.
12. Miyazaki T, Hotta Y. CAD/CAM systems available for the fabrication of crown and bridge restorations. *Aust Dent J*. 2011;56(SUPPL. 1):97–106.
13. Patzelt SBM, Lamprinos C, Stampf S, Att W. The time efficiency of intraoral scanners: an in vitro comparative study. *J Am Dent Assoc*. 2014;145(6):542–51.
14. Ender A, Mehl A. Accuracy of complete-arch dental impressions: a new method of measuring trueness and precision. *J Prosthet Dent*. 2013;109(2):121–8.
15. Ender A, Attin T, Mehl A. In vivo precision of conventional and digital methods of obtaining complete-arch dental impressions. *J Prosthet Dent*. 2016 Mar;115(3):313–20.
16. Güth JF, Runkel C, Beuer F, Stimmelmayer M, Edelhoff D, Keul C. Accuracy of five intraoral scanners compared to indirect digitalization. *Clin Oral Investig*. 2016;21:1–11.
17. Su ST, Sun J. Comparison of repeatability between intraoral digital scanner and extraoral digital scanner: an in-vitro study. *J Prosthodont Res*. 2015; 59(4):236–42.
18. Vecsei B, Joós-Kovács G, Borbély J, Hermann P. Comparison of the accuracy of direct and indirect three-dimensional digitizing processes for CAD/CAM systems – an in vitro study. *J Prosthodont Res*. 2017;61:177–84.
19. Denissen H, Crossed D, Signozic A, Van Der Zel J, Van Waas M. Marginal fit and short-term clinical performance of porcelain-veneered CICERO, CEREC, and Procera onlays. *J Prosthet Dent*. 2000;84(5):506–13.
20. Schätzle M, Lang NP, Ånerud Å, Boysen H, Bürgin W, Loe H. The influence of margins of restorations on the periodontal tissues over 26 years. *J Clin Periodontol*. 2008;28(1):57–64.
21. Lee B, Oh KC, Haam D, Lee JH, Moon HS. Evaluation of the fit of zirconia copings fabricated by direct and indirect digital scanning procedures. *J Prosthet Dent*. 2018;120(2):225–231.
22. Nissan J, Rosner O, Bukhari MA, Ghelfan O, Pilo R. Effect of various putty-wash impression techniques on marginal fit of cast crowns. *Int J Periodontics Restor Dent*. 2013;33(1):e37–42.
23. Rudolph H, Quaas S, Haim M, Preißler J, Walter MH, Koch R, et al. Randomized controlled clinical trial on the three-dimensional accuracy of fast-set impression materials. *Clin Oral Investig*. 2013;17(5):1397–406.
24. Mann K, Davids A, Range U, Richter G, Boening K, Reitemeier B. Experimental study on the use of spacer foils in two-step putty and wash impression procedures using silicone impression materials. *J Prosthet Dent*. 2015;113(4):316–22.
25. Ahmad M, Balakrishnan D, Narayan A. A comparative evaluation of linear dimensional accuracy of the dies obtained using three conceptually different die systems in the fabrication of implant prosthesis: an in vitro study. *Indian J Dent Res*. 2014;25(2):197.
26. Persson ASK, Odén A, Andersson M, Sandborgh-Englund G. Digitization of simulated clinical dental impressions: virtual three-dimensional analysis of exactness. *Dent Mater*. 2009;25(7):929–36.
27. Rudd KD, Strunk RR, Morrow RM. Removable dies for crowns, inlays, and fixed partial dentures. *J Prosthet Dent*. 1970;23(3):337–45.
28. Miranda FJ, Dilts WE, Duncanson MG, Collard EW. Comparative stability of two removable die systems. *J Prosthet Dent*. 1975;36:326–33.
29. Myers M, Hembree JH. Relative accuracy of four removable die systems. *J Prosthet Dent*. 1982;48(2):163–5.
30. Aramouni P, Millstein P. A comparison of the accuracy of two removable die systems with intact working casts. *Int J Prosthodont*. 1993;6(6):533–9.
31. Dogan S, Schwedhelm ER, Heindl H, Mancl L, Raigrodski AJ. Clinical efficacy of polyvinyl siloxane impression materials using the one-step two-viscosity impression technique. *J Prosthet Dent*. 2015;114(2):217–22.
32. Nissan J, Laufer BZ, Brosh T, Assif D. Accuracy of three polyvinyl siloxane putty-wash impression techniques. *J Prosthet Dent*. 2000;83(2):161–5.
33. Dugal R, Railkar B, Musani S. Comparative evaluation of dimensional accuracy of different polyvinyl siloxane putty-wash impression techniques-in vitro study. *J Int oral Heal*. 2013;5(5):85–94.
34. Vandeweghe S, Vervack V, Vanhove C, Dierens M, Jimbo R, De Bruyn H. Accuracy of optical dental digitizers: an in vitro study. *Int J Periodontics Restor Dent*. 2015;35(1):115–21.
35. Mandelli F, Gherlone E, Gastaldi G, Ferrari M. Evaluation of the accuracy of extraoral laboratory scanners with a single-tooth abutment model: a 3D analysis. *J Prosthodont Res*. 2017;61(4):363–70.
36. Keul C, Stawarczyk B, Erdelt KJ, Beuer F, Edelhoff D, Güth JF. Fit of 4-unit FDPs made of zirconia and CoCr-alloy after chairside and labside digitalization - a laboratory study. *Dent Mater*. 2014;30:400–7.
37. Holst S, Persson A, Wichmann M, Karl M. Digitizing implant position locators on master casts: comparison of a noncontact scanner and a contact-probe scanner. *J Prosthet Dent*. 2013;109(1):52.
38. Council on Dental Materials, Instruments, and Equipment. Revised ANSI/ADA specification no. 2. *J Am Dent Assoc*. 1985;111(6):1003.
39. Nedelcu RG, Persson ASK. Scanning accuracy and precision in 4 intraoral scanners: an in vitro comparison based on 3-dimensional analysis. *J Prosthet Dent*. 2014;112(6):1461–71.
40. Wöstmann B, Salmen H, Kuhn K, Rudolph H, Sichwardt V, Moldan M, et al. Accuracy of intraoral and extraoral digital data acquisition for dental restorations. *J Appl Oral Sci*. 2016;24(1):85–94.
41. Jeon J-H, Kim H-Y, Kim J-H, Kim W-C. Accuracy of 3D white light scanning of abutment teeth impressions: evaluation of trueness and precision. *J Adv Prosthodont*. 2014;6(6):468.

Publisher's Note

Springer Nature remains neutral with regard to jurisdictional claims in published maps and institutional affiliations.

Ready to submit your research? Choose BMC and benefit from:

- fast, convenient online submission
- thorough peer review by experienced researchers in your field
- rapid publication on acceptance
- support for research data, including large and complex data types
- gold Open Access which fosters wider collaboration and increased citations
- maximum visibility for your research: over 100M website views per year

At BMC, research is always in progress.

Learn more biomedcentral.com/submissions



RESEARCH ARTICLE

Open Access



Zirconia crowns cemented on titanium bars using CAD/CAM: a five-year follow-up prospective clinical study of 9 patients

Antonio Scarano^{1,2*} , Marco Stoppaccioni³ and Tommaso Casolino⁴

Abstract

Background: The purpose of this prospective clinical study was to evaluate clinical results of the passive fit of the substructure in the Toronto bridge and the chipping or delamination of the ceramic veneering on the zirconia-support, after 5 years, in nine patients rehabilitated with zirconia crowns cemented on titanium bars using CAD/CAM technology.

Methods: A total of nine healthy patient fully edentulous in the upper and lower jaws with non-contributory past medical anamnesis needing full fixed total prosthesis maxilla and mandible were included in this clinical study, where a total 9 mandibles and 9 jaws were treated. The inclusion criteria in order for a patient to participate in the study were: a signed consent form, fully edentulous in the upper and lower jaws, required a full fixed total prosthesis restoration. The exclusion criteria were age limitation of less than 18 years old, chemotherapy, head and neck radiation therapy, diabetes or periodontal disease, smoking and severe illness. All patients received zirconia crowns cemented on titanium bars using CAD/CAM technology. The primary outcome of this study was to examine the survival rate of the zirconia crowns cemented on titanium bars using CAD/CAM technology during the observation period. Any chipping or delamination of the zirconia crowns of the restorations was considered as failure. The secondary outcome was to evaluate the passive fit of the substructure on the implants, loose of occlusal screws, implant survival and satisfactory occlusion.

Results: In 5 years of follow-up no evidence of chipping or delamination of the ceramic veneering on the zirconia crown supported were observed. Fifteen finished prothesis (93.75%) showed satisfactory occlusion and only one case (6.25%) required significant occlusal adjustment. During the first year recall all bars were stable (100%) no mobility of protheses was recorded. After 5 years all bars were stable (100%) and no mobility of protheses was recorded.

Conclusion: The computerized workflow for the process of building bar and prosthesis ensures reproducible results and excellent adaptation and passive insertion of them, as well as conditions for avoiding mechanical complications and guarantees stability of screw-implant abutments.

Keywords: CAD/CAM, Zirconia, Dental implants, Digital workflow, Toronto bridge, Computerized workflow

* Correspondence: ascarano@unich.it

¹Department of Medical, Oral and Biotechnological Sciences, University "G. D'Annunzio" of Chieti-Pescara, Via Dei Vestini, 31, 66100 Chieti, Italy

²Zirconia Implant Research Group (Z.I.R.G), International Academy of Ceramic Implantology, Silver Spring, USA

Full list of author information is available at the end of the article



© The Author(s). 2019 **Open Access** This article is distributed under the terms of the Creative Commons Attribution 4.0 International License (<http://creativecommons.org/licenses/by/4.0/>), which permits unrestricted use, distribution, and reproduction in any medium, provided you give appropriate credit to the original author(s) and the source, provide a link to the Creative Commons license, and indicate if changes were made. The Creative Commons Public Domain Dedication waiver (<http://creativecommons.org/publicdomain/zero/1.0/>) applies to the data made available in this article, unless otherwise stated.

Background

The long-term predictability of the restoration involves several aspects concerning the implant surface [1], surgical techniques [2, 3] and the anchorages used. Screw-retained prosthesis, cemented, or a combined approach have been proposed as prosthetic connections between the implant and the restoration. The screwed prosthesis has the advantage of the possibility of later removal for eventual restoration, repair, treatment of the implants, retightening of the abutment screw and hygiene measurements [4]. Frequently, the position of the screw hole of tilted implants may produce complications in terms of occlusion and aesthetic outcome [5]. Moreover, it might lead to fracture of the porcelain if the metal framework design does not support the porcelain around the access hole [6].

A cemented approach for implant restorations has been proposed to improve the aesthetic outcome in tilted implants by means of customized abutments [7]. This technique presents many benefits over screw-retained restorations. These advantages include higher potential for achieving a passive fit of the superstructure, easy fabrication, improved aesthetic results and an easier positioning in posterior regions of the oral cavity [8, 9].

However, this technique has some disadvantages such as difficulty in removing the cement excess around the implant restoration. High priority should be given to the removal of excess cement after cementation in the implant-mucosal interface, to avoid bleeding on probing in most cases and suppuration in some [10].

The fixed prosthesis on Toronto Bridge implants or abutment-hybrid overdenture, have been proposed in order to overcome problems of both types of screw or cemented restorations while benefiting from their merits [11]. The Toronto Bridge procedure mixes the advantages of screw- and cement-retained prostheses by a screwed in mesostructure and milled abutments for the cementation of single or multiple superstructures. Individual crowns are cemented on the superstructures with a pink characterization or gingiva-coloured laboratory composite or porcelain to simulate the soft tissues. The fixed prosthesis on Toronto Bridge implants takes its name from the Canadian city where it was presented for the first time by Zarb GA [12] in early 1980s.

Full tooth therapy with Toronto Bridge in the totally edentulous patients is frequently indicated for implant therapy. The fixed prosthesis on Toronto Bridge implants is a fixed full total prosthesis with flange that can replace an entire dental arch and is a good alternative solution to be taken into consideration. It usually consists of 10/12 teeth per arch and is directly secured, by abutments, to dental osseointegrated titanium implants. In many cases, immediate load implants can be used, and for this purpose, the All-on-4 surgical protocol is

one of the most used [13–15]. The Toronto Bridge is used when the patient requires a supported implant with need of a good support of the lips with a flange. Today the term Toronto Bridge has taken on a broader meaning, including all cases of full-arch rehabilitation with reconstruction of hard and soft tissues, including cases with tilted implants. Toronto bridge technique or abutment-hybrid overdenture have a bar on which individual crowns can be cemented and pink composite or gingiva-colored porcelain is used for mimicking the soft tissues.

Computer-aided design and computer-aided manufacturing (CAD/CAM) systems for the design and manufacture of Toronto bridges are now used in clinical practice. The CAD/CAM compound prostheses were formerly introduced in clinical practice for single elements over 30 years ago, and advancements in technology now permit the manufacture of full or multi-unit rehabilitations [16]. Nowadays, digital impression with intraoral scanning or indirect digitization of casts derived from conventional impressions, can generate a stereolithography (STL) [17]. The intraoral situation can be moved to a virtual 'cast-free working environment and, in case of necessity, physical casts can be made from the STL files [18]. The intraoral scanner (IOS) is used to transform conventional prosthetic workflows with the possibility of immediately obtaining digital models of the arches. The IOS are also used for the design and fabrication of implant-supported monolithic translucent zirconia crowns cemented on customized hybrid abutments [19]. The classic Toronto have a titanium bar with teeth and resin flange, this prosthesis has a good prognosis, but it is, unfortunately, not equally valid over time from an aesthetic point of view, and acrylic resin does not allow an adequate resistance response when the prosthesis is subjected to a load [20]. To avoid this, in the present study, we have used a cemented zirconia superstructure above a milled metal substructure.

The aim of this prospective clinical study was to evaluate clinical results after 5 years in nine patients rehabilitated with Toronto prostheses and zirconia crowns cemented on titanium bars using CAD/CAM compound prostheses.

Methods

The present prospective clinical study was based in a private practice in Termoli (Italy), in full accordance with ethical principles, including the World Medical Association Declaration of Helsinki and the additional requirements of Italian law. Furthermore, the University of Chieti-Pescara, Italy, classified the study to be exempt from ethical review as it carries only negligible risk and involves the use of existing data that contains only non-identifiable data about human beings. All patients signed

a written informed consent form. A total of nine healthy patients fully edentulous in the upper and lower jaws with non-contributory past medical anamnesis needing full fixed total prosthesis (5 women and 4 men, all non-smokers, mean age 51 years, range 47–69 years) were included in this study, where a total 9 mandibles and 9 jaws were treated. A total of 18 superstructures were made from a prefabricated CAD/CAM framework, connected directly to the implants, using flat abutments. The patients were selected for full fixed total prosthesis and signed a written informed consent. The inclusion criteria in order for a patient to participate in the study were: a signed consent form, fully edentulous in the upper and lower jaws, required a full fixed total prosthesis restoration. The exclusion criteria were age limitation of less than 18 years old, chemotherapy, head and neck radiation therapy, diabetes or periodontal disease, smoking and severe illness. The primary outcome of this study was to examine the survival rate of the zirconia crowns cemented on titanium bars using CAD/CAM technology during the observation period. Any chipping or delamination of the ceramic veneering on zirconia-supports zirconia crowns of the restorations was considered as failure. The secondary outcome was to evaluate the passive fit of the substructure on the implants, loose of occlusal screws, implant survival and satisfactory occlusion. At the initial visit, all candidates underwent a clinical and occlusal evaluation, and orthopantomographic radiographs were evaluated. A three-dimensional cone beam computed tomography scan (CBCT) (Vatech Ipax 3D PCH-6500, Fort Lee, NJ USA) was performed to investigate clinically evident pathologies such as residual teeth, cists, height and thickness of the bone ridge. Before implant surgery, rinses of chlorhexidine digluconate solution 0.2% for 2 min (Curaden Healthcare S.p.A., Saronno, Italy) were administered to the patients. Local anaesthesia was performed using Articaine® (Pierrel, Milano Italy) with epinephrine 1:100.000. A total 90 implants were used, each mandible received four implants while the jaws received six dental implants (Intra-Lock International, Inc. - Florida, USA) inserted according to manufacturer's recommendations. The procedure consisted of a computer guided surgery (Figs. 1 and 2). The case was planned to use the Implant3d (Milan, Italy) surgical planning software package. The radiographic guide, that duplicates the future prosthesis, allows the prediction of the diameter and length, positioning and orientation of the dental implants to anticipate the dimensions, locations and axes of the implants and abutments. The treatment planning software allows maximal exploitation of the available bone volume. One investigator (A.S) performed all virtual planning. Surgical guides were designed and exported from the virtual planning and then 3D printed, using a printer (Isomed, Padova,

Italy). The Implants were placed with flapless technique. All guides were produced using transparent resin with thickness of 3 mm. Each operator visually checked guides for fit. Minor adjustments were permitted to the outer surface, in order to ensure full access of the surgical handpiece. After a healing period of 4 months, a healing screw was placed. During this phase a percussion test on the implants was carried out, and a control radiograph was taken for evaluation of grade of osseointegration of the implants. After another 2 weeks a Flatone® flat abutment (Intra-Lock- Salerno-Italy) was placed and definitively torqued to 30Ncm according to the manufacturer's recommendation using a torque control system and an impression was taken (Fig. 3b).

Flatone® flat abutment systems, adopted to design the bars, improve the level of precision (Figs. 2 and 3). Digitization of casts derived from conventional impression made from polyether material. Also, the models were developed by the laboratory and mounted on an articulator to establish the interarch relationship (Figs. 3 and 4) and then reacquired on the digital platform (Figs. 3 and 5).

After entering the data, with a dedicated software, titanium bars were designed by the same company supplying the implants, having received the design files. After approval of the virtual model, the bar was milled from a titanium block, by a five-axis milling machine Newancorvis (Bologna, Italy).

After being tested in the oral cavity, the bars were delivered to the laboratory to create the zirconia frame using stored data of the temporary and functionalized prosthesis. A trial prosthesis was made on the wax-up, taking into account the aesthetic needs of the patient and, then, a new long-term temporary prosthesis was built, using a systematic CAD/CAM; the advantage of this technique is represented by the possibility of storing useful information that can be used in the next working phases (Figs. 5 and 6). The frame consists of a functional and occlusal part, which is totally anatomical, while the buccal and gingival part is provided with fine ceramic coating (Fig. 6). This protocol does not require any testing of the zirconia frames within the oral cavity, since the correspondence between the model and the mouth was evaluated when testing titanium bars. An Anatomical framework and digital veneering by lithium disilicate and fusion porcelain was produced to reduce the chipping and delamination of the materials. After the final step of ceramization, the prostheses were cemented on the bars with a temporary cement Temp bond (Kerr Italy). The titanium bar was not sandblasted. The large contact surface between bar and prosthesis ensures maximum adhesion. The recall visits were done after 6 weeks, 1 year, 2 years, 3 years, 4 years, and 5 years from delivery of final restorations. During the recall visits the stability of the prostheses and the

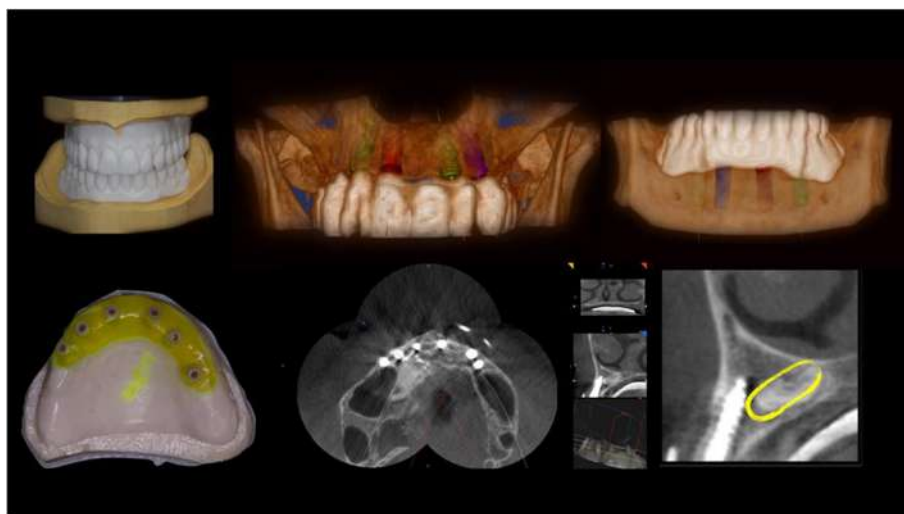


Fig. 1 Initial case. Radiographic moulds, Implant planning through software (Implant3D), surgical moulds and post-surgical X-Ray. Yellow circle highlights the Impacted canine

integrity of the ceramic of crowns were clinically evaluated. CBCTs were taken at annual recalls and were used to evaluate adaption of bar to the Flatone® abutment.

Results

In 5 years, no fractures of the ceramic or titanium bars were observed. No other mechanical complications were registered.

At 5 years, no chipping or delamination of ceramic veneering on zirconia-supports were observed. During the observation period, all the crowns were intact, resulting in a survival rate of 100%.

A passive fit of the substructure on the implants was observed in all 18 bars. The passive fit of the titanium

bar with multiple individual abutments was confirmed in the oral cavity by periapical radiographs and means of a one-screw test. No gaps were observed at any time between bar and abutment by CBCT. Fifteen finished prothesis (93.75%) showed satisfactory occlusion and only one case (6.25%) required significant occlusal adjustment. During the first year recall all bars were stable (100%) no mobility of protheses was recorded. After 5 years all bars were stable (100%) and no mobility of protheses was recorded. During the first-year recall there was no need for re-tightening of occlusal screws. After 5 years only three screws needed re-tightening (3.33%) and occlusal screws were observed in one patient (11.11%). Before loading two implants (2.22%) were removed due to excessive crestal bone resorption and were replaced after 2

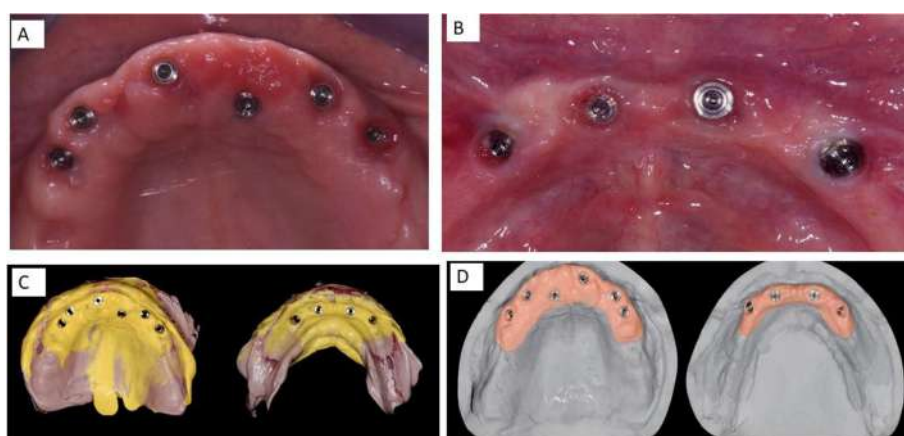


Fig. 2 a The Upper arch. Occlusal view showing the six Intra-Lock System® implants with FlatOne® abutment, one implant was placed palatally to avoid extraction of impacted canine (The patient refused this surgery). b Lower arch with four Intra-Lock System® implants with FlatOne® abutment. c Impressions. d Master cast with silicone gingiva

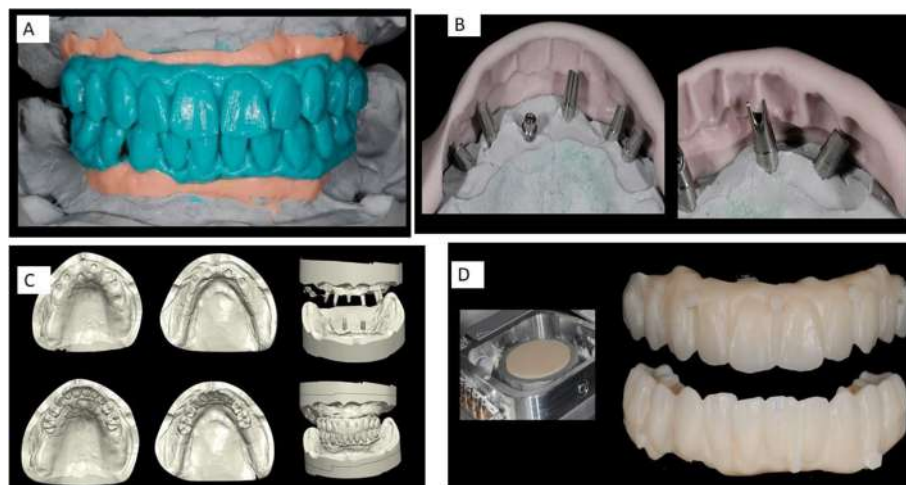


Fig. 3 **a** Diagnostic Project designed with an analog wax-up. **b** Preparation of the prosthetic components for the temporary prosthesis. **c** Wax-up acquisition through a 3D scanner and planning of the temporary prosthesis using the modelling software. **d** Creation of a temporary upper and lower prosthesis through a numerically controlled milling machine with use of long-duration resins

months. During the observation period, all implants were asymptomatic without gingival inflammation, resulting in a survival rate of 100%.

Discussion

The success of an implant surgery depends on the bone and soft tissue healing after the process of implant site preparation [2, 21]. During healing and function of a prosthesis the bacterial adhesion is very important for a high success of an implant [22]. Also, the resistance to corrosion of metals for intra oral and dental rehabilitation is important to avoid ions being released as a result of such corrosion [23]. Zirconia is a material used for

prosthetic rehabilitation of anterior teeth due to its high biocompatibility, its aesthetic (white color) and mechanical properties [24, 25]. In this case prospective clinical study no chipping nor delamination of ceramic veneering were observed in 5 years. This good result achieved thanks to the marginal fit, which is critical for the success and longevity of a dental restoration [26]. The protocol adopted in this clinical trial leads to a substantial and advantageous reduction in costs and treatment times; it is supported by a high, long-term prognosis that, according to the studies carried out, ranges from 92 to 100% [19–21]. In fact conventional casting techniques are technically difficult for producing a

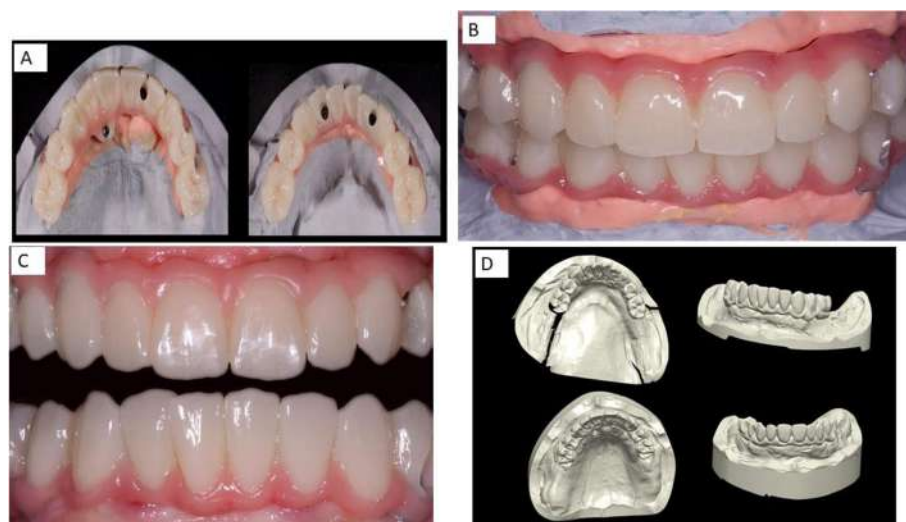


Fig. 4 **a** Temporary prosthesis completed with a pink composite material. **b** Temporary prosthesis. **c** Temporary prosthesis in the mouth. **d** Temporary functionalized scanned prosthesis

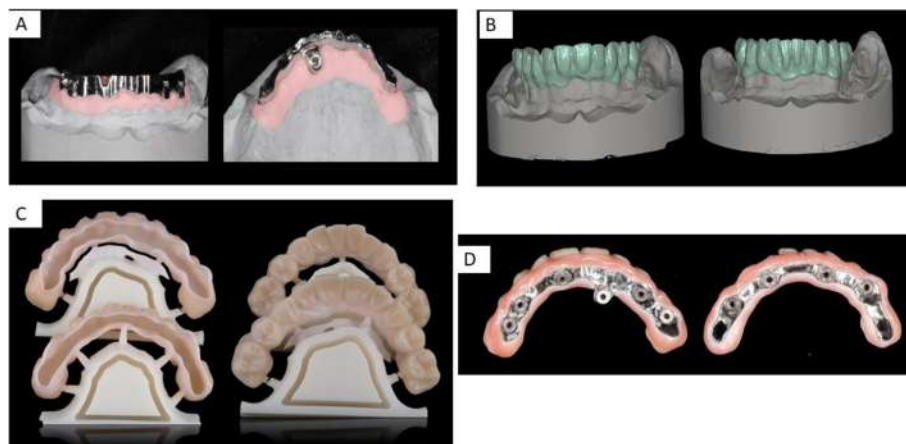


Fig. 5 **a** Milled bars designed with systematic CAD/CAM. **b** Zirconia frame design. **c** Just zirconia frame. **d** View of the final prosthesis

substructure for implant-supported rehabilitation, and the passive fit is difficult in cases of more elements and volume of the substructure [27]. This protocol was recently adopted when restoring implants having unfavorable angulation [28]. The conventional fabrication process of a prosthesis requires multiple materials as well as clinical and laboratory skills. A passive fit of the substructure is necessary for the crestal bone physiology of implants, eliminates overloading of the screw-implant abutments and long term reliability of implant-retained rehabilitation [29, 30]. The Toronto bridges have been used with success in clinical practice for a long time and the only real innovation is the CAD/CAM technology [31] and the data acquisition that can be with or without intraoral scanners. Today the digital technologies and the CAD/CAM technique have an impact on the fabrication of titanium bars for Toronto bridges. CAD/CAM is an important tool for simplifying the prosthetic workflow technologically due to its high-level precision. In dentistry practice several variants have been developed and with them different surgical protocols which, however, are all based on the idea developed by the Swedish school of implantology. One of the main characteristics of this type of prosthesis used in the present prospective clinical study is the flange which reproduces a portion of

the alveolar bone and the pink tissue that have been lost by the patient; they become real orthopaedic prostheses, because they do not just replace the teeth, but also the lost bone. The classic Toronto proposed by Brånemark consists of a titanium bar with teeth and resin flange; it is a screwed solution [32, 33]. Although this prosthesis has a good prognosis, it is, unfortunately, not equally valid over time from an aesthetic point of view. Furthermore, the characteristics of acrylic resin do not allow an adequate resistance response when the prosthesis is subjected to a load in the presence of an antagonist other than a full denture. The technique designed by Brånemark consists of a fixed prosthesis on the lower arch, with implants in the intraforaminal area and a removable prosthesis in the upper arch [34]. After this type of prosthetic rehabilitation it is important to maintain hygienic-care of the prosthesis. To ensure a professional and domestic hygienic procedure, it is important to avoid flanges on the intaglio and that the intaglio surface of the bridge is convex and hygienic, to plan the proper number of implants to balance support of the bridge with the patient's ability to keep the bridge clean. Also the materials used to make the prosthesis are important. For this reason, in this study Zirconia was used, because it is a material with high biocompatibility [35] and

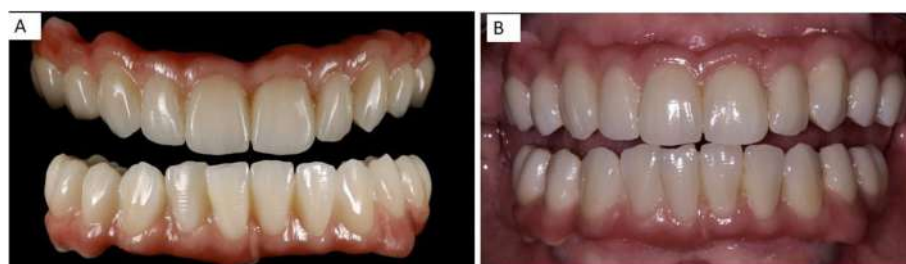


Fig. 6 **a** Prosthesis completed. **b** Prosthesis completed and inserted in the mouth

reduces bacterial adhesion [36]. Over the years the use of implants has become more and more common, even for the upper arch and this has resulted in an increase in resin fractures, which occur in 15% of cases; sometimes they are also accompanied by the fracture of the metal structure. Therefore, protocols aimed at finding a solution are constantly changing, in order to improve aesthetic and functional aspects, which are considered essential. Besides choosing the materials, the techniques used for constructing the prosthesis are important. In recent years, computer-aided design (CAD) and computer-aided manufacturing (CAM) have been used in implant rehabilitation. These digital techniques eliminate the need for making an impression using elastomeric impression material. These techniques capture images of the implant, adjacent, and opposing teeth with elimination of the dimensional stability of impression materials and the pouring of stone casts [37]. They use milling restoration from a sintered ceramic block with a very homogeneous structure which improves the quality of the material compared with conventional ceramic processing techniques [38–40].

According to the literature, zirconia crowns cemented on titanium abutments have an excellent prognosis [41]. This technique was used currently in the anterior region of the maxilla, especially when a patient has a thin gingival biotype and it is an aesthetic alternative to other dental materials.

The stiffness typical of this material does not seem to be a problem, because the superstructure is cemented on a titanium bar, which is the gold standard material for this type of prosthesis, as it is soft and has excellent shock absorption. Moreover, the cementation with a material based on zinc oxide ensures good retention but can also be easily removed [42–47]. For the superstructure material zirconia was chosen because it is a material that can replicate, with a fully digital workflow, the data acquired from the diagnostic prosthesis, which makes it possible to use already tested parameters.

Finally, there is a further advantage, that is a reduction of the time required by the laboratory for a similar work, which translates into a reduction of costs for the laboratory, for the clinician and the patient.

Conclusion

After 5 years clinical observation, this clinical study demonstrates that the zirconia crowns cemented on titanium bars using the CAD/CAM compound prosthesis can be used in clinical practice with high success. Moreover, the computerized workflow of this manufacturing process ensures reproducible results and excellent adaptation and passive insertion of these bars. A condition that guarantees stability of the crestal bone and screw-implant abutments and avoids biological or mechanical complications.

In fact, no evidence of chipping or delamination of the ceramic veneering on the zirconia crown supported were observed and a good satisfactory of occlusion are recorded with 100% of implant survival. The importance of the present paper on 5-year results, although on a relatively limited number of patients, reports a restorative principle where mid-term data are absent from the literature. However, due to the limitations associated with the use of only nine case reports and 90 implants, further research is required to confirm this.

Abbreviations

3D: Three-dimensional; CAD/CAM: Computer-aided design and computer-aided manufacturing; CBCT: Cone-beam computed tomography

Acknowledgements

We wish to thank all the staff of Dental Team Work and in particular Raoul Pietropaolo for his valuable contribution to this project and his diagnostic temporary prosthesis.

Authors' contributions

AS performed the main study and drafted the manuscript. MS and TC helped to acquire data. TC analyzed and interpreted the data. AS was a major contributor in designing the manuscript. AS designed the main scheme of the research and modified the manuscript. All authors read and approved the final manuscript.

Funding

No funding was obtained for this study.

Availability of data and materials

The datasets used and/or analysed during the current study are available from the corresponding author on reasonable request.

Ethics approval and consent to participate

The University of Chieti-Pescara, Italy, classified the study to be exempt from ethical review as it is not carries risk and involves the use of existing data that contains only non-identifiable data about human beings. A consent to participate was requested for this research. All patients signed a written informed consent form.

Consent for publication

Not applicable.

Competing interests

The authors declare that they have no competing interests.

Author details

¹Department of Medical, Oral and Biotechnological Sciences, University "G. D'Annunzio" of Chieti-Pescara, Via Dei Vestini, 31, 66100 Chieti, Italy. ²Zirconia Implant Research Group (Z.I.R.G), International Academy of Ceramic Implantology, Silver Spring, USA. ³L'Aquila, Italy. ⁴Termoli, Italy.

Received: 10 September 2019 Accepted: 11 December 2019

Published online: 19 December 2019

References

1. Scarano A, Lorusso F, Orsini T, Morra M, Iviglia G, Valbonetti L. Biomimetic surfaces coated with covalently immobilized collagen type I: an X-ray photoelectron spectroscopy, atomic force microscopy, micro-CT and histomorphometrical study in rabbits. *Int J Mol Sci*. 2019;20(3):724–40.
2. Scarano A, Carinci F, Lorusso F, Festa F, Bevilacqua L, Santos de Oliveira P, et al. Ultrasonic vs drill implant site preparation: post-operative pain measurement through VAS, swelling and crestal bone remodeling: a randomized clinical study. *Materials*. 2018;11(12):2516–29.
3. Mangano C, Piattelli A, Scarano A, Raspanti M, Shibli JA, Mangano FG, et al. A light and scanning electron microscopy study of human direct

- laser metal forming dental implants. *Int J Periodontics Restorative Dent*. 2014;34:e9–17.
4. Nissan J, Narobai D, Gross O, Ghelfan O, Chaushu G. Long-term outcome of cemented versus screw-retained implant-supported partial restorations. *Int J Oral Maxillofac Implants*. 2011;26:1102–7.
5. Chee W, Felton DA, Johnson PF, Sullivan DY. Cemented versus screw-retained implant prostheses: which is better? *Int J Oral Maxillofac Implants*. 1999;14:137–41.
6. Hebel KS, Gajjar RC. Cement-retained versus screw-retained implant restorations: achieving optimal occlusion and esthetics in implant dentistry. *J Prosthet Dent*. 1997;77:28–35.
7. Lewis S, Beumer J, Hornburg W, Moy P. The "UCLA" abutment. *Int J Oral Maxillofac Implants*. 1988;3:183–9.
8. Michalakakis KX, Hirayama H, Garefis PD. Cement-retained versus screw-retained implant restorations: a critical review. *Int J Oral Maxillofac Implants*. 2003;18:719–28.
9. Karl M, Taylor TD, Wichmann MG, Heckmann SM. In vivo stress behavior in cemented and screw-retained five-unit implant FPDs. *J Prosthodont*. 2006;15:20–4.
10. Korsch M, Obst U, Walther W. Cement-associated peri-implantitis: a retrospective clinical observational study of fixed implant-supported restorations using a methacrylate cement. *Clin Oral Implants Res*. 2014;25:797–802.
11. Montero J, Macedo de Paula C, Albaladejo A. The "Toronto prosthesis", an appealing method for restoring patients candidates for hybrid overdentures: a case report. *J Clin Exp Dent*. 2012;4:e309–12.
12. Zarb GA, Bolender CL. *Prosthodontic treatment of edentulous patients: complete dentures and implant-supported prostheses*. 12th ed. St. Louis: Mosby; 2004.
13. Maló P, de Araujo Nobre M, Petersson U, Wigren S. A pilot study of complete edentulous rehabilitation with immediate function using a new implant design: case series. *Clin Implant Dent Relat Res*. 2006;8:223–32.
14. Maló P, de Araujo Nobre M, Lopes A, Francischone C, Rigolizzo M. "All-on-4" immediate-function concept for completely edentulous maxillae: a clinical report on the medium (3 years) and long-term (5 years) outcomes. *Clin Implant Dent Relat Res*. 2012;14(Suppl 1):e139–50.
15. Maló P, Rangert B, Nobre M. "All-on-four" immediate-function concept with Brånemark system implants for completely edentulous mandibles: a retrospective clinical study. *Clin Implant Dent Relat Res*. 2003;5(Suppl 1):2–9.
16. Cappare P, Sannino G, Minoli M, Montemezzi P, Ferrini F. Conventional versus digital impressions for full arch screw-retained maxillary rehabilitations: a randomized clinical trial. *Int J Environ Res Public Health*. 2019;16(5):829–44.
17. Mangano F, Gandolfi A, Luongo G, Logozzo S. Intraoral scanners in dentistry: a review of the current literature. *BMC Oral Health*. 2017;17:149.
18. Ferrini F, Sannino G, Chiola C, Cappare P, Gastaldi G, Gherlone EF. Influence of Intra-Oral Scanner (I.O.S.) on The Marginal Accuracy of CAD/CAM Single Crowns. *Int J Environ Res Public Health*. 2019;16(4):544–53.
19. Mangano F, Margiani B, Admakin O. A novel full-digital protocol (SCAN-PLAN-MAKE-DONE®) for the design and fabrication of implant-supported monolithic translucent zirconia crowns cemented on customized hybrid abutments: a retrospective clinical study on 25 patients. *Int J Environ Res Public Health*. 2019;16(3):317–37.
20. Attard NJ, Zarb GA. Long-term treatment outcomes in edentulous patients with implant-fixed prostheses: the Toronto study. *Int J Prosthodont*. 2004;17:417–24.
21. Scarano A, Noubissi S, Gupta S, Inchingolo F, Stilla P, Lorusso F. Scanning electron microscopy analysis and energy dispersion X-ray microanalysis to evaluate the effects of decontamination chemicals and heat sterilization on implant surgical drills: zirconia vs. steel. *Appl Sci*. 2019;9:2837.
22. Candotto V, Lauritano D, Carinci F, Bignozzi CA, Pazzi D, Cura F, et al. Silver-based chemical device as an adjunct of domestic oral hygiene: a study on periodontal patients. *Materials*. 2018;11(8):1483–90.
23. Noubissi S, Scarano A, Gupta S. A literature review study on atomic ions dissolution of titanium and its alloys in implant dentistry. *Materials*. 2019;12(3):368–383.
24. Sarikaya I, Hayran Y. Effects of dynamic aging on the wear and fracture strength of monolithic zirconia restorations. *BMC Oral Health*. 2018;18:146.
25. Dauti R, Cvikl B, Franz A, Schwarze UY, Lilaj B, Rybaczek T, et al. Comparison of marginal fit of cemented zirconia copings manufactured after digital impression with lava™ C.O.S and conventional impression technique. *BMC Oral Health*. 2016;16:129.
26. Meirowitz A, Bitterman Y, Levy S, Mijiritsky E, Dolev E. An in vitro evaluation of marginal fit zirconia crowns fabricated by a CAD-CAM dental laboratory and a milling center. *BMC Oral Health*. 2019;19:103.
27. Papadiouhou S, Pissiotis AL. Marginal adaptation and CAD-CAM technology: a systematic review of restorative material and fabrication techniques. *J Prosthet Dent*. 2018;119:545–51.
28. Faeghinejad M, Proussaefs P, AlHelal A, Lozada J. The CAD/CAM compound prosthesis: digital workflow for fabricating cement-retained zirconia prosthesis over screw-retained milled titanium bars. *Int J Periodontics Restorative Dent*. 2019;39:39–47.
29. Abdou J, Bennani V, Waddell N, Lyons K, Swain M. Assessing the fit of implant fixed prostheses: a critical review. *Int J Oral Maxillofac Implants*. 2010;25:506–15.
30. Jemt T. Failures and complications in 391 consecutively inserted fixed prostheses supported by Brånemark implants in edentulous jaws: a study of treatment from the time of prosthesis placement to the first annual checkup. *Int J Oral Maxillofac Implants*. 1991;6:270–6.
31. Mangano F, Veronesi G. Digital versus analog procedures for the prosthetic restoration of single implants: a randomized controlled trial with 1 year of follow-up. *Biomed Res Int*. 2018;2018:5325032.
32. Adell R, Lekholm U, Rockler B, Brånemark PI. A 15-year study of osseointegrated implants in the treatment of the edentulous jaw. *Int J Oral Surg*. 1981;10:387–416.
33. Brånemark PI, Engstrand P, Ohnrell LO, Gröndahl K, Nilsson P, Hagberg K, et al. Brånemark Novum: a new treatment concept for rehabilitation of the edentulous mandible. Preliminary results from a prospective clinical follow-up study. *Clin Implant Dent Relat Res*. 1999;1:2–16.
34. Maló P, Araújo Nobre MD, Lopes A, Rodrigues R. Double full-arch versus single full-arch, four implant-supported rehabilitations: a retrospective, 5-year cohort study. *J Prosthodont*. 2015;24:263–70.
35. Scarano A, Di Carlo F, Quaranta M, Piattelli A. Bone response to zirconia ceramic implants: an experimental study in rabbits. *J Oral Implantol*. 2003;29:8–12.
36. Scarano A, Piattelli M, Caputi S, Favero GA, Piattelli A. Bacterial adhesion on commercially pure titanium and zirconium oxide disks: an in vivo human study. *J Periodontol*. 2004;75:292–6.
37. Souza ROA, Özcan M, Pavanelli CA, Buso L, Lombardo GHL, Michida SMA, et al. Marginal and internal discrepancies related to margin design of ceramic crowns fabricated by a CAD/CAM system. *J Prosthodont*. 2012;21:94–100.
38. Renne W, McGill ST, Forshee KV, DeFee MR, Mennito AS. Predicting marginal fit of CAD/CAM crowns based on the presence or absence of common preparation errors. *J Prosthet Dent*. 2012;108:310–5.
39. Martins LM, Lorenzoni FC, de Melo AO, de Silva LM, de Oliveira JLG, de Oliveira PCG, et al. Internal fit of two all-ceramic systems and metal-ceramic crowns. *J Appl Oral Sci*. 2012;20:235–40.
40. Tezulas E, Yildiz C, Kucuk C, Kahramanoglu E. Current status of zirconia-based all-ceramic restorations fabricated by the digital veneering technique: a comprehensive review. *Int J Comput Dent*. 2019;22:217–30.
41. Gehrke P, Bleuel K, Fischer C, Sader R. Influence of margin location and luting material on the amount of undetected cement excess on CAD/CAM implant abutments and cement-retained zirconia crowns: an in-vitro study. *BMC Oral Health*. 2019;19:111.
42. Woelber JP, Ratka-Krueger P, Vach K, Frisch E. Decementation rates and the peri-implant tissue status of implant-supported fixed restorations retained via zinc oxide cement: a retrospective 10-23-year study. *Clin Implant Dent Relat Res*. 2016;18:917–25.
43. Pjetursson BE, Asgeirsson AG, Zwahlen M, Sailer I. Improvements in implant dentistry over the last decade: comparison of survival and complication rates in older and newer publications. *Int J Oral Maxillofac Implants*. 2014;29(Suppl):308–24.
44. Schwarz S, Schröder C, Corcodel N, Hassel AJ, Rammelsberg P. Retrospective comparison of semipermanent and permanent cementation of implant-supported single crowns and FDPs with regard to the incidence of survival and complications. *Clin Implant Dent Relat Res*. 2012;14(Suppl 1):e151–8.
45. Testori T, Del Fabbro M, Capelli M, Zuffetti F, Francetti L, Weinstein RL. Immediate occlusal loading and tilted implants for the rehabilitation of the atrophic edentulous maxilla: 1-year interim results of a multicenter prospective study. *Clin Oral Implants Res*. 2008;19:227–32.
46. Agliardi E, Panigatti S, Clericò M, Villa C, Maló P. Immediate rehabilitation of the edentulous jaws with full fixed prostheses supported by four implants:

interim results of a single cohort prospective study. *Clin Oral Implants Res.* 2010;21:459–65.

47. Di P, Lin Y, Li J, Qiu L, Chen B, Cui H. Clinical study of "All-on-4" implant immediate function in edentulous patients. *Zhonghua Kou Qiang Yi Xue Za Zhi.* 2010;45:357–62.

Publisher's Note

Springer Nature remains neutral with regard to jurisdictional claims in published maps and institutional affiliations.

Ready to submit your research? Choose BMC and benefit from:

- fast, convenient online submission
- thorough peer review by experienced researchers in your field
- rapid publication on acceptance
- support for research data, including large and complex data types
- gold Open Access which fosters wider collaboration and increased citations
- maximum visibility for your research: over 100M website views per year

At BMC, research is always in progress.

Learn more biomedcentral.com/submissions



The Digital Dentistry Society (DDS) Global Conference 2019 Baden Baden, Germany



Digital
Dentistry
Society

The **Digital Dentistry Society** (DDS) Global Conference in Baden Baden, in october 2019. A beautiful venue, an incredible number of great speakers from all over the world, an impressive series of lectures and workshop, an intense social activity.

Digital Dentistry
Society



MEETING ABSTRACTS

Open Access



Proceeding of the International Digital Dentistry Society World Congress, Baden Baden 2019

Baden Baden, Germany. 3-6 October 2019

Published: 3 December 2019

The Digital Dentistry Society Poster Session- 3rd October 2019, Kurhaus Baden Baden, 9am- 3pm Science

P01

Quantitative accuracy of cone-beam computerised tomography (CBCT) derived biomodels

Sohaib Shujaat, Eman Shaheen, Constantinus Politis, Reinhilde Jacobs OMFS IMPATH Research Group, Department of Imaging and Pathology, Faculty of Medicine, University of Leuven and Oral & Maxillofacial Surgery, University Hospitals Leuven, Leuven, Belgium

Correspondence: Sohaib Shujaat (sohaib.shujaat@kuleuven.be)

BMC Oral Health 2019, 19(Suppl 1):P01

Abstract

Background: Biomodeling in integration with digital imaging techniques such as intra-oral scanning and cone-beam computerized tomography (CBCT) is being commonly practiced in dental implantology for pre-operative treatment planning, clinical teaching and evaluating bone density and drilling techniques. The objective of following study was to assess the quantitative accuracy of CBCT-derived mandibular biomodels.

Methods: A CBCT dataset was segmented and mandible was isolated. Fifteen mandibular biomodels were fabricated utilizing multi-jet (MJ=4), digital light processing (DLP=4), stereolithography (SLA=2), fused deposition modeling (FDM=2), colorjet (CJ=2) and selective laser sintering (LS=1) based high-end commercial and in-house printers. Printed models were superimposed onto the original mandible for comparing surface accuracy. A part comparison analysis with color-coded map was carried out for evaluating the difference between each printed and original model surface.

Results: MJ technology showed least amount of error associated with both erupted and impacted teeth. Highest bony surface accuracy was achieved with SLA and LS based biomodels. Trabecular structures were most accurately printed with MJ printers. FDM technology had the highest overall absolute mean error associated with both teeth and bone. No significant differences were observed between each surface of original and printed models.

Conclusions: Overall biomodels were able to well replicate skeletal and dental anatomical surfaces. However, some models showed shortcomings in relation to depicting trabecular architecture which might influence bone density for drilling bone and placing dental implants.

P02

A new system for augmented reality composite dynamic vision of a surgical site for medical device guided placement

Marco Farronato¹, Davide Farronato²

¹Department of Orthodontics, Fondazione IRCCS Ca' Granda, Ospedale Maggiore Policlinico, University of Milan, via Francesco Sforza 35, 20122 Milano, MI, Italy; ² School of Medicine and Surgery, University of Insubria, Via G. Piatti 10, 21100 Varese, Italy.

Correspondence: Marco Farronato (marcofarronato@msn.com)

BMC Oral Health 2019, 19(Suppl 1):P02

Abstract

Background. On the base of the state of the art on the applications of augmented reality (AR) in dentistry from previous studies a new system was developed and *in vivo* tested with Institutional Review Board approval of the Ethics Committee of Policlinico of Milan (n. 421). The purpose of the new system is to provide a new light, portable hand-held smart device which provides a compound superimposed dynamic vision of the anatomical structures of the patient, radiologic exams and digitally positioned medical devices for AR-guided operations.

Methods. CBCT data and the .stl files of miniscrews (TADs), (Leone, Firenze, Italy), were imported in a dicom viewer, placed in the correct position and fixed, then exported to .stl format separately. The digital images were uploaded to a server and opened with a smart, light hand-held hardware. The hardware was placed in front of the patient placed in N.H.P and the new software was started. Superimposition was regulated with pinch gesture on the touch screen until correct positioning of the frontal teeth of the patient, the opacity of digital images were regulated with a function of the software. The superimposition was automatically stabilized by a function of the software using software development kit (SDK) engines. Tads were placed under the guide of the compound vision. Time measurements were taken on superimposition by different operators and the error was calculated with a digital caliper.

Results. The new system provided effectively a dynamic functional compound superimposition of anatomical structures and previously digitally placed medical devices. The error in the positioning of the TADs was calculated as < of 0.3 mm for both while time measurements of the superimposition session were less than 5 minutes for each session.

Conclusions. The new proposed system effectively provides a simple and light dynamic AR superimposition of digital data on a surgical site



providing the clinician a compound vision of anatomical structures. The TADs were placed with AR assisted surgery with a acceptable error, further in vivo and in vitro studies are needed.

P03

Flat to Flat Vs Magic Five Cone Morse Connection regarding height/width ratio of peri-implant buccal soft tissues

Cristian Scognamiglio¹, Stefano Ponti², Veronica Campana³, Davide Farronato⁴

Correspondence: Cristian Scognamiglio (c.scognamiglio93@gmail.com)

¹DDs, Private Practitioner, Milan, Italy; ²DDs, Private Practitioner, Varese, Italy; ³Dentistry Student, University of Insubria, Varese, Italy; ⁴PhD, PD, AP, Assistant Professor, University of Insubria, Varese, Italy
BMC Oral Health 2019, 19(Suppl 1):P03

Abstract

Purpose. Modern implantology has been focused on the peri-implant mucosa maturation patterns, with particular attention on the frontal area, aiming to obtain an optimal aesthetic result. The purpose of the following study is to analyze height/width proportion in the peri-implant buccal tissues between two different types of connection: Flat to Flat and Magic Five Cone Morse Connection (Anyridge®).

Methods. The present study analyzes 294 implants, the measurements were done with digital 3D technology at one year from the provisional crown placement. Every single implant was matched with its own Scan Body and was scanned with 3Shape D700, in order to obtain a tridimensional section of the model. Peri-implant measurements included the width of the peri-implant mucosa (HV), calculated from the implant connection to the buccal mucosa surface on a line perpendicular to the main implant axis. For the height of the peri-implant tissues (VV), we considered as well, the same geometrical line as the apical point of the measure to calculate the perpendicular distance to the most coronally gingiva point. All the recorded data were analyzed with Test Pearson 2-Tailed (95% Confidence Interval) by IBM® SPSS® Statistics Software. The study protocol was approved by the local Ethics Committee.

Results. The average ratio between height/width of the two different types of connection were compared. Flat to Flat Connection shows an average VV:HV ratio equal to 1:1.54. Meanwhile, Magic Five Cone Morse Connection has an average ratio of 1:1.18. This results are statistically significant at $p \leq 0,001$ (Pearson 2-Tailed).

Conclusions. This study based on 294 implants approved Nozawa's past observations on 14 cases: the average ratio of VV:HV in Flat to Flat connection is 1:1.54. Analyzing the new Magic Five Cone Morse Connection results, the average ratio VV:HV is 1:1.18, showing higher efficiency on biological integration tending to the natural tooth parameters investigated by Wennström: VV:HV = 1,5:1. The differences discovered between the two types of connections can be linked to the "Pumping Effect" described by Zipprich and these data refers to one year maturation period. Therefore, when a transverse load is applied on a Flat to Flat Connection, there is a tendency to create a micro gap between the implant and the prosthetic abutment interface. The presence of the gap induces micro movements that may work as a pump allowing bacterial endotoxins contamination, compromising the peri-implant soft tissue trophism.

P04

How to optimize tissue for the Coronally Advanced Flap. Interaction between emergence profile and tissue tropism

Luciano Laveglia¹, Veronica Campana², Marco Colombo³, Davide Farronato⁴

¹Dentistry Student, University of Insubria, Varese, Italy; ²Dentistry Student, University of Insubria, Varese, Italy; ³DDs, Private Practitioner, Milan, Italy; ⁴PhD, PD, AP, Assistant Professor, University of Insubria, Varese, Italy

Correspondence: Luciano Laveglia (llaveglia@outlook.it)

BMC Oral Health 2019, 19(Suppl 1):P04

Abstract

Background. Several operative protocols recommend the realisation of cervical restorations to restore CEJ in patients undergoing mucogingival plastic surgery. The purpose was to evaluate the response of gingival tissues following the emergency profile restoration with , in patients subsequently subjected to Mucogingival surgery.

Methods. Data were collected from 50 teeth, 47 of which were affected by vestibular recession and 3 without recession. The STL files for the 2 stone models made after the alginate imprint detected prior the conservative therapy (T0) and after at least 60 days (T1) were analyzed. The three dimensional matching of the 2 models was carried out by the Geomagic Software and subsequently, with Mesh-mixer, a series of ortho-shaped and parallel (cutter) planes were superimposed (0 + 0.5 mm, 0 + 1mm, 0 + 1.5 mm) in the Coronal and apical direction considering how to plan 0 the T0 buccal zenith of the analyzed element. The desired measurements were obtained using 3D Viewer visualization software, going to measure the distance between the cutter intersections with the models T0 and T1. The study was conducted in accordance with the fundamental principles of the Helsinki Declaration and was approved by the Ethics Committee at Insubria University.

Results. After the modification of the emergency profile, the thickness and height of the gingival tissue at the level of the free gingival margin has increased statistically significantly with a ratio of the 2 variables is equal to 1.183. Moreover, the increase in tooth thickness corresponds to an increase in the thickness of the gingival margin at the zenith according to a ratio of 1.8:1. Moreover, in subjects with Biotype 2 (festoneate), a greater reduction in the recession was detected compared to those with biotype 1 (thin).

Conclusions. The realization of 5-class restorations with an increased emergence profile performed 2 months prior to the periodontal surgery shows clinical advantages.

P05

Implementation of Automated Digital Odontometry in Studies of Tooth Crown Morphology

Armen Gaboutchian¹, Kristina Goryainova², Samvel Apresyan², Vladimir Knyaz^{3,4}

¹Moscow State Medical-Stomatological University, Moscow, Russia; ²Peoples Friendship University of Russia, Moscow, Russia; ³State Research Institute of Aviation System, Moscow, Russia; ⁴Moscow Institute of Physics and Technology, Moscow, Russia

Correspondence: Kristina Goryainova (kristina@dda-russia.ru)

BMC Oral Health 2019, 19(Suppl 1):P05

Abstract

Background. To propose a method for objective, robust and precise assessment of tooth crown (natural of artificially designed) morphology, where tooth crown can be taken as a whole or in its integral parts, being analysed through variability of measured or calculated parameters. Related matters dealing with basic interpretation of dental morphology, formalisation of measurements and orientating of measured teeth are presented as well.

Methods. Experimental part of the study has been carried out on a sequence of 3D images obtained from dental arch casts, experimentally prepared teeth on the same stone cast models and modelled (digitally and manually) artificial crowns. Digitally modelled crowns were assessed in their default morphology and after reshaping by technician. A significant source of studied samples relates to palaeo-anthropological findings, which refer to various historical periods: Upper Palaeolithic, Early and Middle Bronze, Middle Ages and Modern Era. The studied images were obtained on dental and technical professional equipment (intraoral and laboratory scanners), custom designed photogrammetric scanners as well as on CBCT and micro-CT scanners. The scanning equipment, being chosen in accordance with the studied objects' characteristics, provided high resolution digital images. Merged images of objects, obtained on various stages

of the study or obtained on various equipment, were used as well. Measurements based on the proposed methods were carried out by means of software which provided, after 3D image loading, automated procedures of orientating, multidirectional sectioning modes, measurement landmark (point) detection, distance measurements, contour measurements, calculations, parameter presentation and analytical tools. Up to two hundred parameters are suggested in the current software version on each studied tooth section; the number of studied sections in the existing software version is limited by one hundred. The odontometric data includes linear, angular, contour parameters and coefficients referring to the whole crown or its parts. Results. Automatically generated odontometric data, obtained on series of images: intact tooth – manually modelled crown – suggested “on default” digital crown shape – reshaped digitally modelled crown, was compared in reference to maximal vestibular-oral dimension. Assessments included estimation of value and localisation of measured areas on tooth crown. Conclusions. Automated digital odontometry has demonstrated a potential for conducting measurements of tooth crowns. According to the obtained data, digital method of crown modelling can be considered more accurate and preferable in various terms of their usability. The work was performed with the support by Grant 17-29-04509 of Russian Foundation for Basic Research (RFBR).

P06

Analysis of the Height/Width ratio of peri-implant soft tissues in the different oral sectors

Stefano Ponti¹, Cristian Scognamiglio², Veronica Campana³, Davide Farronato⁴

¹DDs, Private Practitioner, Varese, Italy; ²DDs, Private Practitioner, Milan, Italy; ³Dentistry Student, University of Insubria, Varese, Italy; ⁴PhD, PD, AP, Assistant Professor, University of Insubria, Varese, Italy

Correspondence: Stefano Ponti (steponti@hotmail.it)

BMC Oral Health 2019, 19(Suppl 1):P06

Abstract

Purpose. During the past years, frontal areas rehabilitation has been one of the most important topic of discussion in Implantology. The aim of a good anterior restoration, implant supported, is to achieve function and aesthetic result. The purpose of the following study is to analyze using 3D technology the height/width proportion in the peri-implant buccal tissues comparing different areas in the oral cavity.

Methods. The present study analyzes 294 implants, the measurements were done with digital 3D technology at one year from the provisional crown placement. Every single implant was matched with its own Scan Body and was scanned with 3Shape D700, in order to obtain a tridimensional section of the model. Peri-implant measurements included the width of the peri-implant mucosa (HV), calculated from the implant connection to the buccal mucosa surface on a line perpendicular to the main implant axis. For the height of the peri-implant tissues (VV), we considered as well, the same geometrical line as the apical point of the measure to calculate the perpendicular distance to the most coronally gingiva point. The Implants were split into four main groups on the base of their position in the oral cavity:

1. Anterior Maxilla
2. Anterior Mandible
3. Posterior Maxilla
4. Posterior Mandible

All the recorded data were analyzed with Test Pearson 2-Tailed (95% Confidence Interval) by IBM® SPSS® Statistics Software.

Results. The average height/width ratio in the different areas of the oral cavity shows a significative difference between the anterior sectors and the posterior one.

1. Anterior Maxilla 1:1.23
2. Anterior Mandible 1:1.24
3. Posterior Maxilla, 1:1.45
4. Posterior Mandible, 1:1.77

These results are statistically significative at $p \leq 0,001$ (Pearson 2-Tailed).

Conclusions. This study based on 294 implants approves Nozawa's past observations on 14 cases: the average ratio of VV:HV is overall 1:1.54. Analyzing the differences between the four areas, we can assert that in the aesthetic sectors there is a ratio that follows the height of peri-implant soft tissue; on the other hand in the posterior sectors the ratio is unfavorable to the tissue height. These results might be linked to two different factors: a greater thickness of posterior soft tissues and the role of Buccinator Muscle which during the impression phases is able to pull the vestibular fornix reducing its height. In addition we should not forget that the aesthetic areas requires a specific attention regarding transparency of the abutment caused by thin width of the soft tissues.

P07

Key role in impression accuracy: transfer types or implant placement angulation? An in vitro 3D evaluation

Veronica Campana¹, Cristian Scognamiglio², Giada Goffredo³, Davide Farronato⁴

¹Dentistry Student, University of Insubria, Varese, Italy; ²DDs, Private Practitioner, Milan, Italy; ³DDs, Private Practitioner, Milan, Italy; ⁴PhD, PD, AP, Assistant Professor, University of Insubria, Varese, Italy

Correspondence: Veronica Campana

(v.campana@studenti.uninsubria.it)

BMC Oral Health 2019, 19(Suppl 1):P07

Abstract

Background. Accurate impression making is a fundamental prerequisite such to achieve a passive fit between the implant and the prosthetic structures. The aim of this study is to evaluate if there are differences in the accuracy of the impression using three different types of transfer and to analyze their efficiency in comparative situations given by different angles of implant placement.

Methods. An acrylic resin master model with four implant analogues placed at 0, 15 and 35 degrees towards the horizontal plan was used. Twenty-seven polyvinyl siloxane impressions of the model were made using acrylic resin individual impression trays with the aim of evaluating three different types of transfer: a closed tray technique transfer, a classic open tray technique transfer and a telescopic open tray transfer. The impressions were poured with type IV die stone. After matching each analogue with a digital scan body, an STL file was achieved with the scanner “3SHAPE D2000”. An implant bar was projected from all the different STL files with “3 Shape Dental System” software. Each project is originated from each different impression in order to gain the implant position referred by the transfer under analysis. A comparison between this bars and the one projected from the master model was obtained with “Magic Materialise 13.0” software. Both a linear and angular measurement (heads in x, y and z axes) for every type of transfer, valuated in different angulation, was achieved. The collected data have been processed by the statistical software “IBM SPSS Statistics, Armonk, New York, United States” and analyzed with student's T test and Kruskal-Wallis not parametric test.

Results. Even if the student's T test revealed a statistical significance of the different linear and angular measurements in Δx , Δy , Δz changing the transfer's type, more restrictive tests have highlighted a not statistical significance related to the transfer's type. However, when considering a variation of the implant positioning angle, the same tests revealed a statistically significant difference.

Conclusions. Considering the limitations of this study, it could be concluded that the type of transfer used is not a significant parameter

rather than the implant positioning showed a significant key role in the precision success of impressions.

P08

Drilling protocols in guided surgery: an in vitro study

Nicolò Vercellini¹, Veronica Campana²

¹Nicolò Vercellini DDS; Research Fellow, ITEB "Innovative Technology and Engineered Biomaterial" Research Centre, director Prof. Alberto Caprioglio. Department of Medicine and Surgery; University of Insubria, Varese, Italy; ²Dentistry Student, University of Insubria, Varese, Italy

Correspondence: Veronica Campana (veronica.campana93@gmail.com)
BMC Oral Health 2019, 19(Suppl 1):P08

Abstract

Background. Demonstrate the better accuracy of a computer-guided surgery that follows a complete drilling protocol which includes all the steps in order to reach the whole depth of implant placement. The most apical point is where may occurs the largest angle of deviation from the projected one and where the drill may not be initially guided by the sleeve. As a conclusion, this in-vitro-study is meant to demonstrate the better precision of a real double-guided surgery both from the progressive osteotomies and from the guide of the entry point.

Methods. A 3D model was created, projecting the positioning of a Ø3.8 x 13mm Camlog Conelog implant and a teeth supported template for guided surgery, with incisal-level windows in order to verify its right positioning on the dental elements. Dental SG resin (Formlabs) is the printing material used. Two kind of preparations are compared:

- A complete sequence from this moment indicated as CIP (complete implant preparation)
- A reduced sequence, indicated as RIP (reduced implant preparation), which doesn't include all the gradual steps of drilling preparation in length.

The osteotomies of the two sequences, CIP and RIP, are performed. The implants are positioned in the two models and subsequently, after the connection to a scan body, the model are acquired with an industrial certified scanner "3SHAPE D2000" (documented 5 micron accuracy ISO 12836; 4 x 5.0 MP cameras). Two STL files are obtained. The STL files are upload in Magics Materialize software and both implant positions (obtained with CIP and RIP) are compared with the initial implant positioning project.

In this way it was possible to verify the real implant position obtained with the complete CIP sequence and with the reduced sequence RIP.

Results. The superiority of the complete protocol (CIP) on the reduced one (RIP) is demonstrated. Compared to the implant placement of the initial project the RIP protocol gave a distance of 0.7823 mm and an angle of 1.42 deg; Instead, with the CIP protocol the implant was placed at a distance of 0.5235 mm and at an angle of 0.56 deg, always referred to the initial project.

Conclusions. Within the limitations of this in-vitro study it can be concluded that, in order to achieve a greater accuracy in guided surgery, it is recommend a progressive drilling protocol that guarantees a guidance provided not only by the sleeve, but also by the progressive osteotomies.

P09

Implants placed at 35 degrees: is a telescopic transfer more reliable? An in vitro 3D evaluation

Veronica Campana¹, Luciano Laveglia², Marco Colombo³, Davide Farronato⁴

¹Dentistry Student, University of Insubria, Varese, Italy; ²Dentistry Student, University of Insubria, Varese, Italy; ³DDs, Private Practitioner, Milan, Italy; ⁴PhD, PD, AP, Assistant Professor, University of Insubria, Varese, Italy

Correspondence: Veronica Campana (v.campana@studenti.uninsubria.it)
BMC Oral Health 2019, 19(Suppl 1):P09

Abstract

Background. The aim of this study is to compare the accuracy of three different transfers and to analyze their impression's accuracy in an high implant angulation at 35°. In addition to the classic transfers for the open tray and closed-tray impression techniques, it's tested also a telescopic open tray transfer. This last one is characterized by an inner hexagon that can sweep inside the outer body such to eliminate any extension of the connection under the conical interface. Moreover this study is meant to verify the incidence of the relative angulations between the transfer as well as if a 35° angulation pre-pone a favorite choice depending on this angle. The null hypothesis to validate was that there would be no differences in 3D accuracy between 3 different transfers when tested at 35°.

Methods. A resin master model with 4 implant analogues placed at 0 and 35 degrees towards the horizontal plan was used. 27 polyvinyl siloxane impressions were made using acrylic resin individual impression trays with the aim of evaluating 3 different types of transfers. The impressions were poured with type IV stone. After matching each analogue with a digital scan body a STL file of the impressions was achieved with "3SHAPE D2000" scanner. An implant bar was projected from all the STL files with "3 Shape Dental System" software. These bars indicate the implant positions referred by the transfer under analysis. A comparison between this bars and the one projected on the master model was obtained with "Magic Materialise 13.0" software. Both a linear and angular measurement for every type of transfer, valuated in different angulation, was achieved.

Results. All the measurements collected have been processed by the statistical software "IBM SPSS Statistics". The not parametric Jonckheere-Terpstra test was performed and astatistically significant difference between the transfer types at 35° inclination was found (p=0.023) when considering the angular displacement between them.

Conclusions. Within the limitations of this study it can be concluded that, even if the presence in the telescopic transfer of an inner hexagon that can sweep inside the outer body represents one more element of tolerance between the transfer body and the internal retractor hexagon, when tested at 35° it shows a greater precision and so the advantage to use a telescopic transfer in presence of tilted implants at high angulations seems the ideal solution.

P10

ROBOTA: From Digitalization to Automation & Data Analytics

Giorgio Castagno¹, Veronica Campana², Riccardo Castagno³

¹Doctor of Dental Surgery, Private Practitioner, Borgosesia, Italy;

²Dentistry Student, University of Insubria, Varese, Italy; ³Management

Engineering Student, LIUC University, Giussanella, Italy

Correspondence: Giorgio Castagno (giorgiocastagno@yahoo.it)

BMC Oral Health 2019, 19(Suppl 1):P10

Abstract

Background. Expose the project of an automated sterilization chain and the related advantages, such as the reduction of high cycle-times, of the elevate risk of contaminations and of the huge production of waste. These are enemies that make the daily process stressful. We are reorienting the sterilization chain into a manufacturing system in order to obtain jobs' continuous flow. Through value stream mapping, a method for analyzing the current state of events that take place from the beginning of the process to its end, we in fact observed that a change in the sterilization process is needed.

Methods. The low value processes in dentistry operations are analyzed with "Lean and Six Sigma Dentistry". An analysis of "Industry 4.0 system" that handle the sterilization is performed from the infected utensils' carriage, with an Automated Guided Vehicle, to the disinfection, continuing to the wrapping process and storage using robots (Kr3 Agilus KUKA, Grugliasco, Italy). An integrated vision system scan which tools the system is processing: data are acquired during the entire process. ROBOTA can represent a powerful tool to optimize sterilization routine processes and to increase utensils fulfillment.

Results. ROBOTA can reduce the time spent to sterilize surgical instruments. It can works 24/24h so operators can dispose of a bigger amount of envelopes' stock such to satisfy every demand. In this way

it's not necessary to buy same utensils multiples time. It's also able to track the tools consumption so that the utensils' lifespan can be exploited as maximum as possible. In addition, optimizing the whole process chain, less energy is required from the autoclave, whereas less heat is dissipated from the waiting time between one cycle to the next. The digital processes are automated, so manpower's presence and human error is not only reduced, but also eliminated, and not only for patients, but also for operators. ROBOTA can change the medical world, eliminating risky jobs and creating a higher level of service. This is an impactful tool that ensure to patients that the risk of contamination is close to 0 and the service can be faster. We're now able to connect ROBOTA with our agenda through Data Analytics: an algorithm examines data created from the system and draws info that can improve the way our Customer Management System program our daily clinical schedule.

Conclusions. ROBOTA can help to achieve the goal of reducing contamination risks and errors, ensuring at the same time higher level of sterilization.

P11

Jaw elevator muscles activity and pain on palpation with clear aligners. A prospective observational study

Alessandro Nota, Atanaz Darvizeh, Simona Tecco

Correspondence: Alessandro Nota (dr.alessandro.nota@gmail.com)

University Vita and Salute San Raffaele, Milan, Italy

BMC Oral Health 2019, 19(Suppl 1):P11

Abstract

Background. It is not clear, from the available literature, whether the orthodontic treatment with clear aligners, which has a not negligible thickness between the dental arches, is accompanied by adaptive changes in the electrical activity of the jaw elevator muscles. The aim of this study was to report the jaw elevator muscles activity and their pain on palpation during the early stages of orthodontic dental alignment with clear aligners.

Methods. Surface electromyography (sEMG) and pain level on muscle palpation of masseter and anterior temporalis muscles, were recorded in a sample of 16 adult subjects (18-32 years old; mean 22.5 +/- 3.5 SD) undergoing to orthodontic treatment with clear aligners. Data were recorded before the treatment (T0), after 1 month of treatment (two clear aligners) (T1), and after 3 months of treatment (T2).

Results. No statistically significant differences in muscular pain were observed over the time in the whole sample. At T1, in the test group, the electrical activity in the masseter area at mandibular rest position showed a statistically significant reduction respect to the baseline values, but after 3 months (T2), data appeared similar to T0 ($p=0.03$ and $p=0.02$).

Conclusions. During the early stages of an orthodontic treatment with clear aligners, the subjects could experience an initial reduction of the basal electrical activity of jaw elevator muscles, which tends to disappear quickly. The behavior of the muscles during the orthodontic dental alignment deserves to be investigated in the future because preliminary data indicate a certain muscular adaptation to orthodontic movements, that could occur at least during the very early stages of treatment with aligners.

P12

Comparison of the accuracy of 3-dimensional printed dental models manufactured with different additive technologies

Török Gréta, Borbély Judit, Hermann Péter, Barbara Kispélyi

Department of Prosthodontics, Semmelweis, Budapest, Hungary

Correspondence: Török Gréta (dtorokgreta@gmail.com)

BMC Oral Health 2019, 19(Suppl 1):P12

Abstract

Background. There are several different types of three-dimensional 3D printing technology that are appropriate for constructing dental models. In some cases, the cast has only a holder and carrier function during the whole digital workflow. Models with dies manufactured

by additive technology can be used during the construction of extended fixed partial denture. The purpose of this in vitro study was to assess the accuracy (precision and trueness) of 3D printed dental models and models with removable dies manufactured with scan LED technology (SLT) and stereolithography (SLA) and PolyJet printers.

Methods. A digital upper jaw model serves as a reference. In the initial model, the 15 and 16 teeth are missing, the 11, 14 and 17 teeth are prepared with supragingival chamfer preparation for fixed prosthetic appliance. The 26 tooth was prepared for inlay. To standardize the measurements 16 markers (1 mm diameter) were created on the digital model. After designing the reference markers the model was sectioned to get a model with removable dies using 3Shape Model Builder program. The physical dental models were printed 3 types of 3D printers and printed 5 times with each printer. 1. SLA technology (FormLabs Form2 printer, Dental Model Resin, with layer thicknesses 50 µm). 2. SLT technique (MediTech D30 printer, FotoDent Model material, layer thickness 50 µm) 3. PolyJet technique (Objet Eden 350V 3D printer, VeroFlexWhite, layer thickness 14 µm). The 3D printed models and sectioned models were scanned using a high-resolution industrial 3D scanner (3D System) within two weeks after printing. The accuracy of 3D scanning is ± 0.05 mm. The scanned models were saved as stl format and imported into the Geomagic Verify software to analyse the precision and trueness of 3D printers. After the superimposition, the whole deviation and distances between predefined reference points were measured with a digital caliper. Measurements for the 3 types of printed models were compared with the initial digital model. The deviation of 50 µm has been defined as the allowed deviation interval in prosthetic aspect.

Results. The accuracy of the investigated Objet, Meditech D30 and FormLabs Form2 printers is within the allowed deviation interval.

Conclusions. Within the limitation of this study it was concluded that PolyJet, SLT and SLA technologies are able to fabricate a clinically acceptable physical model that is essential for construction of high-precision fixed prosthetic appliances.

P13

In vitro study on digital splint effect to the accuracy of digital dental implant impression

Gedrimiene Agne¹, Rutkunas Vygandas², Auskalnis Liudas³, Jeglevicius Darius^{4,5}, Dirse Julius⁶, Bilius Vytautas⁷, Pletkus Justinas⁸

¹Phd Student, Department of Prosthodontics, Institute of Odontology,

Faculty of Medicine, Vilnius University; ²"Prodentum" Private Practice,

Vilnius, Lithuania; ³Associate Professor, Department of Prosthodontics,

Institute of Odontology, Faculty of Medicine, Vilnius University;

"Prodentum" Private Practice. Vilnius, Lithuania; ⁵Student, Institute of

Odontology, Faculty of Medicine, Vilnius University. Vilnius, Lithuania;

⁴Head of Laboratory, Biomedical Engineering Institute, Kaunas University

of Technology. Kaunas, Lithuania; ⁵Associate Professor, Department of

Electronics Engineering, Kaunas University of Technology. Kaunas,

Lithuania; ⁶Dentist, "Prodentum" Private Practice. Vilnius, Lithuania;

⁷Dentist, "Vilnius University Hospital Clinic of Žalgiris". Vilnius, Lithuania;

⁸Dentist, Institute of Odontology, Faculty of Medicine, Vilnius University,

Lithuania; "Prodentum" Private Practice. Vilnius, Lithuania

Correspondence: Pletkus Justinas (justinas.pletkus@gmail.com)

BMC Oral Health 2019, 19(Suppl 1):P13

Abstract

Background. Since IOS devices can only capture part of the object at a time, images have to be stitched together to form a 3D object and therefore it is the source of possible errors of the scan. The aim of this in vitro study was to compare the trueness and precision of three different IOS scanning partially and fully edentulous models with 2 or 4 implants with attached scan bodies and digital splints.

Methods. Two types of maxilla models were printed with AsigaMax 3D printer. The first model was missing both premolars and molars on the right side, so Straumann BL dental implants were inserted instead first premolar (straight) and second molar (tilted 20°mesially). Four implants were inserted in the second edentulous model symmetrically at second incisors (straight) and first molar areas (tilted 20°

mesially). Scan bodies were attached to the implants and models were scanned with Nikon Altera 10.7.6. coordinate measurement machine (CMM) to form a reference scan. DII was taken with a Primescan (version 5.0.1), CS 3600 (version 3.1.0), Trios3 (version 1.18.2.10) IOS ten times each (n=10) without digital splint. After that, tablets of hardened Fuji Plus cement was glued in edentulous areas to form digital splint and all models were scanned with three different IOS. Scanning data was exported in standard tessellation language format for analysis. All scans were aligned on the reference scan precisely by applying best-fit alignment procedure. Distance and angulation between scan bodies were measured aligning CAD models of scan bodies to the scanned surfaces of scan bodies.

Results. Trueness of distance and angle in Carestream partially edentulous models was 185 µm in the group with splint and 280 µm without one and 0.22° in the group with splint and 0.29° in the group without respectively. Precision of distance and angle measurements in the splint groups were 87 µm and 0.13°, in the groups without-202 µm and 0.25°. In fully edentulous models trueness of distance varied 53-106 µm in the groups with splint and 67-8µm in the groups without.

Trueness of Primescan in partially edentulous models with splints was 21µm and 0.16° in distance and angular measurements. Without splints-27µm and 0.21°. For fully edentulous models trueness and precision of distance and angle was better in groups with splint than without. Trueness of distance and angle of Trios3 in partially edentulous splinted models was 15 µm and 0.3°; 53 µm and 0.11° in unsplinted models respectively. For fully edentulous splinted models trueness of distance and angle varied 32-122µm and 0.19-0.51°, for unsplinted models-17-80µm and 0.1-0.45°.

Conclusions. Primescan showed the best results of trueness and precision of distance and angle measurements. Since digital splints improve the accuracy of DII, the impact of their forms and materials should be more researched.

P14

Effect of intraoral scanner, printer and digital analog system on accuracy of 3D printed models

L. Auskalnis¹, D. Jeglevičius^{2,3}, M. Akulauskas², A. Gedrimienė⁴, T. Simonaitis⁵, R. Jurgaitė⁵, Vygasdas Rutkunas⁶

¹Student, Institute of Odontology, Faculty of Medicine, Vilnius University, LITHUANIA; ²Engineer and Head of laboratory, Biomedical Engineering Institute, Kaunas University of Technology, LITHUANIA; ³Associate Professor, Department of Electronics Engineering, Kaunas University of Technology, LITHUANIA; ⁴PhD student, Department of Prosthodontics, Institute of Odontology, Faculty of Medicine, Vilnius University, LITHUANIA; ⁵Dental technician, UAB "ProDentum", Vilnius, LITHUANIA; ⁶Associate Professor, Department of Prosthodontics, Institute of Odontology, Faculty of Medicine, Vilnius University, LITHUANIA

Correspondence: Vygasdas Rutkunas (vygandasr@gmail.com)

BMC Oral Health 2019, 19(Suppl 1):P14

Abstract

Background. Digital workflow for producing implant-supported restorations involves the usage of intraoral scanners (IOS). From IOS data 3D printed master model is often fabricated using the selected type of digital analogs. There is a lack of data regarding the effects of IOS, 3D printer, and digital analog type on the local and global accuracy of digital analog positions in 3D printed master model. Moreover, errors arising in each step/stage should be identified.

Methods. Two Straumann BLT 4.1 mm RC implants were inserted in the reference model (REF) left quadrant, in the location of second premolar with 0° angulation and second molar with 5° angulation. Three calibration spheres of 5 mm in diameter (±1 µm) were placed

on the left quadrant at the model base. Scan bodies (3Shape) were attached to the implants and model was scanned with Nikon Altera 10.7.6. industrial scanner (REF-stl). REF model was scanned 10 times with E3 (3Shape) scanner for validation. Ten digital impressions were taken with Trios3 (3Shape) intraoral scanner (IOS-stl). The closest to the overall average of intraoral digital impressions STL file was selected for 3D printing. Asiga MAX and Next Dent 5100 3D printers were used to duplicate the reference model. Two types of digital implant analog systems were placed into the models: ELOS Print Model Analog and NT-trading DIM-ANALOG. In total 4 groups containing 10 quadrant 3D printed models were created. Later models were scanned with a validated E3 scanner (3D-print-stl). STL file superimpositions and measurements were performed using Geomagic Control X 2018 software. Distance, vertical shift, rotation and angulation measurements were made locally and globally.

Results. Validation procedure of E3 scanner showed the trueness of 26 µm and precision of 16.8 µm. Digital impression procedure with Trios 3 introduced 53 µm distance between the implants, 34.7 µm vertical shift, 0.283° angulation and 0.230° rotation errors locally. Comparison of REF_stl and 3D_print_stl files showed most accurate Asiga MAX and Elos PMA analog combination: 37.2 µm distance between the implants, 39.7 µm vertical shift, 0.212° angulation and 0.769° rotation errors locally. Majority of detected differences were statistically significant (p<0.05).

Conclusions. Asiga MAX 3D printer performed more accurately than NextDent 5100. ELOS Print Model Analog showed most accurate result both locally and globally than NT trading. Implant angulation of 5° provides more accurate analog position in the master model than 0° angulation. Intraoral scanning had significant influence in overall error propagation. Further studies are needed to evaluate other factors.

P15

Assessment of distortion caused by stitching during full arch intraoral scanning

János Vág, Evelin Kövér, Ákos Mikolicz, Zsolt Nagy

Department of Conservative Dentistry, Semmelweis University, Budapest, Hungary

Correspondence: János Vág (drvagianos@gmail.com)

BMC Oral Health 2019, 19(Suppl 1):P15

Abstract

Background. The field of application of today's intraoral scanners is extending from making single tooth restorations towards full arch rehabilitations. Scanning technique (scan pattern) are suggested to influence the scanning accuracy especially in case of full arch. The aim of this study was to measure distortion of 3D models created with full arch digital impressions by a novel method and compare with two existing methods.

Methods. Maxillary and mandibular models were captured with an intraoral scanner using four different scan patterns. Accuracy and distortion were assessed by comparing master scans to the intraoral scans using the following three methods: 1: Mean surface deviation was measured after complete arch superimposition. 2: 28 points were selected identically on the experimental and on the master reference models. Deviation between identical points was assessed after superimposition over the complete arch. 3: (Novel technique) The same 28 points were compared after superimposition limited to the scanning origin.

Results. Significant differences were found between the three different methods regardless of the arch and pattern. The overall mean deviation between identical points when models were aligned at the scanning origin was the highest and the mean deviation between

the non-identical values was the lowest. The new method revealed local, tooth-wise differences between scan pattern as well as pattern of error increasing with distance from scanning origin.

Conclusions. The new method better detects the cumulative deviation of stitching error in complete arch intraoral scans, and is suitable to investigate the effect of scanning pattern in a very sensitive manner.

P16

Comparison of distortion of seven intraoral scanners caused by stitching mechanism

Zsolt Nagy¹, János Vág¹, Anthony Mennito², Walter Renne²

¹Department of Conservative Dentistry, Semmelweis University, Budapest, Hungary; ²Department of Oral Rehabilitation, Medical University of South Carolina College of Dental Medicine, Charleston, South Carolina

Correspondence: Zsolt Nagy (nagyzsolt.dent@gmail.com)

BMC Oral Health 2019, 19(Suppl 1):P16

Abstract

Background. Usually full-arch accuracy of intraoral scanners (IOS) are measured by average deviation and does not taking into consideration the origin of scanning. However, during scanning, deviation is accumulating from the scanning origin till the last tooth on the arch. The aim of this work was to compare tooth wise kinetics of deviation of seven different IOS, all starting from the same scanning origin utilizing various hardware and software techniques.

Methods. Test digital models were produced by IOS of 7 different types on a human cadaver maxilla. All scans were started on occlusal surface of tooth 27 and ended up at tooth 17. Superimposition of test models with a master model were done in GOM Inspect software using a local best fit algorithm localized at the scanning origin. Deviation was measured between identical points and accumulated deviation (AD) was calculated at tooth 17. Deviation was also calculated separately on three axis, mesio-distal, bucco-lingual and apico-coronal. Data was statistically analyzed by generalized linear mixed model.

Results. The average full-arch deviation was 365±130 for CS, 535±116 for Element1, 247±27 for Element2, 320±48 for Emerald, 174±16 for Omnicam, 906±122 for Planscan, 156±25 for Trios3. AD was 524±92 for CS, 521±102 for Element1, 321±23 for Element2, 480±49 for Emerald, 408±21 for Omnicam, 1697±64 for Planscan, 235±18 for Trios3. These were not statistically different from each other except AD of Planscan which was significantly higher than all others. Deviation on apico-coronal axis at tooth 17 was higher than deviation measured on mesio-distal or bucco-lingual axis for Element2, Emerald, Omnicam, Planscan except CS, Element1 and Trios3. CS and Element1 had the highest coefficient of variation (56% and 79%) which might mask the difference in accuracy results.

Conclusions. Further away from scanning origin higher deviation values for all IOS were found and with most scanners, the deviation at apico-coronal axis related to the occlusal view was the highest. This suggests that proper selection of the tooth and the surface of origin may help to reduce deviation. The accuracy was improved considerably by manufacturers at the new generation of the same brand.

P17

Optical Properties of Monolithic CAD/CAM Zirconia Reinforced Lithium-Silicate Crowns

Alexandra Czizola¹, Zoltan Imre-Kovacs², Peter Hermann¹, Judit Borbely¹

¹Department of Prosthodontics, Faculty of Dentistry, Semmelweis University - Hungary - Budapest; ²Department of General Dental Preclinical Practice, Faculty of Dentistry, Semmelweis University - Hungary - Budapest

Correspondence: Alexandra Czizola (czizola.alexandra@dent.semmelweis-univ.hu)

BMC Oral Health 2019, 19(Suppl 1):P17

Abstract

Background. All-ceramic systems and CAD/CAM technics allow dentists to make monolithic restorations with reduced wall thickness. Glass-ceramic restorations are in the focus of interest. When the right color block of glass-ceramic material is selected for the restoration it must be taken into consideration, that the final esthetics are influenced by underlying tooth color due to their translucency. The aim of this in vitro study was to determine how substrate colors, ceramic thickness and translucency, cement shades effect the final shade of CAD/CAM monolithic zirconia reinforced lithium-silicate (VITA Suprinity) crowns.

Methods. According to our previously published study 1 premolar teeth (14) were prepared on a study model for 1.0 and 1.5-mm thick full ceramic monolithic crowns. Intraoral scanner was used (Trios, 3Shape) to create digital impressions. CAD/CAM technics were used to design (Dental Designer) and make crowns with identical shape and size. Shade A1 crowns were milled (Everest, Kavo) from HT (high translucency) and T (translucent) Vita Suprinity (Vita Zahnfabrik) zirconia reinforced lithium-silicate blocks. 9 substrates were made of different color and materials (6 of Vita Simulate composite material and zirconia, Co-Cr, gold-colored alloy) to imitate substrate effects on the final shade. Three different try-in pastes were used to simulate the color effect of cements (Variolink Esthetic Try-In paste, Ivoclar). Shade measurement was done 3 times for each crown by spectrophotometer (Vita, Easyshade Advance) and averages were compared to a reference crown (A1, 1.5mm, T, 2M35 abutment, neutral try-in paste). ΔE00 was calculated (CIEDE 2000 formula).

Results. All of the examined parameters influenced ΔE00 of the CAD/CAM monolithic crowns. The weakest effect was exerted by the color of the try-in paste. When ΔE value smaller than 1.8 is regarded as a clinically not acceptable color change 2, out of 108 measured combinations none of the HT and 19 of T crowns were below this threshold.

Conclusions. Before choosing the ceramic block translucency and restoration wall thickness we should consider the underlying abutment color, but final color was just barely affected by luting cement shade in case of 1.0 and 1.5 mm thick ceramic crowns.

Clinics

P18

Post-Extractive Implant Placement in Upper Molar region: Implant Preparation Guided by Dental Roots

Christian Monti (monti.christian@libero.it)

Lake Como Institute, Como (ITA); Dental Student, University of Varese, Italy

BMC Oral Health 2019, 19(Suppl 1):P18

Abstract

Background. The correct positioning of post-extractive implants in the upper posterior area is always a challenge, especially because of the maxillary sinus presence. The aim is therefore to propose, in selected cases, after a careful CT analysis, to use the roots themselves as an insertion-guide in order to obtain a clinical success.

Methods. A 45-years-old woman presented an important vestibular recession and a palatal fracture of element 16, requiring a morpho-functional restoration through implant-prosthetic rehabilitation. A CBCT was performed to evaluate the root trunk anatomy, the presence of inter-radicular bone and the maxillary sinus physiology. The 3D images showed divergent roots with a well-represented bone septum. In order to avoid drill off-setting through axial vibration, because not properly supported during the insertion, it was decided to prepare the implant site before extracting the roots: the tooth was uncrowned and the roots, thanks to their density and inclination, forming an effective guide for the correct three-dimensional osteotomy. The roots were then atraumatically removed, and the implant inserted. To avoid any buccal-bone resorption, a L-PRF Collagen Block was introduced in the peri-implant gap.

Results. A correct osseo-integration of the implant was documented, as well as an excellent response of the peri-implant tissues in the

follow-up carried out in the two years succeeding the placement. A gingival re-modeling was achieved with the disappearance of the vestibular recession, because of the wound being allowed to heal by secondary intention and using the L-PRF membranes as a tissue healing boost.

Conclusions. The illustrated procedure remains a valid alternative, although not a substitute, of traditional surgical techniques which are already fully described in literature. This particular site preparation has allowed the obtainment of a perfect implant axis, a predictable implant positioning and osteo-integration, favoring the success of the implant-prosthetic rehabilitation.

P19

Fractured Premolar Replacement with Post-Extraction Implant and Immediate Loading with Guided Gingival Recession Regeneration - Fully Digital in Office

Fabrizio Pedrinis¹, Jessica Dana²

¹Dental Studio Digitale – Via Pelli 13B Lugano (CH); ²Dental Student, University of Varese, Italy

Correspondence: Fabrizio Pedrinis (fabrizio@pedrinis.ch)

BMC Oral Health 2019, 19(Suppl 1):P19

Abstract

Background. The replacement of the first upper premolar of a patient who showed up with a root fracture, with a post-extraction implant; delivering also a temporary crown in the same session, which aims a spontaneous gingival regeneration of the pre-existing buccal recession, for an additional aesthetic rehabilitation.

Methods. The CBCT confirmed the radicular fracture and showed a bone structure with a conserved vestibular theca that allowed the insertion of an implant right after the extraction. This 3D radiological exam was imported into the RealGuide (3Diemme) implant design software together with the dental arches scan obtained with the Omnicam intraoral camera (Sirona). The ideal positioning of the fixture was planned with the same RealGuide software, as well as the surgical guide which was designed and printed in office with a Form2 printer (Formlabs). The extraction was performed in an atraumatic way and a 4 x 13 mm Megagen implant was placed with the help of the surgical guide. The ISQ value was 78, which confirmed the good primary stability. In the same session a temporary PMMA crown was formed with the Cerec Chairside method (Sirona). Particular attention was paid to the creation of an S-shaped emergency profile in order to promote gingival regeneration.

Results. The implant was well osseointegrated and after 3 months it was possible to observe a great gingival regeneration, which is always a prerequisite for a stable, aesthetic and functional result.

Conclusions. The fully-digital procedure performed entirely in office allowed the replacement of the fractured tooth within 2 hours. Thanks to the three-dimensional positioning guided according faithfully to the planification, and because of an accurate emergence profile design, a spontaneous gingival regeneration without any connective grafts was also obtained.

P20

Full Mouth Restoration with Immediate Loading

Alessandro Perucchi¹, Christian Monti², Jessica Dana³, Marco Del Prete⁴

¹Studio Odontoiatrico Dr. Alessandro Perucchi – Mendrisio (CH); ²Lake Como Institute, Como, Italy; ³Dental Student, University of Varese, Italy; ⁴Private Practice, Lugano, Switzerland

Correspondence: Alessandro Perucchi (alessandroperucchi@sunrise.ch)

BMC Oral Health 2019, 19(Suppl 1):P20

Abstract

Background. To rehabilitate both jaws of a patient in bad oral conditions is already a challenge in itself. It was intentional to try a motivational training in order to obtain the perfect prerequisites for an implant-prosthetic rehabilitation with a digital workflow. **Methods.** A woman showed up with a poor oral hygiene, without been going to any dentist for 6 years. She went through a depression and was

hospitalized for a year. Hence her desire to fix her teeth in a definitive way, in order to smile again. All the periodontal upper teeth were firstly extracted, and a removable prosthesis was delivered. Short after that her oral situation went really better, that's why it was decided to subsequently rehabilitate the mandibular arch with a Toronto prosthesis immediately loaded on 6 post-extractive Megagen implants, all digitally planned. Considering that her oral hygiene was definitively ameliorated, it was chosen to deliver also in the upper jaw a fixed prosthetic solution immediately loaded on six BLX implants. The vertical dimension was reproduced with a digital wax up, and on the six BLX implants were screwed six SRA (screw retained abutment).

Results. The patient has shown to have definitively improved her oral hygiene, and for this reason there are all the good conditions for a long-term maintenance of the implants. After a year she is very glad, satisfied and has finally returned to smile without being ashamed of her appearance.

Conclusions. With the digital workflow it has been possible to deliver on both jaws an immediate prosthesis in a very short time. The result is extremely satisfying, since it was not only a technical and clinical challenge, but also a matter of caring this lady on a path of personal growth and reconquering her self-esteem.

P21

Development of an evidence-based application for dental grinding evaluation and sleep bruxism monitoring

Patricia Tersi, Cristiane Macedo

Department of Evidence-Based Medicine, Paulista Medical School, Federal University of São Paulo, São Paulo, Brazil.

Correspondence: Patricia Tersi (drapatriciaterse@gmail.com)

BMC Oral Health 2019, 19(Suppl 1):P21

Abstract

Background. There are issues not clarified in the sleep bruxism (SB) field, some of them are associated to the present restrictions related to validity, sensitivity, specificity and poor correspondence between instrumental and non-instrumental diagnostic approaches. The current challenge is to establish more accurate, applicable, affordable and accessible approaches.

Aim: The aim of this study is to present and recommend the use of an innovative and technological smartphone-based approach for SB assessment. It is an evidence-based toll for tooth grinding evaluation and long-term sleep bruxism monitoring, enabling systematic data collection from SB self-report (I), clinical inspection (II) and tooth wear pattern (III).

Methods. The application uses principles of Artificial Intelligence (AI), bruxism consensus grade system statement and Ecological Momentary Assessment (EMA) to collect data from non-instrumental approaches with literature supported questions about self-report and clinical inspections. The image processing algorithms developed measure data from tooth wear pattern and its possible association with symptoms, comorbidities and risk factors.

Results. The findings of this study resulted in a smartphone-based approach for multifactorial SB assessment. With cloud storage, the data from this app can be used for clinical and research purposes.

Conclusions. This APP is an applicable and accessible approach for SB assessment, with algorithms that can contribute to a better understanding of the relationships between clinical assessment, self-report and tooth wear measurements.

P22

From intraoral scan to CAD-CAM no-prep partial veneers: a case report

Veronica Campana¹, Giada Goffredo², Luciano Laveglia³, Stefano Ponti⁴

¹Dentistry Student, University of Insubria, Varese, Italy; ²DDS, Private Practitioner, Varese, Italy; ³Dentistry Student, University of Insubria, Varese, Italy; ⁴DDS, Private Practitioner, Varese, Italy

Correspondence: Veronica Campana (v.campana@studenti.uninsubria.it)

BMC Oral Health 2019, 19(Suppl 1):P22

Abstract

Background. To present the esthetic and orthodontic outcome of multiple lithium disilicate ceramic partial veneers, produced through a full digital process that includes an IOS impression and the computer-aided design/manufacturing phases. In this case report the advantages of this digital technique are presented.

Methods. A digital scan was taken with 3Shape TRIOS 3 Intraoral Scanner (1). Data were sent to the digital laboratory service where the veneers were designed using CAD/CAM design software (3Shape dental system) and milled (2) from low translucency IPS e.max lithium disilicate (Vita A3) blocks (Ivoclar-Vivadent, Amherst, NY, USA) with a four axes milling machine (Vhf N4). A minimum thickness of 0.3 mm for the veneer and of 0.1 for the margins were set. A virtual marginal design was performed (3), checking with a 2D cross section the accuracy of the positioning of the veneer closing margin. The direction of insertion of the veneer was also designed and the occlusion was controlled through a virtual articulator. Veneers were then verified intraorally using a translucent try-in paste (Multilink Automix Try In, Ivoclar-Vivadent). All internal surfaces of the veneers were etched with 5% hydrofluoric acid for 25 seconds and silanated (Monobond Plus, Ivoclar-Vivadent). After conditioning the teeth surfaces with a primer (Multilink primer base/catalyst Ivoclar-Vivadent) the laminate veneers were cemented using a translucent light-cure resin cement (Multilink Automix Ivoclar-Vivadent). An occlusal check was performed, revealing the absence of interfering contact points both in protrusive and laterality. The study was conducted in accordance with the fundamental principles of the Helsinki Declaration and was approved by the Ethics Committee at Insubria University.

Results. The adaption and cementation to the teeth surfaces was clinically easy due to a well-designed planning phase that included not only the selection of the margin but also the detection of the axis of insertion: when this axis was involved in an undercut area, the software reports the error such to modify the design of the veneer. The aesthetic outcome of the lithium disilicate veneers was natural-looking and conservative, while providing high optical properties.

Conclusions. No-prep adhesive restorations are an excellent rehabilitative option for situations in which the dental elements are healthy and can be modified exclusively by an additive plane of treatment, for example if there is a need to compensate the limitations of an orthodontic treatment. The digital workflow allowed the fabrication of satisfying clinical results in terms of marginal fit, shape and aesthetics.

Science

P23

Application of intraoral scanner to identify monozygotic twins

Botond Simon¹, János Vág², Ádám D. Tárnoki³, Dávid L. Tárnoki³

¹SCRUNCH Ltd., Budapest, Hungary; ²Department of Conservative Dentistry, Semmelweis University, Budapest, Hungary; ³Department of Radiology, Semmelweis University, Budapest, Hungary

Correspondence: Botond Simon (dr.simon.botond@gmail.com)

BMC Oral Health 2019, 19(Suppl 1):P23

Abstract

Background. Current methods for identify the monozygotic (MZ) twinning are either invasive such as blood sample taking or expensive as DNA sequencing. Palatal rugae has been suggested previously as a marker of human identity. The aim of this study was to evaluate the 3D digital pattern of the palatum and rugae acquired by intraoral scanner in order to distinguish identical monozygotic twins from one another and to differentiate MZ from dizygotic twins (DZ).

Methods. Palatal area of 36 participants (MZ: 25; DZ: 11) was scanned three times with an intraoral scanner. The age of twins was between 18 and 60 years. Ethical approval was granted on July 26, 2018 by the Hungarian authority called Committee of the Health Registration and Training Center (approval number: 36699-2/2018/EKU). From the scanned data STL file was created and exported into GOM Inspect® inspection software. Each scan within a twin pair was superimposed to each other. The average deviation between scans of the same subject

(reproducibility) and between scans of two subjects within a twin pair (intertwin comparison) were calculated with 95% confidence interval.

Results. The mean reproducibility of the palatal scan was 33 µm (31-36 µm). The intertwin deviation of MZ was 361 µm (324-402 µm) which was significantly ($p < 0.001$) higher than the reproducibility values. The deviation of dizygotic twin pairs was significantly higher (+642 µm, 491-838 µm, $p < 0.001$) than the deviation of monozygotic pairs.

Conclusions. MZ twins can be differentiated from each other accurately by palatal morphology obtained by intraoral scanner. This method may differentiate MZ and DZ twins as well but it requires further study. The alignment method is capable to identify monozygotic twin pairs. This could be a great advantage in forensic science and in twin studies.

Clinics

P24

The facilitated esthetic orthodontic treatment with clear aligners and minimally invasive corticotomy: the importance of digital planning

Simona Tecco (simtecc@gmail.com)

San Raffaele University, Milan, Italy

BMC Oral Health 2019, 19(Suppl 1):P24

Abstract

Background. During the last decades, accelerating orthodontic tooth movement, has become a topical issue and there have been many attempts to shorten treatment duration. Among the different techniques described in the literature, the corticotomy seem to be an effective and safe mean. Corticotomy is an intentional injury to the cortical bone able to accelerate orthodontic tooth movement and dramatically reduce treatment times because it leads to a biological stage called regional acceleratory phenomenon (RAP) characterized an intensified osteoclastic activity, resulting in osteopenia and increased bone modeling. Nevertheless recently, the piezocision technique was introduced, performed under local anesthesia through a tunnel approach overcoming most of the disadvantages of traditional corticotomy. Simultaneously, orthodontic treatment with removable clear aligners has become an increasingly common treatment choice because of adult patients that desire aesthetic and comfortable alternatives to conventional fixed appliances. Being aesthetics and treatment duration the principal adult patients expectations, the aim is to illustrate the planning of a combined approach with piezocision corticotomy and clear aligners orthodontic treatment.

Methods. Two case reports are described, an open-bite and a closure of extraction spaces. After performing polyvinylsiloxane or digital impressions of the dental arches and sending it to the manufacturer a proper aligners orthodontic planning using the digital software (Clin-Check, Align Technology, Santa Clara, CA, USA) the orthodontist identified the time window in which the most difficult orthodontic movements had to be performed. The surgical procedure was planned and executed as starting point of this period in which each aligner will be used for 4 days rather than 15 days for a total time of 4 months. A careful planning of the ideal attachments for correctly expressing the aligner execution of these movements was necessary.

Results. Clinical results obtained were satisfactory results, as seen in figure 1 and figure 2 for the openbite and the space closure, respectively.

Conclusions. In order to underwent to accelerated esthetic orthodontic treatment (AEOT) applying a corticotomy surgical technique to orthodontic clear aligners treatment (Invisalign, Align Technology, Santa Clara, CA, USA), each subject should be carefully evaluated. A cone-beam computed tomography should be added to the standard orthodontic examination (anamnesis, extraoral and intraoral examination and photographs, dental casts, orthopantomography, cephalometry). The primary objective of this combination should be to facilitate difficult and less predictable orthodontic movement in addition to reduce the treatment duration, simultaneously, the long term risk of relapse should be reduced.

P25

Implant open-flap and flapless placement using dynamic navigation: a pilot controlled clinical trial

Gerardo Pellegrino (gerardo.pellegrino2@unibo.it)

University of Bologna, Italy

BMC Oral Health 2019, 19(Suppl 1):P25

Abstract

Background. Dynamic navigation is a computer-guided technique offering different advantages with respect to conventional free-hand implant insertion. Some of these are an accurate and prosthetic-based implant placement, the surgical time reduction and safe use of a less invasive surgical procedure, like the flapless technique. This technique allows a higher patients comfort but is more challenging and is usually associated with less accurate placement of the fixture with respect to an open-flap method. The aim of this controlled clinical trial is to investigate the accuracy of implant placement comparing open-flap and flapless technique using a dynamic navigation system.

Methods. 12 patients were consecutively recruited and allocated to the flapless or open-flap group depending on soft tissue parameters. Implant position was planned on the preoperative CBCT according to the prosthetic project using dedicated software. A total of 20 implants were placed: 11 with a flapless technique and 9 with the conventional open-flap method. The surgery was performed with the navigation system according to the virtual planning. The deviation between the real implant position obtained from the post-operative cone-beam computed tomography and the planned one was measured. Data were statistically analyzed using a Mann-Whitney U test.

Results. The errors of implant placement using a flapless approach were 0.88 ± 0.50 mm (range 0.46-1.84 mm) at the insertion point and 1.09 ± 0.62 mm (range 0.48-2.28 mm) at the apical point. The depth error was 0.37 ± 0.29 mm (range 0.03-0.86 mm) and the angular deviation was $4.78 \pm 2.58^\circ$ (range 1-9.7°). Using a conventional open-flap technique, the errors were 1.06 ± 0.48 mm (range 0.45-2.21 mm), 1.40 ± 0.58 mm (range 0.59-2.21 mm), 0.45 ± 0.37 mm (range 0.18-1.41 mm), and $7.13 \pm 4.76^\circ$ (range 1.4-15.9°), respectively. The values of the two groups were not significantly different ($p=0.43$, $p=0.27$, $p=0.59$, $p=0.20$). No difference was found between the conventional open-flap and flapless approaches in terms of the accuracy of implant placement.

Conclusions. Therefore, the use of a navigation system can overcome the drawback of a "blind" technique and ensure a high level of accuracy.

P26

Conventional and tilted implants placement using dynamic navigation: a case series

Gerardo Pellegrino (gerardo.pellegrino2@unibo.it)

University of Bologna, Italy

BMC Oral Health 2019, 19(Suppl 1):P26

Abstract

Background. Tilted implants are used instead of bone regenerative techniques, allowing a more conservative approach. Dynamic navigation is a computer-guided technique allowing accurate implant placement and safe use of minimally invasive surgical procedures, like flapless and tilted implant insertion. The aim of this study is to report a series of cases in which implant placement was performed using a dynamic navigation system combining tilted approach and flapless technique. The secondary objective was to assess implants placement accuracy.

Methods. Three patients needing implant-prosthetic rehabilitation in the maxilla and having atrophy of the posterior area are treated (Ethics Committee approval number 104/2018/DISP/AUSLBO). For each

patient, two implants (BTK, Biotec Srl, Italy) are planned, one of these tilted engaging the available alveolar bone and avoiding the maxillary sinus. The surgeries were performed with a dynamic navigation system (ImplaNav, BresMedical, Sydney, Australia) and all the implants were placed using a flapless approach. The implants were exposed after three months. The accuracy of implant placement was assessed measuring the deviations between the positioned and the planned implants comparing pre- and post-operative CBCT.

Results. No complications occurred and both tilted and conventional implants reached the osseointegration. The mean deviations of implants placed with a conventional technique were 0.93 ± 0.61 mm at the insertion point, 1.27 ± 0.78 mm at the apical point and 0.42 ± 0.29 mm in depth. The angular deviation was $4.53 \pm 2.44^\circ$. The mean deviations of tilted implants were 1.03 ± 0.64 mm at the insertion point, 1.39 ± 0.81 mm at the apical point and 0.43 ± 0.24 mm in depth. The angular deviation was $4.62 \pm 2.94^\circ$.

Conclusions. The use of dynamic navigation can be considered a reliable and safe technique in implantology. It allows the placement of implants using a conservative and safe approach even though more challenging procedures are performed. The accuracy values seem to be similar using a tilted or a conventional technique of implant placement.

P27

Augmented reality for dynamic navigation displaying: a report of two cases

Gerardo Pellegrino (gerardo.pellegrino2@unibo.it)

University of Bologna, Italy

BMC Oral Health 2019, 19(Suppl 1):P27

Abstract

Background. Dynamic navigation is a computer-guided surgery technique used in dental implantology. The employment of navigation systems offers different advantages, as accurate placement of the fixtures. Many authors reported good results in terms of implant placement accuracy using this method. A drawback of this technique is the need to turn away from the surgical field to look at the monitor of the navigation system. Augmented reality (AR) is a technology employed in different surgical fields, as neurosurgery, vascular surgery, and maxillofacial surgery. Nevertheless, only few dentistry studies are available to date. The aim of this study was to present two clinical cases of navigated implant surgery associated with the use of augmented reality and to report the accuracy of implant placement using both the devices.

Methods. Two patients needing implant-supported rehabilitation in the upper premolar area were treated. Implant position was planned on the preoperative CBCT according to the prosthetic project using dedicated software. For each patient, an implant (WinSix, Ancona, Italy; Straumann, Switzerland) was placed by the same surgeon using a dynamic navigation system (ImplaNav, BresMedical, Sydney, Australia) and AR glasses (Fifthingenium, Milan, Italy).

Results. The navigation system allowed the operator to see the implant planning and to follow drills and implant position on the CBCT of the patient. With the association of the augmented reality device, the navigation screen was directly displayed near the surgical field. Both the implants were placed with a flapless technique. The accuracy of implant placement was evaluated measuring into CBCTs the deviation between real and planned positions of the implants. The deviation values for the first implant were 0.53 mm at the entry point and 0.50 mm at the apical point; for the second implant were 0.46 mm at the entry point and 0.48 mm at the apical point. The angular deviations were respectively 3.05° and 2.19° .

Conclusions. The use of AR glasses allowed the surgeon to have at the same time both the view of the surgical field and the position of the virtual drills without the need to turn away from the working

position. The use of augmented reality applied to dynamic navigation allowed a reduced operating time and led to accurate values of implant placement. The association of these two technologies seems to be promising in dental implantology. More studies are needed to confirm these results.

P28

Esthetic performance of different CAD/CAM all-ceramic implant-supported crowns via digital workflows in the esthetic zone: a case report

Krisztina Mikulas¹, Tamás Chikány², Peter Hermann¹

¹Department of Prosthodontics Semmelweis University, Maxdental - Hungary – Budapest; ²Intellident - Hungary – Budapest

Correspondence: Krisztina Mikulas (dr.mikulas@gmail.com, mikulas.krisztina@dent.semmelweis-univ.hu)

BMC Oral Health 2019, 19(Suppl 1):P28

Abstract

Background. Successful esthetic outcome in implant rehabilitation can be resulted through accurate implant placement, management of supraimplant soft tissues and appropriate biomaterials. Provisional restorations (PR) have a decisive role in soft-tissue contouring and preservation during maturation period after implant placement. Correct 3D capturing of the supraimplant emergence profile of PR allow predictable definitive restorations. This case report follows a recently known indirect scanning technique recommended in case of rapidly collapsed supraimplant mucosa and based on production of three different anterior all-ceramic implant-supported crowns via complete or semi digital workflow. **Methods.** At baseline a 49 year old female patient with fracture of tooth 22 was treated. Immediate implant placement (BL, Straumann AG) was performed in a correct palatal and apico-coronal position, buccal gap was grafted with xenograft (Creos, Nobel Biocare AG). Immediate provisionalisation was carried out chairside. After healing period and creating harmonious supraimplant emergence profile we performed intraoral digital impression (CARES Intraoral Scanner) generating standard triangulation language files (STL) based on three digital impressions. The merged file of STL1, 2, 3 was used to design CAD/CAM abutments made of Y-TZP (Straumann CARES), single crowns and then a 3D stereolithographic model was printed for the semi-digital way. Two different CAD/CAM abutments were designed and milled for three different all-ceramic restorations. The outcome variables were the esthetic outcomes of the three all-ceramic crowns. Firstly a cement-retained monolithic zirconia crown on individualized CAD/CAM abutment was fabricated via complete digital workflow without any physical model. Next cement-retained pressed ceramic crown (IPS e.max CAD HT) was performed. Finally a one-piece screw-retained single crown based on CAD/CAM abutment veneered with hand buildup technique was delivered, which was finally inserted after the esthetic evaluation.

Results. The esthetic outcomes (PES and WES values) were pleasing overall for the three all-ceramic restorations.

Conclusions. Ideal shaping of provisional at immediate implant placement helps stabilize the bone graft material within the blood clot during healing and develop the desired emergence profile. The individualized zirconia abutment may provide an ideal surface for soft tissue adhesion with less plaque accumulation. Both complete digital and semi digital prosthetic pathways resulted in appropriate clinical performance in the esthetic zone and simplified the clinical procedures.

Written, informed consent for publication was obtained from the patient [or parent/guardian for patients under 16]

P29

Digital workflow to perform esthetic and functional rehabilitation of oligodontia with occlusal veneers and implant supported crowns, case report

Judit Borbely¹, Peter Hermann¹, Peter Windisch², Szandra Körmendi¹

¹Department of Prosthodontics Semmelweis University, Hungary – Budapest; ²Department of Periodontics Semmelweis University, Hungary – Budapest

Correspondence: Judit Borbely (borbely.judit@dent.semmelweis-univ.hu)

BMC Oral Health 2019, 19(Suppl 1):P29

Abstract

Background. Agenesis of teeth is one of the most common of human developmental anomalies. Oligodontia is the congenital agenesis of 6 or more permanent teeth. Multidisciplinary treatment approach calls for pre-prosthetic orthodontic space opening for proper positioning of the missing teeth and correction of inter-maxillary relations. High-quality CAD/CAM materials processed by digital workflow offer predictable and reliable treatment options for surgical and prosthetic phases of therapy.

Methods. A 23-year old girl presented with oligodontia and no stable occlusion in premolar, molar region. Two years of orthodontic treatment created space for implant placement but stable occlusion could not be achieved. Diagnostic wax-up was made on casts mounted on articulator (Kavo Protar 5B, Kavo Dental GmbH, Germany) programmed to individual patient parameters. Optical impression (TRIOS 3, 3Shape, Denmark) was taken as prepreparation scan to record occlusal morphology and contour of crowns. Mock-up served as a guide to follow a minimal invasive preparation approach. Prepared teeth scan was aligned under prepreparation scan and fit to occlusal morphology. Following adhesive cementation of milled hybridceramic occlusal veneers (Vita Enamic, Vita Zahnfabrik, Germany) and stabilizing occlusion digital workflow was used for fixed implant rehabilitation.

Results. A prosthetic-driven backward implant planning and guided implant placement (AstraTech EV Implant System, diameter 3 mm, DentsplySirona Implants, Sweden)(SMART Guide, dicomLAB, Hungary) was performed. The protocol required conventional impression and cone beam computed tomography (CBCT), the superimposition of dental-gingival information on bone anatomy, surgical planning, 3D-printed teeth-supported surgical templates, and implant placement. After 3 months optical impression was carried out to detect 3D implant position to digitally design temporary crowns(Vita CadTemp, Vita Zahnfabrik, Germany) and soft tissue conditioning was done slightly by flow resin composite. After creating harmonious supraimplant emergence profile intraoral scan was taken and customized titanium-nitride abutments and milled zirconia cut-back crowns (Atlantis, Dentsply Sirona Implants, Sweden) were delivered. Model manufacturing was performed using a 3D printer and screw retained veneered ceramic crowns attached to implants.

Conclusions. This article describes a conventional protocol for creating a mock up to preview esthetics and create proper occlusion using individually programmed articulator and digital workflow of

milled occlusal veneers and implant supported crowns for predictable esthetic and reliable functional result. Written, informed consent for publication was obtained from the patient [or parent/guardian for patients under 16]

P30

CAD/CAM Chairside Monolithic Restoration in Esthetic Region with Minimally Invasive Preparation

Mariann Danko¹, Judit Borbely¹, Zoltan Imre-Kovacs²

Correspondence: Mariann Danko (dankomariann@upcmil.hu)

¹Semmelweis University, Faculty of Dentistry Department of Prosthodontics - Hungary - Budapest; ²Semmelweis University, Faculty of Dentistry, Department of General Dental Preclinical Practice - Hungary - Budapest

BMC Oral Health 2019, 19(Suppl 1):P30

Abstract

Background. During the development of CAD/CAM technology in dentistry, numerous new ceramic material were introduced for monolithic restorations. Improved optical features of the materials make it possible to produce monolithic restorations also in esthetic region. Reduced wall thickness compared to veneered restorations allows minimally invasive preparation. Chairside design and production unnecessary 3D printed model. The aim of the study was to describe the chairside CAD/CAM method of making a monolithic crown in the esthetic region with minimally invasive preparation and to compare esthetic features and wall thickness of different material selection: monolithic zirconia, hybridceramic and glass-ceramic.

Methods. A 17-year old girl presented with the need of an esthetic solution for her microdont maxillary central incisor after orthodontic treatment. A minimally invasive treatment concept was used with 0,6 mm reduction. After the rounded shoulder preparation an intraoral scan was taken by Trios POD Wireless scanner. (TRIOS, 3Shape, Denmark) Monolithic crown was designed in 3Shape Design Studio chairside software with the mirroring technique of the contralateral first incisor. Because of the limited space, materials were selected which can be produced with 0,8 mm wall thickness:

1. hybrid ceramic (VITA Enamic HT Multilayer)
2. zirconia-reinforced lithium silicate ceramic (VITA Suprinity PC HT)
3. high-translucency zirconia (VITA YZ HT Color)
4. medium-translucency zirconia (Ivoclar IPS e.max ZirCAD MT Multilayer)
5. low-translucency zirconia (Ivoclar IPS e.max ZirCAD LT)

During the production, the instructions of the manufacturers and clinically proven facts according to the minimum wall thickness were followed. Prosthodontists were asked to compare the crowns using Pink Esthetic Score and White Esthetic Score (PES/WES).

Result. On the basis of the prosthodontists' comparison and patient choice, the zirconia-reinforced lithium silicate glass ceramic crown had been cemented with adhesive technique.

Conclusions. According to this study it seems that the optical features of the monolithic zirconia and hybrid ceramic restorations in the anterior region are not satisfying yet. Only zirconia and hybrid ceramics can be used in minimally invasive case of 0,8 mm according to the instructions of the manufacturers. Glass-ceramic is not indicated under 1,2 mm circumferential and 1,5 incisal wall thickness. However clinical experiences proved, that with adhesive cementation of a glass-ceramic crown, the reduction is allowed, so the most esthetic zirconia-reinforced lithium silicate ceramic could be cemented. Written, informed consent for publication was obtained from the patient [or parent/guardian for patients under 16]

P31

Digital mockup: evaluation of masticatory muscles function. An observational study

Francesca Cattoni, Atanaz Darvizeh, Vincenzo Sanci, Simona Tecco
University Vita-Salute San Raffaele, I.R.C.C.S. Ospedale San Raffaele - Italy - Milano

Correspondence: Simona Tecco (simtecc@gmail.com)

BMC Oral Health 2019, 19(Suppl 1):P31

Abstract

Background. Recently, the roles of occlusion and masticatory muscles have become fundamental in dental rehabilitations. The mockup is used to pre-visualize the final rehabilitations and it can be utilised to test both esthetic and functional patterns before realising the final treatment. The aim of this observational study was to investigate the impact on masticatory muscles by means of measuring electromyographic activity and making a comparison between computer-aided designed/manufactured mockup (digital mockup) and traditional mockup.

Methods. The sample included 22 adult patients, aged 20 to 55 years who were about to receive a prosthetic rehabilitation and did not have any signs of periodontal or systemic disease. A digital or traditional mockup was made for each of the patients. Electromyographic activity of masticatory muscles were evaluated before initiating the treatment (T0), after the mockup insertion (T1), and after treatment (T2) by using the occlusal contact analyzer software called Teethan (Teethan s.p.a., Garbate Milanese, Milan, Italy).

Results. Analysis of parameters at different times for both groups revealed significant variations for most of parameters. The analysis of traditional group revealed a significant variation in POC AT and IMP at "T0 vs. T1" and "T0 vs. T2", BAR at "T0 vs. T2" and TOT at all 3 time comparisons. In digital group, POC MM and TORS at "T1 vs. T2" and "T0 vs. T2", BAR at "T0 vs. T1" and "T0 vs. T2" and TOT at all 3 time comparisons showed a significant difference. The comparison between the two groups (traditional and digital) at different time gaps revealed that at Δ1 (T1-T0) only POC AT and IMP showed significant differences and no other significant variation was observed between the two groups at Δ2 (T2-T1) and Δ3 (T2-T0). It concludes that traditional and digital methods generally have nonsignificant differences. **Conclusions.** Useful reduction in working time and higher degree of precision in fabrication process of mockup can be obtained by applying the digital technique. Therefore new technological advancement can greatly assist the operator, with a substantially valuable impact. But for ensuring the final restoration of a muscular symmetric function both traditional and digital methods can still be considered to be effective and applicable procedures.

Science

P32

Eagle syndrome: a rare case of calcified ligament with an articulated structure inside

Simona Tecco (simtecc@gmail.com)

San Raffaele University, Milan, Italy

BMC Oral Health 2019, 19(Suppl 1):P32

Abstract

Background. Eagle syndrome, or calcification of the stylohyoid ligament, is a rare condition characterized by a mineralization of Mineralization of the stylohyoid ligament occurs infrequently and is usually only an incidental finding noted on routine radiographic examination. Eagle syndrome is diagnosed only when the facial or neck pain originates from a stylohyoid ligament that is calcified. This clinical presentation was identified in 1937 by W.W. Eagle. From a radiographic perspective, Eagle syndrome may be a common incidental finding on routine panoramic radiographs, although only a

very small percentage of patients with calcified stylohyoid ligaments present with clinically significant symptoms. Currently, the use of computed tomography (CT) or cone beam CT (CBCT) scanning, with or without three-dimensional reconstruction, is essential to establish an Eagle syndrome diagnosis and to appropriately plan individual patient management.

Methods. This paper reports a case of Eagle syndrome individuated with a CBCT 3D reconstruction, and reviews the literature regarding management options for Eagle syndrome. A case-report of an adult Caucasian patient is reported. The patient has referred to a private practice office in Milan, due to a Temporomandibular joint disorder with neck pain. A complete examination with also a CBCT scanning revealed the presence of an articulated calcified stylohyoid ligament, very particular due to the particular articulation, similar to a knee useful to maintain a mobility of the ligament.

Results. Eagle syndrome may be appropriately diagnosed via a detailed history, physical examination, and radiological evaluation. CBCT and 3D digital reconstructions represent the main diagnostic tool.

Conclusions. This disease process can be confused with many other conditions that must be excluded in the differential diagnosis, mostly through 3D digital reconstructions, to allow appropriate prompt patient management.

Clinics

P33

Digital Orthodontics: Technology in Modern Practice

Alessandro Nota, Darvizeh Atanaz, Valter Firbo, Simona Tecco
University Vita- Salute San Raffaele, Milan Italy

Correspondence: Alessandro Nota (dr.alessandro.nota@gmail.com)
BMC Oral Health 2019, 19(Suppl 1):P33

Abstract

Background. The aim of this study is to describe the integration of technology with clinical orthodontics. New digital technologies appear essential to the success of any orthodontic practice seeking to increase efficiency and communication. The aim of the present study is to describe a practical digital workflow in clinical orthodontics.

Methods. A useful workflow to integrate digital impression, model storage, orthodontic treatment planning, and customizing the orthodontic appliances with the support of a dental laboratory is described. Advantages are exposed, and limits are discussed, with a particular focus on the clinical point of view.

Results. Digital technology could enhance the ability of the orthodontist to diagnose and treatment plan, using high resolution graphics and model analysis measurements. It also could allow the orthodontist to easily interact with the laboratory, improving the final satisfaction of the patients.

Conclusions. A whole digital workflow appears particularly useful in orthodontics also to reduce estimates costs for manufacturing of oral appliances.

P34

Effectiveness of Shade Measurement Using Intraoral Scanner Compared with Digital Spectrophotometer and Visual Shade Assessment

Ivett Roth (yvettroth@gmail.com)
Semmelweis University, Budapest, Hungary
BMC Oral Health 2019, 19(Suppl 1):P34

Abstract

Background. In digital shade measurement digital spectrophotometer is used as a gold standard. New intraoral scanner system was developed with a tool for teeth shade measurement, but there is less information about its efficiency. The aim of this study was to evaluate shade measurement function of a digital scanning system in relation to visual shade determination and digital spectrophotometric device.

Methods. 10 dental students from Semmelweis University took digital impressions and measured tooth shade for 10 different patients using 3Shape Trios intraoral scanner (TR). Students also selected

shade using 2 visual methods: Vita A1-D4 (VC) and Vita Linearguide 3D-Master (LG) shade guides and an instrumental method: Vita Easyshade (ES). The study was ethically approved by the Semmelweis University Institutional Review Board (SE-TUKEB 61/2016). The inclusion criteria of patients were full dentition and no prosthetic restorative treatment. Students had no previous experience in intraoral scanning and tooth color matching, they attended an education course: lecture and training on intraoral scanning and shade matching methods with shade tabs and digital devices. The students matched the color of 3 teeth for each patient: 11 – cervical, central, incisal, 14 – central, 16 – central. Time spent on shade matching were recorded. For each tooth there was a VC shade- tab, an LG shade- tab and LG-shade tab according to ES measurement. Four selected shade tabs were presented to the patient, the student and an experienced dentist to select the best match. The results were recorded and evaluation of percentage was calculated.

Results. The percentages of the selected best matching shade tabs out of the 4 methods: LG: 35,08%, ES: 26,58%, TR: 21,64%, VC: 16,7%. Time spent on shade matching by the 4 different shade matching methods: ES: 14,12 sec, TR:40,06 sec, VC: 52,42 sec, LG: 70,47 sec.

Conclusions. Intraoral scanner (TR) was acceptable for shade measurement. In case of digital impression taking using another device for shade matching wasn't necessary, color results were showed automatically. The fastest shade matching procedure was digital spectrophotometer (ES) followed by intraoral scanner. Most "best fit shade tabs" were selected with visual method (LG). Shade selection with visual method took the most time.

P35

A sport injury of the left mandibular angle in a young adult allows to discover a morphological alteration of the other condyle. A case report

Atanaz Darvizeh, Alessandro Nota, Simona Tecco
University Vita- Salute San Raffaele, Milan, Italy
Correspondence: Atanaz Darvizeh (atanazdarvizeh@gmail.com)
BMC Oral Health 2019, 19(Suppl 1):P35

Abstract

Background. The purpose of this work is to present a clinical case in which digital image analysis has allowed a more accurate diagnosis in the context of Temporomandibular disorders (TMDs)

Methods. The clinical case of a patient who presented himself to our observation due to a sports trauma (a calcium) directed to the left mandibular angle, is described. Immediately after trauma, the patient was hospitalized in a maxillofacial unit of another structure, where he was subjected to a two-jaws block in protruded mandibular position for a period of some weeks, after which he has been resigned. After some months, he has turned to our structure for signs and symptoms of TMD, and malocclusion. The patient was prescribed an RMI of the Temporo-mandibular joints, a CBCT and routine investigations.

Results. The analysis of digital records allowed the diagnosis of a morphological anomaly of the right condyle, which had not been detected previously, since at the maxillofacial department only an analysis of the left side (involved in the trauma) has been performed

Conclusions. The present clinical case suggests that, in contrast to the current clinical guidelines, in case of trauma involving the jaw, mostly the Temporo-mandibular joints, a gnathological evaluation by a specialist dentist should always be considered.

P36

Guided, socket shield, immediate loaded implantation, case report

Lukasz Zadrozny, Leopold Wagner
Medical University of Warsaw - Poland
Correspondence: Lukasz Zadrozny (lukasz.zadrozny@gmail.com)
BMC Oral Health 2019, 19(Suppl 1):P36

Abstract

Background. Proper implant positioning in the post-extraction socket is crucial for the function, durability and aesthetics of the future

prosthetics. In the esthetic zone even more challenging and very difficult is to maintain the shape and structure of the tissues surrounding the tooth after its removal. Literature presents many techniques aimed at preserving tissues after tooth extraction in the best possible condition. One of them, described in 2010 by M. Hurzeller, whom proposed the retention of the buccal root segment after extraction- Socket-Shield technique. Other authors analyse it histologically and have presented many clinical cases. Furthermore, socket shield technique was classified as one of partial extraction techniques which is highly promising and may significantly influence management of the failing dentition, changing a concept from extract and augment to salvaging the patient's own tissues where possible.

Methods. This clinical report presents digitally guided approach to perform partial extraction therapy where the tooth has to be replaced by an implant immediately. A 38-year-old female patient presented fracture of clinical crown in tooth 21. Clinical examination revealed total mobility of composite crown from palatal site. Because of direction and depth of crown fracture the tooth was classified to be extracted. Digital model of patient dentition was prepared as the stl file and superimposed over dicom files from CBCT examination. Implant position and surgical guide were digitally planned in DDS-Pro software (DDS-Pro). Temporary crown was designed in Exocad (Exocad GmbH) software and milled in PMMA. After preparing of buccal root segment the osteotomy for 4,0x11,5 implant (Hiossen TSIII NH, Osstem Implants) was performed through 3D printed sleeveless guide with OneGuide Kit (Osstem Implants). Implant was placed palatal to the shield with initial stability 35 Ncm. PMMA crown was bonded to temporary abutment and attached to an implant with torque of 20 Ncm.

Results. Postoperative CBCT revealed proper implant positioning and maintaining a buccal root shield.

Conclusion. The modern dental care philosophy aims to preserve dental tissue as much as possible, even when tooth extraction is required. Very important are also time of treatment and addressing aesthetic and functional expectations of the patient. Presented case required a thorough planning phase but offered a possibility of not losing a tooth from aesthetic point of patient's view. Considering perfect implant positioning and maintaining the best condition of hard and soft tissues, presented in this study technique, combining PET with guided implantation, could be a valuable tool to restore teeth especially in the aesthetic region.

Written, informed consent for publication was obtained from the patient [or parent/guardian for patients under 16]

Science

P37

Graphical principle of STL superimposition: approbation of complex approach in peri-implant results evaluation

Goncharuk-Khomyn Myroslav (myroslav.goncharuk-khomyn@uzhnu.edu.ua)

DDS, MMSc, PhD-candidate, Head of the Scientific and Research Centre of Forensic Dentistry, Teaching Assistant at Uzhhorod National University (Ukraine)

BMC Oral Health 2019, 19(Suppl 1):P37

Abstract

Background. The objective of research was to appraise integrated approach for evaluation the results of dental implant treatment using customized image analysis algorithm of CBCT scans.

Methods. Primary stage of the research was dedicated to the formation of a study sample, consisted of a set of 156 CBCT data pairs (dicom-files, voxel size 100 µm, isotropic) of 78 patients who had undergone dental implantation at the University Dental Clinic. Peri-implant bone changes evaluation was following originally developed algorithm which included, segmentation of the area of interest from the CBCT data set with the isolation of the implant installation region, transformation of the formatted image of region of interest from the *.dcm format to the *.stl format, superimpose of obtained stl-files from the data sets, calculation of the absolute bone volume loss around dental implant due to the amount of non-matched

image parts. Evaluation of bone parameters conducted in the adapted software ImageJ with additional plug-in BoneJ (the Wellcome Trust). Implant stability was measured with Ostell Mentor (Ostell). Statistical analysis of numerical data performed using software Microsoft Excel software (Microsoft Office, 2016).

Results. Method of STL-superimposition helped to calculate absolute volumetric parameter of radiused bone loss at periimplant region. Such average values for the implants installed in the distal part of maxilla were 3,547 cubed mm., around maxillary frontal implants its volume reached 3,118 cubed mm., mean bone loss around mandibular distal implants was 2,614 cubed mm., and mandibular frontal implants lost 2,456 cubed mm. of circular bone volume. Statistically tested correlation value between mean vertical bone loss and radiused volumetric bone reduction reached $r=0,784$ ($p \leq 0,05$). Also specific regressions between parameters of bone loss and prosthetic designs were found. In addition correlation level were estimated between ISQ values, volumetric bone loss measured by the superimposition principle and marginal bone loss measured by the sagittal slices of CBCT.

Conclusions. The proposed approach ensures possibilities for objectification not only geometrical, but also qualitative changes of bone at peri-implant region and takes into account the impact of functional stability of titanium infra-structures to prognose the success of treatment. The possibility of considering customized values of volumetric peri-implant bone loss instead of simple geometrical bone height reduction value, allows to individualize treatment algorithm by adapting different prosthetic designs due to the patient rehabilitation group with different trends of bone loss.

Clinics

P38

CAD/CAM Monolithic Restoration in Molar Region without Occlusal Adjustment

Zoltán Imre Kovács¹, Judit Borbely², Peter Schmidt², Peter Hermann²

¹Semmelweis University, Faculty of Dentistry, Department of General Dental Preclinical Practice - Hungary – Budapest; ²Semmelweis University, Faculty of Dentistry, Department of Prosthodontics - Hungary – Budapest

Correspondence: Zoltán Imre Kovács (dr.csonti@gmail.com)

BMC Oral Health 2019, 19(Suppl 1):P38

Abstract

Background. Development of digital technology in dentistry gives the opportunity to produce CAD/CAM temporary and definitive monolithic restorations. A usual problem with monolithic restorations is the occlusal correction after sintering procedures. During dental treatment, usually a temporary restoration is needed, which fits the preparation margin and the occlusion is adjusted in the patient mouth. If the morphology of this restoration is perfect, the need of making an absolutely alike definitive restoration appears. Laboratory design software makes it possible to use shapes recorded in prepreparation scan during the computer aided design. The aim of this study was to compare the adjusted occlusal contact of the temporary restoration to the monolithic definitive restoration's, which shape is copied from the temporary in the design software.

Methods. A 36 year old woman presented with the need of a treatment for her lost left mandibular first molar. The treatment plan was a 3 unit monolithic zirconia bridge. The preparation was made with 1-1,5 mm reduction and rounded shoulder finishing line. An intraoral scan was taken by Trios POD Wireless scanner. (TRIOS, 3Shape, Denmark). A 3 unit temporary PMMA bridge (Yamahachi) was designed in 3Shape Dental Designer software. After milling, the occlusion was adjusted in the mouth with the help of a T-scan device (Tekscan, U.S.). A prepreparation intraoral scan was taken from the temporary bridge, which was copied in the design software for the definitive monolithic zirconia restoration. (GLI Bruxzir shaded, Glidewell Dental, U.S.).

Results. The measured occlusal contacts with T-scan of the definitive restoration did not show significant difference from the temporary restorations.

Conclusions. Using the recorded shape of the temporary bridge as a prepreparation scan, the production of the monolithic zirconia bridge was possible. The patient felt the zirconia bridge as comfortable as the PMMA. With this method, the occlusal correction and repolishing of the definitive restoration was not needed.

Written, informed consent for publication was obtained from the patient [or parent/guardian for patients under 16]

P39

Complete digital workflow and immediate functional loading of implant-supported monolithic glass ceramic crowns

Justinas Pletkus¹, Adomas Auškalnis², Marius Kubilius³, Jotautas Kaktys⁴, Ieva Gendvilienė⁵, Rokas Borusevičius⁶, Agnė Gečiauskaitė⁷, Vygasdas Rutkūnas⁸

¹Resident at Department of Prosthodontics, Institute of Odontology, Faculty of Medicine, Vilnius University, Lithuania; Private practice; ²PhD, lector at Department of Dental and Oral Pathology, Faculty of Odontology, Lithuanian University of Health Sciences; Private practice ("Restauracines odontologijos centras", Kaunas, Lithuania); ³PhD, DDS, Private practice ("Restauracines odontologijos centras", Kaunas, Lithuania); ⁴Private practice ("Restauracines odontologijos centras", Kaunas, Lithuania); ⁵Department of Prosthodontics, Institute of Odontology, Faculty of Medicine, Vilnius University, Lithuania; Private practice ("Prodentum", Vilnius, Lithuania); ⁶Rokas Borusevičius, PHD student at Department of Periodontology, Institute of Odontology, Faculty of Medicine, Vilnius University, Private practice; ⁷PhD student, Department of Prosthodontics, Institute of Odontology, Faculty of Medicine, Vilnius University, Lithuania; Private practice ("Prodentum", Vilnius, Lithuania); ⁸Associate Professor, Department of Prosthodontics, Institute of Odontology, Faculty of Medicine, Vilnius University, Lithuania; Private practice ("Prodentum", Vilnius, Lithuania).

Correspondence: Justinas Pletkus (justinas.pletkus@gmail.com)

BMC Oral Health 2019, 19(Suppl 1):P39

Abstract

Background. Survival and success rates of immediate implant loading may vary widely according to literature. Advances in digital technologies create an opportunity for fast fabrication and delivery of final restorations. There is a very limited data on clinical outcomes of immediate loading of implants with final full-contour ceramic restorations produced using completely digital workflow. The aim of this study was to evaluate surgical and prosthetic aspects of immediate implant loading with glass ceramic screw-retained single crowns that could be associated with biologic and prosthetic outcomes.

Methods. Nineteen subjects, who required single tooth implant supported crown in the posterior region of the mandible received one or more implant (patients with bad or parafunctional habits were excluded). In total 22 implants were placed. Primary stability measured and recorded in Ncm and ISQ values. Cerec® (Densply Sirona) implant scan post and scanbody was attached to the implant. Omnicam® (Densply Sirona) intraoral scanner (IOS) (CEREC AC software 4.3) was used to take the digital impressions and bite registrations. Within 24hours functional glass ceramic (NICE, Straumann) crowns were delivered (Fig. 1 and Fig. 2). For every crown occlusal and interproximal contacts were adjusted and recorded. Quality of contact points were measured with shimstock occlusal foil (Hanel, Coltene). Restorations were followed-up for 1, 3, 6 months.

Results. 1 implant failed and was removed after 4 weeks. The rest implants and crowns were in function with no technical or biological complications after 6 months of use (survival rate of our study was 95,5%). Statistically significant effect on MBL was not found considering factors such as implant size, time after extraction, bone type, soft tissue thickness, and primary stability measured in Ncm and ISQ values. Mean MBL mesially was 0.3mm (SD 0.42) and distally – 0.4mm (SD 0.66). These findings are similar to those in other studies reporting MBL on delayed or immediate loading. One distal and one mesial proximal contacts were missing during 6 months check-up, similarly as during insertion of the crowns - 1 and 2, accordingly.

Conclusions. Fully digital workflow without 3D printed model could be successfully employed for immediate functional loading with a

single-unit implant-supported crowns fabricated from glass ceramics. When patients are carefully selected, it can provide clinically acceptable biologic and prosthetic outcomes in a follow-up period of 6 months. The protocol should be further evaluated with longer observational periods.

P40

Unconventional Implant Placement Through Impacted Maxillary Canine – A Case Report

Ivona Bjenjaš¹, Nenad Milinković², Đorđe Pejanović³, Tamara Ristić³
¹Dental clinic "BGD Osmeh" Francuska 25 11158 Belgrade; ²Dental SM D.O.O. Bulevar Oslobođenja 152 11040 Belgrade; ³Faculty of Dentistry Pancevo Žarka Zrenjanina 179, 26000 Pancevo; Faculty of Dentistry Pancevo Žarka Zrenjanina 179, 26000 Pancevo

Correspondence: Ivona Bjenjaš (ivonabjenjas@gmail.com)

BMC Oral Health 2019, 19(Suppl 1):P40

Abstract:

Background. Female patient 66 years old needed dental therapy of the upper right partial edentulism of maxilla. Old PMF fixed partial denture was loosened and the extraction of the tooth 12 was indicated. Tooth 15 was indicated for the root treatment and post. Region 14 and 13 were indicated for implant therapy.

Methods. Dental status was taken. To reduce the patient x-ray exposure following ALARA recommendation only small FOV on CBCT was done. The impacted right upper canine was discovered. Patient knew about it, but it was completely asymptomatic for years and no other surrounding pathology couldn't be seen on CBCT. Extraction of the impacted tooth was avoided because of expected massive bone loss and possible complications. The tooth 12 was extracted. There was no buccal plate after extraction, so this site was excluded for immediate implant placement. Two C-Tech implants were placed through the impacted tooth in region 13 (EL 3,5x11) and 14 (EL 3,5x9). Primary stability was achieved on 60N/cm. The wound was sutured with 4,0 Nylon. Control CBCT was taken, expected positions of implants were achieved. Patient was prescribed with antibiotic therapy Sinacilin 0.5g 3x1 for seven days and Ibuprofen 0.4 if needed.

Results. No postoperative pain, swelling or bleeding was reported by the patient. After seven days sutures were removed, the wound healing was uneventful. Tooth 15 was treated and CoCrMo post was made. After four months implants were uncovered without any difficulties and healing caps were placed.

Conclusions. There are only a few case reports done with placing implants into impacted teeth. From our experience protocol deviation is justified in situations when expected bone loss is compromising implant therapy afterward. There should be more studies confirming the safety of such procedures.

Written, informed consent for publication was obtained from the patient [or parent/guardian for patients under 16]

P41

Treatment of Ameloblastoma in posterior mandible with resection, reconstruction by free fibula graft and dental rehabilitation of conventional dental implants

Ashwini Bhalerao^{1,2} (ashwinib1170@gmail.com)

¹Private Practice, Mumbai, India; ²Consultant oral and maxillofacial surgeon, Criticare group of hospitals, Mumbai, India

BMC Oral Health 2019, 19(Suppl 1):P41

Abstract

Background. Ameloblastoma is a benign, locally infiltrative epithelial odontogenic tumour with cortical expansion and a high local recurrence rate. Clinically; the long standing lesions are characterized by looseness of teeth, root resorption and usually combined with unerupted tooth. Tumour cells have a great tendency to invade the surrounding healthy tissue which is considered to be the essential step in tumour progression. In the mandible majority of ameloblastomas are found in the molar ramus region. There are 7 types of ameloblastomas, follicular ameloblastoma having the highest rate of recurrence,

therefore these cases are treated by surgical excision and reconstruction by iliac crest or free fibula graft. The challenge in dental rehabilitation of such patients, aim is to rehabilitate the dentition not with removable but with dental implants restoring form and function.

Methods. A 28 years old male came with complaint of pain, swelling and discharge from right retromolar region since 3 weeks' revealed presence of a huge cystic lesion in the right ramus of mandible which had pushed the third molar superiorly. What was first thought to be a routine dentigerous cyst turned out to be a follicular ameloblastoma, confirmed by biopsy. Under general anaesthesia, the patient was operated for complete enucleation of the tumour. The Mandible was partially resected, simultaneously a free fibula graft was harvested and fixed in place with a reconstruction plate. The patient was placed on intravenous antibiotics and painkillers, after 8 days, he was discharged. Liquid diet was advised for 3 weeks post-surgery. After 10 months, the soft tissue healing was complete, CT scan showed a well-integrated graft. The cortico cancellous component was deemed to be satisfactory and dental implants placed by a flapless procedure as we did not want to disturb the mucosal attachment to the graft. 8 weeks later, they were loaded with screw retained prosthesis to prevent cement leaching through the mucosa till the fibula. Occlusion was checked with a T scan to ensure equal distribution.

Results. Satisfactory dental rehabilitation was achieved by placing dental implants in the optimal stage when the cortico cancellous proportion of fibula graft was favourable for achieving primary stability.

In the follow up of two years, we saw good remodelling of fibula under favourable load **Conclusions.** Patients with resected mandible can be given fixed prosthetic options, provided the planning and placing of dental implants is done in a calculated phased manner and the patient is counselled on the need of strict oral hygiene measures in the absence of attached gingiva. Giving such patients a removable denture or obturator works against them as food collection, non-loading, leads to resorption of graft and facial asymmetry with loss of function.

Written, informed consent for publication was obtained from the patient [or parent/guardian for patients under 16]

Science

P42

The Impact of an Augmented Reality Application on Perception and Anxiety Level in Students during Administration of First Local Anesthetic Injection

Rasa Mladenovic¹, Leandro Pereira², Kristina Mladenovic³

¹Faculty of Medicine, University of Pristina, Kosovska Mitrovica, Serbia;

²Blantus Endodontic Center, Campinas, Brazil; ³Faculty of Medical Sciences, University of Kragujevac, Serbia

Correspondence: Rasa Mladenovic (rasa.mladenovic@med.pr.ac.rs)

BMC Oral Health 2019, 19(Suppl 1):P42

Abstract

Background. Although local anesthesia (LA) is an imperative of modern dentistry, many dental students feel insufficiently prepared for administration of their first injection in a clinical setting. Augmented Reality (AR) is a technology that superimposes a computer-generated image on a user's view of the real world, thus providing a composite view. Visualization and interaction are fundamental components of AR technology. The objective of this study was to examine the impact of an AR application in students administering LA for the first time.

Methods. Students were categorized into two groups. In addition to the theoretical and practical training, the students of the experimental group used the AR simulator. The trigger for acute stress was LA administration. The concentration of salivary cortisol was measured before and after LA. Patients were children who had indications for anesthesia. Mann-Whitney test, t-test and Wilcoxon test were used to test statistical hypotheses.

Results. The level of cortisol after anesthesia was statistically significant in all subjects, but there was no statistically significant difference between the groups. The time required for the LA administration was significantly longer in the control group ($p = 0.014$).

Conclusions. Given that blood sampling is a stressful process that could add up to the anxiety level, in the study we measured the concentration of salivary cortisol. We opted for afternoon measurements when the levels of salivary cortisol are considered to be stable according to the circadian rhythm. Increased cortisol concentration in all students after LA supports the opinion of many clinicians that LA administration is one of the more stressful aspects of clinical practice. Having the syringe in the patient's line of sight and performing lengthy treatments may result in unsatisfactory analgesia, specifically in children. Using the AR, the anatomical structures in the oral cavity are easy and convenient to use and give a good introduction to clinical anesthesia due to user interaction, as demonstrated in our study - students who received AR training had significantly less time for the anesthetic procedure. This form of learning provides an innovative and interactive way of presenting material, and therefore should be used in addition to conventional learning or as a self-improvement tool that can result in a positive response and student motivation. AR application can influence better understanding of anatomy structure and the correct and faster technique for administering local anesthesia, but cannot reduce acute stress.

Clinics

P43

Influence of malocclusion and cranio-cervical dysfunction in facial paralysis

Diego Tatis^{1,2} (dtatis@orthokinetic.com)

¹Isaac Newton University Costa Rica; ²Orthokinetic Training Center – Colombia

BMC Oral Health 2019, 19(Suppl 1):P43

Abstract

Background. To present and to explain the influence of dental occlusion, the cranio-masticatory system and the cranio-cervical system in the etiology and prognosis in the therapeutic management of peripheral paralysis of the facial nerve. In this work, the paralysis of the VII cranial nerve refers to an acute unilateral peripheral facial paresis, monosymptomatic, until now, in most cases unknown.

Methods. The material of this poster includes a literature review and two clinical cases of perispheric facial nerve palsy from the group of cases studied and treated by the author over a period of 20 years. Patients previously evaluated and diagnosed by neurosurgery with facial paralysis or Bell's palsy. A common clinical pattern was observed in the treated patients: skeletal class II, facial asymmetry, temporo-mandibular dysfunction and cranio-cervical dysfunction. A standard test was performed at the first consultation, which included a detailed description of the degree and location of the tests. of paresis, taste, extra-oral clinical examination and intra-oral clinical examination, electromyographic examination, MRI and audio-spectrometric analysis of temporomandibular joints. The immediate suspension of any type of medication indicated previously for the treatment of the pathology is ordered. OrthokineticTM splints of Neuro Muscular and Skull-cervical Articular Repositioning Splints (Patent No. 978627) are adapted and controlled with T-Scan Analysis and follow-up once every two days, second control at week and third at two weeks and then once a month. Complementary physical therapy was used.

Results. The clinical examination revealed 100% unilateral complete paralysis. The follow-up showed in 100% of the patients the function was partially restored on the second day and total at 6 days. In 100% of the patients the function of the normal mimicry was obtained. The sequelae of dysfunction were 0% for the total of the patients

Conclusions. Cranio-masticatory dysfunction could have an influence on skeletal mechanics and neuro-muscular mechanics in the anatomical course of the facial nerve, which could lead to its dysfunction, with the consequent paralysis of the muscles of the affected side. The use of prednisone poses a great ethical problem because there is no evidence of its efficacy and the euphoric side effect induces a false sense of benefit in patients. Dental occlusion is directly and intimately related with the temporo-mandibular and cranio-cervical balance. Occlusal imbalances could influence neuro-muscular imbalance, temporo-mandibular imbalance and cranio-cervical imbalance, which

would affect the normal function of any cranial nerve involved, including the facial nerve or VII cranial nerve.

P44

Guided implant placement in patient with Multiple Idiopathic Cervical Resorption

Lukasz Zadrozny, Katarzyna Brus-Sawczuk
Medical University of Warsaw - Poland

Correspondence: Lukasz Zadrozny (lukasz.zadrozny@gmail.com)
BMC Oral Health 2019, 19(Suppl 1):P44

Abstract

Background. Multiple Idiopathic Cervical Resorption is very a rare disease and proceed asymptomatic until teeth mobility occurs or accidental X-ray reveals different degree of cervical resorption in more than one tooth. Infected teeth stays vital with proper pulp reactions. MICR may run and develop in different time on another teeth even if previously founded illness teeth were treated or extracted. Potential reasons for this disease development are trauma or injury or systemic diseases such as hyperparathyroidism.

Methods. A 41-year-old female patient with good general health complained on increased mobility of front teeth in the mandible. Clinically teeth 32-42 has 3rd grade of mobility. Patient had a face trauma about 30 years ago. OPG X-Ray revealed severe cervical resorption in teeth 33-43 and 15-11, 21 has RCT done many years ago. CBCT was taken for more accurate diagnostics and additional blood test were done. Mandible treatment plan based on virtual planning with CBCTs DICOM data and an optical scans STLs files of both dental arches (DentiqGuide) and preparing temporary bridge (Exocad) obtains extracting of teeth 33-43 and guided immediate implants placement in positions 33, 31, 43 and immediate loading. In local anesthesia teeth 33-43 were sectioned and extracted. Sleeveless 3D printed guide with OneGuide Kit (Osstem Implant) were used to place implants in positions corresponding with virtual planning to be restore immediate by already milled from PMMA six units temporary bridge. ISQ values for each implant was over 75 what provides condition for immediate loading. Bridge was positioned in occlusion with positioning splint and bonding to abutments. After unscrewing, bridge was polished and screwed back, access holes were closed with composite.

Results. Teeth supported 3D printed guide provides 3 implants placement with accuracy allowing for fixing and screw retaining of six points unit bridge, in proper occlusion.

Conclusion. Virtual, backward planning of complex cases may offer possibilities for an esthetic restoration of implant supported fixed prosthesis. In the presented case of MICR, treatment plan includes potential development of resorption on remaining teeth. Basing on that fact long time temporary reconstruction was attached to the implants through multiunits. Implants positioned in sites 33, 31 and 43 and multiunit abutments creates open condition to exchange bridge to more expand if potential further extractions would be required and offers even full arch reconstruction with only two additional implants in premolar or molar sites if the initial disease would still develop.

Written, informed consent for publication was obtained from the patient [or parent/guardian for patients under 16]

P45

Potentially mortal complication during guided implant placement in anterior mandible

Lukasz Zadrozny, Leopold Wagner
Medical University of Warsaw - Poland

Correspondence: Lukasz Zadrozny (lukasz.zadrozny@gmail.com)
BMC Oral Health 2019, 19(Suppl 1):P45

Abstract

Background. Frontal mandible is common described as a safe zone for implant procedures. Besides of inferior alveolar nerves and vessels injuries much more dangerous may be hurting of sublingual artery or its branches what can happen if implant drill perforate lingual plate of mandible. Hurting these arteries may provoke severe bleeding to the sublingual space and creation of sublingual hematoma and subsequently obstruct the airways, what can be potentially mortal.

Methods. A 62-year-old female patient presented with hopeless teeth 33-41 in anterior mandible and toothless maxilla. Teeth extractions were planned and because of big discrepancy in bone height of front and back segments of mandible, bone reduction in front segment was planned. Two implants with Locator attachments in positions of canines were planned to support future removable prosthesis. Two-pieces bone supported surgical guide was designed and 3D printed. First- lower part fixed to the bone with two anchor screws determines range of planned bone reduction. Second- upper part of guide with attachments to the first and another bone anchor pin provides implants positioning with sleeveless OneGuide Kit (Osstem Implants). After flap opening, teeth were extracted and first part of guide were set on the bone and stabilize with two anchor screws. Bone was reduced according to the guide. Second guide part was then attached to the already fixed part and additionally fixed with third anchor. Osteotomy for implant in position 33 was performed. During preparation of osteotomy in position 43 high bone density was felt. Probing revealed lingual plate bone perforation at the end of osteotomy. No severe bleeding occurred and no distortion of lingual soft tissue were found. Osteotomy was filled with hemostatic sponge (Ferrosan) and medially another osteotomy was prepared freehand. Implants were placed and wound was closed.

Results. Check up examinations and communication with patient didn't revealed any signs of increasing bleeding and development of intraoperative complication.

Conclusion. Guided surgeries provide new possibilities and improve accuracy of implant procedures. Very important is to not forget about still existing range of inaccuracy especially when tissue or bone supported guides are used. Clinician has to consider that drills for guided surgeries are about 10mm longer than standard and the longer the drill the farer its tip may deflect even with minor guide setting inaccuracy. That may leads to destroy anatomical structures, and it's extremely important to calculate safety zones even in guided surgeries.

Written, informed consent for publication was obtained from the patient [or parent/guardian for patients under 16]

Publisher's Note

Springer Nature remains neutral with regard to jurisdictional claims in published maps and institutional affiliations.

